NTS2 NEUROTENSIN RECEPTORS:

Distribution, Interactions, and Cellular Dynamics in Model Systems and Rat Brain

Amélie Perron

Department of Neurology and Neurosurgery
McGill University, Montreal, Canada

June 2006

A thesis submitted to the Faculty of Graduate Studies and Research in partial fulfillment of the requirements for the degree of Doctorate in Science

Your file Votre référence
ISBN: 978-0-494-27829-1
Our file Notre référence
ISBN: 978-0-494-27829-1

ABSTRACT

Although available evidence suggests that NTS1 receptors play a key role in the transduction of many of the central effects of neurotensin (NT), recent data indicate that the NTS2 subtype may be responsible for mediating NT-induced analgesia. However, little is known about the cellular and molecular mechanisms underlying NTS2 function. It is also unclear whether endogenous NT is an agonist at the NTS2 site and to which second messenger system(s) this receptor is coupled since conflicting data has emerged from studies carried out in systems heterologously expressing the NTS2 receptor. In this context, the overall objective of the present study was to characterize the distribution of the NTS2 protein in rat brain, to further document the role played by NTS2 receptors in antinociception, and to unravel the cellular mechanisms underlying NTS2-mediated transduction of NT's effects. Our immunohistochemical studies revealed that NTS2 receptors are widely expressed within the rat CNS with high densities of labeled neurons and/or processes in descending antinociceptive pathways including the periaqueductal gray (PAG), and the rostroventral medial medulla. Both the full-length and alternatively-spliced isoforms induced a rapid and sustained activation of the mitogen-activated protein kinase (ERK1/2) pathway in both transfected CHO and COS-7 cells upon stimulation with NT. Combined biochemical and confocal microscopic studies revealed that NTS2 receptors were maintained at the cell surface following long-term agonist exposure despite efficient internalization mechanisms. This preservation was neither due to NTS2 neosynthesis nor recycling but rather appeared to involve translocation of spare receptors from intracellular stores as observed in both transfected cells and rat spinal cord neurons. NTS2 was demonstrated to heterodimerize with NTS1 in cells co-transfected with the two receptors. This heterodimerization was found to affect cell surface recruitment of NTS1, making it more similar to that of NTS2. Also, upon prolonged NT stimulation, cell surface NTS1 were more resistant to down-regulation in cells co-expressing NTS1 and NTS2 than in cells expressing NTS1 alone. Such maintenance of NT receptors bioavailability might prove of great importance for the use of NTS2-selective agonists for the treatment of chronic pain.

RÉSUMÉ

Bien que la plupart des effets de la neurotensine (NT) soient reliés à la stimulation des récepteurs de sous-type NTS1, certains restent intouchés par l'administration d'antagonistes sélectifs, suggérant qu'ils sont induits par d'autres sous-types de récepteur. Afin d'évaluer l'implication éventuelle des récepteurs NTS2 dans l'effet analgésique de la NT, nous avons étudié la distribution régionale et cellulaire de ce récepteur dans le système nerveux central (SNC) du rat. Nos analyses immunohistochimiques ont révélé que le récepteur NTS2 est exclusivement neuronal, et qu'il est exprimé de façon ubiquitaire dans le SNC avec des concentrations particulièrement importantes dans les régions impliquées dans l'antinoception telles que la substance grise periaqueductale et le bulbe rachidien rostro-ventral. Nos travaux ont par ailleurs démontré l'existence de deux isoformes de NTS2 dans le SNC du rat: une forme complète à sept domaines transmembranaires et une forme variante tronquée à cinq domaines transmembranaires (vNTS2). La liaison de la NT à ces deux sous-types de récepteurs induit une internalisation du complexe ligand/récepteur de même qu'une activation rapide et soutenue de la voie de la famille des MAP kinases dans les cellules COS-7 et CHO transfectées. Des études de radioliaison ont d'autre part révélé que, contrairement au NTS1, les récepteurs NTS2 sont maintenus à la membrane cellulaire suite à une stimulation prolongée par la NT. Cette préservation des récepteurs NTS2 à la membrane est indépendante de leur recyclage ou de la synthèse de nouveaux récepteurs mais semble impliquer un adressage de récepteurs de réserve à partir du complexe Golgi/TGN, selon nos observations en microscopie confocale et électronique dans les cellules COS-7 et neurones de la moelle épinière de rat, respectivement. Finalement, nous avons démontré que dans des cellules co-exprimant le NTS1 et le NTS2, les deux récepteurs forment des complexes hétérodimériques. Cette hétérodimérisation réduit l'adressage membranaire du NTS1 et amoindrit la perte de sa densité de surface suite à une exposition prolongée à la neurotensine. L'utilisation d'agonistes spécifiques du récepteur NTS2 pourrait par conséquent s'avérer une stratégie intéressante pour le traitement de la douleur chronique par des agonistes de la neurotensine.

TABLE OF CONTENTS

CHAPTER 8: General Discussion

LIST OF FIGURES

LIST OF TABLES

ACKNOWLEDGEMENTS

Je tiens à remercier en tout premier lieu mon directeur de thèse, le professeur Alain Beaudet, pour m'avoir accueillie dans son laboratoire et pour avoir su me conseiller efficacement tout au long de mon doctorat. Ce fut un plaisir de travailler avec un groupe de scientifiques aussi dynamiques et polyvalents, qui m'ont également appris les rudiments du travail d'équipe.

Je tiens particulièrement à remercier le Dr. Philippe Sarret, l'expert en NTS2, qui m'a prise sous son aile dès mon arrivée. Je tiens aussi à rendre hommage à son humour et à sa patience. Merci au Dr. Thomas Stroh pour m'avoir appris à ordonner mes idées et pour m'avoir aidée dans la rédaction de nombreux manuscrits. Je remercie le Dr. Ongali pour nos échanges scientifiques et pour m'avoir permis de participer à ses recherches. Je lui souhaite la meilleure des chances dans sa carrière de futur chercheur. Je tiens aussi à remercier Mariette Lavallée, avec qui j'ai pu partager ma passion pour les arts et échanger sur de nombreux sujets intéressants. Naomi Takeda, pour son aide et son efficacité sans pareil. Merci à Nadder Sharif pour son expertise en photographie et son soutien moral. Je souhaite également exprimer ma gratitude envers le Dr Louis Gendron pour son esprit critique et sa disponibilité, qui ont été fort appréciés lors de la dernière partie de ma thèse.

Un grand merci finalement à Pablo, Phil, Mandana, Frédéric, Chris, Dany, Motoharu, Anne-Julie, Marie-France, Babak, Claudine, Alby, Sofiane et Oum pour leur amitié et leurs précieux conseils.

PUBLICATIONS

Journals:

A. Perron, N. Sharif, P. Sarret, T. Stroh, and A. Beaudet. (2006) NTS2 Modulates the intracellular distribution and trafficking of NTS1 via heterodimerization. Submitted to *Journal of Biological Chemistry* (manuscript M6:05442).

A. Perron, N. Sharif, L. Gendron, M. Lavallée, T. Stroh, J. Mazella, and A. Beaudet. (2006) Sustained neurotensin exposure promotes cell surface recruitment of NTS2 receptors. *Biochemical Biophysical Research Communications* **343**: 799-808.

P. Sarret, M. J. Esdaile, A. Perron, J. Martinez, T. Stroh, and A. Beaudet. (2005) Potent spinal analgesia elicited through stimulation of NTS2 neurotensin receptors. *Journal of Neuroscience* **25**: 8188-96.

A. Perron, P. Sarret, L. Gendron, T. Stroh, and A. Beaudet. (2005) Identification and functional characterization of the 5-transmembrane domain variant isoform of the NTS2 neurotensin receptor in rat central nervous system. *Journal of Biological Chemistry* **280**: 10219-27.

L. Gendron, A. Perron, D. Payet, N. Gallo-Payet, P. Sarret, and A. Beaudet. (2004) Low-affinity neurotensin Receptor (NTS2) signaling: internalization-dependent activation of ERK1/2. *Molecular Pharmacology* **66**: 1421-30.

A. Perron, P. Sarret, T. Stroh, and A. Beaudet. (2003) Immunohistochemical distribution of NTS2 receptors in the rat central nervous system. *Journal of Comparative Neurology,* **461**: 520-38.

Sequence:

A. Perron, P. Sarret, and A. Beaudet. (2005) Rattus norvegicus variant neurotensin receptor 2 (Ntsr2) mRNA, complete cds. *GenBank*, Accession Number: AY946024.

Conferences/Abstracts:

A. Perron, N. Sharif, T. Stroh, J. Mazella, and A. Beaudet. (2005) Neurotensin stimulation promotes recruitment of NTS2 receptors to the cell surface. 35th Annual meeting, Society for Neuroscience, Washington DC, USA.

B. Ongali, A. Perron, T. Stroh, and A. Beaudet. (2005) Dehydratation-induced up-regulation of apelin receptors in the hypothalamus and cortex of adult rats. 35th Annual meeting, Society for Neuroscience, Washington DC, USA.

A. Perron, P. Sarret, L. Gendron, t. Stroh and A. Beaudet. (2004) Carboxy-terminal tail of the rat NTS2 receptor modulates NTS2-vNTS2 heterodimerization. 34th Annual meeting, Society for Neuroscience, San Diego CA, USA.

P. Sarret, M.J. Esdaile, A. Perron, T. Stroh, J. Martinez, and A. Beaudet. (2004) Implication of NTS2 Receptors in the regulation of primary afferent nociceptive pathways. 34th Annual meeting, Society for Neuroscience, San Diego CA, USA.

A. Perron, P. Sarret, L. Gendron, T. Stroh, A. Beaudet. (2004) Distribution, caractérisation moléculaire et couplage fonctionnel des récepteurs de basse affinité de la neurotensine (NTS2) dans l'hypothalamus de rat. 32e Colloque de la Société de Neuroendocrinologie, Montpellier, France.

A. Perron, P. Sarret, L. Gendron, T. Stroh, and A. Beaudet. (2003) Identification and functional characterization of a short variant isoform of the NTS2 neurotensin receptor in rat CNS. 33rd Annual meeting, Society for Neuroscience, New Orleans LA, USA.

P. Sarret, A. Perron, T. Stroh, and A. Beaudet. (2003) Immunohistochemical localization of NTS2 neurotensin receptors in rat spinal cord and dorsal root ganglia. 33rd Annual meeting, Society for Neuroscience, New Orleans LA, USA.

L. Gendron, P. Sarret, A. Perron, N. Gallo-Payet, and A. Beaudet. (2003) The rat NTS2 is functionally coupled to ERK1/2: activation by an internalization-dependent mechanism. 33rd Annual meeting, Society for Neuroscience, New Orleans LA, USA.

A. Perron, P. Sarret, T. Stroh, and A. Beaudet. (2002) Immunohistochemical distribution of NTS2 neurotensin receptors in adult rat brain. 32nd Annual meeting, Society for Neuroscience, Orlando FL, USA.

A. Perron, P. Sarret, T. Stroh, and A. Beaudet. (2002) Identification of the 5-transmembrane domain variant isoform of NTS2 in the rat CNS. 3rd Annual meeting, Great Lakes GPCR Retreat, Ann Arbor MI, USA.

GUIDELINES FOR THESIS PREPARATION

As stated in the "Guidelines Concerning Thesis Preparation" of the Faculty of Graduate Studies and Research of McGill University:

> 1. Candidates have the option of including, as part of the thesis, the text of one or more papers submitted, or to be submitted, for publication, or the clearly-duplicated text (not the reprints) of one or more published papers. These texts must conform to the "Guidelines for Thesis Preparation" with respect to font size, line spacing and margin sizes and must be bound together as an integral part of the thesis. (Reprints of published papers can be included in the appendices at the end of the thesis.)
>
> 2. The thesis must be more than a collection of manuscripts. All components must be integrated into a cohesive unit with a logical progression from one chapter to the next. In order to ensure that the thesis has continuity, connecting texts* that provide logical bridges preceding and following each manuscript are mandatory.
>
> 2. The thesis must conform to all other requirements of the "Guidelines for Thesis Preparation" in addition to the manuscripts. The thesis must include the following (1) a table of contents; (2) a brief abstract in both English and French; (3) an introduction which clearly states the rational and objectives of the research; (4) a comprehensive review of the literature (in addition to that covered in the introduction to each paper); (5) a final conclusion and summary; (6) a thorough bibliography; (6) Appendix containing an ethics certificate in the case of research involving human or animal subjects, microorganisms, living cells, other biohazards and/or radioactive material.
>
> 3. As manuscripts for publication are frequently very concise documents, where appropriate, additional material must be provided (e.g., in appendices) in sufficient detail to allow a clear and precise judgement to be made of the importance and originality of the research reported in the thesis.
>
> 5. In general, when co-authored papers are included in a thesis the candidate must have made a substantial contribution to all papers included in the thesis. In addition, the candidate is required to make an explicit statement in the thesis as to who contributed to such work and to what extent. This statement should appear in a single section entitled "Contributions of Authors" as a preface to the thesis. The supervisor must attest to the accuracy of this statement at the doctoral oral defence. Since the task of the examiners is made more difficult in these cases, it is in the candidate's interest to clearly specify the responsibilities of all the authors of the co-authored papers.

*Note: connecting texts that provide the logical bridges between each chapter in this thesis were grouped together and are presented in **CHAPTER 2: RATIONALE OF THE THESIS**.

CONTRIBUTION OF AUTHORS

Dr. Alain Beaudet was the candidate's research and thesis supervisor. He assisted in the conception of the experiments and provided direction to the candidate. Hence, Dr. Beaudet is an author on all research papers and manuscripts included in this thesis.

ORIGINAL RESEARCH ARTICLES

1. IMMUNOHISTOCHEMICAL DISTRIBUTION OF NTS2 NEUROTENSIN RECEPTORS IN THE RAT CENTRAL NERVOUS SYSTEM

Philippe Sarret, **Amélie Perron**, Thomas Stroh, and Alain Beaudet.
Journal of Comparative Neurology (2003) 461: 520-538.

- A. Perron was co-first author with P. Sarret. They both conceived all of the studies described in this manuscript.
- P. Sarret, A. Perron and T. Stroh participated in the design of the N-terminally directed NTS2 peptide antibody.
- A. Perron tested the specificity of 12 different bleeds through confocal microscopic and Western blotting studies in both tranfected cells and brain membranes. She also determined the conditions for the peptide blocking experiments that were conducted in tissue samples. She wrote the sections in the manuscript (Materials and Methods, Results, Discussion, Figure Legends) concerning the work that she had performed.
- P. Sarret accomplished all the light immunohistochemical studies and the mapping of the NTS2 receptor in rat brain. He prepared most of the figures and wrote a substantial portion of the manuscript.
- T. Stroh participated in the interpretation of the data, helped in the mapping, and supervised the writing of the manuscript.

2. LOW-AFFINITY NEUROTENSIN RECEPTOR (NTS2) SIGNALING: INTERNALIZATION-DEPENDENT ACTIVATION OF EXTRACELLULAR SIGNAL-REGULATED KINASES 1/2

Louis Gendron, **Amélie Perron**, Marcel Daniel Payet, Nicole Gallo-Payet, Philippe Sarret, and Alain Beaudet.

Molecular Pharmacology (2004) 66: 1421-1430.

- L. Gendron conceived, planned, and performed most of the studies described in the paper. He prepared the figures and wrote a substantial portion of the paper.
- A. Perron carried out the cloning and binding experiments. She wrote the introduction of the manuscript as well as the sections (Materials and Methods, Results, Discussion, Figure Legends) concerning the work that she had performed.
- M. D. Payet and N. Gallo-Payet are professors of the Department of Physiology and Biophysics at the University of Sherbrooke. The intracellular calcium measurement experiments were performed under their direction.
- P. Sarret established the CHO cell line stably expressing the rat NTS2 receptor. He also participated in the interpretation of the data.

3. IDENTIFICATION AND FUNCTIONAL CHARACTERIZATION OF THE 5-TRANSMEMBRANE DOMAIN VARIANT ISOFORM OF THE NTS2 NEUROTENSIN RECEPTOR IN RAT CENTRAL NERVOUS SYSTEM

Amélie Perron, Philippe Sarret, Louis Gendron, Thomas Stroh, and Alain Beaudet.

Journal of Biological Chemistry (2005) 280: 10219-10227.

- A. Perron and P. Sarret conceived all of the studies described in this article.
- A. Perron performed all of the experiments described in this manuscript. She prepared the figures and wrote the manuscript.
- L. Gendron trained A. Perron to determine the measurement of MAP Kinases activity and participated in the interpretation of the data.
- T. Stroh provided a substantial help in writing the manuscript.

4. SUSTAINED NEUROTENSIN EXPOSURE PROMOTES CELL SURFACE RECRUITMENT OF NTS2 RECEPTORS

Amélie Perron, Nadder Sharif, Louis Gendron, Mariette Lavallée, Thomas Stroh, Jean Mazella, and Alain Beaudet.

Biochemical and Biophysical Research Communications (2006) 343: 799-808.

- A. Perron conceived and performed most of the experiments described in this manuscript. She prepared the figures and wrote the manuscript.
- N. Sharif assisted A. Perron in the acquisition of images by confocal microscopy. He also participated in the interpretation of the data.
- L. Gendron performed the intrathecal injections and conducted the rat perfusions for electron microscopic studies. He also assisted A. Perron in the acquisition of images at the electron microscope.
- M. Lavallée performed the final steps of immunogold labeling experiments.
- T. Stroh participated in electron microscopic data analysis and provided assistance in writing the manuscript.
- L. Gendron, T. Stroh, N. Sharif, and J. Mazella assisted in the editing of the manuscript.

5. NTS2 MODULATES THE INTRACELLULAR DISTRIBUTION AND TRAFFICKING OF NTS1 VIA HETERODIMERIZATION

Amélie Perron, Nadder Sharif, Philippe Sarret, Thomas Stroh, and Alain Beaudet.

Manuscript submitted to *Journal of Biological Chemistry* (M6:05442)

- A. Perron conceived, planned and coordinated all of the studies described in this manuscript. She arranged the figures and wrote the manuscript.
- N. Sharif assisted A. Perron in the confocal microscopic studies. He took part in data analysis as well.
- P. Sarret provided a considerable help in the radioligand binding studies.
- P. Sarret and T. Stroh participated in the editing of the manuscript.

Note: Underlining indicates co-authorship.

ORIGINALITY

This thesis furthers our knowledge of the molecular and cellular characterization of NTS2 receptors. It demonstrates that NTS2 receptors are expressed as two different isoforms, which are widely distributed throughout the rat central nervous system. Additionally, this thesis provides functional evidence that these receptors behave as bona fide NT receptors but are not down-regulated following persistent agonist exposure, providing physiological relevance for the use of NTS2-selective agonist for the treatment of chronic pain. Finally, it reveals that NTS2 receptor expression influences the intracellular trafficking of other NT receptor subtypes through heterodimerization.

CHAPTER 3:

Immunohistochemical Distribution of NTS2 Neurotensin Receptors in the Rat Central Nervous System. This chapter provides the first comprehensive description of the immunohistochemical distribution of NTS2 receptors in the rat CNS at the light microscopic level. For this purpose, we have designed and sub-contracted the production of a NTS2 antibody directed toward a 15-amino acid synthetic sequence derived from the N-terminal portion of the rat NTS2 receptor, common to both short and long receptor isoforms. Our study indicated that NTS2 receptors are broadly distributed within the rat CNS with high levels of NTS2 receptor proteins detected in regions involved in the descending control of nociceptive inputs, in keeping with its postulated role in antinociception. It also showed that NTS2 receptors are essentially neuronal and that they are mostly, although not solely targeted to dendrites.

CHAPTER 4:

Low-affinity Neurotensin Receptor (NTS2) Signaling: Internalization-Dependent Activation of Extracellular Signal-Regulated Kinases 1/2. In this study, we investigated NTS2 signaling pathways in heterologously expressing cell systems. In contrast to what has previously been reported in the literature, our data revealed that NT, as well as many of the known NTS2 receptor ligands, act as

agonists at the rat NTS2 receptor site, in that all induced a NTS2-mediated activation of the MAP Kinase cascade. Furthermore, this agonist-induced phosphorylation of ERK1/2 was completely abolished by both overexpression of a dominant-negative mutant of dynamin-1 (DynK44A) and preincubation with endocytosis inhibitors (i.e. phenylarsine oxide and monodansylcadaverine), indicating that internalization was required for this activation to occur. Contrary to previous studies in which NT was shown to act as an antagonist at the human NTS2 site, we observed the same NT-triggered ERK1/2 phosphorylation in human and rat NTS2 receptor expressing CHO cells. This finding is important in that it lends further support to the premise that NT is an endogenous ligand at this receptor.

CHAPTER 5:

Identification and Functional Characterization of the 5-Transmembrane Domain Variant Isoform in the Rat Central Nervous System. We presented here a novel spliced variant isoform of the NTS2 receptor that we have isolated from rat brain RNA (GenBank accession number AY946024; see Appendix D). Most importantly, we showed that this 5-transmembrane domain receptor is functional, in that is specifically binds and internalizes NT and is coupled to the activation of the ERK1/2 pathway. To our knowledge, this truncated NTS2 isoform is the first transmembrane spliced GPCR variant cloned to date that was found to maintain its signaling properties. Furthermore, we have demonstrated that the variant NTS2 isoform is expressed in conjunction with the full-length NTS2 isoform throughout the CNS. Our data also indicate that this truncated NTS2 receptor associates both with itself and with the full-length NTS2 receptor to form large molecular weight homo- and heterodimer species in the rat CNS.

CHAPTER 6:

Sustained Agonist Exposure Promotes Cell Surface Recruitment of NTS2 Neurotensin Receptors. In this chapter, we demonstrated that in contrast to what is observed in cells transfected with NTS1, NTS2-expressing cells retain the same surface receptor density during persistent NT exposure despite efficient internalization mechanisms. This preservation of cell surface NTS2 receptors is neither due to receptor recycling nor neosynthesis but rather involves translocation of spare receptors from intracellular stores to the plasma membrane. Additionally, our confocal immunolocalization studies revealed that as opposed to NTS1, internalized NTS2 receptors are not targeted to lysosomes for degradation. The physiological relevance of these observations was provided by immunogold electron microscopic studies on neurons of the superficial laminae of the rat spinal cord in which agonist stimulation was found to trigger an extensive relocalization of intracellular receptors from intracellular stores to the plasma membrane. This report also represents the first account of the subcellular localization of NTS2 by electron microscopy.

CHAPTER 7:

NTS2 Modulates the Intracellular Distribution and Trafficking of NTS1 via Heterodimerization. This section demonstrates that NTS1 and NTS2 receptors form heterodimeric complexes in a transfected cell system. This report also shows that the formation of NTS1/NTS2 heterodimers markedly inhibits cell surface recruitment of NTS1 binding sites, which remain accumulated in the perinuclear region (i.e. in the same compartment that harbours the bulk of NTS2 receptors when they are expressed alone). Additionally, radioligand binding studies have demonstrated that NTS1 cell surface binding sites are more resistant to down-regulation when the two NT receptor subtypes are expressed together, suggesting that NTS1/NTS2 heterodimerization might represent an additional mechanism in the regulation of NT-induced responses mediated by NTS1 and NTS2 receptors.

CHAPTER 1: INTRODUCTION

1. NEUROTENSIN AS A NEUROTRANSMITTER

The tridecapeptide neurotensin (NT) (Glu-Leu-Tyr-Glu-Asn-Lys-Pro-Arg-Arg-Pro-Tyr-Ile-Leu) originally isolated from bovine hypothalamus (Carraway and Leeman, 1973), is broadly distributed throughout the central nervous system (CNS) and peripheral tissues. NT acts as a neuromodulator/neurotransmitter in the CNS, while it fulfills a function of local hormone in the periphery (Vincent et al., 1999).

1.1 Physiological and Pathological Effects

1.1.1 Neurotensin-dopamine Interactions

NT has been shown to modulate dopaminergic (DA) transmission in the nigrostriatal and mesocorticolimbic pathways (Nemeroff, 1986; Kitabgi et al., 1989), thereby implicating this neuropeptide in the pathophysiology of several CNS disorders including Parkinson's disease and schizophrenia (Garver et al., 1991; Rostène et al., 1992; Binder et al., 2001a). Indeed, NT was formally proposed to be a potential endogenous neuroleptic 25 years ago based on the fact that central NT elicited a range of effects similar to those of antipsychotics drugs (APD) (reviewed in Binder et al., 2001a; Kinkead and Nemeroff, 2002). For instance, both intracerebroventricular NT injections and peripherally administrated APD blocked stimulant-induced hyperlocomotion (Kalivas et al., 1984; Skoog et al., 1986; Sarhan et al., 1997) and decreased spontaneous locomotor activity (Jolicoeur et al., 1983; Dubuc et al., 1994; Gully et al., 1995). However, NT was reported to mediate contrary effects on DA transmission, depending on the injection site in the brain. Accordingly, microinjection of NT into the nucleus accumbens, a projection area of mesolimbic DA neurons, was shown to produce neuroleptic-like effects, while NT injections into the ventral tegmental area (VTA), which contains DA neurons that project to the nucleus accumbens, triggered psychostimulant-like effects (e.g. hyperlocomotion and turning behavior) (Kalivas and Steketee, 1992; Kalivas et al., 1993; Steinberg et al., 1994; Kitabgi, 2002; Dobner et al., 2003). Finally, intrastriatal administration of NT was shown to trigger vacuous chewing movements, suggesting that increased levels

of endogenous NT within the ventrolateral striatum may play a critical role in the development of tardive dyskinesia (Stoessl, 1995).

1.1.2 Neurotensin and Neuroendocrine Systems

Several studies have shown that NT participates in the regulation of mammalian neuroendocrine systems (reviewed in Rostène and Alexander, 1997). At the hypothalamic level, NT was reported to modulate the release of gonadotropin-releasing hormone (GnRH) (Alexander et al., 1989a), somatostatin (Sheppard et al., 1979), corticotropin-releasing hormone (CRH) (Nussdorfer et al., 1992), and growth hormone releasing hormone (GHRH) (Niimi et al., 1991). NT was also shown to have a variety of effects on the release of pituitary hormones (Rowe et al., 1992). For instance, NT injection in the preoptic area was shown to regulate the preovulatory surge of luiteinizing hormone (LH) in female rats (Ferris et al., 1984). Additionally, NT was reported to modulate the secretion of prolactin (McCann et al., 1982) and growth hormone (GH) (McCann and Vijayan, 1992). Finally, NT was shown to have a regulatory effect on corticotropin-releasing factor (CRF) and adrenocorticotropic hormone (ACTH) release from adrenal medulla (Mazzocchi et al, 1997).

1.1.3 Neurotensin and Hypothermia

Various studies support the proposition that NT may act endogenously to mediate heat-loss mechanisms in mammals (Nemeroff et al., 1977; Kalivas et al., 1985; Benmoussa et al., 1996; Yamada et al. 1995). For instance, intracisternal or intraventricular administration of NT is followed by a drop in core temperature in mouse, rat, gerbil and monkey (Bissette et al., 1976; Loosen et al., 1978; Prange et al., 1979). In particular, microinjection studies in rodents have demonstrated that NT produced a rapid onset of hypothermia ranging in the magnitude of 0.8-2.3°C below the baseline rectal temperature following administration in the medial preoptic region of the hypothalamus as well as in the periaqueductal area (Martin et al., 1980). This thermal response was shown to result from a significant dose and time-dependent increase in heat loss, while oxygen consumption was not affected (Handler et al., 1994). However, the fact that the core temperature is more sensitive to intracisternally-injected NT than a dose given intraventricularly (Martin et al., 1980)

suggest that the main site of action of NT in inducing hypothermia may be distant from the forebrain hypothalamic structures which have been classically implicated in temperature homeostasis (Prange et al., 1979). Interestingly, recent studies have demonstrated that NT-induced hypothermia provided marked neuroprotection in both models of global and focal cerebral ischemia (Babcock et al., 1993; Torup et al., 2003; Gordon et al., 2003; Katz et al., 2004a and 2004b). However, the mechanisms of NT-induced hypothermic protection are not entirely understood.

1.1.4 Neurotensin and Pain Modulation

Pharmacological studies in rodents have revealed that centrally administrated NT exerts analgesic actions both spinally and supraspinally (reviewed in Yaksh et al., 1982; Clineschmidt et al., 1982; Behbehani, 1992). Of great interest is the finding that these effects are not antagonized by naloxone, implying an opioid-independent mechanism (Clineschmidt et al., 1979; Osbahr et al., 1981; Martin and Naruse, 1982; Coquerel et al., 1986). At the spinal level, intrathecal NT injection produced a nociceptive threshold increase in the hotplate test and altered the tail-flick and acid-induced writhing response latency (Yaksh et al., 1982; Martin and Naruse, 1982; Spampinato et al., 1988). Moreover, NT has been shown to be effective in another model of chemically induced-nociception, the hypertonic saline assay, following intrathecal injection in mice (Hylden and Wilcox, 1983). At supraspinal levels, microinjection of NT into the preoptic area, the central nucleus of the amygdala, the hypothalamic medial nucleus, the rostrovendral medulla (RVM), and the periaqueductal gray (PAG) triggered antinociceptive responses in both tonic and acute pain models (Kalivas et al., 1982a; Kalivas et al., 1982b; Behbehani and Pert, 1984; Fang et al, 1987; Urban and Smith, 1993; Benmoussa et al., 1996). Interestingly, lesions of the stria terminalis and the nucleus raphe magnus both totally abolished the antinociceptive effects of NT following injections into the amygdala (Kalivas et al., 1982a) and the PAG (Behbehani and Pert, 1984), respectively. PAG neurons are known to be innervated by NT-immunoreactive nerve terminals, which originate from the bed nucleus of the stria terminalis, the central nucleus of the amygdala, and the lateral hypothalamus (Behbehani et al., 1988; Gray and

Magnuson, 1992; Rizvi et al., 1991). Conversely, current and voltage clamp recording studies have shown that NT depolarized retrogradely PAG-RVM neurons and evoked action potentials by opening voltage-insensitive and nonselective cation channels (Behbehani et al., 1988; Li et al., 2001). It is thus very likely that NT produces its analgesic effect by directly exciting PAG neurons that project to the RVM. However, NT was also shown to have bipolar effects on pain modulation following administration in the PAG, RVM, and brain regions that project to these structures (reviewed in Dobner, 2005). For instance, microinjection of NT into the RVM elicited analgesia at higher doses (nanomolar), whereas lower doses (picomolar) facilitated both somatic and visceral pain (Urban and Smith, 1993; Urban et al., 1999; Gui et al., 2004). Conversely, intense stress (i.e. forced swimming in cold water) was shown to trigger both inhibitory and facilitatory pathways that modulate visceral nociception (Gui et al., 2004). Finally, NT was also implicated in the development of secondary hyperalgesia following topical application of the skin irritant, mustard oil (Urban et al., 1996a). However, the pain facilitatory effects of exogenous NT are relatively small and have not been observed in all studies (Urban et al., 1996b; Smith et al., 1997). These nociceptive responses are thought to rely on spinal cholecystokinin signaling (Urban et al., 1996b). The mechanisms underlying NT-mediated pain modulation remain unclear. However, there is limited evidence that NT produces analgesia through the activation of descending noradrenergic and serotonergic neurons that project to the dorsal horn of the spinal columns (Naranjo et al., 1989).

1.1.5 Neurotensin and Blood Pressure

In vitro studies have revealed that NT elicited the contraction of isolated blood vessels including the rat portal vein (Rioux et al., 1980) and the coronary vasculature of guinea pigs (Nisato et al., 1994). When given intravenously, NT was shown to dilate the cutaneous vessels and to increase vascular permeability in rodents (Chahl et and Walker, 1981). Administrated at low doses, NT evoked hypotension in anesthetized rats (Carraway and Leeman, 1973; Quirion et al., 1980; Rioux et al., 1980), rabbits (Kataoka et al., 1978), and dogs (Rosell et al., 1976). Atropine,

phenoxybenzamine or propanolol did not alter the vasodepressor effect of NT *in vivo*, suggesting the lack of involvement of the muscarinic or β and α adrenoreceptors (Carraway and Leeman, 1973). In contrast, higher doses of NT induced a slight increase in rat blood pressure (Carraway and Leeman, 1973; Quirion et al., 1979; Di Paola and Richelson, 1990; Gully et al., 1996). This hypertensinve effect is thought to be mediated by an activation of the sympathetic nervous system (Di Paola and Richelson, 1990). Additionally, the sensitivity of species to histamine was proposed to play a role in the NT vasopressor response, rats being the most sensitive (Gully et al., 1996).

1.1.6 Neurotensin and Food Intake

Several reports have indicated that NT also plays a key role in the regulation of food consumption in rodents (Luttinger et al., 1982; Sahu et al., 2001; Wilding, 2002). Accordingly, early microinjection experiments have demonstrated that NT produced anorexigenic effects following administration in the nucleus of the solitary tract (de Beaurepaire and Suaudeau, 1988), the paraventricular hypothalamic nucleus (Stanley et al., 1983), the VTA (Cador et al., 1986), and the substantia nigra (Vaughn et al., 1990). Moreover, hypothalamic NT expression levels were shown to be reduced in genetic models of obese rats (i.e. Zucker *falfa)* and mice (i.e. *ob/ob*), further supporting a role of NT in food intake (Beck et al. 1989; Wilding et al., 1993). This action most likely involves a co-inhibitory effect of leptin and NT, which reciprocally stimulate each other (Beck et al., 1998).

1.1.7 Neurotensin and the Gastrointestinal Tract

NT is known to function as a hormone in the gastrointestinal tract (Andersson et al., 1976; Polak and Bloom, 1978; Bloom and Polak, 1980; Blackburn et al., 1980; Rosell, 1980). Indeed, NT was found in endocrine cells of the distal jejunum and terminal ileum (Polak et al., 1977), which were shown to release NT upon fat ingestion (Rosell, 1982). However, NT was shown to exert opposite actions in the intestine (reviewed in Kitabgi, 1982). For instance, it has inhibitory and excitatory effects on the peristaltic activity (Ohashi et al., 1996), while it produces contractile and relaxant responses in intestinal smooth muscle (Kitabgi and Freychet 1979;

Huidobro-Toro and Zhu, 1984; Ohashi et al., 1994). In particular, studies with rat proximal colon have shown that NT exerts its contractile effects acting both directly on smooth muscle cells and indirectly on nerves through acetylcholine release (Ohashi et al., 1994; Mulè et al., 1995). Conversely, NT was shown to induce a direct myogenic relaxation (Allescher et al., 1992) and to block the spontaneous phasic mechanical activity in rat proximal colon (Mulè and Serio, 1997). Nevertheless, these data are in contrast with studies using isolated smooth muscle preparations from human colon, which have indicated only direct, contractile actions of NT (Bennett et al., 1992; Maselli et al., 1998; Croci et al., 1999).

1.1.8 Neurotensin and Cancer

Increasing evidence suggests that NT plays an important role in growth regulation of carcinomas from diverse organs (reviewed in Kitabgi, 2002). Indeed, NT has been detected in a number of colon cell lines (Evers et al., 1992; Rovère et al., 1998) as well as in human pancreatic (Go et al., 1984; Townsend et al., 1994), prostate (Gu et al., 1983), and lung (Goedert et al., 1984a; Moody et al., 1985) cancer tissues in which NT is thought to act as an autocrine/paracrine trophic factor. In particular, the androgen-sensitive prostate cancer cell line LNCaP was shown to produce and secrete NT during androgen deprivation as a result of both neuropeptide synthesis/secretion and decreased neuropeptide-directed proteolytic activity (Sehgal et al., 1994). Additionally, recent studies have demonstrated that NT triggers a rapid Ca^{2+} mobilization from intracellular stores (Ryder et al., 2001) and PKC activation (Guha et al., 2002), leading to c-Raf-1-dependent phosphorylation of ERK1/2 in human ductal pancreatic cancer cell lines (Guha et al., 2003). Interestingly, treatment with the MEK-1/2 inhibitors prevented NT-induced DNA synthesis and colony formation, indicating that activation of MAPK cascade plays a central role in mediating NT-induced mitogenesis (Guha et al., 2003). NT-induced cell growth has also been reported in small-cell lung cancers (Davis et al., 1989; Sethi and Rozengurt, 1991). This proliferative effect was shown to rely on the activation of focal adhesion kinases (FAK), which are involved in cell adhesion, spreading, migration, and survival mechanisms (Leyton et al., 2002).

1.2 Biosynthesis, Processing, and Inactivation of NT and its Related Peptides

1.2.1 Structure of the Neurotensin/neuromedin N Gene

NT and its structurally related analogue neuromedin-N (NN) (Lys-Ile-Pro-Tyr-Ile-Leu) are synthesized as part of a common precursor protein in mammalian brain (Kislauskis et al., 1988) and intestine (Dobner et al., 1987). This gene consists of a 10.2-kb segment containing four exons and three introns (Kislauskis et al., 1988). The transcription of the rat NT/NN gene generates two mRNA species (1.0 and 1.5 kb), arising from different consensus polyadenylation signals (Kislauskis et al., 1988). Elements involved in the regulation of NT/NN mRNA expression are located in the upstream 200-bp flanking region of the rat gene in which several cis-regulatory elements function cooperatively to integrate multiple environmental stimuli into a concerted transcriptional response (Kislauskis and Dobner, 1990). In the rat NT/NN gene, these sites include one consensus AP-1 site that binds c-Jun and Jun D, two nearby cyclic AMP response elements (CRE), and a glucocorticoid response element (GRE), which is not expressed in the human (Kislauskis and Dobner, 1990; Bean et al., 1992; Evers et al., 1995). In particular, analysis of NT/NN gene expression in PC12 cells revealed that combined treatment with NGF, dexamethasone, and the adenylate cyclase activator forskolin triggered a large increase in NT/NN mRNA (Dobner et al., 1988; Kislauskis and Dobner, 1990; Tischler et al., 1991).

1.2.2 Processing of the Neurotensin/neuromedin N Precursor

Neurotensin and neuromedin N are both located in the C-terminal region of the 169-amino acid prohormone (pro-NT) where they are flanked and separated by four Lys-Arg sequences (Fig. 1.1), which represent putative sites for proteolytic maturation enzymes. Of these sites, the three that are closest to the C-terminus flank and separate NT and NN, whereas the fourth precedes a NN-like sequence. However, previous biochemical and immunological studies have shown that this most-terminal site is less extensively maturated than the remaining three (Nadai et al., 1994; Woulfe et al., 1994). Finally, the active NT and NN peptides have been shown to be released from their precursor in a tissue-specific manner. For instance, processing of the

NT/NN precursor was shown to essentially lead to the formation of NT and NN in the mammalian brain (Carraway and Mitra, 1990; Kitabgi et al., 1992), whereas NT and predominantly extended forms of NN were found in the intestine following food ingestion (Carraway et al., 1992; Vincent et al., 1999).

Previous immunohistochemical studies have shown a high degree of overlap between the Ca^{2+}-dependent prohormone convertases (PC) PCA5 and PCA2 in most NT-rich areas throughout the rat brain, suggesting that these two convertases may act jointly to process pro-NT/NN (Villeneuve et al., 2000a). According to this scheme, the C-terminal most dibasic sites, which are preferentially cleaved by PCA5 (Barbero et al., 1998) are processed first to release NT, whereas the third dibasic site, which is specifically cleaved by PC2, is then processed to release NN (Villeneuve et al., 2000a). However, in certain regions such as the nucleus accumbens and periventricular nucleus of the hypothalamus, there were only a few cells in which NT co-localized with either PC5A or PC2, suggesting that NT/NN can also be processed in the absence of either PC5A or PC2. Indeed, PC1 was shown to be selectively expressed in NT-positive neuronal and endocrine cells throughout the rat brain neuraxis (Schäfer et al. 1993; Winsky-Sommerer et al., 2000; Villeneuve et al., 2000b). Additionally, PC1 has also been shown to cleave pro-NT/NN with a pattern similar to that observed in the gut (Rovère et al., 1996).

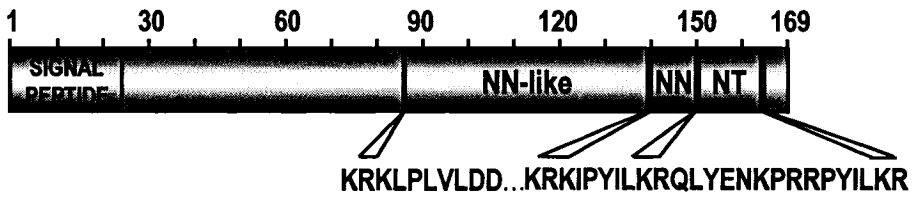

Figure 1.1: Schematic Representation of the Rat NT/NN Precursor Protein. The position of the four Lys-Arg doublets is illustrated. The amino acid sequence of NT and its related peptides are shown. Numbers indicate the length of the precursor amino acid sequence.

1.2.3 Neurotensin as a Peptide

The carboxyl-terminal hexapeptide portion of NT is preserved among vertebrate species, whereas the amino terminus exhibits considerably more phylogenic variability as shown in Table 1.1 (Rostène and Alexander, 1997). For instance, human and bovine NT gave rise to the same fragments when treated with papain, which were indistinguishable in radioimmunoassays and in their hypotensive effect on anesthetized rats (Hammer et al., 1980). However, chicken NT purified from extracts of intestine displayed 3 amino acid substitutions located in its NH_2-terminal (Carraway and Bhatnagar, 1980). Structure-activity relationship studies have established that the 8-13 C-terminal hexapeptide portion of NT contains all the structural elements responsible for its biological activity.

TABLE 1.1

Phylogenic Variations in NT Primary Structure Among Vertebrates

Species	Sequence (position)													Reference
	1	2	3	4	5	6	7	8	9	10	11	12	13	
Human	*Glu*	*Leu*	*Tyr*	*Glu*	*Asn*	*Lys*	*Pro*	*Arg*	*Arg*	*Pro*	*Tyr*	*Ile*	*Leu*	Hammer et al., 1980
Cow	*Glu*	*Leu*	*Tyr*	*Glu*	*Asn*	*Lys*	*Pro*	*Arg*	*Arg*	*Pro*	*Tyr*	*Ile*	*Leu*	Carraway et al, 1975
Dog	*Glu*	*Leu*	*Tyr*	*Glu*	*Asn*	*Lys*	*Pro*	*Arg*	*Arg*	*Pro*	*Tyr*	*Ile*	*Leu*	Dobner et al., 1987
Rat	*Glu*	*Leu*	*Tyr*	*Glu*	*Asn*	*Lys*	*Pro*	*Arg*	*Arg*	*Pro*	*Tyr*	*Ile*	*Leu*	Kislauskis et al., 1988
Guinea pig	*Glu*	*Leu*	***Tyr***	*Glu*	*Asn*	*Lys*	***Ser***	*Arg*	*Arg*	*Pro*	*Tyr*	*Ile*	*Leu*	Shaw et al., 1986
Chicken	*Glu*	*Leu*	***His***	***Val***	*Asn*	*Lys*	***Ala***	*Arg*	*Arg*	*Pro*	*Tyr*	*Ile*	*Leu*	Carraway et al., 1980
Frog	*Glu*	***Ser***	***His***	***Ile***	***Ser***	*Lys*	***Ala***	*Arg*	*Arg*	*Pro*	*Tyr*	*Ile*	*Leu*	Shaw et al., 1992

1.2.4 Proteolytic Degradation of Neurotensin and Neuromedin N

Since NT and NN appear to be co-localized within the same vesicles (Carraway and Mitra, 1987; Kitabgi et al., 1990) and hence are most likely co-released, their differential degradation presides over the relative concentration at which they will reach and activate their receptors on target cells. Indeed, these two peptides were shown to be degraded via proteolytic cleavage by a distinct set of peptidases with characteristic kinetic properties (Kitabgi et al., 1992). In the rat brain, NT is mainly inactivated by a combination of three zinc-containing metallo-endopeptidases, referred to as 24.11, 24.15, and 24.16, cleaving the peptide in its C-terminal domain (Checler et al., 1986a; 1986b). In particular, endopeptidase 24.16 was shown to

ubiquitously participate in the catabolism of NT in various tissues and cell cultures from central and peripheral origin, giving rise to the biologically inert catabolites neurotensin 1-10 and 11-13 (Checler et al., 1988). However, this endopeptidase was shown to be both secreted and expressed at the plasma membrane in neurons, whereas the membrane associate form of the enzyme was absent in astrocytes (Vincent et al., 1996). It was thus suggested that the secreted form would act in the extracellular space, thereby restricting diffusion of released NT, while the neuronal membrane-associated activity would be responsible for the physiological inactivation of the peptide in the synaptic cleft (Vincent et al., 1996). On the other hand, NN is primarily inactivated by bestatin-sensitive aminopeptidases, which are directed towards its N-terminal Lys residue (Barelli et al., 1995). Since aminopeptidases are quite abundant in tissues, NN is usually degraded more rapidly than NT (Vincent et al., 1999). Indeed, the half-life of NT is in the order of 15 min, which is about 2.5 times longer than that of NN in mammalian CNS (Kitabgi et al., 1992).

1.3 Expression of Neurotensin in Mammalian CNS

1.3.1 Ontogenic Patterns of Neurotensin in the Developing Brain

In the rat, expression of NT/NN mRNA and immunoreactive-NT is known to change during brain development in a region-specific manner (Hara et al., 1982; Bissette et al., 1984; Sato et al., 1991a). Accordingly, NT/NN mRNA was detected in most brain regions (e.g. hypothalamus) in the perinatal period, reaching maximal levels by adulthood. On the contrary, a second development profile was reported in different regions including the subiculum and CA1 region of the hippocampus in which mRNA appeared early in the perinatal period and reached maximal levels within the first postnatal week, decreasing thereafter (Nicot et al., 1992). Finally, in regions such as the olfactory bulb and hypoglossal nucleus, NT/NN mRNA was first detected during embryonic development (day 14), reached maximal levels perinatally, and decreased to very low or undetectable levels within several weeks (Kiyama et al., 1991a and 1991b). The transient expression of NT/NN mRNA during the synaptogenesis peek (first postnatal week) suggests that NT and/or NN released from these cells might subserve a trophic function (Vincent et al, 1999).

1.3.2 Neurotensin Distribution in Adult CNS

Radioimmunoassays and immunohistochemical studies concerning the distribution of NT in adult brain have revealed that NT is most abundant in areas in which dopaminergic systems are present (Fig. 1.2). In particular, dense networks of NT-positive cell bodies and/or axonal fibers were observed in the substantia nigra and the VTA, and in projections areas of both nigrostriatal and mesolimbic dopaminergic pathways, such as the striatum, the nucleus accumbens, the bed nucleus of the stria terminalis, the amygdala, and the frontal cortex (Jennes et al., 1982; Emson et al., 1985a and 1985b; Woulfe and Beaudet, 1989; Binder et al., 2001b). Also, electron microscopic studies have shown direct synaptic connections between NT-immunoreactive axon terminals and tyrosine hydroxylase-immunopositive perikarya and dendrites within the substantia nigra and VTA, suggesting a predominantly parasynaptic mechanism of action for NT (Woulfe and Beaudet, 1992). In the rat hypothalamus, neurosecretory cells capable of NT synthesis were found in the arcuate nucleus, parvocellular division of the paraventricular nucleus (PVN), and periventricular nucleus (Kiss et al., 1987; Merchenthaler and Lennard, 1991).

Although most research on the role of NT in the CNS has focused on its interaction with dopaminergic systems (reviewed in Binder et al., 2001b; Kinkead and Nemeroff, 2004), the interaction of NT with serotoninergic neurons has recently become a target of investigation due to the presence of abundant NT-immunoreactive neurons, fibers and terminals within the raphe complex (reviewed in Jolas and Aghajanian, 1997). Moreover, immunohistochemical studies of the basal forebrain have documented the presence NT-immunoreactive fibers in cholinergic systems extending from the medial septum and the diagonal band of Broca through the magnocellular preoptic area and the substantia innominata into the the globus pallidus (Uhl and Snyder, 1976; Jennes et al., 1982; Uhl, 1982; Zahm and Heimer, 1988; Woulfe et al., 1994). At high magnification, neurotensinergic fibers were shown to form a dense plexus of varicose axons in close proximity to cholinergic neurons within the posterior substantia innominata and the globus pallidus (i.e. caudal basal forebrain), suggesting that NT effects could be exerted synaptically upon

distal dendrites of basal forebrain neurons (Morin et al., 1996). Also, retrograde NT labeling studies have identified projections from the lateral hypothalamus and pontomesencephalic tegmentum to the magnocellular preoptic nucleus and posterior substantia innominata, which project to the cerebral cortex and amygdala, suggesting that NT neurons might be part of the ascending reticular formation involved in the regulation of sleep and wakefulness (Morin and Beaudet, 1998).

It is worth noting that NT was also found in nonneuronal cells such as those in the anterior pituitary, which indicates that it may also play a role in cell-to-cell signaling on autocrine, paracrine, and endocrine levels (Vincent et al., 1999).

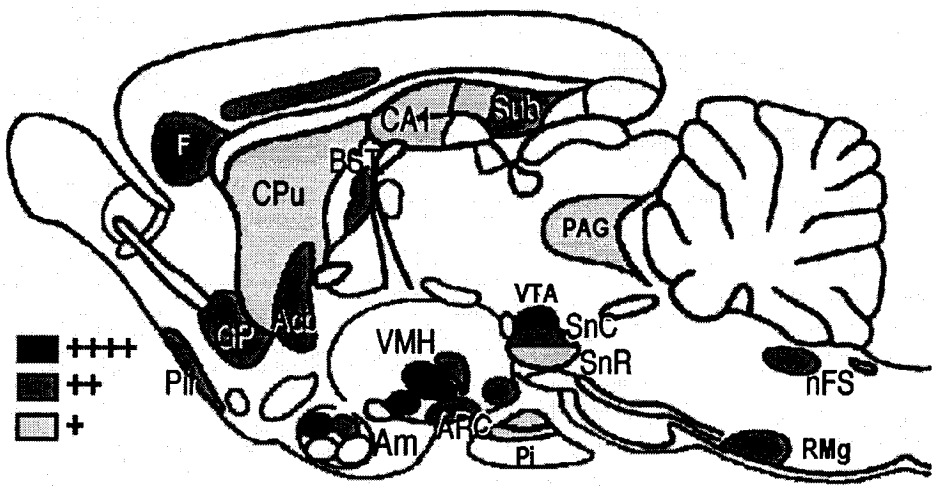

Figure 1.2: Topographic Distribution of NT-containing Neurons in Rat CNS. Schematic midsagittal section through the rat brain provides an overview of the distribution of NT-immunoreactivity throughout the neuraxis (according to Jennes et al., 1982).

However, some discrepancies exist between the NT/NN mRNA distribution and NT immunoreactivity within the rat CNS (Alexander et al., 1989b; Smits et al., 2004). For instance, NT/NN mRNA was abundant in the CA1 region of the hippocampus, a region devoid of NT-immunoreactive neurons (Alexander et al., 1989b). These data suggest that in specific regions of the forebrain, NT/NN precursor is processed to yield other products than NT. Interestingly, comparative studies using an NH_2-terminally directed anti-NN antiserum in rat brain revealed that distributions of NT and NN were generally parallel, with NT being usually more abundant than NN (e.g. dopaminergic areas) (Kitabgi et al., 1991). Indeed, high immunonoreactive-NT over NN ratio values (>3) were found in the globus pallidus, the posterior hypothalamus, the substantia nigra pars compacta, and the VTA. On the other hand, values close to one were observed in most cortical areas in addition to the striatum and the hippocampus.

2. NEUROTENSIN RECEPTORS

Early autoradiographic studies using radiolabeled NT first suggested the existence of two binding sites in both rodent (Goedert et al., 1984b; Kitabgi et al., 1987) and human (Sadoul et al., 1984; Zsurger et al., 1992) CNS. These sites were distinguished by their binding affinity for NT, displaying high (K_d = 0.15-0.5 nM) and low (K_d = 5-7 nM) affinity (Mazella et al., 1983; Kitabgi et al., 1985). NT is now known to mediate its central and peripheral effects through interaction with three different receptor subtypes, referred to as NTS1, NTS2, and NTS3 (reviewed in Vincent et al., 1999; Kitabgi, 2002; Dobner, 2005). NTS1 and NTS2 (both illustrated in Fig. 1.3) belong to the G protein-coupled receptor (GPCR) family of receptors, whereas NTS3 is a single transmembrane domain receptor. The pharmacological properties of NTS1 and NTS2 are reviewed in Table 1.2 and 2.3, respectively, and a summary of their binding properties is provided in Table 1.4.

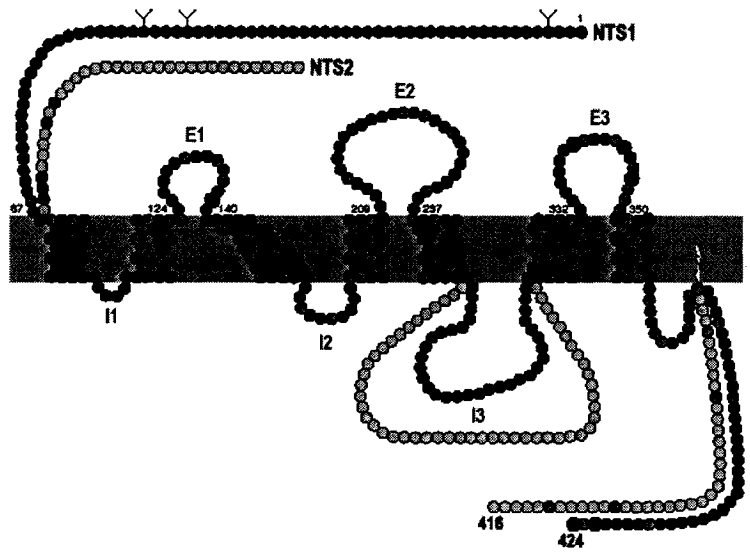

Figure 1.3: Schematic Representation of Rat NTS1 and NTS2 Receptors. Amino acids exclusive to NTS1 are represented in blue, while those that strongly differ from NTS1 are indicated in yellow. Invariants residues between NTS1 and NTS2 are shown in green. Glycosylation sites (Y) and regions corresponding to extracellular (E) and intracellular (I) domains are illustrated *(Adapted from Vincent et 1999).*

2.1 Cloning and Structural Features

2.1.1 NTS1 Receptor

NTS1 was first cloned from rat brain by Nakanishi and colleagues using the oocyte expression technique (Tanaka et al., 1990). This gene occurs as a single copy in the rat haploid genome and contains three introns in its coding region (Maeno et al., 1996). In addition, the upstream putative promoter region was shown to contain a consensus sequence for the transcription factor Sp-1 (Maeno et al., 1996). The open reading frame of rat NTS1 cDNA encodes a 424 amino acids protein with seven putative transmembrane (TM) domains, sharing 84% homology with its human counterpart isolated from the colon carcinoma HT-29 cell line (Vita et al., 1993). Western blotting analysis using an anti-peptide raised against a fragment of the third intracellular loop of the receptor, revealed the presence of immunoreactive bands between 62 and 72 kDa, while only a faint labeling was observed at 47 kDa, corresponding to the molecular mass deduced from the rat NTS1 cDNA sequence (Boudin et al., 1995). The bands of higher molecular mass were no longer present after deglycosylation of membrane proteins by peptide N-glycosidase F, indicating that they represented glycosylated forms of the receptor. Interestingly, the receptor was only observed as the 47 kDa band in membrane extracts prepared from recombinant sf9 cells (Boudin et al., 1995), which are unable to process N-linked oligosaccharides (Luckow and Summers, 1988). A second translation initiation site (Met 27) was also reported in the cDNA sequence encoding the NTS1 receptor, generating a truncated form of the receptor (i.e. 44 kDa) by using a reticulocytes lysate-based *in vitro* transcription-translation system (Botto et al., 1997a).

2.1.2 NTS2 Receptor

A second type of NT receptor (i.e. NTS2) was cloned form murine (Mazella et al., 1996), rat (Chalon et al., 1996), and human (Vita et al., 1998) brain. The cDNA sequence of the mouse NTS2 is composed of four exons separated by three introns (Sun et al., 2001). The first exon encodes the region containing TM domains 1-4, whereas exons 2-4 encode the region containing TM 5-6, TM 6 and TM 7, correspondingly. The existence of a C-terminally truncated form of NTS2 mRNA

lacking a 181-bp internal sequence has also been reported in the mouse (Botto et al., 1997b). Both mouse NTS2 mRNA isoforms are derived from a single NTS2 gene, the short form resulting from alternative splicing of the primary transcript at intron 2a (Sun et al., 2001). The promoter region of NTS2 includes putative binding sites for neuronal transcriptional factors, GATA-2, CREB (cAMP-responsive element binding protein), Oct-2, and Ikarous 2 (Sun et al., 2001). Whether or not these sites are true regulatory elements remains to be determined.

The full-length rat NTS2 cDNA contains a large open-reading frame encoding a 416 amino acid protein, sharing extensive similarity with that of the mouse (96% identity and 98% homology) and human (79% identity and 87% homology) receptors (Vita et al., 1998). Nonetheless, the rat and mouse NTS2 (416 amino acids) are also slightly longer than their human counterpart (410 amino acids) and differ the most in their C-terminal domain. However, most theronine and serine residues within this region are conserved. Other features of the NTS2 receptor include the presence of a cysteine residue in each of the extracellular loops, which might enable the formation of intra- or intermolecular disulfide bonds as well as a putative palmytoylation site in the C-terminal region (Vita et al., 1998). Photoaffinity labeling experiments carried out on HEK 293 cells expressing the mouse NTS2 using a photoreactive NT analogue revealed the presence of a labeled protein with an apparent molecular weight of 45 kDa (Botto et al., 1998).

The rat NTS2 receptor protein shares 43% identity and 64% homology with the NTS1 amino acid sequence as shown in Fig. 1.4 (Chalon et al., 1996; Vincent et al., 1999). Although the lengths of both proteins are very similar, the NTS2 receptor has a shorter N-terminal extracellular region devoid of potential N-glycosylation sites. NTS1 and NTS2 differ most in their third cytoplasmic loops and C-terminal domains, two regions bearing specificity to G-protein coupling and receptor regulation (Yamada 1994; Vincent et al., 1999). In particular, the third intracellular loop is much longer in the NTS2 (~ 50 residues) than in the NTS1 (~ 30 residues) and shares only five identical residues between the two receptor subtypes (Richard et al., 2001a).

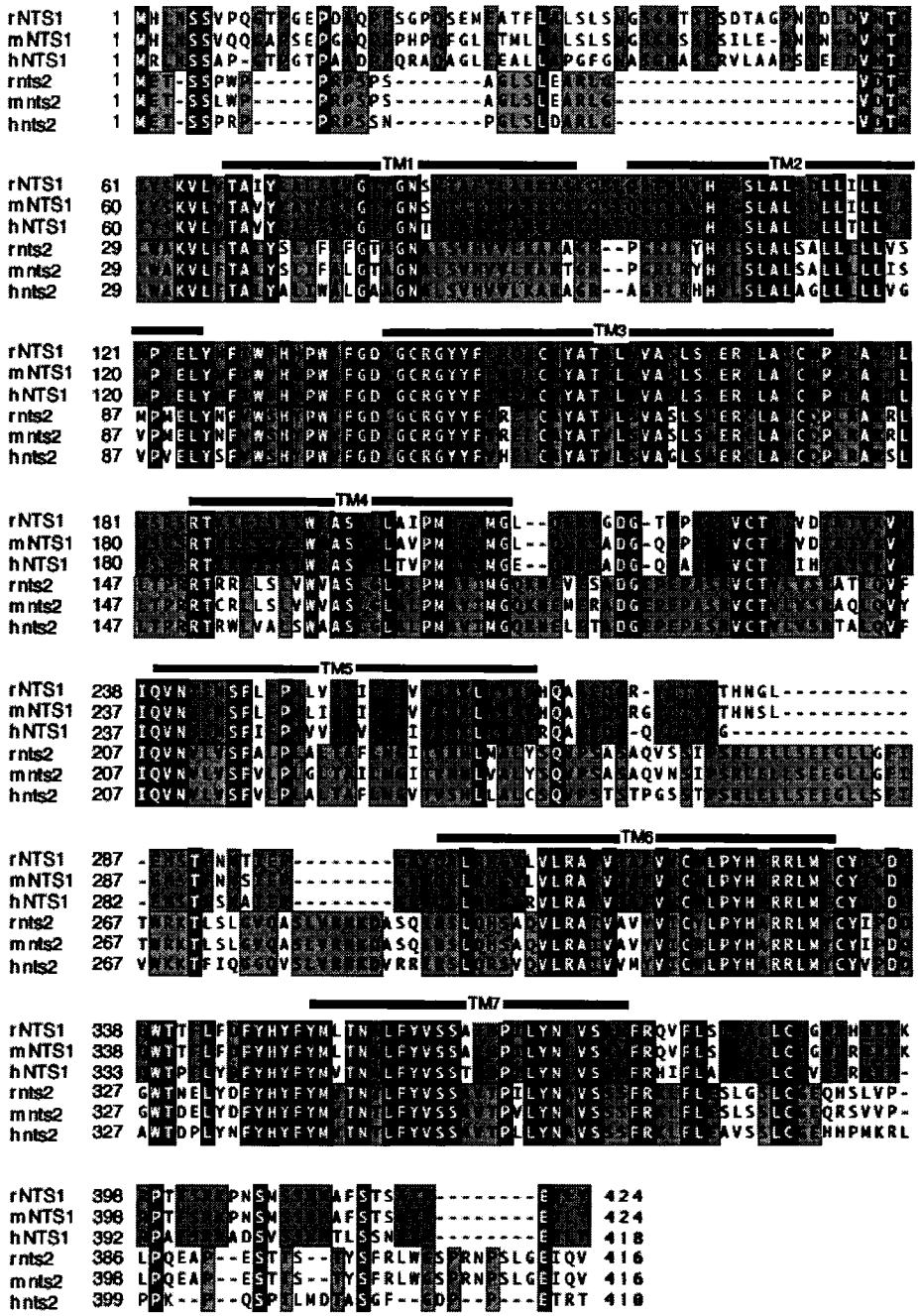

Figure 1.4: Alignment of Rat (r), Mouse (m), and Human (h) NTS1 and NTS2 Amino Acid Sequences. Invariant residues found in NT receptors are shown in green, whereas those that are common in either NTS1 or NTS2 sequences are illustrated in blue and yellow, respectively. The solid line above the sequences indicates the putative transmembrane (TM) segments. Gaps for alignments are represented by dots *(Adapted from Vincent et al., 1999).*

2.1.3 NTS3 Receptor

NTS3 was first cloned from a human brain cDNA library (Mazella et al., 1998; reviewed in Mazella, 2001) and found to be 100% identical to sortilin, which was previously isolated from human brain homogenates based on its interacting properties with RAP, an endoplasmic reticulum-resident protein (Petersen et al., 1997). In addition to the brain, NTS3/sortilin has been localized to several peripheral cell types including 3T3-L1 adipocytes (Lin et al., 1997; Morris et al, 1998), as well as prostatic, colonic, and pancreatic cancer cell lines (Dal Farra et al., 2001; Martin et al., 2002a). NTS3/sortilin is a non-G protein coupled receptor that is 833 amino acid residues long and encodes a single TM domain protein (Mazella et al., 1998). Interestingly, insulin was shown to trigger the translocation of NTS3/sortilin from glucose transporter GLUT4 vesicles to the plasma membrane, suggesting that this receptor is also involved in the sorting of lumenal proteins from the trans-Golgi in addition to its role as a NT receptor (Lin et al., 1997; Morris et al., 1998). NTS3/sortilin belongs to the type-I receptor family including the receptors SorLA and SorCS (Jacobsen et al., 1996; Yamazaki et al., 1996; Hermey et al., 1999). This family is characterized by the presence of a luminal extracellular region containing a cysteine-rich domain homologous to the yeast sorting protein Vps10p (Marcusson et al., 1994), as shown in Fig. 1.5. The NTS3/sortilin C-terminus is also homologous to the mannose-6-phosphate receptor MPR300 (Johnson and Kornfeld, 1992).

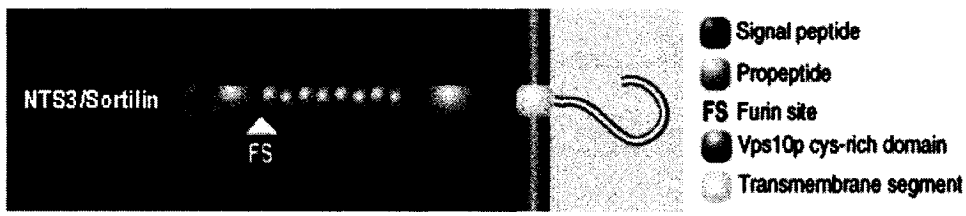

Figure 1.5: Schematic diagram of NTS3/sortilin receptor. NTS3/sortilin is composed of an N-terminal signal peptide, a propeptide released by furin cleavage (FS), a cysteine-rich domain, a transmembrane domain, and a cytoplasmic tail *(Adapted from Mazella, 2001).*

NTS3/sortilin is synthesized as a precursor protein that is converted to its mature form through proteolytic cleavage by furin (see Fig. 1.5) in late Golgi compartments (Mazella, 2001). This step was shown to be crucial for both ligand recognition and functional activity of the receptor (Mazella et al., 1998). Accordingly, binding experiments showed that the NTS3/sortilin was processed into a higher affinity protein receptor upon co-transfection with furin (Mazella et al., 1998). In line with these results, photoaffinity labeling experiments revealed the presence of a 100 and 110 kDa-band in the presence or absence of furin, respectively (Mazella et al., 1998).

2.2 Binding Properties and Transduction Mechanisms

2.2.1 NTS1 Receptor

Experiments on mammalian cells transfected with recombinant NTS1 revealed that this receptor is insensitive to levocabastine ((-)-*trans*-1-[*cis*-4-cyano-4-(p-fluoro-phenyl)-cyclohexyl]-3-methyl-4-phenylisonipecotic acid monohydrochloride) and binds NT with high affinity (K_d in the subnanomolar range; see Table 1.4) (Mazella et al., 1989; Tanaka et al., 1990). This interaction is known to be sensitive to Na^+ and GTP, which decrease the affinity of the receptor for NT (Vincent et al., 1999). The NT binding pocket encompasses aromatic residues located in the third extracellular loop in addition to hydrophobic residues in TM 6 and 7 of rat NTS1 (Barroso et al., 2000; Richard et al., 2001a). Additionally, nuclear magnetic resonance studies have revealed that residues 8-13 in NT peptide are essential for its interaction with the agonist-binding site (Williamson et al., 2002).

Pharmacological and biochemical studies have indicated that NTS1 is involved in the modulation of intracellular second messengers levels, including cGMP (Gilbert et al., 1988; Amar et al., 1985; Slusher et al., 1994), cAMP (Bozou et al., 1989a; Yamada et al., 1993; Richard et al., 2001a; Barroso et al., 2002), and inositol phosphates (Snider et al., 1986; Amar et al., 1986; Amar et al., 1987; Hermans et al., 1992; Watson et al., 1992; Choi et al., 1999). Previous studies have suggested that the third intracellular loop and carboxy terminal portion of NTS1 play a critical role in its coupling to $G_{q/11}$ and $G_{i/o}$, respectively (Yamada et al., 1994; Najimi et al.,

2002). Functional properties of NTS1 receptors also include the activation of extracellular signal-regulated kinases 1/2 (ERK1/2) through coupling with both pertussis toxin-sensitive and insensitive G-proteins in transfected CHO cells (Poinot-Chazel et al., 1996). This MAPK phosphorylation leads in turn to the expression of proliferative genes, such as c-*fos*, *Krox*-24, and c-*jun* (Poinot-Chazel et al., 1996; Portier et al., 1998). NT was shown to trigger the phosphorylation of ERK1/2 through a PKC-dependent mechanism in human pancreatic carcinoma PANC-1 cells (Guha et al., 2003), as well as in human androgen-insensitive prostate cancer PC3 cells (Hassan et al., 2004), which are both known to endogenously express the NTS1 receptor.

TABLE 1.2

NT-induced Signaling Cascades Modulated by NTS1 Receptors

Model	Response measured	Reference
Cell lines		
N1E-115	↑ [IP_3]	Snider et al., 1986; Amar et al., 1987
	↑ [Ca^{2+}]	Snider et al., 1986
	↑ [cGMP]	Gilbert et al., 1988; Amar et al., 1985
NG108-15	↑ [IP_3]	Imaizumi et al., 1989
	↑ [Ca^{2+}]	Imaizumi et al., 1989
HT-29	↑ [IP_3]	Amar et al., 1986
	↑ [Ca^{2+}]	Bozou et al., 1989b; Turner et al., 1990
HL-60	↑ [IP_3]	Choi et al., 1999
	↑ [Ca^{2+}]	Choi et al., 1999
PANC-1	MAPK	Guha et al., 2003
PC3	MAPK	Hassan et al., 2004
Transfected cells		
CHO	↑ [IP_3]	Hermans et al., 1992; Watson et al., 1992
	↑ [Ca^{2+}]	Hermans et al., 1995
	↑ [cAMP]	Yamada et al., 1993
PC12	↑ [Ca^{2+}]	Hermans et al., 1994
HEK 293	↑ [cGMP]	Slusher et al., 1994
LTK	↑ [IP_3]	Chabry et al., 1994
	↑ [Ca^{2+}]	Chabry et al., 1994
COS	↑ [IP_3]	Richard et al., 2001a; Barroso et al., 2002
	↑ [cAMP]	Richard et al., 2001a; Barroso et al., 2002
CHO	MAPK	Poinot-Chazel et al., 1996; Portier et al., 1998

(Adapted from Hermans et al, 1998)

A significant advance in the understanding of NT interactions with its receptors came with the development of the non-peptide NT antagonist SR48692 (2-[1-(7-chloroquinoline-4-yl)-5-(2,6-dimethoxyphenyl)-1H-pyrasol-3-carbonyl]-amino-adamantane-2-carboxylic acid; illustrated in Fig. 1.6), which displays a much higher affinity for NTS1 (IC_{50} = 5.6 μM) than for NTS2 (IC_{50} = 300 nM) (Gully et al., 1993). This antagonist was shown to competitively inhibit [^{125}I]-NT binding in rat, guinea pig, and human brain homogenates (Gully et al., 1993; Azzi et al., 1994; Brouard et al., 1994a). It was also reported to antagonize the inositol production evoked by NT in NTS1 expressing sf9 cells (Boudin et al., 1996a). Recent mutagenesis studies have demonstrated that contact with hydrophobic residues in TM 6 and 7 of NTS1 are crucial for SR48692 binding. These residues include Tyr 342, Phe 331, and Tyr 359, which also appeared to interact with NT, suggesting a basis for the ability of SR48692 to compete for NT binding to the receptor (Labbé-Jullié et al., 1998; Barroso et al., 2000).

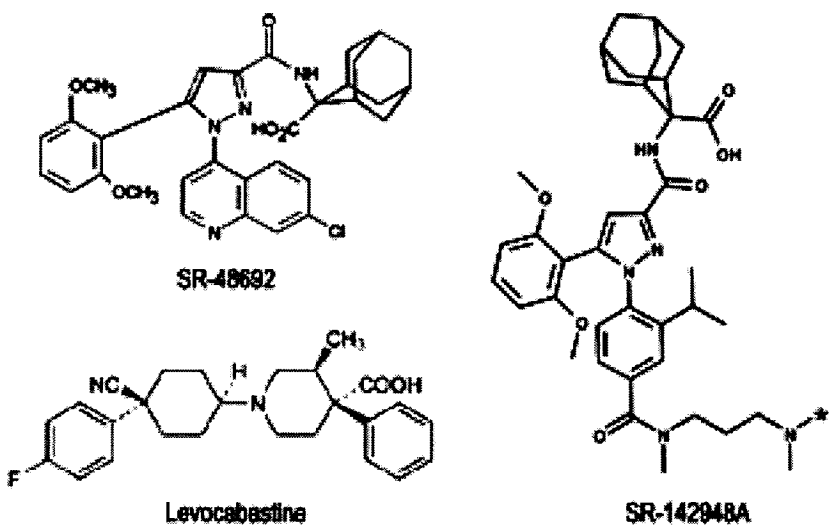

Figure 1.6: Chemical Structure of Non-peptide Ligands for NT Receptors. SR48692 and SR124948A were developed by Sanofi-Synthélabo Inc. through random screening and chemical optimization (see Gully et al., 1993 and Gully et al., 1997). Levocabastine is an original product of Janssen Pharmaceuticals, Inc.

A follow-up compound, SR142948A (2-[5-(2,6-dimethoxylphenyl)-1-(4-(*N*-(3-dimethylaminopropyl)-*N*-methyl-carbamoyl]-amino-adamantane-2-carboxylic acid) was also introduced (illustrated in Fig. 1.6), displaying a better solubility and an increased affinity in the rat brain as compared with SR48692 (Gully et al., 1997). This nonpeptide antagonist was shown to recognize both NTS1 and NTS2 receptors with high affinity (IC_{50} = 6.8 μM and 4.8 μM, respectively) (Bétancur et al., 1998). SR142948A was also shown to antagonize the classical NT's *in vitro* effects (i.e. the inositol phosphate production in HT-29 cells or intracellular calcium mobilization in NTS1 expressing CHO cells (Gully et al., 1997)).

2.2.2 NTS2 Receptor

Binding studies on transfected cells showed that NTS2 binds NT with a lower affinity (K_d = 2 nM) than NTS1 (Mazella et al., 1996). Conversely, the NT analogue JMV 431 (Boc-Arg-Arg-Pro-Tyr-φ(CH_2-NH)-Ile-Leu-OH) has a higher affinity for the mouse NTS2 (K_d = 38 nM) than for the rat NTS1 (K_d = 3315 nM) (Dubuc et al., 1999b). As opposed to NTS1, binding of NT to NTS2 is insensitive to Na^+ and GTP analogs (Martin et al., 1999). NTS2 is also recognized by the histamine H_1-antagonist drug levocabastine, which is known to selectively inhibits NT binding to NTS2 without affecting its binding to NTS1 (Schotte et al., 1986). Finally, NTS2 was shown to specifically bind β-lactotensin (His-Ile-Arg-Leu), an ileum-contracting peptide derived from the chymotrypsin digestion of β-lactoglobulin (Yamauchi et al., 2003b). Interestingly, this peptide was found to be about 47 times more selective for NTS2 (K_d = 7.7 μM) than NTS1 (K_d = 363 μM). The binding properties of NTS2 are reviewed in Table 1.4.

However, the signaling properties of NTS2 are still controversial. In particular, there is inconsistency between reported agonistic and antagonistic properties of NT in systems heterologously expressing NTS2. For instance, in mammalian cells transfected with human NTS2, the NT antagonist SR48692, but neither NT nor levocabastine was reported to activate classical second messenger systems such as phosphoinositide hydrolysis, Ca^{2+} mobilization, arachidonic acid (AA) release or MAPK phosphorylation (Vita et al., 1998). In addition, these SR48692-induced

activities were blocked by NT, NN and levocabastine, suggesting that the endogenous peptide was acting as a competitive antagonist at NTS2 sites. Similarly, NT was reported to reverse the SR48692-induced inositol phosphate production in COS-M6 cells transfected with the human NTS2 receptor cDNA (Richard et al., 2001b). In contrast, in *Xenopus* oocytes expressing the mouse NTS2 receptor, NT, NN, and levocabastine were all found to activate Ca^{2+}-dependent chloride currents (Mazella et al., 1996; Botto et al., 1997c). Additionally, studies on rat cerebellar granule cells in culture showed that both NT and levocabastine, but not SR48692, induced a sustained MAPK p42/p44 activation, indicating that these ligands act as agonists on endogenously expressed rat NTS2 receptors (Sarret et al., 2002). Surprisingly, the human NTS2 was shown to exhibit a robust constitutive activity on inositol phosphate production when transiently expressed in COS-M6 cells (Richard et al., 2001b). However, this spontaneous phospholipase C activity was reported for neither rat NTS2, mouse NTS2 nor human NTS1, suggesting that this constitutive activation might result from the divergent structure of the third intracellular loop among different species or receptor subtypes.

TABLE 1.3

NTS2-Mediated Signaling Pathways in Different Expression Systems

Species	Expression system	Transduction pathway	Agonist	Antagonist	Reference
Human	CHO	↑ [IP_3, Ca^2] AA, MAPK	SR48692 SR142948A	NT Levocabastine	Vita et al., 1998
	COS	↑ [IP_3]	SR48692	NT	Richard et al., 2000a
Mouse	*Xenopus* oocyte	↑ [Ca^{2+}]	NT, NN Levocabastine SR48692		Mazella et al., 1996 Botto et al., 1997c
Rat	CHO	↑ [Ca^{2+}]	NT Levocabastine SR48692		Yamada et al., 1998
	Cerebellar cells	MAPK	NT Levocabastine		Sarret et al., 2002

2.2.3 NTS3 Receptor

Binding experiments on COS-7 cells transfected with the human NTS3 cDNA have revealed that CHAPS solubilized extracts bind to NT with a K_d of 10 nM (Mazella et al., 1998). However, no NT binding was detected either on whole cells or crude homogenates, indicating that the receptor is not expressed at the cell surface (Mazella et al., 1998). This observation is in agreement with several studies that have revealed a predominant association of NTS3/sortilin with intracellular organelles such as the endoplasmic reticulum, the Golgi apparatus and GLUT4 glucose transporter-positive vesicles (Petersen et al., 1997; Nielsen et al., 2001; Li et al., 1997). The NTS3/sortilin was also shown to bind several ligands including RAP (Petersen et al., 1997), lipoprotein lipase (Nielsen et al., 1999), and the precursor of nerve growth factor (Nykjaer et al., 2004), suggesting that its role probably exceeds that of a NT signaling receptor.

Recent RT-PCR studies have revealed that NTS3/sortilin is co-expressed with the NTS1 receptor in most of human colonic and pancreatic cancer cell lines (Dal Farra et al., 2001). Of interest is the finding that NTS3 forms endogenous heterodimers with NTS1 in HT-29 cells (Martin et al., 2002a). This interaction was shown to modulate both NTS1-mediated ERK1/2 MAPK signaling and phosphoinositide turnover (Martin et al., 2002a). However, NTS3 was also found to be expressed without other NT receptor subtypes in different cancer cell lines (e.g. LnCaP and LoVo), suggesting that it might also be specifically involved in the NT-induced growth response (Dal Farra et al., 2001). In addition, the stimulation of NTS3/sortilin with NT was shown to lead to the activation of both ERK1/2 and Akt phosphorylation in the human microglial C13NJ cell line (Martin et al., 2003). This activation was found to promote a phosphatidylinositol 3-kinase-dependent formation of filopodia, which was then followed by a marked activation of cell migration (Martin et al., 2003).

TABLE 1.4

Binding Properties of NT Receptor Subtypes for NT and Different Compounds

	K_d			
Compound	**NTS1**	**NTS2**	**NTS3**	**Reference**
Neurotensin	0.1-0.3 nM	2-4 nM	10 nM	Tanaka et al., 1990 Chalon et al., 1996 Mazella et al., 1998
JMV 431	3315 nM	38 nM	N.A	Dubuc et al., 1999b
JMV 449	0.04 nM	0.56 nM	N.A	Labbé-Jullié et al., 1994 Yamada et al., 1998
Neuromedin N	2.6	1.5-2.5	N.A	Tanaka et al., 1990 Vita et al., 1993 Mazella et al., 1996
Levocabastine	N.A	1-9 nM	N.A	Yamada et al., 1998 Mazella et al., 1996
β-Lactotensin	363 μM	77 μM	N.A	Yamauchi et al., 2003b
SR48692	5-6 nM	300 nM	N.A	Gully et al., 1993
SR142948A	1-7 nM	4.8 nM	N.A	Gully et al., 1997 Bétancur et al., 1998

2.3 Desensitization of Responses to Neurotensin

2.3.1 NTS1 Receptor

Carraway first reported that NT's systemic hypotensive effects exhibited acute tachyphylaxis following subsequent applications of the peptide, suggesting that responses to NT were susceptible to rapid desensitization (Carraway and Leeman, 1973). Likewise, Richelson's group found that NT-induced cGMP reduction declined within the first minutes of agonist stimulation and that the concentration-response curve shifted to higher doses for ensuing applications (Gilbert et al., 1988). Desensitization of NTS1-mediated second messenger systems response has also been reported in cultures of neurons (Sato et al., 1991b) as well as in HT-29 (Turner et al., 1990) and N1E-115 (Yamada and Richelson, 1993a and 1993b) cells. However, few reports have shown NT responses in which desensitization was not observed (reviewed in Hermans and Maloteaux, 1998). For instance, electrophysiological studies on cholinergic neurons of the basal forebrain have reported that NT

application produced a slow and long-lasting membrane potential depolarization associated with a decrease in apparent input conductance (Alonso et al., 1994). In addition, persistent activation of p42/p44 mitogen-activated protein kinases was detected in non-differentiated NTS1 expressing N1E-115 cells following a 24 h exposure to JMV 449 (Toy-Miou-Leong et al., 2004a).

Nonetheless, there is only limited information on the molecular and cellular mechanisms underlying NTS1 desensitization. Several studies on GPCRs have shown that the phosphorylation of serine and threonine residues in the carboxy terminus and/or the third intracellular loop plays an important role in the desensitization of receptor responsiveness (Bouvier et al., 1988; Ferguson, 2001). Likewise, the NT-induced dopamine release observed in mesencephalic cell cultures was suppressed by both short- and long-term treatment with phorbol esters, suggestive of a PKC-dependent desensitization process (Brouard et al., 1994b). Accordingly, the NTS1 third intracellular loop and carboxy-terminal tail contain 13 and 6 serine/threonine residues, respectively (Tanaka et al., 1990). It is thus likely that these residues participate in NTS1 desensitization as a result of phosphorylation. However, agonist-induced phosphorylation of NTS1 has never been directly demonstrated so far.

Receptor internalization has also been proposed to play a critical role in the control of cell responsiveness to NT (reviewed in Hermans and Maloteaux, 1998; Vincent et al., 1999; Kitabgi, 2002). For instance, incubation of rat cultured neurons with NT was shown to be followed by a dramatic decrease in the number of receptors from the cell surface (Vanisberg et al., 1991). Autoradiographic and/or biochemical studies have then shown radioactive NT to be rapidly taken up by mouse and rat neurons in culture in a receptor-dependent manner (Mazella et al., 1991; Vanisberg et al., 1991; Beaudet et al., 1994). Accordingly, photoaffinity labeling experiments indicated that the intracellular NT was associated with a protein of a molecular weight similar to that of NTS1 receptor (Chabry et al., 1993). To gain insight into the mechanisms underlying the internalization process of NTS1, the intracellular migration of NTS1 was monitored by confocal microscopic studies using a fluorescent analogue of NT (Faure et al., 1994; Alonso et al., 1994; Faure et al.,

1995a; Faure et al., 1995b; Nouel et al., 1997; Vandenbulcke et al., 2000; Cape et al., 2000). Indeed, results show that Fluo-NT was internalized at the somatodendritic level both in DA (Nouel et al., 1997) and cholinergic neurons (Faure et al., 1995a; Faure et al., 1995b). However, light microscopic evidence for retrograde transport of intrastriatal neurotensin within nigrostriatal dopaminergic neurons was provided, suggesting that the peptide may also be internalized presynaptically and transported back to nigrostriatal nerve cell bodies (Castel et al., 1990).

NTS1 endocytosis was shown to be prevented by hypertonic sucrose, potassium depletion and cytosol acidification, suggesting that the internalization process was mediated via clathrin-coated vesicles (Faure et al., 1995a: Faure et al., 1995b; Nouel et al., 1997: Vandenbulcke et al., 2000; Nguyen et al., 2002). In particular, confocal microscopic studies demonstrated that β-arrestin 1 and 2 were both translocated to NTS1 following NT exposure (Oakley et al., 2000). As opposed to class A receptors (i.e. β_2-adrenergic (AR), μ opioid receptor, endothelin type A receptor), both β-arrestin isoforms remained associated with NTS1 and internalized with the receptor into endocytic vesicles. These vesicles concentrated the transferrin receptor and displayed colocalization with the low pH indicator Acridine orange, and rab 5, indicating that they corresponded to early endosomes (see Fig. 1.7; Vandenbulcke et al., 2000). The NTS1 internalization process was also shown to depend on dynamin (Savdie et al., 2006), which is known for its role in the scission of newly formed vesicles from the plasma membrane (for reviews, see Schmid et al., 1998; Sever, 2002). However, the molecular pathways involved in NTS1 endocytosis were shown to differ among cell types. In particular, it required the participation of the endocytic scaffolding protein intersectin in COS-7 cells but not in HEK-293 cells (Savdie et al., 2006). Mutagenesis studies have revealed that the C-terminal tail of NTS1 is involved in receptor internalization and desensitization (Chabry et al., 1993; Hermans et al., 1996). More precisely, the substitution of Thr-422 and Tyr-424 virtually abolished ligand-induced receptor internalization in transfected COS-7 cells (Chabry et al., 1995).

Current biochemical and immunocytochemical data suggest that internalized NTS1 receptors are not recycled back to the plasma membrane, but rather targeted to lamp-1-immunopositive lysosomes via rab 7-immunopositive late endosomes (Hermans et Maloteaux, 1998; Vandenbulcke et al., 2000). Accordingly, the lysosomotropic drugs chloroquine and methylamine were reported to partially reduce the progressive loss of cell surface binding sites observed in rat primary cultured neurons following persistent agonist exposure, indicating that lysosomal degradation may be involved in the down-regulation of NTS1 receptors (Hermans et al., 1997). Interestingly, chronic exposure to JMV 449 ([Lys^8-(CH_2NH)-Lys^9]Pro-Tyr-Ile-Leu) was shown to induce the degradation of NTS1 mRNA in cultures of rat embryonic cerebral cortex neurons, suggesting that post-transcriptional events may also be directly implicated in the down-regulation process (Lépée-Lorgeoux et al., 2000). This phenomenon is in agreement with the destabilization of NTS1 mRNA that was previously reported in N1E-115 cells after long-term agonist exposure (Najimi et al., 1998). Finally, it has been established that *de novo* synthesis is required for the recovery of NTS1 receptor-binding sites and function (Donato di Paola et al., 1993; Hermans et al., 1997). Specific autoradiographic NT labeling was also detected in the nucleus of DA neurons and human lung cancer cells, suggesting that NT alone, or complexed to its receptor, might be involved in the regulation of gene expression through direct or indirect interactions with nuclear DNA (Castel et al., 1990; Toy-Miou Leong, 2004b).

However, radioligand binding on synaptosomes from rat neostriatum revealed that NT internalizes in nerve terminals via an endocytic pathway that is related to, but is mechanistically distinct from that responsible for NT internalization in nerve cell bodies (Nguyen et al., 2002). Contrary to what was reported at the somatodendritic level, NTS1-mediated internalization of NT was insentitive to the endocytosis inhibitor phenylarsine oxide (Nguyen et al., 2002). Additionally, treatment of synaptosomes with monensin reduced NT binding and internalization, suggesting that presynaptic NTS1 receptors are recycled back to the plasma membrane (Nguyen et al., 2002). In line with these data, a study in NTS1 expressing N1E-115 cells has demonstrated that internalized NTS1 receptors are recycled back to the cell surface

under prolonged treatment with saturating concentrations of NT agonist (Toy-Miou Leong et al., 2004a). Indeed, confocal microscopic studies revealed that these receptors accumulated slowly (> 6 h) in the perinuclear recycling compartment upon returning to the cell surface, restoring NT binding capacity to half of baseline values after 24 h of agonist exposure (Toy-Miou Leong et al., 2004a).

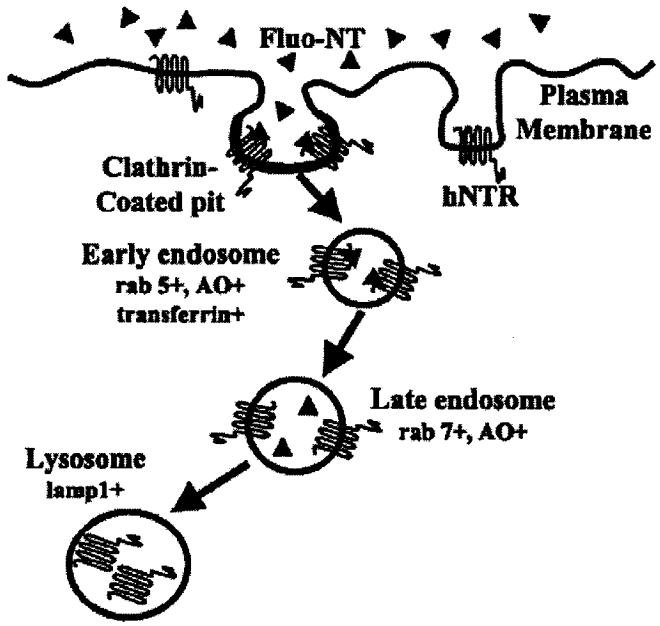

Figure 1.7: Model for the NTS1-mediated Endocytosis of Neurotensin. Fluo-NT and human NTS1 receptors are internalized together into rab 5-immunopositive acidic endosomes via a clathrin-dependent mechanism. The receptors are then translocated to late endosomes and targeted to lamp1-immunopositive lysosomes for intracellular degradation (Adapted from Vandenbulcke et al., 2000).

2.3.2 NTS2 Receptor

Little is known about the regulation of the NTS2 receptor, except that its stimulation with NT induces long-term metabolic effects due to prolonged and sustained activation of ERK1/2 in rat cerebellar granules cells (Sarret et al., 2002). Furthermore, biochemical and cell imaging evidence suggested that NTS2 receptors are sequestered rapidly upon NT exposure either in cells expressing the recombinant mouse NTS2 (Botto et al., 1998) or in rat cultured neurons (Sarret et al., 2002). This process was proposed to occur via a clathrin-coated pit dependent mechanism since it was abolished by either hypertonic sucrose or phenylarsine oxide (Sarret et al., 2002). On the other hand, ligand-receptor complexes were found to form clusters at the cell surface but not to internalize in cultured astrocytes following stimulation with NT at 37°C, suggesting that NTS2 internalization capacities might be cell type-dependent (Nouel et al., 1997). Nevertheless, RT-PCR studies have demonstrated that cortical glial cells in culture expressed a combine population of NTS2 and NTS3 receptor subtypes, which might influence NTS2 behavior (Nouel et al., 1999).

Several lines of evidence suggest that mouse NTS2 receptors are recycled back to the cell surface through a monensin-sensitive mechanism following their sequestration, as observed in HEK 293 and COS-7 cells (Botto et al., 1998; Debaigt et al., 2004). Recycling of NTS2 receptors was shown to involve both phosphatidylinositol 3-kinase (wortmannin-sensitive) and endosome (Brefeldin A-sensitive) pathways (Debaigt et al., 2004). In addition, the suppression of the neuron-enriched endosomal protein of 21 kDa (NEEP21) was shown to strongly inhibited NTS2 recycling in transfected COS-7 cells, indicating that NEEP21 is essential for the correct recycling of internalized receptors (Debaigt et al., 2004). Site-directed mutagenesis studies have revealed that phosphorylation of Tyr 237 is a critical step in the recycling process of NTS2 receptors (Martin et al., 2002b). Indeed, the human NTS2 in which a cysteine residue naturally replaces the tyrosine in position 237 does not undergo recycling following internalization. Interestingly, the single substitution of this cysteine for a tyrosine gives rise to a human NTS2 receptor mutant that is able to recycle as efficiently as the mouse NTS2 (Martin et al., 2002b).

2.3.3 NTS3 Receptor

A striking feature of NTS3/sortilin is its low cell surface expression (10% of total receptors) (Mazella et al., 2001; Morinville et al., 2004). Indeed, a major pool of NTS3/sortilin was found in association with Golgi vesicles in adipocytes (Morris et al., 1998). However, NT was shown to internalize efficiently after binding to NTS3/sortilin receptors on the surface of transfected COS-7 cells (Navarro et al., 2001). Intriguingly, this sequestration process involved no detectable loss of cell surface receptors, suggesting compensation through either recycling or intracellular receptor recruitment mechanisms (Morinville et al., 2004). Indeed, NTS3 was shown to be recruited to the cell surface following stimulation of neuronal cell cultures with NT (Chabry et al., 1993).

2.4 Ontogeny and Localization of NT Receptors Subtypes

One general feature in the development profile of NT receptors is the very low levels of NTS2 mRNA observed in the perinatal period, which is in sharp contrast with the presence of high amounts of NTS1 mRNA (Lépée-Lorgeoux et al. 1999). Indeed, NTS2 mRNA was shown to first appear in mouse brain tissues around postnatal day 7 and to increase progressively thereafter, reaching a plateau between 30 and 60 days of life (Schotte and Laduron, 1987; Mazella et al., 1996; Sarret et al., 1998).

Quite the opposite, NTS1 is known to appear in rat embryo on day 18 and to peak within the first postnatal week as demonstrated by *in situ* hybridization (Sato et al., 1992) and autoradiographic (Palacios et al., 1988; Hermans et al., 1993) studies. Afterward, NTS1 mRNA was found to decrease dramatically reaching adult levels at the end of the third postnatal week (Sato et al., 1992). Interestingly, previous studies have demonstrated that NTS1 exists as two differentially glycosylated forms in developing rat brain: a heavily glycosylated form corresponding to that found in adult brain, which is largely associated with neuronal processes, and a incompletely glycosylated form transiently expressed between postnatal days 10 and 15, which is concentrated within nerve cell bodies (Boudin et al., 1995; Boudin et al. 2000). This selective expression of the short form at early development stages suggests that it might play a role in the establishment of neuronal circuitry (Boudin et al., 2000).

Less is known about the ontogeny of NTS3/sortilin, expect that its mRNA was detected during embryonic development (from day 7.5 to 16.5), suggesting that it might be involved in proliferation of neuronal precursors (Hermans-Borgmeyer et al., 1999).

2.4.1 NTS1 Receptor

Autoradiographic ligand binding (Quirion et al., 1982; Schotte et al., 1986; Kitabgi et al., 1987; Kessler et al., 1987), *in situ* hybridization (Elde et al., 1990; Nicot et al., 1995; Alexander and Leeman, 1998) and immunohistochemical (Boudin et al., 1996b; Fassio et al., 2000) studies have yielded extensive information on the distribution of NTS1 receptors in mammalian brain (see Table 1.5).

Briefly, prominent NTS1 expression levels were found in association with selective neuronal populations throughout the basal forebrain, hypothalamus, thalamus, limbic system, and brainstem (Boudin et al., 1996b; Alexander and Leeman, 1998). More precisely, high concentrations of NTS1 mRNA immunoreactive proteins and radiolabeled binding sites were observed in the substantia nigra and VTA in association with dopaminergic neurons (Palacios et al., 1981; Quirion et al., 1985; Szigethy and Beaudet, 1987; Szigethy and Beaudet, 1989; Dana et al., 1989; Fassio et al., 2000) as well as in the diagonal band of Broca and magnocellular preoptic nucleus where they were shown to be selectively associated with cholinergic cells (Szigethy et al., 1988; Szigethy et al., 1990; Faure et al., 1995b; Morin et al., 1996; Morin and Beaudet, 1998). Additionally, dual labeling immunohistochemistry demonstrated precise overlap between [^{125}I]-NT binding sites and both vasoactive intestinal peptide (VIP)-containing nerve cell bodies and serotonin (5-HT)-containing axons throughout the suprachiasmatic nucleus (SCN) of the rat hypothalamus (François-Bellan et al., 1992). Both VIP and 5-HT innervations of the SCN have been implicated in the control of phasic gonadotropin release (Hery et al., 1978; Hery and Faudon, 1984). Conversely, NTS1 binding sites were shown to be down-regulated by gonadal steroids (Moyse et al., 1987). Taken together these data suggest evidence for an integrated involvement of NT, 5-HT, and VIP innervations of the SCN in the regulation of gonadotropin secretion (François-Bellan et al., 1992).

Within the pons, high affinity NT labeling was detected in the periventricular region, particularly within the dorsal tegmental nucleus and the laterodorsal tegmental nucleus (Kessler et al., 1987). More dorsally, NTS1-labeled neurons were detected within the ventral tegmental nucleus as well as the median raphe nucleus (Boudin et al., 1996b). Intense NTS1 immunolabeling was also found throughout the pontine nuclei, where it pervaded both perikarya and neutropil (Boudin et al., 1996b).

In the medulla, high affinity NT binding sites and NTS1 immunolabeling were mainly concentrated within the nucleus of the solitary tract, the medial vestibular nucleus, inferior olive, and the cuneate nucleus (Young and Kuhar, 1981; Kessler et al., 1987; Boudin et al., 1996b). NTS1 receptors were also found in vagal projections, providing an anatomical correlate for the NT-induced hypotensive and gastrointestinal functions since vagus nerve components are involved in the control of both cardiovascular and gastrointestinal functions (Roman and Gonella, 1981; Hellstrom, 1986).

In the rat spinal cord, NTS1-immunoreactivity was found exclusively within the substantia gelatinosa (laminae II) of the dorsal horn, suggesting that this receptor might play a role in the spinal NT antinociceptive action (Fassio et al., 2000). Finally, quantitative RT-PCR studies in rat peripheral tissues revealed that NTS1 mRNA is also found in the colon, liver, duodenum and pancreas (Mendez et al., 1997).

Mapping of NTS1 at the cellular level by a antipeptide antibody approach using photonic and electon microscopy demonstrated that this receptor is broadly distributed both post and presynaptically in rat CNS (Boudin et al. 1996b; Boudin et al., 1998; Pickel et al., 2001). This cellular distribution is consistent with electrophysiological and pharmacological evidence for postsynaptic effects of NT in mammalian brain. Indeed, NT was shown to directly activate mesencephalic dopaminergic (Pinnock, 1985) and basal forebrain cholinergic (Alonso et al., 1994) neurons, which both exhibit widespread dendritic and somatic NTS1-like immunoreactivity (Boudin et al., 1996b). Additionally, the NTS1-like labeling associated with axonal arborizations within the cerebral cortex (Boudin et al., 1996b)

is in agreement with the NT-induced increase in acetylcholine release reported in slices from rat frontal cortex (Lapchak et al., 1993). However, a few structures (e.g. the amygdala, the PAG, and the superior colliculus) that are known to be innervated by NT fibers were devoid of NTS1 immunohistochemical signal (Boudin et al., 1996b; Fassio et al., 2000), suggesting the existence of another NT receptor subtype that would be detectable by autoradiography but not by immunohistochemistry.

TABLE 1.5

Regional Distribution of NTS1 Receptors in the Adult Rat Brain

Structure	**[^{125}I]-NT binding[a]**	**mRNA levels[b]**	**NTS1 immunoreactivity[c]**	
			Cell bodies and dendrites	Axons and nerve terminals
Telencephalon				
Cerebral cortex				
Frontal cortex	+	+/++	++	+
Parietal cortex	+	+	++	
Cingulate cortex	+++	++		++
Perihinal cortex	+++	+/++	++	++
Entorhinal cortex	+++	++/+++	++	+
Retrosplenial cortex	+++	+	++	++/+++
Basal ganglia				
Caudate putamen	++	-	-/+	++
Nucleus accumbens	++	+	+	+
Olfactory tubercle				
Islands of Calleja	++++	+	++++	
Basal forebrain				
Medium septum	++	++++	++	
Diagonal band of Broca	++/+++	++++	++++	+
Magnocellular preoptic area	+++	++++	++++	
Substantia innominata	++	++++	++	
Lateral septum	++	++/+++	-/+	+++
Bed nucleus of the stria terminalis	++	++/+++	-/+	+++
Amygdala				
Posterior cortical nucleus	++++	++	++	++
Basomedial nucleus	++	+		+
Central nucleus	++	++/+++		-/+
Lateral nucleus	++	+		+
Hippocampal formation				
Pre, parasubiculum	++++	+/++	+++	++
CA1, CA2, CA3	+	++	+	
Dentate gyrus	++		+	

TABLE 1.5 (continued)

Diencephalon				
Thalamus				
Anterior dorsal nucleus	++++	+++	+++	
Paraventrucular nucleus	+	+		+++
Hypothalamus				
Suprachiasmatic nucleus	+++	+++	+++	+
Periventricular nucleus	++	+/++	++	++
Paraventricular nucleus	+/++	+/++	+	++
Lateral hypothalamic area	++/+++	+++	++	++
Mesencephalon				
Substantia nigra	+++/++++		+++/++++	
Ventral tegmental area	++++		+++	
Periaqueductal gray	++		-/+	+
Dorsal raphe nucleus			++	
Superior colliculus	+++		++	+++
Pons				
Pontine nuclei			++++	
Reticulotegmental nucleus			+++	
Ventral tegmental nucleus			++	
Median raphe nucleus			+	
Medulla				
Medial vestibular nucleus			++	
Dorsal cochlear nucleus			++	
Retrofacial nucleus			+++	
Inferior olive			+++	
Nucleus of the vagus			++++	
Nucleus of the solitary tract				+++
Cuneate nucleus			+++	

[a]Density of [^{125}I]-NT binding sites as described in Moyse et al., 1987; [b]NTS1 mRNA levels as stated by Alexander et al., 1998; [c]NTS1 immunoreactivity as per Boudin et al., 1996b. - = no labeling; +/- = limit of detection, + = low signal; ++ = moderate signal; +++ = high signal; ++++ = very high signal.

2.4.2 NTS2 Receptor

Expression of NTS2 mRNA was first investigated by Northern blot analysis (Chalon et al., 1996; Mazella et al., 1996; Vita et al., 1998). These studies revealed that the NTS2 mRNA is mainly expressed in the brain, cerebellum, and to a lesser extent in the heart, kidney, lung and uterus (Vita et al., 1998). Northern blot studies also disclosed the presence of two alternatively spliced transcripts of 1.6 and 1.4 kb in mouse brain (Botto et al., 1997b). Using NTS2-specific oligonucleotides, these two isoforms were then detected by RT-PCR analysis in the rat olfactory bulb, neocortex, cerebellum, striatum and hypothalamus (Botto et al., 1997b). Interestingly, only the long form of the receptor was detected in cortical glial cells, whereas both forms were observed in rat cerebellar granule cells in culture, suggesting that the shorter

variant NTS2 (vNTS2) isoform may be exclusively neuronal (Nouel et al., 1999; Sarret et al., 2002).

As opposed to NTS1, much less is known about the distribution of NTS2 within the mammalian CNS (reviewed in Table 1.6). Early autoradiographic studies based on displacement of [^{125}I]-NT, [^{3}H]-NT, or [^{3}H]-SR142948A binding by levocabastine reported a widespread distribution of NTS2 in the adult rat brain (Schotte et al., 1986; Kitabgi et al., 1987; Bétancur et al., 1998), which was subsequently confirmed by direct labeling carried out with [^{3}H]-levocabastine (Asselin et al., 2001). Accordingly, these studies demonstrated that specific NTS2 binding sites are particularly abundant in cerebral cortex, limbic areas (e.g. the amygdala and the hippocampal formation) and regions involved in pain perception (e.g. the PAG and the superior colliculus).

In conformity with these results, *in situ* hybridization studies using probes that did not discriminate between the two spliced isoforms have shown that NTS2 mRNAs are diffusely distributed throughout the rodent CNS (Sarret et al., 1998; Walker et al., 1998; Lépée-Lorgeoux et al., 1999). In particular, moderate to dense hybridization signal was observed in the cerebral and cerebellar cortices, PAG, superior colliculus, amygdaloid complex, and hippocampal formation (Sarret et al 1998). Expression of NTS2 mRNA was also found in association with a collection of auditory, visual, olfactory, and somatosensory nuclei, suggesting that this receptor might be implicated in virtually all primary afferent pathways (Sarret et al., 1998). A high degree of correspondence exists between NTS2 biding sites distribution with that of NTS2 mRNA within the rat CNS (Asselin et al., 2001). These studies also revealed that the distribution of NTS2 mRNA overlapped to some extent with that of NTS1 (e.g. the enthorhinal and retrosplenial cortices, the medial septum, and the hypothalamic suprachiasmatic nucleus), implying that certain neurons might jointly express NTS1 and NTS2.

Finally, *in situ* hybridization studies have shown that central NTS2 receptors are predominantly expressed by neurons in homeostatic conditions (Sarret et al., 1998). However, NTS2 receptor expression was also detected in astrocytes and found to be up-regulated during astrocytic reaction, suggesting that NTS2 may play a role in regulating glial response to injury (Nouel et al., 1999). At the subcellular level, labeling with [^{3}H]-levocabastine revealed that NTS2 receptors are mainly intracellular, signifying that they might correspond to newly synthesized receptors or receptors recycled to the cell surface (Asselin et al., 2001). Additionally, [^{3}H]-NT binding studies on synaptosomal preparations have proposed that a proportion of NTS2 receptors located to the molecular layer of the rat cerebellar cortex are expressed presynaptically on parallel fibers (Sarret et al., 2002).

TABLE 1.6

Regional Distribution of NTS2 Binding Sites and mRNA in Mammalian CNS

Brain region	[^{3}H]-levocabastine labeling[a]	mRNA levels[b]
Telencephalon		
Cerebral cortex		
Piriform cortex	N.A	++++
Cingulate cortex	+++	++
Perihinal cortex	N.A	+/++
Entorhinal cortex	+++	+++
Retrosplenial cortex	N.A	+++
Basal ganglia		
Caudate/Putamen	++	+
Nucleus accumbens	++	+
Basal forebrain		
Olfactory tubercle	N.A	++++
Medium septum	++	+
Diagonal band of Broca	N.A	+++
Magnocellular preoptic nucleus	N.A	+/++
Lateral septal nucleus	N.A	-/+
Bed nucleus of the stria terminalis	N.A	++
Amygdala	+++	
Cortical nucleus		++++
Basolateral nucleus		++++
Basomedial nucleus		++++
Medial nucleus		++++
Hippocampal formation	++	
Pre, parasubiculum		++++
CA1, CA2, CA3		++++
Dentate gyrus		++++

TABLE 1.6 (continued)

Diencephalon		
Thalamus	++++	
Reticular nucleus		++
Parafascicular nucleus		+++
Medial geniculate nucleus		++
Lateral geniculate nucleus		+/++
Hypothalamus	+++	
Suprachiasmatic nucleus		+++
Paraventricular nucleus		++++
Lateral hypothalamic area		+
Arcuate nucleus		++++
Ventromedial nucleus		++++
Dorsomedial nucleus		++++
Mesencephalon		
Substantia nigra	+	+/++
Ventral tegmental area	+	-/+
Periaqueductal gray	++	+++
Superior colliculus	+++	+++
Dorsal raphe nucleus	+/++	+/++
Pons	N/A	
Pontine nuclei		+++
Superior olivary nucleus		+++
Motor trigeminal nucleus		++
Medulla		
Vestibular complex	+/++	++
Ventral cochlear nucleus	N.A	++
Gigantocellular reticular nucleus, pars alpha	N.A	++
Inferior olivary nucleus	N.A	+
Dorsal motor nucleus of the vagus	N.A	-/+
Nucleus of the solitary tract	N.A	+

[a]Density of [^{3}H]-levocabastine binding sites in rat brain as described by Asselin et al., 2001. +/- = limit of detection (1-10 fmol/mg/tissue equivalent), + = low signal (10-20 fmol/mg/tissue equivalent); +/++ = low to moderate signal (20-30 fmol/mg/tissue equivalent); ++ = moderate signal (30-40 fmol/mg/tissue equivalent); +++ = high signal (40-50 fmol/mg/tissue equivalent); ++++ = very high signal (50-60 fmol/mg/tissue equivalent). [b]NTS2 mRNA levels in mouse CNS as stated by Sarret et al., 1998. +/- = limit of detection (0-25 arbitrary optical density units (OD)), += low signal (25-40 OD); +/++ = low to moderate signal (40-55 OD); ++ = moderate signal (55-70 OD); +++ = high signal (70-85 OD); ++++ = very high signal (85-100 OD).

2.4.3 NTS3 Receptor

NTS3/sortilin expression was first detected in various tissues by Northern and Western blotting analysis (Petersen et al., 1997; Lin et al., 1997). Indeed, the NTS3 mRNA appeared particularly abundant in brain, spinal cord, skeletal muscle, heart, thyroid, placenta, and testis (Petersen at al., 1997). More recently, *in situ* hybridization and immunohistochemical studies displayed a widespread distribution of NTS3/sortilin throughout the rat brain (see Table 1.7) including neuronal cell

bodies and dendrites of the olfactory bulb, piriform cortex, amygdaloid nuclei, substantia nigra, lateral septum, diagonal band of Broca, and thalamic nuclei (Sarret et al., 2003b). The distribution and labeling intensity of NTS3-immunoreactive cell bodies basically matched with the localization and levels of NTS3/sortilin mRNA, except in the nucleus accumbens, medial geniculate nucleus, dorsal raphe nucleus, and cerebellar granule cell layer, in which there were neurons displaying a weak NTS3/sortilin mRNA signal without receptor immunolabeling (Sarret et al., 2003b). This divergence may be due to variations in the messenger stability among brain regions or to differential translation regulatory mechanisms (Sarret et al., 2003b).

NTS3/sortilin expression was also found within neurons and oligodendrocytes in major fiber tracks (Sarret et al., 2003b). In particular, electron microscopy revealed that NTS3/sortilin immunoreactivity was mainly associated with the Golgi apparatus, saccules of the endoplasmic reticulum, and vesicular organelles, whereas only a small proportion of NTS3/sortilin was found in association with neuronal plasma membranes (Sarret et al., 2003b).

TABLE 1.7

Distribution of NTS3/sortilin mRNA and Immunoreactivity in the Adult Rat Brain

Structure	mRNA levels[a]	NTS1 immunoreactivity[b]	
		Cell bodies and dendrites	Axons and nerve terminals
Telencephalon			
Cerebral cortex			
Frontal cortex	++	+/++	+
Parietal cortex	++	++	+
Temporal cortex	++	++	+/++
Cingulate cortex	+++	+/++	+
Piriform cortex	+++	++/+++	-
Entorhinal cortex	++/+++	++	+
Retrosplenial cortex	++/+++	+/++	+
Basal ganglia			
Caudate/Putamen	+/++	++	-
Nucleus accumbens	+/++	-	-
Basal forebrain			
Olfactory tubercle	+/++	++	++
Islands of Calleja	++	++	++
Lateral septum	++/+++	+++	-/+
Medium septum	++	++/+++	++
Diagonal band of Broca	+	++/+++	++/+++
Magnocellular preoptic area	+/++	+++	+++
Bed nucleus of the stria terminalis	+/++	++	-

TABLE 1.7 (continued)

Amygdala			
Central nucleus	++	+/++	-/+
Basomedial nucleus	+	++	+
Basolateral nucleus	++	++	+
Cortical nucleus	++	++	++
Hippocampal formation			
Pre, parasubiculum	+	+/++	-
CA1, CA2, CA3	+++	++	-
Dentate gyrus	+	+/++	-
Diencephalon			
Thalamus			
Anterior dorsal nucleus	++	++/+++	+/++
Paraventricular nucleus	+	+++	+
Reticular nucleus	++	++/+++	-
Medial nucleus	+/++	+/++	-/+
Medial geniculate nucleus	++	-	-
Lateral geniculate nucleus	+/++	++	+/++
Hypothalamus			
Anterior hypothalamic area	+	+	+
Suprachiasmatic nucleus	+++	+	-
Supraoptic nucleus	+++	++/+++	+
Paraventricular nucleus	++	++	++
Arcuate nucleus	+++	++	-
Mesencephalon			
Substantia nigra pars compacta	++	++/+++	++
Substantia nigra pars reticulata	-/+	+/++	++
Ventral tegmental area	++	+/++	-
Periaqueductal gray	+	+/++	-
Superior colliculus	++	+/++	+/++
Dorsal raphe nucleus	++	-	-
Red nucleus	++	++/+++	-
Pons			
Pontine nuclei	+	++	++
Superior olivary nucleus	++	++	+/++
Median raphe nucleus	++	+/++	-
Medulla			
Vestibular complex	++	++	+/++
Cochlear nuclei	+	++	+
Inferior olivary nucleus	++	+++	+/++
Nucleus of the solitary tract	+	+/++	++
Cuneate nucleus	+/++	+/++	-/+
Gracile nucleus	+/++	+/++	-/+
Abducens nucleus	++	++	+
Facial nucleus	++	++	+
Dorsal motor nucleus of the vagus	+	++	-/+

[a]NTS3/sortilin mRNA levels as stated by Sarret et al., 2003b; [b]NTS3/sortilin immunoreactivity as per Sarret et al., 2003b. - = no labeling; +/- = limit of detection, + = low signal; +/++ = low to moderate signal; ++ = moderate signal; ++/+++ = moderate to high signal; +++ = high signal; ++++ = very high signal (referring to both labeling intensity and the number of labeled elements).

2.5 Physiological Roles of NT Receptor Subtypes

2.5.1 Nonpeptide Antagonists and NT Analogues

A better understanding of the central effects of endogenous NT was provided by pharmacological studies using the NTS1-specific antagonist SR48692. Indeed, this compound was shown to reverse both the turning behavior induced by intrastriatal NT injections in mice (Gully et al., 1993) and the hypolocomotor response elicited by intracerebroventricular NT administration (Dubuc et al., 1994; Pugsley et al., 1995). It also antagonized the locomotor activity evoked by NT injection into the VTA (Steinberg et al., 1994). On the other hand, it did not antagonize the hypothermic and analgesic response to NT in rodents, suggesting that these central effects are not mediated through NTS1 (Dubuc et al., 1994). Likewise, SR48692 failed to inhibit NT-mediated excitation of PAG-RVM neurons (Li et al., 2000). However, SR48692 was used over a narrow dose range in these studies and other investigations have shown that this antagonist has a triphasic effect on the increase in tail-flick response latencies triggered by an antinociceptive dose of NT (Smith et al., 1997). For instance, NT-induced analgesia following administration into the RVM was attenuated, overturned, or partially blocked by femtomolar, picomolar, or higher doses of SR48692, respectively.

Unlike SR48692, SR142948 recognizes both NTS1 and NTS2 receptors with high affinity (IC_{50} = 1-4 nM) (Gully et al., 1997). SR142948A inhibited the NT-mediated turning behavior in mice and had no effect on DA release elicited by NT injection into the VTA (Gully et al., 1997). Interestingly, it also blocked both the analgesic and hypothermic responses induced by central injection of NT, as well as the depolarization induced by exogenously applied NT on PAG neurons, suggesting that the NTS2 receptor subtype may mediate these effects (Gully et al., 1997; Kreitel et al., 2002). In line with these results, structure-activity studies have suggested that the hypothermic and analgesic actions of NT in the mouse brain appear to be mediated through a receptor, whose pharmacological properties are distinct from those of the high affinity NT receptor (Al Rhodan et al., 1991; Labbé-Jullié et al., 1994; Tyler et al., 1998a). However, only the NT-induced analgesia was reversed by

the NTS2-specific ligand levocabastine, suggesting that NT receptors involved in hypothermia differ from those involved in analgesia (Tyler et al., 1998b; Dubuc et al., 1999a). A similar effect on NT-mediated antinociception was observed following pretreatment with another specific H_1 antagonist (i.e. diphenhydramine) (Tyler et al., 1998b). This antagonist also blocked the responses of PAG neurons to stimulation of the medial preoptic (MPO) nucleus in anesthetized rats, suggesting that the MPO-PAG interaction is, in part, mediated by activation of NTS2 receptors (Kreitel et al., 2002).

2.5.2 Knock-down Strategies

Experiments in knock-out mice have shown that NTS1 gene deletion resulted in the loss of NT-induced hypothermia and contractile effects in both isolated distal colon and stomach fundus (Pettibone et al., 2002; Remaury et al., 2002). Additionally, NTS1 deficient mice did not respond to intracerebroventricular NT-mediated hypolocomotion and feeding regulation, indicating that NTS1 mediates several of the central and peripheral effects of NT (Pettibone et al., 2002; Remaury et al., 2002).

However, several lines of evidence suggest that NTS2 may play a particularly important role in mediating the antinociceptive effects of NT (Gully et al., 1997; Dubuc et al., 1999b). For instance, injection of antisense oligonucleotides designed to knock-down NTS2 receptors markedly inhibited NT-induced analgesia (Dubuc et al., 1999b). This response was specific for the NTS2 receptor subtype since treatment with oligonucleotides raised against NTS1 did not induce any effects. Similarly, the antinociceptive activity of β-lactotensin, a NTS2 specific agonist, was blocked by treatment with NTS2 antisense oligonucleotides while treatment with NTS1 antisense oligonucleotides had no effect (Yamauchi et al., 2003a). Structure-activity studies also revealed a close correlation between the analgesic potencies of NT analogues and their affinity for the levocabastine-sensitive NT receptor (Labbé-Jullié et al., 1994; Dubuc et al., 1999b). In line with these observations, levocabastine was shown to behave as a partial agonist in the writhing test following intracerebroventricular administration in mice (Dubuc et al., 1999b). Nonetheless,

this analgesic effect was not additive to that of NT, but rather decreased its effect to a level not significantly different from that observed with levocabastine alone.

On the other hand, these results are in contrast with those of Tyler et al (1998c) who demonstrated that the inhibition of NTS1 receptor synthesis after gene blockade by complementary peptide nucleic acids resulted in a loss of analgesic response to NT. Nonetheless, recent demonstration that NTS1 knockout mice displayed defects in NT-induced analgesia in the hot plate (Pettibone et al., 2002), but not in the writhing test (Remaury et al., 2002) suggested that the NT receptor subtype required for NT-mediated antinociception might depend on the stimulus. However, it is hazardous to compare these analgesic effects with one another since they implicate different signaling pathways (i.e. thermal vs. visceral pain). Finally, NTS2, but not NTS1 knockout mice have been reported to exhibit increased jump latency in the hot plate test, suggesting that NT facilitates pain transmission via NTS2, which might play a different role under physiological conditions (Maeno et al., 2004). Taken together, these results indicate that multiple NT receptors with distinct antagonist binding affinities seem to be involved in NT-induced modulation of inhibitory and facilitatory nociceptive systems.

CHAPTER 2: RATIONALE OF THE THESIS

NOTE: This section corresponds to the connecting texts that provide the logical bridges between each chapter.

CHAPTER 3:

Immunohistochemical Distribution of NTS2 Neurotensin Receptors in the Rat Central Nervous System

Little is known concerning the distribution of the NTS2 receptors in the mammalian brain except that *in situ* hybridization and radioligand binding studies have shown that NTS2 is diffusely expressed throughout the rodent CNS (refer to Section 2.4.2 for details and references). However, no data are currently available on the distribution of NTS2 receptor proteins, nor of their putative colocalization with other NT receptor subtypes in the brain. A precise knowledge of neuronal networks harbouring NTS2 receptors was thus crucial to our understanding of their function in mammalian CNS.

In order to address these questions, the subcellular distribution of NTS2 receptor proteins was first investigated by confocal microscopy in NTS2-expressing COS-7 cells using a custom-synthesized antibody raised against a synthetic peptide corresponding to the 7-21 amino acid sequence in the N-terminal segment of the rat receptor. These studies revealed the presence of a prominent pool of intracellular receptors in the perinuclear region, suggesting that NTS2 receptors are poorly expressed at the cell surface. Additionnally, immunohistochemical studies on rat brain sections showed that NTS2 immunoreactivity was selectively associated with neurons and for the most part, although not exclusively, with their dendritic arbors. Of particular interest from a functional perspective was the intense labelling of brain structures involved in pain control (e.g. PAG and dorsal raphe). Interestingly, many of the regions which displayed NTS2-like immunoreactivity had previously been shown to contain high levels of NTS1 immunostaining (e.g. anterodorsal thalamic nucleus, substantia nigra, VTA), suggesting that NTS2 is in a position to interact with NTS1 in mediating NT's central effects.

CHAPTER 4:

Low-Affinity Neurotensin Receptor (NTS2) Signaling: Internalization-Dependent Activation of Extracellular Signal-Regulated Kinases 1/2.

The role and signaling properties of NTS2 are still controversial. In particular, it is unclear whether NT acts as an agonist, inverse agonist, or antagonist at this site (refer to Section 2.2.2 for details and references). However, our immunohistochemical studies (refer to Chapter 3) have shown that NTS2 receptors are expressed in structures implicated in the descending control of nociceptive inputs, suggesting that NTS2 may mediate certain analgesic effects of NT.

In order to elucidate the functional role of NTS2, we have investigated the pharmacological and signaling properties of this receptor in NTS2-expressing CHO cells. We found that NT activates the mitogen-activated protein kinase cascade through its interaction with either rat or human NTS2 receptors. The present NT-induced effects on ERK1/2 phosphorylation are unlikely to be caused by neutral antagonistic or inverse agonistic properties of the drug since there was no evidence of constitutive NTS2 receptor activity in our system. The similarity of this NT-mediated ERK1/2 phosphorylation with that obtained in cultured neurons (refer to Section 2.2.2 for details and references) suggests that this activation is physiological and not caused by artifactual coupling of the receptor subsequent to its aberrant expression in CHO cells. In addition, the fact that NT was found to induce NTS2 internalization further argues in favour of its putative role as an agonist at the NTS2 receptor. Finally, we found that blocking internalization with phenylarsine oxide or monodansylcadaverine completely impaired the ability of NT to activate ERK1/2 in NTS2-expressing CHO cells, suggesting that the NTS2-mediated activation of the MAP kinase pathway is predicated on the internalization of receptor-ligand complexes.

CHAPTER 5:

Identification and Functional Characterization of the 5-Transmembrane Domain Variant Isoform in the Rat Central Nervous System.

The mouse NTS2 receptor exists in two different isoforms referred to as NTS2 (full-length receptor) and vNTS2, an alternatively spliced form in which the last two transmembrane domains have been deleted (see Section 2.1.2 for more information). However, the latter protein failed to bind NT after transient expression in COS-7 cells, suggesting that the variant NTS2 isoform was non-functional protein (Botto et al., 1997b). Interestingly, our previous Western blotting analysis of NTS2 receptors in rat brain membrane preparations (refer to Chapter 3) had revealed the presence of high molecular weight immunoreactive species that could correspond to either NTS2 homodimers or putative heterodimers of NTS2 and vNTS2, suggesting that this truncated isoform might also be found in the rat CNS.

Hence, to clarify whether vNTS2 is a true NT receptor, we first investigated the binding and internalization properties of this truncated receptor in COS-7 cells stably transfected with the HA-tagged vNTS2 cDNA that we isolated from rat brain tissue (refer to Appendix D for GenBank accession number). As opposed to what had been reported for the mouse vNTS2, our results demonstrated that the rat vNTS2 bound NT, albeit with a considerably lower affinity than the full-length receptor (as demonstrated in Chapter 4). Immunocytochemical analysis using the NTS2 N-terminally directed antiserum (refer to Chapter 3 for characterization) revealed that the bulk of immunoreactive receptors was intracellular and concentrated in a Golgi-like structure surrounding the nucleus. This subcellular localization is in agreement with what was observed for NTS2 in cells expressing the full-length receptor (as demonstrated in Chapter 3), suggesting that the greater part of NTS2 receptors (i.e. full-length and variant isoforms) is concentrated intracellularly. Despite its poor trafficking to the cell surface, confocal microscopic experiments demonstrated specific vNTS2 receptor-mediated internalization of fluorescent NT following incubation at 37°C with a pattern consistent with former report on internalization via the full-length NTS2 receptor (see Chapter 4). We then investigated whether the

truncated NTS2 receptor retained the MAP Kinase activation properties exhibited by the long NTS2 isoform (as described in Chapter 4). Our results indicated that stimulation with NT induced a rapid and sustained increase in ERK1/2 phosphorylation in CHO cells transfected with vNTS2, suggesting that the two NTS2 isoforms are functionally responsive to NT.

In order to determine if it was possible that the high molecular weight species of NTS2 receptors detected in rat brain membrane preparations corresponded to vNTS2/NTS2 heterodimers as hypothesised earlier (see Chapter 3), we co-expressed HA-tagged vNTS2 together with untagged NTS2 receptors in COS-7 cells and subjected cell lysates to immunoprecipitation with the anti-HA antibody. Immunoblotting with our custom-synthesized C-terminally directed NTS2 antiserum revealed the presence of immunoreactive bands corresponding to NTS2, indicating that it has been co-immunoprecipitated with the variant NTS2 via heterodimerization.

CHAPTER 6:

Sustained Agonist Exposure Promotes Cell Surface Recruitment of NTS2 Neurotensin Receptors

Receptor internalization has been shown to play a critical role in the control of cell responsiveness to NT (see Section 2.3 for more details). Also, current biochemical and immunocytochemical data suggest that internalized NTS1 are not recycled back to the plasma membrane but rather targeted to lysosomes for degradation. However, little is known about the regulation of NTS2 except that its stimulation with NT induces long-term metabolic effects as demonstrated in our ERK1/2 activation experiments (see Chapter 4).

The next study was thus initiated in order to determine whether extended stimulation of NTS2 leads to down-regulation of cell surface receptor densities as in the case of NTS1. We have found that, contrary to NTS1, cell surface NTS2 receptors are resistant to down-regulation despite efficient internalization mechanisms. By tracking the intracellular routing of NTS2 receptors using confocal microscopy, we established that cell surface NTS2 receptors are maintained through

recruitment of spare receptors from internal stores. This intracellular pool of NTS2 receptors is congruent with what was observed in our earlier studies (refer to Chapter 3). The cell surface binding sites maintained during persistent NT exposure corresponded to functional NTS2 receptors since NT-induced ERK1/2 phosphorylation levels in cells exposed to NT for 24 h were comparable to those previously reported in transfected CHO cells (see Chapter 4). To ascertain the physiological relevance of these observations, we monitored by electron microscopy the effect of intrathecal NT injection on the subcellular distribution of NTS2 in neurons of the superficial laminae of the rat spinal cord by using our NTS2 peptide antiserum (previously characterized in Chapter 3). Twenty minutes after NT injection, we found an enhanced NTS2 receptor density on neuronal plasma membranes without any change in NTS2 total density suggesting that *in vivo*, as *in vitro*, exposure to NT triggers a relocalization of intracellular receptors to the plasma membrane.

CHAPTER 7:

NTS2 Modulates NTS1 Expression and Internalization via Heterodimerization.

Our previous immunohistochemical studies have shown that NTS2 receptor distribution shares similarities with that of NTS1 within the rat CNS (see Chapter 3), supporting the hypothesis that NTS2 might co-localize within the same neurons as NTS1 and that, within these neurons, NTS2 and NTS1 might either interact together or be found in the same protein complex.

We thus combined biochemical, pharmacological, and immunocytochemical approaches to determine whether NTS2 can physically interact with NTS1 and to investigate the effect of NTS2 expression on NTS1 regulation. Our results indicated that NTS2 is able to form heterodimers with NTS1 *in vitro* via hydrophobic interactions. They also showed that coexpression of NTS2 markedly inhibited cell surface expression of NTS1 by causing its accumulation in the perinuclear region, where it colocalized with NTS2 immunoreactivity (as described in Chapter 6).

Chronic exposure of NTS1 to its ligand was previously shown to result in time-dependent decline in cell surface receptors (see Section 2.3.1 for more details and references). By contrast, we have shown that NTS2 cell surface binding sites are resistant to down-regulation (see Chapter 6). We thus hypothesized that NTS2 expression might affect the regulation of NTS1 cell surface densities upon extended NT stimulation. Indeed, we found that NTS1 binding sites were more resistant to down-regulation when the two NT receptor subtypes were expressed together than when expressed alone. These data suggest that NTS2 influences intracellular trafficking of NTS1, likely mediated through heterodimerization of these two receptor subtypes.

CHAPTER 3

IMMUNOHISTOCHEMICAL DISTRIBUTION OF NTS2 NEUROTENSIN RECEPTORS IN THE RAT CENTRAL NERVOUS SYSTEM

Philippe Sarret[1], Amélie Perron[1], Thomas Stroh, and Alain Beaudet

[1]Authors contributed equally to the work.

Montreal Neurological Institute, Department of Neurology and Neurosurgery, McGill University, Montreal, Québec, Canada

Journal of Comparative Neurology (2003) **461**, 520-538.

3.1 ABSTRACT

In the present study, we localized the levocabastine-sensitive neurotensin receptor (NTS2) protein in adult rat brain by using an N-terminally directed antibody. NTS2-like immunoreactivity was broadly distributed throughout the rat brain. At the cellular level, the reaction product was exclusively associated with neurons and predominantly, although not exclusively, with their dendritic arbors. No NTS2 signal was observed in astrocytes, as confirmed by dual confocal microscopic immunofluorescence studies using the astrocytic marker S100β. High densities of NTS2-like immunoreactive nerve cell bodies and/or processes were detected in many regions documented to receive a dense neurotensinergic innervation, such as the olfactory bulb, bed nucleus of the stria terminalis, magnocellular preoptic nucleus, amygdaloid complex, anterodorsal thalamic nucleus, substantia nigra, ventral tegmental area, and several brainstem nuclei. Most conspicuous among the latter were structures implicated in the descending control of nociceptive inputs (e.g., the periaqueductal gray, dorsal raphe, gigantocellular reticular nucleus, pars alpha, lateral paragigantocellular and raphe magnus), in keeping with the postulated role of NTS2 receptors in the mediation of neurotensin's supraspinal antinociceptive actions. However, the distribution of NTS2-like immunoreactivity largely exceeded that of neurotensin terminal fields, and some of the highest concentrations of the receptor were found in areas devoid of neurotensinergic inputs such as the cerebral cortex, the hippocampus, and the cerebellum, suggesting that neurotensin may not be the exclusive endogenous ligand for this receptor subtype.

3.2 INTRODUCTION

The tridecapeptide neurotensin (NT), originally isolated from bovine hypothalamus (Carraway and Leeman, 1973), was subsequently localized throughout the central nervous system (CNS) of several mammalian species (for review, see Uhl, 1982 and Emson, 1985a) and shown to be involved in a variety of central functions including thermoregulation, nociception, food consumption, regulation of dopaminergic and cholinergic neurotransmission, and neuroendocrine control (for reviews, see Kitabgi et al., 1985; Kitabgi and Nemeroff, 1992; Rostène and Alexander, 1997; Sarret and Beaudet, 2002).

Neurotensin effects are exerted through a variety of receptor subtypes, two of which have been distinguished pharmacologically on the basis of their affinities for NT and sensitivity to the histamine antagonist levocabastine: a NT high-affinity site, which does not bind levocabastine (NTS1; K_d = 0.3 nM) and a NT low-affinity site, which recognizes levocabastine (NTS2; K_d = 2-4 nM) (Mazella et al., 1983; Schotte et al., 1986; Kitabgi et al., 1987). These two receptors have been molecularly identified in recent years and shown to belong to the seven transmembrane domain, G protein-coupled receptor family (GPCR, for review, see Hermans and Maloteaux, 1998; Vincent et al., 1999; Sarret and Beaudet, 2002). A third NT receptor (NTS3) was recently cloned from human brain (Mazella et al., 1998). This receptor is a type I amino-acid receptor with a single transmembrane-spanning region corresponding to the previously cloned gp95/sortilin (Petersen et al., 1997).

Autoradiographic ligand binding, *in situ* hybridization, and immunohisto-chemical studies have yielded abundant information on the distribution of the NTS1 receptors in mammalian brain. In brief, high concentrations of NTS1 were found in association with selective neuronal populations throughout the hypothalamus, basal forebrain and limbic system (Sarrieau et al., 1985; Schotte et al., 1986; Moyse et al., 1987; Kitabgi et al., 1987; Palacios et al., 1988; Dana et al., 1989; Elde et al., 1990; Sato et al., 1992; Nicot et al., 1994a,b, 1995; Boudin et al., 1996b; Alexander and Leeman, 1998; Fassio et al., 2000). They were markedly enriched over dopaminergic neurons of the ventral midbrain (Palacios and Kuhar, 1981; Quirion et al., 1985;

Hervé et al., 1986; Szigethy and Beaudet, 1989, Schotte and Leysen, 1989; Goulet et al., 1999), cholinergic neurons of the basal forebrain (Szigethy and Beaudet, 1987; Szigethy et al., 1988; Faure et al., 1995; Cape et al 2000), and VIPergic neurons of the suprachiasmatic nucleus of the hypothalamus (François-Bellan et al., 1992). This distribution is consistent with reported NTS1-mediated NT effects on locomotion and cognition, as well as on the sleep-wake cycle, memory, and regulation of hypothalamo-pituitary functions (Cape et al., 2000; for review, see Rostène and Alexander, 1997; Binder et al., 2001a ; Sarret and Beaudet, 2002).

Much less is known concerning the distribution, particularly at the cellular level, of the levocabastine-sensitive NTS2 receptors. Early autoradiographic binding studies, based on the displacement of specific ^{125}I-labeled NT, [^{3}H]-NT, or [^{3}H]-SR142948A binding by levocabastine, reported a widespread distribution of levocabastine-sensitive NTS2 receptor sites in adult rat brain (Kitabgi et al., 1987; Schotte et al., 1986, 1988; Schotte and Laduron, 1987; Bétancur et al., 1998). This widespread distribution of NTS2 binding sites was confirmed recently by using direct autoradiographic localization of [^{3}H]-levocabastine (Asselin et al., 2001). Based on their ubiquitous distribution, as well as on their pattern of ontogenetic development (Schotte and Laduron, 1987) and recovery after local destruction of neurons with kainic acid (Schotte et al., 1988), low-affinity NT binding sites were originally surmised to be mainly associated with glial cells. Accordingly, NTS2 binding and/or mRNA were detected in association with astrocytes both *in vivo* and *in vitro* (Nouel et al., 1997; Walker et al., 1998; Lépée-Lorgeoux et al., 1999) and NTS2 expression was found to be markedly up-regulated in reactive astrocytes surrounding a cortical stab wound (Nouel et al., 1999). However, *in situ* hybridization studies also demonstrated that, in homeostatic conditions, NTS2 was predominantly expressed by neurons within the CNS (Sarret et al., 1998). Further evidence for the expression of functional NTS2 receptors in neurons was provided recently by studies in rat cerebellar granule cells in culture, which demonstrated cell surface NTS2 binding, ligand-induced receptor internalization, and NT-induced MAP kinase activation in these cells (Sarret et al., 2002).

The contribution of NTS2 to the mediation of central NT functions is not as clearly established as that of NTS1. Nonetheless, pharmacologic data based on the use of selective NTS2 agonists (Labbé-Jullié et al., 1994) and antisense oligonucleotides (Dubuc et al., 1999b) have suggested that NTS2 may play a role in the mediation of NT antinociceptive effects. Further insight into the functional role of NTS2 requires precise knowledge of the distribution of this receptor at both regional and cellular levels. To this aim, we have investigated here the localization of NTS2 receptor proteins in rat brain by immunohistochemistry, using an antibody raised against the N-terminal segment of the cloned rat NTS2 receptor.

3.3 MATERIAL AND METHODS

All animal-related procedures were approved by the McGill University Animal Care Committee and carried out according to the regulations of the Canadian Council on animal care.

3.3.1 Primary Antibody for NTS2 Immunodetection

Rabbit anti-NTS2 peptide antiserum was generated by using a synthetic peptide (WPPRPSPSAGLSLEA), corresponding to the 7-21 predicted amino acid sequence in the N-terminal segment of the rat receptor (Chalon et al., 1996), and showing no homology with other known neurotensin receptor subtypes. The peptide was conjugated via maleimide to ovalbumin. The conjugate was used to immunize two rabbits (Affinity BioReagents, ABR, Golden, CO). The initial immunization was followed by five additional booster injections. Serum samples were analyzed separately for reactivity by Western blotting and immunohistochemistry. One of the sera proved more sensitive than the other for immunohistochemistry and, therefore, was used throughout the present study.

3.3.2 Preparation of Rat NTS2 Construct

The *HA*-tagged NTS2 cDNA was obtained through reverse transcription of rat brain mRNA isolated by polymerase chain reaction (PCR) using nucleotide sequences 35-61 bp (5'-ACAGAGATGGCATACCCATACGACGTCCCAGACTACGC TGAGA-CCAGCAGTCCGTGG-3') and 1268-1291 bp (5'-TCATACTTGTATTTCTCCC-AGGCT-3') of the open reading frame of NTS2 mRNA (Chalon et al., 1996) as sense and antisense oligonucleotides, respectively. The PCR product was purified from a 1% low melting temperature agarose gel and subcloned into the pTARGET expression vector (Promega, Madison, WI). That the proper rat NTS2 sequence had been cloned was confirmed by base pair sequencing.

3.3.3 Culture and Transfection of COS-7 Cells

COS-7 cells were maintained in Dulbecco's modified Eagle's medium with high glucose supplemented with 5% fetal bovine serum in the presence of 100 U/ml penicillin/streptomycin (GibcoBRL, Life Technologies, Burlington, Ontario, CAN).

Cells were grown at 37°C in a humidified atmosphere with 5% CO_2 and plated in 100-mm Petri dishes at a density of 10^6 cells/dish. On the following day, semiconfluent cells were transiently transfected with the rat *HA*-tagged NTS2 receptor cDNA by the diethylaminoethanol-dextran/chloroquine method, as described previously (Innamorati et al., 2001). Cells were collected 48-72 hours after the beginning of the transfection and processed for immunoprecipitation or immunocytochemistry as described below.

3.3.4 Preparation of Brain Membranes

Adult Sprague-Dawley rats (200-250g; Charles River, St-Constant, Québec, Canada) were killed by decapitation. Their brains were removed quickly and placed on ice. Cerebellum and brain were dissected, homogenized separately with a Polytron in buffer A containing 50 mM Tris-HCl (pH 7.0) and 4 mM ethylenediaminetetraacetic acid (EDTA) with protease inhibitors (Complete Protease inhibitors tablets, Roche Molecular Biochemicals, Laval, Québec, Canada), and centrifuged at 1,000 rpm for 10 minutes at 4°C. The supernatant was collected and the pellet resuspended in buffer A and centrifuged again for 10 minutes at 4°C. The supernatant from the second spin was combined with that of the first for each sample and centrifuged at 4°C for 10 minutes at 46,000 rpm. The pellets were then resuspended in buffer B, consisting of 50 mM Tris-HCl (pH 7.0) and 0.2 mM EDTA with protease inhibitors, by vortexing and brief sonication. Protein concentration was determined by the Bio-Rad procedure with bovine serum albumin (BSA) as standard (Bradford, 1976).

3.3.5 Immunoblotting Analysis

Membranes from rat brain and cerebellum were denatured by using Laemmli sample buffer (Laemmli, 1970) containing 5% β-mercaptoethanol, resolved by using 8% Tris-glycine precast gels (Invitrogen, Burlington, Ontario, CAN), and transferred to nitrocellulose membranes (Bio-Rad laboratories, Mississauga, Ontario, Canada). Nonspecific sites were blocked by 0.1% Tween 20 and 10% milk powder (Carnation, Don Mills, Ontario, Canada) in phosphate-buffered saline (PBS; pH 7.4) overnight at 4°C. Nitrocellulose membranes were then incubated overnight at 4°C with the N-terminal specific anti-NTS2 rabbit antibody (1/10,000) in PBS with 1% BSA and 1%

ovalbumin. After washing with PBS-Tween, blots were incubated for 1 hour at room temperature (RT) with an horseradish peroxidase (HRP)-conjugated goat anti-rabbit secondary antibody (1/4000; Amersham Pharmacia Biotech, Baie d'Urfé, Québec, Canada) in PBS with 5% milk powder and proteins were visualized by using an enhanced chemiluminescent detection system (Perkin Elmer, Life Sciences, Boston, MA). Specificity of antiserum was confirmed by preadsorption of the NTS2 antibody overnight with an excess of immunizing peptide (2 μg/ml of adsorbing peptide at a final antibody dilution of 1/10,000).

3.3.6 Immunoprecipitation

COS-7 cells were rinsed with PBS 72 hour after transfection, detached from the dishes, and centrifuged. The cell pellet was disrupted in RIPA buffer (150 mM NaCl, 50 mM Tris-HCl, pH 7.5, 5 mM EDTA, 1%, IGEPAL, 0.5% deoxycholic acid, 0.1% sodium dodecyl sulfate) containing protease inhibitors and incubated for 30 minutes on ice. Lysates were then precleared with 25 μg of protein A-Sepharose (Sigma, St-Louis, MO) for 45 minutes at 4°C and incubated overnight at 4°C with the NTS2 rabbit antibody (1/800) or with a rat monoclonal antibody (clone 3F10) directed toward the *HA*-epitope (1/400; Roche Molecular Biochemicals, Indianapolis, IN). The protein A-sepharose was gently shaken in lysis buffer containing 1% BSA for 30 minutes at room temperature before use. HA epitope-tagged NTS2 receptors were precipitated by incubation with 100 μg of protein A-sepharose for 2 hours at 4°C. After washing three times in lysis buffer, complexes were dissolved in Laemmli sample buffer and resolved as described above. Nitrocellulose membranes were then incubated overnight at 4°C in PBS with a solution containing 1% BSA and 1% ovalbumin and a 1/2,500 dilution of a mouse monoclonal antibody (clone 12CA5) directed toward the *HA*-epitope (samples precipitated with NTS2 antibody) or with a 1/10,000 dilution of the NTS2 antibody (samples precipitated with anti-HA antibody). After washing with PBS-Tween, blots were incubated for 1 hour at RT with HRP-conjugated goat anti-rabbit or anti-mouse secondary antibodies in PBS with 5% milk powder (1/4,000; Amersham Pharmacia Biotech, Baie d'Urfé, Québec,

CAN) and proteins were visualized using an enhanced chemiluminescent detection system.

3.3.7 Immunocytochemistry on COS-7 Cells

Transfected COS-7 cells, plated on poly-L-lysine-coated glass coverslips, were fixed for 20 minutes with 4% paraformaldehyde (PFA; Polysciences, Warington, PA) in 0.1 M phosphate buffer (PB), pH 7.4, rinsed with 0.1 M Trisma base-buffered saline (TBS), pH 7.4, and preincubated for 30 minutes at RT with a blocking solution consisting of 5% normal goat serum (NGS), 2% BSA and 0.1% Triton X-100 (BDH, Inc., Toronto, Ontario, Canada) in 0.1 M TBS. Double immunostaining was performed by incubating cells overnight at 4°C with the anti-NTS2 peptide antiserum (1/15,000) or with the anti-NTS2 peptide antiserum preadsorbed with the antigenic peptide, together with the mouse monoclonal antibody (clone 12CA5) directed toward the HA epitope, diluted 1/500 in 0.1 M TBS, pH 7.4, containing 1% NGS and 0.05% Triton X-100. After washing with TBS, cells were incubated for 1 hour at RT with a mixture of Alexa 488-conjugated goat anti-mouse and Alexa 594-conjugated goat anti-rabbit (1/750; Molecular Probes, Eugene, OR), washed twice in TBS and mounted on glass slides with Aquamount.

Double-labeled cells were analyzed by confocal microscopy using a Zeiss 510 laser scanning microscope equipped with a Zeiss inverted microscope and Argon2 (488 nm) and He/Ne1 (543 nm) lasers (Carl Zeiss Micro Imaging Inc. Thornwood, NY). Images were acquired simultaneously for both fluorophores (Alexa-488 and Alexa-594) by using the multitrack configuration mode and processed using the Zeiss 510 laser scanning microscope software. Identical parameters were used to acquire the images for cells immunolabeled in the presence or absence of NTS2 blocking peptide.

3.3.8 Light Microscopic Immunolabeling of Rat Brain Sections

3.3.8.1 Tissue Fixation

Adult male Sprague-Dawley rats (200-250 g; n = 10) were anesthetized with sodium pentobarbital (Somnotol; 1.2 ml/kg) and perfused transaortically with a freshly prepared solution of 4% PFA in 0.1 M PB, pH 7.4. Brains were rapidly removed, cryoprotected overnight in 0.1 M PB containing 30% sucrose at 4°C, and frozen for 1 minute in isopentane at -40°C.

3.3.8.2 Single-Labeling Immunohistochemistry

Coronal sections (30 μm thick) were cut on a freezing microtome along the whole rostrocaudal extent of the brain from bregma 6.70 to –14.60 and collected in 0.1 M PB. Immunohistochemistry was performed according to the avidin biotinylated-HRP complex (ABC) method by using a Elite ABC kit (Vector Laboratories, Burlingame, CAN). Briefly, free-floating sections were washed twice with 0.1 M TBS, pH 7.4, pretreated for 30 minutes with 3% hydrogen peroxide in 0.1 M TBS to quench endogenous peroxidase. Serial sections were then washed twice with TBS (2 x 10 minutes), preincubated for 1 hour at RT in a blocking solution containing 3% NGS and 0.2% Triton X-100 in TBS, and incubated overnight at 4°C with the primary NTS2 antibody (1/10,000) diluted in TBS containing 0.05% Triton X-100 and 0.5% NGS. After two rinses in TBS containing 1% NGS (2 x 10 minutes), sections were incubated for 1 hour at RT in biotinylated goat anti-rabbit immunoglobulin diluted 1/400 in TBS (Vector laboratories), and then 1 hour in Elite ABC solution (Vector; prepared according to the manufacturer's instructions). Visualization of bound peroxidase was achieved by reaction in a solution of 0.1 M Tris-HCl (TB; pH 7.4) containing 0.05% 3-3'-diaminobenzidine (DAB, Sigma-Aldrich), 0.04% nickel chloride, and 0.001% H_2O_2. The DAB reaction was monitored under a microscope to determine the optimal duration of incubation (5 minutes maximum) for yielding intense immunolabeling with minimal background staining. This reaction was stopped by several washes with 0.1 M TB.

The same procedure was used for control experiments except that sections were processed either with antibodies preabsorbed overnight with an excess of immunizing peptide (as for Western blotting procedures) or in the absence of primary antibody. Sections were mounted on chrome alum/gelatin-coated slides, dehydrated in graded ethanols, defatted in xylene, and mounted with Permount (Fisher Scientific, Montreal, Québec, Canada). Labeled structures were examined under bright-field illumination with a Leitz Aristoplan miscroscope (Leica, Dollard Desormeaux, Québec, Canada) and labeling densities were assessed for each region and visually scored on a scale of – /+ to +++ according to both the number of labeled elements and the intensity of immunoreactive signal.

3.3.8.3 Double-Labeling Immunohistochemistry

Frozen sections, prepared as above (n = 4 rats), were treated for 30 minutes in 3% NGS in TBS and incubated overnight at 4°C in a mixture of rabbit NTS2 antibody (1/10,000) and monoclonal mouse anti-S100 β-subunit (1/500; Sigma) diluted in TBS containing 0.05% Triton X-100 and 0.5% NGS. The following day, sections were rinsed twice in TBS containing 1% NGS and incubated for 1 hour in the same buffer containing a mixture of biotinylated goat anti-rabbit immunoglobulin (1/400; Vector) and Alexa 488-tagged goat anti-mouse (1/500; Molecular Probes). Sections were then rinsed in TBS, incubated for 1 hour in ABC complex solution, rinsed again in TBS, and incubated as above for 10 minutes in a biotinylated tyramine solution (Adam, 1992; NEN-Dupont, Wilmington, DE). After several buffer washes, sections were incubated for 1 hour in a solution of Texas-Red-conjugated streptavidin (1/250; Jackson, West Grove, PA). Sections were then rinsed and mounted with Aquamount. The absence of cross-reactivity of the secondary antibodies was verified by omitting one or both primary antibodies during the overnight incubation. Double-labeled sections were analyzed by confocal microscopy by using a Zeiss 510 laser scanning microscope equipped with a Zeiss inverted microscope and Argon2 (488 nm) and He/Ne1 (543 nm) lasers. Images were acquired simultaneously for both fluorophores (Alexa-488 and Texas Red) by using the multitrack configuration mode and processed by using the Zeiss 510 laser scanning microscope software.

3.3.9 Data Analysis

Light microscopic photomicrographs and color images from double-labeling experiments were adjusted for contrast and brightness by using Adobe Photoshop 6.0 software (Adobe, San Jose, CA). The final composites were processed by using Deneba's Canvas 7.0 imaging software (Deneba Software, Miami, FL) on an Apple PowerBook G3. Brain structures were identified according to the nomenclature of Paxinos and Watson's atlas (Paxinos and Watson, 1986).

3.4 RESULTS

3.4.1 Characterization of NTS2 Antiserum

To demonstrate the specificity of the NTS2 antiserum, Western blotting was performed on membranes prepared from rat brain and cerebellum (Fig. 3.1*A*). In both structures, anti-NTS2 specifically detected a band at 46 kDa, consistent with the molecular weight of the monomeric form of the receptor as deduced from its cDNA sequence (Fig. 3.1*A*, *lanes 1* and *2*). Specific immunoreactive bands, which might reflect multimeric species of NTS2 receptors, were also detected at approximately 80-85 kDa and 124-206 kDa in both whole brain (Fig. 3.1*A*, *lane 1*) and cerebellar membranes (Fig. 3.*1A*, *lane 2*). All of these bands were absent when the antibody was presaturated with the immunizing peptide (Fig. 3.1*A*, *lanes 3* and *4*).

To confirm that these immunoreactive bands corresponded to the NTS2 receptor, crude membrane preparations from COS-7 cells expressing *HA*-tagged rat NTS2 receptors were immunoprecipitated with the NTS2 antiserum (Fig. 3.1*B*, *lane 2*) or with the 3F10 antibody specific for the *HA*-epitope tag (Fig. 3.1*B*, *lane 4*), and respectively, immunoblotted with the 12CA5 HA antibody (Fig. 3.1*B*, *lane 2*) or with the NTS2 antiserum (Fig. 3.1*B*, *lane 4*). These experiments revealed the presence of 46- and 83-kDa protein bands, as observed in rat brain and cerebellum, in both immunoprecipitates (Fig. 3.1*B*, *lanes 2* and *4*). In addition, immunoreactive bands were detected at approximately 124-206 kDa in both preparations (Fig. 3.1*B*, *lane 2* and *4*), which presumably correspond to multimeric complexes of the receptor. No specific bands were detected in membranes prepared from nontransfected cells (Fig. 3.1*B*, *lanes 1* and *3*).

3.4.2 Specificity of Immunolabeling

To demonstrate the applicability of the NTS2 antiserum to immunohistochemical detection of the receptor in PFA-fixed material, double immunofluorescent staining was carried out on COS-7 cells expressing the *HA*-tagged NTS2 receptor. Confocal microscopy revealed that HA (Fig. 3.1*C*) and NTS2 (Fig. 3.1*D*) antibodies produced very similar patterns of immunostaining. No signal was detected in untransfected

cells or in the absence of primary antibodies (data not shown). Preincubation of the anti-NTS2 antiserum with the N-terminal immunogenic peptide completely abolished NTS2-like (*NTS2-l*) immunolabeling (Fig. 3.1*F*). However, the same cells were still positively stained for the *HA*-epitope, indicating that they did express the receptor (Fig. 3.1*E*).

Immunolabeling of rat brain sections with a 1/10,000 dilution of NTS2 antiserum gave rise to selective immunostaining patterns throughout the neuraxis (e.g. Figs. 3.2*A*, 3.4-11). By contrast, sections incubated with antiserum pre-adsorbed with the immunogenic peptide were completely devoid of immunolabeling (Figs. 3.2*B*, 3.6*C*).

3.4.3 Cellular Distribution of NTS2-l Immunoreactivity

NTS2-l immunoreactivity was selectively concentrated over neurons, and most prominently within neuronal processes (Table 3.1). Thus, in many regions such as the piriform cortex (Fig. 3.3*A*) and other cortical areas, *NTS2-l* immunolabeling was highly concentrated over pyramidal cell dendrites, whereas the vast majority of the corresponding perikarya were only moderately labeled. However, in other regions, such as the central amygdaloid nucleus (Fig. 3.3*B*), the bed nucleus of the stria terminalis (Fig. 3.3*D*, 3.5*A*), or CA1 of Ammon's horn (Fig. 3.6*A and B*), both perikarya and dendrites showed moderate to intense *NTS2-l* immunolabeling. *NTS2-l* immunoreactivity was also detected in axons and axon terminals throughout the neuraxis, e.g. in the diagonal band of Broca (Fig. 3.3*C*) and in the anterior hypothalamus (Fig. 3.3*G*). Labeling of the ependyma was observed in some of our sections (e.g. Fig. 3.5*A*, 3.8*A* and *E*), but this labeling was non-specific as it was still present in sections incubated with preadsorbed antiserum.

No obvious *NTS2-l* immunolabeling was evident over glial cells in our single-labeling experiments. To formally exclude astrocytic involvement, dual immunolabeling experiments were performed by using our NTS2 antiserum and the astrocytic marker S100β in regions exhibiting either prominent somatic (Fig. 3.3*D-F*) or process labeling (Fig. 3.3*G-I*). In the bed nucleus of the stria terminalis, strongly *NTS2-l*-positive perikarya as well as small fluorescent puncta resembling cross-

sectioned processes were evident by confocal microscopy (Fig. 3.3*D*). None of these structures exhibited S100β immunolabeling within the same sections (Fig. 3.3*E* and *F*). In the anterior hypothalamus, *NTS2-l* immunoreactivity was localized to punctate structures reminiscent of transected dendrites and/or glial elements (Fig. 3.3*G*). Here again, none of these structures were dually labeled with the S100β antibody, which revealed a number of astrocytic cell bodies as well as the entire ependyma (Fig. 3.3*H* and *I*).

3.4.4 Regional Distribution of NTS2-l Immunoreactivity

3.4.4.1 Telencephalon

Within the telencephalon, strong and selective *NTS2-l* immunolabeling was apparent in the olfactory bulb and tubercle, the basal forebrain, the basal ganglia, the amygdaloid complex, the hippocampal formation, and the cerebral cortex (Table 3.1; for topographical overview, see Fig. 3.4).

In the main olfactory bulb, *NTS2-l* immunoreactivity was distributed throughout the granule cell, mitral cell, external plexiform, and glomerular layers (Fig. 3.2*A*; Table 3.1). Immunopositive perikarya were most intensely labeled in the mitral cell layer (Table 3.1). Moderately labeled mitral cell dendrites also extended through the external plexiform layer into the glomerular layer. In the glomerular layer, a moderate meshwork of *NTS2-l*-positive neuronal processes surrounded the glomeruli. Periglomerular cells were occasionally labeled (Table 3.1). Labeling in the granule cell layer was abundant although quite diffuse, making it difficult to identify individual immunoreactive cells. The accessory olfactory bulb displayed very strong immunolabeling of neuronal processes (Fig. 3.2*A*; Table 3.1). In the olfactory cortex, only the olfactory tubercle displayed substantial numbers of immunolabeled nerve cell bodies. A few *NTS2-l*-positive perikarya were also present in the taenia tecta, the islands of Calleja, the piriform and prepiriform cortex (Fig. 3.3*A*), and the lateral olfactory nucleus (Table 3.1). All of these structures, as well as the anterior olfactory nucleus (Fig. 3.4) and the dorsal and ventral endopiriform nuclei displayed at least low levels of fiber labeling. In contrast, the piriform and prepiriform cortex stood out by exhibiting a dense network of strongly immunostained dendrites (Fig. 3.3*A*).

In the basal forebrain, *NTS2-l*-immunoreactive neuronal cell bodies were observed in the ventral pallidum, the substriatal area, the medial and lateral septum (Fig. 3.4*A*), the diagonal band of Broca (Fig. 3.4*A*), the magnocellular preoptic nucleus, and most prominently the bed nucleus of the stria terminalis (Fig. 3.5*A*). With the exception of the latter two nuclei, labeling of processes and terminals in all of these structures was more prominent than that of neuronal perikarya (Fig. 3.3*C*; Table 3.1). In addition, immunoreactive processes and terminals were encountered in the septohippocampal nucleus and the substantia innominata (Table 3.1).

With the exception of the caudate-putamen, which displayed low to moderate numbers of relatively small, *NTS2-l*-positive neurons (Fig. 3.5*C*; Table 3.1), the basal ganglia exhibited only low numbers of immunolabeled nerve cells or none at all (Table 3.1). The nucleus accumbens (core and shell), the caudate-putamen, and the fundus striati also contained sparse *NTS2-l*-immunoreactive processes and terminals. By contrast, the globus pallidus (Fig. 3.5*B*) and the entopeduncular nucleus exhibited a dense network of immunolabeled fibers (Table 3.1). The central amygdaloid nucleus (Fig. 3.3*B*) and the sub-nuclei of the cortical amygdala (*cf.* posteromedial amygdaloid nucleus in Fig. 3.4*B*) both exhibited a moderate number of strongly *NTS2-l*-immunoreactive multipolar neurons (Table 3.1). In addition, sparse immunolabeled cells were found in the medial nucleus of the amygdala. All of these nuclei, as well as the basomedial nucleus, exhibited low to moderate densities of labeled processes and terminals (Table 3.1).

The hippocampal formation was among the most heavily labeled regions of the brain (Fig. 3.4*B*; Table 3.1). The most striking pattern of staining was found in the CA fields of the hippocampus proper. CA1 exhibited extremely strong immunostaining of pyramidal cell bodies and apical dendrites (Figs. 3.4 and 3.6*A* and *B*). These processes coursed through the stratum radiatum and ramified into the stratum lacunosum moleculare, forming a mesh of transected dendritic profiles (Fig. 3.6*A* and *B*). In CA2, the labeling diminished in intensity (Fig. 3.6*A*; Table 1) and in CA3, no labeling was apparent at low magnification except for a light staining of the stratum lacunosum moleculare (Fig. 3.6*A*). At high magnification, however, it

became obvious that the apical dendrites of CA3 pyramidal cells were in fact labeled, although less intensely so than in CA1 or CA2. CA3 nerve cell bodies were not labeled (Table 3.1). In the dentate gyrus, granule cells were immunonegative (Fig. 3.6*A*; Table 3.1) but a few faintly labeled cell bodies, as well as sparse fibers, showed *NTS2-l* immunolabeling (Table 3.1). No immunolabeling was apparent in the hippocampus in sections incubated with antiserum pre-adsorbed with 2 μg/ml antigenic peptide (Fig. 3.6*C*). The entorhinal cortex, as well as the pre- and parasubiculum, exhibited moderately to intensely labeled nerve cell bodies in layer II (Fig. 3.6*D* and *E*). The enthorinal cortex also exhibited moderate staining of neuronal processes (Fig. 3.6*E*, Table 3.1).

In all neocortical areas, apical dendrites of layer V pyramidal neurons were the most strongly immunoreactive structures (Fig. 3.7*A*, Table 3.1). These could be traced all the way to layer I in which they ramified (Fig. 3.7*A*). Allocortical areas, represented by the retrosplenial cortex, also displayed strongly labeled pyramidal cells (Fig. 3.7*B*, *insert*). Moderate numbers of *NTS2-l*-positive neuronal somata were observed in the frontal, parietal (Fig. 3.7*A*, *insert*), occipital, temporal, retrospenial, and insular cortex. Cingulate and perirhinal cortices exhibited only low numbers of immunoreactive somata (Table 3.1).

3.4.4.2 Diencephalon

In the thalamus, the paraventricular (Fig. 3.8*A*), anterior dorsal and anterior ventral (Fig. 8*B*), ventromedial, mediodorsal, lateral and medial geniculate (Fig. 3.8*C*, *insert*) nuclei displayed low to moderate numbers of *NTS2-l*-immunoreactive somata (Table 3.1). Most of these nuclei also exhibited intensely labeled neuronal processes except for the anterior ventral and medial geniculate nuclei or the dorsal tier of the lateral geniculate body, which were completely devoid of *NTS2-l*-positive processes (Table 3.1). The reuniens, reticular, central medial, rhomboid, parafascicular (Fig. 3.4*B*), and subparafascicular nuclei all exhibited moderate to dense networks of *NTS2-l*-positive fibers but no immunopositive nerve cell bodies (Table 3.1). Within the hypothalamus, low to moderate numbers of immunoreactive nerve cell bodies were evident in the supraoptic, arcuate (Fig. 3.8*E* and *F*), and ventromedial nucleus (Fig.

3.4), as well as in the retrochiasmatic area (Fig. 3.4), the lateral hypothalamic area, and the lateral mammillary nucleus (Fig. 3.8*F*). All of these nuclei also displayed moderate to high levels of immunolabeled neuronal processes (Table 3.1). As in the thalamus, light to moderate labeling of processes was detected in a number of additional nuclei, namely the anterior hypothalamus (Fig. 3.3*G*), suprachiasmatic nucleus, para- (Fig. 3.8*D*) and periventricular nuclei (Fig. 3.3*G*), tuber cinereum (Fig. 3.3*G*), medial mammillary nucleus (Figs. 3.4 and 3.8*F*), and lateral and medial preoptic area (Fig. 3.4; Table 3.1). The outer zone of the median eminence (Fig. 3.8*E*) as well as the supramammillary nucleus (Fig. 3.8*F*) exhibited strong *NTS2-l* fiber labeling (Table 3.1).

In the zona incerta, sparse, lightly stained nerve cell bodies were detected amidst intensely labeled neuronal processes (Fig. 3.8*C*; Table 3.1). The subthalamic nucleus exhibited moderate levels of *NTS2-l*-positive processes, but no immunoreactive nerve cell bodies (Table 3.1). Both subdivisions of the habenula displayed sparse, lightly labeled nerve cell bodies (Fig. 3.8*A*; Table 3.1). The lateral habenula also exhibited a moderately dense plexus of *NTS2-l*-positive processes (Fig. 3.8*A*; Table 3.1). The subfornical organ, while devoid of immunopositive cell bodies, harbored a moderately dense network of immunoreactive processes (Table 3.1).

3.4.4.3 Mesencephalon

In the midbrain, the oculomotor (Figs. 3.4 and 3.9*A*) and magnocellular part of the red nucleus (Fig. 3.9*C*) contained medium numbers of intensely stained NTS2-positive nerve cell bodies. Lightly labeled and/or less numerous neurons were also observed in the substantia nigra, pars reticulata (Fig. 3.9*D* and *E*), ventral tegmental area (Figs. 3.4 and 3.9*D*), interpeduncular (Figs. 3.4 and 3.9*D*) and interfascicular nuclei, periaqueductal gray (Figs. 3.4 and 3.9*A,B*), dorsal raphe nucleus (Figs. 3.4 and 3.9*A*), and superior and inferior colliculi (Fig. 3.4, Table 3.1). In most of these structures, and most prominently in the periaqueductal gray, dorsal raphe nucleus, and substantia nigra pars reticulata, these labeled perikarya were embedded in a dense meshwork of immunolabeled processes (Figs. 3.4 and 3.9). In the superior

colliculus, labeled perikarya were exclusively observed in the inner gray layer, immediately adjacent to the optic nerve layer, and in the deep gray, where they were concentrated laterally. The substantia nigra, pars compacta (Fig. 3.9*D*), peripeduncular nucleus, deep mesencephalic nucleus (Fig. 3.9*D*), and precommissural nucleus were devoid of immunopositive perikarya but displayed low to moderate to labeling of neuronal processes (Table 3.1). The caudal linear raphe nucleus (Fig. 3.4*C*), while devoid of perikaryal immunolabeling displayed intensely labeled processes (Table 3.1).

3.4.4.4 Pons

The pontine nuclei (Fig. 3.4*C*) and nucleus of the trapezoid body (Figs. 3.4*D* and 3.9*H*) displayed a moderate number of strongly immunostained neuronal perikarya. Less numerous and/or more lightly stained cell bodies were also evident in the superior olivary complex and superior paraolivary nucleus (Figs. 3.4*D* and 3.9*F*) as well as in the principal sensory (Fig. 3.4*D*) and motor trigeminal nuclei (Table 3.1). Except for the nucleus of the trapezoid body, these structures were also pervaded by moderately abundant immunoreactive neuronal processes (Fig. 3.9*F*,*G*; Table 3.1). The paramedian raphe nucleus displayed no *NTS2-l*-positive nerve cell bodies, but a moderately dense network of immunolabeled processes (Fig. 3.9*G*; Table 3.1).

3.4.4.5 Medulla Oblongata

In the medulla oblongata, variable numbers of moderately to intensely labeled *NTS2-l* immunoreactive cell bodies and processes were observed in all sensory and most of the motor cranial nerve nuclei (Table 3.1), including the vestibular complex (Fig. 3.10*A*,*B*), the cochlear nuclei (Figs. 3.4*D*, 3.10*A*), the subnuclei of the spinal trigeminal nucleus (Fig. 3.10*A*-*C*), the nucleus of the solitary tract (Figs. 3.4*D* and 3.10*B*,*C*) as well as the trochlear, abducens (Fig. 3.10*D*), facial (Fig. 3.10*A*), vagal (Fig. 3.10*B*) and hypoglossal (Fig. 3.10*B* and *C*) nuclei. In addition, the inferior olive (Fig. 3.10*B* and *C*), the gigantocellular reticular nucleus, pars alpha (rostroventral medial medulla; Fig. 3.10*A* and *F*), the lateral paragigantocellular (Fig. 3.10*A*) and lateral reticular nuclei, the parvocellular reticular nucleus (Fig. 3.10*A*, *B*, and *G*), the external cuneate and cuneate nuclei (Fig. 3.10*B*, *C*, and *E*), the linear nucleus of the

raphe (Fig. 3.10*B*), and the nuclei raphe magnus and pallidus (Fig. 3.10*A* and *F*) displayed low to moderate perikaryal *NTS2-l* immunolabeling as well as moderate to dense labeling of neuronal processes (Table 3.1). Structures in which immunolabeled processes but no cell bodies were observed include the gigantocellular and intermediate reticular nuclei (Fig. 3.10*A* and *B*), the medullary reticular field (Fig. 3.10*C*), the paratrigeminal (Fig. 3.10*H*) and gracile (Fig. 3.10*C*) nuclei, nucleus X (Fig. 3.10*B*), and the nucleus raphe obscurus (Fig. 3.10*B*) (Table 3.1).

3.4.4.6 Cerebellum

The deep cerebellar nuclei displayed a moderate number of strongly immunoreactive nerve cell bodies interspersed among a plexus of immunopositive processes (Fig. 3.11*A*; Table 3.1). The lateral nucleus was slightly more intensely stained than intermediate and medial nuclei (Figs. 3.4*D* and 3.11*A*). In the cerebellar cortex, *NTS2-l* immunoreactivity was present in all three layers. Purkinje cell perikarya and dendritic processes ascending in the molecular layer were the most strongly labeled elements (Figs. 3.11*B* and *C*; Table 3.1). Labeling in the granule cell layer was less pronounced and essentially accounted for by the immunolabeling of a subpopulation of granule cells (Fig. 3.11*D*; Table 3.1). In the molecular layer, sparse, strongly labeled neuronal perikarya (not shown) were evident among the pervasive Purkinje cell dendrites (Fig. 3.11*C* and *D*).

3.5 DISCUSSION

The present study provides the first description of the distribution of NTS2 receptor proteins in mammalian brain. The NTS2 antiserum used here was raised against a sequence from the N-terminus of the rat receptor unique among known NT receptor sequences. The specificity of the antiserum was initially established by Western blotting of membranes prepared from whole brain and cerebellum (which previously had been shown to express among the highest levels of NTS2 mRNA and binding sites in rodent brain; cf. Sarret et al., 1998, 2002; Walker et al., 1998). The NTS2 antiserum specifically recognized a band at 46 kDa, which corresponds to the molecular weight of the monomeric receptor deduced from its cDNA sequence. In addition, other specific bands were detected at molecular weights corresponding to multiples of the monomeric receptor's size, thus possibly representing multimeric complexes of NTS2. None of these bands were present when the blots were incubated with antiserum preadsorbed with the antigenic peptide, indicating that the NTS2 antiserum selectively recognized the native receptor protein. To further support the notion that the immunoreactive bands detected in brain homogenates indeed corresponded to the NTS2 receptor, immunoprecipitation experiments were carried out on membranes from COS-7 cells transfected or not with cDNA encoding the N-terminally *HA*-tagged NTS2 receptor. Both immunoprecipitation with an anti-HA epitope antibody and detection with anti-NTS2 and the reverse experiment gave rise to the same major bands pattern as detected in rat brain and cerebellum homogenates. These findings confirm that our antiserum selectively cross-reacts with the rat NTS2 receptor.

To establish the applicability of the antiserum to the immunohistochemical detection of NTS2 receptors, double-labeling studies were performed on COS-7 cells transiently expressing the N-terminally *HA*-tagged NTS2 receptor. The NTS2 antiserum exclusively labeled cells that also exhibited *HA*-immunoreactivity, indicating that it selectively recognized cells expressing the NTS2 receptor. Preadsorption of the NTS2 antiserum with immunogenic peptide completely abolished immunostaining, confirming that it was attributable to the NTS2 antibody.

Similarly, sections of rat brain incubated with preadsorbed antiserum were virtually devoid of immunostaining, suggesting that as in transfected cells, the antibody selectively recognized the NTS2 receptor.

Within the brain, *NTS2-l* immunoreactivity was exclusively found in neurons. However, its subcellular compartmentalization varied markedly between brain regions. Thus, whereas in some areas, such as the hippocampus, the immunolabeling was associated with both perikarya and dendrites, in others, such as the cerebral cortex or the globus pallidus, it clearly predominated over dendrites. In yet others, such as the diagonal band of Broca and the anterior hypothalamus, it was mainly associated with axons and axon terminals. These data suggest that unlike NTS1 receptors, which are reportedly more or less uniformly distributed over perikarya, dendrites, and axons of neurons in which they are expressed (Boudin et al., 1996b; Fassio et al., 2000), NTS2 receptors may be selectively targeted to specific neuronal elements, and most prominently to dendritic processes.

Previous *in situ* hybridization studies have reported the presence of NTS2 mRNA expression in glial and ependymal cells in intact adult rat brain (Walker et al., 1998; Lépée-Lorgeoux et al., 1999). Furthermore, double-labeling experiments have demonstrated NTS2 mRNA expression in glial fibrillary acidic protein-immunolabeled reactive astrocytes, both *in vitro* and *in vivo* (Nouel et al., 1999). No glial and/or ependymal labeling was readily apparent here in NTS2-immunoreacted sections. To confirm the lack of association of *NTS2-l* immunoreactivity with astrocytes, we performed dual-labeling experiments using the astroglial marker S100β. In none of the regions examined did S100β immunoreactivity co-localize with *NTS2-l* immunostaining, suggesting that under basal conditions, NTS2 receptor proteins are not present in astrocytes. This is not to say, however, that they would not be detectable under conditions of reactive gliosis.

The topographic distribution of the *NTS2-l* immunoreactivity was extensive, as expected from earlier subtractive autoradiographic binding studies based on the displacement of specific ^{125}I-labeled NT, [^{3}H]-NT, or [^{3}H]-SR142948A binding by levocabastine (Kitabgi et al., 1987; Schotte et al., 1986, 1988; Schotte and Laduron,

1987; Bétancur et al., 1998) or on direct binding of [^{3}H]-levocabastine (Asselin et al., 2001). Thus, *NTS2-l* immunolabeling was detected in all regions previously reported to exhibit high levels of NTS2 binding sites including olfactory bulb, all olfactory relay nuclei, septum, bed nucleus of the stria terminalis, amygdaloid nuclei, CA1 of the hippocampus, pre- and parasubiculum, cerebral cortex, several thalamic nuclei, arcuate nucleus, mammillary bodies, interpeduncular nucleus, superior colliculus, periaqueductal gray, dorsal raphe nucleus, red nucleus, substantia nigra, ventral tegmental area, nucleus raphe magnus, vestibular complex, and cerebellum. However, the present study also demonstrated that if widespread, the distribution of NTS2 receptor proteins was also more selective than previously surmised from the diffuse distributional patterns yielded by autoradiographic binding studies (Kitabgi et al., 1987; Schotte et al., 1986, 1988; Schotte and Laduron, 1987; Bétancur et al., 1998; Asselin et al., 2001).

The distribution of *NTS2-l*-immunoreactive nerve cell bodies was also in good agreement with that of NTS2-expressing cells as determined by *in situ* hybridization in both rat (Walker et al., 1998; Lépée-Lorgeoux et al., 1999) and mouse (Sarret et al., 1998) brain. By and large, all regions reported to exhibit medium to strong NTS2 mRNA levels, such as the olfactory bulb, cerebral cortex, hippocampal formation, periaqueductal gray, and cerebellar cortex to name but a few, were immunolabeled here. There were several regions, however, in which *NTS2-l* immunolabeling appeared more restricted than expected from *in situ* hybridization data. For instance, the medial habenula, which was reported to contain high levels of NTS2 mRNA (Sarret et al., 1998; Lépée-Lorgeoux et al., 1999), was barely immunoreactive in the present study. Similarly, the hippocampus, which was shown to express very high levels of NTS2 mRNA throughout all subfields of Ammon's horn and the dentate gyrus (Sarret et al., 1998; Walker et al., 1998; Lépée-Lorgeoux et al., 1999), exhibited NTS2-immunoreactive cell bodies only in CA1 and CA2 subfields. These discrepancies could reflect poor translation of the NTS2 message in certain sub-population of neurons or could be due to selective targeting of NTS2 proteins to neuronal processes. Thus, NTS2 mRNA-positive/NTS2-immunonegative neurons in the medial habenula could account for the terminal immunolabeling observed in their

projection field within the interpeduncular nucleus (Butcher, 1995). Alternatively, the lack of apparent cellular immunoreactivity in areas containing high levels of NTS2 mRNA could reflect selective targeting of NTS2 receptor proteins to plasma membranes. Indeed, the diffuse *NTS2-l* immunolabeling observed here over the CA3 subfield and dentate gyrus was reminiscent of the pattern of labeling described for the sst_{2A} somatostatin receptor in brain areas in which this receptor was found by electron microscopy to be selectively addressed to plasma membranes (Dournaud et al., 1996).

In contrast to NTS1 mRNA (Elde et al., 1990; Sato et al., 1992; Nicot et al., 1994a,b; Alexander and Leeman, 1998) or immunoreactivity (Boudin at al., 1996b; Fassio et al., 2000), which are more or less restricted to regions innervated by neurotensinergic axons, *NTS2-l* immunoreactivity considerably exceeded that of NT terminal fields. Thus, some of the most heavily labeled regions in the brain, such as the hippocampus, the cerebral and cerebellar cortices, and medullary cranial nerve nuclei had been described as being innervated only sparsely if at all by NT fibers (Jennes et al., 1982, Emson et al., 1985a and 1985b). These findings provide further support to the hypothesis that NT may not be the exclusive endogenous ligand for this receptor subtype (Sarret et al., 1998). There were, however, regions in which *NTS2-l* immunoreactivity showed considerable overlap with NT terminal fields, including the olfactory bulb, bed nucleus of the stria terminalis, magnocellular preoptic nucleus, anterior dorsal thalamic nucleus, substantia nigra, ventral tegmental area, periaqueductal gray, nucleus raphe dorsalis and magnus, and lateral paragigantocellular nucleus (Jennes et al., 1982; Emson et al., 1985b). All of these regions (except for nuclei raphe magnus and lateral paragigantocellular nucleus), as well as several others in which NT axons are less prominent, such as the entorhinal, frontal, and retrosplenial cortices, the pre-and parasubiculum, the cortical amygdala, the pontine nuclei, and various medullary nuclei, also display high levels of NTS1 (Boudin et al., 1996b; Fassio et al., 2000), indicating that in many brain structures, NTS2 is in a position to interact with NTS1 in mediating NT's central effects.

The distribution of *NTS2-l* immunoreactivity also overlapped extensively with that of the single-transmembrane domain receptor NTS3/sortilin (except in the granule cell layer of the cerebellar cortex and medullary reticular formation which were enriched in NTS2-, but not in NTS3-immunoreactive neurons; Sarret et al., submitted). This widespread co-distribution of NTS2 with NTS3/sortilin raises the possibility of interactions between these two receptors for the mediation of the NT signal, particularly in light of recent studies showing that NTS3 can interact with NTS1 to enhance the NT-induced phosphorylation of mitogen-activated protein kinases and turnover of phosphoinositides in the HT29 human cancer cell line (Martin et al., 2002a).

A striking feature of NTS2 distribution was its association with every single sensory system in the brain. Thus, all olfactory relay nuclei, including the olfactory bulb, exhibited *NTS2-l* immunoreactivity. The auditory system was also labeled from the cochlear nuclei, through the superior olive, the inferior colliculus, and the medial geniculate nucleus, all the way to the temporal cortex. Likewise, the visual system exhibited *NTS2-l* immunolabeling throughout the lateral geniculate body, suprachiasmatic nucleus, superior colliculus, and occipital cortex. The nucleus of the solitary tract, a major relay for visceral and gustatory input, exhibited moderate immunolabeling. Finally, *NTS2-l* immunoreactivity was associated with relay nuclei of ascending somatosensory information, including the gracile and cuneate nuclei, spinal and principal sensory trigeminal nuclei, and parietal cortex.

Of particular interest from a functional perspective was the intense labeling of brainstem structures involved in pain control. Indeed, recent pharmacological studies have demonstrated that the NT antagonist SR142948A, which does not distinguish between NTS1 and NTS2, blocks NT-induced antinociception (Gully et al., 1997), whereas the NTS1-specific antagonist SR48692 does not (Gully et al., 1993; Dubuc et al., 1994; Labbé-Jullié, 1994). Furthermore, the NTS2-selective ligand, levocabastine (Tyler et al., 1998; Dubuc et al., 1999a) and NTS2 antisense oligonucleotides (Dubuc et al., 1999b) both inhibit the antinociceptive effects of intracerebroventricularly administered NT, whereas knocking down the NTS1 gene

in mice is without effect (Remaury et al., 2002; but also see Pettibone et al., 2002). Microinjection studies have long identified regions involved in the descending control of nociceptive inputs as sites of NT-induced antinociception (Kalivas et al., 1982b; Mayer and Price 1989; McHaffie et al., 1989). The strong *NTS2-l* immunolabeling found here in regions such as the periaqueductal gray, dorsal raphe nucleus, raphe magnus and pallidus, gigantocellular nucleus, pars alpha, and lateral paragigantocellular nucleus suggests that NTS2 receptors are ideally poised to regulate NT's supraspinal antinociceptive actions.

Strong *NTS2-l* immunoreactivity was associated with cerebellum-related brainstem nuclei such as the external cuneate nucleus, pontine nuclei, inferior olive, and vestibular complex, suggesting that NTS2 is associated with both mossy and climbing fiber afferent cerebellar systems. NTS2 immunolabeling was also observed over Purkinje cells, deep cerebellar nuclei, vestibular complex, and red nucleus suggesting that NTS2 receptors are equally involved in the regulation of the cerebellar output. In cerebellar cortex, *NTS2-l* immunoreactivity was evident over a sub-population of granule cells, in conformity with the recent demonstration of functionally coupled NTS2 receptors in these cells in primary culture (Sarret et al., 2002). Taken together, the present results suggest a prominent involvement of NTS2 in the regulation of cerebellar function. However, because the cerebellum is essentially devoid of NT innervation, the stimulus responsible for NTS2 activation in this structure remains to be established.

In conclusion, the present study demonstrates that NTS2 receptors are widely distributed in the rat CNS. It also indicates that this receptor is essentially neuronal and that it is predominantly, although not exclusively, targeted to dendrites. High levels of NTS2 receptor proteins were detected in regions documented to receive a dense neurotensinergic innervation (namely the hypothalamus, the basal forebrain and ventral midbrain, and several limbic and brainstem structures), in keeping with the postulated role of this receptor in transducing NT's actions, and most specifically its antinociceptive effects. However, the distribution of NTS2 largely exceeded that of NT's terminal fields, suggesting that it may also serve as receptor for other endogenous ligand(s).

3.6 ACKNOWLEDGEMENTS

This work was supported by Canadian Institutes of Health Research grants MT-7366 to Alain Beaudet. The authors extend their gratitude to Naomi Takeda for secretarial help in the preparation of this manuscript. Philippe Sarret is the recipient of a fellowship from the Fonds de la Recherche en Santé du Québec (FRSQ).

3.7 ABBREVIATIONS

V	Layer of the cerebral cortex
3V	3rd ventricle
4V	4th ventricle
3n	Oculomotor nucleus
6n	Abducens nucleus
7n	Facial nucleus
12n	Hypoglossal nucleus
Acb	Accumbens nucleus
AD	Anterodorsal thalamic nucleus
AHC	Anterior hypothalamic area, central part
AOB	Accessory olfactory bulb
AON	Anterior olfactory nucleus
Aq	Aqueduct (Sylvius)
Arc	Arcuate hypothalamic nucleus
AV	Anteroventral thalamic nucleus
CA1-3	Fields CA1-3 of Ammon's horn
CLi	Caudal linear nucleus of the raphe
cp	Cerebral peduncle, ventral part
Cpu	Caudate putamen (striatum)
Cu	Cuneate nucleus
DC	Dorsal cochlear nucleus
DG	Dentate gyrus
DLG	Dorsal lateral geniculate nucleus
DMSp5	Dorsomedial spinal trigeminal nucleus
DR	Dorsal raphe nucleus
Ecu	External cuneate nucleus
Ent	Entorhinal cortex

Epl	External plexiform layer of the olfactory bulb
f	Fornix
Fr1	Frontal cortex, area 1
Gcl	Granule cell layer of the cerebellum
Gi	Gigantocellular reticular nucleus
GiA	Gigantocellular reticular nucleus, alpha part
Gl	Glomerular layer of the olfactory bulb
Gr	Gracile nucleus
GrA	Granular cell layer of the accessory olfactory bulb
ic	Internal capsule
icp	Inferior cerebellar peduncle (restiform body)
Igr	Internal granular layer of the olfactory bulb
Int	Interposed cerebellar nucleus
IO	Inferior olive
IP	Interpeduncular nucleus
Ipl	Internal plexifom layer of the olfactory bulb
Lat	Lateral (dentate) cerebellar nucleus
LHb	Lateral habenular nucleus
Li	Linear nucleus of the medulla
LM	Lateral mammillary nucleus
LPGi	Lateral paragigantocellular nucleus
LRt	Lateral reticular nucleus
LSD	Lateral septal nucleus, dorsal part
LSO	Lateral superior olive
LSV	Lateral septal nucleus, ventral part
LVe	Lateral vestibular nucleus
m5	Motor root of the trigeminal nerve
MD	Mediodorsal thalamic nucleus
MdD	Medullary reticular nucleus, dorsal part
MdV	Medullary reticular nucleus, ventral part
ME	Median eminence

Med	Medial (fastigial) cerebellar nucleus
MG	Medial geniculate nucleus
MHb	Medial habenular nucleus
Mi	Mitral cell layer of the olfactory bulb
ml	Medial lemniscus
Ml	Molecular layer of the cerebellum
MnR	Median raphe nucleus
mol	Lacunosum molecular stratum of Ammon's horn
MSO	Medial superior olive
mt	Mammillothalamic tract
MVe	Medial vestibular nucleus
OB	Olfactory bulb
or	Stratum oriens of Ammon's horn
Pa	Paraventricular hypothalamic nucleus
Pa5	Paratrigeminal nucleus
PaS	Parasubiculum
PAG	Periaqueductal gray
Pcl	Purkinje cell layer of the cerebellum
Pe	Periventricular hypothalamic nucleus
PF	Parafascicular thalamic nucleus
PFL	Paraflocculus
Pir	Piriform cortex
PMCo	Posteromedial cortical amygdaloid nucleus
PMR	Paramedian raphe nucleus
PMV	Premammillary nucleus, ventral part
Pn	Pontine nuclei
Pr5	Principal sensory trigeminal nucleus
PrS	Presubiculum
PV	Paraventricular thalamic nucleus
py	Pyramidal tract
pyr	Stratum pyramidale of Ammon's horn

pyx	Pyramidal decussation
rad	Stratum radiatum of Ammon's horn
RCh	Retrochiasmatic area
RMg	Raphe magnus nucleus
ROb	Raphe obscurus nucleus
RPa	Raphe pallidus nucleus
Rt	Reticular thalamic nucleus
s5	Sensory root of the trigeminal nerve
SC	Superior colliculus
sm	Stria medullaris of the thalamus
SNc	Substantia nigra, pars compacta
SNr	Substantia nigra, pars reticulata
Sol	Nucleus of the solitary tract
Sp5C	Spinal trigeminal nucleus, caudal part
Sp5I	Spinal trigeminal nucleus, interpolar part
Sp5O	Spinal trigeminal nucleus, oral part
SPO	Superior paraolivary nucleus
SuM	Supramammillary nucleus
SuVe	Superior vestibular nucleus
TC	Tuber cinereum area
Tu	Olfactory tubercle
Tz	Trapezoid nucleus
VCA	Ventral cochlear nucleus, anterior part
VCP	Ventral cochlear nucleus, posterior part
VDB	Nucleus vertical limb diagonal band
VLG	Ventral lateral geniculate nucleus
VMH	Ventromedial hypothalamic nucleus
VTA	Ventral tegmental area
X	Nucleus X
ZI	Zona incerta

3.8 FIGURES

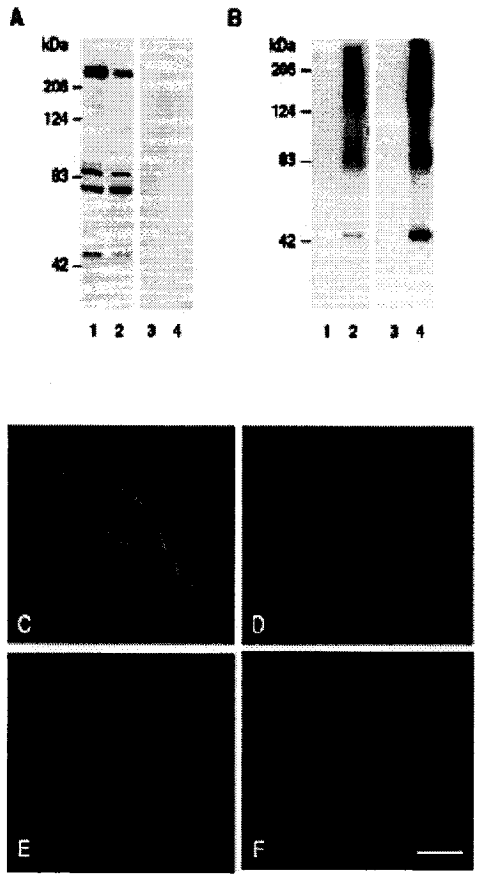

Figure 3.1

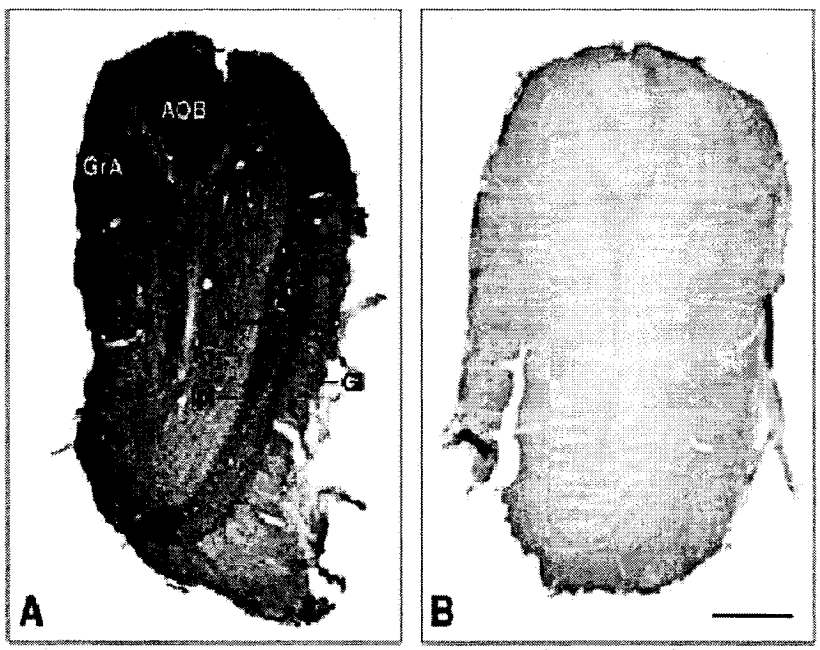

Figure 3.2

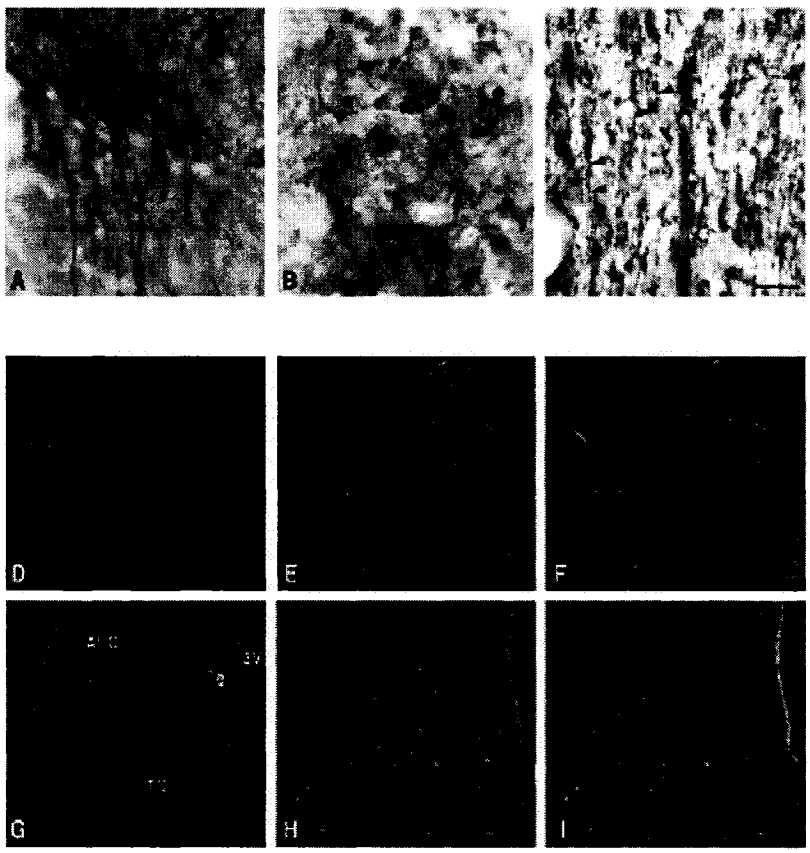

Figure 3.3

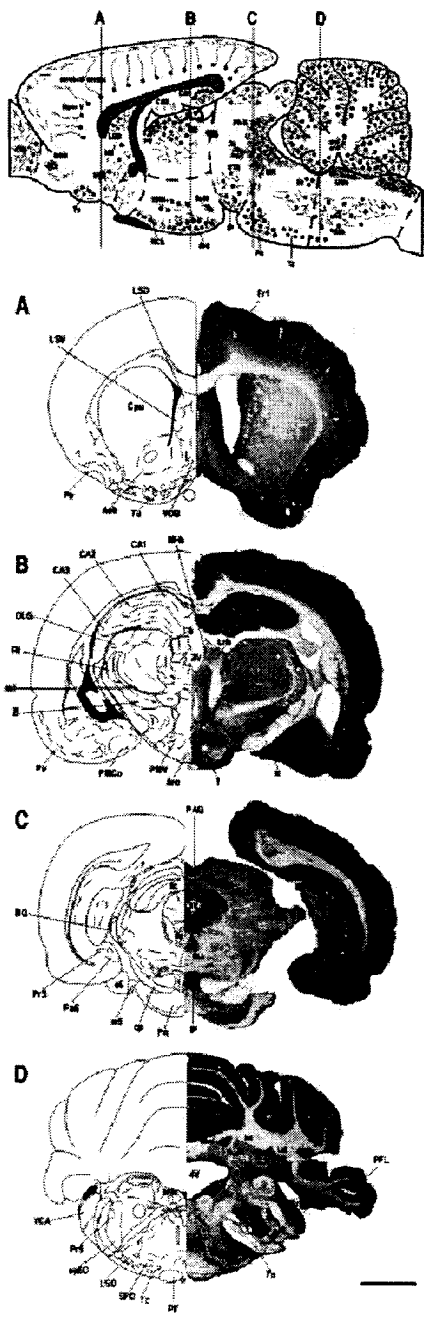

Figure 3.4

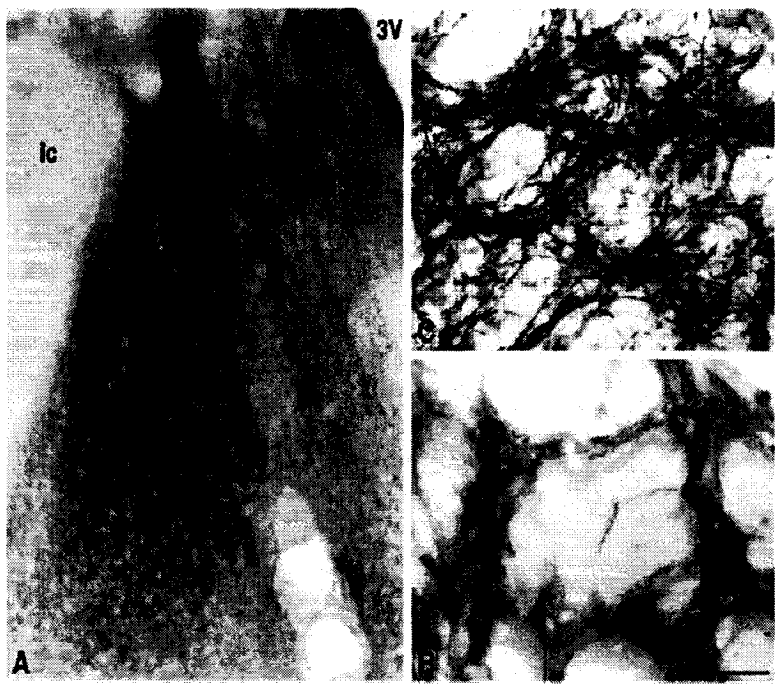

Figure 3.5

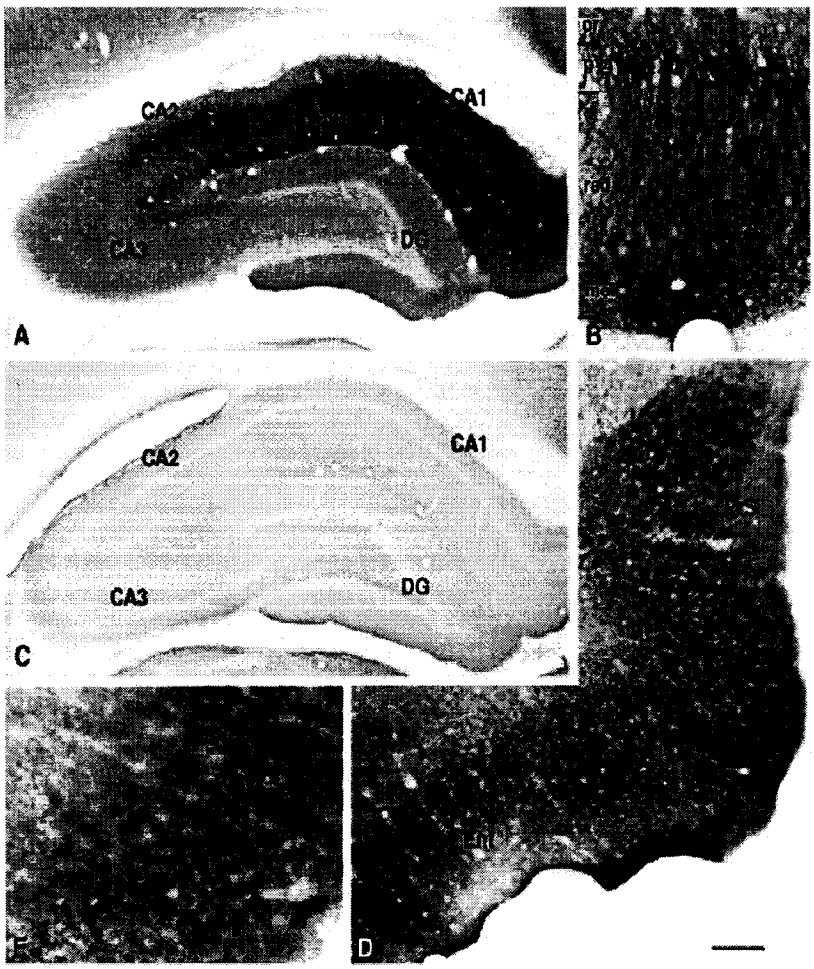

Figure 3.6

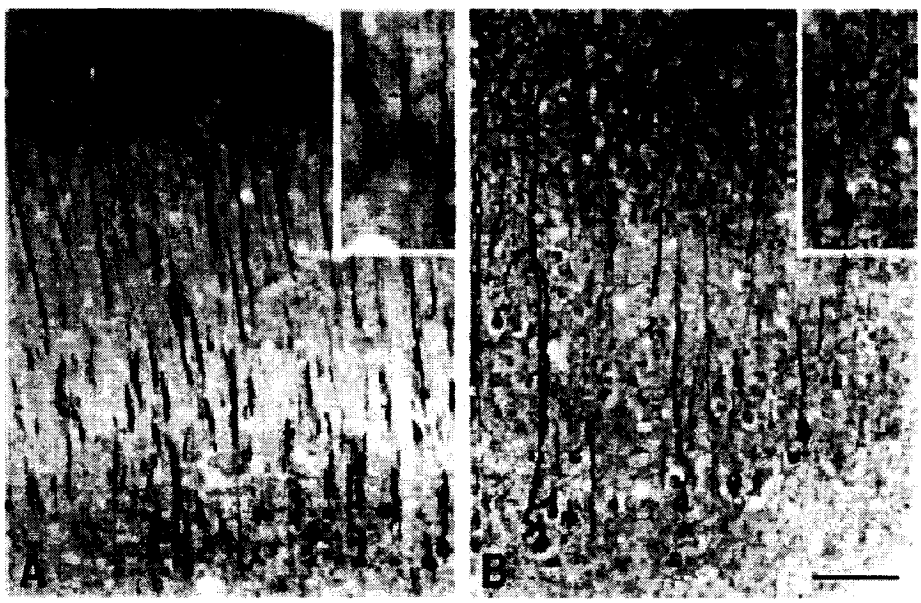

Figure 3.7

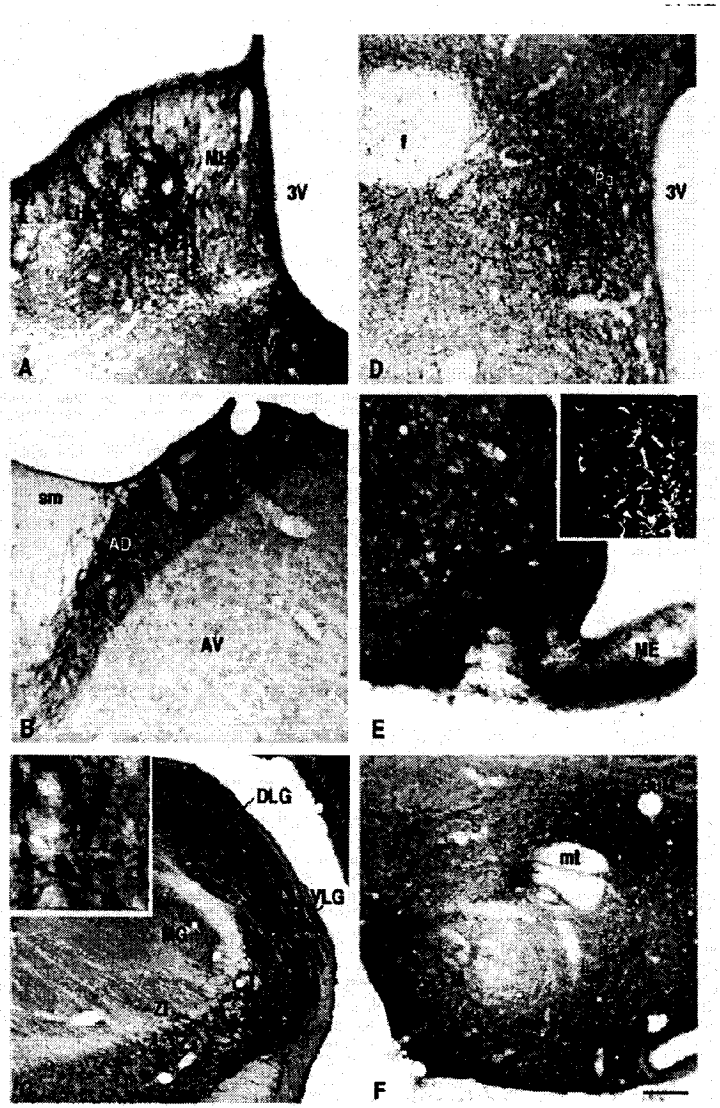

Figure 3.8

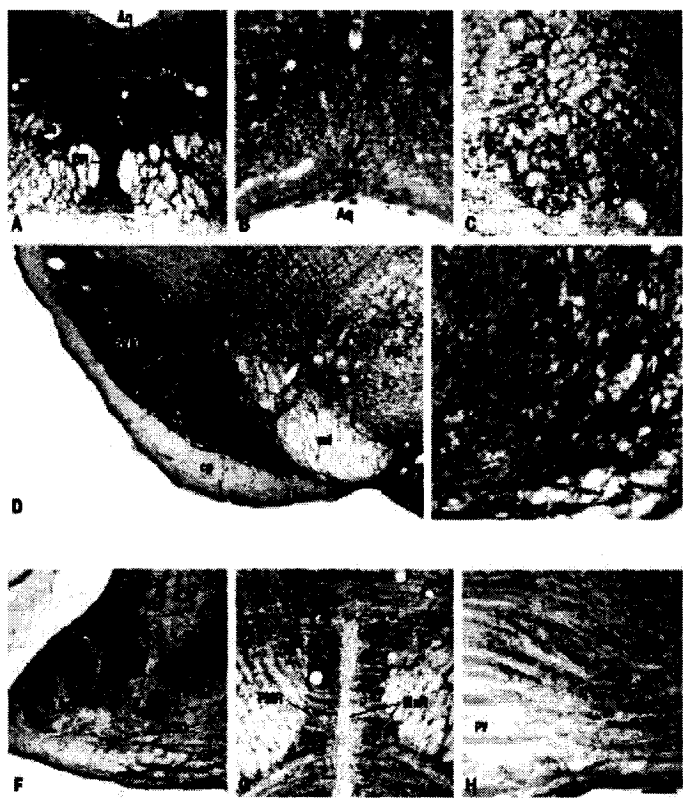

Figure 3.9

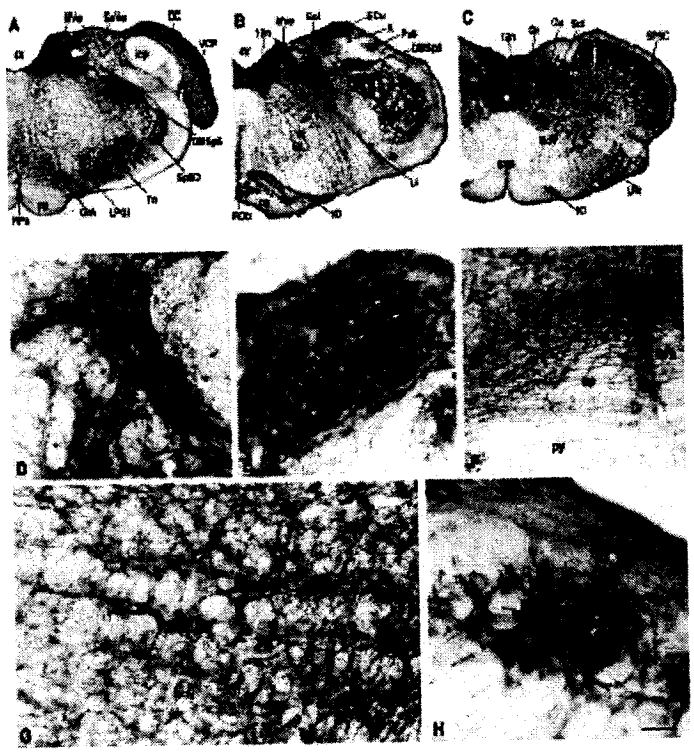

Figure 3.10

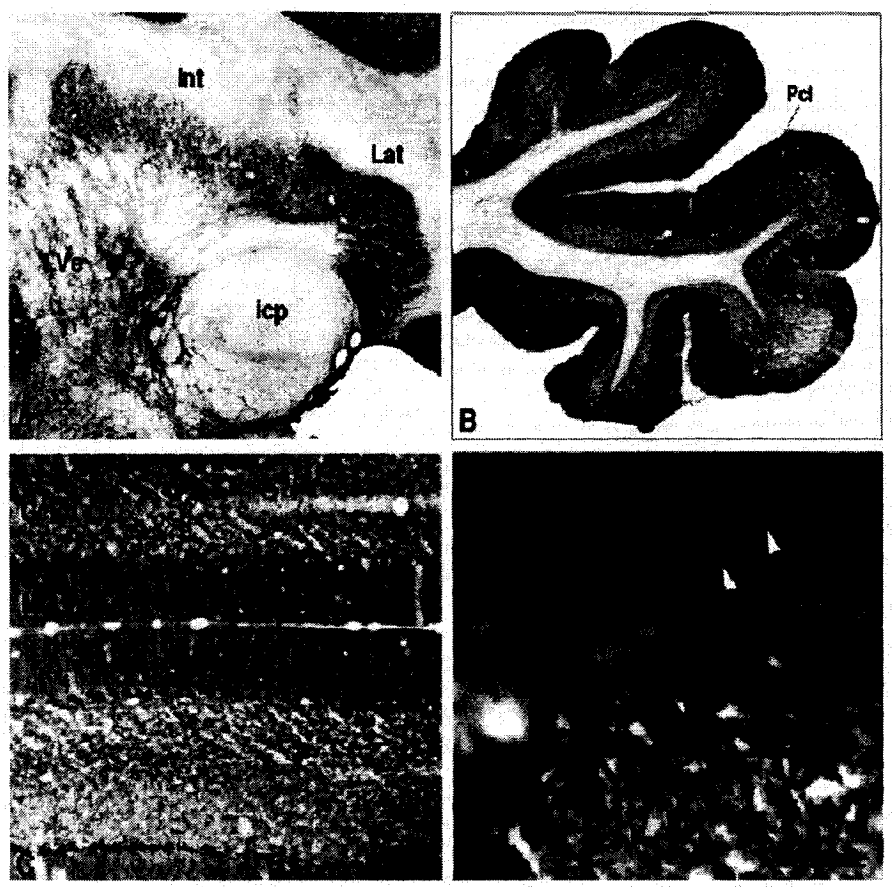

Figure 3.11

3.9 FIGURE LEGENDS

Fig. 3.1: Characterization of Levocabastine-sensitive NTS2 Antiserum. ***A*** and ***B*****:** Identification by Western blotting of endogenously vs. heterologously expressed NTS2 receptors. ***A*****:** Blot from whole brain (*lanes 1, 3*) and cerebellar (*lanes 2, 4*) membranes incubated with the NTS2 antiserum. As a control, the antiserum was preadsorbed with 2 μg/ml of antigenic peptide (*lanes 3, 4*). Specific immunoreactive bands are apparent at estimated molecular weights of 46, 80-85 and 124-206 kDa. Each lane represents the transfer of 60 μg of membrane protein. Data are representative of four independent experiments. ***B*****:** Immunoprecipitation with NTS2 antiserum and blotting with anti-HA antibody (*lane 2*) or immunoprecipitation with anti-HA antibody and blotting with anti-NTS2 antiserum (*lane 4*) of homogenates from COS-7 cells expressing (*lanes 2, 4*) or not (*lane 1, 3*) *HA*-NTS2. Both approaches reveal translation products of approximately 46, 83 and 125-206 kDa in transfected, but not in untransfected cells. Data are representative of three independent experiments. Migration of molecular weight markers is indicated on the left. ***C-F*****:** Dual immunofluorescence labeling of COS-7 cells transfected with cDNA encoding *HA*-epitope-tagged NTS2 receptor. Labeling of the *HA*-epitope (***C***) overlaps with staining produced by the NTS2 antiserum. (***D***). Preadsorption of NTS2 antiserum with antigenic peptide completely abolishes *NTS2-l* immunostaining (***F***) in cells expressing the epitope-tagged receptor (***E***). Trans-nuclear confocal microscopic images representative of three separate experiments. Scale bar = 5 μm in *F* (applies to *C-F*).

Fig. 3.2.: Specificity of Levocabastine-sensitive Neurotensin Receptor-like (*NTS2-l*) Immunolabeling in Rat Brain Sections. ***A*****:** Section from the olfactory bulb, immunostained with anti-NTS2 serum diluted 1:10,000. All layers of the main olfactory bulb are strongly immunopositive. Most intensely stained are the external plexiform layer (Epl) and the accessory olfactory bulb (AOB). ***B*****:** Section from the same region incubated with primary antiserum preadsorbed with 2 μg/ml of antigen at the same final dilution as in ***A***. Note the complete suppression of the

immunolabeling. For other abbreviations, see list. Scale bar = 0.6 mm in B (applies to *A* and *B*)

Fig. 3.3: Cellular Distribution of Levocabastine-sensitive Neurotensin Receptor-like (*NTS2-l*) Immunoreactivity in Rat Brain Sections. ***A*:** In many areas such as the piriform cortex, *NTS2-l* immunoreactivity is mainly apparent over dendrites. In regions such as the central amygdaloid nucleus (***B***) or the bed nucleus of the stria terminalis (***D***), *NTS2-l* immunoreactivity is predominantly associated with nerve cell bodies. ***C*:** *NTS2-l*-immunoreactive axons and axonal varicosities (*arrowheads*) are visible in several regions such as here in the diagonal band of Broca. ***D-I*:** Dual immunofluorescence labeling of NTS2 and of the astrocyte antigen S100β. ***D*:** In the bed nucleus of the stria terminalis, *NTS2-l* immunoreactivity is apparent over somata and small processes. ***E-F*:** None of these structures are immunoreactive for the S100β antigen within the same section. ***G*:** In the anterior hypothalamus, *NTS2-l* labeling is detected in the form of small puncta pervading the neuropil, predominantly in its dorso-medial aspect. ***H-I*:** Here again, none of the *NTS2-l*-immunoreactive structures co-localize S100β within the same section. For abbreviations, see list. Scale bar in *C* = 60 μm in *A-B*; 40 μm in *C*; 25 μm in *D-F*; 200 μm in *G-I*.

Fig. 3.4: Topographic Distribution of Levocabastine-sensitive Neurotensin Receptor-like (*NTS2-l*) Immunoreactivity. A schematic midsagittal section through the rat brain provides an overview of the distribution of *NTS2-l* immunoreactivity throughout the neuraxis and indicates the rostrocaudal levels of the coronal sections illustrated below. Symbols in schematic sagittal section: *dots*, *NTS2-l*-positive neuronal perikarya; *twisted lines*, labeled neuronal processes. ***A*:** At anterior levels, the neocortex (most notably layer V and supragranular layers), piriform cortex, olfactory tubercle, and lateral septum all display moderate to strong immunoreactivity. The mediodorsal aspect of the caudate-putamen is also moderately labeled. ***B*:** Further caudally, very strong immunolabeling is evident in CA1 and CA2 hippocampal subfields. Moderate to dense immunostaining is again

evident in cerebral cortex. The posteromedial cortical amygdaloid nucleus also displays intense *NTS2-l* immunoreactivity. Finally, moderate immunolabeling is evident in the parafascicular nucleus of the thalamus and throughout the hypothalamus. ***C*:** At caudal mesencephalic and rostral pontine levels, the strongest immunoreactive signal is observed in the interpeduncular nucleus, the caudal linear raphe, and the periaqueductal gray. The superior colliculus also displays moderate immunolabeling, differentialy distributed among its layers. The pontine nuclei are strongly labeled. ***D*:** In the caudal pons, the superior olivary complex and the nucleus of the trapezoid body are conspicuously labeled. In the same section, rostral medullary nuclei such as the principal sensory and spinal trigeminal nuclei, the medial vestibular nucleus, and the cochlear nuclei display medium to strong immunoreactivity. In the cerebellum, both the deep nuclei and the cerebellar cortex display high levels of *NTS2-l* immunoreactivity. For abbreviations, see list. Scale bar = 2.5 mm in *D* (applies to *A-D*)

Fig. 3.5: Distribution of Levocabastine-sensitive Neurotensin Receptor-like (*NTS2-l*) Immunoreactivity in the Basal Forebrain (*A*) and Basal Ganglia (*B,C*). ***A*:** In the bed nucleus of the stria terminalis, numerous cell bodies are strongly immunoreactive. In addition, there is a moderate staining of the neuropil surrounding the somata. ***B*:** Within the globus pallidus, *NTS2-l* immunoreactivity is associated with neuronal processes coursing in between fascicles of myelinated axons. ***C*:** In the caudate-putamen, small spiny type II-like immunopositive neuronal perikarya are visible between the fiber bundles of the internal capsule. A light staining of the neuropil is evident as well. For abbreviations, see list. Scale bar in *B* = 75 μm in *A*; 160 μm in *B*; 40 μm in *C*.

Fig. 3.6: Distribution of Levocabastine-sensitive Neurotensin Receptor-like (*NTS2-l*) Immunoreactivity in the Hippocampal Formation. ***A*:** In Ammon's horn, intense *NTS2-l* immunolabeling is evident in stratum pyramidale, radiatum, and lacunosum moleculare of CA1 and CA2. CA3 displays only moderate, diffuse labeling except in the stratum lacunosum moleculare, where the labeling is more

pronounced. The dentate gyrus is likewise moderately, but diffusely labeled except for the granule cell layer which is totally devoid of immunostaining. ***B*:** At high magnification, virtually all CA1 pyramidal cells are seen to be immunopositive. Their apical dendrites pass through the stratum radiatum and ramify in the stratum lacunosum moleculare. ***C*:** Preadsorption of the antiserum with 2 μg/ml of antigen result in a complete loss of *NTS2-l* immunoreactivity. ***D*:** The entorhinal cortex as well as the pre- and parasubiculum all display numerous, strongly labeled nerve cell bodies in layer II. ***E*:** At high magnification, labeling over neurons in the entorhinal cortex is seen to spare the nucleus and to extend for a short distance within proximal dendrites. For abbreviations, see list. Scale bar in *D* = 400 μm in *A* and *C*; 80 μm in *B*; 150 μm in *D*; 60 μm in *E*.

Fig. 3.7: Distribution of Levocabastine-sensitive Neurotensin Receptor-like (*NTS2-l*) Immunoreactivity in the Cerebral Cortex. ***A*:** In neocortical areas such as the parietal cortex illustrated here, a sub-population of layer V pyramidal cells (*insert*) exhibit intense immunolabeling of their cell bodies and apical dendrites. The latter may be followed up to the superficial layers, in which they ramify. ***B*:** Allocortical areas, represented here by the retrosplenial cortex, display a similar pattern of labeling. Scale bar in *B* = 150 μm in *A* (60 μm in *insert*); 75 μm in *B* (45 μm in *insert*).

Fig. 3.8: Distribution of Levocabastine-sensitive Neurotensin receptor-like (*NTS2-l*) Immunoreactivity in the Diencephalon. *A*: Habenular complex. The lateral habenula exhibits moderate to dense fiber staining whereas the medial habenula is only lightly and diffusely stained. The ventromedially adjoining paraventricular thalamic nucleus displays strong immunolabeling. ***B*:** The anterior dorsal thalamic nucleus displays intense perikaryal and neuropil immunostaining, whereas the neighboring anterior ventral nucleus is only lightly reactive. ***C*:** Intense immunoreactivity is apparent over the dorsal lateral and ventral tiers of the lateral geniculate nucleus as well as in the adjoining zona incerta. As seen in the *insert*, most of this immunostaining is accounted for by dendritic processes. ***D*:** Within the

paraventricular nucleus, *NTS2-l* immunoreactivity is selectively detected within small punctate processes. ***E*:** The arcuate nucleus (Arc) displays both immunoreactive nerve cell bodies (*arrowheads*, *insert*) and a dense network of strongly immunoreactive processes. Diffuse immunolabeling is also evident over the external zone of the median eminence. ***F*:** At the level of the mammillary bodies, the lateral mammillary (LM) and supramammillary (SuM) nuclei show moderate to strong neuropil immunolabeling. For other abbreviations, see list. Scale bar in *F* = 130 μm in *A*, *B,* and *D*; 500 μm in *C* (40 μm in *insert*); 80 μm in *E* (50 μm in *insert*); 200 μm in *F*.

Fig. 3.9: Distribution of Levocabastine-sensitive Neurotensin Receptor-like (*NTS2-l*) Immunoreactivity in Mesencephalon (A-E) and Pons (F-H). ***A*:** The ventral periaqueductal gray (PAG) and dorsal raphe nucleus both exhibit a dense network of immunopositive processes. Intensely immunoreactive nerve cell bodies are also evident within the oculomotor nucleus. ***B*:** In the dorsal part of the PAG, labeled neuronal perikarya (*arrowheads*) are apparent amidst a less intensely stained plexus of immunoreactive processes. ***C*:** Intensely immunostained nerve cell bodies are detected in the ventral, magnocellular portion of the red nucleus. ***D*:** The substantia nigra, pars compacta (SNc) and reticulata (SNr), exhibit a dense network of immunopositive processes. In the ventral tegmental area, the labeling is less intense and concerns nerve cell bodies as well as processes. ***E*:** At high magnification, *NTS2-l*-positive nerve cell bodies (*arrowheads*) can be identified amongst the dense plexus of processes pervading the SNr. ***F*:** In the rostral pons, the superior olivary complex exhibits a mix of labeled somata and processes. ***G*:** The paramedian raphe nucleus displays a high density of immunolabeled processes, whereas the median raphe nucleus is completely devoid of NTS2 immunoreactivity. ***H*:** In the nucleus of the trapezoid body, *NTS2-l* immunoreactivity is predominantly associated with small neuronal perikarya. For other abbreviations, see list. Scale bar in *H* = 280 μm in *A*; 65 μm in *B*; 120 μm in *C*; 350 μm in *D*; 50 μm in *E*; 240 μm in *F*; 150 μm in *G* and *H*.

Fig. 3.10: Distribution of Levocabastine-sensitive Neurotensin Receptor-like (*NTS2-l*) Immunoreactivity in the Medulla Oblongata. ***A-C*:** Low magnification micrographs illustrating labeling of cranial nerve sensory nuclei. Some of these, such as the medial vestibular (*A-B*) and dorsal cochlear nuclei (*A*) are more or less uniformly and very strongly stained. Others, such as the superior (*A*) and spinal vestibular (*B*) nuclei and ventral cochlear nucleus (*A*) exhibit lighter staining of the neuropil and NTS2-positive nerve cell bodies are visible even at low magnification. ***D*:** The abducens nucleus diplays numerous intensely stained neurons as well as a strong labeling of the neuropil. ***E*:** The external cuneate nucleus exhibits a moderate number of *NTS2-l*-positive perikarya in its lateral aspect. The neuropil is strongly stained and pervaded by a dense network of immunolabeled processes. ***F*:** The gigantocellular reticular nucleus, pars alpha, exhibits numerous labeled perikarya as well as processes. Medially, the nucleus raphe magnus is intensely stained and the raphe pallidus displays moderate immunoreactivity. ***G*:** Intensely *NTS2-l* immunoreactive neurons in the parvocellular reticular nucleus are surrounded by a moderately dense plexus of immunopositive fibers. ***H*:** The paratrigeminal nucleus is pervaded by a dense plexus of intensely stained processes. For abbreviations, see list. Scale bar in *H* = 700 μm, in *A-C*; 60 μm in *D-E*, *H*; 170 μm in *F*; 75 μm in *G*.

Fig. 3.11: Distribution of Levocabastine-sensitive Neurotensin Receptor-like (*NTS2-l*) Immunoreactivity in the Cerebellum. ***A*:** Intensely labeled nerve cell bodies are detected among a network of immunoreactive processes within the lateral and intermediate cerebellar nuclei. To the left of the inferior cerebellar peduncle, light to moderate immunoreactivity is observed in the lateral vestibular nucleus. ***B*:** Sagittal section through the paraflocculus illustrating the presence of *NTS2-l* immunolabeling in all three layers of cerebellar cortex. ***C*:** At higher magnification, labeling of Purkinje cells and of their apical dendrites traversing the molecular layer is evident. ***D*:** At high magnification, individual immunopositive granule cells can be identified (black *arrowheads*). In addition, the plexus of Purkinje cell dendrites is resolved in the molecular layer (white *arrowheads*). For abbreviations, see list. Scale bar in *D* = 400 μm in *A*, 500 μm in *B*, 130 μm in *C*, 30 μm in *D*.

3.10 TABLE

TABLE 3.1. Regional Distribution of NTS2 Immunoreactivity in Adult Rat Brain[1]

Structure	NTS2 immunoreactivity: Cell bodies	NTS2 immunoreactivity: Processes and Terminals
Telencephalon		
Cerebral cortex		
Frontal	+/++	+/++
Parietal	++	+++
Cingulate	+	++
Occipital	+/++	+/++
Temporal	+/++	+++
Insular	+/++	++/+++
Perirhinal	+	+/++
Retrosplenial	++	++
Olfactory bulb		
Accessory olfactory bulb	–	+++
Internal granular layer	+	+
Mitral cell layer	++	–
External plexiform layer	–	++
Glomerular layer	–/+	+/++
Olfactory system		
Lateral olfactory nucleus	–/+	+/++
Piriform cortex	+	++/+++
Prepiriform cortex	+	++/+++
Anterior olfactory nucleus	–	++
Dorsal endopiriform nucleus	–	–/+
Ventral endopiriform nucleus	–	+/++
Taenia tecta	+	–/+
Olfactory tubercle	++	+/++
Islands of Calleja	+	+/++
Basal forebrain		
Septohippocampal nucleus	–	++
Lateral septum	+/++	++
Medial septum	–/+	+/++
Diagonal band of Broca		
Vertical limb	–/+	+/++
Horizontal limb	–/+	++
Magnocellular preoptic nucleus	+/++	+/++
Bed nucleus of the stria terminals	++/+++	+/++
Ventral pallidum	–/+	++
Substantia innominata	–	++
Substriatal area	+	+/++
Basal ganglia		
Nucleus accumbens		
Core	–/+	–/+
Shell	–/+	+
Caudate putamen	+/++	–/+
Fundus striati	+	–/+
Globus pallidus	–	++/+++
Entopeduncular nucleus	–	++/+++
Amygdala		
Central nucleus	++	++
Basomedial nucleus	–	+
Medial nucleus	–/+	+/++
Cortical nucleus	++	++
Hippocampal formation		
Entorhinal cortex	++/+++	+/++
Presubiculum	++	–/+
Parasubiculum	++/+++	–/+
CA1	+++	+++
CA2	++	++
CA3	–	–/+
Dentate gyrus		
Granule cells	–	–
Hilus	–/+	+
Diencephalon		
Thalamus		
Anterior dorsal nucleus	–/+	++/+++
Anterior ventral nucleus	+	+
Paraventricular nucleus	+	++
Reuniens nucleus	–	+
Reticular thalamic nucleus	–	++/+++
Central medial thalamic nucleus	–	+
Ventromedial thalamic nucleus	+	+
Mediodorsal thalamic nucleus	+/++	–/+
Rhomboid thalamic nucleus	–	+
Parafascicular nucleus	–	++
Subparafascicular nucleus	–	+/++
Medial geniculate nucleus	+	–
Ventral lateral geniculate nucleus	+	++
Dorsal lateral geniculate nucleus	+	–
Hypothalamus		
Anterior hypothalamus	–	+/++
Suprachiasmatic nucleus	–	++
Supraoptic nucleus	+	++
Paraventricular nucleus	–/+	+/++
Arcuate nucleus	+/++	++/+++
Retrochiasmatic area	++	++
Ventromedial nucleus	–/+	+/++
Dorsomedial nucleus	–	+
Periventricular nucleus	–	++
Lateral hypothalamic area	–/+	++
Tuber cinereum	–	+/++
Medial mammillary nucleus	–	++
Lateral mammillary nucleus	+	++
Supramammillary nucleus	–	++/+++
Lateral preoptic area	–	–/+
Medial preoptic area	–	++
Median eminence	–	++/+++
Subthalamus		
Zona incerta	–/+	++/+++
Subthalamic nucleus	–	+/++
Epithalamus		
Medial habenula nucleus	–/+	–/+
Lateral habenula nucleus	–/+	++
Sublomical organ	–	++
Mesencephalon		
Substantia nigra pars compacta	–	+/++
Substantia nigra pars reticulata	–/+	++/+++
Ventral tegmental area	+	+
Deep mesencephalic nucleus	–	+/++
Red nucleus	++	+
Peripeduncular nucleus	–	++
Interpeduncular nucleus	–/+	++
Interfascicular nucleus	–/+	+/++
Precommissural nucleus	–	++
Periaqueductal gray (central gray)	+	++/+++
Oculomotor nucleus (3n)	++	+/++
Dorsal raphe nucleus	+	++/+++
Caudal linear nucleus raphe	–	++/+++
Superior colliculus	+	++
Inferior colliculus	+	+/++
Pons		
Pontine nuclei	++	++
Superior olivary complex	+/++	++/+++
Superior paraolivary nucleus	+	++
Nucleus of the trapezoid body	++	–
Paramedian raphe nucleus	–	+/++
Motor trigeminal nucleus	+/++	+/++
Principal sensory nucleus (5n)	–/+	+/++
Medulla		
Medial vestibular nucleus	–/+	++/+++
Lateral vestibular nucleus	+/++	+
Ventral cochlear nucleus	++/+++	+/++
Dorsal cochlear nucleus	+/++	+
Linear nucleus of the raphe	–/+	+/++
Inferior olive	+/++	+++
Nucleus of the solitary tract	–/+	++
Gigantocellular reticular nucleus, pars alpha	+	+/++
Gigantocellular reticular nucleus	–	+
Lateral paragigantocellular nucleus	+	+/++
Lateral reticular nucleus	+	++/+++
Intermediate reticular nucleus	–	–/+
Parvocellular reticular nucleus	–/+	++/+++
Medullary reticular field, dorsal	–	++
Medullary reticular field, ventral	–	–/+
Paratrigeminal nucleus	–	+++
External cuneate nucleus	+/++	++/+++
Cuneate nucleus	–/+	++
Gracile nucleus	–	++
Nucleus X	–	++/+++
Raphe magnus nucleus	–/+	++
Raphe obscurus nucleus	–	+/++
Raphe pallidus nucleus	–/+	+/++
Trochlear nucleus (4n)	+/++	+/++
Spinal trigeminal nucleus (5n)	+	++
Abducens nucleus (6n)	+	++/+++
Facial nucleus (7n)	+	++/+++
Dorsal motor nucleus of the vagus (10n)	–/+	++
Hypoglossal nucleus (12n)	+	++/+++
Cerebellum		
Cerebellar cortex		
Granule cell layer	++	–
Purkinje cell layer	++/+++	–
Molecular layer	–/+	++/+++
Cerebellar nuclei (int, lat, medial)	++	+/++

[1]The intensity of immunolabeling was qualitatively scored using the CA1 (+++) and CA3 (–) subfields of Ammon's horn as references. Intensity of NTS2 immunoreactivity:- no labeling, + low signal, ++ moderate signal, +++ high signal, referring to both labeling intensity and the number of labeled elements. NTS2, levocabastine-sensitive neurotensin receptor.

CHAPTER 4

LOW-AFFINITY NEUROTENSIN RECEPTOR (NTS2) SIGNALING: INTERNALIZATION-DEPENDENT ACTIVATION OF EXTRACELLULAR SIGNAL-REGULATED KINASES ERK 1/2

Louis Gendron[1], Amélie Perron[1], Marcel Daniel Payet[2], Nicole Gallo-Payet[3], Philippe Sarret[1], and Alain Beaudet[1]

[1] Montreal Neurological Institute, Department of Neurology and Neurosurgery, McGill University, Montreal, Québec, Canada

[2] Department of Physiology and Biophysics, Faculty of Medicine, University of Sherbrooke, Sherbrooke, Québec, Canada

[3] Service of Endocrinology, Faculty of Medicine, University of Sherbrooke, Sherbrooke, Québec, Canada

Molecular Pharmacology (2004) **66**, 1421-1430.

4.1 ABSTRACT

The role and signaling properties of the low-affinity neurotensin receptor (NTS2) are still controversial. In particular, it is unclear whether neurotensin acts as an agonist, inverse agonist, or antagonist at this site. In view of the growing evidence for a role of NTS2 in antinociception, the elucidation of the pharmacological and coupling properties of this receptor is particularly critical. In the present study, we demonstrate that in Chinese hamster ovary (CHO) cells expressing the rat NTS2 receptor, neurotensin (NT), levocabastine, neuromedin N, and the high-affinity NT receptor antagonist SR48692 [2-{[1-(-7-chloroquinolin-4-yl)-5-(2,6-dimethoxyphenyl)-1H-pyrazole-3-carbonyl]amino}adamantane-2-carboxylic acid] all bind to and activate the NTS2 receptor. This activation is followed by ligand-induced internalization of receptor-ligand complexes, as evidenced by confocal microscopy using a fluorescent NT analog. All compounds tested produced a rapid and sustained activation of extracellular signal-regulated kinases 1/2 (ERK1/2) but were without specific effect on Ca^{2+} mobilization. The agonist-induced activation of ERK1/2 was completely abolished by preincubation of the cells with the endocytosis inhibitors phenylarsine oxide and monodansylcadaverine as well as overexpression of a dominant-negative mutant of dynamin 1 (DynK44A), indicating that receptor internalization was required for ERK1/2 activation. NTS2-induced activation of ERK1/2 was not species-specific, because the same agonistic effects of NT and analogs were observed in CHO cells transfected with the human NTS2 receptor. In conclusion, this study demonstrates that NTS2 is a bona fide NT receptor and that activation of this receptor by NT or NT analogs results in an internalization-dependent activation of the ERK1/2 signaling cascade.

4.2 INTRODUCTION

Neurotensin (NT) is a tridecapeptide that exerts neuromodulatory functions in the central nervous system and has endocrine/paracrine actions in the periphery (Vincent, 1995; Rostène and Alexander, 1997). NT has been shown to modulate dopaminergic transmission in the nigrostriatal and mesocorticolimbic pathways (Nemeroff, 1986; Kitabgi et al., 1989), thereby implicating this neuropeptide in the patho-physiology of several central nervous system disorders, including Parkinson's disease and schizophrenia (for review, see Kitabgi et al., 1989; Binder et al., 2001a; Kinkead and Nemeroff, 2002). In addition, NT injection in the brain or ventricular system produces hypothermia (Martin et al., 1980), changes in blood pressure (Rioux et al., 1981), and nonopioid-dependent analgesia (Kalivas et al., 1982a).

NT mediates its central and peripheral effects through interaction with three receptor subtypes, referred to as NTS1, NTS2, and NTS3. NTS1 and NTS2 belong to the seven transmembrane domain/G protein-coupled receptor family (Tanaka et al., 1990; Vita et al., 1993, 1998; Chalon et al., 1996; Mazella et al., 1996), whereas NTS3 is a single transmembrane domain sorting receptor predominantly associated with vesicular organelles and the Golgi apparatus (Petersen et al., 1997; Mazella et al., 1998). Pharmacological and biochemical studies have indicated that the high-affinity (subnanomolar range) NT receptor NTS1 is coupled to cGMP, cAMP, and inositol phosphate signaling cascades (for review, see Hermans and Maloteaux, 1998; Vincent et al., 1999). Stimulation of NTS1 also induces the activation of extracellular signal-regulated kinases 1/2 (ERK1/2) through coupling with both pertussis toxin-sensitive and -insensitive G proteins. This activation leads in turn to the expression of proliferative genes such as *c-fos*, *Krox-24*, and *elk-1* (Poinot-Chazel et al., 1996; Ehlers et al., 1998, 2000; Portier et al., 1998; Martin et al., 2002a). These effects are selectively blocked by the nonpeptide NT antagonist SR48692, which displays a nanomolar affinity for NTS1 (Gully et al., 1993).

The low-affinity (nanomolar range) NT receptor NTS2 differs from the NTS1 site not only by its 10-fold lower affinity for NT, but also by its selective recognition of levocabastine, a nonpeptide histamine H1 receptor antagonist that selectively inhibits NT binding to NTS2 without affecting its binding to NTS1 (Schotte et al., 1986; Kitabgi et al., 1987). NTS2 also displays a much lower affinity (IC_{50} = 300 nM) than NTS1 (IC_{50} = 5.6 nM) for the SR48692 compound (Gully et al., 1993); however, the pharmacological and signaling properties of NTS2 are still extremely controversial. In particular, doubts have been cast regarding the agonistic properties of NT at this site and, hence, about whether or not this protein may be regarded as a true NT receptor. Indeed, in CHO cells stably transfected with human NTS2, SR48692, but neither NT nor levocabastine, was found to activate classic second messenger systems, such as phosphoinositide hydrolysis, Ca^{2+} mobilization, or ERK1/2 phosphorylation (Vita et al., 1998). Furthermore, in transfected CHO and COS-7 cells, this SR48692-induced activation of the human NTS2 was blocked by NT, suggesting that the endogenous peptide was acting as a competitive antagonist at these sites (Vita et al., 1998; Richard et al., 2001b).

By contrast, in *Xenopus laevis* oocytes expressing the mouse NTS2 receptor, NT, neuromedin N (NN), and levocabastine were all found to activate Ca^{2+}-dependent chloride currents (Mazella et al., 1996). In addition, application of NT or levocabastine on rat cerebellar granule cells, which endogenously express the NTS2 but not the NTS1 receptor, induced a sustained activation of the ERK1/2 signaling cascade (Sarret et al., 2002). Congruent with an agonist role of NT at this site, rodent NTS2 receptors were found to efficiently internalize via clathrin-coated pits upon NT binding both in stably transfected human embryonic kidney 293 cells (Botto et al., 1998) and in rat cerebellar granule cell cultures (Sarret et al., 2002).

It is unclear whether the reported agonistic/antagonistic effects of NT on the human versus rodent NTS2 receptor are caused by species differences between the two receptors or by variations in receptor coupling as a result of the cell type in which the receptor is expressed. In view of the growing evidence for a role of NTS2 (Dubuc et al., 1999a and 1999b; Remaury et al., 2002; Yamauchi et al., 2003a), in

addition to that of NTS1 (Tyler et al., 1999; Pettibone et al., 2002), in antinociception, and therefore of the possibility that NTS2 might represent a new target for the development of nonopioid analgesic drugs, the need for precise knowledge of the pharmacological and signaling properties of this receptor seems particularly critical. Thus, the aim of the present study was to characterize the pharmacological and signaling properties of the rat NTS2 receptor expressed in stably transfected CHO cells and to compare these properties with those of the human NTS2 receptor expressed in the same cell line as well as with our own earlier data on the properties of the rat NTS2 receptor endogenously expressed in rat cerebellar granule cells.

4.3 MATERIALS AND METHODS

4.3.1 Materials

The chemicals used in the present study were obtained from the following sources: Dulbecco's modified Eagle's medium (DMEM) and F-12 medium, fetal bovine serum (FBS), glutamine, G-418, gentamicin, and LipofectAMINE were from Invitrogen (Carlsbad, CA); NT, monodansylcadaverine (MDC), phenylarsine oxide (PAO), sodium orthovanadate (Na_3VO_4), pertussis toxin (PTX), and staurosporine were from Sigma-Aldrich (St. Louis, MO); antiphosphorylated ERK1/2 and anti-ERK1/2 antibodies were from New England Biolabs (Beverly, MA); horseradish peroxidase-conjugated anti-rabbit antibodies and the enhanced chemiluminescence detection system were from Amersham Biosciences Inc. (Piscataway, NJ); Complete protease inhibitor and polyvinylidene difluoride (PVDF) membranes were from Roche (Montreal, QC, Canada); NN was from Bachem California (Torrance, CA). Levocabastine and SR48692 were kindly provided by Janssen Pharmaceuticals (Antwerp, Belgium) and Sanofi Synthelabo (Toulouse, France), respectively.

4.3.2 Transfection of CHO Cells

CHO/K1 cells were cultured in DMEM/F-12 medium mixture (1:1) supplemented with 10% FBS and 50 mg/l gentamicin at 37°C in 75-cm^2 Falcon flasks in a humidified atmosphere of 95% air and 5% CO_2. For transfection, CHO/K1 cells were grown to subconfluence (70-80%) in 24-well Petri dishes and incubated for 4 h at 37°C in transfection medium [mixture of pTargeT-rNTS2 (1 μg/ml) (Sarret et al., 2003a) or pTargeT-hNTS2 and 40 μg/ml LipofectAMINE in serum-free DMEM. Transfection medium was then replaced with DMEM/F-12 medium, and the cells were transferred 36 h later to a 75-cm^2 flask containing fresh medium supplemented with G-418 at a concentration of 800 μg/ml. After 2 weeks of selection with G-418, a total of 23 and 12 individual clones were isolated for CHO/rNTS2 and CHO/hNTS2, respectively. Each clone was separately grown and tested for its capacity to internalize *Nα*-BODIPY-neurotensin-(2-13) (Fluo-NT) as described below. CHO/rNTS2 clone no. 16 and CHO/hNTS2 clone no. 1 were used for all experiments.

4.3.3 Reverse Transcription-Polymerase Chain Reaction Analysis

Total RNAs (2 μg) were extracted from CHO/rNTS2 and CHO/K1 cells using QIAGEN RNeasy Mini Spin columns (QIAGEN, Mississauga, ON, Canada) and submitted to reverse transcription (reverse transcription system kit; Promega, Madison, WI) for 1 h at 42°C. First-strand cDNAs were then subjected to 35 cycles of PCR in a final reaction volume of 50 μl of the reaction buffer (50 mM KCl, 10 mM Tris, pH 9.0, 1.5 mM $MgCl_2$, 0.1% Triton X-100, 0.02% BSA, 200 μM dNTPs, and 0.5 units of *Taq* DNA polymerase) containing 100 ng of either one of the following three pairs of sense and antisense primers as described previously (Sarret et al., 2002). The first pair (5'-ACACCCATTGTGGACACAGCC-3' and 5'-TTCATCCGAGATATAGCAGAA-3') provided for the amplification of a fragment of rNTS1 receptor cDNA with a predicted size of 335 bp. The second pair (5'-GAATGTGCTGGTGTCCTTCGC-3' and 5'-ACTTGTATTTCTCCCAGGCTG-3') provided for the amplification of a fragment of rNTS2 receptor cDNA with a predicted size of 620 bp. The third pair (5'-TCCCGAGAACTCTGGAAAGGT-3' and 5'-CACAGAGGCGAAGAGGAAACG-3') provided for the amplification of a fragment of rNTS3 receptor cDNA with a predicted size of 426 bp. Amplification was carried out with the first cycle at 95°C for 3 min, 54°C for 2 min, 72°C for 45 s, followed by 34 cycles at 95°C for 40 s, 54°C for 35 s, 72°C for 45 s, and a final extension step at 72°C for 5 min. PCR products were then analyzed on a 1.5% agarose gel.

4.3.4 Binding of ^{125}I-NT to CHO/rNTS2 Cells

For binding experiments, cells were grown on 24-well plates and incubated at 37°C in DMEM/F-12 medium 48 h before the assay. Cells were equilibrated for 10 min at 37°C in Earle's buffer (130 mM NaCl, 5 mM KCl, 1.8 mM $CaCl_2$, 0.8 mM $MgCl_2$, and 20 mM HEPES, pH 7.4) supplemented with 0.2% BSA and 0.1% glucose. Cells were then incubated with 2.5 nM ^{125}I-NT (100 Ci/mmol) for 30 min at 37°C in 250 μl of Earle's buffer containing 0.8 mM *ortho*-phenanthroline in the presence of increasing concentrations (from 10^{-11}-10^{-5} M) of nonradio-active NT, levocabastine, NN, or SR48692. Cells were then washed twice with Earle's buffer and harvested in

1 ml of 0.1 M NaOH, and the radioactivity content was measured in a γ counter. IC_{50} values were determined from competition curves as the concentration of unlabeled ligand necessary to inhibit 50% of ^{125}I-NT-specific binding.

4.3.5 Intracellular Calcium Measurements

For intracellular calcium ($[Ca^{2+}]_i$) measurements, the CHO/rNTS2 and CHO/K1 cells were cultured on 22-mm glass coverslips and incubated in serum-free DMEM supplemented with 4 μM Fluo-4/acetoxymethyl ester (Molecular Probes, Eugene, OR) at 37°C for 30 min. Cells were then washed three times with 0.5% BSA and further incubated in PBS-HEPES (140 mM NaCl, 5.4 mM KCl, 2 mM $CaCl_2$, 1 mM $MgCl_2 \cdot 6H_2O$, and 10 mM HEPES, pH 7.35) at 37°C for 30 min to allow the acetoxymethyl ester form to be hydrolyzed. The coverslips were then mounted on the stage of a Nikon Eclipse TE300 inverted microscope (Nikon, Melville, NY), and the cells were maintained at 37°C throughout the experiments with a heating Peltier element. NT, NN, levocabastine, or SR48692, diluted in fresh PBS-HEPES containing, for the solubilization of the latter two drugs, 0.01% dimethylsulfoxide (DMSO), were added to the cells at a final concentration of 1 μM, and images of fluorescence were acquired every 5 s using a $CoolSnap_{fx}$ charge-coupled device camera (Roper Scientific, Trenton, NJ) cooled at -35°C. Additional experiments were carried out using 0.01% DMSO in PBS-HEPES alone to test for possible nonspecific effects of the solubilizing agent. Band-pass filters were used for excitation and emission (450-490 and 520-560 nm, respectively). Average fluorescence intensity for each cell was measured using MetaFluor software package (Universal Imaging Corporation, Downingtown, PA). Each Ca^{2+} curve in Fig 4.2 represents the average response of *n* cells.

4.3.6 Western Blotting Analyses of ERK1/2 Activity

CHO/rNTS2, CHO/hNTS2, and CHO/K1 cells were grown for 3 days in DMEM/F-12 medium containing 10% FBS, starved in serum-free DMEM for 1 h, and then stimulated for various time intervals (1-60 min) with NT (100 nM), levocabastine (100 nM or 1 μM), NN (100 nM), or SR48692 (100 nM) at 37°C in serum-free medium. In some experiments, cells were preincubated with PAO or MDC (two endocytosis inhibitors) for 30 min or with PTX (G_i protein inhibitor) for 18 h (100 ng/ml) before stimulation with NT or NT analogs. The reaction was stopped by aspiration of the medium and the addition of ice-cold Hanks' balanced salt solution containing 0.1 μM staurosporine and 1 mM sodium orthovanadate. Cells were then left for 30 min at 4°C and lysed in 50 mM HEPES, pH 7.8, containing 1% Triton X-100, 0.1 μM staurosporine, 1 mM sodium orthovanadate, and Complete protease inhibitor. The cell lysates were centrifuged at 8000g for 15 min at 4°C, and the supernatants were stored at -20°C until use. For each lysate, equal amounts of proteins (25 μg) were separated on 10% SDS-polyacrylamide gels and electrotransferred on PVDF membranes as described previously (Gendron et al., 2003). PVDF membranes containing proteins were incubated for 2 h at room temperature with anti-phosphorylated ERK1/2 (1:1000) or anti-ERK1/2 (1:1000) rabbit antibodies, followed by three washes with Tris-buffered saline/Tween 20. Detection of immunoreactive proteins was accomplished using horseradish peroxidase-conjugated anti-rabbit (1:2000) and an enhanced chemiluminescence detection system.

To quantify the effect of NT and NT analogs on ERK1/2 phosphorylation, the ratios of phosphorylated ERK1/2 over total ERK1/2 levels were determined by densitometry, using Scion Image (Scion Corporation, Frederick, MD). The statistical significance of the activation of ERK1/2 in stimulated versus nonstimulated cells was verified using ANOVA, and the *p* values were obtained from Dunnett's tables.

4.3.7 Binding of Fluo-NT to CHO/rNTS2 Cells

CHO/rNTS2 cells were grown for 2 days on 12-mm poly-L-lysine-coated glass coverslips in DMEM/F-12 medium containing 10% FBS and stimulated for 30 min at 37°C with 50 nM Fluo-NT in serum-free DMEM containing 0.8 mM *ortho*-phenanthroline alone or in the presence of levocabastine (10 μM) or phenylarsine oxide (endocytosis inhibitor) (10 μM). At the end of the incubation, cells were washed twice with ice-cold PBS, air-dried, mounted on glass slides with Aquamount (Polysciences, Warrington, PA) and examined using the Zeiss LSM510 confocal laser-scanning microscope (Carl Zeiss Canada Ltd., Toronto, ON, Canada) equipped with a Zeiss inverted microscope and a helium/neon laser (543 nm).

4.3.8 Immunofluorescence Studies

CHO/rNTS2 cells were grown on 12-mm glass coverslips for 3 days in DMEM/F-12 medium containing 10% FBS and then starved in serum-free DMEM for 1 h. Cells pretreated or not with PAO (10 μM, 10 min at 37°C) were then treated or not with SR48692 (100 nM) for 5 min at 37°C in serum-free DMEM. The reaction was stopped by aspiration of the medium and the addition of ice-cold Hanks' balanced salt solution containing 0.1 μM staurosporine, and 1 mM sodium orthovanadate. After 10 min of incubation on ice, cells were fixed for 20 min with methanol at -20°C and rehydrated with Hanks' balanced salt solution for 30 min at room temperature. Phosphorylated ERK1/2 were labeled overnight at 4°C using anti-phosphorylated ERK1/2 rabbit antibodies (1:100) and revealed using goat anti-rabbit Alexa488- or Alexa594-conjugated secondary antibodies (Molecular Probes; diluted 1:500 in Hanks' balanced salt solution) for 60 min at room temperature. After washing, coverslips were mounted on glass slides using Aquamount and examined using the Zeiss LSM510 confocal laser-scanning microscope equipped with a Zeiss inverted microscope, an argon laser (488 nm), and a helium/neon laser (543 nm). Images were all taken using the same acquisition settings.

To determine whether ligand-induced receptor internalization was necessary for NTS2-induced ERK1/2 phosphorylation, the above immunofluorescence assay was repeated on CHO/rNTS2 cells preincubated for 10 min with PAO (10 μM) as well as on CHO/rNTS2 cells cotransfected with pcDNA1-DynK44A (kindly provided by Dr. Stephen S. Ferguson, Carleton University, Ontario, QC, Canada) and pEGFP-N1 (BD Biosciences, Mississauga, ON, Canada). For this purpose, pcDNA1-DynK44A (1 μg/ml) and pEGFP-N1 (0.1 μg/ml) plasmids were mixed with 40 μg/ml LipofectAMINE, and the mixture was kept at room temperature for 30 min before being added to the culture medium. CHO/rNTS2 cells grown to 25 to 30% subconfluence on 12-mm poly-L-lysine-coated glass coverslips were then transfected for 4 h at 37°C with this DNA-lipid complex. At the end of the incubation, transfection medium was replaced with fresh medium, and cells were processed 36 h later for immunolabeling of the phosphorylated ERK1/2 as described above.

4.4 RESULTS

4.4.1 Expression and Binding Properties of rNTS2 in CHO Cells

Reverse transcription-polymerase chain reaction (RT-PCR) analysis of rat NTS1, NTS2, and NTS3 expression was performed on nontransfected CHO cells (CHO/K1) and on CHO cells transfected with rat NTS2 receptor cDNA (CHO/rNTS2). As shown in Fig. 4.1*A*, a 620-bp band corresponding to the size of the NTS2 receptor fragment was observed in CHO/rNTS2 cells but not in CHO/K1 cells. In contrast, a 425-bp product corresponding to the NTS3 receptor was detected in both transfected and nontransfected cells. The PCR product for the NTS1 receptor (expected at 336 bp) was observed in neither of these cell lines but was present in CHO/rNTS1 cells used as positive controls (not shown). As illustrated in Fig. 4.1*B*, NT, levocabastine, NN, and SR48692 all inhibited competitively specific ^{125}I-NT binding with IC_{50} values of 3.5, 74, 21, and 31 nM, respectively.

4.4.2 Lack of NTS2-Induced Intracellular Ca^{2+} Mobilization

The capacity of NT, levocabastine, NN, and SR48692 to induce Ca^{2+} mobilization was tested in CHO/rNTS2 cells using Fluo-4 as a fluorescent marker of $[Ca^{2+}]_i$. As seen in Fig. 4.2, NT, Levo, and NN were ineffective at modifying $[Ca^{2+}]_i$, even when applied at concentrations as high as 1 μM (*A*, *B*, and *C*, respectively). By contrast, SR48692 (1 μM) markedly increased $[Ca^{2+}]_i$. This effect was caused by the drug itself, because it was not observed after the application of the DMSO containing vehicle alone. The SR48692-induced increase in $[Ca^{2+}]_i$ was neither prevented nor modified by concomitant (not shown) or prior stimulation with NT, levocabastine, or NN (Fig. 4.2, *A*, *B*, and *C*), suggesting that it was not mediated by NTS2. Congruent with this interpretation, SR48692 produced a similar increase in $[Ca^{2+}]_i$ in nontransfected CHO/K1 cells (Fig. 4.2*D*).

4.4.3 NTS2-Mediated ERK1/2 Phosphorylation

To determine whether heterologously expressed rNTS2 were functionally coupled to the ERK1/2 pathway, CHO/rNTS2 cells were stimulated with 100 nM NT for various

periods of time. Western blot analysis of phosphorylated ERK1/2 revealed that NT rapidly enhanced the level of phosphorylation of ERK1/2 (Fig. 4.3, *A* and *B*). This increase in ERK1/2 phosphorylation was already apparent after 1 min of stimulation, peaked at 10 min (2.89 ± 0.80-fold increase over control), and was sustained for at least 1 h. This effect was mediated by NTS2, because it was not observed in nontransfected cells (Fig. 4.3, *B* and *C*). As shown in Fig. 4.3*D*, the NT-induced ERK1/2 activation measured after 5 min of stimulation was dose-dependent and readily detectable at concentrations as low as 10^{-8} M (i.e., within the range of the k_d value of NT for the rNTS2 receptor).

We then tested whether other documented NTS2 ligands similarly affected ERK1/2 phosphorylation. As shown in Fig. 4.4, *A* and *B*, levocabastine (100 nM) and NN (100 nM) both activated ERK1/2 to the same extent as NT (3.2 ± 0.8- and 2.2 ± 0.9-fold increase over control, respectively). Furthermore, the NTS1 antagonist SR48692, which binds the NTS2 receptor with less affinity than NT (Fig. 4.1*B*), induced a phosphorylation of ERK1/2 that was considerably more robust than that produced by either of the other NTS2 agonists tested (15.4 ± 4.2-fold increase over control). This effect of SR48692 was unaffected by the addition of 100 nM NT in the incubation medium (Fig. 4.4, *A* and *B*), suggesting that the two drugs interacted with different sites. Yet the effects of SR48692, as well as those of levocabastine and NN, were mediated by NTS2, because none of these ligands was able to activate ERK1/2 in nontransfected, CHO/K1 cells (Fig. 4.4*C*). These effects were also independent from G_i, because they were unaffected by an overnight preincubation of CHO/rNTS2 cells with PTX (not shown).

To determine whether the NTS2-mediated effects of NT and NT analogs on ERK1/2 activation were species-specific, Western blot analyses of ERK1/2 phosphorylation were repeated on CHO cells transfected with cDNA encoding the human NTS2 receptor (CHO/hNTS2). As shown in Fig. 4.5, *A* and *C*, stimulation of CHO/hNTS2 with 10^{-7} M NT for 3 to 60 min resulted in a significant increase in ERK1/2 phosphorylation. As in CHO/rNTS2 cells, this effect peaked at 10 min but was somewhat less sustained in that phosphorylation levels returned to baseline by 1

h (Fig. 4.5*A*). Stimulation of CHO/hNTS2 cells for 5 min with 10^{-6} M levocabastine or 10^{-7} M SR48692 also induced a robust activation of ERK1/2 phosphorylation (Fig. 4.5, *B* and *C*). As in CHO/rNTS2 cells, the effects of SR48692 were significantly greater than those of NT (3.07 ± 0.57-versus 1.79 ± 0.31-fold increase over control; Fig. 4.5*C*).

4.4.4 Internalization Dependence of the NTS2-Induced ERK1/2 Activation

To determine whether heterologously expressed NTS2 internalized upon agonist binding, CHO/rNTS2 and CHO/K1 cells were incubated with 50 nM Fluo-NT for 30 min at 37°C and examined by confocal microscopy. In CHO/rNTS2 cells, Fluo-NT pervaded the cytoplasm in the form of small, endosome-like fluorescent clusters (Fig. 4.6*A*). By contrast, Fluo-NT labeling was confined to the cell surface after pretreatment with the endocytosis inhibitor PAO (10 μM, 10 min) (Fig. 4.6*B*). Fluo-NT internalization was NTS2-specific, because nontransfected CHO/K1 cells (not shown) and cells coincubated with Fluo-NT and an excess of levocabastine (Fig. 4.6*C*) were entirely fluorescent-negative.

To determine whether ligand-induced NTS2 receptor internalization was necessary for ERK1/2 activation, CHO/rNTS2 cells were pretreated or not with PAO (10 μM) or MDC (400 μM) and stimulated for 5 min with 100 nM NT, levocabastine, or SR48692. PAO and MDC both completely inhibited the effect of stimulation by either ligand on ERK1/2 phosphorylation, as measured by Western blotting (Fig. 4.7*A*).

The effect of stimulation with SR48692 on ERK1/2 activation was also verified by immunofluorescence in CHO/rNTS2 cells, using antibodies against phosphorylated ERK1/2. As ooposed to nonstimulated cells, which were immunonegative (Figs. 4.6*D*,*G*, and 4.7*B*), cells stimulated for 5 min with SR48692 (100 nM) exhibited intense phosphorylated ERK1/2 immunoreactivity, mainly within their nucleus (Fig. 4.7*B*, *arrowheads*). This induction of phosphorylated ERK1/2 immunoreactivity was totally prevented by preincubating the cells with PAO (Fig. 4.7*B*).

To further confirm that the NTS2-induced ERK1/2 activation was dependent on ligand-induced internalization, CHO/rNTS2 cells were transiently transfected with a dominant-negative mutant of dynamin 1, DynK44A, together with the fluorescent protein EGFP (with a ratio of 10:1), to distinguish DynK44A-expressing from -nonexpressing cells. Stimulation of these dually transfected cells with 100 nM SR48692 increased phosphorylated ERK1/2 immunofluorescence in approximately 40% of the cells (Fig. 4.6, *E* and *H*), whereas 100% of the cells expressing only the rNTS2 receptor were activated after stimulation with SR48692 (Fig. 4.7*B*). This decrease was caused by the overexpression of the dynamin 1 dominant-negative mutant, because none of the cells confirmed to overexpress DynK44A, by virtue of their co-expression of EGFP, showed phosphorylated ERK1/2 immunofluorescence (Fig. 4.6, *F* and *I*, *arrows*).

4.5 DISCUSSION

The present study demonstrates that neurotensin activates the mitogen-activated protein kinase cascade through its interaction with either rat or human NTS2 receptors in transfected CHO cells. It also suggests that ligand-induced internalization of this receptor is required for NTS2-mediated signaling.

We previously demonstrated that stimulation of rat cerebellar granule cells, which endogenously express the NTS2 receptor, with either NT or levocabastine resulted in ERK1/2 activation (Sarret et al., 2002). These results differed from those obtained by other groups that had reported antagonistic or inverse agonistic effects of these two drugs on the human NTS2 receptor heterologously expressed in COS (Richard et al., 2001b) and CHO cells (Vita et al., 1998), respectively. A first objective of the present study was therefore to determine whether these discrepancies were caused by species differences or by endogenous versus heterologous expression of the NTS2 receptor. For this purpose, we first established a stable cell line of CHO cells expressing the rat NTS2 receptor (CHO/rNTS2 cells). RT-PCR analysis confirmed that these cells did express the NTS2 receptor, to the exclusion of the NTS1. ^{125}I-NT was accordingly found to bind to these cells with a pharmacology characteristic of that of NTS2, both in terms of affinity for NT and of relative affinity for the NT analogs levocabastine, NN, and SR48692 (Chalon et al., 1996; Mazella et al., 1996; Botto et al., 1998; Vita et al., 1998; Sarret et al., 2002).

We then tested the effects of NT and of various NT analogs on the mobilization of $[Ca^{2+}]_i$ in these transfected cells. As previously reported for cortical cerebellar neurons endogenously expressing the rat NTS2 receptor (Sarret et al., 2002), or for transfected CHO cells expressing the human NTS2 receptor (Vita et al., 1998), neither NT, levocabastine, nor NN affected Ca^{2+} mobilization in CHO/rNTS2 cells. By contrast, incubation with the NTS1 antagonist SR48692 caused a marked elevation of intracellular calcium in the same cells. This increase conformed to earlier reports of SR48692-induced Ca^{2+} mobilization in CHO cells transfected with either human (Vita et al., 1998) or rat (Yamada et al., 1998) NTS2 receptors.

However, whereas in these previous studies the effects of SR48692 were antagonized by concomitant administration of an excess of NT, NN, or levocabastine and could not be elicited in nontransfected cells, in the present study, the effects of SR48692 were not blocked by NT, NN, or levocabastine and were equally strong in nontransfected cells, suggesting that they were not mediated by NTS2. Likewise, in rat cerebellar granule cells, SR48692 induced a robust $[Ca^{2+}]_i$ increase that was unaffected by concomitant application of NT or levocabastine and was therefore interpreted as being NTS2-independent (Sarret et al., 2002).

We then sought to determine whether NT activated ERK1/2 in transfected CHO/rNTS2 cells as in rat cerebellar granule cells (Sarret et al., 2002). Application of 100 nM NT to CHO/rNTS2 cells induced a robust, dose-dependent increase in ERK1/2 phosphorylation. This activation was rapid and sustained over 60 min. It also was mediated by NTS2, because it could not be elicited in nontransfected cells. The similarity of these findings with those obtained in neurons in culture (Sarret et al., 2002) suggests that the observed activation is physiological and not caused by artifactitious coupling of the receptor subsequent to its aberrant expression in CHO cells.

Levels of ERK1/2 activation comparable with those obtained after stimulation with NT were achieved by incubating CHO/rNTS2 cells with either NN or levocabastine. That these two drugs would display effects comparable with those of NT is congruent with results in X. *laevis oocytes*, which showed that NT, NN, and levocabastine all stimulated to the same extent an NTS2-mediated Ca^{2+}-activated inward Cl^- current (Mazella et al., 1996; Botto et al., 1997c; Dubuc et al., 1999b). However, the present results differ from those of Vita et al. (1998), who found no effect of NT, NN, or levocabastine on ERK1/2 activation in CHO cells transfected with the human NTS2 receptor. To determine whether this discrepancy was related to species differences, we repeated the experiments in CHO cells transfected with hNTS2 in lieu of rNTS2. Our results showed the same NTS2-mediated activation of ERK1/2 phosphorylation in cells transfected with the human plasmid as in cells transfected with the rNTS2, suggesting that the differences between the present and

earlier results are not the result of differences between rat and human NTS2 but rather of variations in the sensitivity of the methods employed for the detection of ERK1/2 phosphorylation.

Stimulation with the NTS1 antagonist SR48692 also resulted in a marked increase in ERK1/2 activation in both CHO/rNTS2 and CHO/hNTS2 cells. Unlike the effects of SR48692 on Ca^{2+} mobilization, these effects were mediated by NTS2, because they were not observed in nontransfected CHO cells. Previous studies have reported on the agonistic properties of SR48692 on both rodent (Botto et al., 1997c; Yamada et al., 1998) and human (Vita et al., 1998) NTS2. Surprising here was the fact that, although SR48692 displayed a much lower affinity than NT, NN, or levocabastine for the NTS2 receptor (present study; Gully et al., 1993; Mazella et al., 1996; Botto et al., 1998; Vita et al., 1998; Yamada et al., 1998; Nouel et al., 1999; Richard et al., 2001b; Sarret et al., 2002), it induced ERK1/2 phosphorylation much more efficiently (~7-fold more efficient than NT in cells transfected with the rat receptor). To determine whether this discrepancy could be explained by the binding of SR48692 to a site distinct from the target of NT or its analogs, we repeated the SR48692 stimulation experiments in the presence of 100 nM NT. Despite its higher affinity for the receptor, NT had no competitive inhibiting effect on the SR48692-induced ERK1/2 activation, suggesting that the two drugs interact with different binding pockets as they do on the NTS1 receptor (Labbé-Jullié et al., 1995; Barroso et al., 2000).

Immunofluorescent studies confirmed that stimulation of CHO/rNTS2 cells with SR48692 produced a robust increase in phosphorylated ERK1/2 levels. Furthermore, they demonstrated that this increase mainly occurred in the nucleus, suggesting that some of the targets of activated ERK1/2 may be transcription factors such as Elk-1, Ets, Stat1/3, or c-Myc/N-Myc and, by extension, that the activation of the NTS2 receptor results in the modulation of gene expression.

It was recently shown that in COS-7 cells transfected with the human NTS2 receptor, the receptor was constitutively active and that NT and levocabastine behave as a neutral antagonist and inverse agonist, respectively, on the production of inositol phosphate (Richard et al., 2001b). By contrast, the present NT- or levocabastine-induced effects on ERK1/2 phosphorylation are unlikely to be caused by neutral antagonistic or inverse agonistic properties of the drugs, because there was no evidence of constitutive NTS2 receptor activity in our system. Indeed, no difference was observed between the basal phosphorylation level of ERK1/2 in CHO/rNTS2 and in nontransfected CHO cells. Furthermore, had NT or levocabastine acted as inverse agonists, they should not, as they did, have increased phosphorylation of ERK1/2 to levels higher than those measured in nontransfected cells.

As previously demonstrated for mouse and human NTS2 receptors in transfected cells (Botto et al., 1998; Martin et al., 2002b) and for rat NTS2 receptors in cerebellar granule cells (Sarret et al., 2002), stimulation of rat NTS2 receptors heterologously expressed in CHO cells resulted in a ligand-induced internalization of receptor-ligand complexes. This effect was inhibited by the endocytosis inhibitor phenylarsine oxide, suggesting that it was mediated by clathrin, as documented for most G protein-coupled receptors (Kranenburg et al., 1999; Pierce et al., 2000; Miller and Lefkowitz, 2001; Claing et al., 2002). That a fluorescent analog of NT was able to induce NTS2 internalization is consistent with its agonistic role at the NTS2 receptor.

It is now well documented that seven transmembrane domain/G protein-coupled receptors may activate ERK1/2 via G protein-independent mechanisms, involving interaction of the receptor with endocytic proteins such as dynamin (Kranenburg et al., 1999; Pierce et al., 2000) and -arrestins (Miller and Lefkowitz, 2001; Claing et al., 2002). In the present study, we found that blocking receptor internalization with phenylarsine oxide or monodansylcadaverine completely impaired the ability of NT, as well as of all other NTS2 agonists tested, to activate ERK1/2 in CHO/rNTS2 cells. Furthermore, overexpression of DynK44A, a dominant-negative mutant form of

dynamin 1, was found to selectively inhibit SR48692-induced ERK1/2 activation in cells dually expressing the NTS2 and the dominant-negative mutant. These results strongly suggest that the activation of the mitogen-activated protein kinase pathway (involving either NTS2 itself or other cell surface receptors) is predicated on the internalization of receptor-ligand complexes via a dynamin-dependent and G_i protein-independent mechanism.

In conclusion, the present results reveal that NT, as well as many of the known NTS2 receptor ligands, act as agonists at this site, at least as pertains to the promotion of ERK1/2 phosphorylation. This finding is important in that it lends further support to the premise that NT is an endogenous ligand at this receptor. It also suggests that NTS2-acting NT analogs may constitute a promising new class of nonopioid analgesic drugs, provided that these drugs do not, as does SR48692, exert other actions (e.g., NTS1 antagonism and NTS2-independent induction of Ca^{2+} mobilization). Indeed, recent studies have demonstrated that NT, but not SR48692 (Dubuc et al., 1994), induces antinociceptive effects in the mouse through interaction with NTS2 as well as with NTS1 receptors (Dubuc et al., 1999b; Tyler et al., 1999; Pettibone et al., 2002; Yamauchi et al., 2003a). An intriguing observation is that the sustained, NTS2-mediated activation of ERK1/2 documented here seems to be exerted to the exclusion of other signaling systems. Thus, stimulation of NTS2 does not seem to induce Ca^{2+} mobilization (present study; Sarret et al., 2002) or cAMP or cGMP production (Chalon et al., 1996; Botto et al., 1998). Further studies will obviously be needed to determine how diverse NTS2-mediated signals truly are and whether some account, in contrast to those reported here, for short-term NT signaling.

4.6 ACKNOWLEDGEMENTS

We are grateful to Dr. Stephen S. Ferguson for the pcDNA1-DynK44A construction, Dr. Jean-Pierre Vincent for Fluo-NT, and Lyne Bilodeau for her technical assistance with Ca^{2+} imaging.

4.7 FOOTNOTES

This work was supported by a grant from the Canadian Institutes of Health Research (CIHR) awarded to Alain Beaudet. Louis Gendron was funded by fellowship from CIHR, and Amélie Perron and Philippe Sarret were funded by fellowships from the Fonds de la Recherche en Santé du Québec. Presented in part at the 33rd Annual Meeting for The Society for Neuroscience; 2003 Nov 8-12; New Orleans, LA: Gendron L, Sarret P, Perron A, Gallo-Payet N, Payet MD, and Beaudet A (2003) The rat NTS2 neurotensin receptor is functionally coupled to extracellular signal-regulated protein kinases (ERK1/2) by an internalization dependent-mechanism. Soc Neurosci Abstr 29: 161.3

4.8 ABBREVIATIONS

NT, neurotensin; ERK1/2, extracellular signal-regulated kinases 1/2; SR48692, 2-{[1-(-7-chloroquinolin-4-yl)-5-(2,6-dimethoxy-phenyl)-1*H*-pyrazole-3-carbonyl]amino}adamantane-2-carboxylic acid; Levo, levocabastine; CHO, Chinese hamster ovary; COS, *Cercopithecus aethiops*; NN, neuromedin N; DMEM, Dulbecco's modified Eagle's medium; FBS, fetal bovine serum; G-418, geneticin; MDC, monodansylcadaverine; PAO, phenylarsine oxide; PTX, pertussis toxin; PVDF, polyvinylidene difluoride; Fluo-NT, *Nα*-BODIPY-neurotensin-(2-13); PCR, polymerase chain reaction; BSA, bovine serum albumin; bp, base pair(s); PBS, phosphate-buffered saline; DMSO, dimethyl sulfoxide; ANOVA, analysis of variance; RT-PCR, reverse transcription-polymerase chain reaction; EGFP, enhanced green fluorescent protein.

4.9 FIGURES

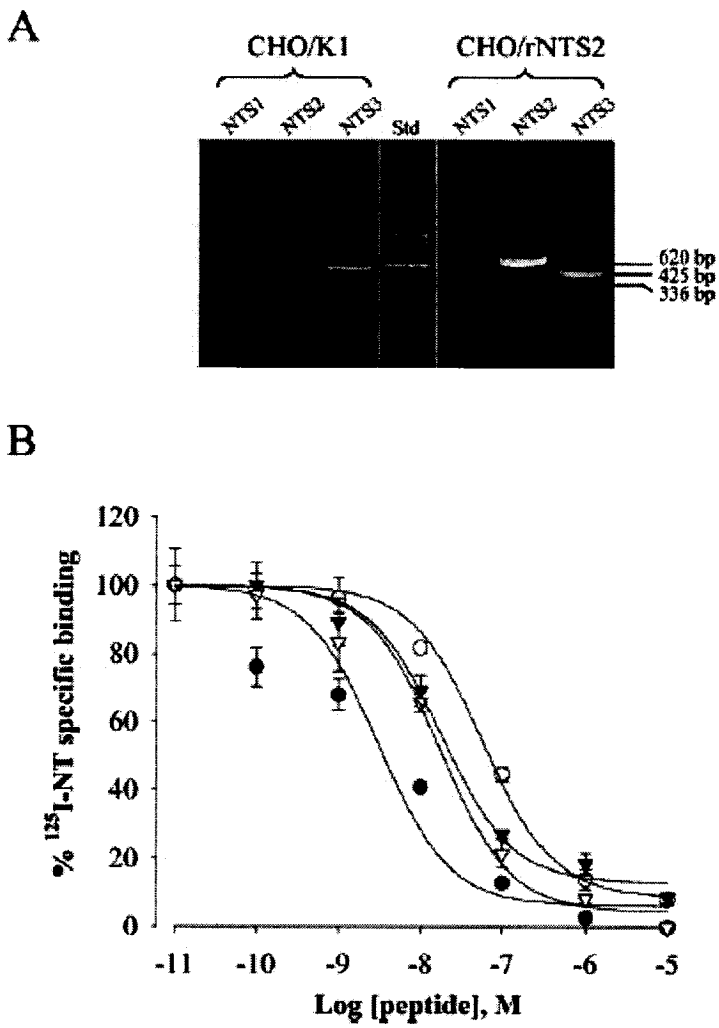

Figure 4.1

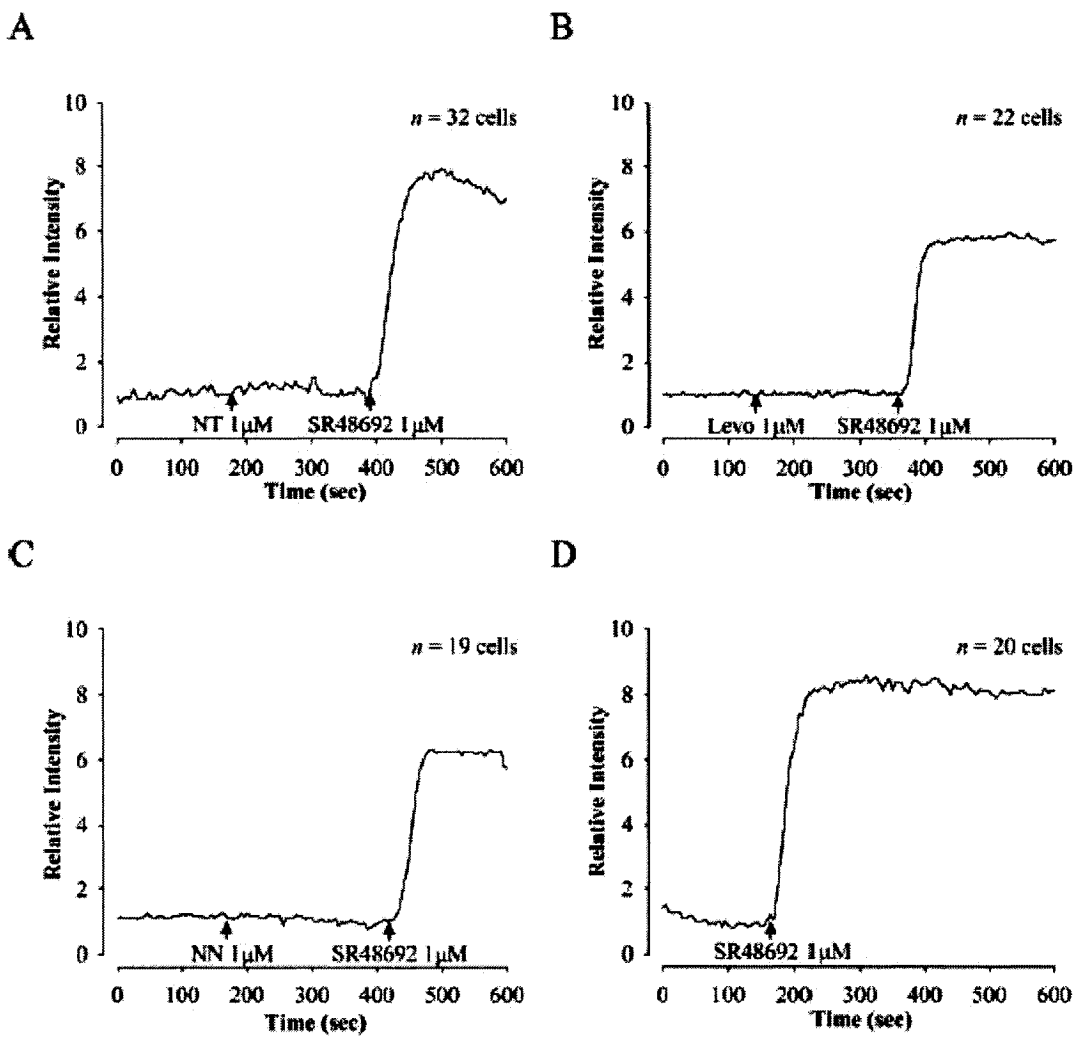
A
B
C
D
n = 32 cells
n = 22 cells
n = 19 cells
n = 20 cells
Relative Intensity
Time (sec)
NT 1μM
SR48692 1μM
Levo 1μM
NN 1μM

Figure 4.2

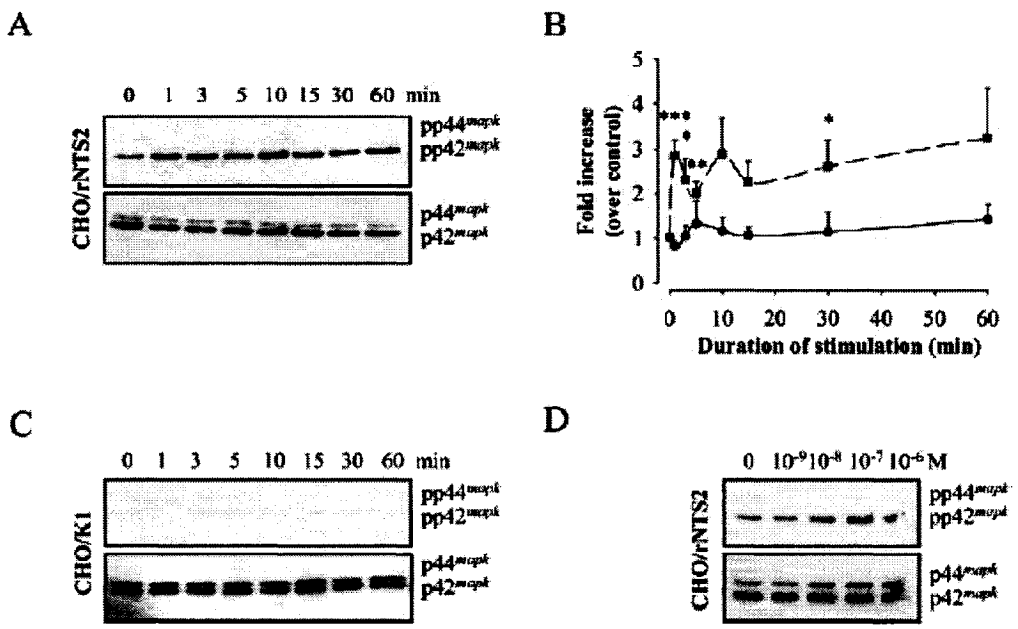
A
0 1 3 5 10 15 30 60 min
CHO/rNTS2
pp44mapk
pp42mapk
p44mapk
p42mapk
B
Fold increase (over control)
Duration of stimulation (min)
C
0 1 3 5 10 15 30 60 min
CHO/K1
D
0 10-9 10-8 10-7 10-6 M
CHO/rNTS2

Figure 4.3

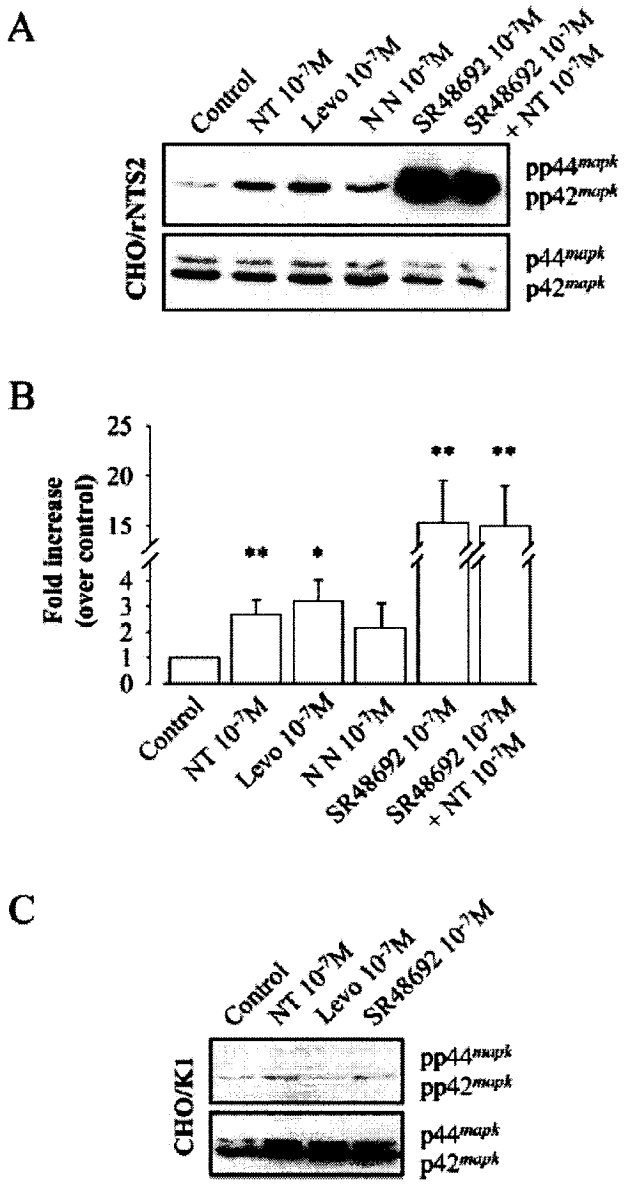
A
Control
NT 10-7M
Levo 10-7M
N N 10-7M
SR48692 10-7M
SR48692 10-7M + NT 10-7M
CHO/rNTS2
pp44mapk
pp42mapk
p44mapk
p42mapk
B
Fold increase (over control)
25
20
15
4
3
2
1
0
**
*
**
**
Control
NT 10-7M
Levo 10-7M
N N 10-7M
SR48692 10-7M
SR48692 10-7M + NT 10-7M
C
Control
NT 10-7M
Levo 10-7M
SR48692 10-7M
CHO/K1
pp44mapk
pp42mapk
p44mapk
p42mapk

Figure 4.4

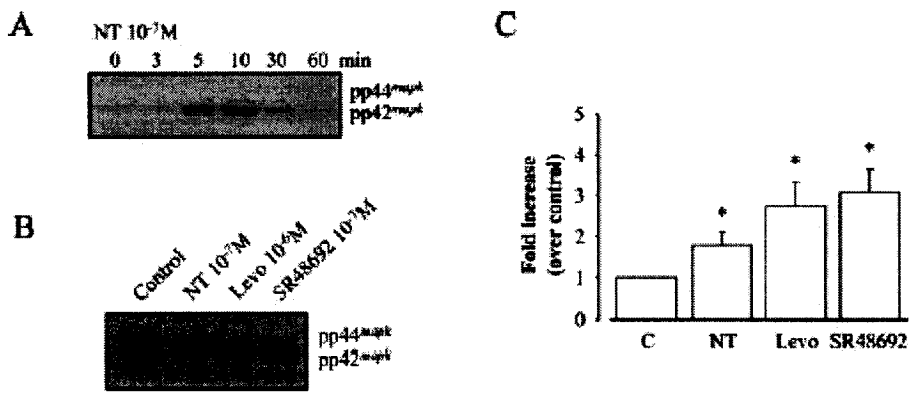
A
NT 10⁻⁷M
0 3 5 10 30 60 min
pp44mapk
pp42mapk
B
Control
NT 10⁻⁷M
Levo 10⁻⁶M
SR48692 10⁻⁷M
pp44mapk
pp42mapk
C
Fold increase (over control)
0
1
2
3
4
5
C
NT
Levo
SR48692

Figure 4.5

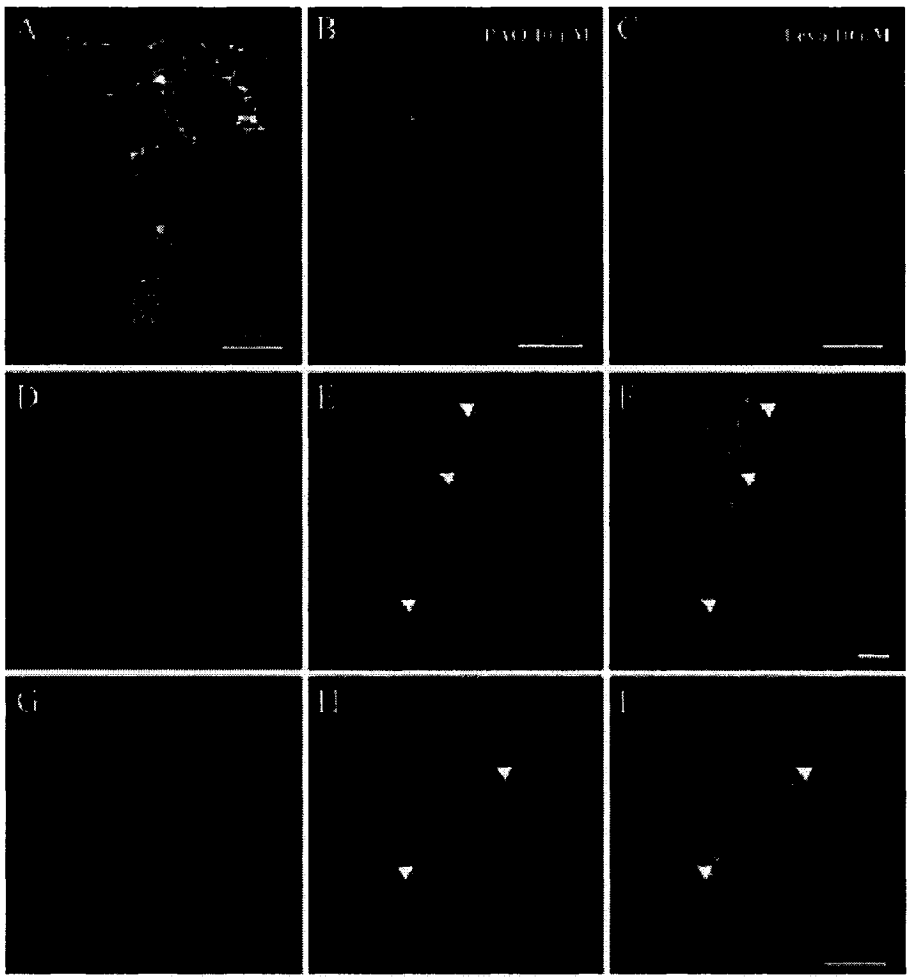

Figure 4.6

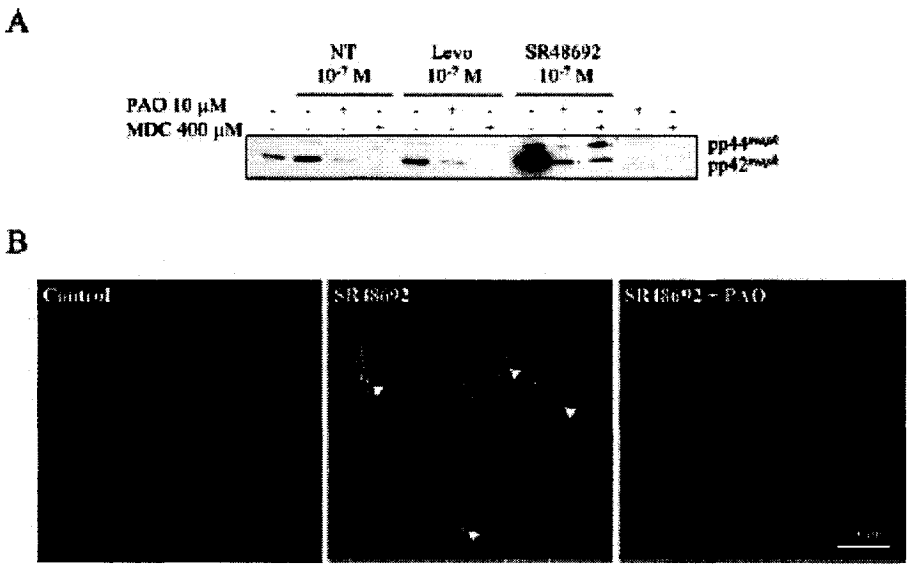
A
NT
10⁻⁷ M
Levo
10⁻⁷ M
SR48692
10⁻⁷ M
PAO 10 µM
MDC 400 µM
B
Control
SR48692
SR48692 + PAO

Figure 4.7

4.10 FIGURE LEGENDS

Fig. 4.1: Expression and Binding Properties of the rNTS2 Receptor Transfected in CHO Cells. *A*, RT-PCR analysis of nontransfected CHO cells (CHO/K1) and CHO cells transfected with the rat NTS2 receptor cDNA (CHO/rNTS2). In CHO/K1 cells, a single band of the size expected for the NTS3 receptor fragment (425 bp) is visible. By contrast, in CHO/rNTS2 cells, a band the size of the rNTS2 receptor fragment (620 bp) is amplified in addition to rNTS3. Neither cell type expressed the rNTS1 receptor (expected size of the rNTS1 receptor fragment is 336 bp). ***B***, competition inhibition of ^{125}I-NT (2 nM) binding to CHO/rNTS2 cells by neurotensin (●), levocabastine (○), neuromedin N (▽), or SR48692 (▼). Each point is the mean of two separate experiments performed in triplicate (mean ± S.D.).

Fig. 4.2: Intracellular Ca^{2+} Mobilization in Fluo-4-loaded CHO Cells. ***A-C***, application of 1 μM SR48692 to CHO/rNTS2 cells induces an increase, followed by a plateau, in intracellular Ca^{2+}. By contrast, no increase in intracellular Ca^{2+} is observed after 1 μM NT, 1 μM Levo, or 1 μM NN, nor are any of these drugs able to prevent the Ca^{2+} mobilization effect of SR48692. ***D***, same type of SR48692-induced response observed in CHO/K1 cells (nontransfected cells). The curves represent the means of *n* responding cells and five experiments.

Fig. 4.3: NT Activation of ERK1/2 in rNTS2-transfected CHO Cells. CHO/rNTS2 (*A*, *B*, and *D*) and CHO/K1 (*C*) cells were stimulated with various concentrations of NT (*D*) for 0 to 60 min (*A-C*), and ERK1/2 phosphorylation levels were determined as described under *Materials and Methods*. *A*, *C*, and *D*, top, phosphorylated ERK1/2; bottom, total ERK1/2. ***A***, stimulation of CHO/rNTS2 cells with 100 nM NT induces a rapid and sustained activation of ERK1/2. ***B***, densitometric measurements of ERK1/2 activation (phosphorylated ERK1/2 over total ERK1/2) expressed as -fold increase over control ± S.E.M. (●, CHO/K1, $n = 3$; ■, CHO/rNTS2, $n = 4$) (ANOVA and Dunnett's). *, $p < 0.05$; **, $p < 0.02$; and ***, $p < 0.01$ compared with control, untreated cells. ***C***, stimulation of wild-type, nontransfected CHO cells with 100 nM NT has no effect on ERK1/2

phosphorylation. ***D***, dose-dependent activation of ERK1/2 after application of 10^{-9} to 10^{-6} M NT for 5 min (representative of two independent experiments).

Fig. 4.4: Effect of NT, Levocabastine, Neuromedin N, and SR48692 on ERK1/2 Phosphorylation in CHO/rNTS2. CHO/rNTS2 (*A* and *B*) and CHO/K1 (*C*) cells were treated or not for 5 min with a battery of NTS2 agonists and harvested for the determination of ERK1/2 phosphorylation levels as described under *Materials and Methods*. NT (100 nM), Levo (100 nM), NN (100 nM), and SR48692 (100 nM) all induce ERK1/2 phosphorylation in CHO/rNTS2 cells (***A***) but not in CHO/K1 cells (***C***). Note that ERK1/2 phosphorylation levels are markedly higher in cells stimulated with SR48692 than with other drugs, an effect that is not modified by coincubation with NT (100 nM). ***B***, densitometric measurements of ERK1/2 activation (phosphorylated ERK1/2 over total ERK1/2) expressed as -fold increase over control ± S.E.M. (n = 3) (ANOVA and Dunnett's). *, $p < 0.1$ and **, $p < 0.05$ compared with control, untreated cells.

Fig. 4.5: Effect of NT, Levocabastine, and SR48692 on ERK1/2 Phosphorylation in CHO/hNTS2 cells. CHO/hNTS2 cells were treated or not for 0 to 60 min with 100 nM NT (***A***) or for 5 min with a battery of NTS2 agonists (***B***) and harvested for the determination of ERK1/2 phosphorylation levels as described under *Materials and Methods*. *C*, densitometric measurements of ERK1/2 activation expressed as -fold increase over control ± S.E.M. (n = 5-7) (ANOVA and Dunnett's). *, $p < 0.001$ compared with control, untreated cells. NT (100 nM), Levo (1 μM), and SR48692 (100 nM) all induce ERK1/2 phosphorylation in CHO/hNTS2 cells.

Fig. 4.6: Role of NTS2 Receptor Internalization in Ligand-induced ERK1/2 Activation. *A-C*, CHO/rNTS2 cells incubated with 50 nM Fluo-NT for 30 min at 37°C and examined by confocal microscopy. ***A***, punctate Fluo-NT labeling is evident throughout the cytoplasm of CHO/rNTS2 cells; ***B***, Fluo-NT labeling is confined to the periphery of the cells in CHO/rNTS2 cells preincubated with the endocytosis inhibitor PAO (10 μM); ***C***, Fluo-NT labeling is specific and receptor-mediated, because the labeling is completely abolished by an excess of levocabastine

(10 μM). Images were acquired using the same parameters and represent three different experiments. ***D-I***, CHO/rNTS2 cells transfected with a 10:1 ratio of dynamin 1 (DynK44A) and pEGFP and processed for immunofluorescence detection of phosphorylated ERK1/2. Because of the transfection ratio, most of the EGFP-positive cells (green) can be assumed to express DynK44A. *D* and *G*, basal level of phosphorylated ERK1/2 immunoreactivity in nontreated cells. *E-H*, phosphorylated ERK1/2-immunoreactive signal is evident within the nucleus of a subpopulation of NTS2-expressing cells after 5-min exposure to 100 nM SR48692. *F* and *I*, in merged images of phosphorylated ERK1/2- and EGFP-labeled fields, all EGFP-positive (e.g., DynK44A-expressing) cells (*white arrows*) are phosphorylated ERK1/2-immunonegative, indicating that internalization blockade prevents ERK1/2 activation (representative of three different experiments).

Fig. 4.7: Inhibitors of Internalization Block NT-Induced ERK Activation. ***A*** (Western Blot analysis), 30-min preincubation with PAO (10 μM) or MDC (400 μM), two endocytosis inhibitors, prevents NT-, Levo-, and SR48692-induced ERK1/2 phosphorylation (5 min of stimulation) in CHO/rNTS2 cells. Immunoblots represent three different experiments. ***B*** (immunofluorescence labeling), 30-min preincubation with PAO (10 μM) prevents immunofluorescence labeling of phosphorylated ERK1/2 in rNTS2-transfected CHO cells treated (100 nM SR48692) for 5 min. Note that ERK1/2 phosphorylation is evident in all cells and that phosphorylated ERK1/2 preferentially accumulates into the nucleus (*arrowheads*). All images were acquired using the same parameters and represent two different experiments.

CHAPTER 5

IDENTIFICATION AND FUNCTIONAL CHARACTERIZATION OF THE 5-TRANSMEMBRANE DOMAIN VARIANT ISOFORM OF THE NTS2 NEUROTENSIN RECEPTOR IN RAT CENTRAL NERVOUS SYSTEM

Amélie Perron, Philippe Sarret[¶], Louis Gendron, Thomas Stroh, and Alain Beaudet

Montreal Neurological Institute, Department of Neurology and Neurosurgery, McGill University, Montreal, Québec, Canada

[¶]Present Address: Department of Physiology and Biophysics, Faculty of Medicine, Sherbrooke, Québec, Canada

Journal of Biological Chemistry (2005) **280**: 10219-10227.

5.1 ABSTRACT

The present study demonstrated that alternative splicing of the rat nts2 receptor gene generates a 5-transmembrane domain variant isoform (vNTS2) that is co-expressed with the full-length NTS2 receptor throughout the brain and spinal cord, as evidenced by reverse transcription-PCR. The vNTS2 polypeptide is 281 amino acids in length, which is 135 amino acids shorter than the full-length isoform. Immunohistochemical and radioligand binding studies revealed that the HA-tagged recombinant vNTS2 receptor is poorly targeted to plasma membranes in transfected COS-7 cells. Binding studies also showed that the truncated receptor displayed a 5000-fold lower affinity for neurotensin (NT) than its full-length counterpart (IC_{50} of 10 μM and 2 nM, respectively). Yet NT binding induced efficient internalization of receptor-ligand complexes in vNTS2-transfected cells. Furthermore, it produced a rapid (<5 min) activation of the mitogen-activated protein kinases (ERK1/2) pathway, indicating functional coupling of the variant receptor. This activation is sustained (>1 h) and is also produced by the NTS2 agonist levocabastine. Western blotting experiments suggested that vNTS2 is not expressed in monomeric form in the rat central nervous system. However, it does appear to form a variety of multimeric complexes, including homodimers and heterodimers, with the full-length NTS2. Indeed, co-immunoprecipitation studies in dually transfected cells demonstrated that the two receptor isoforms can form stable associations. Taken together, the present results indicated that the rat vNTS2 is a functional receptor that may play a role in NT signaling in mammalian central nervous system.

5.2 INTRODUCTION

The tridecapeptide neurotensin (NT) produces a wide array of biological responses when administered peripherally or in the central nervous system (CNS). NT effects include analgesia (Nemeroff et al., 1979; Kalivas et al., 1982a), hypothermia (Martin et al., 1980), antipsychosis (Kinkead and Nemeroff, 1994), catalepsy (Snijders et al., 1982), and change in blood pressure (Rioux et al., 1981). NT is also known for its regulatory role on midbrain dopaminergic and basal forebrain cholinergic neurons (St-Gelais et al., 2004; Cape et al., 2000), and cumulative evidence has implicated the NT system in the pathophysiology of schizophrenia (Binder et al., 2001a).

NT signaling is mediated by interaction of the peptide with either one of three different receptor subtypes, referred to as NTS1, NTS2, and NTS3. NTS1 and NTS2 belong to the family of seven transmembrane-spanning, G protein-coupled receptors (GPCRs) and exhibit high and low affinity for NT, respectively (Tanaka et al., 1990; Chalon et al., 1996). The NTS3 receptor is a single transmembrane domain sorting receptor with 100% homology to gp95/sortilin (Petersen et al., 1997, Mazella et al., 1998). NTS1 is predominantly coupled to $G_{q/11}$ (Hermans et al., 1998; Vincent et al., 1999) and activates phospholipase C (Hermans et al., 1992; Chabry et al., 1994). Pharmacological and biochemical studies have indicated that NTS1 is also involved in the modulation of intracellular levels of cGMP (Amar et al., 1985), cAMP (Bozou et al., 1989a; Yamada et al., 1993), inositol phosphates (Watson et al., 1992; Bozou et al., 1989b), and extracellular signal-regulated kinases (ERK1/2) (Poinot-Chazel et al., 1996). Much less is known about the signaling pathways of NTS2. Stimulation of NTS2 was found to induce Ca^{2+}-dependent chloride currents in *Xenopus* oocytes expressing the mouse receptor (Botto et al., 1997c). More recent studies have shown that stimulation of NTS2 with either NT or the selective NTS2 ligand, levocabastine, activates the ERK1/2 cascade both in CHO cells stably transfected with cDNA encoding rat or human NTS2 (Gendron et al., 2004) or in cultured rat cerebellar granule cells (Sarret et al., 2002).

The cDNA sequence of the mouse NTS2 receptor is composed of four exons separated by three introns (Sun et al., 2001). The first exon encodes the region containing TM domains 1-4, whereas exons 2-4 encode the region containing TM 5-6, TM 6, and TM 7, respectively. The existence of a deletion-type NTS2 mRNA encoding a C-terminally truncated form of the receptor, which lacks an internal 181-bp sequence, has been reported in the mouse (Botto et al., 1997b). Both mouse NTS2 mRNA isoforms are derived from a single *nts2* gene, the short form resulting from alternative splicing of the primary NTS2 transcript at intron 2a (Sun et al., 2001). The corresponding truncated NTS2 mRNA encodes a 282-amino acid protein (Botto et al., 1997b).

Other GPCRs encoding sequences have been shown to similarly generate truncated receptor isoforms through alternative splicing, exon skipping, or intron retention (Kilpatrick et al., 1999). Many of these splice variants, such as the truncated forms of the prostanoid receptor EP_3 and endothelin B receptor (Namba et al., 1993; Nambi et al., 2000), differ from their full-length counterparts in their intracellular C-terminal tail. Others show a disparity in the third intracellular loop (e.g. the D_2 dopamine receptor variant (Monsma et al., 1989)) or in the transmembrane (TM) domains (e.g. the D_3nf dopamine receptor isoform (Schmauss et al., 1993)). Yet others differ from the full-length receptor in their extracellular N-terminal loop as exemplified by the truncated form of the angiotensin II receptor (Nishimatsu et al., 1994).

Splice variations may have little or no effect on ligand binding properties (Minneman, 2001). However, some deletions, particularly in TM domains, were shown to have significant impact on ligand recognition. For example, a short variant of the 5-hydroxytryptamine 2C receptor lacking TM domains 6 and 7 was reported to be totally devoid of serotonergic binding activity (Canton et al., 1996). Similar findings were also found for the truncated endothelin A (Zhang et al., 1998) and D_3nf dopamine (Schmauss et al., 1993) isoforms. Shortened receptor isoforms may also display aberrant or impaired coupling, even in the face of normal ligand binding. For instance, the four alternatively spliced isoforms of the EP_3 receptor, which vary only

in their C-terminal tails, couple to different G proteins and activate diverse second messenger systems (Namba et al., 1993).

The generation of alternatively spliced GPCRs may also affect the function of their full-length counterparts. Thus, co-expression of the full-length gonadotropin-releasing hormone receptor together with that of its C-terminally truncated isoform, which is incapable of ligand binding and signal transduction, was found to impair targeting of the full-length receptor to the plasma membrane (Grosse et al., 1997). Finally, alternative splicing of GPCRs has been associated with a number of genetic disorders (Grabowski and Black, 2001). For instance, splice variants of the growth hormone-releasing hormone receptors have been documented in primary human prostate carcinomas and diverse human cancer cell lines (Rekasi et al., 2000).

This study was initiated to determine whether the splice variant form of the NTS2 receptor originally identified in mouse brain extracts was also expressed in rat brain and to investigate the binding, internalization, and signaling properties of this receptor isoform, as compared with those of the full-length NTS2 receptor, in mammalian cells. Our results demonstrate the existence of a functional 5-TM domain variant form of NTS2 (vNTS2) in rat brain and suggest that this truncated receptor may play a role in the modulation of NT effects in the CNS.

5.3 EXPERIMENTAL PROCEDURES

5.3.1 Expression of Rat vNTS2 mRNA

In order to assess the expression of vNTS2 mRNA in rat CNS and spinal cord, adult male Sprague-Dawley rats (200–250 g; Charles River Breeding Laboratories, St-Constant, Québec, Canada) were killed by decapitation. The brain and spinal cord were rapidly removed, and the areas of interest were dissected on ice. Samples were solubilized in lysis buffer (4 M guanidinium thiocyanate, 0.01 M Tris-HCl, pH 7.5, 0.97% β-mercaptoethanol), and total RNA was extracted using the SV RNA Isolation System kit (Promega, Madison, WI), according to the manufacturer's instructions. These total mRNAs (2 μg) were then reverse-transcribed at 42°C for 1 h using the Reverse Transcription System kit (Promega, Madison, WI). First strand cDNAs were subjected to 35 cycles of PCR in a final reaction volume of 50 μl of reaction buffer (50 mM KCl, 10 mM Tris-HCl, pH 9.0, 1.5 mM $MgCl_2$, 0.1% Triton X-100, 0.02% bovine serum albumin (BSA), 200 μM dNTPs, 0.5 unit of *Taq* DNA polymerase) using a set of primers (5'-GAATGTGCTGGTGTCCTTCGC-3' and 5'-ACT-TGTATTTCTCCCAGGCTG-3') derived from bases 667–1287 in the sequence reported previously (Chalon et al., 1996) for the rat NTS2 receptor. The oligonucleotides used are flanking the region where the deletion occurs in the mouse vNTS2 receptor (Botto et al., 1997b) and allow the amplification of fragments of predicted sizes of 620 and 439 bp, as demonstrated previously (Sarret et al., 2002) in rat cerebellar granule cell cultures. As internal standard for semi-quantitative analysis, the housekeeping gene glyceraldehyde-3-phosphate dehydrogenase (GAPDH) was concurrently amplified using primers 5'-CAAGATTGTCAG-CAATGCAT-3' (sense, nucleotides 511–530) and 5'-CTTGATGTCATCATAC-TTGGC-3' (antisense, nucleotides 856 to 836), which target a 346-bp sequence in the rat GAPDH gene.

The ratios of NTS2 over GAPDH mRNAs and between the NTS2 receptor isoforms were determined by densitometry, using NIH Scion Image Software. Calculations and statistical analyses were performed using Excel 2000 (Microsoft) and Prism 3.02 (Graph Pad Software). Statistical analyses were performed using a

one-way analysis of variance (Bonferroni's multiple comparison test). Total RNA samples were subjected to reverse transcription in the absence of the enzyme to control for intrinsic contamination by genomic DNA, and the reaction was performed without RNA to control for contamination during the experiment.

5.3.2 Gene Constructs

The HA-tagged cDNA encoding the rat variant NTS2 receptor was obtained through reverse transcription of vNTS2 mRNA isolated from rat brain by PCR using nucleotides (5'-ACAGAGATGGCATACCCATACGACGTCCCAGACTACGCTG-AGACCAGCAGTCCGTGG-3') and (5'-TCATACTTGTATTTCTCCCAGGCT-3') as sense and antisense primers, respectively. The former contains the HA tag sequence followed by the 44–61-bp sequence of the rat NTS2 receptor mRNA (Chalon et al., 1996), whereas the latter corresponds to the sequence 1268–1291 bp of the open reading frame of the rat *nts2* receptor gene. The predicted sizes of the amplified fragments were 1.6 kb for the full-length NTS2 and 1.4 kb for the spliced variant form of the receptor. Fidelity of PCR amplification was confirmed by DNA sequence analysis using the ABIPRISM® 3100 Genetic Analyzer in the MOBIX laboratory (McMaster University, Hamilton, Ontario, Canada). The PCR product corresponding to vNTS2 was purified from a 1% low melting agarose gel and subcloned into the pTargeT expression vector (Promega, Madison, WI).

5.3.3 Cell Culture and Transfections

For MAPK kinase activity and radioligand binding experiments, CHO and COS-7 cells were stably transfected with the *HA*-vNTS2 construct. Briefly, cells were maintained at 37°C in a 5% CO_2 atmosphere in Dulbecco's modified Eagle's medium (DMEM) F-12 and DMEM with high glucose, respectively, supplemented with 5% fetal bovine serum in the presence of 100 units/ml penicillin/streptomycin (Invitrogen). Cells were grown in 100-mm dishes to 70–80% confluence and transfected with 4 μg of the *HA*-vNTS2-pTargeT plasmid by using the Lipofectamine™ transfection reagent (Invitrogen) according to the manufacturer's instructions. After 72 h at 37°C, positive cells were selected with a FACSVantage cell sorter (BD Biosciences) following sequential labeling with a mouse monoclonal

antibody (clone 12CA5) directed toward the HA epitope (1/500; Roche Applied Science) and Alexa 488-conjugated goat anti-mouse antibody (1/1000; Molecular Probes, Eugene, OR). Stable CHO (for MAPK kinase activity) and COS-7 (for radioligand binding experiments) transfectants were selected in the presence of 500 μg/ml G418.

For Western blotting and immunocytochemistry experiments, COS-7 cells were transiently transfected with 7 ml of a mixture of 100 μM chloroquine and 0.25 mg/ml DEAE-dextran containing 4 μg of plasmid DNA (*HA*-vNTS2, *HA*-NTS2 (Sarret et al., 2003a), untagged NTS2, or a mixture of *HA*-vNTS2 and untagged NTS2) in DMEM high glucose. After 2 h at 37°C, the solution was removed, and the cells were treated for 1 min with 10% dimethyl sulfoxide in phosphate-buffered saline (PBS), rinsed twice with PBS, and returned to the 37°C incubator in growth medium supplemented with 5% fetal bovine serum.

5.3.4 Immunocytochemistry on COS-7 Cells

To assess the subcellular distribution of vNTS2, COS-7 cells transfected with *HA*-vNTS2 cDNA were plated on poly-L-lysine-coated glass coverslips, fixed for 20 min with 4% paraformaldehyde (Polysciences, Warrington, PA) in PBS, pH 7.4, and preincubated for 30 min at room temperature (RT) with a blocking solution consisting of 5% normal goat serum, 2% BSA, and 0.1% Triton X-100 (BDH, Toronto, Ontario, Canada) in PBS. Cells were incubated overnight at 4°C with a polyclonal antibody directed toward the 7–21-amino acid sequence in the N-terminal segment of the rat NTS2 receptor (1/25,000; made on demand by Affinity BioReagents, ABR, Golden, CO), which recognizes both short and long isoforms of the receptor (Sarret et al., 2003a), together with a mouse monoclonal antibody (clone 12CA5, 1/500) directed toward the HA epitope in PBS containing 1% normal goat serum and 0.05% Triton X-100. Cells were then incubated for 1 h at RT with a mixture of Alexa 594-conjugated goat anti-rabbit and Alexa 488-conjugated goat anti-mouse antibodies (1/750; Molecular Probes, Eugene, OR). For specificity controls, cells were incubated with anti-NTS2 peptide antiserum preadsorbed with the antigenic peptide.

For cell surface immunolabeling experiments, COS-7 cells expressing the HA-tagged vNTS2 receptor were stained using the Alexa 488-conjugated monoclonal anti-HA IgG (1/500; Molecular Probes, Eugene, OR) in serum-depleted medium for 1 h at 37°C. Cells were then washed with PBS, fixed with 10% paraformaldehyde for 30 min at RT, and washed again with PBS prior to examination.

For dual immunolocalization of vNTS2 and NTS2, COS-7 cells co-expressing HA-tagged vNTS2 and the untagged NTS2 were incubated overnight at 4°C with mouse monoclonal anti-HA antibody in concert with rabbit NTS2 peptide antiserum (1/10,000) in PBS containing 1% NGS and 0.05% Triton X-100. This second NTS2 antiserum is directed toward a synthetic peptide (YSFRLWGSPRNPSLG) corresponding to the 397–412 predicted amino acid sequence in the C-terminal tail of the rat NTS2 receptor (custom-raised by Affinity BioReagents, ABR, Golden, CO) that specifically recognizes the full-length receptor. Cells were then incubated for 1 h at RT with a mixture of Alexa 488-conjugated goat anti-mouse and Alexa 594-conjugated goat anti-rabbit antibodies (1/750; Molecular Probes, Eugene, OR).

Cells were examined with a Zeiss 510 laser-scanning confocal microscope equipped with argon2 (488 nm) and He/Ne1 (543 nm) lasers (Carl Zeiss Micro Imaging Inc., Thornwood, NY). Images were processed using the Zeiss 510 laser-scanning microscope software and Adobe Photoshop 6.0.

5.3.5 Immunoprecipitation and Immunoblotting Analysis

For immunoprecipitation studies, COS-7 cells expressing either the HA epitope-tagged vNTS2 or the untagged full-length NTS2 were lysed in RIPA buffer (150 nM NaCl, 50 mM Tris-HCl, pH 7.5, 5 mM EDTA, 1% IGEPAL, 0.5% deoxycholic acid, 0.1% SDS) containing protease inhibitors (Complete™ inhibitor tablets; Roche Applied Science) and incubated for 30 min on ice. Lysates were then precleared with 5 mg of protein A-Sepharose (Sigma) for 45 min at 4°C and incubated overnight at 4°C with a rat monoclonal antibody (clone 3F10) directed toward the HA epitope (1/400; Roche Applied Science). The protein A-Sepharose was gently shaken in lysis buffer containing 1% BSA for 30 min at RT before use. Receptor proteins were immunoprecipitated with 3 mg of protein A-Sepharose for 2 h at 4°C. Complexes

were dissolved in Laemmli sample buffer (Laemmli, 1970) and resolved by using 10% Tris-glycine precast gels (Invitrogen). Nonspecific sites were blocked by 0.1% Tween 20 (EMD Chemicals Inc., Gibbstown, NJ) and 10% milk powder (Carnation, Don Mills, Ontario, Canada) in PBS overnight at 4°C. Nitrocellulose membranes were then incubated with rabbit N-terminally directed NTS2 antibody (1/10,000) overnight at 4°C, followed by horseradish peroxidase (HRP)-conjugated goat anti-rabbit antibody for 1 h at RT (1/4000; Amersham Biosciences). Specificity of antiserum was confirmed by preadsorption of the NTS2 antibody overnight with an excess of immunizing peptide (2 μg/ml of adsorbing peptide at a final antibody dilution of 1/10,000).

For cell surface labeling experiments, COS-7 cells expressing *HA*-vNTS2 or co-expressing *HA*-vNTS2 and untagged full-length NTS2 were washed with ice-cold PBS and incubated with the N-terminally directed NTS2 peptide antiserum (1/10,000) in PBS containing 0.5% BSA for 2 h at RT. Cells were then washed three times with PBS and transferred into 1.5-ml Eppendorf tubes. They were treated with 100 μl of RIPA buffer for 1 h at 4°C, lysed, and centrifuged at 12,500 rpm at 4°C for 30 min. The supernatants were incubated with protein A-Sepharose for 2 h at 4°C to immunoprecipitate antibody-bound cell surface receptors. Immunoprecipitates were processed as described above. Membranes were probed with rabbit N-terminally directed NTS2 antibody (1/2000), followed by a 1-h incubation with HRP-conjugated goat anti-rabbit antibody (1/4000; Amersham Biosciences).

For heterodimerization experiments, COS-7 cells expressing the HA epitope-tagged vNTS2 together with the untagged full-length NTS2 were treated as described above. Receptor proteins were immunoprecipitated using the rat anti-HA antibody (clone 3F10; 1/400), and immunoblotting was then carried out with the N-terminally or C-terminally directed NTS2 antisera (1/10,000).

To determine which molecular forms of the vNTS2 protein are expressed in rat CNS, Western blotting experiments were performed on membranes from rat spinal cord, as this structure had been shown previously (Botto et al., 1997b) to express among the highest levels of vNTS2 mRNA in the mouse. Rat spinal cord membrane

preparations were obtained as described previously (Sarret et al., 2003a). Approximately 70 µg of protein from each sample were loaded onto 8% Tris-glycine gels and transferred to nitrocellulose membranes for immunoblotting. Membranes were incubated with the affinity-purified N-terminal specific anti-NTS2 rabbit antibody (1/1250) overnight at 4°C in PBS containing 1% ovalbumin and 1% BSA, followed by HRP-conjugated anti-rabbit secondary antibody in PBS with 5% milk powder. Specificity of antiserum was confirmed by preadsorption with the antigenic peptide.

5.3.6 Receptor Binding Experiments

For radioactive ligand binding experiments, COS-7 cells expressing *HA*-vNTS2 were grown on 24-well plates and incubated at 37°C in DMEM high glucose medium for 72 h before the assay. Cells were equilibrated for 10 min at 37°C in Earle's buffer (130 mM NaCl, 5 mM KCl, 1.8 mM $CaCl_2$, 0.8 mM $MgCl_2$, HEPES 20 mM, pH 7.4) supplemented with 0.2% BSA and 0.1% glucose and incubated with 0.4 nM ^{125}I-labeled NT (1670 Ci/mmol) for 30 min at 37°C in 250 µl of Earle's buffer containing 0.8 mM *ortho*-phenanthroline in the presence of increasing concentrations (from 10–10 to 10–3 M) of nonradioactive NT. The cells were then washed twice with Earle's buffer and harvested in 1 ml of 0.1 M NaOH, and the radioactivity content was measured in a gamma counter. IC_{50} values were determined from competition curves as the concentration of unlabeled ligand necessary to inhibit 50% of ^{125}I-labeled NT-specific binding. Nonspecific binding was defined as binding in the presence of a 10,000-fold excess of unlabeled ligand, which represented less than 1% of total counts.

For fluorescent ligand labeling, COS-7 cells expressing the HA epitope-tagged vNTS2 were grown on poly-L-lysine-treated glass coverslips and incubated at 37°C in DMEM high glucose medium for 24 h. They were then equilibrated for 10 min at 37°C in Earle's buffer containing 0.2% BSA and 0.1% glucose in the presence or in the absence of 10 µM phenylarsine oxide, an endocytosis inhibitor, and incubated for 30 min in the same buffer with 50 nM of *Nα*-BODIPY-NT-(2–13) (Fluo-NT) in the presence or absence of 1 mM nonfluorescent NT. Cells were air-dried, mounted on

glass slides with Aquamount (Polysciences, Warrington, PA), and examined by confocal microscopy as described above.

5.3.7 Measurement of MAP Kinase Activity

CHO cells stably expressing HA-tagged vNTS2 were split into 6-well plates and incubated for 1–2 days in DMEM-F-12 at 37°C. Cells were then serum-starved overnight, pretreated or not with MEK inhibitors PD98059 (50 μM) (New England Biolabs, Beverly, MA) or U0126 (10 μM) (Promega, Madison, WI) for 30 min, and incubated with NT (0.1–10 μM) or levocabastine (1 μM) at 37°C for the indicated times. The reaction was stopped by aspiration of the medium and the addition of ice-cold PBS containing 0.1 μM staurosporine and 1 mM sodium orthovanadate. After 30 min of incubation on ice, cells were lysed in 50 mM HEPES, pH 7.8, containing 1% Triton X-100, 0.1 μM staurosporine, 1 mM sodium orthovanadate, and protease inhibitors. Cell lysates were then centrifuged at 12,500 rpm for 10 min at 4°C, and the supernatants were stored at -20°C until use. Parallel experiments were done using untransfected cells to determine the specificity of the assay. Protein concentration was determined by the Bio-Rad procedure with BSA as standard. Samples containing 40 μg of protein were denatured in Laemmli sample buffer (Laemmli, 1970), resolved using 10% Tris-glycine precast gels, and transferred to nitrocellulose membranes (Bio-Rad). Nitrocellulose membranes were incubated overnight at 4°C with anti-phosphorylated ERK1/2 or anti-ERK1/2 rabbit antibodies (1/1000; New England Biolabs) in PBS containing 1% ovalbumin and 1% BSA. Detection of immunoreactive proteins was accomplished by using HRP-conjugated anti-rabbit and an enhanced chemiluminescent detection system (PerkinElmer Life Sciences). To quantify the effect of NT on ERK1/2 phosphorylation, the ratios of phosphorylated ERK1/2 over total ERK1/2 levels were determined by densitometry, using NIH Scion Image software. Calculations and statistical analyses were performed using Excel 2000 (Microsoft) and Prism 3.02 (Graph Pad Software). The statistical significance of the activation of ERK1/2 between transfected and nontransfected cells was verified using the paired *t* test, and *p* values were obtained from Dunnett's tables.

5.4 RESULTS

5.4.1 Expression of NTS2 Receptor mRNAs in the CNS

In order to assess expression patterns of NTS2 mRNAs in rat brain and spinal cord, a set of oligonucleotide primers designed to selectively recognize the region flanking the deletion yielding vNTS2 in the mouse (Botto et al., 1997b) was used for reverse transcription-PCR. As shown in Fig. 5.1, PCR amplification of total mRNAs yielded two bands of 620 and 439 bp, corresponding to the expected sizes of NTS2 and vNTS2 receptor fragments, respectively, in all regions examined. No signal was detected when transcribed products from homogenates were amplified with either one of the sense or antisense primers alone (not shown). Semi-quantitative analyses performed using GAPDH as an internal correction standard indicated that mRNA levels for either of the two isoforms, and hence the ratio of vNTS2 over NTS2, were not statistically different between the various regions examined (Table 5.1).

5.4.2 Isolation and Molecular Characterization of the Rat Variant NTS2

Rat vNTS2 receptor cDNA was isolated from brain tissue by reverse transcription-PCR, using a pair of sense and antisense primers corresponding to the open reading frame of the full-length NTS2 receptor. The specificity of the amplification was verified by agarose gel electrophoresis, which revealed two bands of the expected size (full-length = 1251 bp; variant isoform = 1070 bp) (not shown). The nucleic acid sequence of vNTS2 was identical to that of the full-length NTS2 with the exception of a 181-nucleotide deletion corresponding to NTS2 base pairs 760–940. It is worth noting that the nucleotide sequence of the 5'-part of the truncated receptor shares high homology with the consensus sequence of vertebrate splice donor-acceptor sites (Horowitz and Krainer, 1994). The deletion causes a frameshift in the open reading frame, leading to a premature stop codon. The short form of the rat NTS2 contains 281 amino acids, instead of 416 for the long form (Fig. 5.2*A*). It shows a global amino acid sequence homology of 79.9 and 77.4% with its full-length counterpart and the mouse spliced NTS2 isoform, respectively. Hydrophobicity analysis, performed according to the method of Kyte and Doolittle (BioEdit version 5.0.6), indicated that vNTS2 is a 5-transmembrane domain receptor with an

intracellular C-terminal tail. The resulting protein is devoid of the last two transmembrane domains of the full-length NTS2 receptor and contains 37 unique C-terminal amino acids (Fig. 5.2*B*). The C-terminal domain of the variant isoform is rich in cysteine and methionine residues.

5.4.3 Expression of vNTS2 in COS-7 Cells

In order to investigate the pharmacological and functional properties of rat vNTS2, we established a COS-7 cell line stably expressing an HA epitope-tagged vNTS2 receptor, using cDNA transfection. Immunohistochemical analysis revealed that within these cells, the bulk of immunoreactive receptors, visualized using either HA (Fig. 5.3, *A* and *C*) or NTS2 N-terminally directed antibodies (Fig. 5.3*B*), was intracellular and concentrated in a Golgi-like structure surrounding the nucleus. No immunofluorescence signal was detected in nontransfected cells or in cells incubated in the absence of primary antibodies (data not shown). Preincubation of the NTS2 antiserum with its antigenic peptide completely abolished NTS2 immunolabeling (Fig. 5.3*D*) without affecting the HA epitope staining (Fig. 5.3*C*). Surface labeling studies on nonpermeabilized cells indicated that vNTS2 was poorly expressed on the cell surface (data not shown).

To confirm that the immunoreactive protein expressed in transfected cells corresponded to the variant receptor, lysates from COS-7 cells expressing the HA epitope-tagged vNTS2 receptor were immunoprecipitated with the anti-HA antibody. Immunoblotting using the NTS2 peptide antiserum revealed the presence of two distinct translation products as follows: one of ~32 kDa, corresponding to the monomeric form of the receptor as deduced from its cDNA sequence, and another of ~60 kDa, i.e. of the size of putative vNTS2 homodimers (Fig. 5.3*E*, *lane 1*). By contrast, in control COS-7 cells expressing the full-length receptor, immunoreactive bands were detected at 46 kDa, as well as around 80–85 kDa, corresponding to the size of monomeric and dimeric forms of the full-length receptor, respectively (Sarret et al., 2003a) (Fig. 5.3*E*, *lane 2*). No specific bands were evident in homogenates prepared from nontransfected cells (Fig. 5.3*E*, *lane 3*).

To determine whether any particular molecular form of the receptor was targeted to the cell surface, COS-7 cells expressing the HA epitope-tagged vNTS2 were incubated for 2 h with the N-terminally directed NTS2 peptide antiserum, and antibody-bound cell surface receptors were separated from unbound cytoplasmic receptors by using protein A-Sepharose beads. Immunoblotting was then performed by using the NTS2 antiserum. As seen in Fig. 5.3*E*, *lane 4*, the cell surface fraction contained the same two forms (32 and 60 kDa) as fractions from whole cells.

5.4.4 Binding and Internalization Properties of vNTS2

To determine the binding properties of the short NTS2 isoform, COS-7 cells stably expressing vNTS2 were incubated with 0.4 nM ^{125}I-labeled NT for 30 min at 37°C with increasing concentrations of nonradioactive NT. As shown in Fig. 5.4*A*, unlabeled NT inhibited specific ^{125}I-labeled NT binding with an IC_{50} value of 10 μM (Fig. 5.4*A*). No specific ^{125}I-labeled NT binding was observed in nontransfected cells (data not shown).

In order to visualize NT binding and internalization, COS-7 cells expressing vNTS2 were incubated for various periods of time with 50 nM Fluo-NT at 37°C and were examined by confocal microscopy (Fig. 5.4, *B–D*). Following 30 min of incubation with the fluorescent ligand, punctate fluorescent labeling was evident throughout the cytoplasm of transfected cells, sparing the nucleus (Fig. 5.4, *B* and *C*). No fluorescent labeling was visible in nontransfected cells (not shown) or in transfected cells incubated with an excess of NT (Fig. 5.4*D*). When the incubation was carried out in the presence of the endocytosis inhibitor phenylarsine oxide, bound fluorescent molecules remained clustered on the cell surface (data not shown).

5.4.5 Signaling Properties of vNTS2

We then investigated whether the truncated form of the rat NTS2 receptor retained the MAPK activation (ERK1/2 pathway) properties exhibited by the long form of the receptor (Gendron et al., 2004). Stimulation with NT of CHO cells stably expressing the rat vNTS2 induced the phosphorylation of ERK1/2 (p42/44^{mapk}) starting at concentrations of 1 μM (Fig. 5.5*A*). Time course studies in which the cells were

stimulated for 1–60 min with 1 μM NT showed this effect to be rapid (<5 min) and sustained (over 1 h) (Fig. 5.5*B*). Densitometric analysis of the ratio of phosphorylated ERK1/2 over total ERK1/2 levels indicated that the NT-induced increase in MAPK phosphorylation was 1.4 ± 0.1-fold and reached a plateau after 15 min of stimulation (Fig. 5.5*C*, ●). This effect was vNTS2-mediated, as it was not observed in nontransfected cells (Fig. 5.5*C*, ○). A similar activation was observed following 10 min of stimulation with the NTS2 agonist levocabastine (1 μM; Fig. 5.5*D*). Pretreatment with selective MAP kinase kinase (MEK) inhibitors (PD98059 or U0126) significantly inhibited NT-mediated ERK1/2 phosphorylation in these cells (Fig. 5.5*E*).

5.4.6 Heterodimerization of NTS2 Receptors

In rat spinal cord membrane preparations immunoblotted with the N-terminally directed NTS2 antiserum (which recognizes both NTS2 isoforms; Fig. 5.6*A*), a prominent band was evident at 46 kDa, corresponding to the molecular weight of the monomeric form of the full-length NTS2 receptor detected in transfected COS-7 cells (compare Fig. 5.6*A* with Fig. 5.3*E*, *lane 2*). Surprisingly, no band was visible at 32 kDa, i.e. at the size expected for the monomeric form of the truncated receptor (e.g. Fig. 5.3*E*, *lane 1*). However, as in COS-7 transfected with the *HA*-vNTS2 (Fig. 5.3*E*, *lane 1*), an immunoreactive band was detected at 60 kDa, corresponding to the size of putative vNTS2 homodimers (Fig. 5.6*A*). An additional band was also observed at 75–85 kDa (Fig. 5.6*A*, *asterisk*), which might correspond to vNTS2/NTS2 heterodimers. All of these bands were absent when the antibody was pre-saturated with the immunizing peptide (not shown).

To investigate whether the species of NTS2 receptors detected at the 75-85-kDa molecular weight mark could correspond to vNTS2/NTS2 heterodimers, we co-expressed HA-tagged vNTS2 together with untagged NTS2 receptors in COS-7 cells and subjected cell lysates to Western blotting analysis. As shown in Fig. 5.6*B*, both monomeric and putative homodimeric forms of variant (32 and ~60 kDa, *arrows*) and full-length (46 and ~85 kDa, arrowheads) NTS2 receptors were detected using the N-terminally directed NTS2 peptide antiserum. An immunoreactive band was also

observed at the ~75-kDa mark (*asterisk*), consistent with the theoretical molecular weight of a vNTS2/NTS2 heterodimer.

Cell lysates were then subjected to immunoprecipitation with the rat anti-HA antibody. Immunoblotting of these immunoprecipitates with the N-terminally directed NTS2 antiserum showed that they contained HA-tagged vNTS2 as well as untagged NTS2 receptors, suggesting that long and short forms of NTS2 receptors might interact together (Fig. 5.6*C*, *lane 1*). Indeed, immunoreactive bands were detected at both 32 and 46 kDa, i.e. at the molecular weights of the monomeric forms of the variant and full-length receptors, as well as at ~60 kDa, corresponding to the presumptive homodimeric isoform of vNTS2 (Fig. 5.6C, lane 1). Higher molecular weight bands (~75 and ~110 kDa) were also evident, which may represent heteromultimeric forms of NTS2 receptors. Immunoreactive bands corresponding to monomeric and putative homodimeric forms of vNTS2 (32 and 65 kDa, respectively) were also detected in COS-7 cells transfected with the *HA*-vNTS2 cDNA alone (Fig. 5.6*C*, *lane 3*). However, no specific bands were observed in cells expressing the full-length NTS2 alone (Fig. 5.6C, *lane 2*). Immunoprecipitates were also subjected to Western blotting analysis using the C-terminally directed NTS2 antiserum, which selectively recognizes the full-length NTS2. This antibody revealed the presence of the full-length isoform in co-transfected cells subjected to immunoprecipitation with the HA antibody, confirming that NTS2 may be part of the same complex as vNTS2 (Fig. 5.6*D*, *lane 1*). No bands were detected with the C-terminally directed NTS2 peptide antiserum in immunoprecipitates from COS-7 cells expressing either NTS2 (Fig. 5.6*D*, *lane 2*) or *HA*-vNTS2 (Fig. 5.6*D*, *lane 3*) alone, confirming the specificity of the interaction.

To investigate whether vNTS2/NTS2 heterodimerization influenced trafficking of the truncated receptor to the cell surface, COS-7 cells co-expressing the HA epitope-tagged vNTS2 and the untagged full-length NTS2 were incubated for 2 h with the N-terminally directed NTS2 peptide antiserum, and antibody-bound cell surface receptors were separated from unbound cytoplasmic receptors by using protein A-Sepharose beads. Immunoblotting was then performed using the mouse

anti-HA antibody. As seen in Table 5.2, the density of both low (monomers) and high (dimers and multimers) molecular weight forms detected in the cell surface fraction (22 ± 2, 26 ± 3, and 52 ± 4%, respectively) was the same as in the cell fraction from cells transfected with vNTS2 alone (21 ± 2, 28 ± 4, and 51 ± 6%, correspondingly). Confocal microscopy confirmed that as in COS-7 cells transfected with vNTS2 alone (Fig. 5.3), the bulk of vNTS2 immunoreactivity in COS-7 co-expressing NTS2 and *HA*-vNTS2 was intracellular (Fig. 5.7*B*). Predictably, vNTS2 and NTS2 immunoreactive intracellular stores closely overlapped, in keeping with their demonstrated heterodimerization (Fig. 5.7, *A-C*).

5.5 DISCUSSION

In this study, we have demonstrated the presence of an alternatively spliced form of the NTS2 receptor mRNA in rat brain, comparable with the one previously identified in the mouse (Botto et al., 1997b). Most importantly, we have shown that this 5-transmembrane domain truncated receptor protein is functional, in that it specifically binds and internalizes NT and is coupled to the activation of the ERK1/2 pathway.

Alternative splicing is a frequent occurrence in mammalian gene expression, contributing both to proteome diversity and to functional complexity of genomes by generating structurally distinct isoforms from a single gene (Furnham and al., 2004). Nucleic acid sequence analysis demonstrated that the vNTS2 isoform results from a 181-bp deletion in the full-length cDNA that leads to a frameshift in the reading frame, introducing a premature stop codon. The sequence of the cDNA fragment isolated showed partial sequence overlap with the previously published rat full-length NTS2 sequence (Chalon et al., 1996), indicating that vNTS2 was indeed generated by alternative splicing from a donor-acceptor splice site as suggested by Sun *et al.* (Sun et al., 2001). This type of processing does not appear to be regionally selective because mRNA levels and ratios of the two isoforms did not vary significantly between the different regions examined.

Western blotting analysis of COS-7 cells transfected with cDNA encoding an HA-tagged rat vNTS2 revealed the presence of distinct translation products of ~32 and 60 kDa. The former corresponds to the molecular weight of the monomeric form of vNTS2 as deduced from its cDNA sequence, whereas the latter likely represents a homodimeric form of the receptor. Immunocytochemistry revealed that the bulk of these vNTS2 proteins were intracellular. This observation is in agreement with the results of subprograms executed by the PSORT II server (Kenta Nakai, Human Genome Center, Institute for Medical Science, University of Tokyo, Japan), which predict the subcellular localization of vNTS2 from its amino acid sequence in the endoplasmic reticulum (44.4%), intracellular vacuoles (22.2%), Golgi apparatus (11.1%), plasma membrane (11.1%), and mitochondrial compartments (11.1%). Both immunoblotting and immunocytochemical

experiments suggest that the vNTS2 receptor is poorly targeted to plasma membranes. However, this restricted targeting does not appear to be linked to the molecular species recruited to the membrane because both low (monomeric) and high (putative dimeric) molecular weight forms were detected at the cell surface.

Despite its short transmembrane span, the rat vNTS2 still specifically binds ^{125}I-labeled NT, albeit with a considerably lower affinity than the full-length receptor (IC_{50} of 10 μM *versus* 2 nM, for the full-length isoform). This result differs from those of Botto *et al.* (1997b), who found no specific binding of ^{125}I-labeled NT to mouse vNTS2 transiently expressed in COS-7 cells. This discrepancy may be explained by species differences, by variations in the sensitivity of the methods employed, or by the nature of the expression system. Indeed, stable transfectants might express higher levels and/or recruit more efficiently vNTS2 to the membrane than transiently transfected cells. Previous studies have shown that NT binding to rat NTS1 and human NTS2 receptors involved residues located in TM 6 and in the third intracellular loop (Barroso et al., 2000; Richard et al., 2001a). These residues are lost in the variant isoform, due to the splicing of the last two TM domains of NTS2, which may explain the lower affinity of vNTS2 for NT as compared with the full-length receptor.

Confocal microscopic experiments demonstrated specific, receptor-mediated internalization of fluorescent NT. The internalized ligand was concentrated within small endosome-like organelles, a pattern consistent with earlier reports (Gendron et al., 2004; Botto et al., 1998) on internalization via the full-length NTS2 receptor. This finding suggested to us that the NTS2 variant isoform was functionally responsive to NT, as confirmed by MAPK activation experiments. Indeed, stimulation with NT induced a rapid and sustained increase in ERK1/2 phosphorylation in CHO cells transfected with vNTS2, indicating functional coupling of the truncated receptor to the MAPK signaling pathway. Stimulation of these cells with the NTS2-specific agonist levocabastine also resulted in ERK1/2 activation. The time course of ERK1/2 activation corresponded to that observed following stimulation of the full-length receptor in a similar transfection system

(Gendron et al., 2004). Activation of ERK1/2 was already apparent at concentrations of NT lower than the IC_{50} (1 μM), in keeping with the detection of ligand-induced internalization at concentrations of Fluo-NT of 50 nM. However, phosphorylation levels obtained following stimulation with 1 μM NT were lower in cells transfected with the vNTS2 than with the full-length receptor (1.4 *versus* 2.9-fold increase over control (Gendron et al., 2004)). They were also lower than those produced in cultured rat cerebellar granule cells, which endogenously express the two NTS2 isoforms (Sarret et al., 2002). These results suggest that the third intracellular loop and the C-terminal tail of the full-length NTS2 are not essential for but may play an accessory role in MAPK activation. To our knowledge, the vNTS2 is the first TM-spliced GPCR variant cloned to date that was found to maintain signaling properties. Indeed, other TM splice variants of GPCRs, such as the corticotrophin-releasing factor receptor 2, have been reported to retain their agonist binding properties but to totally lose their functional coupling (Miyata et al., 1999).

Western blotting studies using an N-terminally directed NTS2 peptide antiserum revealed that the 32-kDa monomeric form of vNTS2 is not expressed in the spinal cord, whereas a band twice the size of vNTS2 is present, suggesting that the NTS2 receptor variant may exist in homodimeric form in the rat CNS. By contrast, a specific band was detected at 46 kDa, i.e. at the molecular weight of the full-length isoform of the receptor, indicating that in contrast to its variant isoform, the full-length receptor exists in monomeric form in rat CNS. These results are similar to those previously reported for membranes prepared from rat brain and cerebellum (Sarret et al., 2003a). In addition, specific bands were detected at molecular weight marks higher than the putative vNTS2 dimers. One of these was approximately twice the size of the monomeric form of the full-length receptor and was therefore interpreted as a putative NTS2 homodimer. Another migrated slightly lower, as would be expected from a vNTS2/NTS2 heterodimer. Indeed, recent biochemical, biophysical, and functional studies (reviewed in Bouvier, 2001; Devi, 2001) have shown that GPCR can assemble as hetero- as well as homodimeric complexes. To test whether the vNTS2 could actually associate with its full-length counterpart, we carried out immunoprecipitation experiments on COS-7 cells co-expressing HA-

tagged vNTS2 and native NTS2. These experiments demonstrated that the two NTS2 isoforms did associate when co-expressed in COS-7 cells, because both receptors were pulled down using an HA antibody. Furthermore, the presence in these dually transfected cells of a band at the theoretical molecular weight of vNTS2/NTS2 heterodimers indicated that the band detected at the same level in spinal cord membranes might indeed have corresponded to a vNTS2-NTS2 heterodimer. This vNTS2/NTS2 heterodimer was stable during cell lysis and reducing Tris-glycine gel electrophoresis, suggesting that the interaction involves a noncovalent hydrophobic interface between the receptor proteins.

To investigate whether heterodimerization of NTS2 and vNTS2 receptors affected targeting of the truncated receptor to the plasma membrane, we examined by Western blot the expression of vNTS2 on the cell surface of singly transfected *versus* dually transfected cells, and we compared the immunocytochemical distribution of NTS2 and vNTS2 in dually transfected cells. By using either technique, we found that co-expression of the full-length NTS2 did not noticeably increase the cell surface density of the truncated form over that seen in cells expressing *HA*-vNTS2 alone, suggesting that the full-length NTS2 does not act as a chaperone protein for its shorter isoform. However, intracellular vNTS2 stores closely overlapped with those of NTS2, supporting the notion that the two receptors heterodimerize.

In summary, our results indicate that the rat vNTS2 is a functional receptor that is expressed in conjunction with the full-length NTS2 receptor throughout the CNS. Our data also indicate that this truncated 5-TM receptor does not exist in monomeric form in the rat CNS. Rather, it associates both with itself and with the full-length 7-TM receptor to form large molecular weight homo- and heterodimer species. Therefore, it is likely that these associations provide for subtle regulation of the NT signal, as demonstrated previously (Motomura et al., 1998) for the splice variant isoform of the growth hormone-releasing hormone receptor.

5.6 FOOTNOTES

This work was supported in part by a grant from the Canadian Institutes for Health Research. The costs of publication of this article were defrayed in part by the payment of page charges. This article must therefore be hereby marked "advertisement" in accordance with 18 U.S.C. Section 1734 solely to indicate this fact. Amélie Perron and Philippe Sarret were supported by a fellowship from the Fonds de la Recherche en Santé du Québec (FRSQ). Louis Gendron was supported by fellowship from the CIHR.

5.7 ABBREVIATIONS

NT, neurotensin; GPCR(s), G protein-coupled receptor(s); TM, transmembrane domain; CHO cells, Chinese hamster ovary cells; COS-7 cells, green African monkey kidney cells; MAPK, mitogen-activated protein kinase; ERK1/2, extracellular signal-regulated kinases 1/2; DMEM, Dulbecco's modified Eagle's medium; BSA, bovine serum albumin; HRP, horseradish peroxidase; HA, hemagglutinin; RT, room temperature; CNS, central nervous system; PBS, phosphate-buffered saline; GAPDH, glyceraldehyde-3-phosphate dehydrogenase; MEK, MAPK/ERK kinase; Fluo-NT, *Nα*-BODIPY-neurotensin-(2–13).

5.8 FIGURES

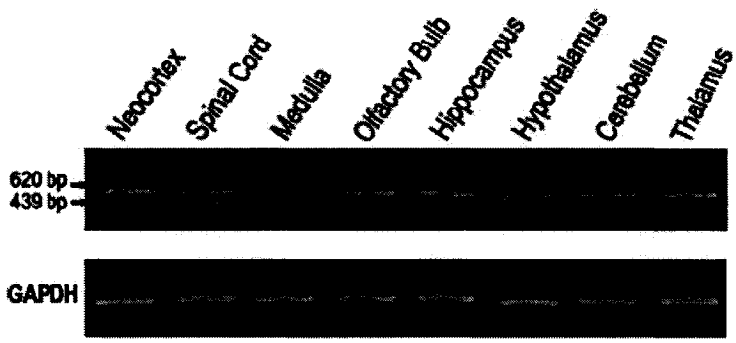

Figure 5.1

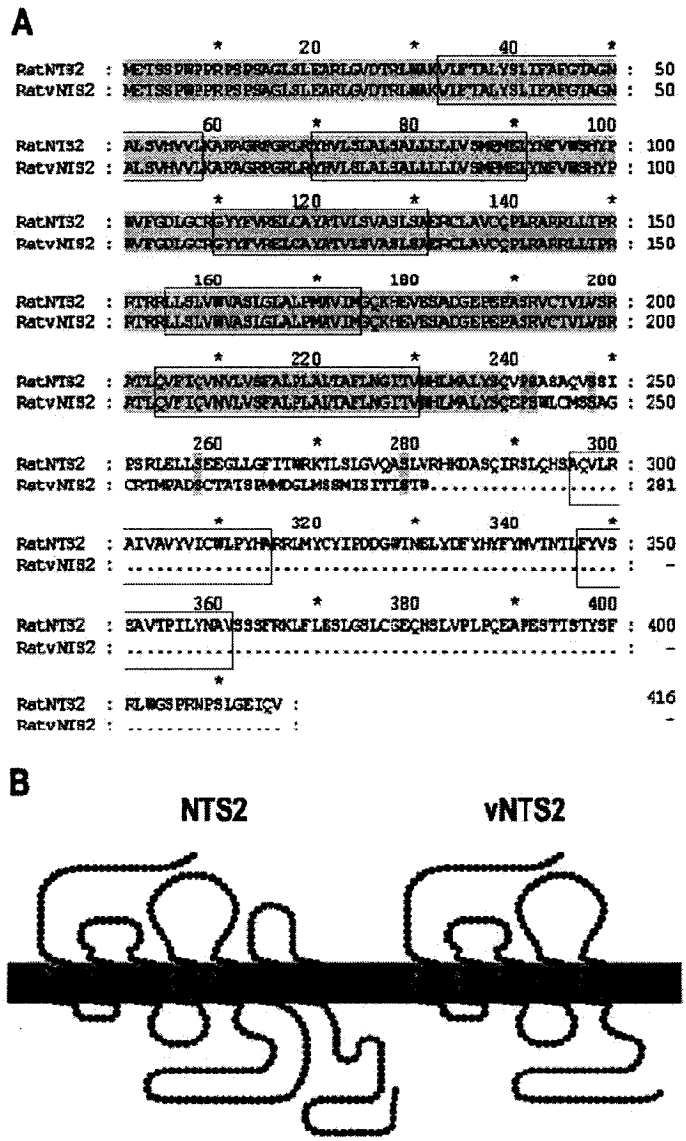

Figure 5.2

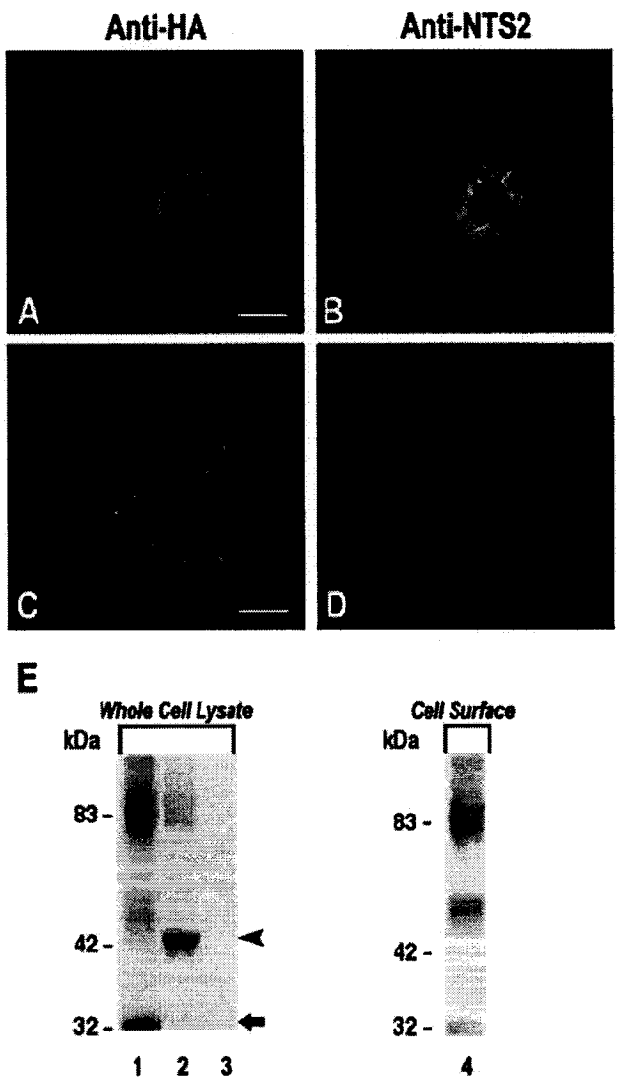
Anti-HA
Anti-NTS2
A
B
C
D
E
Whole Cell Lysate
Cell Surface
kDa
kDa
83 -
42 -
32 -
83 -
42 -
32 -
1 2 3
4

Figure 5.3

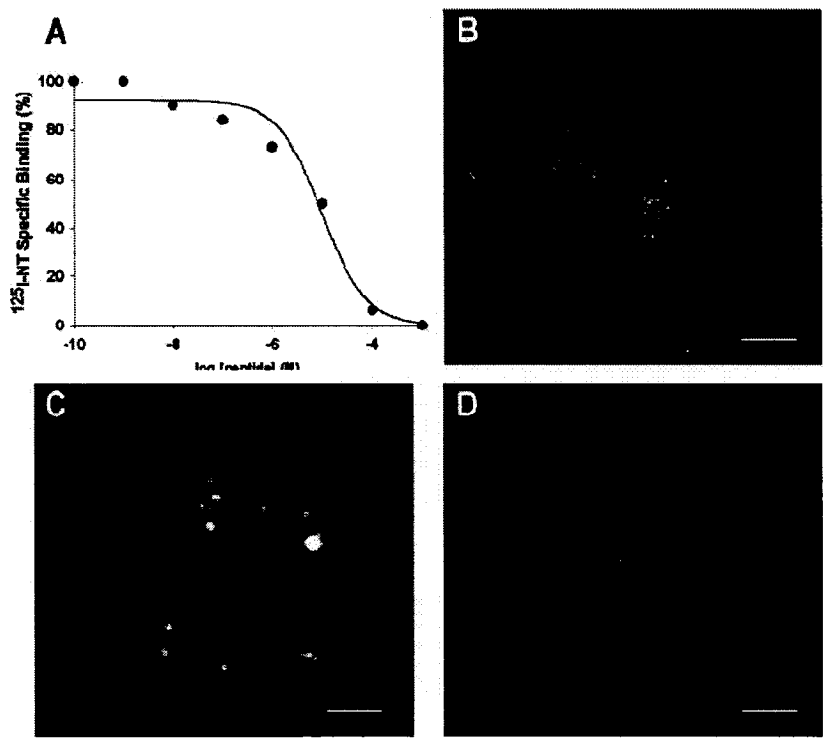

Figure 5.4.

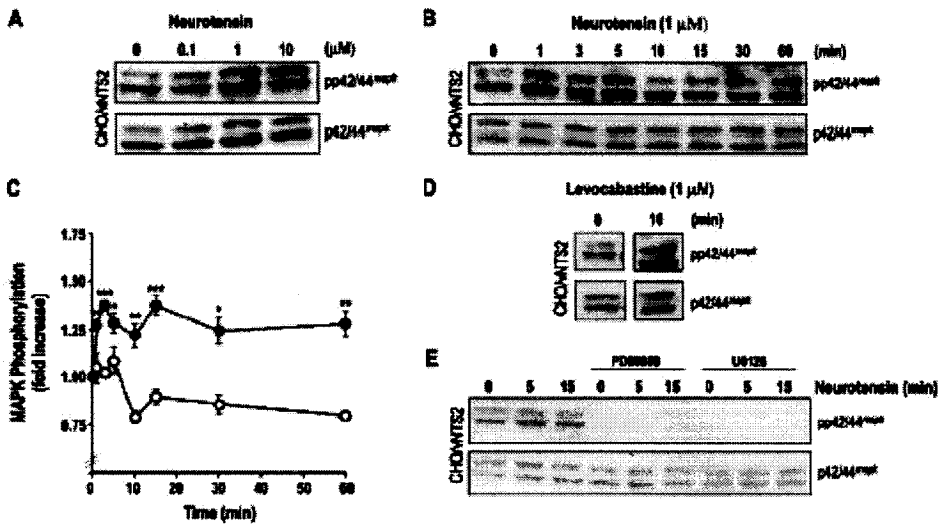
A
Neurotensin
0
0.1
1
10
(μM)
CHO/NTS2
B
Neurotensin (1 μM)
0
1
3
5
10
15
30
60
(min)
CHO/NTS2
C
MAPK Phosphorylation (fold increase)
1.75
1.50
1.25
1.00
0.75
0
10
20
30
40
50
60
Time (min)
D
Levocabastine (1 μM)
0
10
(min)
CHO/NTS2
E
PD98059
U0126
0
5
15
0
5
15
0
5
15
Neurotensin (min)
CHO/NTS2

Figure 5.5

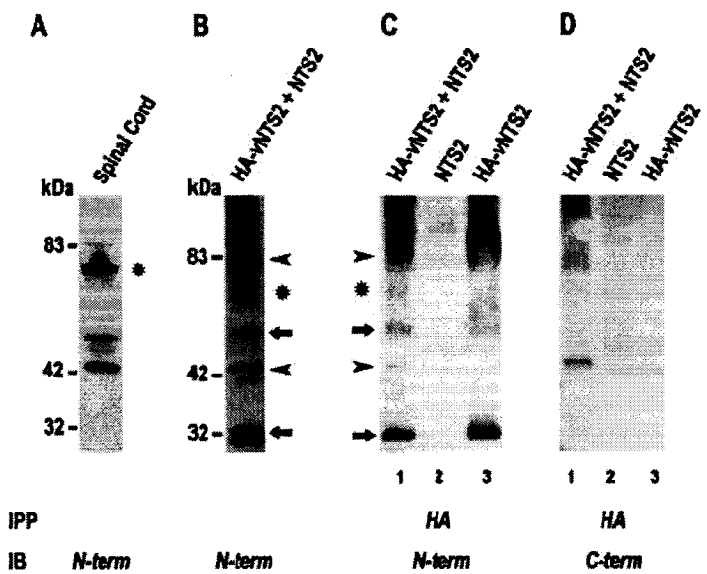
A
B
C
D
Spinal Cord
HA-vNTS2 + NTS2
HA-vNTS2 + NTS2
NTS2
HA-vNTS2
HA-vNTS2 + NTS2
NTS2
HA-vNTS2
kDa
kDa
83
42
32
83
42
32
1 2 3
1 2 3
IPP
HA
HA
IB
N-term
N-term
N-term
C-term

Figure 5.6

Figure 5.7

5.9 FIGURE LEGENDS

Fig 5.1: Reverse Transcription-PCR Analysis of NTS2 mRNAs. Amplification of NTS2 and vNTS2 mRNAs was from various brain regions. PCRs were performed on mRNAs reverse-transcribed using primers flanking the truncated portion of NTS2. The expected sizes of the reverse transcription-PCR products were 620 and 439 bp for the full-length and spliced form of NTS2, respectively. The housekeeping gene GAPDH was also amplified and used as an internal control for semi-quantitative analyses.

Fig. 5.2: Comparison of Rat Full-Length and Variant NTS2 Isoform Sequences. *A*, alignment of rat NTS2 isoform sequences. Identical sequences found in NTS2 receptor isoforms are *shaded*, and the putative transmembrane segments are *boxed*. Gaps for alignment are indicated by *dots*. The short form of NTS2 contains 281 amino acids, instead of 416 for the long form. The resulting protein is devoid of the last two transmembrane domains and contains 37 unique C-terminal amino acids. *B*, schematic representation of the secondary structure of NTS2 receptors. Common amino acids are shown in *black*. Unique amino acid residues in the sequence of NTS2 and vNTS2 are represented in *hatched* and *gray*, respectively.

Fig. 5.3: Expression of vNTS2 Receptor Protein in Transfected COS-7 Cells. ***A-D***, dual immunolabeling of COS-7 cells transfected with cDNA encoding the HA epitope-tagged vNTS2 receptor. Staining for the HA epitope (*A*) co-localizes with NTS2 immunolabeling (*B*), confirming recognition of the vNTS2 by the NTS2 antiserum. Preadsorption of NTS2 antiserum with its antigenic peptide completely abolishes NTS2 immunolabeling (*D*) in cells expressing the epitope-tagged receptor (*C*). Scale bar, 10 μm in *A* and *B*; 5 μm in *C* and *D*. ***E***, Western blotting analysis of NTS2 receptor isoforms. Immunoprecipitation with HA antibody and blotting with N-terminally directed NTS2 antiserum of homogenates from transfected COS-7 cells (*lane 1*, COS-7/*HA*-vNTS2; *lane 2*, COS-7/*HA*-NTS2; *lane 3*, untransfected cells). In cells transfected with vNTS2, specific immunoreactive bands are evident at 32 and 60 kDa, corresponding to the molecular weights of monomeric and dimeric forms of

vNTS2. The same bands were detected in cell surface labeling experiments using the N-terminally directed NTS2 antiserum (*lane 4*). In cells transfected with the full-length NTS2, immunoreactive bands are visible at 46 and 83 kDa, corresponding to the molecular weights of monomeric and dimeric forms of NTS2. *Arrow* and *arrowhead* represent the monomeric isoform of vNTS2 and NTS2, respectively. No specific band is evident in nontransfected cells (*lane 3*).

Fig. 5.4: Binding and Internalization of NT in COS-7 Cells Expressing vNTS2. ***A***, competition inhibition of ^{125}I-labeled NT binding to whole COS-7 cells stably expressing vNTS2. Cells were incubated with 0.4 nM ^{125}I-labeled NT for 30 min at 37°C with increasing concentrations of nonradioactive NT. Binding IC_{50} = 10 μM. The results are representative of three independent experiments. ***B*** and ***C***, confocal microscopic imaging of Fluo-NT internalization in COS-7 cells expressing vNTS2. Cells were incubated for 30 min at 37°C with 50 nM Fluo-NT and air-dried. Internalized fluorescent ligand molecules are detected in the form of small endosome-like particles distributed throughout the cytoplasm. *D*, Fluo-NT labeling is prevented when the incubation is performed in the presence of an excess of nonfluorescent NT. Scale bar, 10 μmin *B*; 5 μm in *C* and *D*.

Fig. 5.5: MAPK Kinase Signaling in vNTS2 Expressing CHO Cells. ***A***, dose-dependent effect of NT on MAPK (ERK1/2) phosphorylation. Cells were treated for 5 min with the indicated concentrations of NT. Phosphorylation levels of MAPK were detected by immunoblotting as described under "Experimental Procedures". *Upper panels* of *A*, *B*, *D*, and *E*, phosphorylated ERK1/2; *lower panels*, total ERK1/2. ***B***, time course of NT-stimulated MAPK phosphorylation in CHO cells stably expressing vNTS2. ***C***, densitometric analysis of the ratio of phosphorylated ERK1/2 over total ERK1/2 levels following incubation with 1 μM of NT. Untransfected (○) and vNTS2-expressing (●) CHO cells were incubated at 37°C for the indicated times. Values represent the means ± S.E. of five independent experiments. Transfected cell values are significantly different from nontransfected cell values at all time points as follows: *, p 0.05; **, p 0.01; and ***, p 0.001. *D*, ERK1/2 phosphorylation levels in vNTS2-expressing CHO cells stimulated with

levocabastine for 10 min at 37°C. *E*, MEK inhibitors prevent ERK1/2 activation by NT in CHO cells expressing vNTS2. Cells were pretreated with PD98059 (50 μM) or U0126 (10 μM) and treated with NT (1 μM) for 5–15 min at 37°C. The results are representative of three individual experiments, each with duplicate determinations.

Fig. 5.6: Characterization of vNTS2/NTS2 Heterodimers by Co-immuno-precipitation. Immunoblotting (*IB*) analysis of NTS2 receptors in spinal cord membrane preparations (***A***) and in COS-7 cells co-expressing NTS2 and *HA*-vNTS2 (***B***) using a N-terminally directed NTS2 antibody. ***C*** and ***D***, co-immunoprecipitation (*IPP*) studies on COS-7 cells heterologously expressing NTS2 (*lanes 2*), *HA*-vNTS2 (*lanes 3*), or a combination of both (*lanes 1*). Cells were lysed and subjected to immunoprecipitation with rat anti-HA antibody. The co-immunoprecipitates were then immunoblotted using N-terminally (*C*) or C-terminally (*D*) directed NTS2 peptide antisera as described under "*Experimental Procedures*". Molecular mass markers are shown to the left of *A* and *B*. Molecular masses for *B* also apply for *C* and *D*. Each illustrated blot is representative of three independent experiments. *Arrows* and *arrowheads* represent isoforms of vNTS2 and NTS2, respectively. *Asterisks* represent the putative vNTS2/NTS2 heterodimer.

Fig. 5.7: Double Immunolabeling of COS-7 cells Co-expressing NTS2 and *HA*-vNTS2. Staining with the C-terminally directed NTS2 antiserum (***A***), which exclusively recognizes the long isoform, co-localizes with immunoreactivity for the HA epitope (***B***) in co-transfected cells, as evident in the overlay (***C***).

5.10 TABLES

TABLE 5.1

Densitometric analysis of the regional expression of vNTS2 and NTS2 mRNAs in the rat CNS

Values represent means ± S.E. of four independent experiments. No regional difference in the expression of either isoforms is detectable ($p > 0.05$, one-way analysis of variance, Bonferroni's multiple comparison test).

Structure	Receptor to GAPDH ratio		vNTS2/NTS2
	vNTS2	NTS2	
	arbitrary units		
Neocortex	0.91 ± 0.15	0.99 ± 0.07	0.92 ± 0.15
Spinal cord	0.93 ± 0.10	1.06 ± 0.01	0.88 ± 0.11
Medulla	0.93 ± 0.10	1.03 ± 0.05	0.91 ± 0.13
Olfactory bulb	0.98 ± 0.10	1.15 ± 0.08	0.88 ± 0.14
Hippocampus	0.91 ± 0.12	1.21 ± 0.13	0.78 ± 0.16
Hypothalamus	1.09 ± 0.14	1.28 ± 0.17	0.89 ± 0.14
Cerebellum	0.73 ± 0.12	0.87 ± 0.05	0.83 ± 0.15
Thalamus	0.90 ± 0.09	1.17 ± 0.12	0.81 ± 0.14

TABLE 5.2

Densitometric analysis of the effect of NTS2 expression on cell surface expression of HA-vNTS2

The relative intensity of HA-vNTS2 is expressed as percent of total surface receptor (monomer + dimer + multimer) immunoreactivity. Values represent the means ± S.E. of four independent experiments.

	HA-vNTS2 isoforms		
	Monomer	Dimer	Multimer
	%	%	%
HA-vNTS2	21 ± 2	28 ± 4	51 ± 6
HA-vNTS2 + NTS2	22 ± 2	26 ± 3	52 ± 4

CHAPTER 6

SUSTAINED NEUROTENSIN EXPOSURE PROMOTES CELL SURFACE RECRUITMENT OF NTS2 RECEPTORS

Amélie Perron[1], Nadder Sharif[1], Louis Gendron[1], Mariette Lavallée[1], Thomas Stroh[1], Jean Mazella[2], and Alain Beaudet[1]

[1]Montreal Neurological Institute, Department of Neurology and Neurosurgery, McGill University, Montreal, Québec, Canada

[2]Institut de Pharmacologie Moléculaire et Cellulaire, CNRS, Sophia Antipolis, Valbonne, France

Biochemical and Biophysical Research Communications (2006) **343**:799-808.

6.1 ABSTRACT

In this study, we investigated whether persistent agonist stimulation of NTS2 receptors gives rise to down-regulation, in light of reports that their activation induced long-lasting effects. To address this issue, we incubated COS-7 cells expressing the rat NTS2 with neurotensin (NT) for up to 24 h and measured resultant cell surface [^{125}I]-NT binding. We found that NTS2-expressing cells retained the same surface receptor density despite efficient internalization mechanisms. This preservation was neither due to NTS2 neosynthesis nor recycling since it was not blocked by cycloheximide or monensin. However, it appeared to involve translocation of spare receptors from internal stores, as NT induced NTS2 migration from trans-Golgi network to endosome-like structures. This stimulation-induced regulation of cell surface NTS2 receptors was even more striking in rat spinal cord neurons. Taken together, these results suggest that sustained NTS2 activation promotes recruitment of intracellular receptors to the cell surface, thereby preventing functional desensitization.

6.2 INTRODUCTION

Neurotensin (NT) is a tridecapeptide that was shown to be involved in a variety of central and peripheral neuromodulatory effects including naloxone-independent analgesia, hypothermia, and neuroleptic-like modulation of dopaminergic pathways (Vincent et al., 1999). Most of these effects result from the specific interaction of the peptide with two cell surface G protein-coupled receptors (GPCRs) referred to as NTS1 and NTS2. The former binds NT with high affinity (K_d = 0.2 nM), whereas the latter binds NT with lower affinity (K_d = 2 nM) and is recognized by the antihistamine drug levocabastine (Tanaka et al., 1990; Chalon et al., 1996). Biochemical studies have indicated that NTS1 is implicated in the modulation of intracellular levels of inositol phosphates (Watson et al., 1992), cAMP (Yamada et al., 1993), and extracellular signal-regulated kinases (Poinot-Chazel et al., 1996), whereas NTS2 induces Ca^{2+}-dependent chloride currents in *Xenopus* oocytes (Botto et al., 1997b) and activates the ERK1/2 cascade, both in transfected CHO cells (Gendron et al., 2004) and in cerebellar granule cells in culture (Sarret et al., 2002).

Most GPCRs are subjected to regulatory processes in order to control their responsiveness to persistent agonist exposure (Tsao and von Zastrow, 2000; Ferguson, 2001). Agonist-induced regulation of GPCRs usually involves receptor desensitization, due to uncoupling from G proteins, followed by receptor internalization and down-regulation. The latter is characterized by a decrease in the total number of receptors and typically involves increased turnover or reduced synthesis of receptors. In the case of the NTS1 receptor, such desensitization processes have been reported in N1E-115 cells as well as in rat cultured neurons after prolonged incubation in the presence of NT (Donato di Paola et al., 1993; Hermans et al., 1997). The disappearance of NT-binding sites was surmised to result from degradation of internalized receptors after fusion with lysosomes, since it was partially inhibited by the lysosomotropic drugs chloroquine and methylamine (Hermans et al., 1997; Vandenbulcke et al., 2000). Moreover, destabilization of NTS1 mRNA was reported in N1E-115 and HT29 cells after long-term agonist

exposure, suggesting that post-transcriptional events may be directly implicated in the down-regulation process (Hermans and Maloteaux, 1998). Finally, it has been established that *de novo* synthesis is required for the recovery of NTS1 receptor-binding sites and function (Donato di Paola et al., 1993; Hermans et al., 1997).

Little is known about the regulation of NTS2, except that its stimulation with NT induces long-term metabolic effects due to prolonged and sustained activation of ERK1/2, either in transfected CHO cells (Gendron et al., 2004) or in neurons in culture (Sarret et al., 2002). Therefore, the present study was initiated in order to determine whether extended stimulation of NTS2 leads to a down-regulation of cell surface receptor density and/or of intracellular receptor protein levels. Our results demonstrate that cell surface NTS2 receptors are maintained following persistent exposure to NT through a recycling-independent mechanism that involves recruitment of receptors from intracellular stores.

6.3 MATERIALS AND METHODS

6.3.1 Gene Constructs

The cDNA encoding the rat and human NTS2 receptors (rNTS2 and hNTS2, respectively) were obtained through reverse transcription of brain mRNA and subcloned into the mammalian expression vector pTargeT (Promega, Madison, WI) as described in (Sarret et al., 2003aa) and (Gendron et al., 2004), respectively. The subcloning of HA-tagged NTS1 into pcDNA3 was described previously (Labbé-Jullié et al., 1998).

6.3.2 Cell Culture and Transfections

COS-7 cells were maintained in Dulbecco's modified Eagle's medium (DMEM) supplemented with 5% Fetal Bovine Serum (FBS) in the presence of penicillin/streptomycin (100 units/ml; Invitrogen Burlington, ON, Canada). Cells were transiently transfected by the DEAE-dextran/chloroquine method with 4 μg of rNTS2, hNTS2, or HA-tagged NTS1 plasmid.

6.3.3 Receptor Binding Experiments

COS-7 cells expressing rNTS2, hNTS2 or HA-NTS1 were incubated with or without 1 μM NT for 1-24 h in DMEM with 2.5% FBS or Earle's buffer (130 mM NaCl, 5 mM KCl, 1.8 mM $CaCl_2$, 0.8 mM $MgCl_2$, 20 mM HEPES, pH 7.4) for long (1-24 h) and short (0-60 min) term experiments, respectively. Cells were washed once with hypertonic acid buffer (Earle's containing 0.2 M acetic acid and 0.5 NaCl, pH 4) for 3 min on ice, twice with Earle's, and incubated with 0.4 nM ^{125}I-labeled NT (1670 Ci/mmol; Perkin Elmer) for 60 min on ice in Earle's supplemented with 0.25% BSA, 0.1% glucose and 0.8 mM *ortho*-phenanthroline. Cells were then washed twice with ice-cold Earle's, harvested in 0.1 M NaOH, and radioactivity content was measured in a gamma counter. Non-specific binding was defined as binding in the presence of a 10,000-fold excess of unlabeled ligand, which corresponded to less than 1% of total counts. Statistical comparisons between groups were performed using a Student's *t* test. Differences were considered significant for $p < 0.05$.

For experiments with recycling inhibitors, transfected COS-7 cells were equilibrated for 10 min at 37°C in Earle's supplemented with 0.25% BSA and 0.1% glucose. Cells were then pre-stimulated for 30 min with 25 μM monensin (Sigma) in Earle's at 37°C and incubated with or without 1 μM NT in the continuous presence of monensin for 60 min at 37°C. Cells were then washed once with hypertonic acid buffer, twice with Earle's and binding with radioligand was performed as described above.

6.3.4 Immunoblotting Analyses

COS-7 cells expressing rNTS2 were stimulated or not with 1 μM NT with or without 70 μM cycloheximide for 1 or 24 h at 37°C and resuspended in ice-cold buffer containing 10 mM Tris-HCl, pH 8.0, and 1 mM EDTA with protease inhibitors (Complete Protease Inhibitors tablets, Roche Molecular Biochemicals, Laval, QC, Canada). Cells were then disrupted by sonication and pelleted by centrifuging at 12,000 g for 30 min at 4°C. Parallel experiments were done using untransfected cells as a negative control. Protein concentration was determined using the Bio-Rad method (Bio-Rad Laboratories, Mississauga, ON, Canada). Samples containing 20 μg of crude membrane proteins were denatured in Laemmli sample buffer, resolved on 10% Tris-glycine precast gels (Invitrogen) and transferred to nitrocellulose membranes (Bio-Rad). Membranes were then incubated with the NTS2 peptide antiserum (1/10,000; previously characterized in (Sarret et al., 2003a)) overnight at 4°C in PBS containing 1% ovalbumin (Sigma, St-Louis, MO) and BSA, followed by HRP-conjugated anti-rabbit secondary antibody (1/3500; Amersham Pharmacia Biotech, Baie d'Urfé, QC, Canada) in PBS with 5% evaporated milk (Carnation, Don Mills, ON, Canada) for 1 h at room temperature (RT). Immunoreactive proteins were detected using an enhanced chemiluminescent system (Perkin Elmer Life Science, Boston, MA). The effects of long-term NT exposure on rNTS2 protein levels were quantified by densitometry using Scion Image. Calculation and statistical analyses were carried out in Excel 2000 (Microsoft).

6.3.5 Immunocytochemistry on COS-7 cells

COS-7 cells expressing rNTS2 were stimulated or not with 1 μM NT for 1 h at 37°C, fixed for 20 min with 4% paraformaldehyde (PFA) (Polysciences, Warrington, PA), preincubated for 30 min with a blocking solution (5% Normal Goat Serum (NGS), 2% BSA, and 0.1% Triton (Sigma)) and incubated overnight at 4°C with the NTS2 antiserum (1/25,000) alone, or in concert with either a monoclonal antibody against syntaxin 6 (1/1000; Transduction Laboratories, Lexington, KY) or guinea pig anti-PIST antibody (1/1000; gift of Dr. Hans-Jürgen Kreienkamp, Institute for Human Genetics, Hamburg, Germany). Cells were then incubated for 1 h at RT with a mixture of Alexa 488-conjugated goat anti-rabbit with either Alexa 596-conjugated goat anti-mouse or anti-guinea pig antibodies (1/750; Molecular Probes, Eugene, OR). Cells were examined with a Zeiss 510 laser scanning confocal microscope equipped with Argon2 (488 nm) and He/Ne1 (543 nm) lasers (Carl Zeiss Micro Imaging Inc., Thornwood, NY). Images were processed using the Zeiss 510 laser-scanning microscope software and Adobe Photoshop 6.0.

To quantify peripheral (as an index of cell surface) versus internal NTS2 immunolabeling in permeabilized cells, a total of 12-15 cells per condition (i.e. untreated or stimulated for 60 min with NT) from 4 independent experiments were randomly selected and analyzed using the ImageJ software (National Institutes of Health, Bethesda, MD). For this purpose, peripheral and intracellular compartment were delineated and integrated fluorescence densities associated with either of these two compartments were measured. Values are expressed as a percentage of the total fluorescence density (peripheral + intracellular) for each condition. Statistical comparisons between conditions were performed using a Student's *t* test.

6.3.6 Measurement of MAP Kinase Activity

COS-7 cells expressing rNTS2 were incubated at 37°C in DMEM, 2.5% FBS with or without 1 μM NT for 24 h, serum-starved for 2 h, and then incubated with 1 μM NT for 0, 5, 15, 30 or 60 min at 37°C. The reaction was stopped by addition of ice-cold PBS containing 0.1 μM staurosporine (Sigma) and 1 mM sodium orthovanadate. Cells

were then lysed in 50 mM HEPES, pH 7.8, containing 1% Triton, 0.1 μM staurosporine, 1 mM sodium orthovanadate, and protease inhibitors. Cell lysates were centrifuged at 12,000 g for 10 min at 4°C and protein concentration was determined by the Bio-Rad procedure as described above. Samples containing 30 μg of protein were denatured in Laemmli buffer and resolved by using 10% Tris-glycine precast gels. Nitrocellulose membranes were incubated overnight at 4°C with anti-phosphorylated ERK1/2 or anti-ERK1/2 rabbit antibodies (1/1000; New England Biolabs, Beverly, MA), followed by HRP-conjugated goat anti-rabbit antibody for 1 h at RT (1/4000; Amersham Pharmacia Biotech). To quantify the effect of NT on ERK1/2 phosphorylation, the ratios of phosphorylated ERK1/2 over total ERK1/2 levels were determined by densitometry using Scion Image software. Calculations and statistical analyses were performed using Excel 2000 and SigmaPlot 2001. Statistical significance of the activation of ERK1/2 between untreated and NT-prestimulated cells was determined using a Student's *t* test.

6.3.7 NTS2 Immunogold Labeling

Adult male Sprague Dawley rats (200-250 g; Charles River, St-Constant, QC, Canada) were anesthetized with halothane and intrathecally injected or not with NT (1200 pmol). After 20 min, rats were transaortically perfused under pentobarbital anesthesia with a mixture of 3.75% acrolein and 2% PFA. Lumbar spinal cords were removed, fixed in 2% PFA and cut (50 μm) using a vibrating microtome. Sections were incubated in 1% sodium borohydride and cryoprotectant solution (25% sucrose and 3% glycerol) prior to snap freezing in isopentane (-70 °C), transfer to liquid nitrogen, and thawing. Section were then incubated for 48 h at 4 °C with NTS2 antiserum (1/1800), followed by 2 h at RT with colloidal gold-conjugated goat anti-rabbit antibody (1/50; Cedarlane Laboratories, Hornby, ON, Canada). Sections were fixed with 2% glutaraldehyde and immunogold deposits were enhanced using the IntenSE kit (Amersham Pharmacia Biotech). Sections were then post-fixed with osmium tetroxide, dehydrated in ethanol, flat-embedded in Epon, counterstained with lead citrate and uranyl acetate, and examined with a JEOL 100CX transmission electron microscope. Negatives were digitized on a scanner and processed using

Adobe Photoshop. Quantitative analysis of the ultrastructural distribution of NTS2 immunoreactivity was performed on three to four grids per experimental condition from three independent experiments (n = 3 rats). A total of 38 and 31 randomly selected labeled dendritic profiles within the superficial layers (laminae I and II) of the spinal cord from respectively non-treated and NT-injected rats were analyzed using the Neurolucida morphometry software. First, density of immunoreactive NTS2 receptor gold particles associated with selected dendrites was calculated per surface area and expressed as immunogold/silver particles per μm^2. Second, gold particles were classified as being intracellular or membrane-associated. The proportion of membrane-associated NTS2 receptors was expressed as a percentage of the total number of gold particles. Statistical comparisons between groups were performed using a Student's *t* test. Differences were considered significant for $p < 0.05$.

6.4 RESULTS

6.4.1 Cell Surface NTS2 Receptors are Resistant to Down-regulation

To investigate the effects of prolonged incubation with NT on NTS2 cell surface density, rNTS2-expressing COS-7 cells were prestimulated with 1 μM NT for up to 24 h at 37°C and cell surface receptor binding was carried out using 0.4 nM [^{125}I]-NT on ice. As shown in Fig. 6.1*A*, NT stimulation resulted in an immediate decrease in the density of cell surface NTS2 binding sites (50 ± 4% of baseline values after 5 min). A similar but weaker response was obtained in NTS1-expressing cells (73 ± 2% of baseline values at 5 min; Fig. 6.1*A*). Upon sustained NT exposure, NTS2 binding progressively returned to baseline values (100 ± 4% of baseline after 24 h) whereas NTS1 binding kept on decreasing (46 ± 1% of baseline after 24 h; Fig. 6.1*B*). NTS2 binding sites were also maintained at baseline levels after a 24 h-stimulation with the metabolically-stable NT analog JMV-431 (106 ± 6%), suggesting that maintenance of NTS2 cell surface binding sites was not due to peptide degradation (not shown). Taken together, these data show that contrary to NTS1, cell surface NTS2 binding sites are maintained following persistent agonist stimulation despite efficient internalization mechanisms (Botto et al., 1998).

6.4.2 Effect of Prolonged NT Exposure on NTS2 Receptor Protein Levels

In order to determine whether prolonged exposure to NT affected total NTS2 protein levels, rNTS2-expressing COS-7 cells were stimulated with 1 μM NT for different periods of time and crude membrane preparations were analyzed by Western blotting using a NTS2 peptide antiserum. As seen in Fig. 6.2, the total levels of immunodetected-NTS2 (45 kDa) were not significantly different after than before NT stimulation (103 ± 15% of control values after 24 h), suggesting that NTS2 is neither up- nor down-regulated following prolonged agonist exposure. To confirm that prolonged NT stimulation did not induce NTS2 neosynthesis, COS-7 cells were incubated with NT in presence of the protein synthesis inhibitor cycloheximide for up to 24 h. Immunoblotting of crude membrane preparations using the NTS2 peptide

antiserum revealed that treatment with cycloheximide did not affect receptor protein levels (not shown).

6.4.3 Maintenance of Cell Surface NTS2 is a Recycling-independent Process

To investigate whether receptor recycling accounted for the preservation of cell surface NTS2 receptors following prolonged NT exposure, rNTS2-expressing COS-7 cells were first preincubated with monensin for 30 min and incubated with 1 μM NT together with monensin for 1 h at 37°C. Monensin is known to hinder late receptor recycling steps beyond the acidification of endocytic vesicles (Tycko et al., 1983). As shown in Fig. 6.3*A* monensin had little if any effect on the preservation of [^{125}I]-NT binding levels following NT exposure. Indeed, cell surface levels of NTS2 receptors represented 92 ± 8% of pre-stimulation values, which were comparable to those measured in the absence of monensin following the same stimulation period with NT (90 ± 4%).

Previous site-directed mutagenesis studies have revealed that Tyr 237 is a critical residue in the recycling process of NTS2 receptors (Martin et al., 2002b). Indeed, the human NTS2 in which a cysteine residue naturally replaces the tyrosine in position 237 does not undergo recycling following ligand-induced internalization (Martin et al., 2002b). In order to study further the potential implication of receptor recycling in the maintenance cell surface NTS2 receptors, hNTS2-expressing COS-7 cells were prestimulated with 1 μM NT for up to 24 h at 37°C and cell surface receptor binding was carried out by using 0.4 nM [^{125}I]-NT on ice. As shown in Fig. 6.3*B*, NT stimulation resulted in rapid decrease in the density of cell surface human NTS2 binding sites (36 ± 8% of baseline values after 5 min), suggesting efficient ligand-induced internalization. However, human NTS2 receptors also progressively resurfaced upon extended agonist exposure (82 ± 5% of baseline after 24 h) despite their inability to undergo recycling (Martin et al., 2002b). Taken together, these results suggest that receptor recycling does not account by itself for the maintenance of cell surface NTS2 receptors, but that other mechanisms must be brought into play.

6.4.4 Effect of Long-term NT Exposure on NTS2 Trafficking and Function

In order to visualize the effect of NT stimulation on NTS2 intracellular trafficking, transfected COS-7 cells were incubated in the presence or absence of 1 μM NT for 60 min at 37°C and the distribution of immunolabeled receptors was examined by confocal microscopy. Immunostaining of non stimulated, permeabilized cells revealed a prominent juxtanuclear pool of NTS2 receptors as well as small peripheral, presumably membrane-associated, receptor clusters (Fig. 6.4*A*). To ensure that the localization of the receptors was not due to an idiosyncratic feature of COS-7 cells, we repeated the experiments using CHO cells stably expressing rNTS2. As in COS-7 cells, NTS2 exhibited a predominantly intracellular distribution (not shown). Following 60 min stimulation with NT at 37°C, intracellular immunoreactive receptors were no longer concentrated next to the nucleus, but became scattered throughout the cytoplasm in the form of small vesicle-like clusters (Fig. 6.4*A*). However, there was no apparent change in the density of cell surface receptor clusters (Fig. 6.4*A*, arrowheads). Indeed, quantitative image analysis confirmed that there was no difference in the relative density of peripheral immunolabeling before and after NT stimulation (15,3 ± 1.8% versus 15.9 ± 3.6%, respectively; $p > 0,95$; Fig. 6.4*B*). These data suggest that receptor activation results in a redistribution of intracellular receptor stores without any apparent loss of cell surface receptors.

To ascertain whether NTS2 receptors present at the cell surface following prolonged NT exposure were functional, rNTS2-expressing COS-7 cells were preincubated or not with 1 μM NT for 24 h at 37°C and serum-starved for 2 h without the agonist. ERK1/2 phosphorylation was then measured in response to subsequent pulse stimulations with NT. As shown in Fig. 6.5, NT induced a rapid (< 5 min) and sustained phosphorylation (over 1 h) of ERK1/2, irrespective of whether cells had been preincubated or not with NT for 24 h. Moreover, densitometric analysis of the ratio of phosphorylated ERK1/2 over total ERK1/2 levels indicated that NT pretreatment did not significantly influence the agonist-induced ERK1/2 activation (5.2 ± 1.6 versus 4.6 ± 0.6-fold increase in ERK1/2 phosphorylation levels at 5 min

in cells pretreated or not with NT, respectively; $p > 0.95$). This effect was NTS2-mediated since it was not observed in untransfected cells (not shown). Thus, these data indicate that NTS2 receptors maintained at the cell surface following sustained ligand exposure are truly functional.

6.4.4 Golgi and TGN as Putative Sources of Newly Recruited NTS2 Receptors

To investigate putative intracellular sources for the membrane recruitment of NTS2 receptors, we co-localized NTS2 with the molecular markers syntaxin 6 or PIST, using dual labeling immunocytochemistry in rNTS2-expressing COS-7 cells. Previous studies have shown that Syntaxin 6 is present mainly in the trans-Golgi network (TGN) and participates in vesicular trafficking between the TGN and endosomes (Bock et al., 1997), whereas PIST (PDZ domain Protein Interacting Specifically with TC10) is known to be associated with the Golgi apparatus (Wente et al., 2005). In unstimulated cells (Fig. 6.6*A-F*), NTS2 immunoreactivity (Fig. 6.6*A* and *D*) was largely intracellular and concentrated in a compact juxtanuclear structure that was immunopositive for endogenous syntaxin 6 (Fig. 6.6*B*) and PIST (Fig. 6.6*E*), as shown in overlays (Fig. 6.6*C* and *F*). These data strongly suggest that NTS2 localizes primarily to the TGN/Golgi complex. This observation was confirmed by the fact that disassembly of the Golgi complex by Brefeldin A induced a total dispersion of NTS2 through the cytoplasm (data not shown). Following a 1 h-incubation with 1 μM NT (Fig. 6.6*G-L*), NTS2 immunolabeling was still noticeable in the TGN/Golgi where it remained co-localized with syntaxin 6 (Fig. 6.6*H*) and PIST (Fig. 6.6*K*). However, NTS2 was also apparent in vesicle-like structures distributed throughout the cytoplasm of the cells. These fluorescent clusters were partially immunopositive for syntaxin 6, but not for PIST, as shown in overlays (Fig 6.6*I* and *L*). Similar experiments using the anti-lamp1 antibody as a molecular marker revealed that NT exposure did not induce the trafficking of NTS2 receptors to lysosomes for degradation (not shown). Taken together, these data suggest that NTS2 receptors targeted to the plasma membrane subsequent to NT stimulation could originate from the TGN/Golgi.

6.4.6 Effect of NT Stimulation on Cell Surface NTS2 Density in Rat Spinal Cord

To determine whether the preservation of cell surface NTS2 receptors observed following sustained stimulation of transfected cells *in vitro* also occurred in neuronal cells *in vivo*, we examined by immunoelectron microscopy the fate of NT-stimulated NTS2 receptors in neurons of the superficial layers of the rat spinal cord, which had previously been reported to contain high concentrations of NTS2 receptor immunoreactivity (Sarret et al., 2005). In both stimulated and unstimulated conditions, the bulk of NTS2 immunoreactivity was associated with dendritic shafts, branches and branchlets (Fig. 6.7*A* and *B*). In saline-injected rats, NTS2 immunolabeling within these dendrites was associated mostly with intracellular vesicles and organelles (Fig. 6.7*A*). Only a small fraction of immunogold particles was found on the plasma membrane (4.7 ± 2.6% of total; Fig 6.7*C*). Following 20 min exposure to intrathecal NT, there was a considerable increase in the proportion of immunogold-receptor complexes associated with the plasma membrane (35.1 ± 8.5% of total; Fig 6.7*B* and *C*). By contrast, the density of immunoreactive receptors (immunogold particles per μm^2) was not statistically significantly different between NT- (4.6 ± 2.3 particles/μm^2) and saline-injected (8.2 ± 4.7 particles/μm^2) animals ($p > 0.95$; Student's t-test), indicating that the NT-induced change in plasma membrane receptor density was a trafficking event.

6.5 DISCUSSION

In the present study, we have demonstrated a preservation of cell surface NTS2 receptor densities following prolonged exposure to NT. This preservation did not depend on receptor neosynthesis or recycling, but appeared to involve recruitment of spare receptors from intracellular stores to the plasma membrane.

Sustained activation of most GPCRs triggers a time-dependent decline of cell surface receptors. This process, which reverses upon agonist removal, is of direct clinical relevance as it accounts in part for cellular desensitization to a variety of GPCR-acting drugs (Roth et al., 1998). As confirmed in the present study, agonist stimulation of NTS1 likewise resulted in a loss of cell surface receptors that is known to occur through internalization and lysosomal degradation degradation (reviewed in Hermans and Maloteaux, 1998). In the case of NTS2, stimulation with NT was found here to first induce a rapid decrease in cell surface receptor density (i.e. 50 % by 5 min). This decrease was previously shown by us (Sarret et al., 2002) and others (Botto et al., 1998) to be due to ligand-induced receptor internalization and, accordingly, to be entirely abolished in the presence of sucrose or phenylarsine oxide, which inhibits internalization. However, this decrease was short-lived and, in spite of persistent ligand exposure, NTS2 receptors rapidly resurfaced. Indeed, binding activity recovered to 80% of pre-stimulation levels by 1 h and to 100% after 24 h of stimulation with NT. This reinstatement of cell surface receptors cannot be ascribed to ligand degradation as the same phenomenon was observed when the incubation was carried out with the protease-resistant NT analog JMV-431, instead of NT. The cell surface binding sites maintained during persistent NT exposure corresponded to functional NTS2 receptors since NT-induced ERK1/2 phosphorylation levels in cells exposed to NT for 24 h were comparable to those measured in control cells and were similar to those previously reported in rat cerebellar granule cells (Sarret et al., 2002) and transfected CHO cells (Gendron et al., 2004).

Maintenance of cell surface receptors in response to sustained activation has been documented for a limited number of GPCRs including the β_3-adrenergic receptor (Thomas et al., 1992), somatostatin receptor subtype 1 (Hukovic et al., 1999), and AT_2 angiotensin II receptors (Dudley et al., 1993). It has also been shown for the single transmembrane domain receptor NTS3, following prolonged stimulation with NT (Navarro et al., 2001; Morinville et al., 2004). Cell surface receptor densities are known to result from the equilibrium between receptor internalization, recycling and recruitment from intracellular stores (Koenig et al., 1997). In the case of NTS2, recycling of internalized receptors, demonstrated under different experimental conditions (Botto et al., 1998; Debaigt et al., 2004), did not appear to account significantly for the reinstatement of the plasma membrane receptor population after prolonged NT exposure. Indeed, cell surface receptor recovery was not affected by blockade of receptor recycling with monensin nor by replacing rat NTS2 with the non-recycling human NTS2 (Martin et al., 2002b). Neither did the maintenance of cell surface NTS2 receptor densities appear to require receptor neosynthesis since NTS2 protein levels, as measured by Western blotting, remained unchanged following NT exposure with or without the protein synthesis inhibitor cycloheximide.

Immunocytochemistry revealed that under baseline conditions, the bulk of NTS2 proteins were intracellular (i.e. 84.7 ± 1.8% of total receptors in basal conditions). This observation is in agreement with the results of subprograms executed by the PSORT II server (Kenta Nakai, Ph.D., Institute for Medical Science, University of Tokyo, Japan), which predicted the subcellular localization of NTS2 from its amino acid sequence to be poorly localized to the plasma membrane (22.2%) and possibly confined to intracellular stores such as the endoplasmic reticulum (33.3%), Golgi apparatus (11.1%), intracellular vacuoles (22.2%), and mitochondrial compartments (11.1%). However, confocal microscopic experiments on permeabilized cells demonstrated that NT induced an extensive redistribution of NTS2 receptors from the TGN/Golgi complex (syntaxin 6 and PIST-positive) to vesicle-like structures, suggesting that the maintenance of surface NTS2 receptors

involved mobilization of spare receptors from internal stores. Although syntaxin 6 was mainly concentrated in the TGN, it was also detected in the NTS2-containing vesicles that formed as a result of NT exposure. This co-localization is consistent with previous results showing that syntaxin 6 co-localizes broadly with the early endosomal autoantigen EEA1 in BHK-21 cells and may therefore be implicated in TGN to endosomes trafficking (Simonsen et al., 1999). Interestingly, an earlier study in NTS2-expressing cerebellar granule cells had demonstrated that following prolonged NT stimulation, internalized fluorescently-labeled NT was targeted to a syntaxin 6-positive juxtanuclear compartment, corresponding to the TGN (Sarret et al., 2002). It is therefore possible that internalized NT is targeted to the TGN and serves as a triggering signal for the translocation of resident NTS2 receptors from this compartment to the cell surface, implying a dynamic regulation of subcellular protein localization.

The physiological and pharmacological relevance of the present results was confirmed by immunogold electron microscopic studies of the superficial laminae of the rat spinal cord. Intrathecal injection of NT resulted in a seven-fold increase in the proportion of immunoreactive NTS2 receptors associated with dendritic plasma membranes as compared with saline-injected controls. This increase in the density of plasma membrane-associated NTS2 was not accompanied by a statistically significant increase in the overall receptor population, suggesting that, as in our *in vitro* studies, the NT-induced increase of NTS2 receptors at the plasma membrane of dorsal horn neurons was a trafficking event. These results are reminiscent of the enhanced recruitment of delta opioid receptors (DOR) to the plasma membrane of dendrites in the same superficial laminae of the dorsal horn following either prolonged morphine treatment (Cahill et al., 2003) or chronic inflammation (Cahill et al., 2001). However, whereas this enhanced DOR targeting was heterologously mediated through stimulation of μ-opioid receptors (Morinville et al., 2003), the present increase in NTS2 externalization likely results from stimulation of NTS2 receptors themselves. The present results may, therefore, explain the highly potent,

long-lasting antinociceptive effects of the NTS2-specific agonist JMV-431 in tests of spinal analgesia (Sarret et al., 2005).

In conclusion, we have demonstrated that cell surface NTS2 receptors are resistant to down-regulation following persistent exposure to NT. By inference from the patterns of intracellular distribution of NTS2 receptors observed using confocal and electron microscopy, we propose that the maintenance of cell surface NTS2 receptors is due in part to the recruitment of spare receptors from internal stores. This stimulation-induced regulation of cell surface NTS2 receptors was even more striking in rat spinal cord neurons *in vivo* (7-fold increase in cell surface receptor density) than in transfected COS-7 cells in vitro (return to baseline). Such maintenance of NTS2 bioavailability upon prolonged agonist treatment might prove of great importance for the use of NTS2-selective agonists for the treatment of chronic pain.

6.6 ACKNOWLEDGMENTS

The authors are grateful to Dr. Hans-Jürgen Kreienkamp for the anti-PIST antibody and Naomi Takeda for secretarial help in the preparation of this article.

6.7 FOOTNOTES

This work was funded by grants from the Canadian Institutes for Health Research (CIHR) (to Alain Beaudet) and from the Institut National de la Santé et de la Recherche Médicale (INSERM)/ Fonds de la Recherche en Santé du Québec (FRSQ) exchange program (to Alain Beaudet and Jean Mazella). Amélie Perron was supported by a fellowship from FRSQ. Nadder Sharif and Louis Gendron were supported by fellowships from the Natural Sciences and Engineering Research Council of Canada (NSERC) and CIHR, respectively.

6.8 ABBREVIATIONS

NT, neurotensin; DMEM, Dulbecco's modified Eagle's medium; FBS, fetal bovine serum; BSA, bovine serum albumin; PB, phosphate buffer; RT, room temperature; GPCR(s), G protein coupled receptor(s); TM, transmembrane domain; COS-7 cells, green African monkey kidney cells; CHO, Chinese hamster ovary; MAPK, mitogen-activated protein kinase; ERK1/2, extracellular signal-regulated kinases 1/2; TGN, trans-Golgi network.

6.9 FIGURES

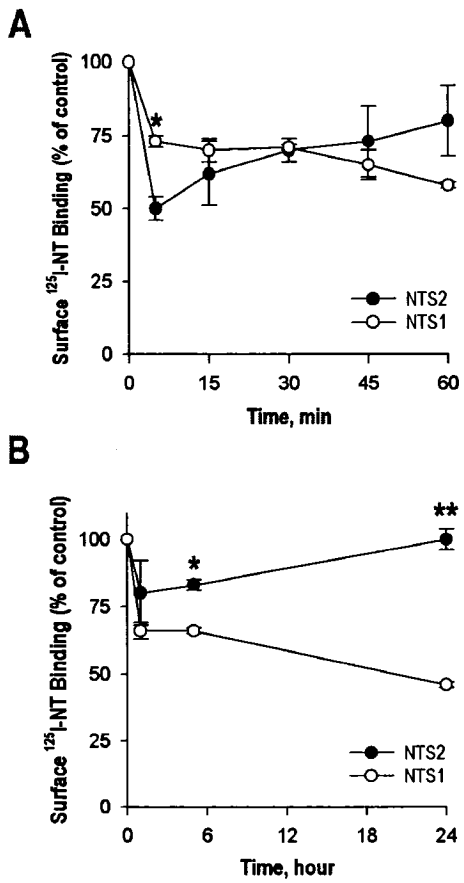

Figure 6.1

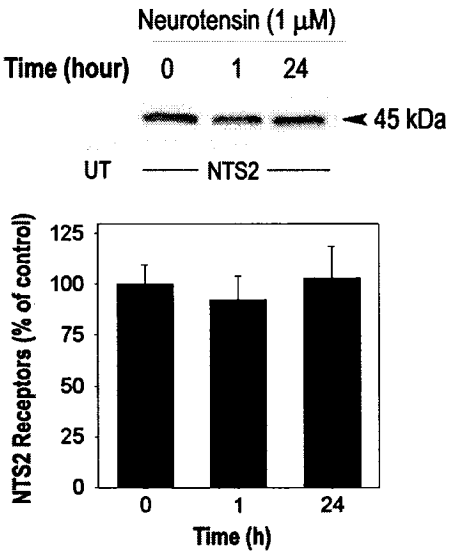
Neurotensin (1 μM)
Time (hour) 0 1 24
45 kDa
UT
NTS2
NTS2 Receptors (% of control)
125
100
75
50
25
0
0
1
24
Time (h)

Figure 6.2

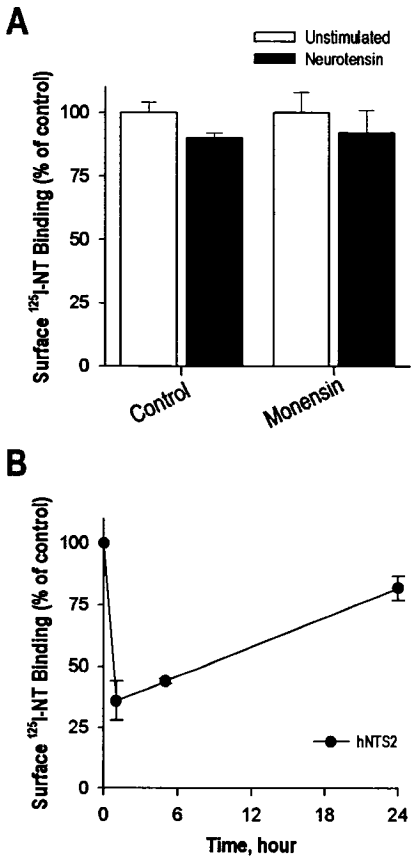
A
Unstimulated
Neurotensin
Surface ^{125}I-NT Binding (% of control)
100
75
50
25
0
Control
Monensin
B
Surface ^{125}I-NT Binding (% of control)
100
75
50
25
0
hNTS2
0
6
12
18
24
Time, hour

Figure 6.3

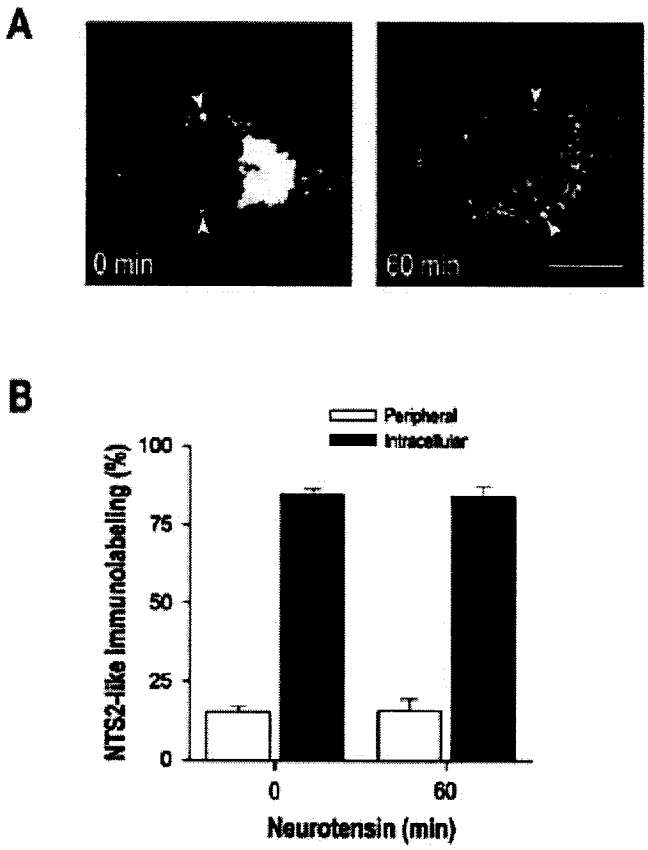
A
0 min
60 min
B
Peripheral
Intracellular
NTS2-like immunolabeling (%)
100
75
50
25
0
0
60
Neurotensin (min)

Figure 6.4

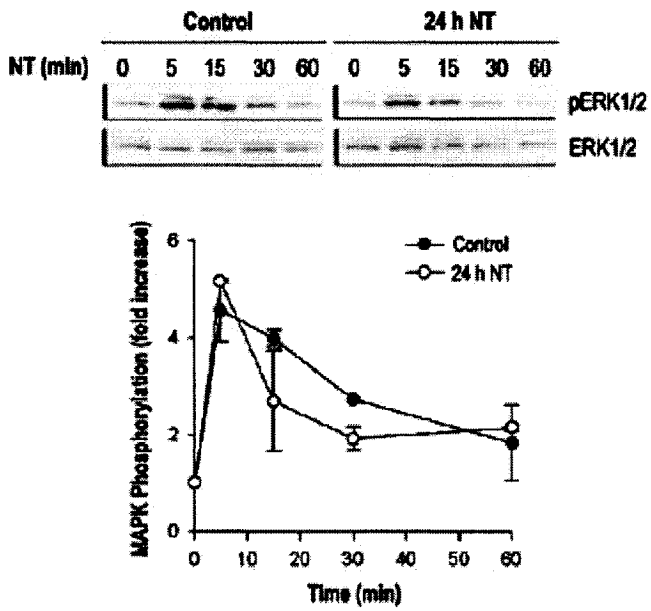
Control
24 h NT
NT (min)
0 5 15 30 60 0 5 15 30 60
pERK1/2
ERK1/2
MAPK Phosphorylation (fold increase)
Control
24 h NT
0 2 4 6
0 10 20 30 40 50 60
Time (min)

Figure 6.5

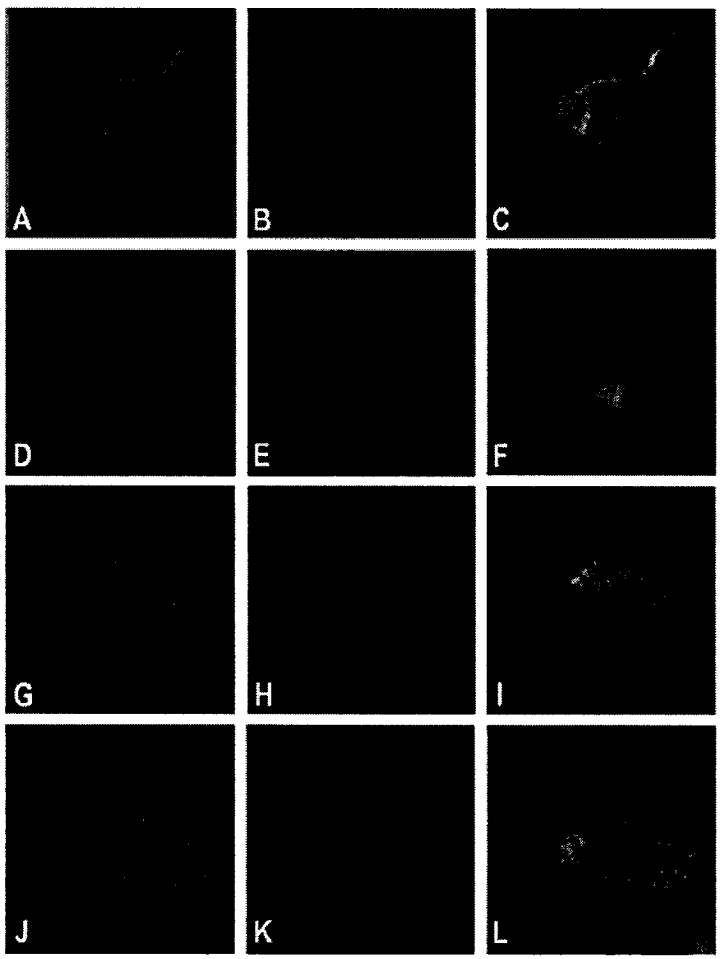

Figure 6.6

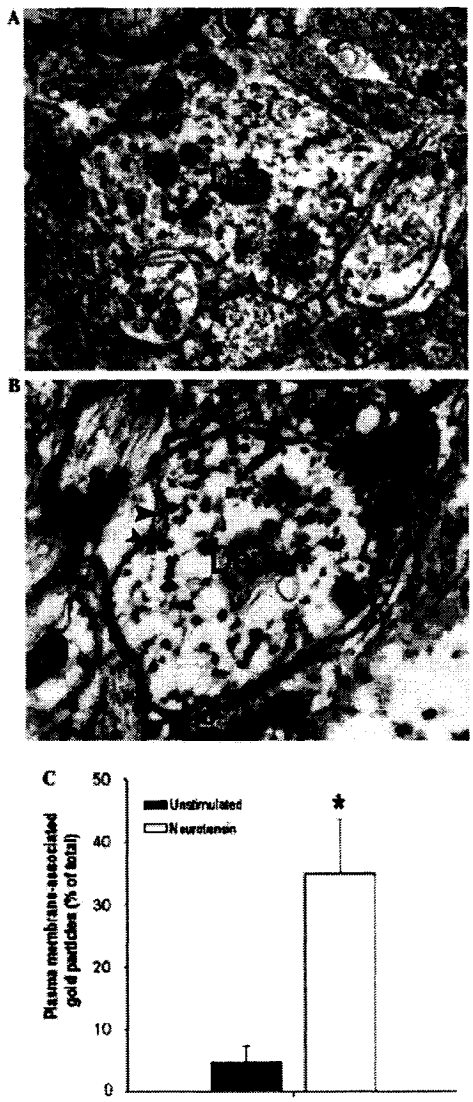
A
B
C
50
40
30
20
10
0
Unstimulated
Neurotensin
*
Plasma membrane-associated gold particles (% of total)

Figure 6.7

6.10 FIGURE LEGENDS

Fig. 6.1: Persistent Agonist-Induced Regulation of Cell Surface NT Receptors. COS-7 cells expressing rNTS2 (●) or NTS1 (○) were exposed to 1 μM NT for 0-60 min (*A*) and up to 24 h (*B*) at 37°C, acid-washed, and incubated with [^{125}I]-NT on ice for monitoring cell surface receptors. The results are representative of three individual experiments ± S.E.M, each with triplicate determinations. Student's *t* tests were used to compare NT cell surface binding sites between rNTS2 and NTS1 expressing COS-7 cells. Values are significantly different at all time points with *, $p < 0.05$ and **, $p < 0.01$.

Fig. 6.2: Effect of NT Stimulation on NTS2 Receptor Protein Levels in COS-7 Cells. COS-7 cells transiently transfected with cDNA encoding the rNTS2 receptor were stimulated with 1 μM NT for different periods of time at 37°C and membranes were isolated as described under "Materials and Methods". Similar experiments were done with untransfected (UT) cells as a negative control. Western blotting analysis was performed using the NTS2 peptide antiserum after a 10% Tris-glycine gel electrophoresis under reducing conditions and NTS2 receptor protein levels were quantified by densitometric analysis. The data represent the mean ± S.E.M of three individual experiments.

Fig. 6.3: Recycling is Not Involved in the Maintenance of Cell Surface NTS2 Binding Sites. *A*, COS-7 cells expressing rNTS2 were preincubated with 25 μM monensin for 30 min and stimulated with NT with the recycling inhibitor for 1 h at 37°C. The peptide was removed by acid wash and cells were incubated with [^{125}I]-NT on ice to determine the amount of cell surface receptors. Each point is the mean ± S.E.M from triplicate determinations of at least two different experiments. *B*, COS-7 cells expressing the non-recycling human NTS2 receptor were exposed to 1 μM NT for up to 24 h at 37°C, acid-washed, and incubated with [^{125}I]-NT on ice for monitoring cell surface receptors. The results are representative of two individual experiments ± S.E.M, each with triplicate determinations.

Fig. 6.4: NT-Induced Intracellular Redistribution of NTS2 Receptors in COS-7 Cells. *A*, rNTS2-expressing COS-7 cells were stimulated or not with 1 μM NT for 60 min at 37°C. Immunolabeling was then performed on permeabilized cells by using the NTS2 peptide antiserum. Scale bar = 5 μm. *B*, Quantitative analysis of NTS2-like immunoreactive staining densities in COS-7 cells stimulated or not with NT. Data are expressed as a percentage of integrated density values associated with peripheral (including cell surface) versus intracellular compartments over total fluorescence (representative of four independent experiments).

Fig. 6.5: Effect of Persistent Stimulation with NT on ERK1/2 Phosphorylation in COS-7 Cells Heterologously Expressing rNTS2. Cells were pretreated (○) or not (●) with 1 μM NT for 24 h at 37°C and subsequently incubated with 1 μM NT for the indicated periods of time (0-60 min). ERK1/2 activity was determined by the ratio of the densitometric analysis of phosphorylated ERK1/2 over total ERK1/2 levels expressed as fold increase over control. Data represent the means ± S.E.M of two individual experiments, each with triplicate determinations.

Fig. 6.6: Dual Immunolabeling of NTS2 and Trans-Golgi Network Markers in COS-7 Cells. Confocal microscopic images of cells transiently expressing rNTS2 preincubated (*G-L*) or not (*A-F*) with 1 μM NT for 1 h at 37°C. In unstimulated cells, NTS2 labeling with the NTS2 peptide antiserum (*A*, *D*) co-localizes with immunoreactivity for the TGN/Golgi markers syntaxin 6 (*B*) and PIST (*E*) in the perinuclear zone as evident in the overlays (*C*, *F*). Following incubation with NT, NTS2 immunostaining is punctate and dispersed throughout the cell. Part of NTS2-positive vesicles also exhibit syntaxin 6 (*H*) but not PIST (*K*) immunoreactivity as shown in the merged images (*I*, *L*). All images were acquired using the same parameters and represent three different experiments.

Fig. 6.7: Electron Microscopic Detection of NTS2 Immunoreactive Receptors in Superficial Laminae of the Rat Lumbar Spinal Cord. *A*, In the absence of the agonist, gold particles (i.e. NTS2 immunolabeling) are mainly intracellular and poorly associated with dendritic (Den) plasma membranes. *B*, In the presence of NT, numerous immunogold particles are associated with dendritic plasma membranes (arrowheads). *C*, Effects of NT exposure on membrane-associated/total NTS2. The asterisk indicates a significant difference ($p < 0.05$) from control.

CHAPTER 7

NTS2 MODULATES THE INTRACELLULAR DISTRIBUTION AND TRAFFICKING OF NTS1 VIA HETERODIMERIZATION

Amélie Perron, Nadder Sharif, Philippe Sarret[¶], Thomas Stroh, and Alain Beaudet

Montreal Neurological Institute, Department of Neurology and Neurosurgery, McGill University, Montreal, Québec, Canada

[¶]Present Address: Department of Physiology and Biophysics, Faculty of Medicine, Sherbrooke, Québec, Canada

Submitted to the *Journal of Biological Chemistry* (2006)
Manuscript M6:05442

7.1 ABSTRACT

G protein-coupled neurotensin (NT) receptors NTS1 and NTS2 show considerable distributional overlap in mammalian central nervous system (CNS). However, studies on transfected cells demonstrate that while NTS1 localizes predominantly to the plasma membrane, the bulk of NTS2 receptors are intracellular when either receptor is expressed alone. Using co-immunoprecipitation approaches, we demonstrate here that in transfected COS-7 cells NTS1 forms constitutive heterodimers with NTS2 via hydrophobic interactions. We also show using radioligand-binding and confocal immunolocalization techniques, that co-expression of NTS2 with NTS1 markedly decreases the cell-surface density of NTS1 as compared to cells expressing NTS1 alone. Functionally, NT-induced increase in ERK1/2 MAPK activity was similar in cells expressing NTS1 alone or together with NTS2, indicating that NTS1/NTS2 heterodimerization did not affect this signaling pathway. Likewise, NT-induced NTS1 internalization was equally efficient in both cell types. However, radioligand-binding studies indicated that upon prolonged NT stimulation, cell surface NTS1 receptors were more resistant to down-regulation in cells co-expressing NTS1 and NTS2 than in cells expressing NTS1 alone. Taken together, these data suggest that NTS1/NTS2 heterodimerization affects the intra-cellular distribution and trafficking of NTS1 by making it more similar to that of NTS2 as witnessed in cells expressing NTS2 alone. NTS1/NTS2 heterodimerization might therefore represent an additional mechanism in the regulation of NT-triggered responses mediated by NTS1 and NTS2 receptors.

7.2 INTRODUCTION

There is now strong evidence that many GPCRs form homo and/or heterodimers and that these molecular interactions are required for their normal functioning and trafficking (Bouvier, 2001; Bai, 2004a and 2004b; Prinster et al., 2005). For instance, the heterodimerization of $GABA_BR1$ and $GABA_BR2$ within the endoplasmic reticulum was shown to be required for the formation of functional $GABA_B$ receptors at the cell surface (Margeta-Mitrovic et al., 2000). Other studies have demonstrated that heterodimerization of taste receptors is necessary for sensing sweet substances or L-amino acids such as monosodium glutamate (Nelson et al., 2001; Nelson et al., 2002). However, heterodimerization between different receptor subtypes can also exert a dominant-negative effect on intracellular signaling. In the case of β adrenergic receptors (AR), heterodimerization of β_1AR with β_2AR has been shown to inhibit both β_2AR-dependent activation of extracellular signal-regulated kinases (ERK1/2) and its ligand-induced internalization (Lavoie et al., 2002). Likewise, the functional properties of the somatostatin receptor subtype 5 (SST5) were found to be modified by its heterodimerization with SST1 (Rocheville et al., 2000).

Neurotensin (NT) is a brain and gastrointestinal peptide that mediates a variety of central and peripheral functions including opioid-independent antinociception, neuroleptic-like modulation of dopamine neurotransmission and inhibition of food intake (Tyler-McMahon et al., 2000; Vincent et al., 1999). Three different NT receptor subtypes have been cloned to date. NTS1 and NTS2 belong to the family of G protein-coupled receptors (GPCRs), whereas NTS3 is a single transmembrane domain sorting receptor with 100% homology to sortilin (Tanaka et al., 1990; Chalon et al., 1996; Mazella et al., 1998; Petersen et al., 1997). The rat NTS1 cDNA contains a large open-reading frame encoding a 424-amino acid protein, sharing 43% identity and 64% homology with NTS2 (Tanaka et al., 1990; Chalon et al., 1996). However, whereas NTS1 binds NT with high affinity (K_d = 0.2 nM), NTS2 binds NT with a tenfold lower affinity (K_d = 2 nM). Furthermore, NTS2 recognizes the

antihistamine drug levocabastine, while NTS1 does not (Vincent et al., 1999). Although the lengths of both receptor proteins are very similar, NTS1 and NTS2 differ markedly in their third intracellular domains and C-terminal tails, two regions bearing specificity for G-protein coupling and receptor regulation. Accordingly, different sets of transduction and trafficking mechanisms have been linked to each receptor subtype. Whereas NTS1 was shown to modulate intracellular levels of cGMP (Amar et al., 1985), inositol phosphates (Watson et al., 1992), cAMP (Bozou et al., 1989a), and ERK1/2 (Poinot-Chazel, et al., 1996), NTS2 was found to induce Ca^{2+}-dependent chloride currents in *Xenopus oocytes* (Botto et al., 1997c) and to activate ERK1/2 signaling cascades, both in CHO (Gendron et al., 2004) and rat cerebellar granule cells (Sarret et al., 2002). Furthermore, while both receptors efficiently internalize upon ligand binding, NTS1 down-regulates from the cell surface and undergoes lysosomal degradation (Hermans and Maloteaux, 1998; Vandenbulcke et al., 2000), whereas NTS2 recycles and does not down-regulate from the cell surface even after prolonged receptor stimulation (Perron et al., 2006).

A recent study has demonstrated that NTS1 and NTS3 formed heterodimers in the HT29 cell line (Martin et al., 2002b). This interaction was shown to modulate both NTS1-mediated ERK1/2 MAPK signaling and phosphoinositide turnover (Martin et al., 2002b). To date, there has been no evidence for heterodimerization between NTS1 and NTS2, but both of these NT receptor subtypes possess a cysteine residue in each of their extracellular loops, which could enable the formation of disulfide bonds between them (Vincent et al., 1999). Indeed, the formation of disulfide bonds was shown to be essential for dimerization and proper trafficking of other types of receptors (Fan et al., 1998). Furthermore, there is considerable regional and cellular overlap between the distributions of NTS1 and NTS2 in rodent brain, suggesting that these receptors are in a position to interact with one another physiologically (Boudin et al., 1996b; Sarret et al., 2003a).

In the present study, we combined biochemical and pharmacological approaches to investigate the ability of NTS1 and NTS2 receptors to interact with one another in heterologous transfection systems. We demonstrate that NTS1 and NTS2 receptor subtypes can form constitutive heterodimers. This heterodimerization does not alter ERK1/2 MAPK signaling but influences the subcellular distribution of NTS1 and decreases its capacity to down-regulate following persistent agonist exposure.

7.3 EXPERIMENTAL PROCEDURES

7.3.1 Expression of NTS1 and NTS2 mRNAs

In order to study the expression patterns of NTS1 and NTS2 mRNAs in the rat CNS and spinal cord, adult male Sprague-Dawley rats (200-250 g; Charles River, St-Constant, Québec, Canada) were killed by decapitation. The brain and spinal cord were rapidly removed and areas of interest dissected on ice. Samples were processed as described in Perron et al., (2005). Total mRNAs (2 μg) were then reverse-transcribed at 42°C for 1 h using the Reverse Transcription System kit (Promega, Madison, WI, USA). First strand cDNAs were subjected to 35 cycles of polymerase chain reaction (PCR) in a final volume of 50 μl reaction buffer (50 mM KCl, 10 mM Tris-HCl, pH 9.0, 1.5 mM $MgCl_2$, 0.1% Triton X-100, 0.02% bovine serum albumin (BSA), 200 μM dNTPs, 0.5 unit of *Taq* DNA polymerase) containing one of the following pairs of sense and antisense primers. The first set (5'-ACACCCATTGTGGACACAGCC-3' and 5'-TTCATCCGAGATATAGCAGAA-3') allows the amplification of a fragment of the rat NTS1 receptor cDNA with a predicted size of 335 bp as demonstrated in (Sarret et al., 2002). The second pair of oligonucleotides (5'-GAATGTGCTGGTGTCCTTCGC-3' and 5'-ACTTGTAT-TTCTCCCAGGCTG-3') is derived from bases 667-1287 in the sequence previously reported for the rat NTS2 receptor (Chalon et al., 1996). These primers are bordering the region where the 181 bp-deletion takes place in the rat vNTS2, allowing the amplification of fragments of 620 and 439 bp as established before in rat cerebellar granule cell cultures (Sarret et al., 2002).

7.3.2 Gene Constructs

The molecular cloning of the cDNA sequence encoding the rat truncated (NTS2-STOP) or full-length NTS2 receptors into the mammalian expression vector pTargeT (Promega, Madison, WI), and HA-tagged NTS1 in pcDNA3 has been described previously (Perron et al., 2005; Sarret et al., 2003a; Labbé-Jullié et al., 1998). The C363A, C621A and C993A (cysteine → alanine) NTS2 mutants were obtained by site-directed mutagenesis on the NTS2 full-length cDNA with the QuickChange® II

Kit (Stratagene, La Jolla, CA), using the respective pairs of sense and antisense primers (MOBIX laboratory, McMaster University, Hamilton, Ontario, Canada): (5'-CTTCGGCGATCTGGGCGCCCGTGGCTATTACTTCG-3'/5'-CGAAGTAATAG-CCACGGGCGCCCAGATCGCCGAAG-3'), (5'-GCCTGCCTCGCGTGTGGCCA-CGGTGCTGGTGAGCC-3'/5'-GGCTCACCAGCACCGTGGCCACACGCGAGC-AGGC-3') and (5'-CGCCGACTCATGTACGCCTACATCCCCGATGATGG-3'/ 5'-CCATCATCGGGGATGTAGGCGTACATGAGTCGGCG-3'). The C621/993A and C363/993A double mutants and the C363/621/993A triple mutant were created by changing cysteine at a given site to alanine throughout the next rounds of mutagenesis. The fidelity of PCR amplification was confirmed by DNA sequence analysis using the ABIPRISM® 3100 Genetic Analyzer in the MOBIX laboratory.

7.3.3 Cell Culture and Transfections

COS-7 cells were cultured in Dulbecco's modified Eagle's medium (DMEM) with high glucose supplemented with 5% fetal bovine serum (FBS) in the presence of penicillin/streptomycin (100 units/ml; Invitrogen Burlington, Ontario, Canada). Cells were grown to 70-80% confluence in 100-mm dishes at 37°C in a humidified atmosphere of 95% air and 5% CO_2. Cells were then transiently transfected with 7 ml of a mixture of 100 μM chloroquine and 0.25 mg/ml DEAE-dextran containing a total of 4 μg of plasmid DNA (2 μg of HA-NTS1 with 2 μg of either pTargeT vector or untagged-NTS2).

7.3.4 Immunoprecipitation and Immunoblotting Analysis

For immunoprecipitation studies, COS-7 cells expressing the HA epitope-tagged NTS1 together with the untagged NTS2 receptor were lysed in RIPA buffer (150 nM NaCl, 50 mM Tris-HCl, pH 7.5, 5 mM EDTA, 1% IGEPAL, 0.5% deoxycholic acid, 0.1% sodium dodecyl sulfate) including protease inhibitors (Complete inhibitor tablets; Roche Laboratories, Montreal, Québec, Canada) and incubated for 30 min on ice. Lysates were then precleared with 25 μg of protein A-Sepharose (Sigma, St-Louis, MO) for 45 min at 4°C and incubated overnight at 4°C with either a mouse monoclonal antibody (clone 12CA5) directed toward the HA epitope (1/500; Roche

Molecular Biochemicals, Indianapolis, IN) or a rabbit NTS2 peptide antiserum (1/1,000; made on demand by Affinity BioReagents, ABR, Golden, CO). Receptor proteins were immunoprecipitated with 100 µg of protein A-Sepharose for 2 h at 4°C. Complexes were dissolved in Laemmli sample buffer (Laemmli, 1970) and resolved on 10% Tris-glycine precast gels (Invitrogen, Burlington, Ontario, Canada). Nitrocellulose membranes (Bio-Rad Laboratories, Mississauga, Ontario, Canada) were then incubated with either NTS2 peptide antiserum (1/10,000) or anti-HA (1/2,500) overnight at 4°C, followed by a 1-h incubation with horseradish peroxidase (HRP)-conjugated goat anti-rabbit or HRP-conjugated goat anti-mouse antibodies (1/3,500; Amersham Pharmacia Biotech, Baie d'Urfé, Québec, Canada), respectively. Immunoreactive proteins were visualized using an enhanced chemiluminescent system (Perkin Elmer Life Science, Boston, MA).

For structural heterodimerization experiments, COS-7 cells expressing HA-NTS1 together with either pTargeT vector or NTS2 mutants (C363A, C621A, C993A, C621/993A, C363/993A, C363/621/993A, and NTS2-STOP) were processed as mentioned above. Receptor proteins were immunoprecipitated using anti-HA antibody (1/400) and immunoblotting was then carried out with the NTS2 peptide antiserum (1/10,000).

7.3.5 Immunocytochemical Detection of NTS1 and NTS2

COS-7 cells transfected with HA-tagged NTS1 alone or together with untagged-NTS2 were plated on poly-L-lysine-coated glass coverslips, fixed for 20 min with 4% paraformaldehyde (PFA; Polysciences, Warrington, PA) in PBS, pH 7.4 and preincubated for 30 min at room temperature (RT) with a blocking solution consisting of 5% Normal Goat Serum (NGS), 2% BSA, and 0.1% Triton X-100 (BDH Inc., Toronto, Ontario, Canada) in PBS. Cells were incubated overnight at 4°C with mouse anti-HA (1/500), together with rabbit NTS2 peptide antiserum (1/15,000) in PBS containing 1% NGS and 0.05% Triton X-100. Cells were then incubated for 1 h at RT with a mixture of Alexa 594-conjugated goat anti-rabbit and Alexa 488-conjugated goat anti-mouse antibodies (1/500; Molecular Probes, Eugene, OR). Results were analyzed using a Zeiss 510 laser scanning confocal microscope

equipped with Argon2 (488 nm) and He/Ne1 (543 nm) lasers (Carl Zeiss Micro Imaging Inc., Thornwood, NY). Images were processed with the Zeiss 510 laser scanning microscope software and Adobe Photoshop 6.0.

7.3.6 Receptor Binding and Internalization Experiments

For cell surface binding experiments, COS-7 cells transiently expressing NTS1 alone or together with NTS2 were transferred to 24-well plates 24 h following transfection. After equilibration for 10 min at 37°C in Earle's buffer (130 mM NaCl, 5 mM KCl, 1.8 mM $CaCl_2$, 0.8 mM $MgCl_2$, HEPES 20 mM, pH 7.4) supplemented with 0.2% BSA/0.1% glucose, saturation experiments were performed by incubating cells with increasing concentrations (0.1 to 4.5 nM) of [^{125}I]-NT (2200 Ci/mmol; Perkin Elmer) isotopically diluted with unlabeled NT, in 250 µl of binding buffer containing 0.8 mM *ortho*-phenanthroline, and 10^{-5} M levocabastine (to prevent NT binding to NTS2). Nonspecific binding was determined in parallel, by adding 10^{-5} M non-radioactive NT to the incubation medium. After 30 min at 37°C, cells were washed twice with Earle's buffer and solubilized with 1 ml of 0.1 M NaOH. The radioactivity content was measured in a gamma counter. Dissociation constant (K_d) and maximal binding capacity (B_{max}) were derived from Scatchard analysis of the data.

For internalization experiments, COS-7 cells transiently transfected with HA-NTS1 together with pTargeT (control) or NTS2 subcloned into pTargeT were transferred into 24-well plates 24 h prior to assay. Cells were equilibrated for 10 min at 37°C in Earle's buffer supplemented with 0.2% BSA/0.1% glucose. The equilibration medium was then replaced by 250 µl of Earle's buffer containing 0.2 nM ^{125}I-labeled NT in the presence of 0.8 mM *ortho*-phenanthroline and an excess of levocabastine (10^{-5} M) for 3-45 min at 37°C. At the indicate times, cells were washed twice with 500 µl of binding buffer. To discriminate between surface-bound and sequestered ^{125}I-labeled NT, cells were washed for 2 min with 500 µl of a hypertonic acid buffer (Earle's buffer containing 0.2 M acetic acid and 0.5 M NaCl, pH 4) to strip off surface-bound radioactivity. Cells were then harvested in 1 ml of 0.1 M NaOH and cell associated radioactivity was measured in a gamma counter.

Non-specific binding was defined as binding in the presence of 10^{-5} M unlabeled NT, which represented less than 5% of total counts.

To determine the effect of prolonged NT exposure on NTS1 cell surface binding, COS-7 cells transiently expressing NTS1 alone or together with NTS2 were transferred to 24-well plates 24 h following transfection. Cells were incubated with or without 1 μM NT for up to 24 h in DMEM supplemented with 2.5% FBS. Cells were then washed once with hypertonic acid buffer, twice with Earle's buffer, and incubated with 0.4 nM [^{125}I]-NT for 60 min on ice in 250 μl of Earle's buffer supplemented with 0.25% BSA, 0.1% glucose and 0.8 mM *ortho*-phenanthroline, in the presence of unlabeled levocabastine. Cells were then processed for counting as described above.

All binding/internalization data were calculated and plotted using Prism 4.0 (Graph Pad Software) and represent the mean ± standard deviation (S.D.) of n determinations (as indicated in "Results"). Statistical comparisons between groups were performed using a two-tailed Student's *t* test. Differences were considered significant for $p < 0.05$.

7.3.7 Measurement of MAP Kinase Activity

COS-7 cells transiently expressing NTS1 alone or together with NTS2 were split into 6-well plates and incubated for 1-2 days in DMEM high glucose at 37°C. Cells were then serum-starved for 2 h and then incubated with 1 μM NT at 37°C for up to 1 h. The reaction was stopped by the addition of ice-cold PBS containing 0.1 μM staurosporine and 1 mM sodium orthovanadate. After 30 min incubation on ice, cells were lysed in 50 mM HEPES, pH 7.8, containing 1% Triton X-100, 0.1 μM staurosporine, 1 mM sodium orthovanadate, and protease inhibitors. Cell lysates were then centrifuged at 12,500 rpm for 10 min at 4°C and protein concentration was determined using the Bio-Rad procedure with BSA as standard. Parallel experiments were done using untransfected cells to determine the specificity of the assay. Samples containing 30 μg of protein were denatured in Laemmli sample buffer and resolved on 10% Tris-glycine precast gels. Nitrocellulose membranes were then

incubated overnight at 4°C with anti-phosphorylated ERK1/2 or anti-ERK1/2 rabbit antibodies (1/1,000; New England Biolabs, Beverly, MA) in PBS containing 1% ovalbumin and 1% BSA, followed by a 1 h-incubation with HRP-conjugated anti-rabbit antibody (1/3,500).

In order to quantify the effect of NT on ERK1/2 phosphorylation, the ratios of phosphorylated ERK1/2 over total ERK1/2 levels were determined by densitometry, using Scion Image Software. Calculations and statistical analyses were carried out in Excel 2000 (Microsoft) and SigmaPlot for Windows version 7.0. The statistical significance of the activation of ERK1/2 between cells expressing NTS1 alone or together with NTS2 was determined using a two-tailed Student's *t* test. Differences were considered significant for $p < 0.05$.

7.4 RESULTS

7.4.1 NTS1 and NTS2 Receptor mRNAs are Co-expressed in Rat CNS

In order to investigate the expression pattern of NTS1 and NTS2 mRNAs in rat brain and spinal cord, two sets of oligonucleotides designed to selectively recognize each NT receptor subtype were used for reverse-transcription PCR. As illustrated in Fig. 7.1, PCR amplification of total mRNA using NTS1 primers gave rise to a single band migrating at 335 bp, as observed in earlier studies of rat whole brain extracts (Sarret et al., 2002). NTS1 mRNA was detected in all brain regions examined, as well as in the spinal cord and pituitary (Fig. 7.1). PCR amplification of mRNA using NTS2 probes yielded two bands of 620 and 439 bp in size, corresponding to the full-length and transcriptionally-spliced NTS2 receptor mRNAs, respectively (Fig. 7.1). Both NTS2 transcripts were present throughout the brain and spinal cord but not in the pituitary (Fig. 7.1). No signal was detected when amplification was carried out with either one of the sense or antisense primers alone, demonstrating the specificity of the probes. Semi-quantitative analysis performed using GAPDH as an internal correction standard indicated that the levels of NTS1 and NTS2 mRNAs were not statistically different between the various regions examined (not shown). Taken together, these data revealed that NTS1 and NTS2 mRNAs are co-expressed throughout the brain and spinal cord.

7.4.2 Heterodimerization of NTS1 and NTS2 Receptors

To assess whether NTS1 and NTS2 formed hetero-oligomers, HA-tagged NTS1 and untagged NTS2 cDNAs were co-expressed in COS-7 cells. These cells were then stimulated or not with 1 μM NT for 1 h at 37°C, lysed and the lysates subjected to immunoprecipitation using a HA antibody (Fig. 7.2; *lanes 1 and 2*). Western blotting analysis of these immunoprecipitates with the NTS2 peptide antiserum showed that they contained NTS2 monomers and homodimers (45 and 83 kDa, respectively; *arrowheads*), which had been co-immunoprecipitated with the HA-tagged NTS1. Conversely, co-immunoprecipitation experiments using the NTS2 peptide antiserum followed by immunoblotting with anti-HA revealed the presence of immunoreactive

bands at approximately 51 and 100 kDa, corresponding to the size expected for monomeric and homodimeric forms of NTS1 (Fig. 7.2; *lanes 3-4*, *asterisks*). No specific bands were detected in cell lysates prepared from untransfected cells or in immunoprecipitates from cells expressing either HA-NTS1 or NTS2 alone, confirming the specificity of the interaction (not shown). Additionally, no co-immunoprecipitation was observed when lysates derived from cells expressing each receptor individually were mixed together, suggesting that solubilization did not promote non-specific dimerization (not shown). However, NTS1/NTS2 heterodimerization was not influenced by NT treatment (Fig. 7.2; *lanes 2 and 4*), indicating that NTS1 and NTS2 form constitutive heterodimers in transfected COS-7 cells.

7.4.3 Structural Requirements for NTS1/NTS2 Heterodimerization

To investigate whether the formation of disulfide bonds played a role in NTS1/NTS2 heterodimerization, we tested the ability of a series of NTS2 cysteine mutants to heterodimerize with NTS1. Each construct was expressed in COS-7 cells, together with HA-tagged NTS1, and cell lysates were subjected to immunoprecipitation by using the HA antibody. As illustrated in Fig. 7.3, immunoblotting with the NTS2 peptide antiserum revealed significant amounts of NTS2 monomers (45 kDa; *asterisk*) for all NTS2 cysteine mutants (C363A; *lane 1*, C621A; *lane 2*, C993A; *lane 3*, C363/621A; *lane 4*, C363/993A; *lane 5*, and C363/621/993A; *lane 6*), implying that NTS2 had been effectively co-immunoprecipitated with NTS1. These results thus suggest that disulfide bridging is not necessary for NTS1/NTS2 heterodimerization. In addition, a second band was also visible around 83 kDa, indicating that NTS2 homodimers are not influenced by cysteine mutations (*arrowhead*).

We also investigated the importance of the NTS2 C-terminal tail in NTS1/NTS2 heterodimer formation, using a truncated receptor lacking the last 55 amino acids of NTS2. This construct was co-expressed with HA-tagged NTS1 and immunoprecipitation was carried out with the HA antibody, as described above. Western blotting of immunoprecipitates using the NTS2 peptide antiserum revealed

the presence of a translation product of approximately 35 kDa as well as a faint band around 70 kDa, corresponding respectively to the monomeric and dimeric forms of the truncated NTS2 receptor as deduced from its cDNA sequence (Fig. 7.3; *lane 7, arrows*). These results therefore suggest that the NTS2 C-terminal tail is not essential for NTS1/NTS2 heterodimerization and that other domains of the receptors are taking part in the physical interaction.

7.4.4 Co-expression of NTS2 Modifies NTS1 Localization

To determine whether the physical interaction of NTS2 with NTS1 affected the binding properties of NTS1, saturation binding studies were carried out on cells expressing NTS1 alone or together with NTS2. As shown in Fig. 7.4*A*, incubation of either cell type with increasing doses of [^{125}I]-NT in the presence of an excess of levocabastine to ensure selective labeling of NTS1 (addition of levocabastine displaced >95% of [^{125}I]–NT binding in cells expressing NTS2 alone; data not shown) revealed the presence of specific (i.e. NT-displaceable) and saturable [^{125}I]-NT binding. No significant difference in binding affinity was observed between cells expressing NTS1 alone (K_d = 0.28 ± 0.14 nM) or in combination with NTS2 (K_d = 0.25 ± 0.11 nM). However, Scatchard analysis of the data revealed that the density of surface [^{125}I]-NT binding sites was nearly 2-fold lower in cells co-expressing NTS1 and NTS2 as compared to cells expressing NTS1 alone (B_{max} = 1538 ± 81 fmol/mg versus 2596 ± 89 fmol/mg, Fig. 7.4*B*). Taken together, these results indicate that co-expression of NTS2 influences cell surface NTS1 receptor densities, but not the affinity of NTS1 for [^{125}I]–NT.

7.4.5 Confocal Microscopic Localization of NTS1 Receptors

To confirm the influence of NTS2 co-expression on the cell surface density of NTS1, we examined the distribution of HA-tagged NTS1 immunostaining in cells expressing NTS1 alone or together with NTS2, using confocal microcopy. Immunocytochemistry revealed distinct distributional patterns for NTS1 receptors in NTS1 and NTS1/NTS2-transfected cells. In cells expressing HA-NTS1 alone, immunoreactive receptors were predominantly located at the cell surface (Fig. 7.5*A*

and C; *arrowheads*). Only weak NTS1 immunolabeling was evident intracellularly (Fig. 7.5*A and C*). By contrast, in cells co-expressing NTS1 and NTS2, the bulk of NTS1 immunoreactivity was detected intracellularly, within a juxtanuclear compartment (Fig. 7.5*D-F*; *arrowheads*). This NTS1 intracellular immunolabeling was co-extensive with NTS2 immunoreactivity (Fig. 7.5*E and F*). Since previous studies have shown NTS2 to co-localize with the trans-Golgi network (TGN) marker syntaxin 6 (Sarret et al., 2002; Perron et al., 2006), it may be surmised that in cells co-expressing NTS1 and NTS2, the two receptors are concentrated within the TGN. Therefore, immunocytochemical data confirm that the cell surface density of NTS1 is decreased upon NTS2 expression in COS-7 cells.

7.4.6 Effects of NTS1/NTS2 Heterodimerization on NTS1 Internalization

To determine whether co-expression of NTS2 affected ligand-induced endocytosis of NTS1 receptors, internalization assays were carried out on COS-7 cells transiently expressing HA-tagged NTS1 alone or in combination with NTS2. Association kinetics of [^{125}I]-NT binding were determined on whole cells incubated for 3-45 min at 37°C in the presence of levocabastine and the proportion of sequestered radioactivity was assessed after hypertonic acid wash of surface-bound ligand. As shown in Fig. 7.6, [^{125}I]-NT bound specifically to both NTS1 (Fig. 7.6*A*) and NTS1/NTS2-expressing cells (Fig. 7.6*B*) in a time-dependent manner, reaching a plateau within 20 min of incubation. This labeling was specific since it was entirely competed for by an excess of unlabeled NT (not shown). In conformity with the results of saturating binding studies, the total amount of cell-associated radioactivity at plateau was markedly lower in cells co-expressing NTS1 and NTS2 than in cells expressing NTS1 alone (compare Figs. 7.6*A* and *B*), reflecting the lower density of cell surface receptors in the former. However, the proportion of internalized radioactivity remained the same between the two cell types (87 ± 3.8% versus 86 ± 2.9% after 20 min; Fig 7.6*B* and 7.6*A*, respectively), indicating that NTS2 expression had no effect on the efficiency of NTS1 receptor internalization.

7.4.7 Functional Characterization of NTS1/NTS2 Interaction

We next investigated the functional consequences of NTS1/NTS2 heterodimerization by measuring receptor-mediated activation of the MAPK kinase pathway. In COS-7 cells transiently expressing NTS1 alone, stimulation with NT for up to 60 min induced a rapid (< 5 min) phosphorylation of ERK1/2 (Fig 7.7*A*, *left panel; B)*. This effect was NTS1-mediated, since it was not observed in untransfected cells (not shown). Similar increases in MAPK kinase activity were observed after 5 min of stimulation with NT in cells co-expressing NTS1 and NTS2 (7.5 ± 0.9 and 7.1 ± 0.4-fold-increase, respectively; $p > 0.95$; Fig. 7A, *right panel;* B), suggesting that co-expression of NTS2 did not significantly influence NTS1 signaling.

7.4.8 Effects of NTS2 Expression on NTS1 Down-Regulation

Previous studies have demonstrated that cell surface NTS1 receptors are rapidly down-regulated following prolonged NT stimulation (Hermans and Maloteaux, 1998; Donato di Paola et al., 1993). By contrast, cell surface NTS2 receptors are maintained at the cell surface during persistent NT exposure (Perron et al., 2006). To investigate the effects of NTS2 expression on NTS1 cell surface binding sites during prolonged NT exposure, COS-7 cells expressing NTS1 alone or together with NTS2 were pre-stimulated with 1 μM NT for up to 24 h at 37°C and cell surface receptor binding was carried out at 4°C using 0.4 nM [^{125}I]-NT in the presence of an excess of levocabastine. In COS-7 cells expressing NTS1 alone, NT application induced a rapid decrease in cell surface NTS1 binding, which was down to 66 ± 1% of control values after 60 min and to 46 ± 3% of control values after 24 h of incubation with NT (Fig. 7.8). By contrast, in cells co-expressing NTS1 and NTS2, cell surface NTS1 binding was only decreased to 72 ± 3% of control values after 60 min and to 75 ± 1% of control values after 24 h of incubation with NT (Fig. 7.8). These values were significantly higher than those recorded at each of these two time points in cells transfected with NTS1 alone ($p < 0.05$ and $p < 0.01$, respectively). The present data therefore suggest that NTS1/2 heterodimerization reduces the down-regulation of cell surface NTS1 binding after persistent NT exposure.

7.5 DISCUSSION

The present study demonstrates that NTS1 and NTS2 form constitutive heterodimers in transiently transfected COS-7 cells. Although NTS1/NTS2 heterodimerization does not affect NTS1 responsiveness to NT, our results indicate that it impedes NTS1 trafficking both to and from the cell surface.

It is now well established that many GPCRs exist as homodimers or heterodimers and that dimerization may alter their functional, pharmacological, and regulatory properties (Bouvier, 2001; Maggio et al., 2005). Previous immunohistochemical studies have revealed extensive overlap in the distribution of NTS1 and NTS2 receptor proteins in rat CNS, namely in the olfactory bulb, bed nucleus of the stria terminalis, anterodorsal thalamic nucleus, substantia nigra, ventral tegmental area, periaqueductal gray, and magnus paragigantocellular nucleus (Boudin et al., 1996b; Sarret et al., 2003a; Fassio et al., 2000). Accordingly, the present RT-PCR data demonstrated that NTS1 and NTS2 mRNAs were co-expressed in virtually all CNS regions examined including the spinal cord, suggesting that these two receptor subtypes are in a position to interact with one another in mediating NT's central effects.

To determine whether NTS1 could form heterodimers with NTS2, co-immunoprecipitation experiments were carried out in dually transfected COS-7 cells. Using two different combinations of antibodies, we were able to demonstrate that NTS1 and NTS2 did heterodimerize and that the extent of their heterodimerization was unaltered by NT treatment, suggesting that NTS1/ NTS2 heterodimers are constitutive. A similar agonist-independent mechanism was also reported for CXCR1/CXCR2 receptor heterodimerization, implying that GPCRs might exist as stable, preformed dimers (Wilson et al., 2005). Several studies have investigated the structural determinants involved in GPCR oligomerization (reviewed in Rios et al., 2001). In particular, the C-terminal tail has often been found to be critical for receptor-receptor interaction (e.g. $GABA_BR1/GABA_BR2$ heterodimerization; Margeta-Mitrovic et al., 2000). However, our findings suggest that the integrity of

NTS2's C-terminal tail is not crucial for NTS1/NTS2 heterodimerization. Likewise, C-truncation mutants of α_1-ARs were found to be ineffective in preventing either homo- or heterodimerization of this receptor subtype (Uberti et al., 2003). GPCR oligomerization may also be mediated by covalent interactions, as shown for metabotropic glutamate receptor 5 (Romano et al., 2001) and calcium-sensing receptor (Zhang et al., 2001). However, cysteine mutations in NTS2 extracellular loops were found here not to interfere with NTS1/NTS2 heterodimerization, indicating that disulfide-bonding arrangements are not required for this interaction and that other domains might be brought into play.

We then sought to determine whether NTS2 co-expression induced changes in NTS1 binding properties since heterodimerization, for instance between delta and kappa opioid receptors, had previously been shown to result in the generation of sites with novel ligand-binding properties (Jordan and Devi, 1999). For this purpose, radioligand binding experiments were carried out in COS-7 cells transiently expressing NTS1 alone or together with NTS2 by using [^{125}I]-NT in the presence of an excess of levocabastine in order to selectively inhibit [^{125}I]-NT binding to NTS2. The results revealed a significant decrease in cell surface binding densities in cells co-expressing NTS1 and NTS2 as compared to NTS1 alone, although the affinity of NTS1 for [^{125}I]-NT was identical in both cell types. Immunocytochemical experiments confirmed that the cell surface NTS1 immunoreactivity was considerably reduced in cells dually transfected as compared to cells expressing NTS1 alone, suggesting that NTS1/NTS2 heterodimerization affected the membrane recruitment of NTS1. Several studies have reported that receptor oligomerization could influence trafficking of GPCRs (reviewed in (Prinster et al., 2005)). For example, expression of dominant-negative V2 vasopressin receptors led to a significant decrease in cell surface targeting of the wild-type V2 receptor (Zhu and Wess, 1998). In cells co-expressing NTS1 and NTS2, intracellularly sequestered NTS1 receptors were concentrated in the same juxtanuclear zone, previously identified as the TGN/Golgi complex, as NTS2 in cells expressing NTS2 alone (Perron et al., 2006; Sarret et al., 2003a). It is therefore likely that the decrease in the

membrane recruitment of NTS1 is the consequence of its heterodimerization with NTS2 within the Golgi/TGN. However, why NTS1/NTS2 heterodimers, like NTS2 receptors, should be retained in the TGN/Golgi remains unclear. Some GPCRs, including the $GABA_BR$, contain retention or export motifs that are thought to play a role in their cell surface expression (Pagano et al., 2001; Tan et al., 2004). Thus, heterodimerization might induce a conformational change that either unmasks a retention signal or masks an export signal in NTS1, thereby conferring this receptor the trafficking properties of NTS2.

We then tested whereas NTS1/NTS2 heterodimerization affected the rate and/or efficiency of ligand-induced receptor endocytosis, as reported for other heterodimers (reviewed in Maggio et al., 2005). For instance, co-expression of β_1AR had been shown to inhibit agonist-promoted internalization of β_2AR in co-transfected HEK-293 cells (Lavoie et al., 2002). However, our kinetic analysis revealed that NTS2 co-expression did not influence [^{125}I]-NT-induced NTS1 internalization. This finding is coherent with the fact that when expressed alone, NTS1 and NTS2 are equally efficiently internalized via clathrin-coated pits upon NT binding (Vandenbulcke et al., 2000; Botto et al., 1998).

Recent studies have demonstrated that heterodimerization could also affect coupling and function of GPCRs. For instance, heterodimerization of NTS1 with NTS3 has been found to modulate NTS1-dependent activation of the ERK1/2 pathway (Martin et al., 2002a). In contrast, another report has indicated that heterodimerization of β_2AR with either delta- or kappa-opioid receptors did not alter its coupling properties (Jordan et al., 2001). To investigate whether NTS1 and NTS2 co-expression led to altered functional properties due to heterodimerization, MAPK kinase activation experiments were carried out in COS-7 cells expressing NTS1 alone or together with NTS2. We found that co-expression of these two NT receptor subtypes did not affect NT-mediated ERK1/2 phosphorylation. This observation may seem at odds with the results of earlier studies which had shown that in CHO cells transfected with either receptor alone, NTS2 had a lower efficacy than NTS1 in

activating the MAPK kinase pathway (Gendron et al., 2004; Poinot-Chazel et al., 1996). However, it is unclear how many receptor molecules of either subtype undergo heterodimerization and it is therefore possible that the density of monomeric (or homodimeric) NTS1 receptors at the cell surface of dually transfected cells might be sufficient for triggering an ERK1/2 phosphorylation response similar to that observed in cells expressing NTS1 alone.

Chronic exposure of GPCRs to their ligands commonly results in a time-dependent decline of their cell surface receptor density, referred to cell surface down-regulation (Ferguson, 2001; Tsao and von Zastrow, 2000). Such is the case for NTS1, which has been shown to rapidly enter the lysosomal degradation pathway instead of being recycled to the cell surface after prolonged NT exposure (Vandenbulcke et al., 2000; Hermans et al., 1997). By contrast, NTS2 cell surface binding sites were found to be resistant to down-regulation upon sustained NT exposure (Perron et al., 2006). It was therefore of interest to determine whether co-expression of NTS1 with NTS2 would affect the regulation of NTS1 cell surface density during persistent agonist stimulation. Transiently transfected COS-7 cells expressing NTS1 alone or together with NTS2 were stimulated for up to 24 h and cell surface receptors were labeled using ^{125}I- NT on ice. Whereas less than 50% of NTS1 binding sites were maintained at the cell surface following prolonged NT exposure in cells expressing NTS1 alone, more than 75% of them were still present at the surface after prolonged NT exposure in cells dually expressing NTS1 and NTS2. This difference is likely attributable to NTS1/NTS2 heterodimerization, again suggesting that NTS1/NTS2 heterodimers have trafficking properties akin to those of NTS2 rather than NTS1, and therefore that interaction between the two receptors reduces the capacity of NTS1 to desensitize upon ligand exposure.

In conclusion, our data provide clear evidence for a functional role of NTS1/NTS2 heterodimerization in NTS1 receptor trafficking in co-transfected COS-7 cells. These two receptor subtypes associate with each other via agonist-independent heterodimerization, which appears to involve primarily hydrophobic interactions. The coexistence of NTS1 and NTS2 in numerous CNS regions supports the view that heterodimerization of these two receptor subtypes may play a physiological role in the regulation of their cell surface density, and hence of their responsiveness to NT, in the mammalian CNS.

7. 6 FOOTNOTES

This work was supported by a grant from the Canadian Institutes for Health Research (CIHR). Amélie Perron and Nadder Sharif were supported by fellowships from the Fonds de la Recherche en Santé du Québec (FRSQ) and from the Natural Sciences and Engineering Research Council of Canada (NSERC), respectively.

7.7 ABBREVIATIONS

NT, neurotensin; GPCR(s), G protein-coupled receptor(s); TM, transmembrane domain; CHO cells, Chinese hamster ovary cells; COS-7 cells, green African monkey kidney cells; MAPK, mitogen-activated protein kinase; ERK1/2, extracellular signal-regulated kinases 1/2; ER, endoplasmic reticulum; AR, adrenergic receptor; NGS, normal goat serum.

7.8 FIGURES

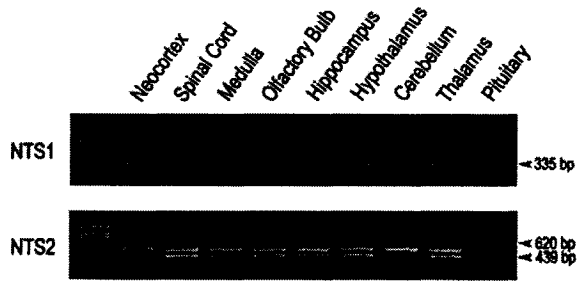

Figure 7.1

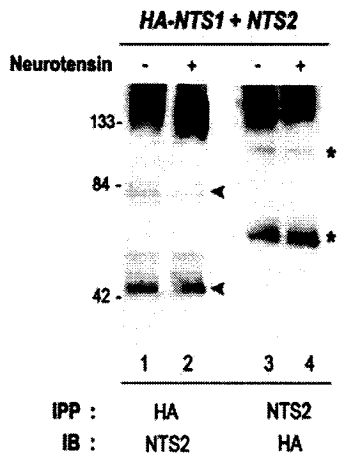

Figure 7.2

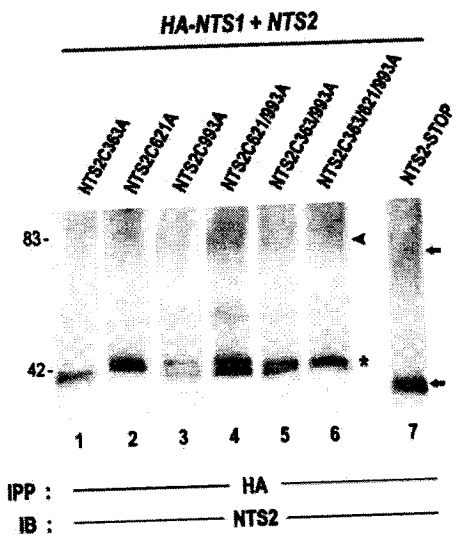
HA-NTS1 + NTS2
NTS2C363A
NTS2C621A
NTS2C993A
NTS2C621/993A
NTS2C363/993A
NTS2C363/621/993A
NTS2-STOP
83-
42-
*
1 2 3 4 5 6 7
IPP : HA
IB : NTS2

Figure 7.3

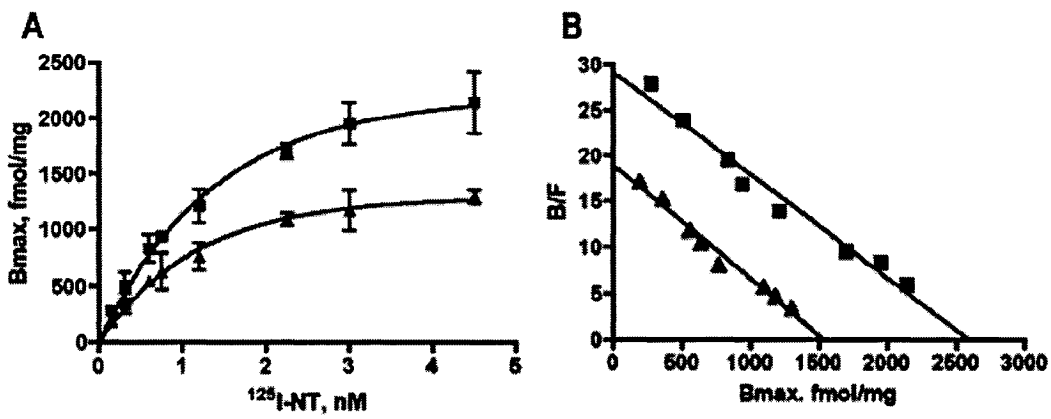
A
Bmax, fmol/mg
2500
2000
1500
1000
500
0
0
1
2
3
4
5
125I-NT, nM
B
B/F
30
25
20
15
10
5
0
0
500
1000
1500
2000
2500
3000
Bmax. fmol/mg

Figure 7.4

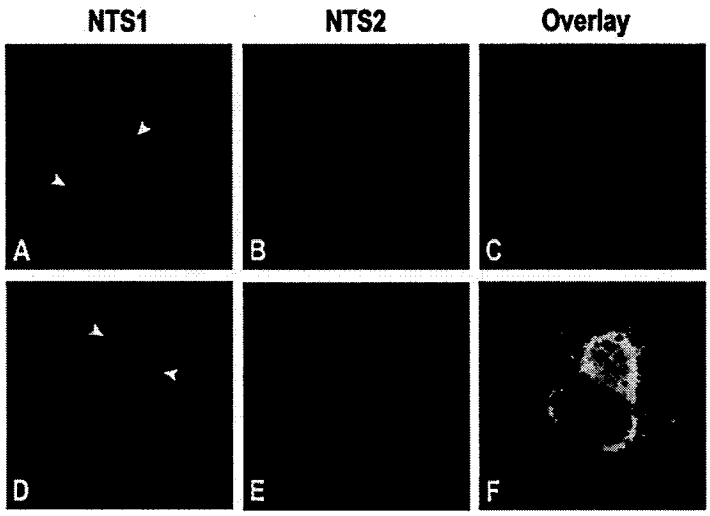

Figure 7.5

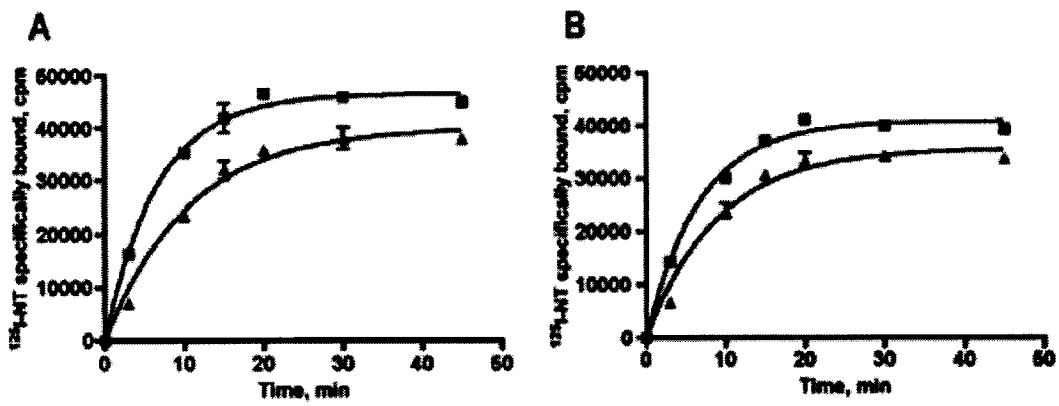

Figure 7.6

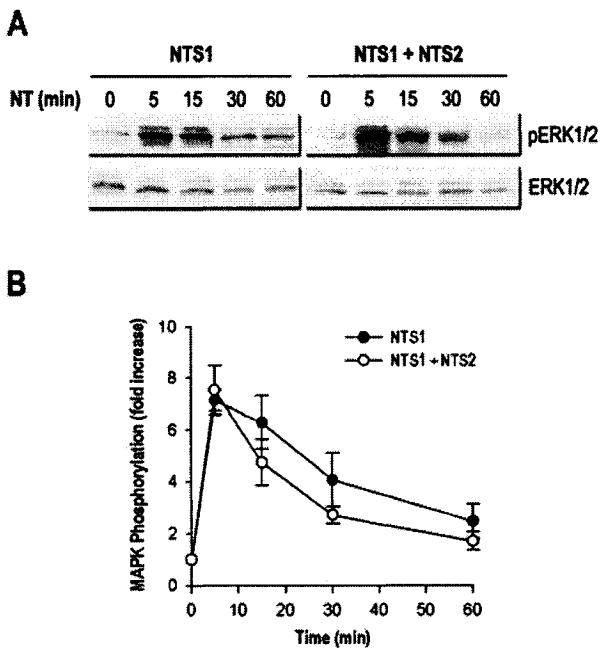
A
NTS1
NTS1 + NTS2
NT (min) 0 5 15 30 60 0 5 15 30 60
pERK1/2
ERK1/2
B
MAPK Phosphorylation (fold increase)
NTS1
NTS1 + NTS2
Time (min)

Figure 7.7

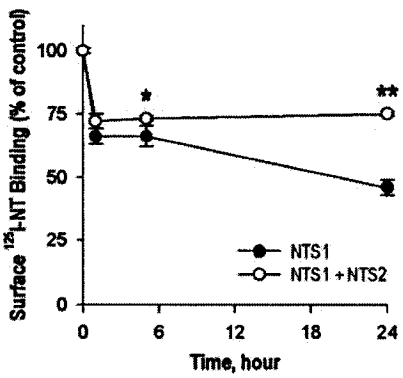
Surface ^{125}I-NT Binding (% of control)
100
75
50
25
0
0
6
12
18
24
Time, hour
*
**
NTS1
NTS1 + NTS2

Figure 7.8

7.9 FIGURE LEGENDS

Fig. 7.1: RT-PCR Analysis of NTS1 and NTS2 mRNAs in Rat CNS. PCRs were performed on mRNAs reverse-transcribed using specific primers for rat NTS1 (upper panel) or NTS2 (lower panel). A 335-bp band corresponding to NTS1 is visible in all brain regions sampled as well as in the spinal cord and pituitary gland. Two different isoforms of NTS2 mRNAs, corresponding to the full-length and alternatively spliced forms of 620 and 439 bp, respectively, are evident in the same CNS regions, but not in the pituitary. Results are representative of three independent experiments.

Fig. 7.2: Co-immunoprecipitation of NTS2 and HA-tagged NTS1 in Transfected Cells. COS-7 cells heterologously expressing a combination of HA-NTS1 and NTS2 were stimulated (*lanes 2* and *4*) or not (*lanes 1* and *3*) with 1 μM NT for 1 h, lysed, and subjected to immunoprecipitation with either HA antibody (*lanes 1* and *2*) or NTS2 peptide antiserum (*lanes 3* and *4*), as described under "Experimental Procedures". Immunoprecipitated receptors were revealed by Western blotting using NTS2 peptide antiserum (*lanes 1* and *2*) or HA antibody (*lanes 3* and *4*). Molecular mass markers are shown on the right. The illustrated blot is representative of three independent experiments. *IPP*, immunoprecipitation; *IB*, immunoblot. *Arrowheads:* bands corresponding to NTS2 monomers and dimers; *asterisks:* bands corresponding to NTS1 monomers and dimers.

Fig. 7.3: Effect of Cysteine Mutations or Truncation of NTS2 on NTS1/NTS2 Dimerization. COS-7 cells heterologously expressing HA-NTS1 with either NTS2 cysteine mutants (C363A, C621A, C993A, C621/993A, and C363/621/993A; *left panel*) or C-terminally truncated NTS2 receptors (*right panel*) were lysed and subjected to immunoprecipitation using the HA antibody. The co-immunoprecipitates were then immunoblotted with the NTS2 peptide antiserum as described under "Experimental Procedures". Molecular mass markers are illustrated on the left. Each blot is representative of three independent experiments. *Asterisk* and *arrowhead* point to monomeric and dimeric forms of NTS2 cysteine mutants,

respectively. *Arrows* point to monomeric and dimeric forms of the C-terminal tail deletion mutant NTS2-STOP.

Fig. 7.4: Effect of Co-expression of NTS1 and NTS2 on NTS1 Binding Properties. COS-7 cells expressing NTS1 alone (■) or together with NTS2 (▲) were incubated whole for 30 min at 37°C with increasing concentrations of [^{125}I]-NT in the presence of an excess of levocabastine in order to prevent binding to NTS2. *A*, Saturation binding curves. [^{125}I]-NT binding to NTS1 is saturable in both cell types, although the B_{max} is lower in cells co-expressing NTS1 and NTS2 than in cells expressing NTS1 alone. *B*, Scatchard analysis of the data indicates that in both cell types, [^{125}I]-NT binds to a single population of sites with K_d and B_{max} values of 0.28 ± 0.14 nM and 2596 ± 89 fmol/mg versus 0.25 ± 0.11 nM and 1538 ± 81 fmol/mg in cells expressing NTS1 alone or together with NTS2, respectively. The values correspond to the mean ± S.D. of two independent experiments, each performed in triplicates.

Fig. 7.5: Co-expression of NTS2 Impairs Cell Surface Recruitment of NTS1 Receptors. COS-7 cells co-expressing HA-tagged NTS1 together with pTargeT (control; *A-C*) or NTS2 subcloned into pTargeT (*D-F*) were permeabilized and stained with a combination of HA and NTS2 antibodies. The subcellular distribution of immunoreactive receptors was then revealed by confocal microscopy. In cells expressing NTS1 alone, immunostained receptors are most prominent peripherally, at the level of the plasma membrane (*A* and *C*). By contrast, in cells co-expressing NTS1 and NTS2, NTS1 immunoreactivity is concentrated in a juxtanuclear intracellular compartment (*D-F*). *Arrowheads* point to NTS1 immunoreactivity.

Fig. 7.6: Co-expression of NTS2 Does not Affect NT-induced NTS1 Internalization. Kinetics (0-45 min) of [^{125}I]-NT binding to whole COS-7 cells transiently expressing NTS1 alone (*A*) or together with NTS2 (*B*). Cells were incubated at 37°C, in the presence of an excess of levocabastine. Association curves before (cell surface + intracellular radioactivity; ■) and after (intracellular

radioactivity; ▲) hypertonic acid stripping of surface-bound ligand. The data are representative of one experiment performed twice in triplicate.

Fig. 7.7: NT-activated MAPK Kinase Signaling is not Affected by Co-expression of NTS2. *A*, Time course of NT-induced MAPK activation in COS-7 cells transiently expressing NTS1 alone or together with NTS2. Upper panels, phosphorylated ERK1/2; *lower panels*, total ERK1/2. *B,* Densitometric analysis of the ratio of phosphorylated ERK1/2 over total ERK1/2 levels following incubation with 1 μM of NT. COS-7 cells expressing NTS1 (●) or co-expressing NTS1 and NTS2 (○) were incubated at 37°C for the indicated times. Patterns of MAPK kinase activation are identical in both cell types. The results are representative of three independent experiments, each with duplicate determinations.

Fig. 7.8: NTS2 Co-expression Reduces Down-regulation of Cell Surface NTS1 Receptors Consequent to Persistent NT Exposure. COS-7 cells transiently transfected with NTS1 alone (●), or together with NTS2 (○) were exposed to 1 μM NT for or up to 24 h at 37°C, washed, and incubated on ice with 0.4 nM [^{125}I]-NT in the presence of 100 μM levocabastine for cell surface binding measurements. In cells expressing NTS1 alone, prolonged NT stimulation results in a loss of 54% of surface [^{125}I]-NT binding sites by 24h, whereas in cells co-expressing NTS1 and NTS2, this loss is reduced to 25%. The results are representative of three individual experiments, each with triplicate determinations. Student's *t* tests were used to compare NT cell surface binding sites between NTS2 and NTS1 expressing COS-7 cells. Values are significantly different at all time points as follows: * $p < 0.05$; ** $p < 0.01$.

CHAPTER 8: GENERAL DISCUSSION

The studies presented in this thesis were aimed at further understanding the molecular and cellular mechanisms underlying NTS2 receptor function and to shed light on the implication of this receptor subtype in mediating NT's effects in the rat CNS. A specific discussion for individual studies has already been provided in each chapter. Thus, the general discussion here shall present a concise overview of the new findings and concepts emerging from previous chapters and include them in the context emanating from the situation described earlier in the introduction. This discussion will also focus on topics that were not detailed in each of the individual manuscripts. Finally, I will suggest some possible molecular mechanisms that may underlie the NTS2 receptor's behavior and propose new areas for further investigations.

8.1 Localization of NTS2 Receptors in the Rat CNS

Our knowledge of the distribution of NTS2 receptors in the mammalian brain was until now exclusively derived from radioligand binding and *in situ* hybridization studies (Schotte et al., 1986; Kitabgi et al., 1987; Bétancur et al., 1998; Asselin et al., 2001; Sarret et al., 1998). However, these techniques do not afford the cellular resolution to ascribe NTS2 to any specific neuronal element. With the aim of localizing NTS2 receptor proteins at both regional and cellular/subcellular levels in the rat CNS, we developed an antiserum directed towards a 15-amino acid synthetic peptide derived from the N-terminal domain of the rat NTS2 receptor, common to both long and short isoforms. We also developed a second antibody directed towards the C-terminal segment of NTS2, allowing the selective recognition of the long NTS2 isoform. It is important to note that these peptide sequences show no homology with other known NT receptor subtypes. This type of antipeptide antibody approach was previously applied to the immunohistochemical detection of other neuropeptide receptors in the rat CNS, such as the neurotensin receptor subtypes 1 (NTS1) (Boudin et al., 1996b) and 3 (Sarret et al., 2003b) as well as the calcitonin gene-related peptide (Ma et al., 2003), μ- (Arvidsson et al., 1995), δ-opioid (Cahill et al., 2001)

and substance P (Shigemoto et al., 1993; Liu et al., 1994; Horie et al., 2000) receptors, to name a few.

The characterization of NTS2 peptide antisera revealed that the N-terminal peptide NTS2 antiserum provided a better immunocytochemical NTS2-like signal in paraformaldehyde-fixed material than the C-terminally directed antibody. Immunohistochemical studies were thus performed using the N-terminal NTS2 peptide antiserum, which recognizes both NTS2 receptor isoforms. Our studies provided the first mapping of NTS2 receptor proteins at the regional, cellular and subcellular levels and demonstrated that these receptors are widely, but selectively distributed within the mammalian CNS. By and large, our results demonstrated that the localization of NTS2-like immunoreactivity conformed for the most part to that previously depicted in previous mRNA hybridization studies (Sarret et al., 1998; Walker et al., 1998; Lépée-Lorgeoux et al., 1999; see Table 2.6 for more details). Indeed, we found the highest NTS2-like immunolabeling levels in sensory areas including the olfactory, auditory and visual systems (see Chapter 3). Strong NTS2-like immunoreactivity was also associated with relay nuclei of ascending somatosensory pathways including gracile and cuneate nuclei as well as spinal and principal sensory trigeminal nuclei. In addition, NTS2 receptor proteins were heavily expressed in structures involved in descending control of nociceptive inputs including the periacqueductal gray, gigantocellular nucleus pars alpha, lateral paragigantocellular nucleus as well as the dorsal and raphe magnus nuclei. However, our results also demonstrated that if widespread, the distribution of NTS2 receptor proteins was also more selective than the NTS2 mRNA distributional patterns obtained by *in situ* hybridization techniques (Sarret et al., 1998; Walker et al., 1998). For instance, the hippocampus, known to express high levels of NTS2 mRNA throughout the dentate gyrus and all of Ammon's horn subfields, exhibited NTS2-like immunoreactivity only in CA1 and CA2 subfields (Sarret et al., 1998; Walker et al., 1998; Lépée-Lorgeoux et al., 1999). These discrepancies might reflect poor translation of NTS2 mRNA in certain subpopulations of neurons. Our immunohistochemical studies also revealed that the distribution of NTS2-like

immunoreactivity largely exceed that of NT terminal fields (see Section 1.3.2). In fact, some of the highest concentration of NTS2 receptors were found in areas devoid of NT inputs such as the cerebral cortex, hippocampus and cerebellum (see Chapter 3), suggesting that NTS2 may also serve as receptor for endogenous ligands other than NT. Indeed, shortly after the publication of the manuscript related to these results (Sarret et al., 2003a), β-Lactotensin, an ileum-contracting peptide derived from bovine β-Lactoglobulin, was shown to selectively bind to NTS2 receptors (Yamauchi et al., 2003b).

At the cellular level, NTS2 receptors were mostly concentrated within neurons, as reported for NTS1 (Boudin et al., 1996b; Fassio et al., 2000). Of interest is the fact that NTS2 subcellular compartmentization varied strikingly throughout the rodent brain (see Chapter 3 for details). Indeed, immunolabeling was associated with axons and terminals within some brain areas (e.g. diagonal band of Broca and the anterior hypothalamus) whereas it was mainly associated with perikarya and dendrites within other areas, such as the hippocampus. As a rule, NTS2 immunolabeling was mainly associated with dendritic neuronal elements. The immunohistochemical distribution of NTS2 receptors was further investigated throughout primary spinal nociceptive pathways using the same N-terminal peptide NTS2 antiserum in the course of a complement study, which is not included in the present thesis (Sarret et al., 2005). In this work, we established that NTS2 was associated with both cell bodies of primary afferent fibers in the dorsal root ganglia and their arborizations in the superficial laminae of the spinal cord, providing the first evidence for an implication of this receptor subtype in NT-induced analgesia at the spinal level. However, our subsequent electron microscopic studies revealed that within the spinal cord (see Chapter 6 for details), the bulk of NTS2 immunoreactivity was associated with dendritic shafts, branches and branchlets, suggesting that the spinal NTS2-mediated nociceptive effects of NT may also be exerted postsynaptically.

It is worth noting that previous *in situ* hybridization studies had demonstrated that NTS2 mRNA expression is up-regulated in glial fibrillary acidic protein-immunolabeled reactive astrocytes both *in vitro* and *in vivo*, suggesting that NTS2 may be involved in neuronal regeneration and/or inflammatory reaction (Nouel et al., 1999). However, none of the brain regions that displayed NTS2 immunoreactivity was immunopositive for the astroglial marker S100β, indicating that NTS2 receptor proteins are not expressed by astrocytes under basal conditions. It would be interesting therefore to determine whether astrocytes specifically express NTS2 in response to injury. To do so, immunohistochemical detection of NTS2 receptors would have to be carried out at various time points in stab-wound animals in order to monitor NTS2 expression during an inflammatory reaction. Protein levels could be quantified in parallel though Western blotting experiments.

8.2 Splicing of the NTS2 Receptor: Is the Isoform Functional ?

The heptahelical G protein-coupled receptors correspond to the largest superfamily in the human genome, including more than 600 genes (Venter, 2001; Sadee et al., 2001). Also, the chemical diversity among endogenous ligands is without equal. Indeed, GPCRs recognize signals as varied as biogenic amines, hormones, glycoproteins, neurotransmitters, nucleotides, ions, proteases, as well as several sensory messages (e.g. light, odors and gustative molecules) (reviewed in Gether, 2000; Bockaert et al., 1999). Within the GPCR family, functional diversity is most often managed by the existence of multiple receptor subtypes, each encoded by a different gene. Alternative splicing of GPCR pre-mRNA is also a mechanism observed in some receptor subtypes to further increase the number of receptor isoforms that can be synthesized from a single receptor gene (reviewed in Minneman, 2001; Kilpatrick. et al., 1999). In the case of NTS2, such a mechanism has been reported in the mouse CNS, in which two NTS2 mRNA isoforms are derived from a single NTS2 gene, the short form resulting from alternative splicing of the primary NTS2 transcript (Sun et al., 2001).

As shown for the mouse NTS2 receptor (Botto et al., 1997b), we have demonstrated that alternative splicing of the rat NTS2 gene generates a 5-transmembrane domain variant isoform, lacking an internal 181-bp sequence. Splice variants for several GPCRs have been shown to be differentially distributed (Minneman, 2001). These include isoforms of the calcitonin (Yamin et al., 1994), CRF (De Souza, 1995) and dopamine D_3 (Sokoloff et al., 1992) receptors. However, this situation is not universal. For instance, *in situ* hybridization studies have shown that the 5-HT_4 receptor splice variants are similarly distributed within the rat CNS (Claeysen et al., 1996). Such is the case for NTS2 receptor isoforms in that mRNA levels and ratios did not varied significantly within the different regions examined (e.g. neocortex, thalamus, hypothalamus, medulla, cerebellum). However, other RT-PCR studies have shown that while the two NTS2 isoforms were detected in whole brain extracts, only the full-length NTS2 isoform was detected in cultured astrocytes

(Nouel et al., 1999). At the protein level, our immunoblotting analyses revealed that the 45 kDa form (i.e. the monomeric full-length NTS2 receptor) was ubiquitously expressed in the CNS (e.g. brain, cerebellum and spinal cord), whereas the 32 kDa form (i.e. the monomeric vNTS2) was detected in none of the regions examined. However, a band twice the size of the variant NTS2 isoform similar to that seen in transfected COS-7 cells was detected in the spinal cord, suggesting the truncated NTS2 receptor may selectively exist in its dimeric form within this region. In order to discriminate the cellular expression of these two NTS2 receptor proteins within the rat CNS, we developed an antibody directed towards the unique C-terminal tail of the variant NTS2 receptor, allowing the specific detection of the short NTS2 isoform. Unfortunally, this antibody gave rise to a noisy signal that was not specific enough to draw conclusions in both immunocytochemical and Western blotting studies. As an alternative approach, immunolabeling could be carried out through a differential approach in which the signal detected with the NTS2 C-terminal peptide antiserum, which recognizes only the long isoform, would be subtracted from that obtained with the N-terminal peptide antiserum. The resulting signal would thus correspond to that of the variant NTS2 isoform.

In contrast to the results of Botto et al. (1997b) who found that the mouse variant counterpart displayed no specific NT binding, we demonstrated that the rat vNTS2 specifically binds NT, although with a lower affinity than the full-length receptor (i.e. IC_{50} of 10 μM versus 2 nM, for the long NTS2 isoform). Most of the GPCR spliced variants were shown to remain functional if their binding site was preserved. This was shown to be the case for both C-terminally spliced endothelin B (Nambi et al., 2000) and somatostatin 2B (Vanetti et al., 1992) receptors. On the other hand, several transmembrane spliced receptors including the 5-TM domain D_3nf dopamine receptor and the corticotropin-releasing factor receptor 2 (CRF2) were shown to display deficient functional activity due to the disappearance of critical segments (Schmauss et al., 1993; Miyata et al., 1999). We thus investigated whether the truncated NTS2 receptor retained the MAPK activation properties exhibited by the full-length receptor (see Chapter 4). We found that stimulation of

vNTS2-expressing CHO cells with NT induced a rapid and sustained phosphorylation of ERK1/2 as demonstrated for the long NTS2 isoform in a similar transfection system. To our knowledge, the rat variant NTS2 isoform is the first transmembrane spliced GPCR variant cloned so far that was shown to preserve its functional properties. However, vNTS2-mediated phosphorylation levels were lower than those obtained with the full-length isoform. Comparison of these two NTS2 amino acid sequences revealed that only a few residues (i.e. 3 serines; refer to Fig. 5.2) of the third intracellular domain of the full-length isoform are conserved in the corresponding part (i.e. C-terminal tail) of the variant isoform, suggesting that the third intracellular loop, although not essential, may play a complementary role in MAPK activation.

Variations in G-protein coupling have been reported among several splice variants (reviewed in Minneman et al., 2001). In particular, the full-length and spliced-variants of both pituitary adenylate cyclase activating polypeptide (PACAP) and prostanoid EP_3 receptors were shown to modulate distinct second messenger systems (Spengler et al., 1993; Namba et al., 1993). It is important to note that the variant NTS2 isoform lacks the third intracellular loop of the full-length receptor and contains 37 unique C-terminal amino acids (see Chapter 5). These two regions are well known for their critical role in GPCR coupling specificity (Ferguson, 2001; Havlickova et al., 2002; Kang et al., 2005). Thus, we cannot rule out the possibility that vNTS2 might activate different signals than those observed in cells expressing the full-length isoform since we have only examined the ERK1/2 activation pathway. It would thus be important to investigate whether the stimulation of vNTS2 receptors elicits other biological responses using complementary second messenger measurements (e.g. cAMP, Ca^{2+}, inositol phosphates). Results of subprograms executed by the NetPhos 2.0 server (Nikolaj Blom, Center for Biological Sequence Analysis, Technical University of Denmark, Denmark) predicted 21 and 12 potential phosphorylation sites within the full-length and variant NTS2 isoform sequences, respectively (illustrated in Fig. 8.1). These consensus motifs may promote the binding of different GPCR interacting proteins, which specifically recognize a

phosphorylated domain and alter G protein specificity (reviewed in Ferguson, 2001; Bockaert et al., 2004; Sato et al., 2006). Whether NTS2 isoforms interact with different proteins needs to be clarified.

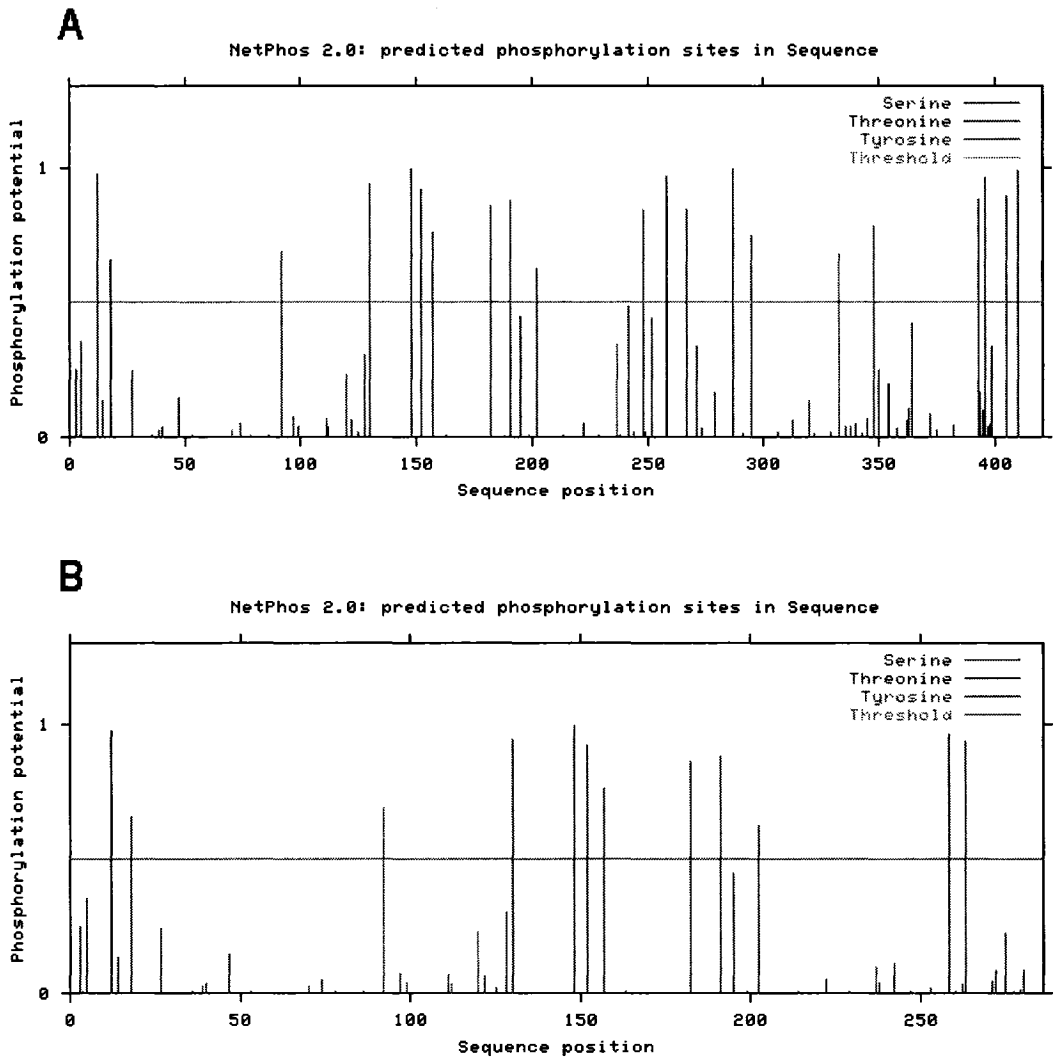

Figure 8.1: Schematic Diagram of NTS2 (A) and vNTS2 (B) Phosphorylation Sites. The phosphorylation sites (serine, threonine and tyrosine) were predicted by the neural network-based method of Nikolaj Blom according to the NetPhos 2.0 server. The position of the amino acid sequence is indicated below each diagram.

According to our immunoblotting studies in rat CNS, vNTS2 appeared to form multimeric complexes that might correspond to vNTS2 homodimers and putative heterodimers with NTS2. Several studies have shown GPCRs to behave structurally in a manner related to multiple-subunits receptors (reviewed in Bouvier, 2001; Bai, 2004a; Prinster et al., 2005). Indeed, our co-immunoprecipitation studies in COS-7 cells expressing both NTS2 receptors confirmed that the short NTS2 isoform interacts physically with its full-length counterpart. Previous studies have demonstrated that heterodimerization between GPCR splice variant isoforms (e.g. D_3 and D_3nf dopamine receptor isoforms (Elmhurst et al., 2000)) may influence cell surface receptor expression. Nevertheless, our immunoblotting and immunocytochemical studies in dually transfected cells revealed that co-expression of the full-length NTS2 isoform did not modify the cell surface density of the truncated form over that seen in cells expressing vNTS2 alone, suggesting that NTS2 does not act as a chaperone protein in vNTS2 trafficking. On the other hand, immunological studies have revealed that co-expression of the gonadotropin-releasing hormone (GnRH) receptor with with its C-terminally truncated isoform resulted in impaired receptor insertion into the plasma membrane (Grosse et al., 1997; Cheung et al., 2005). Whether the variant NTS2 influences the cell surface expression of the full-length isoform remains to be established. To do so, cell surface expression of NTS2 receptors would have to be monitored by confocal immunocytochemistry using the C-terminally directed NTS2 antiserum in cells expressing NTS2 alone or together with the variant isoform. Cell surface receptors could also be quantified in parallel immunolabeling experiments through Fluorescent Activated Cell Sorting (FACS) analysis.

Molecular association with different GPCR subtypes was also shown to result in dramatic effects on receptor signaling (reviewed in Prinster et al., 2005; Terrillon and Bouvier, 2004). However, the fact that ERK1/2 activation levels obtained in CHO cells expressing the full-length NTS2 (see Chapter 4 for details) alone were comparable to those observed in rat cerebellar granule cells, which are known to express both NTS2 isoforms (Sarret et al., 2002), suggests that the truncated NTS2

receptor does not modify signaling efficiency of the full-length NTS2 isoform. Further investigations will require the development of specific ligands for either the short or long isoforms in order to discriminate vNTS2- from NTS2-mediated signaling cascades, respectively.

8.3 NTS2 Receptors and Long-term Neurotensin Exposure

Upon prolonged agonist exposure, nearly all GPCRs display a concomitant reduction of cell responsiveness to the stimulus, a process known as desensitization (reviewed in Gainetdinov et al., 2004; Claing and Laporte, 2005). Such is the case for NTS1 receptors, which were shown to desensitize after NT exposure (Vandenbulcke et al., 2000; Hermans and Maloteaux, 1998). Indeed, confocal microscopic studies have shown that NTS1 receptors were targeted to lysosomes for degradation rather than being recycled back to the plasma membrane, which may account in part for receptor desensitization after prolonged agonist stimulation (Hermans et al., 1997; Vandenbulcke et al., 2000). Furthermore, there is evidence that *de novo* synthesis is required for the recovery of NTS1 binding sites and function (Donato di Paola et al., 1993: Hermans et al., 1997). On the other hand, little was known about the regulation of NTS2 receptors except that their stimulation triggers extended activation of ERK1/2 both in neurons in culture (Sarret et al., 2002) and in transfected CHO cells (as shown in Chapter 4 and Chapter 5 for the full-length NTS2 and its short isoform, respectively).

To determine whether persistent agonist stimulation of NTS2 receptors gives rise to down-regulation, we investigated the effect of prolonged NT exposure on resultant cell surface [^{125}I]-NT binding. We found that in contrast to cells transfected with NTS1, NTS2-expressing cells retained the same surface receptor density despite efficient ligand-induced internalization mechanisms. Since this maintenance of cell surface receptors was also observed when the incubation was carried out with the protease-resistant NT analogue JMV-431, we could not ascribe this mechanism to ligand degradation. Cell surface NTS2 binding sites preserved during persistent NT

exposure corresponded to functional receptors since NT-induced ERK1/2 phosphorylation levels in cell exposed to NT for 24 h were equivalent to those previously reported in rat cerebellar granule cells (Sarret et al., 2002) and NTS2-expressing CHO cells (refer to Chapter 4).

Preservation of cell surface receptors in response to extended agonist stimulation has been documented for a limited number of GPCRs so far (e.g. the β_1 and β_3-adrenergic receptors (Liang et al., 2003; Thomas et al., 1992), the somatostatin receptor subtype 1 (Hokovic et al., 1999; Ramirez et al., 2005), the AT_2 angiotensin receptor (Dudlez and Summerfelt, 1993), the GnRH receptor (Loumaye et al., 1982), and the long form of the dopamine 2 ($D2_L$) receptor (Zhang et al., 1994; Starr et al., 1995; Filtz et al., 1994). The same phenomenon has also been shown for the single transmembrane domain NTS3 receptor upon sustained NT exposure (Navarro et al., 2001; Morinville et al., 2003). Unlike receptor down-regulation, the molecular mechanisms responsible for cell surface receptor maintenance, and hence for preventing functional desensitization, are poorly understood. Depending on the type of receptor, mechanisms involved in surface receptor maintenance include transcriptional and post-translational induction of receptor synthesis, recycling of internalized receptors, impaired receptor degradation and/or targeting of reserve receptors to the cell surface (Thomas et al., 1992; Hukovic et al., 1999; Navarro et al., 2001; Liang et al., 2003; Liang and Fishman, 2004). In the case of NTS2, prolonged NT exposure did not influence the total levels of immunodetected NTS2, indicating that receptor up/down-regulation is not involved in the resensitization mechanism. Neither did it require receptor neosynthesis since protein levels remained unchanged following NT exposure in the presence of the protein synthesis inhibitor cycloheximide. In addition, recycling of internalized receptors did not account significantly for the reinstatement of the plasma membrane NTS2 receptor population since it was not affected by the recycling inhibitor monensin nor by replacing the rat NTS2 receptor with its non-recycling human counterpart. However, it appeared to involve translocation of spare receptors form intracellular stores since stimulation with NT was found to induce migration of NTS2 from Golgi/TGN to

endosome-like structures as evidenced by dual-labeling confocal microscopy (see Chapter 6 for details). To ascertain the functional relevance of this resensitization mechanism, we monitored by electron microscopy the effect of intrathecal NT injection on the subcellular distribution of NTS2 in neurons of the superficial laminae of rat spinal cord. We found that agonist stimulation induced an extensive relocalization of intracellular receptors to the plasma membrane of these cells (7-fold increase). Taken together, these results suggest that sustained activation of NTS2 receptors promotes recruitment of intracellular receptors from the Golgi/TGN complex to the cell surface, thereby preventing functional desensitization of NTS2-expressing cells.

Previous studies have shown that upon prolonged stimulation with fluorescently-labeled NT, internalized ligand molecules were translocated from the cell surface to a juxtanuclear compartment corresponding to the TGN (Vandenbulcke et al., 2000; Sarret et al., 2002). It is therefore possible that internalized NT might serve as a triggering signal for the translocation of resident NTS2 receptors from this compartment to the cell surface, implying a dynamic regulation of subcellular protein localization. For instance, the insulin-responsive glucose transporter GLUT4 was shown to be targeted from a post-endocytic compartment to the cell surface in response to extracellular stimuli such as insulin (Slot et al., 1991; Morris et al., 1996). In order to determine whether receptor endocytosis is a necessary prerequisite for the resensitization of NTS2 receptors, cell surface receptors will be further quantified throughout radioligand binding studies following extended agonist exposure in the presence of internalization blockers (e.g. concanavalin A, sucrose, phenylarsine oxide). Similar experiments could also be carried out in COS-7 cells expressing NTS2 together with a dominant negative mutant of dynamin. It is also unclear whether NT regulates NTS2 surface receptor levels at a step prior to initial insertion in the plasma membrane rather than by altering their endosome trafficking following internalization. Studies have reported that protein trafficking between TGN and the cell surface via endosomes is regulated by targeting signals, which have been identified in a variety of membrane proteins (reviewed in Tan et al, 2004). These

motifs referred to as "acidic clusters" are usually flanked by either tyrosine-based, or dileucine targeting signals and frequently contain consensus casein kinase (CK2) sites that also serve as TGN retrieval signals (Jones et al., 1995). For instance, efficient TGN localization of furin cannot occur unless the serines of the acidic cluster are phosphorylated by CK2 (Dittie et al., 1997). This phosphorylated acidic cluster motif was shown to be linked to AP-1 adaptor complexes via the cytosolic protein PACS-1, playing a role in the clathrin-coated vesicle formation on the TGN, as well as in their endosomal translocation (Crump et al., 2001).

Such consensus CK2 phosphorylation sites are found in the third intracellular and C-terminal domains of NTS2. Moreover, the third intracellular loop of the NTS2 receptor contains an acidic cluster motif that is surrounded by two dileucine signals, as shown in Fig. 8.2. However, a study using a truncated form of NTS2 receptor lacking the entire C-terminus (361-Stop; Fig. 8.2) showed that receptors are still maintained at the cell surface following sustained agonist exposure, indicating that the C-terminal tail of NTS2 is not involved this resensitization process (Perron et al., unpublished data). In view of the presence of numerous TGN-targeting motifs and consensus CK2 phosphorylation sites in the third intracellular loop, it is tempting to speculate that NT-induced phosphorylation of NTS2 and/or conformational change might be involved in the trafficking of the receptor. It would thus be important to investigate the effect of site-directed mutagenesis of these putative TGN motifs and CK2 posphorylation sites on the trafficking of NTS2 receptors following persistent NT exposure in order to determine whether the TGN to endosome transport of NTS2 receptors is mediated via these targeting signals.

Finally, GPCRs are also known to interact with numerous proteins that are implicated in cellular trafficking (Tan et al., 2004). In particular, a single transmembrane domain protein, called the receptor-activity-modifying protein (RAMP) 1, was shown to function as a chaperone in the transport of calcitonin receptor-like (CRLR) receptors from the endoplasmic reticulum to the plasma membrane (McLatchie et al., 1998). In addition, other proteins have been shown to stabilize GPCRs at the cell surface. For instance, Homer-1a was found to allow the

insertion of the metabotropic glutamate receptor 1 into the plasma membrane (Ciruela et al., 2000). Further characterization of cargo sorting proteins involved in the targeting of NTS2 from intracellular pools will therefore provide additional insight into the molecular mechanism leading to the maintenance of cell surface NTS2 binding sites after persistent exposure to NT.

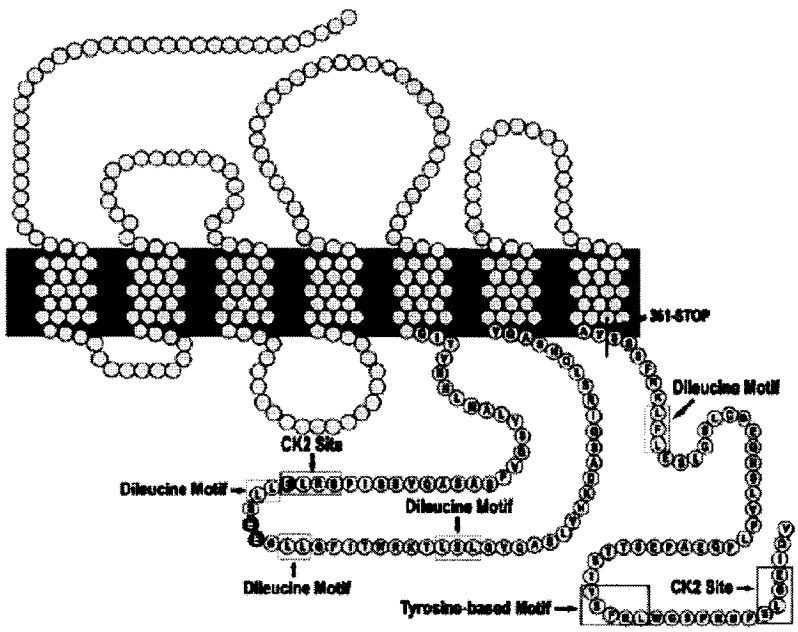

Figure 8.2: Two-Dimensional Model of the Rat NTS2 Receptor. Residues in the third intracellular and C-terminal domains of NTS2 are marked. Putative casein kinase 2 (CK2) phosphorylation sites, dileucine motifs, and tyrosine-based sequences are boxed. Dark circles highlight an acidic cluster. The C-terminal tail deletion mutant of NTS2 was created by introducing a stop codon after position 361.

8.4 Heterodimerization of NTS1/NTS2 and Intracellular Trafficking of NTS1

According to our immunohistochemical mapping studies (see Chapter 3 for details), there were a number of regions in which the distribution of NTS2 overlapped with that of NTS1 including the anterodorsal thalamic nucleus, olfactory bulb, bed nucleus of the stria terminalis, substantia nigra, and VTA. This observation might imply that certain neurons jointly express NTS1 and NTS2 receptors, which might thus be in a position to interact with one another physiologically.

Using two different combinations of NTS2- and NTS1-selective antibodies, we were able to demonstrate that NTS2 and NTS1 indeed interacted physically together. We also found that the extent of their heterodimerization was unaltered by NT treatment, suggesting that NTS1/NTS2 heterodimers are constitutive. Available structural data strongly suggest that many GPCRs can form oligomers in the absence of ligand stimulation (Bouvier et al., 2001; Terrillon and Bouvier, 2004). Indeed, crystallization of the extracellular N-terminal domain of the metabotropic glutamate receptor is consistent with such a model of constitutive dimerization (Kunishima et al., 2000). Our findings also suggest that neither the integrity of NTS2's C-terminal tail nor disulphide bounding were critical for NTS1/NTS2 heterodimerization. The formation of NTS1/NTS2 heterodimers might thus involve non-covalent interactions involving both extracellular and transmembrane domains. Such idea was indeed proposed and demonstrated for the β_2-adrenergic (Hebert et al., 1996) and dopamine D2 (Ng et al., 1996) receptors. In order to unravel the molecular determinants that stabilize NTS1/NTS2 heterodimers, it would be interesting to carry out a series of experiments that would combine the use of synthetic peptides, site-directed mutagenesis and biophysical techniques. In addition, we should investigate whether the 5-TM variant NTS2 isoform is able to form heterodimers with the NTS1 receptor as well.

Radioligand binding experiments in COS-7 cells expressing NTS1 alone or together with NTS2 revealed that the presence of NTS2 did not affect the affinity of NTS1 for [^{125}I]-NT. However, our data suggested that NTS2 expression influenced cell surface NTS1 receptor densities (B_{max}). In parallel, confocal microscopic studies in dually transfected cells revealed that NTS1/NTS2 heterodimerization markedly affected the subcellular localization of NTS1. Indeed, immunoreactive NTS1 receptors were principally located at the cell surface in cells expressing NTS1 alone whereas the bulk of NTS1 immunoreactivity was detected intracellularly within the perinuclear region in cells co-expressing NTS1 and NTS2 (see Chapter 7 for details). A similar juxtanuclear location was previously reported for NTS2 in single-transfected COS-7 cells (Perron et al., 2006) as well as in cerebellar granule cells, which do not express NTS1 (Sarret et al., 2002). Our data thus suggest that NTS2 acts as a negative dominant of the NTS1 receptor by preventing its cell surface expression, presumably by retaining it in the Golgi/TGN through heterodimerization. Several studies have also shown that heterodimerization of GPCRs may also lead to intracellular retention of receptors (Terrillon and Bouvier, 2004; Prinster et al., 2005). This phenomenon may have pathophysiological consequences. For instance, a series of the frizzled (Fz) family of Wnt receptors was shown to be involved in the autosomal-dominant retinal degenerative disease by interfering with the maturation of the wild-type receptor (Kaykas et al., 2004). Surprisingly, our functional studies have revealed that NTS1-mediated ERK1/2 MAPK activity was not affected by NTS2 co-expression. However, it is possible that the density of monomeric (or homodimeric) NTS1 receptors at the cell surface of dually transfected cells had been sufficient for triggering an ERK1/2 phosphorylation response similar to that observed in cells expressing NTS1 alone. Despite the lack of effect on NTS1 signaling, our findings suggest that NTS1/NTS2 heterodimerization might have functional implications in receptor trafficking upon sustained agonist exposure. Indeed, we found that NTS1 cell surface binding sites were more resistant to NT-induced down-regulation when the two NT receptor subtypes were expressed together than in cells expressing NTS1 alone.

Some GPCRs contain retention or export motifs that are thought to play a role in their cell surface expression (reviewed in Duvernay et al., 2005). For instance, association of the $GABA_BR1$ coiled-coil domain with that of $GABA_BR2$ serves to mask the $GABA_BR1$ ER retention signal, allowing the trafficking of the heterodimer to the cell surface (Margeta-Mitrovic et al., 1999; Pagano et al., 2001). NTS1/NTS2 heterodimerization might induce a conformational change as well, which either unmasks a retention signal or masks an export signal in the NTS1 sequence, thereby conferring to this receptor the trafficking properties of NTS2 (as described in Chapter 6).

One of the most striking features in NTS1 and NTS2 amino acid sequences is the absence of glycosylation motifs in the N-terminal domain of NTS2, contrary to NTS1, which presents three potential sites within its extracellular domains at position Asn4, Asn38 and Asn42 (Rostène et al., 1997). Glycosylation is a post-translational modification common in GPCRs and plays an important role in their structural maturation. Accordingly, reports have demonstrated that *N*-linked glycosylation of bradykinin B_2 (Michineau et al., 2004) and AT_1 angiotensin II (Deslauriers et al., 1999) receptors is essential for their proper trafficking from the ER to the plasma membrane. Heterodimerization between NTS1 and NTS2 receptors may therefore impede NTS1 glycosylation due to steric hindrance and its consequent cell surface expression. In order to confirm this hypothesis, NTS1 putative glycosylation sites would be mutated into alanine by site-specific mutagenesis and subcellular localization of the receptor investigated by confocal microscopy in transiently transfected COS-7 cells. The subcellular distribution of NTS1 could then be compared with that obtained in cells co-expressing NTS1 and NTS2 receptors in order to determine whether glycosylation sites deletion gives rise to the same NTS1 localization pattern as when the receptor is co-expressed with NTS2.

CONCLUDING REMARKS

The present study revealed that NTS2 receptors (i.e. the full-length and its spliced-variant isoform) are widely distributed in the rat CNS. It also indicated that these receptors are essentially neuronal in normal conditions and are mainly targeted to dendrites, as demonstrated in our electron microscopic studies. Most importantly, this study demonstrated that NTS2 receptors are associated with structures involved in the descending control of nociceptive inputs, in accordance with their postulated role in the mediation of NT's supraspinal antinociceptive effects. We also confirmed that NT acts as an agonist at both full-length and variant NTS2 receptor sites and demonstrated that these cell surface receptors are resistant to down-regulation following persistent agonist exposure. Interestingly, NTS2 was shown to exert a dominant-negative effect on the intracellular trafficking and down-regulation properties of the NTS1 receptor through NTS1/NTS2 heterodimerization. The coexistence of NTS1 and NTS2 in numerous CNS regions and their complementary role in the mediation of NT's analgesic effects support the view that heterodimerization of these two receptor subtypes may play a physiological role in the regulation of their cell surface density, and hence of their responsiveness to NT. Further studies will thus be required to determine how we can take advantage of the NTS2 behavior in the treatment of chronic pain without the disadvantages associated with opioid tolerance.

LITERATURE CITED

Adams JC (1992) Biotin amplification of biotin and horseradish peroxidase signals in histochemical stains. *J Histochem Cytochem* **40**:1457-63.

Alexander MJ, Mahoney PD, Ferris CF, Carraway RE and Leeman SE (1989a) Evidence that neurotensin participates in the central regulation of the preovulatory surge of luteinizing hormone in the rat. *Endocrinology* **124**:783-8.

Alexander MJ, Miller MA, Dorsa DM, Bullock BP, Melloni RH, Jr., Dobner PR and Leeman SE (1989b) Distribution of neurotensin/neuromedin N mRNA in rat forebrain: unexpected abundance in hippocampus and subiculum. *Proc Natl Acad Sci U S A* **86**:5202-6.

Alexander MJ and Leeman SE (1998) Widespread expression in adult rat forebrain of mRNA encoding high-affinity neurotensin receptor. *J Comp Neurol* **402**:475-500.

Allescher HD, Fick H, Schusdziarra V and Classen M (1992) Mechanisms of neurotensin-induced inhibition in rat ileal smooth muscle. *Am J Physiol* **263**:G767-74.

Alonso A, Faure MP and Beaudet A (1994) Neurotensin promotes oscillatory bursting behavior and is internalized in basal forebrain cholinergic neurons. *J Neurosci* **14**:5778-92.

al-Rodhan NR, Richelson E, Gilbert JA, McCormick DJ, Kanba KS, Pfenning MA, Nelson A, Larson EW and Yaksh TL (1991) Structure-antinociceptive activity of neurotensin and some novel analogues in the periaqueductal gray region of the brainstem. *Brain Res* **557**:227-35.

Amar S, Mazella J, Checler F, Kitabgi P and Vincent JP (1985) Regulation of cyclic GMP levels by neurotensin in neuroblastoma clone N1E115. *Biochem Biophys Res Commun* **129**:117-25.

Amar S, Kitabgi P and Vincent JP (1986) Activation of phosphatidylinositol turnover by neurotensin receptors in the human colonic adenocarcinoma cell line HT29. *FEBS Lett* **201**:31-6.

Amar S, Kitabgi P and Vincent JP (1987) Stimulation of inositol phosphate production by neurotensin in neuroblastoma N1E115 cells: implication of GTP-binding proteins and relationship with the cyclic GMP response. *J Neurochem* **49**:999-1006.

Andersson S, Chang D, Folkers K and Rosell S (1976) Inhibition of gastric acid secretion in dogs by neurotensin. *Life Sci* **19**:367-70.

Arvidsson U, Riedl M, Chakrabarti S, Lee JH, Nakano AH, Dado RJ, Loh HH, Law PY, Wessendorf MW and Elde R (1995) Distribution and targeting of a mu-opioid receptor (MOR1) in brain and spinal cord. *J Neurosci* **15**:3328-41.

Asselin ML, Dubuc I, Coquerel A and Costentin J (2001) Localization of neurotensin NTS2 receptors in rat brain, using. *Neuroreport* **12**:1087-91.

Azzi M, Gully D, Heaulme M, Bérod A, Pélaprat D, Kitabgi P, Boigegrain R, Maffrand JP, LeFur G and Rostène W (1994) Neurotensin receptor interaction with dopaminergic systems in the guinea-pig brain shown by neurotensin receptor antagonists. *Eur J Pharmacol* **255**:167-74.

Babcock AM, Baker DA, Hallock NL, Lovec R, Lynch WC and Peccia JC (1993) Neurotensin-induced hypothermia prevents hippocampal neuronal damage and increased locomotor activity in ischemic gerbils. *Brain Res Bull* **32**:373-8.

Bai M (2004a) Dimerization of G-protein-coupled receptors: roles in signal transduction. *Cell Signal* **16**:175-86.

Bai M (2004b) Structure-function relationship of the extracellular calcium-sensing receptor. *Cell Calcium* **35**:197-207.

Barbero P, Rovère C, De Bie I, Seidah N, Beaudet A and Kitabgi P (1998) PC5-A-mediated processing of pro-neurotensin in early compartments of the regulated secretory pathway of PC5-transfected PC12 cells. *J Biol Chem* **273**:25339-46.

Barelli H, Woskowska Z, Cipris S, Fox-Threlkeld JE, Daniel EE, Vincent JP and Checler F (1995) Pharmacological role and degradation processes of neuromedin N in the gastrointestinal tract: an in vitro and in vivo study. *J Pharmacol Exp Ther* **275**:1300-7.

Barroso S, Richard F, Nicolas-Etheve D, Reversat JL, Bernassau JM, Kitabgi P and Labbé-Jullié C (2000) Identification of residues involved in neurotensin binding and modeling of the agonist binding site in neurotensin receptor 1. *J Biol Chem* **275**:328-36.

Barroso S, Richard F, Nicolas-Ethève D, Kitabgi P and Labbé-Jullié C (2002) Constitutive activation of the neurotensin receptor 1 by mutation of Phe(358) in Helix seven. *Br J Pharmacol* **135**:997-1002.

Bean AJ, Dagerlind A, Hokfelt T and Dobner PR (1992) Cloning of human neurotensin/neuromedin N genomic sequences and expression in the ventral mesencephalon of schizophrenics and age/sex matched controls. *Neuroscience* **50**:259-68.

Beaudet A, Mazella J, Nouel D, Chabry J, Castel MN, Laduron P, Kitabgi P and Faure MP (1994) Internalization and intracellular mobilization of neurotensin in neuronal cells. *Biochem Pharmacol* **47**:43-52.

Beck B, Burlet A, Nicolas JP and Burlet C (1989) Neurotensin in microdissected brain nuclei and in the pituitary of the lean and obese Zucker rats. *Neuropeptides* **13**:1-7.

Beck B, Stricker-Krongrad A, Richy S and Burlet C (1998) Evidence that hypothalamic neurotensin signals leptin effects on feeding behavior in normal and fat-preferring rats. *Biochem Biophys Res Commun* **252**:634-8.

Behbehani MM and Pert A (1984) A mechanism for the analgesic effect of neurotensin as revealed by behavioral and electrophysiological techniques. *Brain Res* **324**:35-42.

Behbehani MM, Park MR and Clement ME (1988) Interactions between the lateral hypothalamus and the periaqueductal gray. *J Neurosci* **8**:2780-7.

Behbehani MM (1992) Physiological mechanisms of the analgesic effect of neurotensin. *Ann N Y Acad Sci* **668**:253-65.

Benmoussa M, Chait A, Loric G and de Beaurepaire R (1996) Low doses of neurotensin in the preoptic area produce hyperthermia. Comparison with other brain sites and with neurotensin-induced analgesia. *Brain Res Bull* **39**:275-9.

Bennett A, Stamford IF, Sanger GJ and Bloom SR (1992) The effects of various peptides on human isolated gut muscle. *J Pharm Pharmacol* **44**:960-7.

Bétancur C, Canton M, Burgos A, Labeeuw B, Gully D, Rostène W and Pélaprat D (1998) Characterization of binding sites of a new neurotensin receptor antagonist, [^{3}H]SR 142948A, in the rat brain. *Eur J Pharmacol* **343**:67-77.

Binder EB, Kinkead B, Owens MJ and Nemeroff CB (2001a) Neurotensin and dopamine interactions. *Pharmacol Rev* **53**:453-86.

Binder EB, Kinkead B, Owens MJ and Nemeroff CB (2001b) The role of neurotensin in the pathophysiology of schizophrenia and the mechanism of action of antipsychotic drugs. *Biol Psychiatry* **50**:856-72.

Bissette G, Nemeroff CB, Loosen PT, Prange AJ, Jr. and Lipton MA (1976) Hypothermia and intolerance to cold induced by intracisternal administration of the hypothalamic peptide neurotensin. *Nature* **262**:607-9.

Bissette G, Richardson C, Kizer JS and Nemeroff CB (1984) Ontogeny of brain neurotensin in the rat: a radioimmunoassay study. *J Neurochem* **43**:283-7.

Blackburn AM, Fletcher DR, Bloom SR, Christofides ND, Long RG, Fitzpatrick ML and Baron JH (1980) Effect of neurotensin on gastric function in man. *Lancet* **1**:987-9.

Bloom SR and Polak JM (1980) Gut hormones. *Adv Clin Chem* **21**:177-244.

Bock JB, Klumperman J, Davanger S and Scheller RH (1997) Syntaxin 6 functions in trans-Golgi network vesicle trafficking. *Mol Biol Cell* **8**:1261-71.

Bockaert J and Pin JP (1999) Molecular tinkering of G protein-coupled receptors: an evolutionary success. *Embo J* **18**:1723-9.

Bockaert J, Fagni L, Dumuis A and Marin P (2004) GPCR interacting proteins (GIP). *Pharmacol Ther* **103**:203-21.

Botto JM, Vincent JP and Mazella J (1997a) Existence of two translation initiation sites leading to the expression of two proteins from the rat high-affinity neurotensin-receptor cDNA: possible regulation by the 5' end non-coding region. *Biochem J* **324 (Pt 2)**:389-93.

Botto JM, Sarret P, Vincent JP and Mazella J (1997b) Identification and expression of a variant isoform of the levocabastine-sensitive neurotensin receptor in the mouse central nervous system. *FEBS Lett* **400**:211-4.

Botto JM, Guillemare E, Vincent JP and Mazella J (1997c) Effects of SR 48692 on neurotensin-induced calcium-activated chloride currents in the Xenopus oocyte expression system: agonist-like activity on the levocabastine-sensitive neurotensin receptor and absence of antagonist effect on the levocabastine insensitive neurotensin receptor. *Neurosci Lett* **223**:193-6.

Botto JM, Chabry J, Sarret P, Vincent JP and Mazella J (1998) Stable expression of the mouse levocabastine-sensitive neurotensin receptor in HEK 293 cell line: binding properties, photoaffinity labeling, and internalization mechanism. *Biochem Biophys Res Commun* **243**:585-90.

Boudin H, Grauz-Guyon A, Faure MP, Forgez P, Lhiaubet AM, Dennis M, Beaudet A, Rostène W and Pélaprat D (1995) Immunological recognition of different forms of the neurotensin receptor in transfected cells and rat brain. *Biochem J* **305 (Pt 1)**:277-83.

Boudin H, Labrecque J, Lhiaubet AM, Dennis M, Rostène W and Pélaprat D (1996a) Pharmacological and molecular characterization of the neurotensin receptor expressed in Sf9 cells. *Biochem Pharmacol* **51**:1243-6.

Boudin H, Pélaprat D, Rostène W and Beaudet A (1996b) Cellular distribution of neurotensin receptors in rat brain: immunohistochemical study using an antipeptide antibody against the cloned high affinity receptor. *J Comp Neurol* **373**:76-89.

Boudin H, Pélaprat D, Rostène W, Pickel VM and Beaudet A (1998) Correlative ultrastructural distribution of neurotensin receptor proteins and binding sites in the rat substantia nigra. *J Neurosci* **18**:8473-84.

Boudin H, Lazaroff B, Bachelet CM, Pélaprat D, Rostène W and Beaudet A (2000) Immunologic differentiation of two high-affinity neurotensin receptor isoforms in the developing rat brain. *J Comp Neurol* **425**:45-57.

Bouvier M, Hausdorff WP, De Blasi A, O'Dowd BF, Kobilka BK, Caron MG and Lefkowitz RJ (1988) Removal of phosphorylation sites from the beta 2-adrenergic receptor delays onset of agonist-promoted desensitization. *Nature* **333**:370-3.

Bouvier M (2001) Oligomerization of G-protein-coupled transmitter receptors. *Nat Rev Neurosci* **2**:274-86.

Bozou JC, de Nadai F, Vincent JP and Kitabgi P (1989a) Neurotensin, bradykinin and somatostatin inhibit cAMP production in neuroblastoma N1E115 cells via both pertussis toxin sensitive and insensitive mechanisms. *Biochem Biophys Res Commun* **161**:1144-50.

Bozou JC, Rochet N, Magnaldo I, Vincent JP and Kitabgi P (1989b) Neurotensin stimulates inositol trisphosphate-mediated calcium mobilization but not protein kinase C activation in HT29 cells. Involvement of a G-protein. *Biochem J* **264**:871-8.

Bradford MM (1976) A rapid and sensitive method for the quantitation of microgram quantities of protein utilizing the principle of protein-dye binding. *Anal Biochem* **72**:248-54.

Brouard A, Heaulme M, Leyris R, Pélaprat D, Gully D, Kitabgi P, Le Fur G and Rostène W (1994a) SR 48692 inhibits neurotensin-induced [^{3}H]dopamine release in rat striatal slices and mesencephalic cultures. *Eur J Pharmacol* **253**:289-91.

Brouard A, Pélaprat D, Vial M, Lhiaubet AM and Rostène W (1994b) Effects of ion channel blockers and phorbol ester treatments on [^{3}H]dopamine release and neurotensin facilitation of [^{3}H]dopamine release from rat mesencephalic cells in primary culture. *J Neurochem* **62**:1416-25.

Butcher LL (1995) Cholinergic neurons and networks, in *The Rat Nervous System* 2nd ed. (Paxinos G, editor), New York: Academic Press. p 1003-1013.

Cador M, Kelley AE, Le Moal M and Stinus L (1986) Ventral tegmental area infusion of substance P, neurotensin and enkephalin: differential effects on feeding behavior. *Neuroscience* **18**:659-69.

Cahill CM, McClellan KA, Morinville A, Hoffert C, Hubatsch D, O'Donnell D and Beaudet A (2001) Immunohistochemical distribution of delta opioid receptors in the rat central nervous system: evidence for somatodendritic labeling and antigen-specific cellular compartmentalization. *J Comp Neurol* **440**:65-84.

Cahill CM, Morinville A, Hoffert C, O'Donnell D and Beaudet A (2003) Up-regulation and trafficking of delta opioid receptor in a model of chronic inflammation: implications for pain control. *Pain* **101**:199-208.

Canton H, Emeson RB, Barker EL, Backstrom JR, Lu JT, Chang MS and Sanders-Bush E (1996) Identification, molecular cloning, and distribution of a short variant of the 5-hydroxytryptamine2C receptor produced by alternative splicing. *Mol Pharmacol* **50**:799-807.

Cape EG, Manns ID, Alonso A, Beaudet A and Jones BE (2000) Neurotensin-induced bursting of cholinergic basal forebrain neurons promotes gamma and theta cortical activity together with waking and paradoxical sleep. *J Neurosci* **20**:8452-61.

Carraway R and Leeman SE (1973) The isolation of a new hypotensive peptide, neurotensin, from bovine hypothalami. *J Biol Chem* **248**:6854-61.

Carraway R and Leeman SE (1975) The amino acid sequence of a hypothalamic peptide, neurotensin. *J Biol Chem* **250**:1907-11.

Carraway R and Bhatnagar YM (1980) Isolation, structure and biologic activity of chicken intestinal neurotensin. *Peptides* **1**:167-74.

Carraway RE and Mitra SP (1987) The use of radioimmunoassay to compare the tissue and subcellular distributions of neurotensin and neuromedin N in the cat. *Endocrinology* **120**:2092-100.

Carraway RE and Mitra SP (1990) Differential processing of neurotensin/neuromedin N precursor(s) in canine brain and intestine. *J Biol Chem* **265**:8627-31.

Carraway RE, Mitra SP and Salmonsen R (1992) Isolation and quantitation of several new peptides from the canine neurotensin/neuromedin N precursor. *Peptides* **13**:1039-47.

Castel MN, Malgouris C, Blanchard JC and Laduron PM (1990) Retrograde axonal transport of neurotensin in the dopaminergic nigrostriatal pathway in the rat. *Neuroscience* **36**:425-30.

Chabry J, Gaudriault G, Vincent JP and Mazella J (1993) Implication of various forms of neurotensin receptors in the mechanism of internalization of neurotensin in cerebral neurons. *J Biol Chem* **268**:17138-44.

Chabry J, Labbé-Jullié C, Gully D, Kitabgi P, Vincent JP and Mazella J (1994) Stable expression of the cloned rat brain neurotensin receptor into fibroblasts: binding properties, photoaffinity labeling, transduction mechanisms, and internalization. *J Neurochem* **63**:19-27.

Chabry J, Botto JM, Nouel D, Beaudet A, Vincent JP and Mazella J (1995) Thr-422 and Tyr-424 residues in the carboxyl terminus are critical for the internalization of the rat neurotensin receptor. *J Biol Chem* **270**:2439-42.

Chahl LA and Walker SB (1981) Responses of the rat cardiovascular system to substance P, neurotensin and bombesin. *Life Sci* **29**:2009-15.

Chalon P, Vita N, Kaghad M, Guillemot M, Bonnin J, Delpech B, Le Fur G, Ferrara P and Caput D (1996) Molecular cloning of a levocabastine-sensitive neurotensin binding site. *FEBS Lett* **386**:91-4.

Checler F, Mazella J, Kitabgi P and Vincent JP (1986a) High-affinity receptor sites and rapid proteolytic inactivation of neurotensin in primary cultured neurons. *J Neurochem* **47**:1742-8.

Checler F, Vincent JP and Kitabgi P (1986b) Purification and characterization of a novel neurotensin-degrading peptidase from rat brain synaptic membranes. *J Biol Chem* **261**:11274-81.

Checler F, Barelli H, Kitabgi P and Vincent JP (1988) Neurotensin metabolism in various tissues of central and peripheral origins: ubiquitous involvement of a novel neurotensin degrading metalloendopeptidase. *Biochimie* **70**:75-82.

Cheung TC and Hearn JP (2005) Dimerizations of the wallaby gonadotropin-releasing hormone receptor and its splice variants. *Gen Comp Endocrinol* **144**:280-8.

Choi SY, Chae HD, Park TJ, Ha H and Kim KT (1999) Characterization of high affinity neurotensin receptor NTR1 in HL-60 cells and its down regulation during granulocytic differentiation. *Br J Pharmacol* **126**:1050-6.

Ciruela F, Soloviev MM, Chan WY and McIlhinney RA (2000) Homer-1c/Vesl-1L modulates the cell surface targeting of metabotropic glutamate receptor type 1alpha: evidence for an anchoring function. *Mol Cell Neurosci* **15**:36-50.

Claeysen S, Sebben M, Journot L, Bockaert J and Dumuis A (1996) Cloning, expression and pharmacology of the mouse 5-HT(4L) receptor. *FEBS Lett* **398**:19-25.

Claing A, Laporte SA, Caron MG and Lefkowitz RJ (2002) Endocytosis of G protein-coupled receptors: roles of G protein-coupled receptor kinases and beta-arrestin proteins. *Prog Neurobiol* **66**:61-79.

Claing A and Laporte SA (2005) Novel roles for arrestins in G protein-coupled receptor biology and drug discovery. *Curr Opin Drug Discov Devel* **8**:585-9.

Clineschmidt BV, McGuffin JC and Bunting PB (1979) Neurotensin: antinocisponsive action in rodents. *Eur J Pharmacol* **54**:129-39.

Clineschmidt BV, Martin GE and Veber DF (1982) Antinocisponsive effects of neurotensin and neurotensin-related peptides. *Ann N Y Acad Sci* **400**:283-306.

Coquerel A, Dubuc I, Menard JF, Kitabgi P and Costentin J (1986) Naloxone-insensitive potentiation of neurotensin hypothermic effect by the enkephalinase inhibitor thiorphan. *Brain Res* **398**:386-9.

Croci T, Aureggi G, Guagnini F, Manara L, Gully D, Fur GL, Maffrand JP, Mukenge S, Ferla G, Ferrara P, Chalon P and Vita N (1999) In vitro functional evidence of different neurotensin-receptors modulating the motor response of human colonic muscle strips. *Br J Pharmacol* **127**:1922-8.

Crump CM, Xiang Y, Thomas L, Gu F, Austin C, Tooze SA and Thomas G (2001) PACS-1 binding to adaptors is required for acidic cluster motif-mediated protein traffic. *Embo J* **20**:2191-201.

Dal Farra C, Sarret P, Navarro V, Botto JM, Mazella J and Vincent JP (2001) Involvement of the neurotensin receptor subtype NTR3 in the growth effect of neurotensin on cancer cell lines. *Int J Cancer* **92**:503-9.

Dana C, Vial M, Léonard K, Beauregard A, Kitabgi P, Vincent JP, Rostène W and Beaudet A (1989) Electron microscopic localization of neurotensin binding sites in the midbrain tegmentum of the rat. I. Ventral tegmental area and the interfascicular nucleus. *J Neurosci* **9**:2247-57.

Davis TP, Burgess HS, Crowell S, Moody TW, Culling-Berglund A and Liu RH (1989) Beta-endorphin and neurotensin stimulate in vitro clonal growth of human SCLC cells. *Eur J Pharmacol* **161**:283-5.

de Beaurepaire R and Suaudeau C (1988) Anorectic effect of calcitonin, neurotensin and bombesin infused in the area of the rostral part of the nucleus of the tractus solitarius in the rat. *Peptides* **9**:729-33.

de Nadai F, Rovère C, Bidard JN, Cuber JC, Beaudet A and Kitabgi P (1994) Post-translational processing of the neurotensin/neuromedin N precursor in the central nervous system of the rat--I. Biochemical characterization of maturation products. *Neuroscience* **60**:159-66.

de Souza EB (1995) Corticotropin-releasing factor receptors: physiology, pharmacology, biochemistry and role in central nervous system and immune disorders. *Psychoneuroendocrinology* **20**:789-819.

Debaigt C, Hirling H, Steiner P, Vincent JP and Mazella J (2004) Crucial role of neuron-enriched endosomal protein of 21 kDa in sorting between degradation and recycling of internalized G-protein-coupled receptors. *J Biol Chem* **279**:35687-91.

Deslauriers B, Ponce C, Lombard C, Larguier R, Bonnafous JC and Marie J (1999) N-glycosylation requirements for the AT1a angiotensin II receptor delivery to the plasma membrane. *Biochem J* **339 (Pt 2)**:397-405.

Devi LA (2001) Heterodimerization of G-protein-coupled receptors: pharmacology, signaling and trafficking. *Trends Pharmacol Sci* **22**:532-7.

Di Paola ED and Richelson E (1990) Cardiovascular effects of neurotensin and some analogues on rats. *Eur J Pharmacol* **175**:279-83.

Dittie AS, Thomas L, Thomas G and Tooze SA (1997) Interaction of furin in immature secretory granules from neuroendocrine cells with the AP-1 adaptor complex is modulated by casein kinase II phosphorylation. *Embo J* **16**:4859-70.

Dobner PR, Barber DL, Villa-Komaroff L and McKiernan C (1987) Cloning and sequence analysis of cDNA for the canine neurotensin/neuromedin N precursor. *Proc Natl Acad Sci U S A* **84**:3516-20.

Dobner PR, Tischler AS, Lee YC, Bloom SR and Donahue SR (1988) Lithium dramatically potentiates neurotensin/neuromedin N gene expression. *J Biol Chem* **263**:13983-6.

Dobner PR, Deutch AY and Fadel J (2003) Neurotensin: dual roles in psychostimulant and antipsychotic drug responses. *Life Sci* **73**:801-11.

Dobner PR (2005) Multitasking with neurotensin in the central nervous system. *Cell Mol Life Sci* **62**:1946-63.

Donato Di Paola E, Cusack B, Yamada M and Richelson E (1993) Desensitization and down-regulation of neurotensin receptors in murine neuroblastoma clone N1E-115 by [D-Lys8] neurotensin(8-13). *J Pharmacol Exp Ther* **264**:1-5.

Dournaud P, Gu YZ, Schonbrunn A, Mazella J, Tannenbaum GS and Beaudet A (1996) Localization of the somatostatin receptor SST2A in rat brain using a specific anti-peptide antibody. *J Neurosci* **16**:4468-78.

Dubuc I, Costentin J, Terranova JP, Barnouin MC, Soubrie P, Le Fur G, Rostène W and Kitabgi P (1994) The nonpeptide neurotensin antagonist, SR 48692, used as a tool to reveal putative neurotensin receptor subtypes. *Br J Pharmacol* **112**:352-4.

Dubuc I, Remande S and Costentin J (1999a) The partial agonist properties of levocabastine in neurotensin-induced analgesia. *Eur J Pharmacol* **381**:9-12.

Dubuc I, Sarret P, Labbé-Jullié C, Botto JM, Honoré E, Bourdel E, Martinez J, Costentin J, Vincent JP, Kitabgi P and Mazella J (1999b) Identification of the receptor subtype involved in the analgesic effect of neurotensin. *J Neurosci* **19**:503-10.

Dudley DT and Summerfelt RM (1993) Regulated expression of angiotensin II (AT2) binding sites in R3T3 cells. *Regul Pept* **44**:199-206.

Duvernay MT, Filipeanu CM and Wu G (2005) The regulatory mechanisms of export trafficking of G protein-coupled receptors. *Cell Signal* **17**:1457-65.

Ehlers RA, Bonnor RM, Wang X, Hellmich MR and Evers BM (1998) Signal transduction mechanisms in neurotensin-mediated cellular regulation. *Surgery* **124**:239-46; discussion 246-7.

Ehlers RA, Zhang Y, Hellmich MR and Evers BM (2000) Neurotensin-mediated activation of MAPK pathways and AP-1 binding in the human pancreatic cancer cell line, MIA PaCa-2. *Biochem Biophys Res Commun* **269**:704-8.

Elde R, Schalling M, Ceccatelli S, Nakanishi S and Hokfelt T (1990) Localization of neuropeptide receptor mRNA in rat brain: initial observations using probes for neurotensin and substance P receptors. *Neurosci Lett* **120**:134-8.

Elmhurst JL, Xie Z, O'Dowd BF and George SR (2000) The splice variant D3nf reduces ligand binding to the D3 dopamine receptor: evidence for hetero-oligomerization. *Brain Res Mol Brain Res* **80**:63-74.

Emson PC, Goedert M and Mantyh PW (1985a) Neurotensin-containing neurons, in *Handbook of Chemical Neuroanatomy* (Björklund A and Hökfelt T eds), Amsterdam: Elsevier, p 355-405.

Emson PC, Horsfield PM, Goedert M, Rossor MN and Hawkes CH (1985b) Neurotensin in human brain: regional distribution and effects of neurological illness. *Brain Res* **347**:239-44.

Evers BM, Ishizuka J, Chung DH, Townsend CM, Jr. and Thompson JC (1992) Neurotensin expression and release in human colon cancers. *Ann Surg* **216**:423-30; discussion 430-1.

Evers BM, Wang X, Zhou Z, Townsend CM, Jr., McNeil GP and Dobner PR (1995) Characterization of promoter elements required for cell-specific expression of the neurotensin/neuromedin N gene in a human endocrine cell line. *Mol Cell Biol* **15**:3870-81.

Fan GF, Ray K, Zhao XM, Goldsmith PK and Spiegel AM (1998) Mutational analysis of the cysteines in the extracellular domain of the human Ca^{2+} receptor: effects on cell surface expression, dimerization and signal transduction. *FEBS Lett* **436**:353-6.

Fang FG, Moreau JL and Fields HL (1987) Dose-dependent antinociceptive action of neurotensin microinjected into the rostroventromedial medulla of the rat. *Brain Res* **420**:171-4.

Fassio A, Evans G, Grisshammer R, Bolam JP, Mimmack M and Emson PC (2000) Distribution of the neurotensin receptor NTS1 in the rat CNS studied using an amino-terminal directed antibody. *Neuropharmacology* **39**:1430-42.

Faure MP, Gaudreau P, Shaw I, Cashman NR and Beaudet A (1994) Synthesis of a biologically active fluorescent probe for labeling neurotensin receptors. *J Histochem Cytochem* **42**:755-63.

Faure MP, Labbé-Jullié C, Cashman N, Kitabgi P and Beaudet A (1995) Binding and internalization of neurotensin in hybrid cells derived from septal cholinergic neurons. *Synapse* **20**:106-16.

Ferguson SS (2001) Evolving concepts in G protein-coupled receptor endocytosis: the role in receptor desensitization and signaling. *Pharmacol Rev* **53**:1-24.

Ferris CF, Pan JX, Singer EA, Boyd ND, Carraway RE and Leeman SE (1984) Stimulation of luteinizing hormone release after stereotaxic microinjection of neurotensin into the medial preoptic area of rats. *Neuroendocrinology* **38**:145-51.

Filtz TM, Guan W, Artymyshyn RP, Facheco M, Ford C and Molinoff PB (1994) Mechanisms of up-regulation of D2L dopamine receptors by agonists and antagonists in transfected HEK-293 cells. *J Pharmacol Exp Ther* **271**:1574-82.

Francois-Bellan AM, Bosler O, Tonon MC, Wei LT and Beaudet A (1992) Association of neurotensin receptors with VIP-containing neurons and serotonin-containing axons in the suprachiasmatic nucleus of the rat. *Synapse* **10**:282-90.

Furnham N, Ruffle S and Southan C (2004) Splice variants: a homology modeling approach. *Proteins* **54**:596-608.

Gainetdinov RR, Premont RT, Bohn LM, Lefkowitz RJ and Caron MG (2004) Desensitization of G protein-coupled receptors and neuronal functions. *Annu Rev Neurosci* **27**:107-44.

Garver DL, Bissette G, Yao JK and Nemeroff CB (1991) Relation of CSF neurotensin concentrations to symptoms and drug response of psychotic patients. *Am J Psychiatry* **148**:484-8.

Gendron L, Oligny JF, Payet MD and Gallo-Payet N (2003) Cyclic AMP-independent involvement of Rap1/B-Raf in the angiotensin II AT2 receptor signaling pathway in NG108-15 cells. *J Biol Chem* **278**:3606-14.

Gendron L, Perron A, Payet MD, Gallo-Payet N, Sarret P and Beaudet A (2004) Low-affinity neurotensin receptor (NTS2) signaling: internalization-dependent activation of extracellular signal-regulated kinases 1/2. *Mol Pharmacol* **66**:1421-30.

Gether U (2000) Uncovering molecular mechanisms involved in activation of G protein-coupled receptors. *Endocr Rev* **21**:90-113.

Gilbert JA, Strobel TR and Richelson E (1988) Desensitization of neurotensin receptor-mediated cyclic GMP formation in neuroblastoma clone N1E-115. *Biochem Pharmacol* **37**:2833-8.

Gilbert JA, McCormick DJ, Pfenning MA, Kanba KS, Enloe LJ, Moore A and Richelson E (1989) Neurotensin(8-13): comparison of novel analogs for stimulation of cyclic GMP formation in neuroblastoma clone N1E-115 and receptor binding to human brain and intact N1E-115 cells. *Biochem Pharmacol* **38**:3377-82.

Go VL, Michener S, Roddy D and Koch M (1984) Clinical relevance of regulatory gastrointestinal peptides. *Clin Biochem* **17**:82-8.

Goedert M, Reeve JG, Emson PC and Bleehen NM (1984a) Neurotensin in human small cell lung carcinoma. *Br J Cancer* **50**:179-83.

Goedert M, Pittaway K, Williams BJ and Emson PC (1984b) Specific binding of tritiated neurotensin to rat brain membranes: characterization and regional distribution. *Brain Res* **304**:71-81.

Gordon CJ, McMahon B, Richelson E, Padnos B and Katz L (2003) Neurotensin analog NT77 induces regulated hypothermia in the rat. *Life Sci* **73**:2611-23.

Goulet M, Morissette M, Grondin R, Falardeau P, Bedard PJ, Rostène W and Di Paolo T (1999) Neurotensin receptors and dopamine transporters: effects of MPTP lesioning and chronic dopaminergic treatments in monkeys. *Synapse* **32**:153-64.

Grabowski PJ and Black DL (2001) Alternative RNA splicing in the nervous system. *Prog Neurobiol* **65**:289-308.

Gray TS and Magnuson DJ (1992) Peptide immunoreactive neurons in the amygdala and the bed nucleus of the stria terminalis project to the midbrain central gray in the rat. *Peptides* **13**:451-60.

Grosse R, Schoneberg T, Schultz G and Gudermann T (1997) Inhibition of gonadotropin-releasing hormone receptor signaling by expression of a splice variant of the human receptor. *Mol Endocrinol* **11**:1305-18.

Gu J, Polak JM, Probert L, Islam KN, Marangos PJ, Mina S, Adrian TE, McGregor GP, O'Shaughnessy DJ and Bloom SR (1983) Peptidergic innervation of the human male genital tract. *J Urol* **130**:386-91.

Guha S, Rey O and Rozengurt E (2002) Neurotensin induces protein kinase C-dependent protein kinase D activation and DNA synthesis in human pancreatic carcinoma cell line PANC-1. *Cancer Res* **62**:1632-40.

Guha S, Lunn JA, Santiskulvong C and Rozengurt E (2003) Neurotensin stimulates protein kinase C-dependent mitogenic signaling in human pancreatic carcinoma cell line PANC-1. *Cancer Res* **63**:2379-87.

Gui X, Carraway RE and Dobner PR (2004) Endogenous neurotensin facilitates visceral nociception and is required for stress-induced antinociception in mice and rats. *Neuroscience* **126**:1023-32.

Gully D, Canton M, Boigegrain R, Jeanjean F, Molimard JC, Poncelet M, Gueudet C, Heaulme M, Leyris R, Brouard A and et al. (1993) Biochemical and pharmacological profile of a potent and selective nonpeptide antagonist of the neurotensin receptor. *Proc Natl Acad Sci U S A* **90**:65-9.

Gully D, Jeanjean F, Poncelet M, Steinberg R, Soubrie P, Le Fur G and Maffrand JP (1995) Neuropharmacological profile of non-peptide neurotensin antagonists. *Fundam Clin Pharmacol* **9**:513-21.

Gully D, Lespy L, Canton M, Rostène W, Kitabgi P, Le Fur G and Maffrand JP (1996) Effect of the neurotensin receptor antagonist SR48692 on rat blood pressure modulation by neurotensin. *Life Sci* **58**:665-74.

Gully D, Labeeuw B, Boigegrain R, Oury-Donat F, Bachy A, Poncelet M, Steinberg R, Suaud-Chagny MF, Santucci V, Vita N, Pecceu F, Labbé-Jullié C, Kitabgi P, Soubrie P, Le Fur G and Maffrand JP (1997) Biochemical and pharmacological activities of SR 142948A, a new potent neurotensin receptor antagonist. *J Pharmacol Exp Ther* **280**:802-12.

Hammer RA, Leeman SE, Carraway R and Williams RH (1980) Isolation of human intestinal neurotensin. *J Biol Chem* **255**:2476-80.

Handler CM, Bradley EA, Geller EB and Adler MW (1994) A study of the physiological mechanisms contributing to neurotensin-induced hypothermia. *Life Sci* **54**:95-100.

Hara Y, Shiosaka S, Senba E, Sakanaka M, Inagaki S, Takagi H, Kawai Y, Takatsuki K, Matsuzaki T and Tohyama M (1982) Ontogeny of the neurotensin-containing neuron system of the rat: immunohistochemical analysis. I. Forebrain and diencephalon. *J Comp Neurol* **208**:177-95.

Hassan S, Dobner PR and Carraway RE (2004) Involvement of MAP-kinase, PI3-kinase and EGF-receptor in the stimulatory effect of Neurotensin on DNA synthesis in PC3 cells. *Regul Pept* **120**:155-66.

Havlickova M, Prezeau L, Duthey B, Bettler B, Pin JP and Blahos J (2002) The intracellular loops of the GB2 subunit are crucial for G-protein coupling of the heteromeric gamma-aminobutyrate B receptor. *Mol Pharmacol* **62**:343-50.

Hebert TE, Moffett S, Morello JP, Loisel TP, Bichet DG, Barret C and Bouvier M (1996) A peptide derived from a beta2-adrenergic receptor transmembrane domain inhibits both receptor dimerization and activation. *J Biol Chem* **271**:16384-92.

Hellstrom PM (1986) Vagotomy inhibits the effect of neurotensin on gastrointestinal transit in the rat. *Acta Physiol Scand* **128**:47-55.

Hermans E, Maloteaux JM and Octave JN (1992) Phospholipase C activation by neurotensin and neuromedin N in Chinese hamster ovary cells expressing the rat neurotensin receptor. *Brain Res Mol Brain Res* **15**:332-8.Hermans E, Jeanjean AP, Laduron PM, Octave JN and Maloteaux JM (1993) Postnatal ontogeny of the rat brain neurotensin receptor mRNA. *Neurosci Lett* **157**:45-8.

Hermans E, Octave JN and Maloteaux JM (1996) Interaction of the COOH-terminal domain of the neurotensin receptor with a G protein does not control the phospholipase C activation but is involved in the agonist-induced internalization. *Mol Pharmacol* **49**:365-72.

Hermans E and Maloteaux JM (1998) Mechanisms of regulation of neurotensin receptors. *Pharmacol Ther* **79**:89-104.Hermans E, Vanisberg MA, Geurts M and Maloteaux JM (1997) Down-regulation of neurotensin receptors after ligand-induced internalization in rat primary cultured neurons. *Neurochem Int* **31**:291-9.

Hermans-Borgmeyer I, Hermey G, Nykjaer A and Schaller C (1999) Expression of the 100-kDa neurotensin receptor sortilin during mouse embryonal development. *Brain Res Mol Brain Res* **65**:216-9.

Hermey G, Riedel IB, Hampe W, Schaller HC and Hermans-Borgmeyer I (1999) Identification and characterization of SorCS, a third member of a novel receptor family. *Biochem Biophys Res Commun* **266**:347-51.

Hervé D, Tassin JP, Studler JM, Dana C, Kitabgi P, Vincent JP, Glowinski J and Rostène W (1986) Dopaminergic control of ^{125}I-labeled neurotensin binding site density in corticolimbic structures of the rat brain. *Proc Natl Acad Sci U S A* **83**:6203-7.

Hery M, Laplante E and Kordon C (1978) Participation of serotonin in the phasic release of luteinizing hormone. II. Effects of lesions of serotonin-containing pathways in the central nervous system. *Endocrinology* **102**:1019-25.

Hery M, Faudon M and Hery F (1984) Effect of vasoactive intestinal peptide on serotonin release in the suprachiasmatic area of the rat. Modulation by oestradiol. *Peptides* **5**:313-7.

Horie M, Miyashita T, Watabe K, Takeda Y, Kawamura K and Kawano H (2000) Immunohistochemical localization of substance P receptors in the midline glia of the developing rat medulla oblongata with special reference to the formation of raphe nuclei. *Brain Res Dev Brain Res* **121**:197-207.

Horowitz DS and Krainer AR (1994) Mechanisms for selecting 5' splice sites in mammalian pre-mRNA splicing. *Trends Genet* **10**:100-6.

Huidobro-Toro JP, Zhu YX, Lee NM, Loh HH and Way EL (1984) Dynorphin inhibition of the neurotensin contractile activity on the myenteric plexus. *J Pharmacol Exp Ther* **228**:293-303.

Hukovic N, Rocheville M, Kumar U, Sasi R, Khare S and Patel YC (1999) Agonist-dependent up-regulation of human somatostatin receptor type 1 requires molecular signals in the cytoplasmic C-tail. *J Biol Chem* **274**:24550-8.

Hylden JL and Wilcox GL (1983) Antinociceptive action of intrathecal neurotensin in mice. *Peptides* **4**:517-20.

Imaizumi T, Osugi T, Misaki N, Uchida S and Yoshida H (1989) Heterologous desensitization of bradykinin-induced phosphatidylinositol response and Ca^{2+} mobilization by neurotensin in NG108-15 cells. *Eur J Pharmacol* **161**:203-8.

Innamorati G, Le Gouill C, Balamotis M and Birnbaumer M (2001) The long and the short cycle. Alternative intracellular routes for trafficking of G-protein-coupled receptors. *J Biol Chem* **276**:13096-103.

Jacobsen L, Madsen P, Moestrup SK, Lund AH, Tommerup N, Nykjaer A, Sottrup-Jensen L, Gliemann J and Petersen CM (1996) Molecular characterization of a novel human hybrid-type receptor that binds the alpha2-macroglobulin receptor-associated protein. *J Biol Chem* **271**:31379-83.

Jennes L, Stumpf WE and Kalivas PW (1982) Neurotensin: topographical distribution in rat brain by immunohistochemistry. *J Comp Neurol* **210**:211-24.

Johnson KF and Kornfeld S (1992) The cytoplasmic tail of the mannose 6-phosphate/insulin-like growth factor-II receptor has two signals for lysosomal enzyme sorting in the Golgi. *J Cell Biol* **119**:249-57.

Jolas T and Aghajanian GK (1997) Neurotensin and the serotonergic system. *Prog Neurobiol* **52**:455-68.

Jolicoeur FB, De Michele G, Barbeau A and St-Pierre S (1983) Neurotensin affects hyperactivity but not stereotypy induced by pre and post-synaptic dopaminergic stimulation. *Neurosci Biobehav Rev* **7**:385-90.

Jones BG, Thomas L, Molloy SS, Thulin CD, Fry MD, Walsh KA and Thomas G (1995) Intracellular trafficking of furin is modulated by the phosphorylation state of a casein kinase II site in its cytoplasmic tail. *Embo J* **14**:5869-83.

Jordan BA and Devi LA (1999) G-protein-coupled receptor heterodimerization modulates receptor function. *Nature* **399**:697-700.

Jordan BA, Trapaidze N, Gomes I, Nivarthi R and Devi LA (2001) Oligomerization of opioid receptors with beta 2-adrenergic receptors: a role in trafficking and mitogen-activated protein kinase activation. *Proc Natl Acad Sci U S A* **98**:343-8.

Kalivas PW, Gau BA, Nemeroff CB and Prange AJ, Jr. (1982a) Antinociception after microinjection of neurotensin into the central amygdaloid nucleus of the rat. *Brain Res* **243**:279-86.

Kalivas PW, Jennes L, Nemeroff CB and Prange AJ, Jr. (1982b) Neurotensin: topographical distribution of brain sites involved in hypothermia and antinociception. *J Comp Neurol* **210**:225-38.

Kalivas PW, Nemeroff CB and Prange AJ, Jr. (1984) Neurotensin microinjection into the nucleus accumbens antagonizes dopamine-induced increase in locomotion and rearing. *Neuroscience* **11**:919-30.

Kalivas PW, Nemeroff CB, Miller JS and Prange AJ, Jr. (1985) Microinjection of neurotensin into the ventral tegmental area produces hypothermia: evaluation of dopaminergic mediation. *Brain Res* **326**:219-27.

Kalivas PW and Steketee JD (1992) Possible transduction mechanisms mediating the acute and sensitized response to neurotensin in the ventral tegmental area. *Ann N Y Acad Sci* **668**:157-64.

Kalivas PW (1993) Neurotransmitter regulation of dopamine neurons in the ventral tegmental area. *Brain Res Brain Res Rev* **18**:75-113.

Kang H, Lee WK, Choi YH, Vukoti KM, Bang WG and Yu YG (2005) Molecular analysis of the interaction between the intracellular loops of the human serotonin receptor type 6 (5-HT6) and the alpha subunit of GS protein. *Biochem Biophys Res Commun* **329**:684-92.

Kataoka K, Taniguchi A, Shimizu H, Soda K, Okuno S, Yajima H and Kitagawa K (1978) Biological activity of neurotensin and its C-terminal partial sequences. *Brain Res Bull* **3**:555-7.

Katz LM, Young A, Frank JE, Wang Y and Park K (2004a) Neurotensin-induced hypothermia improves neurologic outcome after hypoxic-ischemia. *Crit Care Med* **32**:806-10.

Katz LM, Young AS, Frank JE, Wang Y and Park K (2004b) Regulated hypothermia reduces brain oxidative stress after hypoxic-ischemia. *Brain Res* **1017**:85-91.

Kaykas A, Yang-Snyder J, Heroux M, Shah KV, Bouvier M and Moon RT (2004) Mutant Frizzled 4 associated with vitreoretinopathy traps wild-type Frizzled in the endoplasmic reticulum by oligomerization. *Nat Cell Biol* **6**:52-8.

Kessler JP, Moyse E, Kitabgi P, Vincent JP and Beaudet A (1987) Distribution of neurotensin binding sites in the caudal brainstem of the rat: a light microscopic radioautographic study. *Neuroscience* **23**:189-98.

Kilpatrick GJ, Dautzenberg FM, Martin GR and Eglen RM (1999) 7TM receptors: the splicing on the cake. *Trends Pharmacol Sci* **20**:294-301.

Kinkead B and Nemeroff CB (1994) The effects of typical and atypical antipsychotic drugs on neurotensin-containing neurons in the central nervous system. *J Clin Psychiatry* **55 Suppl B**:30-2.

Kinkead B and Nemeroff CB (2002) Neurotensin: an endogenous antipsychotic? *Curr Opin Pharmacol* **2**:99-103.

Kinkead B and Nemeroff CB (2004) Neurotensin, schizophrenia, and antipsychotic drug action. *Int Rev Neurobiol* **59**:327-49.

Kislauskis E, Bullock B, McNeil S and Dobner PR (1988) The rat gene encoding neurotensin and neuromedin N. Structure, tissue-specific expression, and evolution of exon sequences. *J Biol Chem* **263**:4963-8.

Kislauskis E and Dobner PR (1990) Mutually dependent response elements in the cis-regulatory region of the neurotensin/neuromedin N gene integrate environmental stimuli in PC12 cells. *Neuron* **4**:783-95.

Kiss A, Palkovits M, Antoni FA, Eskay RL and Skirboll LR (1987) Neurotensin in the rat median eminence: the possible sources of neurotensin-like fibers and varicosities in the external layer. *Brain Res* **416**:129-35.

Kitabgi P and Freychet P (1978) Effects of neurotensin on isolated intestinal smooth muscles. *Eur J Pharmacol* **50**:349-57.

Kitabgi P and Freychet P (1979) Neurotensin: contractile activity, specific binding, and lack of effect on cyclic nucleotides in intestinal smooth muscle. *Eur J Pharmacol* **55**:35-42.

Kitabgi P (1982) Effects of neurotensin on intestinal smooth muscle: application to the study of structure-activity relationships. *Ann N Y Acad Sci* **400**:37-55.

Kitabgi P, Checler F, Mazella J and Vincent JP (1985) Pharmacology and biochemistry of neurotensin receptors. *Rev Clin Basic Pharm* **5**:397-486.

Kitabgi P, Rostène W, Dussaillant M, Schotte A, Laduron PM and Vincent JP (1987) Two populations of neurotensin binding sites in murine brain: discrimination by the antihistamine levocabastine reveals markedly different radioautographic distribution. *Eur J Pharmacol* **140**:285-93.

Kitabgi P, Hervé D, Studler JM, Tramu G, Rostène W and Tassin JP (1989) Neurotensin/dopamine interactions. *Encephale* **15 Spec No**:91-4.

Kitabgi P, De Nadai F, Cuber JC, Dubuc I, Nouel D and Costentin J (1990) Calcium-dependent release of neuromedin N and neurotensin from mouse hypothalamus. *Neuropeptides* **15**:111-4.

Kitabgi P, Masuo Y, Nicot A, Bérod A, Cuber JC and Rostène W (1991) Marked variations of the relative distributions of neurotensin and neuromedin N in micropunched rat brain areas suggest differential processing of their common precursor. *Neurosci Lett* **124**:9-12.

Kitabgi P, De Nadai F, Rovère C and Bidard JN (1992) Biosynthesis, maturation, release, and degradation of neurotensin and neuromedin N. *Ann N Y Acad Sci* **668**:30-42.

Kitabgi P (2002) Targeting neurotensin receptors with agonists and antagonists for therapeutic purposes. *Curr Opin Drug Discov Devel* **5**:764-76.

Kiyama H, Emson PC, Sato M and Tohyama M (1991a) The transient appearance of proneurotensin mRNA in the rat hypoglossal nucleus during development. *Brain Res Dev Brain Res* **58**:293-6.

Kiyama H, Sato M, Emson PC and Tohyama M (1991b) Transient expression of neurotensin mRNA in the mitral cells of rat olfactory bulb during development. *Neurosci Lett* **128**:85-9.

Koenig JA and Edwardson JM (1997) Endocytosis and recycling of G protein-coupled receptors. *Trends Pharmacol Sci* **18**:276-87.

Kranenburg O, Verlaan I and Moolenaar WH (1999) Dynamin is required for the activation of mitogen-activated protein (MAP) kinase by MAP kinase kinase. *J Biol Chem* **274**:35301-4.

Kreitel KD, Swisher CB and Behbehani MM (2002) The effects of diphenhydramine and SR142948A on periaqueductal gray neurons and on the interactions between the medial preoptic nucleus and the periaqueductal gray. *Neuroscience* **114**:935-43.

Kunishima N, Shimada Y, Tsuji Y, Sato T, Yamamoto M, Kumasaka T, Nakanishi S, Jingami H and Morikawa K (2000) Structural basis of glutamate recognition by a dimeric metabotropic glutamate receptor. *Nature* **407**:971-7.

Labbé-Jullié C, Dubuc I, Brouard A, Doulut S, Bourdel E, Pélaprat D, Mazella J, Martinez J, Rostène W, Costentin J and et al. (1994) In vivo and in vitro structure-activity studies with peptide and pseudopeptide neurotensin analogs suggest the existence of distinct central neurotensin receptor subtypes. *J Pharmacol Exp Ther* **268**:328-36.

Labbé-Jullié C, Botto JM, Mas MV, Chabry J, Mazella J, Vincent JP, Gully D, Maffrand JP and Kitabgi P (1995) [^{3}H]SR 48692, the first nonpeptide neurotensin antagonist radioligand: characterization of binding properties and evidence for distinct agonist and antagonist binding domains on the rat neurotensin receptor. *Mol Pharmacol* **47**:1050-6.

Labbé-Jullié C, Barroso S, Nicolas-Eteve D, Reversat JL, Botto JM, Mazella J, Bernassau JM and Kitabgi P (1998) Mutagenesis and modeling of the neurotensin receptor NTR1. Identification of residues that are critical for binding SR 48692, a nonpeptide neurotensin antagonist. *J Biol Chem* **273**:16351-7.

Laemmli UK (1970) Cleavage of structural proteins during the assembly of the head of bacteriophage T4. *Nature* **227**:680-5.

Lapchak PA, Araujo DM, Pasinetti G and Hefti F (1993) Differential alterations of cortical cholinergic and neurotensin markers following ibotenic acid lesions of the nucleus basalis magnocellularis. *Brain Res* **613**:239-46.

Lavoie C, Mercier JF, Salahpour A, Umapathy D, Breit A, Villeneuve LR, Zhu WZ, Xiao RP, Lakatta EG, Bouvier M and Hebert TE (2002) Beta 1/beta 2-adrenergic receptor heterodimerization regulates beta 2-adrenergic receptor internalization and ERK signaling efficacy. *J Biol Chem* **277**:35402-10.

Lépée-Lorgeoux I, Bétancur C, Rostène W and Pélaprat D (1999) Differential ontogenetic patterns of levocabastine-sensitive neurotensin NT2 receptors and of NT1 receptors in the rat brain revealed by in situ hybridization. *Brain Res Dev Brain Res* **113**:115-31.

Lépée-Lorgeoux I, Bétancur C, Souaze F, Rostène W, Bérod A and Pélaprat D (2000) Regulation of the neurotensin NT(1) receptor in the developing rat brain following chronic treatment with the antagonist SR 48692. *J Neurosci Res* **60**:362-9.

Leyton J, Garcia-Marin L, Jensen RT and Moody TW (2002) Neurotensin causes tyrosine phosphorylation of focal adhesion kinase in lung cancer cells. *Eur J Pharmacol* **442**:179-86.

Li AH, Hwang HM, Tan PP, Wu T and Wang HL (2001) Neurotensin excites periaqueductal gray neurons projecting to the rostral ventromedial medulla. *J Neurophysiol* **85**:1479-88.

Liang W, Austin S, Hoang Q and Fishman PH (2003) Resistance of the human beta 1-adrenergic receptor to agonist-mediated down-regulation. Role of the C terminus in determining beta-subtype degradation. *J Biol Chem* **278**:39773-81.

Liang W and Fishman PH (2004) Resistance of the human beta1-adrenergic receptor to agonist-induced ubiquitination: a mechanism for impaired receptor degradation. *J Biol Chem* **279**:46882-9.

Lin BZ, Pilch PF and Kandror KV (1997) Sortilin is a major protein component of Glut4-containing vesicles. *J Biol Chem* **272**:24145-7.

Liu H, Brown JL, Jasmin L, Maggio JE, Vigna SR, Mantyh PW and Basbaum AI (1994) Synaptic relationship between substance P and the substance P receptor: light and electron microscopic characterization of the mismatch between neuropeptides and their receptors. *Proc Natl Acad Sci U S A* **91**:1009-13.

Liu R, Paxton WA, Choe S, Ceradini D, Martin SR, Horuk R, MacDonald ME, Stuhlmann H, Koup RA and Landau NR (1996) Homozygous defect in HIV-1 coreceptor accounts for resistance of some multiply-exposed individuals to HIV-1 infection. *Cell* **86**:367-77.

Loosen PT, Nemeroff CB, Bissette G, Burnett GB, Prange AJ, Jr. and Lipton MA (1978) Neurotensin-induced hypothermia in the rat: structure-activity studies. *Neuropharmacology* **17**:109-13.

Loumaye E and Catt KJ (1982) Homologous regulation of gonadotropin-releasing hormone receptors in cultured pituitary cells. *Science* **215**:983-5.

Luckow VA and Summers MD (1988) Trends in the development of baculovirus vectors. *Bio/Technology* **6**:47-55.

Luttinger D, King RA, Sheppard D, Strupp J, Nemeroff CB and Prange AJ, Jr. (1982) The effect of neurotensin on food consumption in the rat. *Eur J Pharmacol* **81**:499-503.

Ma W, Chabot JG, Powell KJ, Jhamandas K, Dickerson IM and Quirion R (2003) Localization and modulation of calcitonin gene-related peptide-receptor component protein-immunoreactive cells in the rat central and peripheral nervous systems. *Neuroscience* **120**:677-94.

Maeno H, Yoshimura R, Fujita S, Su Q, Tanaka K, Wada K and Kiyama H (1996) Cloning and characterization of the rat neurotensin receptor gene promoter. *Brain Res Mol Brain Res* **40**:97-104.

Maeno H, Yamada K, Santo-Yamada Y, Aoki K, Sun YJ, Sato E, Fukushima T, Ogura H, Araki T, Kamichi S, Kimura I, Yamano M, Maeno-Hikichi Y, Watase K, Aoki S, Kiyama H, Wada E and Wada K (2004) Comparison of mice deficient in the high- or low-affinity neurotensin receptors, Ntsr1 or Ntsr2, reveals a novel function for Ntsr2 in thermal nociception. *Brain Res* **998**:122-9.

Maggio R, Novi F, Scarselli M and Corsini GU (2005) The impact of G-protein-coupled receptor hetero-oligomerization on function and pharmacology. *Febs J* **272**:2939-46.

Marcusson EG, Horazdovsky BF, Cereghino JL, Gharakhanian E and Emr SD (1994) The sorting receptor for yeast vacuolar carboxypeptidase Y is encoded by the VPS10 gene. *Cell* **77**:579-86.

Margeta-Mitrovic M, Jan YN and Jan LY (2000) A trafficking checkpoint controls GABA(B) receptor heterodimerization. *Neuron* **27**:97-106.

Martin GE, Bacino CB and Papp NL (1980) Hypothermia elicited by the intracerebral microinjection of neurotensin. *Peptides* **1**:333-9.

Martin GE and Naruse T (1982) Differences in the pharmacological actions of intrathecally administered neurotensin and morphine. *Regul Pept* **3**:97-103.

Martin S, Botto JM, Vincent JP and Mazella J (1999) Pivotal role of an aspartate residue in sodium sensitivity and coupling to G proteins of neurotensin receptors. *Mol Pharmacol* **55**:210-5.

Martin S, Navarro V, Vincent JP and Mazella J (2002a) Neurotensin receptor-1 and -3 complex modulates the cellular signaling of neurotensin in the HT29 cell line. *Gastroenterology* **123**:1135-43.

Martin S, Vincent JP and Mazella J (2002b) Recycling ability of the mouse and the human neurotensin type 2 receptors depends on a single tyrosine residue. *J Cell Sci* **115**:165-73.

Martin S, Vincent JP and Mazella J (2003) Involvement of the neurotensin receptor-3 in the neurotensin-induced migration of human microglia. *J Neurosci* **23**:1198-205.

Maselli MA, Piepoli AL, Riezzo G and Pezzolla F (1998) Motor responsiveness of proximal and distal human colonic muscle layers to carbachol and neurotensin. *Dig Dis Sci* **43**:1685-9.

Mayer DJ and Price DD (1989) The neurobiology of pain, in *Clinical electrophysiology: electrotherapy and electrophysiology* (Snyder-Machler LR, A ed), Baltimore: Willian & Wilkins, p 139-202.

Mazella J, Poustis C, Labbé C, Checler F, Kitabgi P, Granier C, van Rietschoten J and Vincent JP (1983) Monoiodo-[Trp11]neurotensin, a highly radioactive ligand of neurotensin receptors. Preparation, biological activity, and binding properties to rat brain synaptic membranes. *J Biol Chem* **258**:3476-81.

Mazella J, Chabry J, Kitabgi P and Vincent JP (1988) Solubilization and characterization of active neurotensin receptors from mouse brain. *J Biol Chem* **263**:144-9.

Mazella J, Chabry J, Zsürger N and Vincent JP (1989) Purification of the neurotensin receptor from mouse brain by affinity chromatography. *J Biol Chem* **264**:5559-63.

Mazella J, Botto JM, Guillemare E, Coppola T, Sarret P and Vincent JP (1996) Structure, functional expression, and cerebral localization of the levocabastine-sensitive neurotensin/neuromedin N receptor from mouse brain. *J Neurosci* **16**:5613-20.

Mazella J, Zsürger N, Navarro V, Chabry J, Kaghad M, Caput D, Ferrara P, Vita N, Gully D, Maffrand JP and Vincent JP (1998) The 100-kDa neurotensin receptor is gp95/sortilin, a non-G-protein-coupled receptor. *J Biol Chem* **273**:26273-6.

Mazella J (2001) Sortilin/neurotensin receptor-3: a new tool to investigate neurotensin signaling and cellular trafficking? *Cell Signal* **13**:1-6.

Mazzocchi G, Malendowicz LK, Rebuffat P, Gottardo G and Nussdorfer GG (1997) Neurotensin stimulates CRH and ACTH release by rat adrenal medulla in vitro. *Neuropeptides* **31**:8-11.

McCann SM and Vijayan E (1992) Control of anterior pituitary hormone secretion by neurotensin. *Ann N Y Acad Sci* **668**:287-97.

McCann SM, Vijayan E, Koenig J and Krulich L (1982) The effects of neurotensin on anterior pituitary hormone secretion. *Ann N Y Acad Sci* **400**:160-71.

McHaffie JG, Kao CQ and Stein BE (1989) Nociceptive neurons in rat superior colliculus: response properties, topography, and functional implications. *J Neurophysiol* **62**:510-25.

McLatchie LM, Fraser NJ, Main MJ, Wise A, Brown J, Thompson N, Solari R, Lee MG and Foord SM (1998) RAMPs regulate the transport and ligand specificity of the calcitonin-receptor-like receptor. *Nature* **393**:333-9.

Mendez M, Souaze F, Nagano M, Kelly PA, Rostène W and Forgez P (1997) High affinity neurotensin receptor mRNA distribution in rat brain and peripheral tissues. Analysis by quantitative RT-PCR. *J Mol Neurosci* **9**:93-102.

Merchenthaler I and Lennard DE (1991) The hypophysiotropic neurotensin-immunoreactive neuronal system of the rat brain. *Endocrinology* **129**:2875-80.

Michineau S, Muller L, Pizard A, Alhenc-Gelas F and Rajerison RM (2004) N-linked glycosylation of the human bradykinin B2 receptor is required for optimal cell-surface expression and coupling. *Biol Chem* **385**:49-57.

Miller WE and Lefkowitz RJ (2001) Expanding roles for beta-arrestins as scaffolds and adapters in GPCR signaling and trafficking. *Curr Opin Cell Biol* **13**:139-45.

Minneman KP (2001) Splice variants of G protein-coupled receptors. *Mol Interv* **1**:108-16.

Miyata I, Shiota C, Ikeda Y, Oshida Y, Chaki S, Okuyama S and Inagami T (1999) Cloning and characterization of a short variant of the corticotropin-releasing factor receptor subtype from rat amygdala. *Biochem Biophys Res Commun* **256**:692-6.

Monsma FJ, Jr., McVittie LD, Gerfen CR, Mahan LC and Sibley DR (1989) Multiple D2 dopamine receptors produced by alternative RNA splicing. *Nature* **342**:926-9.

Moody TW, Carney DN, Korman LY, Gazdar AF and Minna JD (1985) Neurotensin is produced by and secreted from classic small cell lung cancer cells. *Life Sci* **36**:1727-32.

Morin AJ, Tajani M, Jones BE and Beaudet A (1996) Spatial relationship between neurotensinergic axons and cholinergic neurons in the rat basal forebrain: a light microscopic study with three-dimensional reconstruction. *J Chem Neuroanat* **10**:147-56.

Morin AJ and Beaudet A (1998) Origin of the neurotensinergic innervation of the rat basal forebrain studied by retrograde transport of cholera toxin. *J Comp Neurol* **391**:30-41.

Morinville A, Cahill CM, Esdaile MJ, Aibak H, Collier B, Kieffer BL and Beaudet A (2003) Regulation of delta-opioid receptor trafficking via mu-opioid receptor stimulation: evidence from mu-opioid receptor knock-out mice. *J Neurosci* **23**:4888-98.

Morinville A, Martin S, Lavallée M, Vincent JP, Beaudet A and Mazella J (2004) Internalization and trafficking of neurotensin via NTS3 receptors in HT29 cells. *Int J Biochem Cell Biol* **36**:2153-68.

Morris AJ, Martin SS, Haruta T, Nelson JG, Vollenweider P, Gustafson TA, Mueckler M, Rose DW and Olefsky JM (1996) Evidence for an insulin receptor substrate 1 independent insulin signaling pathway that mediates insulin-responsive glucose transporter (GLUT4) translocation. *Proc Natl Acad Sci U S A* **93**:8401-6.

Morris NJ, Ross SA, Lane WS, Moestrup SK, Petersen CM, Keller SR and Lienhard GE (1998) Sortilin is the major 110-kDa protein in GLUT4 vesicles from adipocytes. *J Biol Chem* **273**:3582-7.

Motomura T, Hashimoto K, Koga M, Arita N, Hayakawa T, Kishimoto T and Kasayama S (1998) Inhibition of signal transduction by a splice variant of the growth hormone-releasing hormone receptor expressed in human pituitary adenomas. *Metabolism* **47**:804-8.

Moyse E, Rostène W, Vial M, Léonard K, Mazella J, Kitabgi P, Vincent JP and Beaudet A (1987) Distribution of neurotensin binding sites in rat brain: a light microscopic radioautographic study using monoiodo [^{125}I]Tyr3-neurotensin. *Neuroscience* **22**:525-36.

Mule F, Serio R and Postorino A (1995) Motility pattern of isolated rat proximal colon and excitatory action of neurotensin. *Eur J Pharmacol* **275**:131-7.

Mule F and Serio R (1997) Mode and mechanism of neurotensin action in rat proximal colon. *Eur J Pharmacol* **319**:269-72.

Najimi M, Souaze F, Mendez M, Hermans E, Berbar T, Rostène W and Forgez P (1998) Activation of receptor gene transcription is required to maintain cell sensitization after agonist exposure. Study on neurotensin receptor. *J Biol Chem* **273**:21634-41.

Najimi M, Gailly P, Maloteaux JM and Hermans E (2002) Distinct regions of C-terminus of the high affinity neurotensin receptor mediate the functional coupling with pertussis toxin sensitive and insensitive G-proteins. *FEBS Lett* **512**:329-33.

Namba T, Sugimoto Y, Negishi M, Irie A, Ushikubi F, Kakizuka A, Ito S, Ichikawa A and Narumiya S (1993) Alternative splicing of C-terminal tail of prostaglandin E receptor subtype EP3 determines G-protein specificity. *Nature* **365**:166-70.

Nambi P, Wu HL, Ye D, Gagnon A and Elshourbagy N (2000) Characterization of a novel porcine endothelin(B) receptor splice variant. *J Pharmacol Exp Ther* **292**:247-53.

Naranjo JR, Arnedo A, Molinero MT and Del Rio J (1989) Involvement of spinal monoaminergic pathways in antinociception produced by substance P and neurotensin in rodents. *Neuropharmacology* **28**:291-8.

Navarro V, Martin S, Sarret P, Nielsen MS, Petersen CM, Vincent J and Mazella J (2001) Pharmacological properties of the mouse neurotensin receptor 3. Maintenance of cell surface receptor during internalization of neurotensin. *FEBS Lett* **495**:100-5.

Nelson G, Hoon MA, Chandrashekar J, Zhang Y, Ryba NJ and Zuker CS (2001) Mammalian sweet taste receptors. *Cell* **106**:381-90.

Nelson G, Chandrashekar J, Hoon MA, Feng L, Zhao G, Ryba NJ and Zuker CS (2002) An amino-acid taste receptor. *Nature* **416**:199-202.

Nemeroff CB, Bissette G, Prange AJ, Jr., Loosen PT, Barlow TS and Lipton MA (1977) Neurotensin: central nervous system effects of a hypothalamic peptide. *Brain Res* **128**:485-96.

Nemeroff CB, Osbahr AJ, 3rd, Manberg PJ, Ervin GN and Prange AJ, Jr. (1979) Alterations in nociception and body temperature after intracisternal administration of neurotensin, beta-endorphin, other endogenous peptides, and morphine. *Proc Natl Acad Sci U S A* **76**:5368-71.

Nemeroff CB (1986) The interaction of neurotensin with dopaminergic pathways in the central nervous system: basic neurobiology and implications for the pathogenesis and treatment of schizophrenia. *Psychoneuroendocrinology* **11**:15-37.

Ng GY, O'Dowd BF, Lee SP, Chung HT, Brann MR, Seeman P and George SR (1996) Dopamine D2 receptor dimers and receptor-blocking peptides. *Biochem Biophys Res Commun* **227**:200-4.

Nguyen HM, Cahill CM, McPherson PS and Beaudet A (2002) Receptor-mediated internalization of [^{3}H]-neurotensin in synaptosomal preparations from rat neostriatum. *Neuropharmacology* **42**:1089-98.

Nicot A, Bérod A and Rostène W (1992) Distribution of prepro-neurotensin/neuromedin N mRNA in the young and adult rat forebrain. *Ann N Y Acad Sci* **668**:361-4.

Nicot A, Bérod A, Gully D, Rowe W, Quirion R, de Kloet ER and Rostène W (1994) Blockade of neurotensin binding in the rat hypothalamus and of the central action of neurotensin on the hypothalamic-pituitary-adrenal axis with non-peptide receptor antagonists. *Neuroendocrinology* **59**:572-8.

Nicot A, Rostène W and Bérod A (1995) Differential expression of neurotensin receptor mRNA in the dopaminergic cell groups of the rat diencephalon and mesencephalon. *J Neurosci Res* **40**:667-74.

Nielsen MS, Jacobsen C, Olivecrona G, Gliemann J and Petersen CM (1999) Sortilin/neurotensin receptor-3 binds and mediates degradation of lipoprotein lipase. *J Biol Chem* **274**:8832-6.

Nielsen MS, Madsen P, Christensen EI, Nykjaer A, Gliemann J, Kasper D, Pohlmann R and Petersen CM (2001) The sortilin cytoplasmic tail conveys Golgi-endosome transport and binds the VHS domain of the GGA2 sorting protein. *Embo J* **20**:2180-90.

Niimi M, Takahara J, Sato M and Kawanishi K (1991) Neurotensin and growth hormone-releasing factor-containing neurons projecting to the median eminence of the rat: a combined retrograde tracing and immunohistochemical study. *Neurosci Lett* **133**:183-6.

Nisato D, Guiraudou P, Barthelemy G, Gully D and Le Fur G (1994) SR 48692, a non-peptide neurotensin receptor antagonist, blocks the cardiovascular effects elicited by neurotensin in guinea pigs. *Life Sci* **54**:PL95-100.

Nishimatsu S, Koyasu N, Sugaya T, Ohnishi J, Yamagishi T, Murakami K and Miyazaki H (1994) Isolation and characterization of two alternatively spliced complementary DNAs encoding a Xenopus laevis angiotensin II receptor. *Biochim Biophys Acta* **1218**:401-7.

Nouel D, Faure MP, St Pierre JA, Alonso R, Quirion R and Beaudet A (1997) Differential binding profile and internalization process of neurotensin via neuronal and glial receptors. *J Neurosci* **17**:1795-803.

Nouel D, Sarret P, Vincent JP, Mazella J and Beaudet A (1999) Pharmacological, molecular and functional characterization of glial neurotensin receptors. *Neuroscience* **94**:1189-97.

Nussdorfer GG, Malendowicz LK, Meneghelli V and Mazzocchi G (1992) Neurotensin enhances plasma adrenocorticotropin concentration by stimulating corticotropin-releasing hormone secretion. *Life Sci* **50**:639-43.

Nykjaer A, Lee R, Teng KK, Jansen P, Madsen P, Nielsen MS, Jacobsen C, Kliemannel M, Schwarz E, Willnow TE, Hempstead BL and Petersen CM (2004) Sortilin is essential for proNGF-induced neuronal cell death. *Nature* **427**:843-8.

Oakley RH, Laporte SA, Holt JA, Caron MG and Barak LS (2000) Differential affinities of visual arrestin, beta arrestin1, and beta arrestin2 for G protein-coupled receptors delineate two major classes of receptors. *J Biol Chem* **275**:17201-10.

Ohashi H, Takewaki T, Unno T and Komori S (1994) Mechanical and current responses to neurotensin in the smooth muscle of guinea-pig intestine. *J Auton Pharmacol* **14**:239-51.

Ohashi H, Tanaka K, Kiuchi N, Unno T and Komori S (1996) Modulation of peristalsis by neurotensin in isolated guinea-pig intestinal segments. *Eur J Pharmacol* **301**:129-36.

Osbahr AJ, 3rd, Nemeroff CB, Luttinger D, Mason GA and Prange AJ, Jr. (1981) Neurotensin-induced antinociception in mice: antagonism by thyrotropin-releasing hormone. *J Pharmacol Exp Ther* **217**:645-51.

Overton MC and Blumer KJ (2002) Use of fluorescence resonance energy transfer to analyze oligomerization of G-protein-coupled receptors expressed in yeast. *Methods* **27**:324-32.

Pagano A, Rovelli G, Mosbacher J, Lohmann T, Duthey B, Stauffer D, Ristig D, Schuler V, Meigel I, Lampert C, Stein T, Prezeau L, Blahos J, Pin J, Froestl W, Kuhn R, Heid J, Kaupmann K and Bettler B (2001) C-terminal interaction is essential for surface trafficking but not for heteromeric assembly of GABA(b) receptors. *J Neurosci* **21**:1189-202.

Palacios JM and Kuhar MJ (1981) Neurotensin receptors are located on dopamine-containing neurones in rat midbrain. *Nature* **294**:587-9.

Palacios JM, Pazos A, Dietl MM, Schlumpf M and Lichtensteiger W (1988) The ontogeny of brain neurotensin receptors studied by autoradiography. *Neuroscience* **25**:307-17.

Palkovits M and Zaborszky L (1977) Neuroanatomy of central cardiovascular control. Nucleus tractus solitarii: afferent and efferent neuronal connections in relation to the baroreceptor reflex arc. *Prog Brain Res* **47**:9-34.

Paxinos G and Watson C (1986) *The rat brain in stereotaxic coordinates*. 2nd ed. New York: Academic Press.

Perron A, Sarret P, Gendron L, Stroh T and Beaudet A (2005) Identification and functional characterization of a 5-transmembrane domain variant isoform of the NTS2 neurotensin receptor in rat central nervous system. *J Biol Chem* **280**:10219-27.

Perron A, Sharif N, Gendron L, Lavallée M, Stroh T, Mazella J and Beaudet A (2006) Sustained neurotensin exposure promotes cell surface recruitment of NTS2 receptors. *Biochem Biophys Res Commun* **343**:799-808.

Petersen CM, Nielsen MS, Nykjaer A, Jacobsen L, Tommerup N, Rasmussen HH, Roigaard H, Gliemann J, Madsen P and Moestrup SK (1997) Molecular identification of a novel candidate sorting receptor purified from human brain by receptor-associated protein affinity chromatography. *J Biol Chem* **272**:3599-605.

Pettibone DJ, Hess JF, Hey PJ, Jacobson MA, Leviten M, Lis EV, Mallorga PJ, Pascarella DM, Snyder MA, Williams JB and Zeng Z (2002) The effects of deleting the mouse neurotensin receptor NTR1 on central and peripheral responses to neurotensin. *J Pharmacol Exp Ther* **300**:305-13.

Pickel VM, Chan J, Delle Donne KT, Boudin H, Pélaprat D and Rostène W (2001) High-affinity neurotensin receptors in the rat nucleus accumbens: subcellular targeting and relation to endogenous ligand. *J Comp Neurol* **435**:142-55.

Pierce KL, Maudsley S, Daaka Y, Luttrell LM and Lefkowitz RJ (2000) Role of endocytosis in the activation of the extracellular signal-regulated kinase cascade by sequestering and nonsequestering G protein-coupled receptors. *Proc Natl Acad Sci U S A* **97**:1489-94.

Pinnock RD (1985) Neurotensin depolarizes substantia nigra dopamine neurones. *Brain Res* **338**:151-4.

Poinot-Chazel C, Portier M, Bouaboula M, Vita N, Pecceu F, Gully D, Monroe JG, Maffrand JP, Le Fur G and Casellas P (1996) Activation of mitogen-activated protein kinase couples neurotensin receptor stimulation to induction of the primary response gene Krox-24. *Biochem J* **320 (Pt 1)**:145-51.

Polak JM, Sullivan SN, Bloom SR, Buchan AM, Facer P, Brown MR and Pearse AG (1977) Specific localisation of neurotensin to the N cell in human intestine by radioimmunoassay and immunocytochemistry. *Nature* **270**:183-4.

Polak JM and Bloom SR (1978) Peptidergic innervation of the gastrointestinal tract. *Adv Exp Med Biol* **106**:27-49.

Portier M, Combes T, Gully D, Maffrand JP and Casellas P (1998) Neurotensin type 1 receptor-mediated activation of krox24, c-fos and Elk-1: preventing effect of the neurotensin antagonists SR 48692 and SR 142948. *FEBS Lett* **432**:88-93.

Prange AJ, Jr., Nemeroff CB, Bissette G, Manberg PJ, Osbahr AJ, 3rd, Burnett GB, Loosen PT and Kraemer GW (1979) Neurotensin: distribution of hypothermic response in mammalian and submammalian vertebrates. *Pharmacol Biochem Behav* **11**:473-7.

Prinster SC, Hague C and Hall RA (2005) Heterodimerization of g protein-coupled receptors: specificity and functional significance. *Pharmacol Rev* **57**:289-98.

Pugsley TA, Akunne HC, Whetzel SZ, Demattos S, Corbin AE, Wiley JN, Wustrow DJ, Wise LD and Heffner TG (1995) Differential effects of the nonpeptide neurotensin antagonist, SR 48692, on the pharmacological effects of neurotensin agonists. *Peptides* **16**:37-44.

Quirion R, Rioux F, Regoli D and St-Pierre S (1979) Neurotensin-induced coronary vessels constriction in perfused rat hearts. *Eur J Pharmacol* **55**:221-3.

Quirion R, Rioux F, Regoli D and St-Pierre S (1980) Compound 48/80 inhibits neurotensin-induced hypotension in rats. *Life Sci* **27**:1889-95.

Quirion R, Gaudreau P, St-Pierre S, Rioux F and Pert CB (1982) Autoradiographic distribution of [^{3}H]neurotensin receptors in rat brain: visualization by tritium-sensitive film. *Peptides* **3**:757-63.

Quirion R, Chiueh CC, Everist HD and Pert A (1985) Comparative localization of neurotensin receptors on nigrostriatal and mesolimbic dopaminergic terminals. *Brain Res* **327**:385-9.

Ramirez JL, Watt HL, Rocheville M and Kumar U (2005) Agonist-induced up-regulation of human somatostatin receptor type 1 is regulated by beta-arrestin-1 and requires an essential serine residue in the receptor C-tail. *Biochim Biophys Acta* **1669**:182-92.

Rekasi Z, Czompoly T, Schally AV and Halmos G (2000) Isolation and sequencing of cDNAs for splice variants of growth hormone-releasing hormone receptors from human cancers. *Proc Natl Acad Sci U S A* **97**:10561-6.

Remaury A, Vita N, Gendreau S, Jung M, Arnone M, Poncelet M, Culouscou JM, Le Fur G, Soubrie P, Caput D, Shire D, Kopf M and Ferrara P (2002) Targeted inactivation of the neurotensin type 1 receptor reveals its role in body temperature control and feeding behavior but not in analgesia. *Brain Res* **953**:63-72.

Richard F, Barroso S, Nicolas-Ethève D, Kitabgi P and Labbé-Jullié C (2001a) Impaired G protein coupling of the neurotensin receptor 1 by mutations in extracellular loop 3. *Eur J Pharmacol* **433**:63-71.

Richard F, Barroso S, Martinez J, Labbé-Jullié C and Kitabgi P (2001b) Agonism, inverse agonism, and neutral antagonism at the constitutively active human neurotensin receptor 2. *Mol Pharmacol* **60**:1392-8.

Rios CD, Jordan BA, Gomes I and Devi LA (2001) G-protein-coupled receptor dimerization: modulation of receptor function. *Pharmacol Ther* **92**:71-87.

Rioux F, Quirion R, Regoli D, Leblanc MA and St-Pierre S (1980) Pharmacological characterization of neurotensin receptors in the rat isolated portal vein using analogues and fragments of neurotensin. *Eur J Pharmacol* **66**:273-9.

Rioux F, Quirion R, St-Pierre S, Regoli D, Jolicoeur FB, Belanger F and Barbeau A (1981) The hypotensive effect of centrally administered neurotensin in rats. *Eur J Pharmacol* **69**:241-7.

Rizvi TA, Ennis M, Behbehani MM and Shipley MT (1991) Connections between the central nucleus of the amygdala and the midbrain periaqueductal gray: topography and reciprocity. *J Comp Neurol* **303**:121-31.

Rocheville M, Lange DC, Kumar U, Sasi R, Patel RC and Patel YC (2000) Subtypes of the somatostatin receptor assemble as functional homo- and heterodimers. *J Biol Chem* **275**:7862-9.

Romano C, Miller JK, Hyrc K, Dikranian S, Mennerick S, Takeuchi Y, Goldberg MP and O'Malley KL (2001) Covalent and noncovalent interactions mediate metabotropic glutamate receptor mGlu5 dimerization. *Mol Pharmacol* **59**:46-53.

Rosell S, Burcher E, Chang D and Folkers K (1976) Cardiovascular and metabolic actions of neurotensin and (Gln4)-Neurotensin. *Acta Physiol Scand* **98**:484-91.

Rosell S (1980) Experimental evidence for neurotensin or a metabolite being a hormone. *Acta Physiol Scand* **110**:325.

Rosell S (1982) The role of neurotensin in the uptake and distribution of fat. *Ann N Y Acad Sci* **400**:183-97.

Rostène W, Brouard A, Dana C, Masuo Y, Agid F, Vial M, Lhiaubet AM and Pélaprat D (1992) Interaction between neurotensin and dopamine in the brain. Morphofunctional and clinical evidence. *Ann N Y Acad Sci* **668**:217-31.

Rostène WH and Alexander MJ (1997) Neurotensin and neuroendocrine regulation. *Front Neuroendocrinol* **18**:115-73.

Roth BL, Willins DL and Kroeze WK (1998) G protein-coupled receptor (GPCR) trafficking in the central nervous system: relevance for drugs of abuse. *Drug Alcohol Depend* **51**:73-85.

Rovère C, Barbero P and Kitabgi P (1996) Evidence that PC2 is the endogenous pro-neurotensin convertase in rMTC 6-23 cells and that PC1- and PC2-transfected PC12 cells differentially process pro-neurotensin. *J Biol Chem* **271**:11368-75.

Rovère C, Barbero P, Maoret JJ, Laburthe M and Kitabgi P (1998) Pro-neurotensin/neuromedin N expression and processing in human colon cancer cell lines. *Biochem Biophys Res Commun* **246**:155-9.

Rowe W, Viau V, Meaney MJ and Quirion R (1992) Central administration of neurotensin stimulates hypothalamic-pituitary-adrenal activity. The paraventricular CRF neuron as a critical site of action. *Ann N Y Acad Sci* **668**:365-7.

Ryder NM, Guha S, Hines OJ, Reber HA and Rozengurt E (2001) G protein-coupled receptor signaling in human ductal pancreatic cancer cells: neurotensin responsiveness and mitogenic stimulation. *J Cell Physiol* **186**:53-64.

Sadee W, Hoeg E, Lucas J and Wang D (2001) Genetic variations in human G protein-coupled receptors: implications for drug therapy. *AAPS PharmSci* **3**:E22.

Sadoul JL, Kitabgi P, Rostène W, Javoy-Agid F, Agid Y and Vincent JP (1984) Characterization and visualization of neurotensin binding to receptor sites in human brain. *Biochem Biophys Res Commun* **120**:206-13.

Sahu A, Carraway RE and Wang YP (2001) Evidence that neurotensin mediates the central effect of leptin on food intake in rat. *Brain Res* **888**:343-347.

Sarhan S, Hitchcock JM, Grauffel CA and Wettstein JG (1997) Comparative antipsychotic profiles of neurotensin and a related systemically active peptide agonist. *Peptides* **18**:1223-7.

Sarret P, Beaudet A, Vincent JP and Mazella J (1998) Regional and cellular distribution of low affinity neurotensin receptor mRNA in adult and developing mouse brain. *J Comp Neurol* **394**:344-56.

Sarret P, Gendron L, Kilian P, Nguyen HM, Gallo-Payet N, Payet MD and Beaudet A (2002a) Pharmacology and functional properties of NTS2 neurotensin receptors in cerebellar granule cells. *J Biol Chem* **277**:36233-43.

Sarret P and Beaudet A (2002b) Neurotensin receptors in the central nervous system, in *Handbook of chemical neuroanatomy*, Amsterdam: Elsevier, p 323-400.

Sarret P, Perron A, Stroh T and Beaudet A (2003a) Immunohistochemical distribution of NTS2 neurotensin receptors in the rat central nervous system. *J Comp Neurol* **461**:520-38.

Sarret P, Krzywkowski P, Segal L, Nielsen MS, Petersen CM, Mazella J, Stroh T and Beaudet A (2003b) Distribution of NTS3 receptor/sortilin mRNA and protein in the rat central nervous system. *J Comp Neurol* **461**:483-505.

Sarret P, Esdaile MJ, Perron A, Martinez J, Stroh T and Beaudet A (2005) Potent spinal analgesia elicited through stimulation of NTS2 neurotensin receptors. *J Neurosci* **25**:8188-96.

Sarrieau A, Javoy-Agid F, Kitabgi P, Dussaillant M, Vial M, Vincent JP, Agid Y and Rostène WH (1985) Characterization and autoradiographic distribution of neurotensin binding sites in the human brain. *Brain Res* **348**:375-80.

Sato M, Kiyama H, Yoshida S, Saika T and Tohyama M (1991a) Postnatal ontogeny of cells expressing prepro-neurotensin/neuromedin N mRNA in the rat forebrain and midbrain: a hybridization histochemical study involving isotope-labeled and enzyme-labeled probes. *J Comp Neurol* **310**:300-15.

Sato M, Shiosaka S and Tohyama M (1991b) Neurotensin and neuromedin N elevate the cytosolic calcium concentration via transiently appearing neurotensin binding sites in cultured rat cortex cells. *Brain Res Dev Brain Res* **58**:97-103.

Sato M, Kiyama H and Tohyama M (1992) Different postnatal development of cells expressing mRNA encoding neurotensin receptor. *Neuroscience* **48**:137-49.

Sato M, Blumer JB, Simon V and Lanier SM (2006) Accessory proteins for G proteins: partners in signaling. *Annu Rev Pharmacol Toxicol* **46**:151-87.

Savdie C, Ferguson SS, Vincent J, Beaudet A and Stroh T (2006) Cell-type-specific pathways of neurotensin endocytosis. *Cell Tissue Res* **324**:69-85.

Schafer MK, Day R, Cullinan WE, Chretien M, Seidah NG and Watson SJ (1993) Gene expression of prohormone and proprotein convertases in the rat CNS: a comparative in situ hybridization analysis. *J Neurosci* **13**:1258-79.

Schmauss C, Haroutunian V, Davis KL and Davidson M (1993) Selective loss of dopamine D3-type receptor mRNA expression in parietal and motor cortices of patients with chronic schizophrenia. *Proc Natl Acad Sci U S A* **90**:8942-6.

Schmid SL, McNiven MA and De Camilli P (1998) Dynamin and its partners: a progress report. *Curr Opin Cell Biol* **10**:504-12.

Schotte A, Leysen JE and Laduron PM (1986) Evidence for a displaceable non-specific [^{3}H]neurotensin binding site in rat brain. *Naunyn Schmiedebergs Arch Pharmacol* **333**:400-5.

Schotte A and Laduron PM (1987) Different postnatal ontogeny of two [^{3}H]neurotensin binding sites in rat brain. *Brain Res* **408**:326-8.

Schotte A, Rostène W and Laduron PM (1988) Different subcellular localization of neurotensin-receptor and neurotensin-acceptor sites in the rat brain dopaminergic system. *J Neurochem* **50**:1026-31.

Schotte A and Leysen JE (1989) Further characterization of neurotensin binding in the rat brain: levocabastine-displaceable neurotensin binding sites are not histamine-H1 receptors. *Biochem Pharmacol* **38**:3891-3.

Sehgal I, Powers S, Huntley B, Powis G, Pittelkow M and Maihle NJ (1994) Neurotensin is an autocrine trophic factor stimulated by androgen withdrawal in human prostate cancer. *Proc Natl Acad Sci U S A* **91**:4673-7.

Sethi T and Rozengurt E (1991) Multiple neuropeptides stimulate clonal growth of small cell lung cancer: effects of bradykinin, vasopressin, cholecystokinin, galanin, and neurotensin. *Cancer Res* **51**:3621-3.

Sever S (2002) Dynamin and endocytosis. *Curr Opin Cell Biol* **14**:463-7.

Shaw C, Thim L and Conlon JM (1986) [Ser7]neurotensin: isolation from guinea pig intestine. *FEBS Lett* **202**:187-92.

Shaw C, McKay DM, Halton DW, Thim L and Buchanan KD (1992) Isolation and primary structure of an amphibian neurotensin. *Regul Pept* **38**:23-31.

Sheppard MC, Kronheim S and Pimstone BL (1979) Effect of substance P, neurotensin and the enkephalins on somatostatin release from the rat hypothalamus in vitro. *J Neurochem* **32**:647-9.

Shigemoto R, Nakaya Y, Nomura S, Ogawa-Meguro R, Ohishi H, Kaneko T, Nakanishi S and Mizuno N (1993) Immunocytochemical localization of rat substance P receptor in the striatum. *Neurosci Lett* **153**:157-60.

Simonsen A, Gaullier JM, D'Arrigo A and Stenmark H (1999) The Rab5 effector EEA1 interacts directly with syntaxin-6. *J Biol Chem* **274**:28857-60.

Skoog KM, Cain ST and Nemeroff CB (1986) Centrally administered neurotensin suppresses locomotor hyperactivity induced by d-amphetamine but not by scopolamine or caffeine. *Neuropharmacology* **25**:777-82.

Slot JW, Geuze HJ, Gigengack S, James DE and Lienhard GE (1991) Translocation of the glucose transporter GLUT4 in cardiac myocytes of the rat. *Proc Natl Acad Sci U S A* **88**:7815-9.

Slusher BS, Zacco AE, Maslanski JA, Norris TE, McLane MW, Moore WC, Rogers NE and Ignarro LJ (1994) The cloned neurotensin receptor mediates cyclic GMP formation when coexpressed with nitric oxide synthase cDNA. *Mol Pharmacol* **46**:115-21.

Smith DJ, Hawranko AA, Monroe PJ, Gully D, Urban MO, Craig CR, Smith JP and Smith DL (1997) Dose-dependent pain-facilitatory and -inhibitory actions of neurotensin are revealed by SR 48692, a nonpeptide neurotensin antagonist: influence on the antinociceptive effect of morphine. *J Pharmacol Exp Ther* **282**:899-908.

Smits SM, Terwisscha van Scheltinga AF, van der Linden AJ, Burbach JP and Smidt MP (2004) Species differences in brain pre-pro-neurotensin/neuromedin N mRNA distribution: the expression pattern in mice resembles more closely that of primates than rats. *Brain Res Mol Brain Res* **125**:22-8.

Snider RM, Forray C, Pfenning M and Richelson E (1986) Neurotensin stimulates inositol phospholipid metabolism and calcium mobilization in murine neuroblastoma clone N1E-115. *J Neurochem* **47**:1214-8.

Snijders R, Kramarcy NR, Hurd RW, Nemeroff CB and Dunn AJ (1982) Neurotensin induces catalepsy in mice. *Neuropharmacology* **21**:465-8.

Sokoloff P, Giros B, Martres MP, Andrieux M, Besancon R, Pilon C, Bouthenet ML, Souil E and Schwartz JC (1992) Localization and function of the D3 dopamine receptor. *Arzneimittelforschung* **42**:224-30.

Spampinato S, Romualdi P, Candeletti S, Cavicchini E and Ferri S (1988) Distinguishable effects of intrathecal dynorphins, somatostatin, neurotensin and s-calcitonin on nociception and motor function in the rat. *Pain* **35**:95-104.

Spengler D, Waeber C, Pantaloni C, Holsboer F, Bockaert J, Seeburg PH and Journot L (1993) Differential signal transduction by five splice variants of the PACAP receptor. *Nature* **365**:170-5.

Stanasila L, Perez JB, Vogel H and Cotecchia S (2003) Oligomerization of the alpha 1a- and alpha 1b-adrenergic receptor subtypes. Potential implications in receptor internalization. *J Biol Chem* **278**:40239-51.

Stanley BG, Hoebel BG and Leibowitz SF (1983) Neurotensin: effects of hypothalamic and intravenous injections on eating and drinking in rats. *Peptides* **4**:493-500.

Starr S, Kozell LB and Neve KA (1995) Drug-induced up-regulation of dopamine D2 receptors on cultured cells. *J Neurochem* **65**:569-77.

Steinberg R, Brun P, Fournier M, Souilhac J, Rodier D, Mons G, Terranova JP, Le Fur G and Soubrie P (1994) SR 48692, a non-peptide neurotensin receptor antagonist differentially affects neurotensin-induced behaviour and changes in dopaminergic transmission. *Neuroscience* **59**:921-9.

St-Gelais F, Legault M, Bourque MJ, Rompré PP and Trudeau LE (2004) Role of calcium in neurotensin-evoked enhancement in firing in mesencephalic dopamine neurons. *J Neurosci* **24**:2566-74.

Stoessl AJ (1995) Effects of neurotensin in a rodent model of tardive dyskinesia. *Neuropharmacology* **34**:457-62.

Sullivan R, Chateauneuf A, Coulombe N, Kolakowski LF, Jr., Johnson MP, Hebert TE, Ethier N, Belley M, Metters K, Abramovitz M, O'Neill GP and Ng GY (2000) Coexpression of full-length gamma-aminobutyric acid(B) (GABA(B)) receptors with truncated receptors and metabotropic glutamate receptor 4 supports the GABA(B) heterodimer as the functional receptor. *J Pharmacol Exp Ther* **293**:460-7.

Sun YJ, Maeno H, Aoki S and Wada K (2001) Mouse neurotensin receptor 2 gene (Ntsr2): genomic organization, transcriptional regulation and genetic mapping on chromosome 12. *Brain Res Mol Brain Res* **95**:167-71.

Szigethy E and Beaudet A (1987) Selective association of neurotensin receptors with cholinergic neurons in the rat basal forebrain. *Neurosci Lett* **83**:47-52.

Szigethy E, Wenk GL and Beaudet A (1988) Anatomical substrate for neurotensin-acetylcholine interactions in the rat basal forebrain. *Peptides* **9**:1227-34.

Szigethy E and Beaudet A (1989) Correspondence between high affinity ^{125}I-neurotensin binding sites and dopaminergic neurons in the rat substantia nigra and ventral tegmental area: a combined radioautographic and immunohistochemical light microscopic study. *J Comp Neurol* **279**:128-37.

Szigethy E, Léonard K and Beaudet A (1990) Ultrastructural localization of [^{125}I]neurotensin binding sites to cholinergic neurons of the rat nucleus basalis magnocellularis. *Neuroscience* **36**:377-91.

Tan CM, Brady AE, Nickols HH, Wang Q and Limbird LE (2004) Membrane trafficking of G protein-coupled receptors. *Annu Rev Pharmacol Toxicol* **44**:559-609.

Tanaka K, Masu M and Nakanishi S (1990) Structure and functional expression of the cloned rat neurotensin receptor. *Neuron* **4**:847-54.

Terrillon S, Durroux T, Mouillac B, Breit A, Ayoub MA, Taulan M, Jockers R, Barberis C and Bouvier M (2003) Oxytocin and vasopressin V1a and V2 receptors form constitutive homo- and heterodimers during biosynthesis. *Mol Endocrinol* **17**:677-91.

Terrillon S and Bouvier M (2004) Roles of G-protein-coupled receptor dimerization. *EMBO Rep* **5**:30-4.

Thomas RF, Holt BD, Schwinn DA and Liggett SB (1992) Long-term agonist exposure induces upregulation of beta 3-adrenergic receptor expression via multiple cAMP response elements. *Proc Natl Acad Sci U S A* **89**:4490-4.

Tischler AS, Ruzicka LA and Dobner PR (1991) A protein kinase inhibitor, staurosporine, mimics nerve growth factor induction of neurotensin/neuromedin N gene expression. *J Biol Chem* **266**:1141-6.

Torup L, Borsdal J and Sager T (2003) Neuroprotective effect of the neurotensin analogue JMV-449 in a mouse model of permanent middle cerebral ischaemia. *Neurosci Lett* **351**:173-6.

Townsend CM, Jr., Bold RJ and Ishizuka J (1994) Gastrointestinal hormones and cell proliferation. *Surg Today* **24**:772-7.

Toy-Miou-Leong M, Cortes CL, Beaudet A, Rostène W and Forgez P (2004a) Receptor trafficking via the perinuclear recycling compartment accompanied by cell division is necessary for permanent neurotensin cell sensitization and leads to chronic mitogen-activated protein kinase activation. *J Biol Chem* **279**:12636-46.

Toy-Miou-Leong M, Bachelet CM, Pélaprat D, Rostène W and Forgez P (2004b) NT agonist regulates expression of nuclear high-affinity neurotensin receptors. *J Histochem Cytochem* **52**:335-45.

Tsao P and von Zastrow M (2000) Downregulation of G protein-coupled receptors. *Curr Opin Neurobiol* **10**:365-9.

Turner JT, James-Kracke MR and Camden JM (1990) Regulation of the neurotensin receptor and intracellular calcium mobilization in HT29 cells. *J Pharmacol Exp Ther* **253**:1049-56.

Tycko B, Keith CH and Maxfield FR (1983) Rapid acidification of endocytic vesicles containing asialoglycoprotein in cells of a human hepatoma line. *J Cell Biol* **97**:1762-76.

Tyler BM, Cusack B, Douglas CL, Souder T and Richelson E (1998a) Evidence for additional neurotensin receptor subtypes: neurotensin analogs that distinguish between neurotensin-mediated hypothermia and antinociception. *Brain Res* **792**:246-52.

Tyler BM, Groshan K, Cusack B and Richelson E (1998b) In vivo studies with low doses of levocabastine and diphenhydramine, but not pyrilamine, antagonize neurotensin-mediated antinociception. *Brain Res* **787**:78-84.

Tyler BM, McCormick DJ, Hoshall CV, Douglas CL, Jansen K, Lacy BW, Cusack B and Richelson E (1998c) Specific gene blockade shows that peptide nucleic acids readily enter neuronal cells in vivo. *FEBS Lett* **421**:280-4.

Tyler BM, Jansen K, McCormick DJ, Douglas CL, Boules M, Stewart JA, Zhao L, Lacy B, Cusack B, Fauq A and Richelson E (1999) Peptide nucleic acids targeted to the neurotensin receptor and administered i.p. cross the blood-brain barrier and specifically reduce gene expression. *Proc Natl Acad Sci U S A* **96**:7053-8.

Tyler-McMahon BM, Boules M and Richelson E (2000) Neurotensin: peptide for the next millennium. *Regul Pept* **93**:125-36.

Uberti MA, Hall RA and Minneman KP (2003) Subtype-specific dimerization of alpha 1-adrenoceptors: effects on receptor expression and pharmacological properties. *Mol Pharmacol* **64**:1379-90.

Uhl GR and Snyder SH (1976) Regional and subcellular distributions of brain neurotensin. *Life Sci* **19**:1827-32.

Uhl GR (1982) Distribution of neurotensin and its receptor in the central nervous system. *Ann N Y Acad Sci* **400**:132-49.

Urban MO and Smith DJ (1993) Role of neurotensin in the nucleus raphe magnus in opioid-induced antinociception from the periaqueductal gray. *J Pharmacol Exp Ther* **265**:580-6.

Urban MO, Jiang MC and Gebhart GF (1996a) Participation of central descending nociceptive facilitatory systems in secondary hyperalgesia produced by mustard oil. *Brain Res* **737**:83-91.

Urban MO, Smith DJ and Gebhart GF (1996b) Involvement of spinal cholecystokininB receptors in mediating neurotensin hyperalgesia from the medullary nucleus raphe magnus in the rat. *J Pharmacol Exp Ther* **278**:90-6.

Urban MO, Coutinho SV and Gebhart GF (1999) Biphasic modulation of visceral nociception by neurotensin in rat rostral ventromedial medulla. *J Pharmacol Exp Ther* **290**:207-13.

Vandenbulcke F, Nouel D, Vincent JP, Mazella J and Beaudet A (2000) Ligand-induced internalization of neurotensin in transfected COS-7 cells: differential intracellular trafficking of ligand and receptor. *J Cell Sci* **113 (Pt 17)**:2963-75.

Vanetti M, Kouba M, Wang X, Vogt G and Hollt V (1992) Cloning and expression of a novel mouse somatostatin receptor (SSTR2B). *FEBS Lett* **311**:290-4.

Vanisberg MA, Maloteaux JM, Octave JN and Laduron PM (1991) Rapid agonist-induced decrease of neurotensin receptors from the cell surface in rat cultured neurons. *Biochem Pharmacol* **42**:2265-74.

Vaughn AW, Baumeister AA, Hawkins MF and Anticich TG (1990) Intranigral microinjection of neurotensin suppresses feeding in food deprived rats. *Neuropharmacology* **29**:957-60.

Venter JC, Adams MD, Myers EW, Li PW, Mural RJ, Sutton GG, Smith HO, Yandell M, Evans CA, Holt RA, Gocayne JD, Amanatides P, Ballew RM, Huson DH, Wortman JR, Zhang Q, Kodira CD, Zheng XH, Chen L, Skupski M, Subramanian G, Thomas PD, Zhang J, Gabor Miklos GL, Nelson C, Broder S, Clark AG, Nadeau J, McKusick VA, Zinder N, Levine AJ, Roberts RJ, Simon M, Slayman C, Hunkapiller M, Bolanos R, Delcher A, Dew I, Fasulo D, Flanigan M, Florea L, Halpern A, Hannenhalli S, Kravitz S, Levy S, Mobarry C, Reinert K, Remington K, Abu-Threideh J, Beasley E, Biddick K, Bonazzi V, Brandon R, Cargill M, Chandramouliswaran I, Charlab R, Chaturvedi K, Deng Z, Di Francesco V, Dunn P, Eilbeck K, Evangelista C, Gabrielian AE, Gan W, Ge W, Gong F, Gu Z, Guan P, Heiman TJ, Higgins ME, Ji RR, Ke Z, Ketchum KA, Lai Z, Lei Y, Li Z, Li J, Liang Y, Lin X, Lu F, Merkulov GV, Milshina N, Moore HM, Naik AK, Narayan VA, Neelam B, Nusskern D, Rusch DB, Salzberg S, Shao W, Shue B, Sun J, Wang Z, Wang A, Wang X, Wang J, Wei M, Wides R, Xiao C, Yan C, Yao A, Ye J, Zhan M, Zhang W, Zhang H, Zhao Q, Zheng L, Zhong F, Zhong W, Zhu S, Zhao S, Gilbert D, Baumhueter S, Spier G, Carter C, Cravchik A, Woodage T, Ali F, An H, Awe A, Baldwin D, Baden H, Barnstead M, Barrow I, Beeson K, Busam D, Carver A, Center A, Cheng ML, Curry L, Danaher S, Davenport L, Desilets R, Dietz S, Dodson K, Doup L, Ferriera S, Garg N, Gluecksmann A, Hart B, Haynes J, Haynes C, Heiner C, Hladun S, Hostin D, Houck J, Howland T, Ibegwam C, Johnson J, Kalush F, Kline L, Koduru S, Love A, Mann F, May D, McCawley S, McIntosh T, McMullen I, Moy M, Moy L, Murphy B, Nelson K, Pfannkoch C, Pratts E, Puri V, Qureshi H, Reardon M, Rodriguez R, Rogers YH, Romblad D, Ruhfel B, Scott R, Sitter C, Smallwood M, Stewart E, Strong R, Suh E, Thomas R, Tint NN, Tse S, Vech C, Wang G, Wetter J, Williams S, Williams M, Windsor S, Winn-Deen E, Wolfe K, Zaveri J, Zaveri K, Abril JF, Guigo R, Campbell MJ, Sjolander KV, Karlak B,

Kejariwal A, Mi H, Lazareva B, Hatton T, Narechania A, Diemer K, Muruganujan A, Guo N, Sato S, Bafna V, Istrail S, Lippert R, Schwartz R, Walenz B, Yooseph S, Allen D, Basu A, Baxendale J, Blick L, Caminha M, Carnes-Stine J, Caulk P, Chiang YH, Coyne M, Dahlke C, Mays A, Dombroski M, Donnelly M, Ely D, Esparham S, Fosler C, Gire H, Glanowski S, Glasser K, Glodek A, Gorokhov M, Graham K, Gropman B, Harris M, Heil J, Henderson S, Hoover J, Jennings D, Jordan C, Jordan J, Kasha J, Kagan L, Kraft C, Levitsky A, Lewis M, Liu X, Lopez J, Ma D, Majoros W, McDaniel J, Murphy S, Newman M, Nguyen T, Nguyen N, Nodell M, Pan S, Peck J, Peterson M, Rowe W, Sanders R, Scott J, Simpson M, Smith T, Sprague A, Stockwell T, Turner R, Venter E, Wang M, Wen M, Wu D, Wu M, Xia A, Zandieh A and Zhu X (2001) The sequence of the human genome. *Science* **291**:1304-51.

Villeneuve P, Lafortune L, Seidah NG, Kitabgi P and Beaudet A (2000a) Immunohistochemical evidence for the involvement of protein convertases 5A and 2 in the processing of pro-neurotensin in rat brain. *J Comp Neurol* **424**:461-75.

Villeneuve P, Seidah NG and Beaudet A (2000b) Immunohistochemical evidence for the implication of PC1 in the processing of proneurotensin in rat brain. *Neuroreport* **11**:3443-7.

Vincent B, Beaudet A, Dauch P, Vincent JP and Checler F (1996) Distinct properties of neuronal and astrocytic endopeptidase 3.4.24.16: a study on differentiation, subcellular distribution, and secretion processes. *J Neurosci* **16**:5049-59.

Vincent JP (1995) Neurotensin receptors: binding properties, transduction pathways, and structure. *Cell Mol Neurobiol* **15**:501-12.

Vincent JP, Mazella J and Kitabgi P (1999) Neurotensin and neurotensin receptors. *Trends Pharmacol Sci* **20**:302-9.

Vita N, Laurent P, Lefort S, Chalon P, Dumont X, Kaghad M, Gully D, Le Fur G, Ferrara P and Caput D (1993) Cloning and expression of a complementary DNA encoding a high affinity human neurotensin receptor. *FEBS Lett* **317**:139-42.

Vita N, Oury-Donat F, Chalon P, Guillemot M, Kaghad M, Bachy A, Thurneyssen O, Garcia S, Poinot-Chazel C, Casellas P, Keane P, Le Fur G, Maffrand JP, Soubrie P, Caput D and Ferrara P (1998) Neurotensin is an antagonist of the human neurotensin NT2 receptor expressed in Chinese hamster ovary cells. *Eur J Pharmacol* **360**:265-72.

Walker N, Lépée-Lorgeoux I, Fournier J, Bétancur C, Rostène W, Ferrara P and Caput D (1998) Tissue distribution and cellular localization of the levocabastine-sensitive neurotensin receptor mRNA in adult rat brain. *Brain Res Mol Brain Res* **57**:193-200.

Watson MA, Yamada M, Cusack B, Veverka K, Bolden-Watson C and Richelson E (1992) The rat neurotensin receptor expressed in Chinese hamster ovary cells mediates the release of inositol phosphates. *J Neurochem* **59**:1967-70.

Wente W, Stroh T, Beaudet A, Richter D and Kreienkamp HJ (2005) Interactions with PDZ domain proteins PIST/GOPC and PDZK1 regulate intracellular sorting of the somatostatin receptor subtype 5. *J Biol Chem* **280**:32419-25.

White JH, Wise A, Main MJ, Green A, Fraser NJ, Disney GH, Barnes AA, Emson P, Foord SM and Marshall FH (1998) Heterodimerization is required for the formation of a functional GABA(B) receptor. *Nature* **396**:679-82.

Wilding JP, Gilbey SG, Bailey CJ, Batt RA, Williams G, Ghatei MA and Bloom SR (1993) Increased neuropeptide-Y messenger ribonucleic acid (mRNA) and decreased neurotensin mRNA in the hypothalamus of the obese (ob/ob) mouse. *Endocrinology* **132**:1939-44.

Wilding JP (2002) Neuropeptides and appetite control. *Diabet Med* **19**:619-27.

Williamson PT, Bains S, Chung C, Cooke R and Watts A (2002) Probing the environment of neurotensin whilst bound to the neurotensin receptor by solid state NMR. *FEBS Lett* **518**:111-5.

Wilson S, Wilkinson G and Milligan G (2005) The CXCR1 and CXCR2 receptors form constitutive homo- and heterodimers selectively and with equal apparent affinities. *J Biol Chem* **280**:28663-74.

Winsky-Sommerer R, Benjannet S, Rovère C, Barbero P, Seidah NG, Epelbaum J and Dournaud P (2000) Regional and cellular localization of the neuroendocrine prohormone convertases PC1 and PC2 in the rat central nervous system. *J Comp Neurol* **424**:439-60.

Woulfe J and Beaudet A (1989) Immunocytochemical evidence for direct connections between neurotensin-containing axons and dopaminergic neurons in the rat ventral midbrain tegmentum. *Brain Res* **479**:402-6.

Woulfe J and Beaudet A (1992) Neurotensin terminals form synapses primarily with neurons lacking detectable tyrosine hydroxylase immunoreactivity in the rat substantia nigra and ventral tegmental area. *J Comp Neurol* **321**:163-76.

Woulfe J, Lafortune L, de Nadai F, Kitabgi P and Beaudet A (1994) Post-translational processing of the neurotensin/neuromedin N precursor in the central nervous system of the rat--II. Immunohistochemical localization of maturation products. *Neuroscience* **60**:167-81.

Yaksh TL, Schmauss C, Micevych PE, Abay EO and Go VL (1982) Pharmacological studies on the application, disposition, and release of neurotensin in the spinal cord. *Ann N Y Acad Sci* **400**:228-43.

Yamada M and Richelson E (1993a) Further characterization of neurotensin receptor desensitization and down-regulation in clone N1E-115 neuroblastoma cells. *Biochem Pharmacol* **45**:2149-54.

Yamada M and Richelson E (1993b) Role of signal transduction systems in neurotensin receptor down-regulation induced by agonist in murine neuroblastoma clone N1E-115 cells. *J Pharmacol Exp Ther* **267**:128-33.

Yamada M, Watson MA and Richelson E (1993) Neurotensin stimulates cyclic AMP formation in CHO-rNTR-10 cells expressing the cloned rat neurotensin receptor. *Eur J Pharmacol* **244**:99-101.

Yamada M, Watson MA and Richelson E (1994) Deletion mutation in the putative third intracellular loop of the rat neurotensin receptor abolishes polyphosphoinositide hydrolysis but not cyclic AMP formation in CHO-K1 cells. *Mol Pharmacol* **46**:470-6.

Yamada M, Cho T, Coleman NJ and Richelson E (1995) Regulation of daily rhythm of body temperature by neurotensin receptor in rats. *Res Commun Mol Pathol Pharmacol* **87**:323-32.

Yamada M, Lombet A, Forgez P and Rostène W (1998) Distinct functional characteristics of levocabastine sensitive rat neurotensin NT2 receptor expressed in Chinese hamster ovary cells. *Life Sci* **62**:PL 375-80.

Yamauchi R, Sonoda S, Jinsmaa Y and Yoshikawa M (2003a) Antinociception induced by beta-lactotensin, a neurotensin agonist peptide derived from beta-lactoglobulin, is mediated by NT2 and D1 receptors. *Life Sci* **73**:1917-23.

Yamauchi R, Usui H, Yunden J, Takenaka Y, Tani F and Yoshikawa M (2003b) Characterization of beta-lactotensin, a bioactive peptide derived from bovine beta-lactoglobulin, as a neurotensin agonist. *Biosci Biotechnol Biochem* **67**:940-3.

Yamazaki H, Bujo H, Kusunoki J, Seimiya K, Kanaki T, Morisaki N, Schneider WJ and Saito Y (1996) Elements of neural adhesion molecules and a yeast vacuolar protein sorting receptor are present in a novel mammalian low density lipoprotein receptor family member. *J Biol Chem* **271**:24761-8.

Yamin M, Gorn AH, Flannery MR, Jenkins NA, Gilbert DJ, Copeland NG, Tapp DR, Krane SM and Goldring SR (1994) Cloning and characterization of a mouse brain calcitonin receptor complementary deoxyribonucleic acid and mapping of the calcitonin receptor gene. *Endocrinology* **135**:2635-43.

Young WS, 3rd and Kuhar MJ (1981) Neurotensin receptor localization by light microscopic autoradiography in rat brain. *Brain Res* **206**:273-85.

Zahm DS and Heimer L (1988) Ventral striatopallidal parts of the basal ganglia in the rat: I. Neurochemical compartmentation as reflected by the distributions of neurotensin and substance P immunoreactivity. *J Comp Neurol* **272**:516-35.

Zhang LJ, Lachowicz JE and Sibley DR (1994) The D2S and D2L dopamine receptor isoforms are differentially regulated in Chinese hamster ovary cells. *Mol Pharmacol* **45**:878-89.

Zhang YF, Jeffery S, Burchill SA, Berry PA, Kaski JC and Carter ND (1998) Truncated human endothelin receptor A produced by alternative splicing and its expression in melanoma. *Br J Cancer* **78**:1141-6.

Zhang Z, Sun S, Quinn SJ, Brown EM and Bai M (2001) The extracellular calcium-sensing receptor dimerizes through multiple types of intermolecular interactions. *J Biol Chem* **276**:5316-22.

Zhu X and Wess J (1998) Truncated V2 vasopressin receptors as negative regulators of wild-type V2 receptor function. *Biochemistry* **37**:15773-84.

Zsürger N, Chabry J, Coquerel A and Vincent JP (1992) Ontogenesis and binding properties of high-affinity neurotensin receptors in human brain. *Brain Res* **586**:303-10.

Zsürger N, Mazella J and Vincent JP (1994) Solubilization and purification of a high affinity neurotensin receptor from newborn human brain. *Brain Res* **639**:245-52.

APPENDIX A

THE JOURNAL OF COMPARATIVE NEUROLOGY 461:520–538 (2003)

Immunohistochemical Distribution of NTS2 Neurotensin Receptors in the Rat Central Nervous System

PHILIPPE SARRET,[†] AMÉLIE PERRON,[†] THOMAS STROH, AND ALAIN BEAUDET[*]
Department of Neurology and Neurosurgery, Montreal Neurological Institute, McGill University, Montreal, Quebec H3A 2B4, Canada

ABSTRACT

In the present study, we localized the levocabastine-sensitive neurotensin receptor (NTS2) protein in adult rat brain by using an N-terminally-directed antibody. NTS2-like immunoreactivity was broadly distributed throughout the rat brain. At the cellular level, the reaction product was exclusively associated with neurons and predominantly, although not exclusively, with their dendritic arbors. No NTS2 signal was observed over astrocytes, as confirmed by dual confocal microscopic immunofluorescence studies using the astrocytic marker S100β. High densities of NTS2-like immunoreactive nerve cell bodies and/or processes were detected in many regions documented to receive a dense neurotensinergic innervation, such as the olfactory bulb, bed nucleus of the stria terminalis, magnocellular preoptic nucleus, amygdaloid complex, anterodorsal thalamic nucleus, substantia nigra, ventral tegmental area, and several brainstem nuclei. Most conspicuous among the latter were structures implicated in the descending control of nociceptive inputs (e.g., the periaqueductal gray, dorsal raphe, gigantocellular reticular nucleus, pars alpha, lateral paragigantocellular, and raphe magnus), in keeping with the postulated role of NTS2 receptors in the mediation of neurotensin's supraspinal antinociceptive actions. However, the distribution of NTS2-like immunoreactivity largely exceeded that of neurotensin terminal fields, and some of the highest concentrations of the receptor were found in areas devoid of neurotensinergic inputs such as the cerebral cortex, the hippocampus, and the cerebellum, suggesting that neurotensin may not be the exclusive endogenous ligand for this receptor subtype. J. Comp. Neurol. 461:520–538, 2003.

Indexing terms: light microscopy; neuropeptide; protein; receptor localization; brain

The tridecapeptide neurotensin (NT), originally isolated from bovine hypothalamus (Carraway and Leeman, 1973), was subsequently localized throughout the central nervous system (CNS) of several mammalian species (for review, see Uhl, 1982; Emson et al., 1985) and shown to be involved in a variety of central functions, including thermoregulation, nociception, food consumption, regulation of dopaminergic and cholinergic neurotransmission, and neuroendocrine control (for reviews, see Kitabgi et al., 1985; Kitabgi and Nemeroff, 1992; Rostène and Alexander, 1997; Sarret and Beaudet, 2002).

Neurotensin effects are exerted through a variety of receptor subtypes, two of which have been distinguished pharmacologically on the basis of their affinities for NT and sensitivity to the histamine antagonist levocabastine: an NT high-affinity site, which does not bind levocabastine (NTS1; Kd = 0.3 nM) and a NT low-affinity site, which recognizes levocabastine (NTS2; Kd = 2–4 nM; Mazella et al., 1983; Schotte et al., 1986; Kitabgi et al., 1987). These two receptors have been molecularly identified in recent years and shown to belong to the seven transmembrane domain G-protein–coupled receptor family (GPCR, for review, see Hermans and Maloteaux, 1998;

Grant sponsor: Canadian Institutes of Health; Grant number: MT-7366 (A.B.); Grant sponsor: Fonds de la Recherche en Santé du Québec (FRSQ) (P.S.).

[†]Drs. Sarret and Perron contributed equally to this work.

[*]Correspondence to: Alain Beaudet, Department of Neurology and Neurosurgery, Montreal Neurological Institute, 3801 University Street, Montreal, Quebec H3A 2B4, Canada. E-mail: alain.beaudet@mcgill.ca

Received 6 December 2002; Revised 11 February 2003; Accepted 13 March 2003

DOI 10.1002/cne.10718

Published online the week of May 19, 2003 in Wiley InterScience (www.interscience.wiley.com).

Vincent et al., 1999; Sarret and Beaudet, 2002). A third NT receptor (NTS3) was recently cloned from human brain (Mazella et al., 1998). This receptor is a type I amino-acid receptor with a single transmembrane-spanning region corresponding to the previously cloned gp95/sortilin (Petersen et al., 1997).

Autoradiographic ligand binding, in situ hybridization, and immunohistochemical studies have yielded abundant information on the distribution of the NTS1 receptors in mammalian brain. In brief, high concentrations of NTS1 were found in association with selective neuronal populations throughout the hypothalamus, basal forebrain, and limbic system (Sarrieau et al., 1985; Schotte et al., 1986; Moyse et al., 1987; Kitabgi et al., 1987; Palacios et al., 1988; Dana et al., 1989; Elde et al., 1990; Sato et al., 1992; Nicot et al., 1994a,b, 1995; Boudin et al., 1996; Alexander and Leeman, 1998; Fassio et al., 2000). They were markedly enriched over dopaminergic neurons of the ventral midbrain (Palacios and Kuhar, 1981; Quirion et al., 1985; Hervé et al., 1986; Szigethy and Beaudet, 1989, Schotte and Leysen, 1989; Goulet et al., 1999), cholinergic neurons of the basal forebrain (Szigethy and Beaudet, 1987; Szigethy et al., 1988; Faure et al., 1995; Cape et al., 2000), and VIPergic neurons of the suprachiasmatic nucleus of the

Abbreviations

V	layer V of the cerebral cortex
3V	3rd ventricle
4V	4th ventricle
3n	oculomotor nucleus
6n	abducens nucleus
7n	facial nucleus
12n	hypoglossal nucleus
Acb	accumbens nucleus
AD	anterodorsal thalamic nucleus
AHC	anterior hypothalamic area, central part
AOB	accessory olfactory bulb
AON	anterior olfactory nucleus
Aq	aqueduct (Sylvius)
Arc	arcuate hypothalamic nucleus
AV	anteroventral thalamic nucleus
CA1–3	fields CA1–3 of Ammon's horn
CLi	caudal linear nucleus of the raphe
cp	cerebral peduncle, ventral part
Cpu	caudate putamen (striatum)
Cu	cuneate nucleus
DC	dorsal cochlear nucleus
DG	dentate gyrus
DLG	dorsal lateral geniculate nucleus
DMSp5	dorsomedial spinal trigeminal nucleus
DR	dorsal raphe nucleus
ECu	external cuneate nucleus
Ent	entorhinal cortex
Epl	external plexiform layer of the olfactory bulb
f	fornix
Fr1	frontal cortex, area 1
Gcl	granule cell layer of the cerebellum
Gi	gigantocellular reticular nucleus
GiA	gigantocellular reticular nucleus, alpha part
Gl	glomerular layer of the olfactory bulb
Gr	gracile nucleus
GrA	granular cell layer of the accessory olfactory bulb
ic	internal capsule
icp	inferior cerebellar peduncle (restiform body)
IGr	internal granular layer of the olfactory bulb
Int	interposed cerebellar nucleus
IO	inferior olive
IP	interpeduncular nucleus
Ipl	internal plexiform layer of the olfactory bulb
Lat	lateral (dentate) cerebellar nucleus
LHb	lateral habenular nucleus
Li	linear nucleus of the medulla
LM	lateral mamillary nucleus
LPGi	lateral paragigantocellular nucleus
LRt	lateral reticular nucleus
LSD	lateral septal nucleus, dorsal part
LSO	lateral superior olive
LSV	lateral septal nucleus, ventral part
LVe	lateral vestibular nucleus
m5	motor root of the trigeminal nerve
MD	mediodorsal thalamic nucleus
MdD	medullary reticular nucleus, dorsal part
MdV	medullary reticular nucleus, ventral part
ME	median eminence
Med	medial (fastigial) cerebellar nucleus
MG	medial geniculate nucleus
MHb	medial habenular nucleus
Mi	mitral cell layer of the olfactory bulb
ml	medial lemniscus
Ml	molecular layer of the cerebellum
MnR	median raphe nucleus
mol	lacunosum molecular stratum of Ammon's horn
MSO	medial superior olive
mt	mamillothalamic tract
MVe	medial vestibular nucleus
OB	olfactory bulb
or	stratum oriens of Ammon's horn
Pa	paraventricular hypothalamic nucleus
Pa5	paratrigeminal nucleus
PaS	parasubiculum
PAG	periaqueductal gray
Pcl	Purkinje cell layer of the cerebellum
Pe	periventricular hypothalamic nucleus
PF	parafascicular thalamic nucleus
PFL	paraflocculus
Pir	piriform cortex
PMCo	posteromedial cortical amygdaloid nucleus
PMR	paramedian raphe nucleus
PMV	premamillary nucleus, ventral part
Pn	pontine nuclei
Pr5	principal sensory trigeminal nucleus
PrS	presubiculum
PV	paraventricular thalamic nucleus
py	pyramidal tract
pyr	stratum pyramidale of Ammon's horn
pyx	pyramidal decussation
rad	stratum radiatum of Ammon's horn
RCh	retrochiasmatic area
RMg	raphe magnus nucleus
ROb	raphe obscurus nucleus
RPa	raphe pallidus nucleus
Rt	reticular thalamic nucleus
s5	sensory root of the trigeminal nerve
SC	superior colliculus
sm	stria medullaris of the thalamus
SNc	substantia nigra, pars compacta
SNr	substantia nigra, pars reticulata
Sol	nucleus of the solitary tract
Sp5C	spinal trigeminal nucleus, caudal part
Sp5I	spinal trigeminal nucleus, interpolar part
Sp5O	spinal trigeminal nucleus, oral part
SPO	superior paraolivary nucleus
SuM	supramamillary nucleus
SuVe	superior vestibular nucleus
TC	tuber cinereum area
Tu	olfactory tubercle
Tz	trapezoid nucleus
VCA	ventral cochlear nucleus, anterior part
VCP	ventral cochlear nucleus, posterior part
VDB	vertical limb of the diagonal band of Broca
VLG	ventral lateral geniculate nucleus
VMH	ventromedial hypothalamic nucleus
VTA	ventral tegmental area
X	nucleus X
ZI	zona incerta

hypothalamus (Francois-Bellan et al., 1992). This distribution is consistent with reported NTS1-mediated NT effects on locomotion and cognition, as well as on the sleep–wake cycle, memory, and regulation of hypothalamopituitary functions (Cape et al., 2000; for review, see Rostène and Alexander, 1997; Binder et al., 2001; Sarret and Beaudet, 2002).

Much less is known concerning the distribution, particularly at the cellular level, of the levocabastine-sensitive NTS2 receptors. Early autoradiographic binding studies, based on the displacement of specific ^{125}I-labeled NT, [^{3}H]NT, or [^{3}H]SR142948A binding by levocabastine, reported a widespread distribution of levocabastine-sensitive NTS2 receptor sites in adult rat brain (Schotte et al., 1986, 1988; Kitabgi et al., 1987; Schotte and Laduron, 1987; Betancur et al., 1998). This widespread distribution of NTS2 binding sites was confirmed recently by using direct autoradiographic localization of [^{3}H]levocabastine (Asselin et al., 2001). Based on their ubiquitous distribution, as well as on their pattern of ontogenetic development (Schotte and Laduron, 1987) and recovery after local destruction of neurons with kainic acid (Schotte et al., 1988), low-affinity NT binding sites were originally surmised to be mainly associated with glial cells. Accordingly, NTS2 binding and/or mRNA were detected in association with astrocytes both in vivo and in vitro (Nouel et al., 1997; Walker et al., 1998; Lépée-Lorgeoux et al., 1999) and NTS2 expression was found to be markedly up-regulated in reactive astrocytes surrounding a cortical stab wound (Nouel et al., 1999). However, in situ hybridization studies also demonstrated that, in homeostatic conditions, NTS2 was predominantly expressed by neurons within the CNS (Sarret et al., 1998). Further evidence for the expression of functional NTS2 receptors in neurons was provided recently by studies in rat cerebellar granule cells in culture, which demonstrated cell surface NTS2 binding, ligand-induced receptor internalization, and NT-induced MAP kinase activation in these cells (Sarret et al., 2002).

The contribution of NTS2 to the mediation of central NT functions is not as clearly established as that of NTS1. Nonetheless, pharmacologic data based on the use of selective NTS2 agonists (Labbé-Jullié et al., 1994) and antisense oligonucleotides (Dubuc et al., 1999a) have suggested that NTS2 may play a role in the mediation of NT antinociceptive effects. Further insight into the functional role of NTS2 requires precise knowledge of the distribution of this receptor at both regional and cellular levels. To this aim, we have investigated here the localization of NTS2 receptor proteins in rat brain by immunohistochemistry, using an antibody raised against the N-terminal segment of the cloned rat NTS2 receptor.

MATERIALS AND METHODS

All animal-related procedures were approved by the McGill University Animal Care Committee and carried out according to the regulations of the Canadian Council on animal care.

Primary antibody for NTS2 immunodetection

Rabbit anti-NTS2 peptide antiserum was generated by using a synthetic peptide (WPPRPSPSAGLSLEA), corresponding to the 7-21 predicted amino acid sequence in the N-terminal segment of the rat receptor (Chalon et al., 1996) and showing no homology with other known neurotensin receptor subtypes. The peptide was conjugated by means of maleimide to ovalbumin. The conjugate was used to immunize two rabbits (Affinity BioReagents, ABR, Golden, CO). The initial immunization was followed by five additional booster injections. Serum samples were analyzed separately for reactivity by Western blotting and immunohistochemistry. One of the sera proved more sensitive than the other for immunohistochemistry and, therefore, was used throughout the present study.

Preparation of rat NTS2 construct

The HA-tagged NTS2 cDNA was obtained through reverse transcription of rat brain mRNA isolated by polymerase chain reaction (PCR) by using nucleotide sequences 35-61 bp (5′-ACAGAGATGGCATACCCATACGACGTCCCAGACTACGCTGAGACCAGCAGTCCGTGG-3′) and 1268-1291 bp (5′-TCATACTTGTATTTCTCCCAGGCT-3′) of the open reading frame of NTS2 mRNA (Chalon et al., 1996) as sense and antisense oligonucleotides, respectively. The PCR product was purified from a 1% low melting temperature agarose gel and subcloned into the pTARGET expression vector (Promega, Madison, WI). That the proper rat NTS2 sequence had been cloned was confirmed by base pair sequencing.

Culture and transfection of COS-7 cells

COS-7 cells were maintained in Dulbecco's modified Eagle's medium with high glucose supplemented with 5% fetal bovine serum in the presence of 100 U/ml penicillin/streptomycin (GibcoBRL, Life Technologies, Burlington, Ontario, Canada). Cells were grown at 37°C in a humidified atmosphere with 5% CO_2 and plated in 100-mm Petri dishes at a density of 10^6 cells/dish. On the following day, semiconfluent cells were transiently transfected with the rat HA-tagged NTS2 receptor cDNA by the diethylaminoethanol–dextran/chloroquine method, as described previously (Innamorati et al., 2001). Cells were collected 48–72 hours after the beginning of the transfection and processed for immunoprecipitation or immunocytochemistry as described below.

Preparation of brain membranes

Adult Sprague-Dawley rats (200–250 g; Charles River, St-Constant, Quebec, Canada) were killed by decapitation. Their brains were removed quickly and placed on ice. Cerebellum and brain were dissected, homogenized separately with a Polytron in buffer A containing 50 mM Tris-HCl (pH 7.0) and 4 mM ethylenediaminetetraacetic acid (EDTA) with protease inhibitors (Complete Protease Inhibitors tablets, Roche Molecular Biochemicals, Laval, Quebec, Canada), and centrifuged at 1,000 rpm for 10 minutes at 4°C. The supernatant was collected, and the pellet resuspended in buffer A and centrifuged again for 10 minutes at 4°C. The supernatant from the second spin was combined with that of the first for each sample and centrifuged at 4°C for 10 minutes at 46,000 rpm. The pellets were then resuspended in buffer B, consisting of 50 mM Tris-HCl (pH 7.0) and 0.2 mM EDTA with protease inhibitors, by vortexing and brief sonication. Protein concentration was determined by the Bio-Rad procedure with bovine serum albumin (BSA) as standard (Bradford, 1976).

Immunoblotting analysis

Membranes from rat brain and cerebellum were denatured by using Laemmli sample buffer (Laemmli, 1970), resolved by using 8% Tris-glycine precast gels (Invitrogen, Burlington, Ontario, Canada), and transferred to nitrocellulose membranes (Bio-Rad Laboratories, Mississauga, Ontario, Canada). Nonspecific sites were blocked by 0.1% Tween 20 and 10% milk powder (Carnation, Don Mills, Ontario, Canada in phosphate-buffered saline [PBS; pH 7.4]) overnight at 4°C. Nitrocellulose membranes were then incubated overnight at 4°C with the N-terminal specific anti-NTS2 rabbit antibody (1/10,000) in PBS with 1% BSA and 1% ovalbumin. After washing with PBS-Tween, blots were incubated for 1 hour at room temperature (RT) with an horseradish peroxidase (HRP) -conjugated goat anti-rabbit secondary antibody (1/4,000; Amersham Pharmacia Biotech, Baie d'Urfe, Quebec, Canada) in PBS with 5% milk powder and proteins were visualized by using an enhanced chemiluminescent detection system (Perkin Elmer, Life Sciences, Boston, MA). Specificity of antiserum was confirmed by preadsorption of the NTS2 antibody overnight with an excess of immunizing peptide (2 μg/ml of adsorbing peptide at a final antibody dilution of 1/10,000).

Immunoprecipitation

COS-7 cells were rinsed with PBS 72 hours after transfection, detached from the dishes, and centrifuged. The cell pellet was disrupted in RIPA buffer (150 mM NaCl, 50 mM Tris-HCl, pH 7.5, 5 mM EDTA, 1%, IGEPAL, 0.5% deoxycholic acid, 0.1% sodium dodecyl sulfate) containing protease inhibitors and incubated for 30 minutes on ice. Lysates were then precleared with 25 μg of protein A–Sepharose (Sigma, St. Louis, MO) for 45 minutes at 4°C and incubated overnight at 4°C with the NTS2 rabbit antibody (1/800) or with a rat monoclonal antibody (clone 3F10) directed toward the HA epitope (1/400; Roche Molecular Biochemicals, Indianapolis, IN). The protein A–Sepharose was gently shaken in lysis buffer containing 1% BSA for 30 minutes at room temperature before use. HA epitope-tagged NTS2 receptors were precipitated by incubation with 100 μg of protein A–Sepharose for 2 hours at 4°C. After washing three times in lysis buffer, complexes were dissolved in Laemmli sample buffer and resolved as described above. Nitrocellulose membranes were then incubated overnight at 4°C in PBS with a solution containing 1% BSA and 1% ovalbumin and a 1/2,500 dilution of a mouse monoclonal antibody (clone 12CA5) directed toward the HA epitope (samples precipitated with NTS2 antibody) or with a 1/10,000 dilution of the NTS2 antibody (samples precipitated with anti-HA antibody). After washing with PBS-Tween, blots were incubated for 1 hour at RT with HRP-conjugated goat anti-rabbit or anti-mouse secondary antibodies in PBS with 5% milk powder (1/4,000; Amersham Pharmacia Biotech, Baie d'Urfe, Quebec, Canada) and proteins were visualized using an enhanced chemiluminescent detection system.

Immunocytochemistry on COS-7 cells

Transfected COS-7 cells, plated on poly-L-lysine–coated glass coverslips, were fixed for 20 minutes with 4% paraformaldehyde (PFA; Polysciences, Warington, PA) in 0.1 M phosphate buffer (PB), pH 7.4, rinsed with 0.1 M Trisma base-buffered saline (TBS), pH 7.4, and preincubated for 30 minutes at RT with a blocking solution consisting of 5% normal goat serum (NGS), 2% BSA, and 0.1% Triton X-100 (BDH, Inc., Toronto, Ontario, Canada) in 0.1 M TBS. Double immunostaining was performed by incubating cells overnight at 4°C with the anti-NTS2 peptide antiserum (1/15,000) or with the anti-NTS2 peptide antiserum preadsorbed with the antigenic peptide, together with the mouse monoclonal antibody (clone 12CA5) directed toward the HA epitope, diluted 1/500 in 0.1 M TBS, pH 7.4, containing 1% NGS and 0.05% Triton X-100. After washing with TBS, cells were incubated for 1 hour at RT with a mixture of Alexa 488–conjugated goat anti-mouse and Alexa 594–conjugated goat anti-rabbit (1/750; Molecular Probes, Eugene, OR), washed twice in TBS and mounted on glass slides with Aquamount.

Double-labeled cells were analyzed by confocal microscopy by using a Zeiss 510 laser scanning microscope equipped with a Zeiss inverted microscope and Argon2 (488 nm) and He/Ne1 (543 nm) lasers (Carl Zeiss Micro Imaging, Inc., Thornwood, NY). Images were acquired simultaneously for both fluorophores (Alexa 488 and Alexa 594) by using the multitrack configuration mode and processed by using the Zeiss 510 laser scanning microscope software. Identical parameters were used to acquire the images for cells immunolabeled in the presence or absence of NTS2 blocking peptide.

Light microscopic immunolabeling of rat brain sections

Tissue fixation. Adult male Sprague-Dawley rats (200–250 g; n = 10) were anesthetized with sodium pentobarbital (Somnotol; 1.2 ml/kg) and perfused transaortically with a freshly prepared solution of 4% PFA in 0.1 M PB, pH 7.4. Brains were rapidly removed, cryoprotected overnight in 0.1 M PB containing 30% sucrose at 4°C, and frozen for 1 minute in isopentane at −40°C.

Single-labeling immunohistochemistry. Coronal sections (30 μm thick) were cut on a freezing microtome along the whole rostrocaudal extent of the brain from bregma 6.70 to −14.60 and collected in 0.1 M PB. Immunohistochemistry was performed according to the avidin biotinylated–HRP complex (ABC) method by using a Elite ABC kit (Vector Laboratories, Burlingame, CA). Briefly, free-floating sections were washed twice with 0.1 M TBS, pH 7.4, pretreated for 30 minutes with 3% hydrogen peroxide in 0.1 M TBS to quench endogenous peroxidase. Serial sections were then washed twice with TBS (2 × 10 minutes), preincubated for 1 hour at RT in a blocking solution containing 3% NGS and 0.2% Triton X-100 in TBS, and incubated overnight at 4°C with the primary NTS2 antibody (1/10,000) diluted in TBS containing 0.05% Triton X-100 and 0.5% NGS. After two rinses in TBS containing 1% NGS (2 × 10 minutes), sections were incubated for 1 hour at RT in biotinylated goat anti-rabbit immunoglobulin diluted 1/400 in TBS (Vector laboratories) and then 1 hour in Elite ABC solution (Vector; prepared according to the manufacturer's instructions). Visualization of bound peroxidase was achieved by reaction in a solution of 0.1 M Tris-HCl (TB; pH 7.4) containing 0.05% 3-3'-diaminobenzidine (DAB, Sigma-Aldrich), 0.04% nickel chloride, and 0.001% H_2O_2. The DAB reaction was monitored under a microscope to determine the optimal duration of incubation (5 minutes maximum) for yielding intense immunolabeling with minimal background stain-

ing. This reaction was stopped by several washes with 0.1 M TB.

The same procedure was used for control experiments except that sections were processed either with antibodies preabsorbed overnight with an excess of immunizing peptide (as for Western blotting procedures) or in the absence of primary antibody. Sections were mounted on chrome alum/gelatin-coated slides, dehydrated in graded ethanols, defatted in xylene, and mounted with Permount (Fisher Scientific, Montreal, Quebec, Canada). Labeled structures were examined under brightfield illumination with a Leitz Aristoplan miscroscope (Leica, Dollard Desormeaux, Quebec, Canada), and labeling densities were assessed for each region and visually scored on a scale of – /+ to +++, according to both the number of labeled elements and the intensity of immunoreactive signal.

Double-labeling immunohistochemistry. Frozen sections, prepared as above (n = 4 rats), were treated for 30 minutes in 3% NGS in TBS and incubated overnight at 4°C in a mixture of rabbit NTS2 antibody (1/10,000) and monoclonal mouse anti-S100 β-subunit (1/500; Sigma) diluted in TBS containing 0.05% Triton X-100 and 0.5% NGS. The following day, sections were rinsed twice in TBS containing 1% NGS and incubated for 1 hour in the same buffer containing a mixture of biotinylated goat anti-rabbit immunoglobulin (1/400; Vector) and Alexa 488–tagged goat anti-mouse (1/500; Molecular Probes). Sections were then rinsed in TBS, incubated for 1 hour in ABC complex solution, rinsed again in TBS, and incubated as above for 10 minutes in a biotinylated tyramine solution (Adams, 1992; NEN-Dupont, Wilmington, DE). After several buffer washes, sections were incubated for 1 hour in a solution of Texas-Red–conjugated streptavidin (1/250; Jackson, West Grove, PA). Sections were then rinsed and mounted with Aquamount. The absence of cross-reactivity of the secondary antibodies was verified by omitting one or both primary antibodies during the overnight incubation.

Double-labeled sections were analyzed by confocal microscopy by using a Zeiss 510 laser scanning microscope equipped with a Zeiss inverted microscope and Argon2 (488 nm) and He/Ne1 (543 nm) lasers. Images were acquired simultaneously for both fluorophores (Alexa-488 and Texas Red) by using the multitrack configuration mode and processed by using the Zeiss 510 laser scanning microscope software.

Data analysis

Light microscopic photomicrographs and color images from double-labeling experiments were adjusted for contrast and brightness by using Adobe Photoshop 6.0 software (Adobe, San Jose, CA). The final composites were processed by using Deneba's Canvas 7.0 imaging software (Deneba Software, Miami, FL) on an Apple PowerBook G3. Brain structures were identified according to the nomenclature of Paxinos and Watson's atlas (Paxinos and Watson, 1986).

RESULTS

Characterization of NTS2 antiserum

To demonstrate the specificity of the NTS2 antiserum, Western blotting was performed on membranes prepared from rat brain and cerebellum (Fig. 1A). In both structures, anti-NTS2 specifically detected a band at 46 kDa,

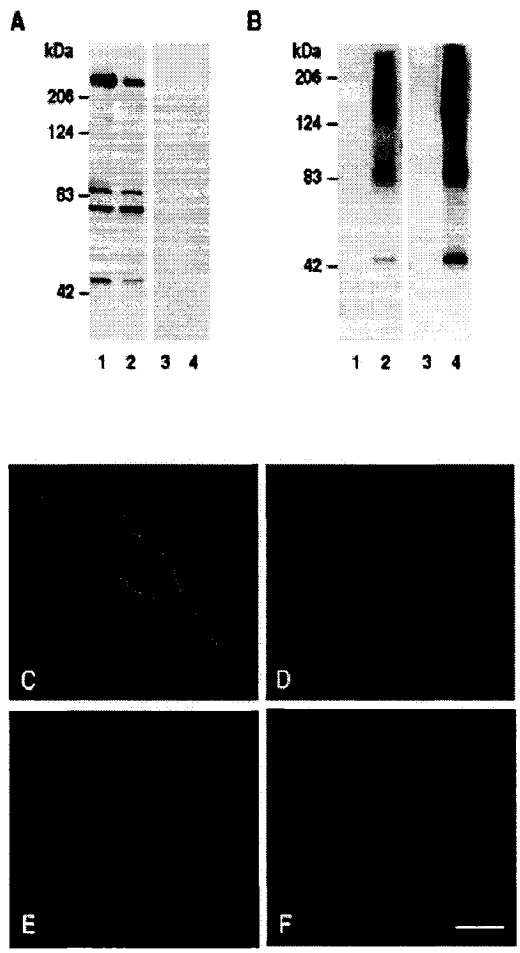

Fig. 1. Characterization of the levocabastine-sensitive neurotensin receptor (NTS2) antiserum. A,B: Identification by Western blotting of endogenously vs. heterologously expressed NTS2 receptors. **A:** Blot from whole brain (lanes 1, 3) and cerebellar (lanes 2, 4) membranes incubated with the NTS2 antiserum. As a control, the antiserum was preadsorbed with 2 μg/ml of antigenic peptide (lanes 3, 4). Specific immunoreactive bands are apparent at estimated molecular masses of 46, 80–85 and 124–206 kDa. Each lane represents the transfer of 60 μg of membrane protein. Data are representative of four independent experiments. **B:** Immunoprecipitation with NTS2 antiserum and blotting with anti-HA antibody (lane 2) or immunoprecipitation with anti-HA antibody and blotting with anti-NTS2 antiserum (lane 4) of homogenates from COS-7 cells expressing (lanes 2, 4) or not (lane 1, 3) HA-NTS2. Both approaches reveal translation products of approximately 46, 83, and 125–206 kDa in transfected but not in untransfected cells. Data are representative of three independent experiments. Migration of molecular weight markers is indicated on the left. C–F: Dual immunofluorescence labeling of COS-7 cells transfected with cDNA encoding *HA*-epitope–tagged NTS2 receptor. Labeling of the *HA* epitope (C) overlaps with staining produced by the NTS2 antiserum (D). Preadsorption of NTS2 antiserum with antigenic peptide completely abolishes NTS2-like immunostaining (F) in cells expressing the epitope-tagged receptor (E). Transnuclear confocal microscopic images representative of three separate experiments. Scale bar = 5 μm in F (applies to C–F).

consistent with the molecular weight of the monomeric form of the receptor as deduced from its cDNA sequence (Fig. 1A, lanes 1 and 2). Specific immunoreactive bands, which might reflect multimeric species of NTS2 receptors, were also detected at approximately 80–85 kDa and 124–206 kDa in both whole brain (Fig. 1A, lane 1) and cerebellar membranes (Fig. 1A, lane 2). All of these bands were absent when the antibody was presaturated with the immunizing peptide (Fig. 1A, lanes 3 and 4).

To confirm that these immunoreactive bands corresponded to the NTS2 receptor, crude membrane preparations from COS-7 cells expressing HA-tagged rat NTS2 receptors were immunoprecipitated with the NTS2 antiserum (Fig. 1B, lane 2) or with the 3F10 antibody specific for the HA-epitope tag (Fig. 1B, lane 4), and, respectively, immunoblotted with the 12CA5 HA antibody (Fig. 1B, lane 2) or with the NTS2 antiserum (Fig. 1B, lane 4). These experiments revealed the presence of 46- and 83-kDa protein bands, as observed in rat brain and cerebellum, in both immunoprecipitates (Fig. 1B, lanes 2 and 4). In addition, immunoreactive bands were detected at approximately 124–206 kDa in both preparations (Fig. 1B, lane 2 and 4), which presumably correspond to multimeric complexes of the receptor. No specific bands were detected in membranes prepared from nontransfected cells (Fig. 1B, lanes 1 and 3).

Specificity of immunolabeling

To demonstrate the applicability of the NTS2 antiserum to immunohistochemical detection of the receptor in PFA-fixed material, double immunofluorescent staining was carried out on COS-7 cells expressing the HA-tagged NTS2 receptor. Confocal microscopy revealed that HA (Fig. 1C) and NTS2 (Fig. 1D) antibodies produced very similar patterns of immunostaining. No signal was detected in untransfected cells or in the absence of primary antibodies (data not shown). Preincubation of the anti-NTS2 antiserum with the N-terminal immunogenic peptide completely abolished NTS2-like (NTS2-l) immunolabeling (Fig. 1F). However, the same cells were still positively stained for the HA epitope, indicating that they did express the receptor (Fig. 1E).

Immunolabeling of rat brain sections with a 1/10,000 dilution of NTS2 antiserum gave rise to selective immunostaining patterns throughout the neuraxis (e.g., Figs. 2A, 4–11). By contrast, sections incubated with antiserum preadsorbed with the immunogenic peptide were completely devoid of immunolabeling (Figs. 2B, 6C).

Cellular distribution of NTS2-l immunoreactivity

NTS2-l immunoreactivity was selectively concentrated over neurons and most prominently within neuronal processes (Table 1). Thus, in many regions such as the piriform cortex (Fig. 3A) and other cortical areas, NTS2-l immunolabeling was highly concentrated over pyramidal cell dendrites, whereas the vast majority of the corresponding perikarya were only moderately labeled. However, in other regions, such as the central amygdaloid nucleus (Fig. 3B), the bed nucleus of the stria terminalis (Fig. 3D, 5A), or CA1 of Ammon's horn (Fig. 6A,B), both perikarya and dendrites showed moderate to intense NTS2-l immunolabeling. NTS2-l immunoreactivity was also detected in axons and axon terminals throughout the neuraxis, e.g., in the diagonal band of Broca (Fig. 3C) and

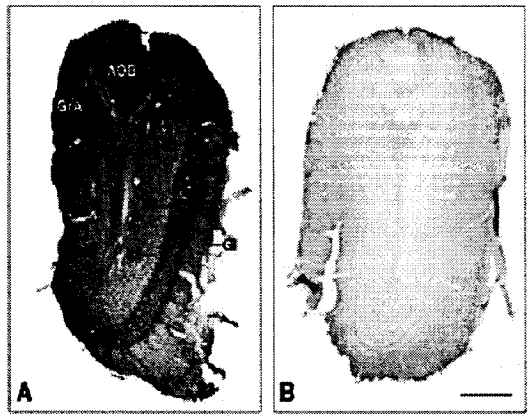

Fig. 2. Specificity of levocabastine-sensitive neurotensin receptor (NTS2)-like immunolabeling in rat brain sections. **A:** Section from the olfactory bulb, immunostained with anti-NTS2 serum diluted 1:10,000. All layers of the main olfactory bulb are strongly immunopositive. Most intensely stained are the external plexiform layer (Epl) and the accessory olfactory bulb (AOB). **B:** Section from the same region incubated with primary antiserum preadsorbed with 2 μg/ml of antigen at the same final dilution as in A. Note the complete suppression of the immunolabeling. For other abbreviations, see list. Scale bar = 0.6 mm in B (applies to A,B).

in the anterior hypothalamus (Fig. 3G). Labeling of the ependyma was observed in some of our sections (e.g., Figs. 5A, 8A,E), but this labeling was nonspecific, because it was still present in sections incubated with preadsorbed antiserum.

No obvious NTS2-l immunolabeling was evident over glial cells in our single-labeling experiments. To formally exclude astrocytic involvement, dual immunolabeling experiments were performed by using our NTS2 antiserum and the astrocytic marker S100β in regions exhibiting either prominent somatic (Fig. 3D–F) or process labeling (Fig. 3G–I). In the bed nucleus of the stria terminalis, strongly NTS2-l–positive perikarya as well as small fluorescent puncta resembling cross-sectioned processes were evident by confocal microscopy (Fig. 3D). None of these structures exhibited S100β immunolabeling within the same sections (Fig. 3E,F). In the anterior hypothalamus, NTS2-l immunoreactivity was localized to punctate structures reminiscent of transected dendrites and/or glial elements (Fig. 3G). Here again, none of these structures were dually labeled with the S100β antibody, which revealed several astrocytic cell bodies as well as the entire ependyma (Fig. 3H,I).

Regional distribution of NTS2-l immunoreactivity

Telencephalon. Within the telencephalon, strong and selective NTS2-l immunolabeling was apparent in the olfactory bulb and tubercle, the basal forebrain, the basal ganglia, the amygdaloid complex, the hippocampal formation, and the cerebral cortex (Table 1; for topographical overview, see Fig. 4).

In the main olfactory bulb, NTS2-l immunoreactivity was distributed throughout the granule cell, mitral cell,

TABLE 1. Regional Distribution of NTS2 Immunoreactivity in Adult Rat Brain[1]

Structure	NTS2 immunoreactivity: Cell bodies	NTS2 immunoreactivity: Processes and Terminals
Telencephalon		
Cerebral cortex		
Frontal	+/++	+/++
Parietal	++	+++
Cingulate	+	++
Occipital	+/++	+/++
Temporal	+/++	+++
Insular	+/++	++/+++
Perirhinal	+	+/++
Retrosplenial	++	++
Olfactory bulb		
Accessory olfactory bulb	–	+++
Internal granular layer	+	+
Mitral cell layer	++	–
External plexiform layer	–	++
Glomerular layer	–/+	+/++
Olfactory system		
Lateral olfactory nucleus	–/+	+/++
Piriform cortex	+	++/+++
Prepiriform cortex	+	++/+++
Anterior olfactory nucleus	–	++
Dorsal endopiriform nucleus	–	–/+
Ventral endopiriform nucleus	–	+/++
Taenia tecta	+	–/+
Olfactory tubercle	++	+/++
Islands of Calleja	+	+/++
Basal forebrain		
Septohippocampal nucleus	–	++
Lateral septum	+/++	++
Medial septum	–/+	+/++
Diagonal band of Broca		
Vertical limb	–/+	+/++
Horizontal limb	–/+	++
Magnocellular preoptic nucleus	+/++	+/++
Bed nucleus of the stria terminalis	++/+++	+/++
Ventral pallidum	–/+	++
Substantia innominata	–	++
Substriatal area	+	+/++
Basal ganglia		
Nucleus accumbens		
Core	–/+	–/+
Shell	–/+	+
Caudate putamen	+/++	–/+
Fundus striati	+	–/+
Globus pallidus	–	++/+++
Entopeduncular nucleus	–	++/+++
Amygdala		
Central nucleus	++	++
Basomedial nucleus	–	+
Medial nucleus	–/+	+/++
Cortical nucleus	++	++
Hippocampal formation		
Entorhinal cortex	++/+++	+/++
Presubiculum	++	–/+
Parasubiculum	++/+++	–/+
CA1	+++	+++
CA2	++	++
CA3	–	–/+
Dentate gyrus		
Granule cells	–	–
Hilus	–/+	+
Diencephalon		
Thalamus		
Anterior dorsal nucleus	–/+	++/+++
Anterior ventral nucleus	+	+
Paraventricular nucleus	+	++
Reuniens nucleus	–	+
Reticular thalamic nucleus	–	++/+++
Central medial thalamic nucleus	–	+
Ventromedial thalamic nucleus	+	+
Mediodorsal thalamic nucleus	+/++	–/+
Rhomboid thalamic nucleus	–	+
Parafascicular nucleus	–	++
Subparafascicular nucleus	–	+/++
Medial geniculate nucleus	+	–
Ventral lateral geniculate nucleus	+	++
Dorsal lateral geniculate nucleus	+	–
Hypothalamus		
Anterior hypothalamus	–	+/++
Suprachiasmatic nucleus	–	++
Supraoptic nucleus	+	++
Paraventricular nucleus	–/+	+/++
Arcuate nucleus	+/++	++/+++
Retrochiasmatic area	++	++
Ventromedial nucleus	–/+	+/++
Dorsomedial nucleus	–	+
Periventricular nucleus	–	++
Lateral hypothalamic area	–/+	++
Tuber cinereum	–	+/++
Medial mammillary nucleus	–	++
Lateral mammillary nucleus	+	++
Supramammillary nucleus	–	++/+++
Lateral preoptic area	–	–/+
Medial preoptic area	–	++
Median eminence	–	++/+++
Subthalamus		
Zona incerta	–/+	++/+++
Subthalamic nucleus	–	+/++
Epithalamus		
Medial habenula nucleus	–/+	–/+
Lateral habenula nucleus	–/+	++
Subfornical organ	–	++
Mesencephalon		
Substantia nigra pars compacta	–	+/++
Substantia nigra pars reticulata	–/+	++/+++
Ventral tegmental area	+	+
Deep mesencephalic nucleus	–	+/++
Red nucleus	++	+
Peripeduncular nucleus	–	++
Interpeduncular nucleus	–/+	++
Interfascicular nucleus	–/+	+/++
Precommissural nucleus	–	++
Periaqueductal gray (central gray)	+	++/+++
Oculomotor nucleus (3n)	++	+/++
Dorsal raphe nucleus	+	++/+++
Caudal linear nucleus raphe	–	++/+++
Superior colliculus	+	++
Inferior colliculus	+	+/++
Pons		
Pontine nuclei	++	++
Superior olivary complex	+/++	++/+++
Superior paraolivary nucleus	+	++
Nucleus of the trapezoid body	++	–
Paramedian raphe nucleus	–	+/++
Motor trigeminal nucleus	+/++	+/++
Principal sensory nucleus (5n)	–/+	+/++
Medulla		
Medial vestibular nucleus	–/+	++/+++
Lateral vestibular nucleus	+/++	+
Ventral cochlear nucleus	++/+++	+/++
Dorsal cochlear nucleus	+/++	+
Linear nucleus of the raphe	–/+	+/++
Inferior olive	+/++	+++
Nucleus of the solitary tract	–/+	++
Gigantocellular reticular nucleus, pars alpha	+	+/++
Gigantocellular reticular nucleus	–	+
Lateral paragigantocellular nucleus	+	+/++
Lateral reticular nucleus	+	++/+++
Intermediate reticular nucleus	–	–/+
Parvocellular reticular nucleus	–/+	++/+++
Medullary reticular field, dorsal	–	++
Medullary reticular field, ventral	–	–/+
Paratrigeminal nucleus	–	+++
External cuneate nucleus	+/++	++/+++
Cuneate nucleus	–/+	++
Gracile nucleus	–	++
Nucleus X	–	++/+++
Raphe magnus nucleus	–/+	++
Raphe obscurus nucleus	–	+/++
Raphe pallidus nucleus	–/+	+/++
Trochlear nucleus (4n)	+/++	+/++
Spinal trigeminal nucleus (5n)	+	++
Abducens nucleus (6n)	+	++/+++
Facial nucleus (7n)	+	++/+++
Dorsal motor nucleus of the vagus (10n)	–/+	++
Hypoglossal nucleus (12n)	+	++/+++
Cerebellum		
Cerebellar cortex		
Granule cell layer	++	–
Purkinje cell layer	++/+++	–
Molecular layer	–/+	++/+++
Cerebellar nuclei (int, lat, medial)	++	+/++

[1]The intensity of immunolabeling was qualitatively scored using the CA1 (+++) and CA3 (–) subfields of Ammon's horn as references. Intensity of NTS2 immunoreactivity: – no labeling, + low signal, ++ moderate signal, +++ high signal, referring to both labeling intensity and the number of labeled elements. NTS2, levocabastine-sensitive neurotensin receptor.

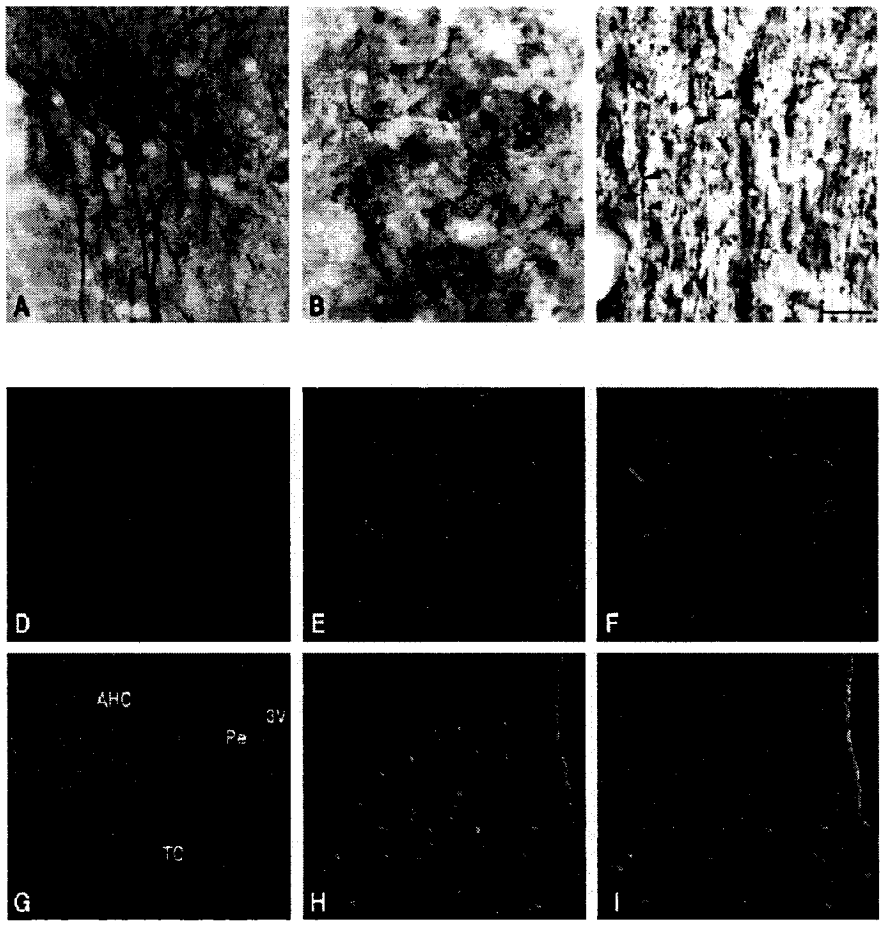

Fig. 3. Cellular distribution of levocabastine-sensitive neurotensin receptor–like (NTS2-l) immunoreactivity in rat brain sections. **A:** In many areas such as the piriform cortex, NTS2-l immunoreactivity is mainly apparent over dendrites. In regions such as the central amygdaloid nucleus (**B**) or the bed nucleus of the stria terminalis (D), NTS2-l immunoreactivity is predominantly associated with nerve cell bodies. **C:** NTS2-immunoreactive axons and axonal varicosities (arrowheads) are visible in several regions such as here in the diagonal band of Broca. D–I: Dual immunofluorescence labeling of NTS2 and of the astrocyte antigen S100β. **D:** In the bed nucleus of the stria terminalis, NTS2-l immunoreactivity is apparent over somata and small processes. **E,F:** None of these structures are immunoreactive for the S100β antigen within the same section. **G:** In the anterior hypothalamus, NTS2-l labeling is detected in the form of small puncta pervading the neuropil, predominantly in its dorsomedial aspect. **H,I:** Here again, none of the NTS2-l–immunoreactive structures colocalize S100β within the same section. For abbreviations, see list. Scale bar in C = 60 μm in A,B, 40 μm in C, 25 μm in D–F, 200 μm in G–I.

external plexiform, and glomerular layers (Fig. 2A; Table 1). Immunopositive perikarya were most intensely labeled in the mitral cell layer (Table 1). Moderately labeled mitral cell dendrites also extended through the external plexiform layer into the glomerular layer. In the glomerular layer, a moderate meshwork of NTS2-l–positive neuronal processes surrounded the glomeruli. Periglomerular cells were occasionally labeled (Table 1). Labeling in the granule cell layer was abundant, although quite diffuse, making it difficult to identify individual immunoreactive cells. The accessory olfactory bulb displayed very strong immunolabeling of neuronal processes (Fig. 2A; Table 1).

In the olfactory cortex, only the olfactory tubercle displayed substantial numbers of immunolabeled nerve cell bodies. A few NTS2-l–positive perikarya were also present in the taenia tecta, the islands of Calleja, the piriform and prepiriform cortex (Fig. 3A), and the lateral olfactory nucleus (Table 1). All of these structures, as well as the anterior olfactory nucleus (Fig. 4) and the dorsal and ventral endopiriform nuclei displayed at least low levels of fiber labeling. In contrast, the piriform and prepiriform cortex stood out by exhibiting a dense network of strongly immunostained dendrites (Fig. 3A).

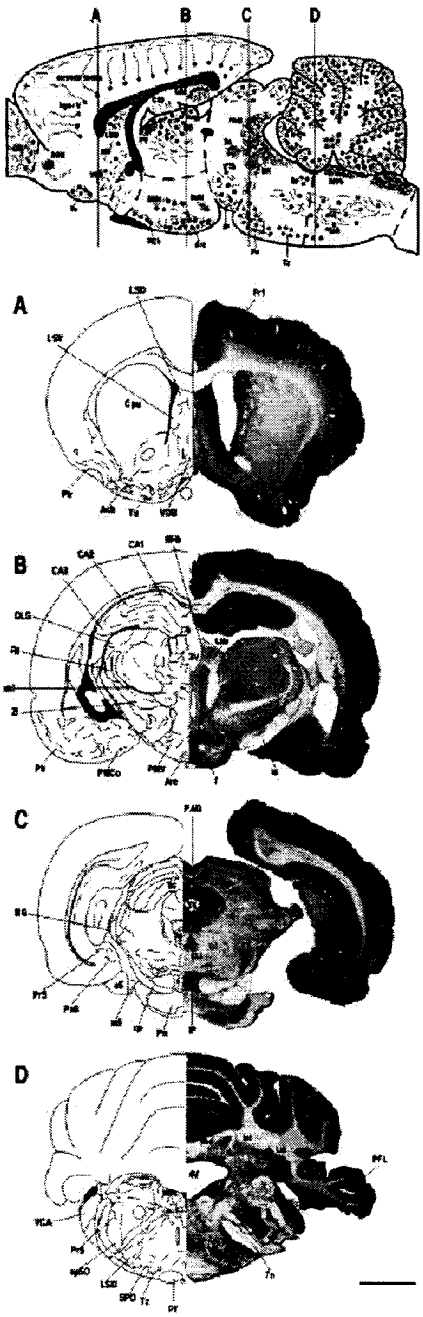

In the basal forebrain, NTS2-1–immunoreactive neuronal cell bodies were observed in the ventral pallidum, the substriatal area, the medial and lateral septum (Fig. 4A), the diagonal band of Broca (Fig. 4A), the magnocellular preoptic nucleus, and most prominently the bed nucleus of the stria terminalis (Fig. 5A). With the exception of the latter two nuclei, labeling of processes and terminals in all of these structures was more prominent than that of neuronal perikarya (Fig. 3C; Table 1). In addition, immunoreactive processes and terminals were encountered in the septohippocampal nucleus and the substantia innominata (Table 1).

With the exception of the caudate putamen, which displayed low to moderate numbers of relatively small, NTS2-1–positive neurons (Fig. 5C; Table 1), the basal ganglia exhibited only low numbers of immunolabeled nerve cells or none at all (Table 1). The nucleus accumbens (core and shell), the caudate putamen, and the fundus striati also contained sparse NTS2-1–immunoreactive processes and terminals. By contrast, the globus pallidus (Fig. 5B) and the entopeduncular nucleus exhibited a dense network of immunolabeled fibers (Table 1).

The central amygdaloid nucleus (Fig. 3B) and the subnuclei of the cortical amygdala (cf. posteromedial amygdaloid nucleus in Fig. 4B) both exhibited a moderate number of strongly NTS2-1–immunoreactive multipolar neurons (Table 1). In addition, sparse immunolabeled cells were found in the medial nucleus of the amygdala. All of these nuclei, as well as the basomedial nucleus, exhibited low to moderate densities of labeled processes and terminals (Table 1).

The hippocampal formation was among the most heavily labeled regions of the brain (Fig. 4B; Table 1). The most striking pattern of staining was found in the CA fields of the hippocampus proper. CA1 exhibited extremely strong immunostaining of pyramidal cell bodies and apical dendrites (Figs. 4, 6A,B). These processes coursed through

Fig. 4. Topographic distribution of levocabastine-sensitive neurotensin receptor–like (NTS2-1) immunoreactivity. A schematic midsagittal section through the rat brain provides an overview of the distribution of NTS2-1 immunoreactivity throughout the neuraxis and indicates the rostrocaudal levels of the coronal sections illustrated below. Symbols in schematic sagittal section: dots, NTS2-1–positive neuronal perikarya; twisted lines, labeled neuronal processes. **A:** At anterior levels, the neocortex (most notably layer V and supragranular layers), piriform cortex, olfactory tubercle, and lateral septum all display moderate to strong immunoreactivity. The mediodorsal aspect of the caudate putamen is also moderately labeled. **B:** Further caudally, very strong immunolabeling is evident in CA1 and CA2 hippocampal subfields. Moderate to dense immunostaining is again evident in cerebral cortex. The posteromedial cortical amygdaloid nucleus also displays intense NTS2-1 immunoreactivity. Finally, moderate immunolabeling is evident in the parafascicular nucleus of the thalamus and throughout the hypothalamus. **C:** At caudal mesencephalic and rostral pontine levels, the strongest immunoreactive signal is observed in the interpeduncular nucleus, the caudal linear raphe, and the periaqueductal gray. The superior colliculus also displays moderate immunolabeling, differentially distributed among its layers. The pontine nuclei are strongly labeled. **D:** In the caudal pons, the superior olivary complex and the nucleus of the trapezoid body are conspicuously labeled. In the same section, rostral medullary nuclei such as the principal sensory and spinal trigeminal nuclei, the medial vestibular nucleus, and the cochlear nuclei display medium to strong immunoreactivity. In the cerebellum, both the deep nuclei and the cerebellar cortex display high levels of NTS2-1 immunoreactivity. For abbreviations, see list. Scale bar = 2.5 mm in D (applies to A–D).

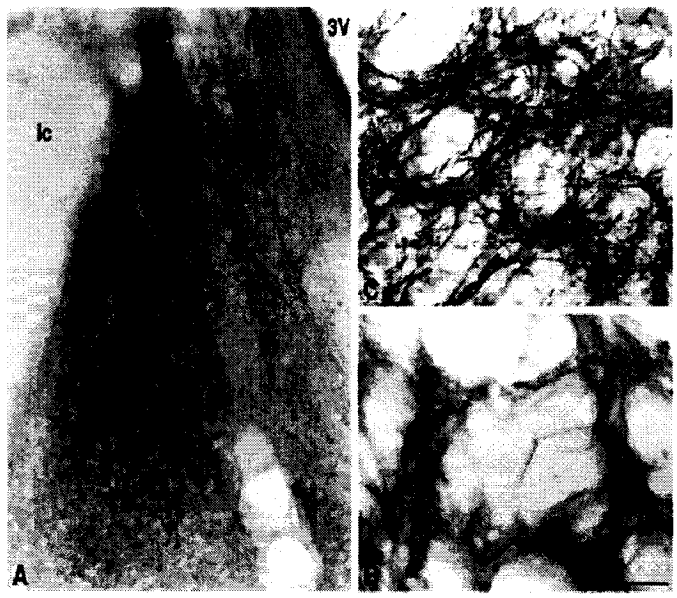

Fig. 5. Distribution of levocabastine-sensitive neurotensin receptor–like (NTS2-l) immunoreactivity in the basal forebrain (A) and basal ganglia (B,C,). A: In the bed nucleus of the stria terminalis, numerous cell bodies are strongly immunoreactive. In addition, there is a moderate staining of the neuropil surrounding the somata. B: Within the globus pallidus, NTS2-l immunoreactivity is associated with neuronal processes coursing in between fascicles of myelinated axons. C: In the caudate putamen, small spiny type II-like immunopositive neuronal perikarya are visible between the fiber bundles of the internal capsule. A light staining of the neuropil is evident as well. For abbreviations, see list. Scale bar in B = 75 μm in A, 160 μm in B, 40 μm in C.

the stratum radiatum and ramified into the stratum lacunosum moleculare, forming a mesh of transected dendritic profiles (Fig. 6A,B). In CA2, the labeling diminished in intensity (Fig. 6A; Table 1) and in CA3, no labeling was apparent at low magnification except for a light staining of the stratum lacunosum moleculare (Fig. 6A). At high magnification, however, it became obvious that the apical dendrites of CA3 pyramidal cells were in fact labeled, although less intensely so than in CA1 or CA2. CA3 nerve cell bodies were not labeled (Table 1). In the dentate gyrus, granule cells were immunonegative (Fig. 6A; Table 1) but a few faintly labeled cell bodies, as well as sparse fibers, in the hilus showed NTS2-l immunolabeling (Table 1). No immunolabeling was apparent in the hippocampus in sections incubated with antiserum preadsorbed with 2 μg/ml antigenic peptide (Fig. 6C). The entorhinal cortex, as well as the pre- and parasubiculum, exhibited moderately to intensely labeled nerve cell bodies in layer II (Fig. 6D,E). The entorhinal cortex also exhibited moderate staining of neuronal processes (Fig. 6E; Table 1).

In all neocortical areas, apical dendrites of layer V pyramidal neurons were the most strongly immunoreactive structures (Fig. 7A; Table 1). These could be traced all the way to layer I in which they ramified (Fig. 7A). Allocortical areas, represented by the retrosplenial cortex, also displayed strongly labeled pyramidal cells (Fig. 7B, insert). Moderate numbers of NTS2-l–positive neuronal somata were observed in the frontal, parietal (Fig. 7A, insert), occipital, temporal, retrosplenial, and insular cortex. Cingulate and perirhinal cortices exhibited only low numbers of immunoreactive somata (Table 1).

Diencephalon. In the thalamus, the paraventricular (Fig. 8A), anterior dorsal and anterior ventral (Fig. 8B), ventromedial, mediodorsal, lateral and medial geniculate (Fig. 8C, insert) nuclei displayed low to moderate numbers of NTS2-l–immunoreactive somata (Table 1). Most of these nuclei also exhibited intensely labeled neuronal processes except for the anterior ventral and medial geniculate nuclei or the dorsal tier of the lateral geniculate body, which were completely devoid of NTS2-l–positive processes (Table 1). The reuniens, reticular, central medial, rhomboid, parafascicular (Fig. 4B), and subparafascicular nuclei all exhibited moderate to dense networks of NTS2-l–positive fibers but no immunopositive nerve cell bodies (Table 1).

Within the hypothalamus, low to moderate numbers of immunoreactive nerve cell bodies were evident in the supraoptic, arcuate (Fig. 8E,F), and ventromedial nucleus (Fig. 4), as well as in the retrochiasmatic area (Fig. 4), the lateral hypothalamic area, and the lateral mammillary nucleus (Fig. 8F). All of these nuclei also displayed moderate to high levels of immunolabeled neuronal processes (Table 1). As in the thalamus, light to moderate labeling of processes was detected in several additional nuclei, namely the anterior hypothalamus (Fig. 3G), suprachiasmatic nucleus, para- (Fig. 8D) and periventricular nuclei (Fig. 3G), tuber cinereum (Fig. 3G), medial mammillary nucleus (Figs. 4, 8F), and lateral and medial preoptic area

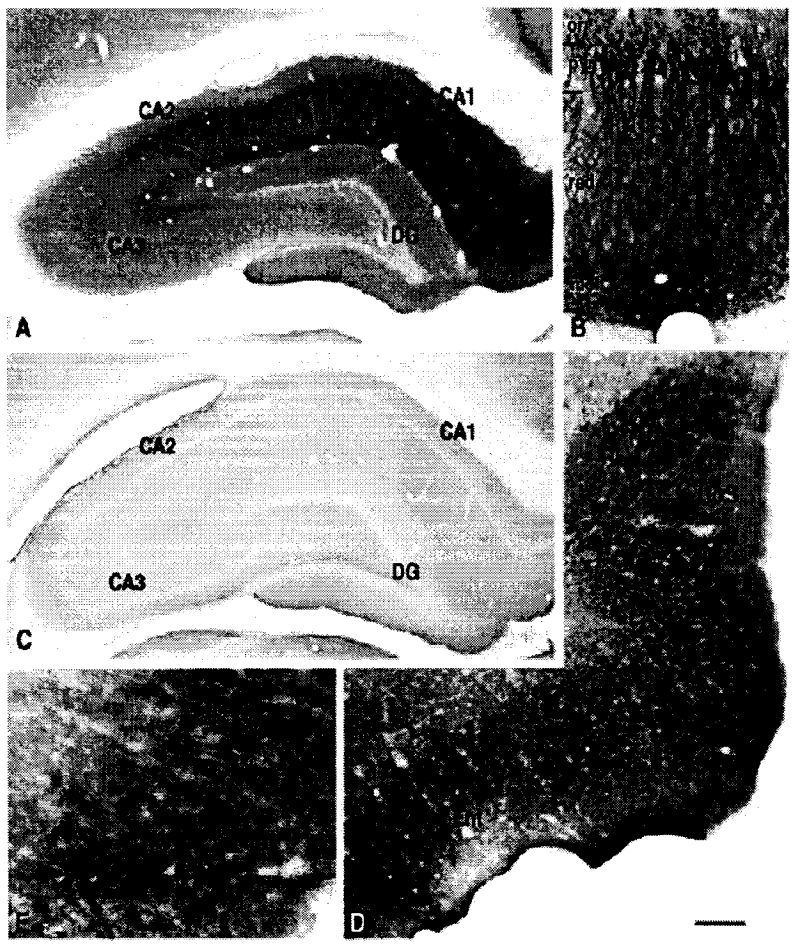

Fig. 6. Distribution of levocabastine-sensitive neurotensin receptor-like (NTS2-l) immunoreactivity in the hippocampal formation. **A:** In Ammon's horn, intense NTS2-l immunolabeling is evident in stratum pyramidale, radiatum, and lacunosum moleculare of CA1 and CA2. CA3 displays only moderate, diffuse labeling, except in the stratum lacunosum moleculare, where the labeling is more pronounced. The dentate gyrus is likewise moderately but diffusely labeled except for the granule cell layer, which is totally devoid of immunostaining. **B:** At high magnification, virtually all CA1 pyramidal cells are seen to be immunopositive. Their apical dendrites pass through the stratum radiatum and ramify in the stratum lacunosum moleculare. **C:** Preadsorption of the antiserum with 2 μg/ml of antigen results in a complete loss of NTS2-l immunoreactivity. **D:** The entorhinal cortex as well as the pre- and parasubiculum all display numerous, strongly labeled nerve cell bodies in layer II. **E:** At high magnification, labeling over neurons in the entorhinal cortex is seen to spare the nucleus and to extend for a short distance within proximal dendrites. For abbreviations, see list. Scale bar in D = 400 μm in A,C, 80 μm in B, 150 μm in D, 60 μm in E.

(Fig. 4; Table 1). The outer zone of the median eminence (Fig. 8E) as well as the supramammillary nucleus (Fig. 8F) exhibited strong NTS2-l fiber labeling (Table 1).

In the zona incerta, sparse, lightly stained nerve cell bodies were detected amidst intensely labeled neuronal processes (Fig. 8C; Table 1). The subthalamic nucleus exhibited moderate levels of NTS2-l–positive processes, but no immunoreactive nerve cell bodies (Table 1).

Both subdivisions of the habenula displayed sparse, lightly labeled nerve cell bodies (Fig. 8A; Table 1). The lateral habenula also exhibited a moderately dense plexus of NTS2-l–positive processes (Fig. 8A; Table 1). The subfornical organ, while devoid of immunopositive cell bodies, harbored a moderately dense network of immunoreactive processes (Table 1).

Mesencephalon. In the midbrain, the oculomotor (Figs. 4, 9A) and magnocellular part of the red nucleus (Fig. 9C) contained medium numbers of intensely stained NTS2-positive nerve cell bodies. Lightly labeled and/or less numerous neurons were also observed in the substan-

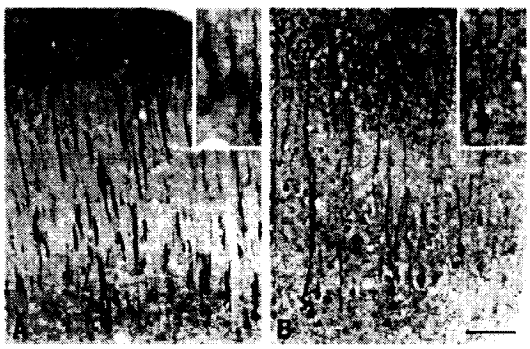

Fig. 7. Distribution of levocabastine-sensitive neurotensin receptor-like (NTS2-l) immunoreactivity in the cerebral cortex. **A:** In neocortical areas such as the parietal cortex illustrated here, a subpopulation of layer V pyramidal cells (insert) exhibit intense immunolabeling of their cell bodies and apical dendrites. The latter may be followed up to the superficial layers, in which they ramify. **B:** Allocortical areas, represented here by the retrosplenial cortex, display a similar pattern of labeling. Scale bar in B = 150 μm in A (60 μm in insert), 75 μm in B (45 μm in insert).

tia nigra, pars reticulata (Fig. 9D,E), ventral tegmental area (Figs. 4, 9D), interpeduncular (Figs. 4, 9D) and interfascicular nuclei, periaqueductal gray (Figs. 4, 9A,B), dorsal raphe nucleus (Figs. 4, 9A), and superior and inferior colliculi (Fig. 4; Table 1). In most of these structures, and most prominently in the periaqueductal gray, dorsal raphe nucleus, and substantia nigra pars reticulata, these labeled perikarya were embedded in a dense meshwork of immunolabeled processes (Figs. 4, 9). In the superior colliculus, labeled perikarya were exclusively observed in the inner gray layer, immediately adjacent to the optic nerve layer, and in the deep gray, where they were concentrated laterally. The substantia nigra, pars compacta (Fig. 9D), peripeduncular nucleus, deep mesencephalic nucleus (Fig. 9D), and precommissural nucleus were devoid of immunopositive perikarya but displayed low to moderate labeling of neuronal processes (Table 1). The caudal linear raphe nucleus (Fig. 4C), while devoid of perikaryal immunolabeling, displayed intensely labeled processes (Table 1).

Pons. The pontine nuclei (Fig. 4C) and nucleus of the trapezoid body (Figs. 4D, 9H) displayed a moderate number of strongly immunostained neuronal perikarya. Less numerous and/or more lightly stained cell bodies were also evident in the superior olivary complex and superior paraolivary nucleus (Figs. 4D, 9F) as well as in the principal sensory (Fig. 4D) and motor trigeminal nuclei (Table 1). Except for the nucleus of the trapezoid body, these structures were also pervaded by moderately abundant immunoreactive neuronal processes (Fig. 9F,G; Table 1). The paramedian raphe nucleus displayed no NTS2-l–positive nerve cell bodies but a moderately dense network of immunolabeled processes (Fig. 9G; Table 1).

Medulla oblongata. In the medulla oblongata, variable numbers of moderately to intensely labeled NTS2-l–immunoreactive cell bodies and processes were observed in all sensory and most of the motor cranial nerve nuclei (Table 1), including the vestibular complex (Fig. 10A,B), the cochlear nuclei (Figs. 4D, 10A), the subnuclei of the spinal trigeminal nucleus (Fig. 10A–C), the nucleus of the solitary tract (Figs. 4D, 10B,C), as well as the trochlear, abducens (Fig. 10D), facial (Fig. 10A), vagal (Fig. 10B), and hypoglossal (Fig. 10B,C) nuclei. In addition, the inferior olive (Fig. 10B,C), the gigantocellular reticular nucleus, pars alpha (rostroventral medial medulla; Fig. 10A,F), the lateral paragigantocellular (Fig. 10A) and lateral reticular nuclei, the parvocellular reticular nucleus (Fig. 10A,B,G), the external cuneate and cuneate nuclei (Fig. 10B,C, E), the linear nucleus of the raphe (Fig. 10B), and the nuclei raphe magnus and pallidus (Fig. 10A,F) displayed low to moderate perikaryal NTS2-l immunolabeling as well as moderate to dense labeling of neuronal processes (Table 1). Structures in which immunolabeled processes but no cell bodies were observed include the gigantocellular and intermediate reticular nuclei (Fig. 10A,B), the medullary reticular field (Fig. 10C), the paratrigeminal (Fig. 10H) and gracile (Fig. 10C) nuclei, nucleus X (Fig. 10B), and the nucleus raphe obscurus (Fig. 10B; Table 1).

Cerebellum. The deep cerebellar nuclei displayed a moderate number of strongly immunoreactive nerve cell bodies interspersed among a plexus of immunopositive processes (Fig. 11A; Table 1). The lateral nucleus was slightly more intensely stained than intermediate and medial nuclei (Figs. 4D, 11A). In the cerebellar cortex, NTS2-l immunoreactivity was present in all three layers. Purkinje cell perikarya and dendritic processes ascending in the molecular layer were the most strongly labeled elements (Fig. 11B,C; Table 1). Labeling in the granule cell layer was less pronounced and essentially accounted for by the immunolabeling of a subpopulation of granule cells (Fig. 11D; Table 1). In the molecular layer, sparse, strongly labeled neuronal perikarya (not shown) were evident among the pervasive Purkinje cell dendrites (Fig. 11C,D).

DISCUSSION

The present study provides the first description of the distribution of NTS2 receptor proteins in mammalian brain. The NTS2 antiserum used here was raised against a sequence from the N-terminus of the rat receptor unique among known NT receptor sequences. The specificity of the antiserum was initially established by Western blotting of membranes prepared from whole brain and cerebellum (which previously had been shown to express among the highest levels of NTS2 mRNA and binding sites in rodent brain; cf. Sarret et al., 1998, 2002; Walker et al., 1998). The NTS2 antiserum specifically recognized a band at 46 kDa, which corresponds to the molecular weight of the monomeric receptor deduced from its cDNA sequence. In addition, other specific bands were detected at molecular weights corresponding to multiples of the monomeric receptor's size, thus possibly representing multimeric complexes of NTS2. None of these bands were present when the blots were incubated with antiserum preadsorbed with the antigenic peptide, indicating that the NTS2 antiserum selectively recognized the native receptor protein. To further support the notion that the immunoreactive bands detected in brain homogenates indeed corresponded to the NTS2 receptor, immunoprecipitation experiments were carried out on membranes from COS-7

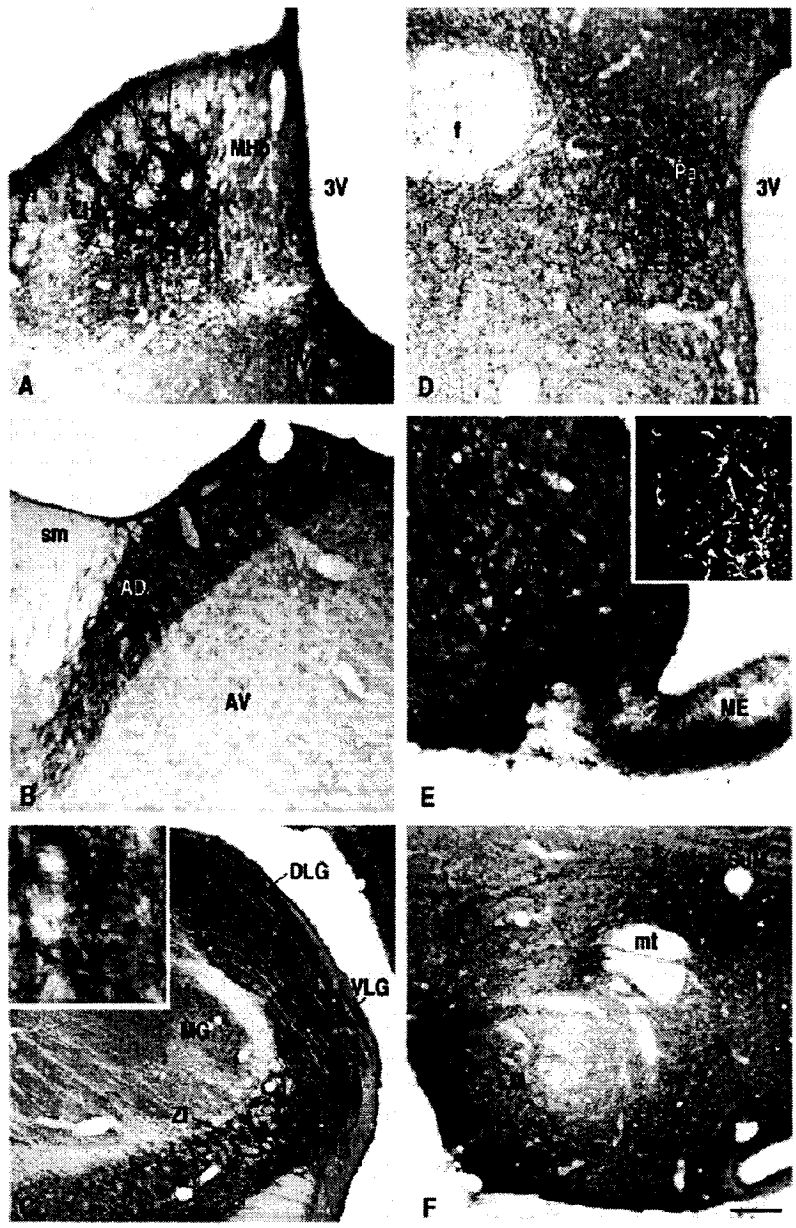

Fig. 8. Distribution of levocabastine-sensitive neurotensin receptor–like (NTS2-l) immunoreactivity in the diencephalon. **A:** Habenular complex. The lateral habenula exhibits moderate to dense fiber staining, whereas the medial habenula is only lightly and diffusely stained. The ventromedially adjoining paraventricular thalamic nucleus displays strong immunolabeling. **B:** The anterior dorsal thalamic nucleus displays intense perikaryal and neuropil immunostaining, whereas the neighboring anterior ventral nucleus is only lightly reactive. **C:** Intense immunoreactivity is apparent over the dorsal lateral and ventral tiers of the lateral geniculate nucleus as well as in the adjoining zona incerta. As seen in the insert, most of this immunostaining is accounted for by dendritic processes. **D:** Within the paraventricular nucleus, NTS2-l immunoreactivity is selectively detected within small punctate processes. **E:** The arcuate nucleus (Arc) displays both immunoreactive nerve cell bodies (arrowheads, insert) and a dense network of strongly immunoreactive processes. Diffuse immunolabeling is also evident over the external zone of the median eminence. **F:** At the level of the mammillary bodies, the lateral mammillary (LM) and supramammillary (SuM) nuclei show moderate to strong neuropil immunolabeling. For other abbreviations, see list. Scale bar in F = 130 μm in A,B,D, 500 μm in C (40 μm in insert), 80 μm in E (50 μm in insert); 200 μm in F.

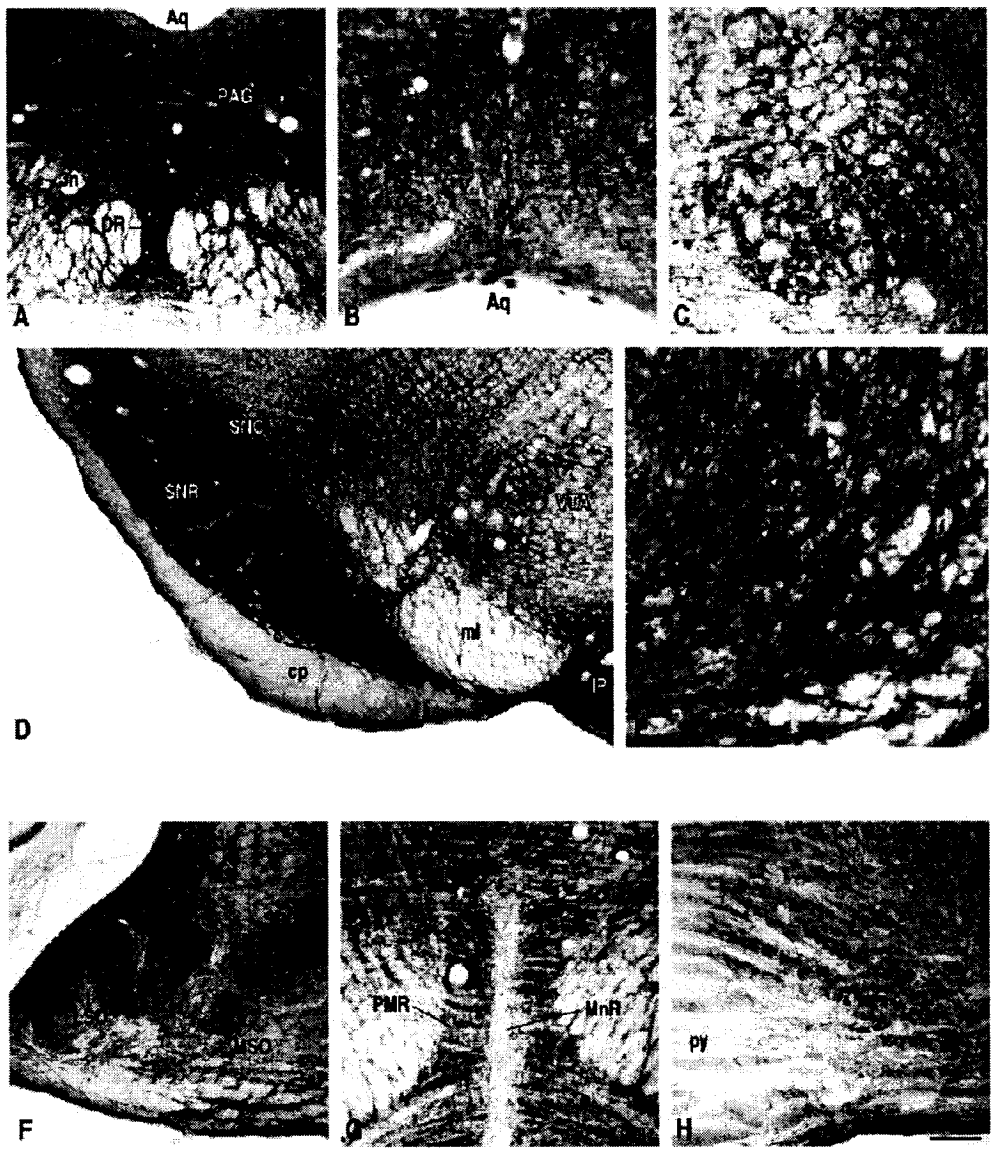

Fig. 9. Distribution of levocabastine-sensitive neurotensin receptor–like (NTS2-l) immunoreactivity in mesencephalon (A–E) and pons (F–H). **A:** The ventral periaqueductal gray (PAG) and dorsal raphe nucleus both exhibit a dense network of immunopositive processes. Intensely immunoreactive nerve cell bodies are also evident within the oculomotor nucleus. **B:** In the dorsal part of the PAG, labeled neuronal perikarya (arrowheads) are apparent amidst a less intensely stained plexus of immunoreactive processes. **C:** Intensely immunostained nerve cell bodies are detected in the ventral, magnocellular portion of the red nucleus. **D:** The substantia nigra, pars compacta (SNc) and reticulata (SNr) exhibit a dense network of immunopositive processes. In the ventral tegmental area, the labeling is less intense and concerns nerve cell bodies as well as processes. **E:** At high magnification, NTS2-l–positive nerve cell bodies (arrowheads) can be identified amongst the dense plexus of processes pervading the SNr. **F:** In the rostral pons, the superior olivary complex exhibits a mix of labeled somata and processes. **G:** The paramedian raphe nucleus displays a high density of immunolabeled processes, whereas the median raphe nucleus is completely devoid of NTS2 immunoreactivity. **H:** In the nucleus of the trapezoid body, NTS2-l immunoreactivity is predominantly associated with small neuronal perikarya. For other abbreviations, see list. Scale bar in H = 280 μm in A, 65 μm in B, 120 μm in C, 350 μm in D, 50 μm in E, 240 μm in F, 150 μm in G,H.

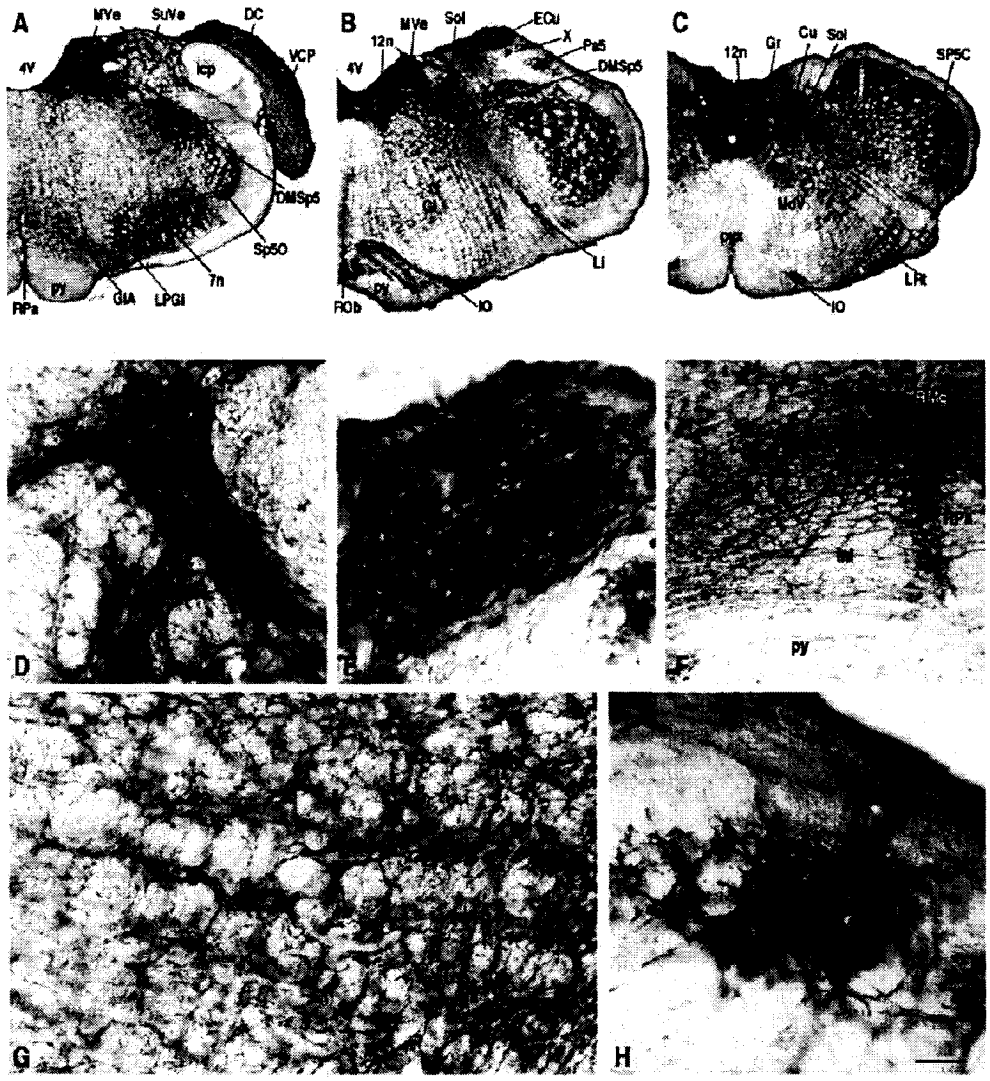

Fig. 10. Distribution of levocabastine-sensitive neurotensin receptor-like (NTS2-l) immunoreactivity in the medulla oblongata. A–C: Low-magnification photomicrographs illustrating labeling of cranial nerve sensory nuclei. Some of these, such as the medial vestibular (A,B) and dorsal cochlear nuclei (A) are more or less uniformly and very strongly stained. Others, such as the superior (A) and spinal vestibular (B) nuclei and ventral cochlear nucleus (A), exhibit lighter staining of the neuropil and NTS2-positive nerve cell bodies are visible even at low magnification. D: The abducens nucleus displays numerous intensely stained neurons as well as a strong labeling of the neuropil. E: The external cuneate nucleus exhibits a moderate number of NTS2-l–positive perikarya in its lateral aspect. The neuropil is strongly stained and pervaded by a dense network of immunolabeled processes. F: The gigantocellular reticular nucleus, pars alpha, exhibits numerous labeled perikarya as well as processes. Medially, the nucleus raphe magnus is intensely stained, and the raphe pallidus displays moderate immunoreactivity. G: Intensely NTS2-l immunoreactive neurons in the parvocellular reticular nucleus are surrounded by a moderately dense plexus of immunopositive fibers. H: The paratrigeminal nucleus is pervaded by a dense plexus of intensely stained processes. For abbreviations, see list. Scale bar in H = 700 μm in A–C, 60 μm in D,E,H, 170 μm in F. 75 μm in G.

cells transfected or not with cDNA encoding the N-terminally HA-tagged NTS2 receptor. Both immunoprecipitation with an anti-HA epitope antibody and detection with anti-NTS2 and the reverse experiment gave rise to the same major bands pattern as detected in rat brain and cerebellum homogenates. These findings confirm that

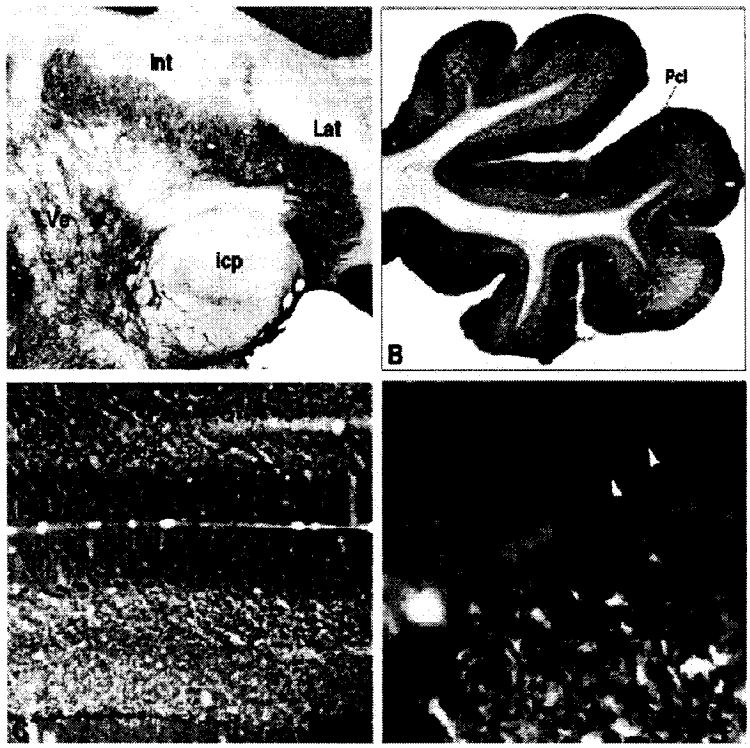

Fig. 11. Distribution of levocabastine-sensitive neurotensin receptor-like (NTS2-l) immunoreactivity in the cerebellum. **A:** Intensely labeled nerve cell bodies are detected among a network of immunoreactive processes within the lateral and intermediate cerebellar nuclei. To the left of the inferior cerebellar peduncle, light to moderate immunoreactivity is observed in the lateral vestibular nucleus. **B:** Sagittal section through the paraflocculus, illustrating the presence of NTS2-l immunolabeling in all three layers of cerebellar cortex. **C:** At higher magnification, labeling of Purkinje cells and of their apical dendrites traversing the molecular layer is evident. **D:** At high magnification, individual immunopositive granule cells can be identified (black arrowheads). In addition, the plexus of Purkinje cell dendrites is resolved in the molecular layer (white arrowheads). For abbreviations, see list. Scale bar in D = 400 μm in A, 500 μm in B, 130 μm in C, 30 μm in D.

our antiserum selectively cross-reacts with the rat NTS2 receptor.

To establish the applicability of the antiserum to the immunohistochemical detection of NTS2 receptors, double-labeling studies were performed on COS-7 cells transiently expressing the N-terminally HA-tagged NTS2 receptor. The NTS2 antiserum exclusively labeled cells that also exhibited HA immunoreactivity, indicating that it selectively recognized cells expressing the NTS2 receptor. Preadsorption of the NTS2 antiserum with immunogenic peptide completely abolished immunostaining, confirming that it was attributable to the NTS2 antibody. Similarly, sections of rat brain incubated with preadsorbed antiserum were virtually devoid of immunostaining, suggesting that as in transfected cells, the antibody selectively recognized the NTS2 receptor.

Within the brain, NTS2-l immunoreactivity was exclusively found in neurons. However, its subcellular compartmentalization varied markedly between brain regions. Thus, whereas in some areas, such as the hippocampus, the immunolabeling was associated with both perikarya and dendrites, in others, such as the cerebral cortex or the globus pallidus, it clearly predominated over dendrites. In yet others, such as the diagonal band of Broca and the anterior hypothalamus, it was mainly associated with axons and axon terminals. These data suggest that, unlike NTS1 receptors, which are reportedly more or less uniformly distributed over perikarya, dendrites, and axons of neurons in which they are expressed (Boudin et al., 1996; Fassio et al., 2000), NTS2 receptors may be selectively targeted to specific neuronal elements, and most prominently to dendritic processes.

Previous in situ hybridization studies have reported the presence of NTS2 mRNA expression in glial and ependymal cells in intact adult rat brain (Walker et al., 1998; Lépée-Lorgeoux et al., 1999). Furthermore, double-labeling experiments have demonstrated NTS2 mRNA expression in glial fibrillary acidic protein-immunolabeled reactive astrocytes, both in vitro and in vivo (Nouel et al., 1999). No glial and/or ependymal labeling was readily apparent here in NTS2-immunoreacted sections. To confirm the lack of association of NTS2-l immunoreactivity

with astrocytes, we performed dual-labeling experiments using the astroglial marker S100β. In none of the regions examined did S100β immunoreactivity colocalize with NTS2-I immunostaining, suggesting that under basal conditions, NTS2 receptor proteins are not present in astrocytes. This is not to say, however, that they would not be detectable under conditions of reactive gliosis.

The topographic distribution of NTS2-I immunoreactivity was extensive, as expected from earlier subtractive autoradiographic binding studies based on the displacement of specific ^{125}I-labeled NT, [^{3}H]NT, or [^{3}H]SR142948A binding by levocabastine (Kitabgi et al., 1987; Schotte et al., 1986, 1988; Schotte and Laduron, 1987; Betancur et al., 1998) or on direct binding of [^{3}H]levocabastine (Asselin et al., 2001). Thus, NTS2-I immunolabeling was detected in all regions previously reported to exhibit high levels of NTS2 binding sites, including olfactory bulb, all olfactory relay nuclei, septum, bed nucleus of the stria terminalis, amygdaloid nuclei, CA1 of the hippocampus, pre- and parasubiculum, cerebral cortex, several thalamic nuclei, arcuate nucleus, mammillary bodies, interpeduncular nucleus, superior colliculus, periaqueductal gray, dorsal raphe nucleus, red nucleus, substantia nigra, ventral tegmental area, nucleus raphe magnus, vestibular complex, and cerebellum. However, the present study also demonstrated that, if widespread, the distribution of NTS2 receptor proteins was also more selective than previously surmised from the diffuse distributional patterns yielded by autoradiographic binding studies (Kitabgi et al., 1987; Schotte et al., 1986, 1988; Schotte and Laduron, 1987; Betancur et al., 1998; Asselin et al., 2001).

The distribution of NTS2-I–immunoreactive nerve cell bodies was also in good agreement with that of NTS2-expressing cells as determined by in situ hybridization in both rat (Walker et al., 1998; Lépée-Lorgeoux et al., 1999) and mouse (Sarret et al., 1998) brain. By and large, all regions reported to exhibit medium to strong NTS2 mRNA levels, such as the olfactory bulb, cerebral cortex, hippocampal formation, periaqueductal gray, and cerebellar cortex, to name but a few, were immunolabeled here. There were several regions, however, in which NTS2-I immunolabeling appeared more restricted than expected from in situ hybridization data. For instance, the medial habenula, which was reported to contain high levels of NTS2 mRNA (Sarret et al., 1998; Lépée-Lorgeoux et al., 1999), was barely immunoreactive in the present study. Similarly, the hippocampus, which was shown to express very high levels of NTS2 mRNA throughout all subfields of Ammon's horn and the dentate gyrus (Sarret et al., 1998; Walker et al., 1998; Lépée-Lorgeoux et al., 1999), exhibited NTS2-immunoreactive cell bodies only in CA1 and CA2 sub-fields. These discrepancies could reflect poor translation of the NTS2 message in certain subpopulations of neurons or could be due to selective targeting of NTS2 proteins to neuronal processes. Thus, NTS2 mRNA-positive/NTS2-immunonegative neurons in the medial habenula could account for the terminal immunolabeling observed in their projection field within the interpeduncular nucleus (Butcher, 1995). Alternatively, the lack of apparent cellular immunoreactivity in areas containing high levels of NTS2 mRNA could reflect selective targeting of NTS2 receptor proteins to plasma membranes. Indeed, the diffuse NTS2-I immunolabeling observed here over the CA3 subfield and dentate gyrus was reminiscent of the pattern of labeling described for the sst_{2A} somatostatin receptor in brain areas in which this receptor was found by electron microscopy to be selectively addressed to plasma membranes (Dournaud et al., 1996).

In contrast to NTS1 mRNA (Elde et al., 1990; Sato et al., 1992; Nicot et al., 1994a,b; Alexander and Leeman, 1998) or immunoreactivity (Boudin at al., 1996; Fassio et al., 2000), which are more or less restricted to regions innervated by neurotensinergic axons, NTS2-I immunoreactivity considerably exceeded that of NT terminal fields. Thus, some of the most heavily labeled regions in the brain, such as the hippocampus, the cerebral and cerebellar cortices, and medullary cranial nerve nuclei have been described as being innervated only sparsely if at all by NT fibers (Jennes et al., 1982, Emson et al., 1985). These findings provide further support to the hypothesis that NT may not be the exclusive endogenous ligand for this receptor subtype (Sarret et al., 1998). There were, however, regions in which NTS2-I immunoreactivity showed considerable overlap with NT terminal fields, including the olfactory bulb, bed nucleus of the stria terminalis, magnocellular preoptic nucleus, anterior dorsal thalamic nucleus, substantia nigra, ventral tegmental area, periaqueductal gray, nucleus raphe dorsalis and magnus, and lateral paragigantocellular nucleus (Jennes et al., 1982; Emson et al., 1985). All of these regions (except for nuclei raphe magnus and lateral paragigantocellular nucleus), as well as several others in which NT axons are less prominent, such as the entorhinal, frontal, and retrosplenial cortices, the pre- and parasubiculum, the cortical amygdala, the pontine nuclei, and various medullary nuclei, also display high levels of NTS1 (Boudin et al., 1996; Fassio et al., 2000), indicating that, in many brain structures, NTS2 is in a position to interact with NTS1 in mediating NT's central effects.

The distribution of NTS2-I immunoreactivity also overlapped extensively with that of the single-transmembrane domain receptor NTS3/sortilin (except in the granule cell layer of the cerebellar cortex and medullary reticular formation, which were enriched in NTS2- but not in NTS3-immunoreactive neurons; (Sarret et al., 2003)). This widespread codistribution of NTS2 with NTS3/sortilin raises the possibility of interactions between these two receptors for the mediation of the NT signal, particularly in light of recent studies showing that NTS3 can interact with NTS1 to enhance the NT-induced phosphorylation of mitogen-activated protein kinases and turnover of phosphoinositides in the HT29 human cancer cell line (Martin et al., 2002).

A striking feature of NTS2 distribution was its association with every single sensory system in the brain. Thus, all olfactory relay nuclei, including the olfactory bulb, exhibited NTS2-I immunoreactivity. The auditory system was also labeled from the cochlear nuclei, through the superior olive, the inferior colliculus, and the medial geniculate nucleus, all the way to the temporal cortex. Likewise, the visual system exhibited NTS2-I immunolabeling throughout the lateral geniculate body, suprachiasmatic nucleus, superior colliculus, and occipital cortex. The nucleus of the solitary tract, a major relay for visceral and gustatory input, exhibited moderate immunolabeling. Finally, NTS2-I immunoreactivity was associated with relay nuclei of ascending somatosensory information, including the gracile and cuneate nuclei, spinal and principal sensory trigeminal nuclei, and parietal cortex.

Of particular interest from a functional perspective was the intense labeling of brainstem structures involved in pain control. Indeed, recent pharmacologic studies have

demonstrated that the NT antagonist SR142948A, which does not distinguish between NTS1 and NTS2, blocks NT-induced antinociception (Gully et al., 1997), whereas the NTS1-specific antagonist SR48692 does not (Gully et al., 1993; Dubuc et al., 1994; Labbé-Jullié, 1994). Furthermore, the NTS2-selective ligand, levocabastine (Tyler et al., 1998; Dubuc et al., 1999b) and NTS2 antisense oligonucleotides (Dubuc et al., 1999a) both inhibit the antinociceptive effects of intracerebroventricularly administered NT, whereas knocking down the NTS1 gene in mice is without effect (Remaury et al., 2002; but also see Pettibone et al., 2002). Microinjection studies have long identified regions involved in the descending control of nociceptive inputs as sites of NT-induced antinociception (Kalivas et al., 1982; Mayer and Price, 1989; McHaffie et al., 1989). The strong NTS2-I immunolabeling found here in regions such as the periaqueductal gray, dorsal raphe nucleus, raphe magnus and pallidus, gigantocellular nucleus, pars alpha, and lateral paragigantocellular nucleus suggests that NTS2 receptors are ideally poised to regulate NT's supraspinal antinociceptive actions.

Strong NTS2-I immunoreactivity was associated with cerebellum-related brainstem nuclei such as the external cuneate nucleus, pontine nuclei, inferior olive, and vestibular complex, suggesting that NTS2 is associated with both mossy and climbing fiber afferent cerebellar systems. NTS2 immunolabeling was also observed over Purkinje cells, deep cerebellar nuclei, vestibular complex, and red nucleus, suggesting that NTS2 receptors are equally involved in the regulation of the cerebellar output. In cerebellar cortex, NTS2-I immunoreactivity was evident over a subpopulation of granule cells, in conformity with the recent demonstration of functionally coupled NTS2 receptors in these cells in primary culture (Sarret et al., 2002). Taken together, the present results suggest a prominent involvement of NTS2 in the regulation of cerebellar function. However, because the cerebellum is essentially devoid of NT innervation, the stimulus responsible for NTS2 activation in this structure remains to be established.

In conclusion, the present study demonstrates that NTS2 receptors are widely distributed in the rat CNS. It also indicates that this receptor is essentially neuronal and that it is predominantly, although not exclusively, targeted to dendrites. High levels of NTS2 receptor proteins were detected in regions documented to receive a dense neurotensinergic innervation (namely the hypothalamus, the basal forebrain and ventral midbrain, and several limbic and brainstem structures), in keeping with the postulated role of this receptor in transducing NT's actions, and most specifically its antinociceptive effects. However, the distribution of NTS2 largely exceeded that of NT's terminal fields, suggesting that it may also serve as receptor for other endogenous ligand(s).

ACKNOWLEDGMENTS

The authors thank Naomi Takeda for secretarial help in the preparation of this article.

LITERATURE CITED

Adams JC. 1992. Biotin amplification of biotin and horseradish peroxidase signals in histochemical stains. J Histochem Cytochem 40:1457–1463.

Alexander MJ, Leeman SE. 1998. Widespread expression in adult rat forebrain of mRNA encoding high- affinity neurotensin receptor. J Comp Neurol 402:475–500.

Asselin ML, Dubuc I, Coquerel A, Costentin J. 2001. Localization of neurotensin NTS2 receptors in rat brain, using. Neuroreport 12:1087–1091.

Betancur C, Canton M, Burgos A, Labeeuw B, Gully D, Rostène W, Pélaprat D. 1998. Characterization of binding sites of a new neurotensin receptor antagonist, [3H]SR 142948A, in the rat brain. Eur J Pharmacol 343:67–77.

Binder EB, Kinkead B, Owens MJ, Nemeroff CB. 2001. Neurotensin and dopamine interactions. Pharmacol Rev 53:453–486.

Boudin H, Pélaprat D, Rostène W, Beaudet A. 1996. Cellular distribution of neurotensin receptors in rat brain: immunohistochemical study using an antipeptide antibody against the cloned high affinity receptor. J Comp Neurol 373:76–89.

Bradford MM. 1976. A rapid and sensitive method for the quantitation of microgram quantities of protein utilizing the principle of protein-dye binding. Anal Biochem 72:248–254.

Butcher LL. 1995. Cholinergic neurons and networks. In: Paxinos G, editor. The Rat Nervous System. 2nd ed. New York: Academic Press. p 1003–1013.

Cape EG, Manns ID, Alonso A, Beaudet A, Jones BE. 2000. Neurotensin-induced bursting of cholinergic basal forebrain neurons promotes gamma and theta cortical activity together with waking and paradoxical sleep. J Neurosci 20:8452–8461.

Carraway R, Leeman SE. 1973. The isolation of a new hypotensive peptide, neurotensin, from bovine hypothalami. J Biol Chem 248:6854–6861.

Chalon P, Vita N, Kaghad M, Guillemot M, Bonnin J, Delpech B, Le Fur G, Ferrara P, Caput D. 1996. Molecular cloning of a levocabastine-sensitive neurotensin binding site. FEBS Lett 386:91–94.

Dana C, Vial M, Leonard K, Beauregard A, Kitabgi P, Vincent JP, Rostène W, Beaudet A. 1989. Electron microscopic localization of neurotensin binding sites in the midbrain tegmentum of the rat. I. Ventral tegmental area and the interfascicular nucleus. J Neurosci 9:2247–2257.

Dournaud P, Gu YZ, Schonbrunn A, Mazella J, Tannenbaum GS, Beaudet A. 1996. Localization of the somatostatin receptor SST2A in rat brain using a specific anti-peptide antibody. J Neurosci 16:4468–4478.

Dubuc I, Costentin J, Terranova JP, Barnouin MC, Soubrié P, Le Fur G, Rostène W, Kitabgi P. 1994. The nonpeptide neurotensin antagonist, SR 48692, used as a tool to reveal putative neurotensin receptor subtypes. Br J Pharmacol 112:352–354.

Dubuc I, Sarret P, Labbé-Jullié C, Botto JM, Honoré E, Bourdel E, Martinez J, Costentin J, Vincent JP, Kitabgi P, Mazella J. 1999a. Identification of the receptor subtype involved in the analgesic effect of neurotensin. J Neurosci 19:503–510.

Dubuc I, Remande S, Costentin J. 1999b. The partial agonist properties of levocabastine in neurotensin-induced analgesia. Eur J Pharmacol 381: 9–12.

Elde R, Schalling M, Ceccatelli S, Nakanishi S, Hokfelt T. 1990. Localization of neuropeptide receptor mRNA in rat brain: initial observations using probes for neurotensin and substance P receptors. Neurosci Lett 120:134–138.

Emson PC, Goedert M, Mantyh PW. 1985. Neurotensin-containing neurons. In: Björklund A, Hökfelt T, editors. Handbook of chemical neuroanatomy. Vol. 4. GABA and neuropeptides in the CNS, Part I. Amsterdam: Elsevier. p 355–405.

Fassio A, Evans G, Grisshammer R, Bolam JP, Mimmack M, Emson PC. 2000. Distribution of the neurotensin receptor NTS1 in the rat CNS studied using an amino-terminal directed antibody. Neuropharmacology 39:1430–1442.

Faure MP, Labbé-Jullié C, Cashman N, Kitabgi P, Beaudet A. 1995. Binding and internalization of neurotensin in hybrid cells derived from septal cholinergic neurons. Synapse 20:106–116.

Francois-Bellan AM, Bosler O, Tonon MC, Wei LT, Beaudet A. 1992. Association of neurotensin receptors with VIP-containing neurons and serotonin-containing axons in the suprachiasmatic nucleus of the rat. Synapse 10:282–290.

Goulet M, Morissette M, Grondin R, Falardeau P, Bedard PJ, Rostène W, Di Paolo T. 1999. Neurotensin receptors and dopamine transporters: effects of MPTP lesioning and chronic dopaminergic treatments in monkeys. Synapse 32:153–164.

Gully D, Canton M, Boigegrain R, Jeanjean F, Molimard JC, Poncelet M, Gueudet C, Heaulme M, Leyris R, Brouard A. 1993. Biochemical and pharmacological profile of a potent and selective nonpeptide antagonist of the neurotensin receptor. Proc Natl Acad Sci U S A 90:65–69.

Gully D, Labeeuw B, Boigegrain R, Oury-Donat F, Bachy A, Poncelet M, Steinberg R, Suaud-Chagny MF, Santucci V, Vita N, Pecceu F, Labbé-Jullié C, Kitabgi P, Soubrié P, Le Fur G, Maffrand JP. 1997. Biochemical and pharmacological activities of SR 142948A, a new potent neurotensin receptor antagonist. J Pharmacol Exp Ther 280:802–812.

Hermans E, Maloteaux JM. 1998. Mechanisms of regulation of neurotensin receptors. Pharmacol Ther 79:89–104.

Hervé D, Tassin JP, Studler JM, Dana C, Kitabgi P, Vincent JP, Glowinski J, Rostène W. 1986. Dopaminergic control of 125I-labeled neurotensin binding site density in corticolimbic structures of the rat brain. Proc Natl Acad Sci U S A 83:6203–6207.

Innamorati G, Le Gouill C, Balamotis M, Birnbaumer M. 2001. The long and the short cycle. Alternative intracellular routes for trafficking of G-protein-coupled receptors. J Biol Chem 276:13096–13103.

Jennes L, Stumpf WE, Kalivas PW. 1982. Neurotensin: topographical distribution in rat brain by immunohistochemistry. J Comp Neurol 210:211–224.

Kalivas PW, Jennes L, Nemeroff CB, Prange AJ Jr. 1982. Neurotensin: topographical distribution of brain sites involved in hypothermia and antinociception. J Comp Neurol 210:225–238.

Kitabgi P, Nemeroff CB, editors. 1992. The neurobiology of neurotensin. Ann N Y Acad Sci 668:1–374.

Kitabgi P, Checler F, Mazella J, Vincent JP. 1985. Pharmacology and biochemistry of neurotensin receptors. Rev Clin Basic Pharmacol 5:397–486.

Kitabgi P, Rostène W, Dussaillant M, Schotte A, Laduron PM, Vincent JP. 1987. Two populations of neurotensin binding sites in murine brain: discrimination by the antihistamine levocabastine reveals markedly different radioautographic distribution. Eur J Pharmacol 140:285–293.

Labbé-Jullié C, Dubuc I, Brouard A, Doulut S, Bourdel E, Pélaprat D, Mazella J, Martinez J, Rostène W, Costentin J. 1994. In vivo and in vitro structure-activity studies with peptide and pseudopeptide neurotensin analogs suggest the existence of distinct central neurotensin receptor subtypes. J Pharmacol Exp Ther 268:328–336.

Laemmli UK. 1970. Cleavage of structural proteins during the assembly of the head of bacteriophage T4. Nature 227:680–685.

Lépée-Lorgeoux I, Betancur C, Rostène W, Pélaprat D. 1999. Differential ontogenetic patterns of levocabastine-sensitive neurotensin NT2 receptors and of NT1 receptors in the rat brain revealed by in situ hybridization. Brain Res Dev Brain Res 113:115–131.

Martin S, Navarro V, Vincent JP, Mazella J. 2002. Neurotensin receptor-1 and -3 complex modulates the cellular signaling of neurotensin in the HT29 cell line. Gastroenterology 123:1135–1143.

Mayer DJ, Price DD. 1989. The neurobiology of pain. In: Snyder-Machler L, Robinson A, editors. Clinical electrophysiology: electrotherapy and electrophysiology. Baltimore: William & Wilkins. p 139–202.

Mazella J, Poustis C, Labbé C, Checler F, Kitabgi P, Granier C, van Rietschoten J, Vincent JP. 1983. Monoiodo-[Trp11]neurotensin, a highly radioactive ligand of neurotensin receptors. Preparation, biological activity, and binding properties to rat brain synaptic membranes. J Biol Chem 258:3476–3481.

Mazella J, Zsürger N, Navarro V, Chabry J, Kaghad M, Caput D, Ferrara P, Vita N, Gully D, Maffrand JP, Vincent JP. 1998. The 100-kDa neurotensin receptor is gp95/sortilin, a non-G-protein- coupled receptor. J Biol Chem 273:26273–26276.

McHaffie JG, Kao CQ, Stein BE. 1989. Nociceptive neurons in rat superior colliculus: response properties, topography, and functional implications. J Neurophysiol 62:510–525.

Moyse E, Rostène W, Vial M, Leonard K, Mazella J, Kitabgi P, Vincent JP, Beaudet A. 1987. Distribution of neurotensin binding sites in rat brain: a light microscopic radioautographic study using monoiodo [125I]Tyr3-neurotensin. Neuroscience 22:525–536.

Nicot A, Bérod A, Gully D, Rowe W, Quirion R, de Kloet ER, Rostène W. 1994a. Blockade of neurotensin binding in the rat hypothalamus and of the central action of neurotensin on the hypothalamic-pituitary-adrenal axis with non-peptide receptor antagonists. Neuroendocrinology 59:572–578.

Nicot A, Rostène W, Bérod A. 1994b. Neurotensin receptor expression in the rat forebrain and midbrain: a combined analysis by in situ hybridization and receptor autoradiography. J Comp Neurol 341:407–419.

Nicot A, Rostene W, Berod A. 1995. Differential expression of neurotensin receptor mRNA in the dopaminergic cell groups of the rat diencephalon and mesencephalon. J Neurosci Res 40:667–674.

Nouel D, Faure MP, St Pierre JA, Alonso R, Quirion R, Beaudet A. 1997. Differential binding profile and internalization process of neurotensin via neuronal and glial receptors. J Neurosci 17:1795–1803.

Nouel D, Sarret P, Vincent JP, Mazella J, Beaudet A. 1999. Pharmacological, molecular and functional characterization of glial neurotensin receptors. Neuroscience 94:1189–1197.

Palacios JM, Kuhar MJ. 1981. Neurotensin receptors are located on dopamine-containing neurones in rat midbrain. Nature 294:587–589.

Palacios JM, Pazos A, Dietl MM, Schlumpf M, Lichtensteiger W. 1988. The ontogeny of brain neurotensin receptors studied by autoradiography. Neuroscience 25:307–317.

Paxinos G, Watson C. 1986. The rat brain in stereotaxic coordinates. 2nd ed. New York: Academic Press.

Petersen CM, Nielsen MS, Nykjaer A, Jacobsen L, Tommerup N, Rasmussen HH, Roigaard H, Gliemann J, Madsen P, Moestrup SK. 1997. Molecular identification of a novel candidate sorting receptor purified from human brain by receptor-associated protein affinity chromatography. J Biol Chem 272:3599–3605.

Pettibone DJ, Hess JF, Hey PJ, Jacobson MA, Leviten M, Lis EV, Mallorga PJ, Pascarella DM, Snyder MA, Williams JB, Zeng Z. 2002. The effects of deleting the mouse neurotensin receptor NTR1 on central and peripheral responses to neurotensin. J Pharmacol Exp Ther 300:305–313.

Quirion R, Chiueh CC, Everist HD, Pert A. 1985. Comparative localization of neurotensin receptors on nigrostriatal and mesolimbic dopaminergic terminals. Brain Res 327:385–389.

Remaury A, Vita N, Gendreau S, Jung M, Arnone M, Poncelet M, Culouscou J, Le Fur G, Soubrie P, Caput D, Shire D, Kopf M, Ferrara P. 2002. Targeted inactivation of the neurotensin type 1 receptor reveals its role in body temperature control and feeding behavior but not in analgesia. Brain Res 25:63–72.

Rostène WH, Alexander MJ. 1997. Neurotensin and neuroendocrine regulation. Front Neuroendocrinol 18:115–173.

Sarret P, Beaudet A. 2002. Neurotensin receptors in the central nervous system. Handbook of chemical neuroanatomy. Vol. 20. Peptide receptors, Part II. Amsterdam: Elsevier. p 323–400.

Sarret P, Beaudet A, Vincent JP, Mazella J. 1998. Regional and cellular distribution of low affinity neurotensin receptor mRNA in adult and developing mouse brain. J Comp Neurol 394:344–356.

Sarret P, Gendron L, Kilian P, Nguyen HM, Gallo-Payet N, Payet MD, Beaudet A. 2002. Pharmacology and functional properties of NTS2 neurotensin receptors in cerebellar granule cells. J Biol Chem 25: 36233–36243.

Sarret P, Krzywkowski P, Segal L, Nielsen MS, Petersen CM, Mazella J, Stroh T, Beaudet A. 2003. Distribution of NTS3 receptor/sortilin mRNA and protein in the rat central nervous system. J Comp Neurol 461:483–505.

Sarrieau A, Javoy-Agid F, Kitabgi P, Dussaillant M, Vial M, Vincent JP, Agid Y, Rostène WH. 1985. Characterization and autoradiographic distribution of neurotensin binding sites in the human brain. Brain Res 348:375–380.

Sato M, Kiyama H, Tohyama M. 1992. Different postnatal development of cells expressing mRNA encoding neurotensin receptor. Neuroscience 48:137–149.

Schotte A, Laduron PM. 1987. Different postnatal ontogeny of two [3H]neurotensin binding sites in rat brain. Brain Res 408:326–328.

Schotte A, Leysen JE. 1989. Further characterization of neurotensin binding in the rat brain: levocabastine-displaceable neurotensin binding sites are not histamine- H1 receptors. Biochem Pharmacol 38:3891–3893.

Schotte A, Leysen JE, Laduron PM. 1986. Evidence for a displaceable non-specific [3H]neurotensin binding site in rat brain. Naunyn Schmiedebergs Arch Pharmacol 333:400–405.

Schotte A, Rostène W, Laduron PM. 1988. Different subcellular localization of neurotensin-receptor and neurotensin-acceptor sites in the rat brain dopaminergic system. J Neurochem 50:1026–1031.

Szigethy E, Beaudet A. 1987. Selective association of neurotensin receptors with cholinergic neurons in the rat basal forebrain. Neurosci Lett 83:47–52.

Szigethy E, Beaudet A. 1989. Correspondence between high affinity 125I-neurotensin binding sites and dopaminergic neurons in the rat substantia nigra and ventral tegmental area: a combined radioautographic and immunohistochemical light microscopic study. J Comp Neurol 279:128–137.

Szigethy E, Wenk GL, Beaudet A. 1988. Anatomical substrate for neurotensin-acetylcholine interactions in the rat basal forebrain. Peptides 9:1227–1234.

Tyler BM, Groshan K, Cusack B, Richelson E. 1998. In vivo studies with low doses of levocabastine and diphenhydramine, but not pyrilamine, antagonize neurotensin-mediated antinociception. Brain Res 787:78–84.

Uhl GR. 1982. Distribution of neurotensin and its receptor in the central nervous system. Ann N Y Acad Sci 400:132–149.

Vincent JP, Mazella J, Kitabgi P. 1999. Neurotensin and neurotensin receptors. Trends Pharmacol Sci 20:302–309.

Walker N, Lépée-Lorgeoux I, Fournier J, Betancur C, Rostène W, Ferrara P, Caput D. 1998. Tissue distribution and cellular localization of the levocabastine- sensitive neurotensin receptor mRNA in adult rat brain. Brain Res Mol Brain Res 57:193–200.

APPENDIX B

0026-895X/04/6606-1421–1430$20.00
MOLECULAR PHARMACOLOGY
Vol. 66, No. 6
2303/1184495
Mol Pharmacol 66:1421–1430, 2004
Printed in U.S.A.

Low-Affinity Neurotensin Receptor (NTS2) Signaling: Internalization-Dependent Activation of Extracellular Signal-Regulated Kinases 1/2

Louis Gendron, Amélie Perron, Marcel Daniel Payet, Nicole Gallo-Payet, Philippe Sarret, and Alain Beaudet

Department of Neurology and Neurosurgery (L.G., A.P., P.S., A.B.), Montreal Neurological Institute, McGill University, Montreal, Quebec, Canada; and Department of Physiology and Biophysics (M.D.P.), Faculty of Medicine, and Service of Endocrinology (N.G.P.), University of Sherbrooke, Sherbrooke, Quebec, Canada

Received May 4, 2004; accepted September 9, 2004

ABSTRACT

The role and signaling properties of the low-affinity neurotensin receptor (NTS2) are still controversial. In particular, it is unclear whether neurotensin acts as an agonist, inverse agonist, or antagonist at this site. In view of the growing evidence for a role of NTS2 in antinociception, the elucidation of the pharmacological and coupling properties of this receptor is particularly critical. In the present study, we demonstrate that in Chinese hamster ovary (CHO) cells expressing the rat NTS2 receptor, neurotensin (NT), levocabastine, neuromedin N, and the high-affinity NT receptor antagonist SR48692 [2-{[1-(-7-chloroquinolin-4-yl)-5-(2,6-dimethoxyphenyl)-1*H*-pyrazole-3-carbonyl]amino}adamantane-2-carboxylic acid] all bind to and activate the NTS2 receptor. This activation is followed by ligand-induced internalization of receptor-ligand complexes, as evidenced by confocal microscopy using a fluorescent NT analog. All compounds tested produced a rapid and sustained activation of extracellular signal-regulated kinases 1/2 (ERK1/2) but were without specific effect on Ca^{2+} mobilization. The agonist-induced activation of ERK1/2 was completely abolished by preincubation of the cells with the endocytosis inhibitors phenylarsine oxide and monodansylcadaverine as well as overexpression of a dominant-negative mutant of dynamin 1 (DynK44A), indicating that receptor internalization was required for ERK1/2 activation. NTS2-induced activation of ERK1/2 was not species-specific, because the same agonistic effects of NT and analogs were observed in CHO cells transfected with the human NTS2 receptor. In conclusion, this study demonstrates that NTS2 is a bona fide NT receptor and that activation of this receptor by NT or NT analogs results in an internalization-dependent activation of the ERK1/2 signaling cascade.

Neurotensin (NT) is a tridecapeptide that exerts neuromodulatory functions in the central nervous system and has endocrine/paracrine actions in the periphery (Vincent, 1995; Rostène and Alexander, 1997). NT has been shown to modulate dopaminergic transmission in the nigrostriatal and mesocorticolimbic pathways (Nemeroff, 1986; Kitabgi et al., 1989), thereby implicating this neuropeptide in the pathophysiology of several central nervous system disorders, including Parkinson's disease and schizophrenia (for review, see Kitabgi et al., 1989; Binder et al., 2001; Kinkead and Nemeroff, 2002). In addition, NT injection in the brain or ventricular system produces hypothermia (Martin et al., 1980), changes in blood pressure (Rioux et al., 1981), and non–opioid-dependent analgesia (Kalivas et al., 1982).

NT mediates its central and peripheral effects through interaction with three receptor subtypes, referred to as NTS1, NTS2, and NTS3. NTS1 and NTS2 belong to the seven

This work was supported by a grant from the Canadian Institutes of Health Research (CIHR) awarded to Alain Beaudet. Louis Gendron was funded by fellowship from CIHR, and Amélie Perron and Philippe Sarret were funded by fellowships from the Fonds de la Recherche en Santé du Québec.

Presented in part at the 33rd Annual Meeting for The Society for Neuroscience; 2003 Nov 8–12; New Orleans, LA: Gendron L, Sarret P, Perron A, Gallo-Payet N, Payet MD, and Beaudet A (2003) The rat NTS2 neurotensin receptor is functionally coupled to extracellular signal-regulated protein kinases (ERK1/2) by an internalization dependent-mechanism. *Soc Neurosci Abstr* **29**:161.3

Article, publication date, and citation information can be found at http://molpharm.aspetjournals.org.

doi:10.1124/mol.104.002303.

ABBREVIATIONS: NT, neurotensin; ERK1/2, extracellular signal-regulated kinases 1/2; SR48692, 2-{[1-(-7-chloroquinolin-4-yl)-5-(2,6-dimethoxyphenyl)-1*H*-pyrazole-3-carbonyl]amino}adamantane-2-carboxylic acid; Levo, levocabastine; CHO, Chinese hamster ovary; COS, *Cercopithecus aethiops*; NN, neuromedin N; DMEM, Dulbecco's modified Eagle's medium; FBS, fetal bovine serum; G-418, geneticin; MDC, monodansylcadaverine; PAO, phenylarsine oxide; PTX, pertussis toxin; PVDF, polyvinylidene difluoride; Fluo-NT, *Nα*-BODIPY-neurotensin-(2-13); PCR, polymerase chain reaction; BSA, bovine serum albumin; bp, base pair(s); PBS, phosphate-buffered saline; DMSO, dimethyl sulfoxide; ANOVA, analysis of variance; RT-PCR, reverse transcription-polymerase chain reaction; EGFP, enhanced green fluorescent protein.

transmembrane domain/G protein-coupled receptor family (Tanaka et al., 1990; Vita et al., 1993, 1998; Chalon et al., 1996; Mazella et al., 1996), whereas NTS3 is a single transmembrane domain sorting receptor predominantly associated with vesicular organelles and the Golgi apparatus (Petersen et al., 1997; Mazella et al., 1998). Pharmacological and biochemical studies have indicated that the high-affinity (subnanomolar range) NT receptor NTS1 is coupled to cGMP, cAMP, and inositol phosphate signaling cascades (for review, see Hermans and Maloteaux, 1998; Vincent et al., 1999). Stimulation of NTS1 also induces the activation of extracellular signal-regulated kinases 1/2 (ERK1/2) through coupling with both pertussis toxin-sensitive and -insensitive G proteins. This activation leads in turn to the expression of proliferative genes such as *c-fos, Krox-24*, and *elk-1* (Poinot-Chazel et al., 1996; Ehlers et al., 1998, 2000; Portier et al., 1998; Martin et al., 2002a). These effects are selectively blocked by the nonpeptide NT antagonist SR48692, which displays a nanomolar affinity for NTS1 (Gully et al., 1993).

The low-affinity (nanomolar range) NT receptor NTS2 differs from the NTS1 site not only by its 10-fold lower affinity for NT, but also by its selective recognition of levocabastine, a nonpeptide histamine H_1 receptor antagonist that selectively inhibits NT binding to NTS2 without affecting its binding to NTS1 (Schotte et al., 1986; Kitabgi et al., 1987). NTS2 also displays a much lower affinity (IC_{50} = 300 nM) than NTS1 (IC_{50} = 5.6 nM) for the SR48692 compound (Gully et al., 1993); however, the pharmacological and signaling properties of NTS2 are still extremely controversial. In particular, doubts have been cast regarding the agonistic properties of NT at this site and, hence, about whether or not this protein may be regarded as a true NT receptor. Indeed, in CHO cells stably transfected with human NTS2, SR48692, but neither NT nor levocabastine, was found to activate classic second messenger systems, such as phosphoinositide hydrolysis, Ca^{2+} mobilization, or ERK1/2 phosphorylation (Vita et al., 1998). Furthermore, in transfected CHO and COS-7 cells, this SR48692-induced activation of the human NTS2 was blocked by NT, suggesting that the endogenous peptide was acting as a competitive antagonist at these sites (Vita et al., 1998; Richard et al., 2001).

By contrast, in *Xenopus laevis* oocytes expressing the mouse NTS2 receptor, NT, neuromedin N (NN), and levocabastine were all found to activate Ca^{2+}-dependent chloride currents (Mazella et al., 1996). In addition, application of NT or levocabastine on rat cerebellar granule cells, which endogenously express the NTS2 but not the NTS1 receptor, induced a sustained activation of the ERK1/2 signaling cascade (Sarret et al., 2002). Congruent with an agonist role of NT at this site, rodent NTS2 receptors were found to efficiently internalize via clathrin-coated pits upon NT binding both in stably transfected human embryonic kidney 293 cells (Botto et al., 1998) and in rat cerebellar granule cell cultures (Sarret et al., 2002).

It is unclear whether the reported agonistic/antagonistic effects of NT on the human versus rodent NTS2 receptor are caused by species differences between the two receptors or by variations in receptor coupling as a result of the cell type in which the receptor is expressed. In view of the growing evidence for a role of NTS2 (Dubuc et al., 1999a,b; Remaury et al., 2002; Yamauchi et al., 2003), in addition to that of NTS1 (Tyler et al., 1999; Pettibone et al., 2002), in antinociception, and therefore of the possibility that NTS2 might represent a new target for the development of nonopioid analgesic drugs, the need for precise knowledge of the pharmacological and signaling properties of this receptor seems particularly critical. Thus, the aim of the present study was to characterize the pharmacological and signaling properties of the rat NTS2 receptor expressed in stably transfected CHO cells and to compare these properties with those of the human NTS2 receptor expressed in the same cell line as well as with our own earlier data on the properties of the rat NTS2 receptor endogenously expressed in rat cerebellar granule cells.

Materials and Methods

Materials. The chemicals used in the present study were obtained from the following sources: Dulbecco's modified Eagle's medium (DMEM) and F-12 medium, fetal bovine serum (FBS), glutamine, G-418, gentamicin, and LipofectAMINE were from Invitrogen (Carlsbad, CA); NT, monodansylcadaverine (MDC), phenylarsine oxide (PAO), sodium orthovanadate (Na_3VO_4), pertussis toxin (PTX), and staurosporine were from Sigma-Aldrich (St. Louis, MO); anti-phosphorylated ERK1/2 and anti-ERK1/2 antibodies were from New England Biolabs (Beverly, MA); horseradish peroxidase-conjugated anti-rabbit antibodies and the enhanced chemiluminescence detection system were from Amersham Biosciences Inc. (Piscataway, NJ); Complete protease inhibitor and polyvinylidene difluoride (PVDF) membranes were from Roche (Montreal, QC, Canada); NN was from Bachem California (Torrance, CA). Levocabastine and SR48692 were kindly provided by Janssen Pharmaceuticals (Antwerp, Belgium) and Sanofi Synthelabo (Toulouse, France), respectively. All other chemicals were of grade A purity.

Transfection of CHO Cells. CHO/K1 cells were cultured in DMEM/F-12 medium mixture (1:1) supplemented with 10% FBS and 50 mg/l gentamicin at 37°C in 75-cm^2 Falcon flasks in a humidified atmosphere of 95% air and 5% CO_2. For transfection, CHO/K1 cells were grown to subconfluence (70–80%) in 24-well Petri dishes and incubated for 4 h at 37°C in transfection medium [mixture of pTARGET-rNTS2 (1 μg/ml) (Sarret et al., 2003) or pTARGET-hNTS2 and 40 μg/ml LipofectAMINE in serum-free DMEM]. Transfection medium was then replaced with DMEM/F-12 medium, and the cells were transferred 36 h later to a 75-cm^2 flask containing fresh medium supplemented with G-418 at a concentration of 800 μg/ml. After 2 weeks of selection with G-418, a total of 23 and 12 individual clones were isolated for CHO/rNTS2 and CHO/hNTS2, respectively. Each clone was separately grown and tested for its capacity to internalize *N*α-BODIPY-neurotensin-(2-13) (Fluo-NT) as described below. CHO/rNTS2 clone no. 16 and CHO/hNTS2 clone no. 1 were used for all experiments.

Reverse Transcription-Polymerase Chain Reaction Analysis. Total RNAs (2 μg) were extracted from CHO/rNTS2 and CHO/K1 cells using QIAGEN RNeasy Mini Spin columns (QIAGEN, Mississauga, ON, Canada) and submitted to reverse transcription (reverse transcription system kit; Promega, Madison, WI) for 1 h at 42°C. First-strand cDNAs were then subjected to 35 cycles of PCR in a final reaction volume of 50 μl of the reaction buffer (50 mM KCl, 10 mM Tris, pH 9.0, 1.5 mM $MgCl_2$, 0.1% Triton X-100, 0.02% BSA, 200 μM dNTPs, and 0.5 units of *Taq* DNA polymerase) containing 100 ng of either one of the following three pairs of sense and antisense primers as described previously (Sarret et al., 2002). The first pair (5′-ACACCCATTGTGGACACAGCC-3′ and 5′-TTCATCCGAGATATAGCAGAA-3′) provided for the amplification of a fragment of rNTS1 receptor cDNA with a predicted size of 335 bp. The second pair (5′-GAATGTGCTGGTGTCCTTCGC-3′ and 5′-ACTTGT-ATTTCTCCCAGGCTG-3′) provided for the amplification of a fragment of rNTS2 receptor cDNA with a predicted size of 620 bp. The third pair (5′-TCCCGAGAACTCTGGAAAGGT-3′ and 5′-CACAGAGGCGAAGAGGAAACG-3′) provided for the amplification of a fragment of rNTS3 receptor cDNA with a predicted size of 426 bp.

Amplification was carried out with the first cycle at 95°C for 3 min, 54°C for 2 min, 72°C for 45 s, followed by 34 cycles at 95°C for 40 s, 54°C for 35 s, 72°C for 45 s, and a final extension step at 72°C for 5 min. PCR products were then analyzed on a 1.5% agarose gel.

Binding of ^{125}I-NT to CHO/rNTS2 Cells. For binding experiments, cells were grown on 24-well plates and incubated at 37°C in DMEM/F-12 medium 48 h before the assay. Cells were equilibrated for 10 min at 37°C in Earle's buffer (130 mM NaCl, 5 mM KCl, 1.8 mM $CaCl_2$, 0.8 mM $MgCl_2$, and 20 mM HEPES, pH 7.4) supplemented with 0.2% BSA and 0.1% glucose. Cells were then incubated with 2.5 nM ^{125}I-NT (100 Ci/mmol) for 30 min at 37°C in 250 μl of Earle's buffer containing 0.8 mM *ortho*-phenanthroline in the presence of increasing concentrations (from 10^{-11}–10^{-5} M) of nonradioactive NT, levocabastine, NN, or SR48692. Cells were then washed twice with Earle's buffer and harvested in 1 ml of 0.1 M NaOH, and the radioactivity content was measured in a γ counter. IC_{50} values were determined from competition curves as the concentration of unlabeled ligand necessary to inhibit 50% of ^{125}I-NT-specific binding.

Intracellular Calcium Measurements. For intracellular calcium ($[Ca^{2+}]_i$) measurements, the CHO/rNTS2 and CHO/K1 cells were cultured on 22-mm glass coverslips and incubated in serum-free DMEM supplemented with 4 μM Fluo-4/acetoxymethyl ester (Molecular Probes, Eugene, OR) at 37°C for 30 min. Cells were then washed three times with 0.5% BSA and further incubated in PBS-HEPES (140 mM NaCl, 5.4 mM KCl, 2 mM $CaCl_2$, 1 mM $MgCl_2 \cdot 6H_2O$, and 10 mM HEPES, pH 7.35) at 37°C for 30 min to allow the acetoxymethyl ester form to be hydrolyzed. The coverslips were then mounted on the stage of a Nikon Eclipse TE300 inverted microscope (Nikon, Melville, NY), and the cells were maintained at 37°C throughout the experiments with a heating Peltier element.

NT, NN, levocabastine, or SR48692, diluted in fresh PBS-HEPES containing, for the solubilization of the latter two drugs, 0.01% dimethylsulfoxide (DMSO), were added to the cells at a final concentration of 1 μM, and images of fluorescence were acquired every 5 s using a CoolSnap$_{fx}$ charge-coupled device camera (Roper Scientific, Trenton, NJ) cooled at −35°C. Additional experiments were carried out using 0.01% DMSO in PBS-HEPES alone to test for possible nonspecific effects of the solubilizing agent. Band-pass filters were used for excitation and emission (450–490 and 520–560 nm, respectively). Average fluorescence intensity for each cell was measured using MetaFluor software package (Universal Imaging Corporation, Downingtown, PA). Each Ca^{2+} curve in Fig 2 represents the average response of *n* cells.

Western Blotting Analyses of ERK1/2 Activity. CHO/rNTS2, CHO/hNTS2, and CHO/K1 cells were grown for 3 days in DMEM/F-12 medium containing 10% FBS, starved in serum-free DMEM for 1 h, and then stimulated for various time intervals (1–60 min) with NT (100 nM), levocabastine (100 nM or 1 μM), NN (100 nM), or SR48692 (100 nM) at 37°C in serum-free medium. In some experiments, cells were preincubated with PAO or MDC (two endocytosis inhibitors) for 30 min or with PTX (G_i protein inhibitor) for 18 h (100 ng/ml) before stimulation with NT or NT analogs. The reaction was stopped by aspiration of the medium and the addition of ice-cold Hanks' balanced salt solution containing 0.1 μM staurosporine and 1 mM sodium orthovanadate. Cells were then left for 30 min at 4°C and lysed in 50 mM HEPES, pH 7.8, containing 1% Triton X-100, 0.1 μM staurosporine, 1 mM sodium orthovanadate, and Complete protease inhibitor. The cell lysates were centrifuged at 8000*g* for 15 min at 4°C, and the supernatants were stored at −20°C until use.

For each lysate, equal amounts of proteins (25 μg) were separated on 10% SDS-polyacrylamide gels and electrotransferred on PVDF membranes as described previously (Gendron et al., 2003). PVDF membranes containing proteins were incubated for 2 h at room temperature with anti-phosphorylated ERK1/2 (1:1000) or anti-ERK1/2 (1:1000) rabbit antibodies, followed by three washes with Tris-buffered saline/Tween 20. Detection of immunoreactive proteins was accomplished using horseradish peroxidase-conjugated anti-rabbit (1:2000) and an enhanced chemiluminescence detection system.

To quantify the effect of NT and NT analogs on ERK1/2 phosphorylation, the ratios of phosphorylated ERK1/2 over total ERK1/2 levels were determined by densitometry, using Scion Image (Scion Corporation, Frederick, MD). The statistical significance of the activation of ERK1/2 in stimulated versus nonstimulated cells was verified using ANOVA, and the *p* values were obtained from Dunnett's tables.

Binding of Fluo-NT to CHO/rNTS2 Cells. CHO/rNTS2 cells were grown for 2 days on 12-mm poly-L-lysine-coated glass coverslips in DMEM/F-12 medium containing 10% FBS and stimulated for 30 min at 37°C with 50 nM Fluo-NT in serum-free DMEM containing 0.8 mM *ortho*-phenanthroline alone or in the presence of levocabastine (10 μM) or phenylarsine oxide (endocytosis inhibitor) (10 μM). At the end of the incubation, cells were washed twice with ice-cold PBS, air-dried, mounted on glass slides with Aquamount (Polysciences, Warrington, PA) and examined using the Zeiss LSM510 confocal laser-scanning microscope (Carl Zeiss Canada Ltd., Toronto, ON, Canada) equipped with a Zeiss inverted microscope and a helium/neon laser (543 nm).

Immunofluorescence Studies. CHO/rNTS2 cells were grown on 12-mm glass coverslips for 3 days in DMEM/F-12 medium containing 10% FBS and then starved in serum-free DMEM for 1 h. Cells pretreated or not with PAO (10 μM, 10 min at 37°C) were then treated or not with SR48692 (100 nM) for 5 min at 37°C in serum-free DMEM. The reaction was stopped by aspiration of the medium and the addition of ice-cold Hanks' balanced salt solution containing 0.1 μM staurosporine, and 1 mM sodium orthovanadate. After 10 min of incubation on ice, cells were fixed for 20 min with methanol at −20°C and rehydrated with Hanks' balanced salt solution for 30 min at room temperature. Phosphorylated ERK1/2 were labeled overnight at 4°C using anti-phosphorylated ERK1/2 rabbit antibodies (1:100) and revealed using goat anti-rabbit Alexa488- or Alexa594-conjugated secondary antibodies (Molecular Probes; diluted 1:500 in Hanks' balanced salt solution) for 60 min at room temperature. After washing, coverslips were mounted on glass slides using Aquamount and examined using the Zeiss LSM510 confocal laser-scanning microscope equipped with a Zeiss inverted microscope, an argon laser (488 nm), and a helium/neon laser (543 nm). Images were all taken using the same acquisition settings.

To determine whether ligand-induced receptor internalization was necessary for NTS2-induced ERK1/2 phosphorylation, the above immunofluorescence assay was repeated on CHO/rNTS2 cells preincubated for 10 min with PAO (10 μM) as well as on CHO/rNTS2 cells cotransfected with pcDNA1-DynK44A (kindly provided by Dr. Stephen S. Ferguson, Carleton University, Ontario, QC, Canada) and pEGFP-N1 (BD Biosciences, Mississauga, ON, Canada). For this purpose, pcDNA1-DynK44A (1 μg/ml) and pEGFP-N1 (0.1 μg/ml) plasmids were mixed with 40 μg/ml LipofectAMINE, and the mixture was kept at room temperature for 30 min before being added to the culture medium. CHO/rNTS2 cells grown to 25 to 30% subconfluence on 12-mm poly-L-lysine-coated glass coverslips were then transfected for 4 h at 37°C with this DNA-lipid complex. At the end of the incubation, transfection medium was replaced with fresh medium, and cells were processed 36 h later for immunolabeling of the phosphorylated ERK1/2 as described above.

Results

Expression and Binding Properties of rNTS2 in Transfected CHO Cells. Reverse transcription-polymerase chain reaction (RT-PCR) analysis of rat NTS1, NTS2, and NTS3 expression was performed on nontransfected CHO cells (CHO/K1) and on CHO cells transfected with rat NTS2 receptor cDNA (CHO/rNTS2). As shown in Fig. 1A, a 620-bp band corresponding to the size of the NTS2 receptor fragment was observed in CHO/rNTS2 cells but not in CHO/K1 cells. In contrast, a 425-bp product corresponding to the NTS3

Amplification was carried out with the first cycle at 95°C for 3 min, 54°C for 2 min, 72°C for 45 s, followed by 34 cycles at 95°C for 40 s, 54°C for 35 s, 72°C for 45 s, and a final extension step at 72°C for 5 min. PCR products were then analyzed on a 1.5% agarose gel.

Binding of ^{125}I-NT to CHO/rNTS2 Cells. For binding experiments, cells were grown on 24-well plates and incubated at 37°C in DMEM/F-12 medium 48 h before the assay. Cells were equilibrated for 10 min at 37°C in Earle's buffer (130 mM NaCl, 5 mM KCl, 1.8 mM $CaCl_2$, 0.8 mM $MgCl_2$, and 20 mM HEPES, pH 7.4) supplemented with 0.2% BSA and 0.1% glucose. Cells were then incubated with 2.5 nM ^{125}I-NT (100 Ci/mmol) for 30 min at 37°C in 250 μl of Earle's buffer containing 0.8 mM *ortho*-phenanthroline in the presence of increasing concentrations (from 10^{-11}–10^{-5} M) of nonradioactive NT, levocabastine, NN, or SR48692. Cells were then washed twice with Earle's buffer and harvested in 1 ml of 0.1 M NaOH, and the radioactivity content was measured in a γ counter. IC_{50} values were determined from competition curves as the concentration of unlabeled ligand necessary to inhibit 50% of ^{125}I-NT-specific binding.

Intracellular Calcium Measurements. For intracellular calcium ($[Ca^{2+}]_i$) measurements, the CHO/rNTS2 and CHO/K1 cells were cultured on 22-mm glass coverslips and incubated in serum-free DMEM supplemented with 4 μM Fluo-4/acetoxymethyl ester (Molecular Probes, Eugene, OR) at 37°C for 30 min. Cells were then washed three times with 0.5% BSA and further incubated in PBS-HEPES (140 mM NaCl, 5.4 mM KCl, 2 mM $CaCl_2$, 1 mM $MgCl_2 \cdot 6H_2O$, and 10 mM HEPES, pH 7.35) at 37°C for 30 min to allow the acetoxymethyl ester form to be hydrolyzed. The coverslips were then mounted on the stage of a Nikon Eclipse TE300 inverted microscope (Nikon, Melville, NY), and the cells were maintained at 37°C throughout the experiments with a heating Peltier element.

NT, NN, levocabastine, or SR48692, diluted in fresh PBS-HEPES containing, for the solubilization of the latter two drugs, 0.01% dimethylsulfoxide (DMSO), were added to the cells at a final concentration of 1 μM, and images of fluorescence were acquired every 5 s using a CoolSnap$_{fx}$ charge-coupled device camera (Roper Scientific, Trenton, NJ) cooled at −35°C. Additional experiments were carried out using 0.01% DMSO in PBS-HEPES alone to test for possible nonspecific effects of the solubilizing agent. Band-pass filters were used for excitation and emission (450–490 and 520–560 nm, respectively). Average fluorescence intensity for each cell was measured using MetaFluor software package (Universal Imaging Corporation, Downingtown, PA). Each Ca^{2+} curve in Fig 2 represents the average response of *n* cells.

Western Blotting Analyses of ERK1/2 Activity. CHO/rNTS2, CHO/hNTS2, and CHO/K1 cells were grown for 3 days in DMEM/F-12 medium containing 10% FBS, starved in serum-free DMEM for 1 h, and then stimulated for various time intervals (1–60 min) with NT (100 nM), levocabastine (100 nM or 1 μM), NN (100 nM), or SR48692 (100 nM) at 37°C in serum-free medium. In some experiments, cells were preincubated with PAO or MDC (two endocytosis inhibitors) for 30 min or with PTX (G_i protein inhibitor) for 18 h (100 ng/ml) before stimulation with NT or NT analogs. The reaction was stopped by aspiration of the medium and the addition of ice-cold Hanks' balanced salt solution containing 0.1 μM staurosporine and 1 mM sodium orthovanadate. Cells were then left for 30 min at 4°C and lysed in 50 mM HEPES, pH 7.8, containing 1% Triton X-100, 0.1 μM staurosporine, 1 mM sodium orthovanadate, and Complete protease inhibitor. The cell lysates were centrifuged at 8000*g* for 15 min at 4°C, and the supernatants were stored at −20°C until use.

For each lysate, equal amounts of proteins (25 μg) were separated on 10% SDS-polyacrylamide gels and electrotransferred on PVDF membranes as described previously (Gendron et al., 2003). PVDF membranes containing proteins were incubated for 2 h at room temperature with anti-phosphorylated ERK1/2 (1:1000) or anti-ERK1/2 (1:1000) rabbit antibodies, followed by three washes with Tris-buffered saline/Tween 20. Detection of immunoreactive proteins was accomplished using horseradish peroxidase-conjugated anti-rabbit (1:2000) and an enhanced chemiluminescence detection system.

To quantify the effect of NT and NT analogs on ERK1/2 phosphorylation, the ratios of phosphorylated ERK1/2 over total ERK1/2 levels were determined by densitometry, using Scion Image (Scion Corporation, Frederick, MD). The statistical significance of the activation of ERK1/2 in stimulated versus nonstimulated cells was verified using ANOVA, and the *p* values were obtained from Dunnett's tables.

Binding of Fluo-NT to CHO/rNTS2 Cells. CHO/rNTS2 cells were grown for 2 days on 12-mm poly-L-lysine-coated glass coverslips in DMEM/F-12 medium containing 10% FBS and stimulated for 30 min at 37°C with 50 nM Fluo-NT in serum-free DMEM containing 0.8 mM *ortho*-phenanthroline alone or in the presence of levocabastine (10 μM) or phenylarsine oxide (endocytosis inhibitor) (10 μM). At the end of the incubation, cells were washed twice with ice-cold PBS, air-dried, mounted on glass slides with Aquamount (Polysciences, Warrington, PA) and examined using the Zeiss LSM510 confocal laser-scanning microscope (Carl Zeiss Canada Ltd., Toronto, ON, Canada) equipped with a Zeiss inverted microscope and a helium/neon laser (543 nm).

Immunofluorescence Studies. CHO/rNTS2 cells were grown on 12-mm glass coverslips for 3 days in DMEM/F-12 medium containing 10% FBS and then starved in serum-free DMEM for 1 h. Cells pretreated or not with PAO (10 μM, 10 min at 37°C) were then treated or not with SR48692 (100 nM) for 5 min at 37°C in serum-free DMEM. The reaction was stopped by aspiration of the medium and the addition of ice-cold Hanks' balanced salt solution containing 0.1 μM staurosporine, and 1 mM sodium orthovanadate. After 10 min of incubation on ice, cells were fixed for 20 min with methanol at −20°C and rehydrated with Hanks' balanced salt solution for 30 min at room temperature. Phosphorylated ERK1/2 were labeled overnight at 4°C using anti-phosphorylated ERK1/2 rabbit antibodies (1:100) and revealed using goat anti-rabbit Alexa488- or Alexa594-conjugated secondary antibodies (Molecular Probes; diluted 1:500 in Hanks' balanced salt solution) for 60 min at room temperature. After washing, coverslips were mounted on glass slides using Aquamount and examined using the Zeiss LSM510 confocal laser-scanning microscope equipped with a Zeiss inverted microscope, an argon laser (488 nm), and a helium/neon laser (543 nm). Images were all taken using the same acquisition settings.

To determine whether ligand-induced receptor internalization was necessary for NTS2-induced ERK1/2 phosphorylation, the above immunofluorescence assay was repeated on CHO/rNTS2 cells preincubated for 10 min with PAO (10 μM) as well as on CHO/rNTS2 cells cotransfected with pcDNA1-DynK44A (kindly provided by Dr. Stephen S. Ferguson, Carleton University, Ontario, QC, Canada) and pEGFP-N1 (BD Biosciences, Mississauga, ON, Canada). For this purpose, pcDNA1-DynK44A (1 μg/ml) and pEGFP-N1 (0.1 μg/ml) plasmids were mixed with 40 μg/ml LipofectAMINE, and the mixture was kept at room temperature for 30 min before being added to the culture medium. CHO/rNTS2 cells grown to 25 to 30% subconfluence on 12-mm poly-L-lysine-coated glass coverslips were then transfected for 4 h at 37°C with this DNA-lipid complex. At the end of the incubation, transfection medium was replaced with fresh medium, and cells were processed 36 h later for immunolabeling of the phosphorylated ERK1/2 as described above.

Results

Expression and Binding Properties of rNTS2 in Transfected CHO Cells. Reverse transcription-polymerase chain reaction (RT-PCR) analysis of rat NTS1, NTS2, and NTS3 expression was performed on nontransfected CHO cells (CHO/K1) and on CHO cells transfected with rat NTS2 receptor cDNA (CHO/rNTS2). As shown in Fig. 1A, a 620-bp band corresponding to the size of the NTS2 receptor fragment was observed in CHO/rNTS2 cells but not in CHO/K1 cells. In contrast, a 425-bp product corresponding to the NTS3

plasm in the form of small, endosome-like fluorescent clusters (Fig. 6A). By contrast, Fluo-NT labeling was confined to the cell surface after pretreatment with the endocytosis inhibitor PAO (10 μM, 10 min) (Fig. 6B). Fluo-NT internalization was NTS2-specific, because nontransfected CHO/K1 cells (not shown) and cells coincubated with Fluo-NT and an excess of levocabastine (Fig. 6C) were entirely fluorescent-negative.

To determine whether ligand-induced NTS2 receptor internalization was necessary for ERK1/2 activation, CHO/rNTS2 cells were pretreated or not with PAO (10 μM) or MDC (400 μM) and stimulated for 5 min with 100 nM NT, levocabastine, or SR48692. PAO and MDC both completely inhibited the effect of stimulation by either ligand on ERK1/2 phosphorylation, as measured by Western blotting (Fig. 7A).

The effect of stimulation with SR48692 on ERK1/2 activation was also verified by immunofluorescence in CHO/rNTS2 cells, using antibodies against phosphorylated ERK1/2. In contradistinction with nonstimulated cells, which were immunonegative (Figs. 6, D and G, and 7B), cells stimulated for 5 min with SR48692 (100 nM) exhibited intense phosphorylated ERK1/2 immunoreactivity, mainly within their nucleus (Fig. 7B, arrowheads). This induction of phosphorylated ERK1/2 immunoreactivity was totally prevented by preincubating the cells with PAO (Fig. 7B).

To further confirm that the NTS2-induced ERK1/2 activation was dependent on ligand-induced internalization, CHO/rNTS2 cells were transiently transfected with a dominant-negative mutant of dynamin 1, DynK44A, together with the fluorescent protein EGFP (with a ratio of 10:1), to distinguish DynK44A-expressing from -nonexpressing cells. Stimulation of these dually transfected cells with 100 nM SR48692 increased phosphorylated ERK1/2 immunofluorescence in approximately 40% of the cells (Fig. 6, E and H), whereas 100% of the cells expressing only the rNTS2 receptor were activated after stimulation with SR48692 (Fig. 7B). This decrease was caused by the overexpression of the dynamin 1 dominant-negative mutant, because none of the cells confirmed to overexpress DynK44A, by virtue of their coexpression of EGFP, showed phosphorylated ERK1/2 immunofluorescence (Fig. 6, F and I, arrows).

Discussion

The present study demonstrates that neurotensin activates the mitogen-activated protein kinase cascade through its interaction with either rat or human NTS2 receptors in transfected CHO cells. It also indicates that ligand-induced internalization of this receptor is required for NTS2-mediated signaling.

We previously demonstrated that stimulation of rat cerebellar granule cells, which endogenously express the NTS2 receptor, with either NT or levocabastine resulted in ERK1/2 activation (Sarret et al., 2002). These results differed from those obtained by other groups that had reported antagonistic or inverse agonistic effects of these two drugs on the

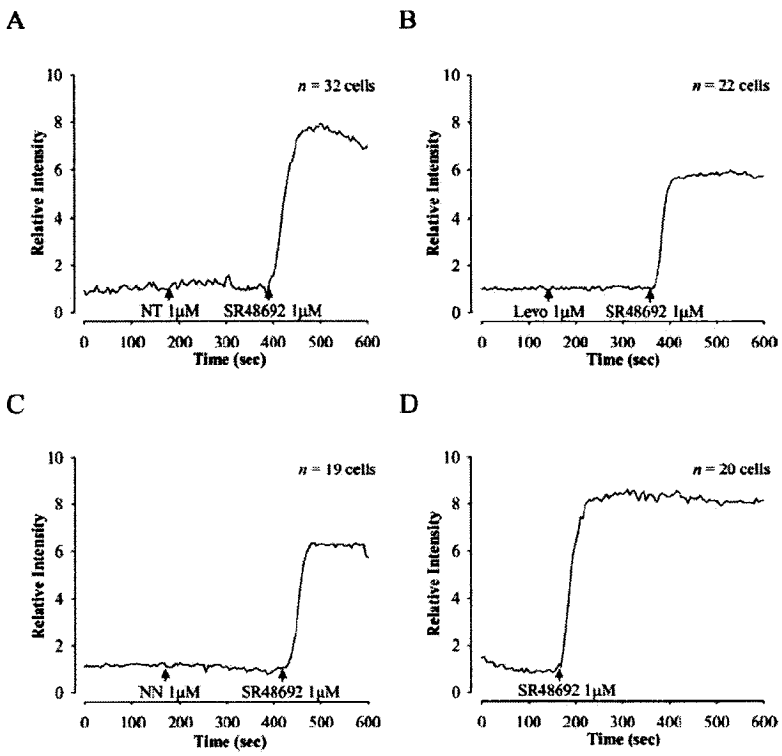

Fig. 2. Intracellular Ca^{2+} mobilization in Fluo-4-loaded CHO cells. A–C, application of 1 μM SR48692 to CHO/rNTS2 cells induces an increase, followed by a plateau, in intracellular Ca^{2+}. By contrast, no increase in intracellular Ca^{2+} is observed after 1 μM NT, 1 μM Levo, or 1 μM NN, nor are any of these drugs able to prevent the Ca^{2+} mobilization effect of SR48692. D, same type of SR48692-induced response observed in CHO/K1 cells (nontransfected cells). The curves represent the means of *n* responding cells and five experiments.

human NTS2 receptor heterologously expressed in COS (Richard et al., 2001) and CHO cells (Vita et al., 1998), respectively. A first objective of the present study was therefore to determine whether these discrepancies were caused by species differences or by endogenous versus heterologous expression of the NTS2 receptor.

For this purpose, we first established a stable cell line of CHO cells expressing the rat NTS2 receptor (CHO/rNTS2 cells). RT-PCR analysis confirmed that these cells did express the NTS2 receptor, to the exclusion of the NTS1. ^{125}I-NT was accordingly found to bind to these cells with a pharmacology characteristic of that of NTS2, both in terms of affinity for NT and of relative affinity for the NT analogs levocabastine, NN, and SR48692 (Chalon et al., 1996; Mazella et al., 1996; Botto et al., 1998; Vita et al., 1998; Sarret et al., 2002).

We then tested the effects of NT and of various NT analogs on the mobilization of $[Ca^{2+}]_i$ in these transfected cells. As previously reported for cortical cerebellar neurons endogenously expressing the rat NTS2 receptor (Sarret et al., 2002), or for transfected CHO cells expressing the human NTS2 receptor (Vita et al., 1998), neither NT, levocabastine, nor NN affected Ca^{2+} mobilization in CHO/rNTS2 cells. By contrast, incubation with the NTS1 antagonist SR48692 caused a marked elevation of intracellular calcium in the same cells. This increase conformed to earlier reports of SR48692-induced Ca^{2+} mobilization in CHO cells transfected with either human (Vita et al., 1998) or rat (Yamada et al., 1998) NTS2 receptors. However, whereas in these previous studies the effects of SR48692 were antagonized by concomitant administration of an excess of NT, NN, or levocabastine and could not be elicited in nontransfected cells, in the present study, the effects of SR48692 were not blocked by NT, NN, or levocabastine and were equally strong in nontransfected cells, suggesting that they were not mediated by NTS2. Likewise, in rat cerebellar granule cells, SR48692 induced a robust $[Ca^{2+}]_i$ increase that was unaffected by concomitant application of NT or levocabastine and was therefore interpreted as being NTS2-independent (Sarret et al., 2002).

We then sought to determine whether NT activated ERK1/2 in transfected CHO/rNTS2 cells as in rat cerebellar granule cells (Sarret et al., 2002). Application of 100 nM NT to CHO/rNTS2 cells induced a robust, dose-dependent increase in ERK1/2 phosphorylation. This activation was rapid and sustained over 60 min. It also was mediated by NTS2, because it could not be elicited in nontransfected cells. The similarity of these findings with those obtained in neurons in culture (Sarret et al., 2002) suggests that the observed activation is physiological and not caused by artifactitious coupling of the receptor subsequent to its aberrant expression in CHO cells.

Levels of ERK1/2 activation comparable with those obtained after stimulation with NT were achieved by incubating CHO/rNTS2 cells with either NN or levocabastine. That these two drugs would display effects comparable with those of NT is congruent with results in *X. laevis* oocytes, which showed that NT, NN, and levocabastine all stimulated to the same extent an NTS2-mediated Ca^{2+}-activated inward Cl^- current (Mazella et al., 1996; Botto et al., 1997; Dubuc et al., 1999b). However, the present results differ from those of Vita et al. (1998), who found no effect of NT, NN, or levocabastine on ERK1/2 activation in CHO cells transfected with the human NTS2 receptor. To determine whether this discrepancy was related to species differences, we repeated the experiments in CHO cells transfected with hNTS2 in lieu of rNTS2. Our results showed the same NTS2-mediated activation of ERK1/2 phosphorylation in cells transfected with the human

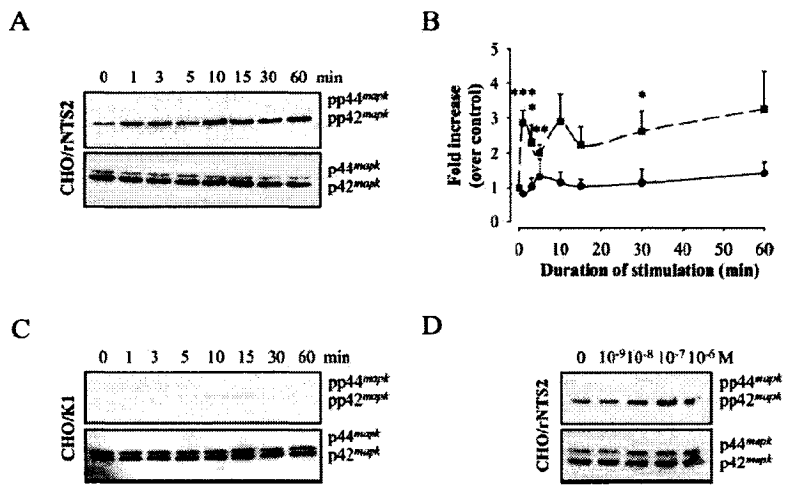

Fig. 3. Neurotensin activation of ERK1/2 in rNTS2-transfected CHO cells. CHO/rNTS2 (A, B, and D) and CHO/K1 (C) cells were stimulated with various concentrations of NT (D) for 0 to 60 min (A–C), and ERK1/2 phosphorylation levels were determined as described under *Materials and Methods*. A, C, and D, top, phosphorylated ERK1/2; bottom, total ERK1/2. A, stimulation of CHO/rNTS2 cells with 100 nM NT induces a rapid and sustained activation of ERK1/2. B, densitometric measurements of ERK1/2 activation (phosphorylated ERK1/2 over total ERK1/2) expressed as -fold increase over control ± S.E.M. (●, CHO/K1, $n = 3$; ■, CHO/rNTS2, $n = 4$) (ANOVA and Dunnett's). *, $p < 0.05$; **, $p < 0.02$; and ***, $p < 0.01$ compared with control, untreated cells. C, stimulation of wild-type, nontransfected CHO cells with 100 nM NT has no effect on ERK1/2 phosphorylation. D, dose-dependent activation of ERK1/2 after application of 10^{-9} to 10^{-6} M NT for 5 min (representative of two independent experiments).

plasmid as in cells transfected with the rNTS2, suggesting that the differences between the present and earlier results are not the result of differences between rat and human NTS2 but rather of variations in the sensitivity of the methods employed for the detection of ERK1/2 phosphorylation.

Stimulation with the NTS1 antagonist SR48692 also resulted in a marked increase in ERK1/2 activation in both CHO/rNTS2 and CHO/hNTS2 cells. Unlike the effects of SR48692 on Ca^{2+} mobilization, these effects were mediated by NTS2, because they were not observed in nontransfected CHO cells. Previous studies have reported on the agonistic properties of SR48692 on both rodent (Botto et al., 1997; Yamada et al., 1998) and human (Vita et al., 1998) NTS2. Surprising here was the fact that, although SR48692 displayed a much lower affinity than NT, NN, or levocabastine for the NTS2 receptor (present study; Gully et al., 1993; Mazella et al., 1996; Botto et al., 1998; Vita et al., 1998; Yamada et al., 1998; Nouel et al., 1999; Richard et al., 2001; Sarret et al., 2002), it induced ERK1/2 phosphorylation much more efficiently (~7-fold more efficient than NT in cells transfected with the rat receptor). To determine whether this discrepancy could be explained by the binding of SR48692 to a site distinct from the target of NT or its analogs, we repeated the SR48692 stimulation experiments in the presence of 100 nM NT. Despite its higher affinity for the receptor, NT had no competitive inhibiting effect on the SR48692-induced ERK1/2 activation, suggesting that the two drugs interact with different binding pockets as they do on the NTS1 receptor (Labbé-Jullié et al., 1995; Barroso et al., 2000).

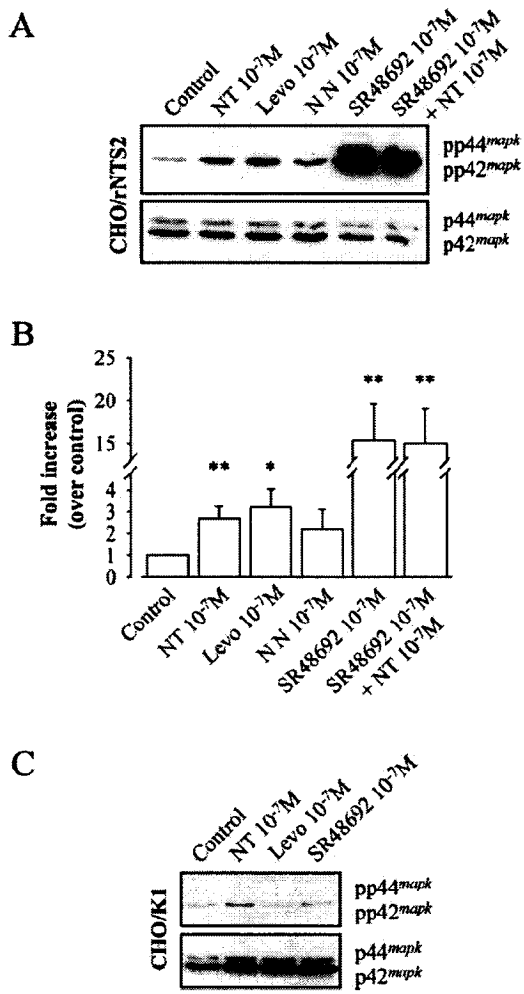

Fig. 4. Effect of neurotensin, levocabastine, neuromedin N, and SR48692 on ERK1/2 phosphorylation in CHO/rNTS2. CHO/rNTS2 (A and B) and CHO/K1 (C) cells were treated or not for 5 min with a battery of NTS2 agonists and harvested for the determination of ERK1/2 phosphorylation levels as described under *Materials and Methods*. NT (100 nM), Levo (100 nM), NN (100 nM), and SR48692 (100 nM) all induce ERK1/2 phosphorylation in CHO/rNTS2 cells (A) but not in CHO/K1 cells (C). Note that ERK1/2 phosphorylation levels are markedly higher in cells stimulated with SR48692 than with other drugs, an effect that is not modified by coincubation with NT (100 nM). B, densitometric measurements of ERK1/2 activation (phosphorylated ERK1/2 over total ERK1/2) expressed as -fold increase over control ± S.E.M. ($n = 3$) (ANOVA and Dunnett's). *, $p < 0.1$ and **, $p < 0.05$ compared with control, untreated cells.

Immunofluorescent studies confirmed that stimulation of CHO/rNTS2 cells with SR48692 produced a robust increase in phosphorylated ERK1/2 levels. Furthermore, they demonstrated that this increase mainly occurred in the nucleus, suggesting that some of the targets of activated ERK1/2 may be transcription factors such as Elk-1, Ets, Stat1/3, or c-Myc/N-Myc and, by extension, that the activation of the NTS2 receptor results in the modulation of gene expression.

It was recently shown that in COS-7 cells transfected with the human NTS2 receptor, the receptor was constitutively active and that NT and levocabastine behave as a neutral antagonist and inverse agonist, respectively, on the production of inositol phosphate (Richard et al., 2001). By contrast, the present NT- or levocabastine-induced effects on ERK1/2 phosphorylation are unlikely to be caused by neutral antagonistic or inverse agonistic properties of the drugs, because there was no evidence of constitutive NTS2 receptor activity in our system. Indeed, no difference was observed between the basal phosphorylation level of ERK1/2 in CHO/rNTS2 and in nontransfected CHO cells. Furthermore, had NT or levocabastine acted as inverse agonists, they should not, as they did, have increased phosphorylation of ERK1/2 to levels higher than those measured in nontransfected cells.

As previously demonstrated for mouse and human NTS2 receptors in transfected cells (Botto et al., 1998; Martin et al., 2002b) and for rat NTS2 receptors in cerebellar granule cells (Sarret et al., 2002), stimulation of rat NTS2 receptors heterologously expressed in CHO cells resulted in a ligand-induced internalization of receptor-ligand complexes. This effect was inhibited by the endocytosis inhibitor phenylarsine oxide, suggesting that it was mediated by clathrin, as documented for most G protein-coupled receptors (Kranenburg et al., 1999; Pierce et al., 2000; Miller and Lefkowitz, 2001; Claing et al., 2002). That a fluorescent analog of NT was able to induce NTS2 internalization further argues in favor of its agonistic role at the NTS2 receptor.

It is now well documented that seven transmembrane domain/G protein-coupled receptors may activate ERK1/2 via G protein-independent mechanisms, involving interaction of the receptor with endocytic proteins such as dynamin

(Kranenburg et al., 1999; Pierce et al., 2000) and β-arrestins (Miller and Lefkowitz, 2001; Claing et al., 2002). In the present study, we found that blocking receptor internalization with phenylarsine oxide or monodansylcadaverine completely impaired the ability of NT, as well as of all other NTS2 agonists tested, to activate ERK1/2 in CHO/rNTS2 cells. Furthermore, overexpression of DynK44A, a dominant-negative mutant form of dynamin 1, was found to selectively inhibit SR48692-induced ERK1/2 activation in cells dually expressing the NTS2 and the dominant-negative mutant. These results strongly suggest that the NTS2-mediated activation of the mitogen-activated protein kinase pathway is predicated on the internalization of receptor-ligand complexes via a dynamin-dependent and G_i protein-independent mechanism.

In conclusion, the present results reveal that NT, as well as many of the known NTS2 receptor ligands, act as agonists at this site, at least as pertains to the promotion of ERK1/2 phosphorylation. This finding is important in that it lends further support to the premise that NT is an endogenous ligand at this receptor. It also suggests that NTS2-acting NT analogs may constitute a promising new class of nonopioid analgesic drugs, provided that these drugs do not, as does SR48692, exert other actions (e.g., NTS1 antagonism and NTS2-independent induction of Ca^{2+} mobilization). Indeed, recent studies have demonstrated that NT, but not SR48692 (Dubuc et al., 1994), induces antinociceptive effects in the mouse through interaction with NTS2 as well as with NTS1 receptors (Dubuc et al., 1999a,b; Tyler et al., 1999; Pettibone et al., 2002; Yamauchi et al., 2003). An intriguing observation is that the sustained, NTS2-mediated activation of ERK1/2 documented here seems to be exerted to the exclusion of other signaling systems. Thus, stimulation of NTS2 does not seem to induce Ca^{2+} mobilization (present study; Sarret et al., 2002) or cAMP or cGMP production (Chalon et al., 1996; Botto et al., 1998). Further studies will obviously be

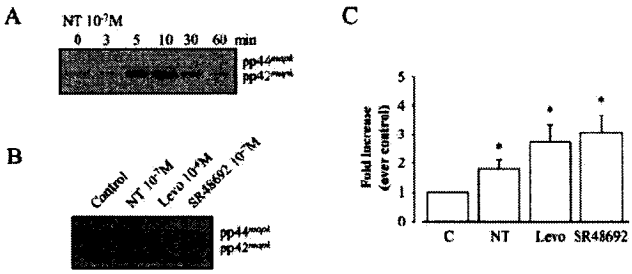

Fig. 5. Effect of neurotensin, levocabastine, and SR48692 on ERK1/2 phosphorylation in CHO/hNTS2 cells. CHO/hNTS2 cells were treated or not for 0 to 60 min with 100 nM NT (A) or for 5 min with a battery of NTS2 agonists (B) and harvested for the determination of ERK1/2 phosphorylation levels as described under *Materials and Methods*. C, densitometric measurements of ERK1/2 activation expressed as -fold increase over control ± S.E.M. (n = 5–7) (ANOVA and Dunnett's). *, $p < 0.001$ compared with control, untreated cells. NT (100 nM), Levo (1 μM), and SR48692 (100 nM) all induce ERK1/2 phosphorylation in CHO/hNTS2 cells.

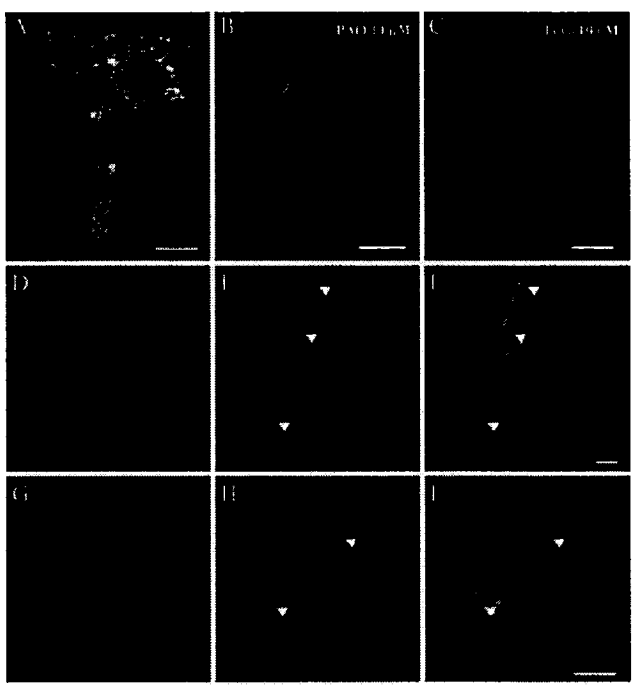

Fig. 6. Role of NTS2 receptor internalization in ligand-induced ERK1/2 activation. A–C, CHO/rNTS2 cells incubated with 50 nM Fluo-NT for 30 min at 37°C and examined by confocal microscopy. A, punctate Fluo-NT labeling is evident throughout the cytoplasm of CHO/rNTS2 cells; B, Fluo-NT labeling is confined to the periphery of the cells in CHO/rNTS2 cells preincubated with the endocytosis inhibitor PAO (10 μM); C, Fluo-NT labeling is specific and receptor-mediated, because the labeling is completely abolished by an excess of levocabastine (10 μM). Images were acquired using the same parameters and represent three different experiments. D–I, CHO/rNTS2 cells transfected with a 10:1 ratio of dynamin 1 (DynK44A) and pEGFP and processed for immunofluorescence detection of phosphorylated ERK1/2. Because of the transfection ratio, most of the EGFP-positive cells (green) can be assumed to express DynK44A. D and G, basal level of phosphorylated ERK1/2 immunoreactivity in nontreated cells. E–H, phosphorylated ERK1/2-immunoreactive signal is evident within the nucleus of a subpopulation of NTS2-expressing cells after 5-min exposure to 100 nM SR48692. F and I, in merged images of phosphorylated ERK1/2- and EGFP-labeled fields, all EGFP-positive (e.g., DynK44A-expressing) cells (white arrows) are phosphorylated ERK1/2-immunonegative, indicating that internalization blockade prevents ERK1/2 activation (representative of three different experiments).

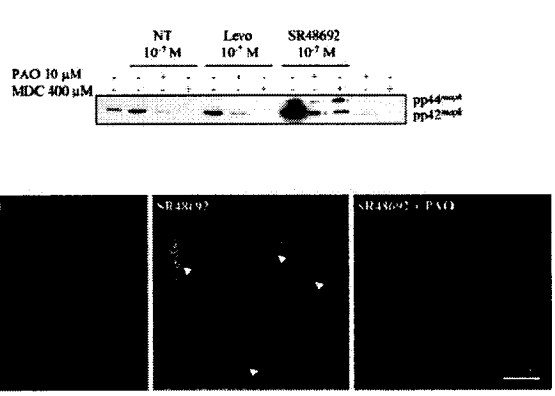

Fig. 7. ERK1/2 activation requires internalization of the NTS2 receptor. A (Western Blot analysis), 30-min preincubation with PAO (10 μM) or MDC (400 μM), two endocytosis inhibitors, prevents NT-, Levo-, and SR48692-induced ERK1/2 phosphorylation (5 min of stimulation) in CHO/rNTS2 cells. Immunoblots represent three different experiments. B (immunofluorescence labeling), 30-min preincubation with PAO (10 μM) prevents immunofluorescence labeling of phosphorylated ERK1/2 in rNTS2-transfected CHO cells treated (100 nM SR48692) for 5 min. Note that ERK1/2 phosphorylation is evident in all cells and that phosphorylated ERK1/2 preferentially accumulates into the nucleus (arrowheads). All images were acquired using the same parameters and represent two different experiments.

needed to determine how diverse NTS2-mediated signals truly are and whether some account, in contrast to those reported here, for short-term NT signaling.

Acknowledgments

We are grateful to Dr. Stephen S. Ferguson for the pcDNA1-DynK44A construction, Dr. Jean-Pierre Vincent for Fluo-NT, and Lyne Bilodeau for her technical assistance with Ca^{2+} imaging.

References

Barroso S, Richard F, Nicolas-Ethève D, Reversat JL, Bernassau JM, Kitabgi P, and Labbé-Jullié C (2000) Identification of residues involved in neurotensin binding and modeling of the agonist binding site in neurotensin receptor 1. *J Biol Chem* **275**:328–336.

Binder EB, Kinkead B, Owens MJ, and Nemeroff CB (2001) Neurotensin and dopamine interactions. *Pharmacol Rev* **53**:453–486.

Botto JM, Chabry J, Sarret P, Vincent JP, and Mazella J (1998) Stable expression of the mouse levocabastine-sensitive neurotensin receptor in HEK 293 cell line: binding properties, photoaffinity labeling and internalization mechanism. *Biochem Biophys Res Commun* **243**:585–590.

Botto JM, Guillemare E, Vincent JP, and Mazella J (1997) Effects of SR 48692 on neurotensin-induced calcium-activated chloride currents in the *X. laevis* oocyte expression system: agonist-like activity on the levocabastine-sensitive neurotensin receptor and absence of antagonist effect on the levocabastine insensitive neurotensin receptor. *Neurosci Lett* **223**:193–196.

Chalon P, Vita N, Kaghad M, Guillemot M, Bonnin J, Delpech B, Le Fur G, Ferrara P, and Caput D (1996) Molecular cloning of a levocabastine-sensitive neurotensin binding site. *FEBS Lett* **386**:91–94.

Claing A, Laporte SA, Caron MG, and Lefkowitz RJ (2002) Endocytosis of G protein-coupled receptors: roles of G protein-coupled receptor kinases and beta-arrestin proteins. *Prog Neurobiol* **66**:61–79.

Dubuc I, Costentin J, Terranova JP, Barnouin MC, Soubrié P, Le Fur G, Rostène W, and Kitabgi P (1994) The nonpeptide neurotensin antagonist, SR 48692, used as a tool to reveal putative neurotensin receptor subtypes. *Br J Pharmacol* **112**:352–354.

Dubuc I, Remande S, and Costentin J (1999a) The partial agonist properties of levocabastine in neurotensin-induced analgesia. *Eur J Pharmacol* **381**:9–12.

Dubuc I, Sarret P, Labbé-Jullié C, Botto JM, Honoré E, Bourdel E, Martinez J, Costentin J, Vincent JP, Kitabgi P, et al. (1999b) Identification of the receptor subtype involved in the analgesic effect of neurotensin. *J Neurosci* **19**:503–510.

Ehlers RA, Bonner RM, Wang X, Hellmich MR, and Evers BM (1998) Signal transduction mechanisms in neurotensin-mediated cellular regulation. *Surgery* **124**:239–246; discussion 246–247.

Ehlers RA, Zhang Y, Hellmich MR, and Evers BM (2000) Neurotensin-mediated activation of MAPK pathways and AP-1 binding in the human pancreatic cancer cell line, MIA PaCa-2. *Biochem Biophys Res Commun* **269**:704–708.

Gendron L, Oligny JF, Payet MD, and Gallo-Payet N (2003) Cyclic AMP-independent involvement of Rap1/B-Raf in the angiotensin II AT2 receptor signaling pathway in NG108-15 cells. *J Biol Chem* **278**:3606–3614.

Gully D, Canton M, Boigegrain R, Jeanjean F, Molimard JC, Poncelet M, Gueudet C, Heaulme M, Leyris R, Brouard A, et al. (1993) Biochemical and pharmacological profile of a potent and selective nonpeptide antagonist of the neurotensin receptor. *Proc Natl Acad Sci USA* **90**:65–69.

Hermans E and Maloteaux JM (1998) Mechanisms of regulation of neurotensin receptors. *Pharmacol Ther* **79**:89–104.

Kalivas PW, Gau BA, Nemeroff CB, and Prange AJ Jr (1982) Antinociception after microinjection of neurotensin into the central amygdaloid nucleus of the rat. *Brain Res* **243**:279–286.

Kinkead B and Nemeroff CB (2002) Neurotensin: an endogenous antipsychotic? *Curr Opin Pharmacol* **2**:99–103.

Kitabgi P, Herve D, Studler JM, Tramu G, Rostène W, and Tassin JP (1989) Neurotensin/dopamine interactions. *Encephale* **15**:91–94.

Kitabgi P, Rostène W, Dussaillant M, Schotte A, Laduron PM, and Vincent JP (1987) Two populations of neurotensin binding sites in murine brain: discrimination by the antihistamine levocabastine reveals markedly different radioautographic distribution. *Eur J Pharmacol* **140**:285–293.

Kranenburg O, Verlaan I, and Moolenaar WH (1999) Dynamin is required for the activation of mitogen-activated protein (MAP) kinase by MAP kinase kinase. *J Biol Chem* **274**:35301–35304.

Labbé-Jullié C, Botto JM, Mas MV, Chabry J, Mazella J, Vincent JP, Gully D, Maffrand JP, and Kitabgi P (1995) [^{3}H]-SR48692, the first nonpeptide neurotensin antagonist radioligand: characterization of binding properties and evidence for distinct agonist and antagonist binding domains on the rat neurotensin receptor. *Mol Pharmacol* **47**:1050–1056.

Martin GE, Bacino CB, and Prupp NL (1980) Hypothermia elicited by the intracerebral microinjection of neurotensin. *Peptides* **1**:333–339.

Martin S, Navarro V, Vincent JP, and Mazella J (2002a) Neurotensin receptor-1 and -3 complex modulates the cellular signaling of neurotensin in the HT29 cell line. *Gastroenterology* **123**:1135–1143.

Martin S, Vincent JP, and Mazella J (2002b) Recycling ability of the mouse and the human neurotensin type 2 receptors depends on a single tyrosine residue. *J Cell Sci* **115**:165–173.

Mazella J, Botto JM, Guillemare E, Coppola T, Sarret P, and Vincent JP (1996) Structure, functional expression and cerebral localization of the levocabastine-sensitive neurotensin/neuromedin N receptor from mouse brain. *J Neurosci* **16**:5613–5620.

Mazella J, Zsürger N, Navarro V, Chabry J, Kaghad M, Caput D, Ferrara P, Vita N, Gully D, Maffrand JP, et al. (1998) The 100-kDa neurotensin receptor is gp95/sortilin, a non-G-protein-coupled receptor. *J Biol Chem* **273**:26273–26276.

Miller WE and Lefkowitz RJ (2001) Expanding roles for beta-arrestins as scaffolds and adapters in GPCR signaling and trafficking. *Curr Opin Cell Biol* **13**:139–145.

Nemeroff CB (1986) The interaction of neurotensin with dopaminergic pathways in the central nervous system: basic neurobiology and implications for the pathogenesis and treatment of schizophrenia. *Psychoneuroendocrinology* **11**:15–37.

Nouel D, Sarret P, Vincent JP, Mazella J, and Beaudet A (1999) Pharmacological, molecular and functional characterization of glial neurotensin receptors. *Neuroscience* **94**:1189–1197.

Petersen CM, Nielsen MS, Nykjaer A, Jacobsen L, Tommerup N, Rasmussen HH, Roigaard H, Gliemann J, Madsen P, and Moestrup SK (1997) Molecular identification of a novel candidate sorting receptor purified from human brain by receptor-associated protein affinity chromatography. *J Biol Chem* **272**:3599–3605.

Pettibone DJ, Hess JF, Hey PJ, Jacobson MA, Leviten M, Lis EV, Mallorga PJ, Pascarella DM, Snyder MA, Williams JB, et al. (2002) The effects of deleting the mouse neurotensin receptor NTR1 on central and peripheral responses to neurotensin. *J Pharmacol Exp Ther* **300**:305–313.

Pierce KL, Maudsley S, Daaka Y, Luttrell LM, and Lefkowitz RJ (2000) Role of endocytosis in the activation of the extracellular signal-regulated kinase cascade by sequestering and nonsequestering G protein-coupled receptors. *Proc Natl Acad Sci USA* **97**:1489–1494.

Poinot-Chazel C, Portier M, Bouaboula M, Vita N, Perceu F, Gully D, Monroe JG, Maffrand JP, Le Fur G, and Casellas P (1996) Activation of mitogen-activated protein kinase couples neurotensin receptor stimulation to induction of the primary response gene Krox-24. *Biochem J* **320 (Pt 1)**:145–151.

Portier M, Combes T, Gully D, Maffrand JP, and Casellas P (1998) Neurotensin type 1 receptor-mediated activation of krox24, c-fos and Elk-1: preventing effect of the neurotensin antagonists SR 48692 and SR 142948. *FEBS Lett* **432**:88–93.

Remaury A, Vita N, Gendreau S, Jung M, Arnone M, Poncelet M, Culouscou JM, Le Fur G, Soubrié P, Caput D, et al. (2002) Targeted inactivation of the neurotensin type 1 receptor reveals its role in body temperature control and feeding behavior but not in analgesia. *Brain Res* **953**:63–72.

Richard F, Barroso S, Martinez J, Labbé-Jullié C, and Kitabgi P (2001) Agonism, inverse agonism and neutral antagonism at the constitutively active human neurotensin receptor 2. *Mol Pharmacol* **60**:1392–1398.

Rioux F, Quirion R, St-Pierre S, Regoli D, Jolicoeur FB, Bélanger F, and Barbeau A

(1981) The hypotensive effect of centrally administered neurotensin in rats. *Eur J Pharmacol* **69**:241–247.
Rostène W and Alexander MJ (1997) Neurotensin and neuroendocrine regulation. *Front Neuroendocrinol* **18**:115–173.
Sarret P, Gendron L, Kilian P, Nguyen HM, Gallo-Payet N, Payet MD, and Beaudet A (2002) Pharmacology and functional properties of NTS2 neurotensin receptors in cerebellar granule cells. *J Biol Chem* **277**:26233–36243.
Sarret P, Perron A, Stroh T, and Beaudet A (2003) Immunohistochemical distribution of NTS2 neurotensin receptors in the rat central nervous system. *J Comp Neurol* **461**:520–538.
Schotte A, Leysen JE, and Laduron PM (1986) Evidence for a displaceable non-specific [^{3}H]neurotensin binding site in rat brain. *Naunyn Schmiedeberg's Arch Pharmacol* **333**:400–405.
Tanaka K, Masu M, and Nakanishi S (1990) Structure and functional expression of the cloned rat neurotensin receptor. *Neuron* **4**:847–854.
Tyler BM, Jansen K, McCormick DJ, Douglas CL, Boules M, Stewart JA, Zhao L, Lacy B, Cusack B, Fauq A, et al. (1999) Peptide nucleic acids targeted to the neurotensin receptor and administered i.p. cross the blood-brain barrier and specifically reduce gene expression. *Proc Natl Acad Sci USA* **96**:7053–7058.
Vincent JP (1995) Neurotensin receptors: binding properties, transduction pathways and structure. *Cell Mol Neurobiol* **15**:501–512.
Vincent JP, Mazella J, and Kitabgi P (1999) Neurotensin and neurotensin receptors. *Trends Pharmacol Sci* **20**:302–309.
Vita N, Laurent P, Lefort S, Chalon P, Dumont X, Kaghad M, Gully D, Le Fur G, Ferrara P, and Caput D (1993) Cloning and expression of a complementary DNA encoding a high affinity human neurotensin receptor. *FEBS Lett* **317**:139–142.
Vita N, Oury-Donat F, Chalon P, Guillemot M, Kaghad M, Bachy A, Thurneyssen O, Garcia S, Poinot-Chazel C, Casellas P, et al. (1998) Neurotensin is an antagonist of the human neurotensin NT2 receptor expressed in Chinese hamster ovary cells. *Eur J Pharmacol* **360**:265–272.
Yamada M, Lombet A, Forgez P, and Rostène W (1996) Distinct functional characteristics of levocabastine sensitive rat neurotensin NT2 receptor expressed in Chinese hamster ovary cells. *Life Sci* **62**:PL375–PL380.
Yamauchi R, Sonoda S, Jinsmaa Y, and Yoshikawa M (2003) Antinociception induced by beta-lactotensin, a neurotensin agonist peptide derived from beta-lactoglobulin, is mediated by NT2 and D1 receptors. *Life Sci* **73**:1917–1923.

Address correspondence to: Dr. Alain Beaudet, Department of Neurology and Neurosurgery, Montreal Neurological Institute, Room 896, 3801 University St., Montreal, Quebec, Canada, H3A 2B4. E-mail: alain.beaudet@mcgill.ca

APPENDIX C

THE JOURNAL OF BIOLOGICAL CHEMISTRY
Vol. 280, No. 11, Issue of March 18, pp. 10219–10227, 2005
Printed in U.S.A.

Identification and Functional Characterization of a 5-Transmembrane Domain Variant Isoform of the NTS2 Neurotensin Receptor in Rat Central Nervous System*

Received for publication, September 14, 2004, and in revised form, December 22, 2004
Published, JBC Papers in Press, January 6, 2005, DOI 10.1074/jbc.M410557200

Amélie Perron‡, Philippe Sarret‡§, Louis Gendron¶, Thomas Stroh, and Alain Beaudet‖

From the Montreal Neurological Institute, Department of Neurology and Neurosurgery, McGill University, Montreal, Quebec H3A 2B4, Canada

The present study demonstrated that alternative splicing of the rat *nts2* receptor gene generates a 5-transmembrane domain variant isoform (vNTS2) that is co-expressed with the full-length NTS2 receptor throughout the brain and spinal cord, as evidenced by reverse transcription-PCR. The vNTS2 polypeptide is 281 amino acids in length, which is 135 amino acids shorter than the full-length isoform. Immunohistochemical and radioligand binding studies revealed that the HA-tagged recombinant vNTS2 receptor is poorly targeted to plasma membranes in transfected COS-7 cells. Binding studies also showed that the truncated receptor displayed a 5000-fold lower affinity for neurotensin (NT) than its full-length counterpart (IC_{50} of 10 μM and 2 nM, respectively). Yet NT binding induced efficient internalization of receptor-ligand complexes in vNTS2-transfected cells. Furthermore, it produced a rapid (<5 min) activation of the mitogen-activated protein kinases (ERK1/2) pathway, indicating functional coupling of the variant receptor. This activation is sustained (>1 h) and is also produced by the NTS2 agonist levocabastine. Western blotting experiments suggested that vNTS2 is not expressed in monomeric form in the rat central nervous system. However, it does appear to form a variety of multimeric complexes, including homodimers and heterodimers, with the full-length NTS2. Indeed, co-immunoprecipitation studies in dually transfected cells demonstrated that the two receptor isoforms can form stable associations. Taken together, the present results indicated that the rat vNTS2 is a functional receptor that may play a role in NT signaling in mammalian central nervous system.

The tridecapeptide neurotensin (NT)[1] produces a wide array of biological responses when administered peripherally or in the central nervous system (CNS). NT effects include analgesia (1, 2), hypothermia (3), antipsychosis (4), catalepsy (5), and change in blood pressure (6). NT is also known for its regulatory role on midbrain dopaminergic and basal forebrain cholinergic neurons (7, 8), and cumulative evidence has implicated the NT system in the pathophysiology of schizophrenia (9).

NT signaling is mediated by interaction of the peptide with either one of three different receptor subtypes, referred to as NTS1, NTS2, and NTS3. NTS1 and NTS2 belong to the family of seven transmembrane-spanning, G protein-coupled receptors (GPCRs) and exhibit high and low affinity for NT, respectively (10, 11). The NTS3 receptor is a single transmembrane domain sorting receptor with 100% homology to gp95/sortilin (12, 13). NTS1 is predominantly coupled to $G_{q/11}$ (14, 15) and activates phospholipase C (16, 17). Pharmacological and biochemical studies have indicated that NTS1 is also involved in the modulation of intracellular levels of cGMP (18), cAMP (19, 20), inositol phosphates (21), and extracellular signal-regulated kinases (ERK1/2) (22). Much less is known about the signaling pathways of NTS2. Stimulation of NTS2 was found to induce Ca^{2+}-dependent chloride currents in *Xenopus* oocytes expressing the mouse receptor (23). More recent studies have shown that stimulation of NTS2 with either NT or the selective NTS2 ligand, levocabastine, activates the ERK1/2 cascade both in CHO cells stably transfected with cDNA encoding rat or human NTS2 (24) or in cultured rat cerebellar granule cells (25).

The cDNA sequence of the mouse NTS2 receptor is composed of four exons separated by three introns (26). The first exon encodes the region containing TM domains 1–4, whereas exons 2–4 encode the region containing TM 5–6, TM 6, and TM 7, respectively. The existence of a deletion-type NTS2 mRNA encoding a C-terminally truncated form of the receptor, which lacks an internal 181-bp sequence, has been reported in the mouse (27). Both mouse NTS2 mRNA isoforms are derived from a single *nts2* gene, the short form resulting from alternative splicing of the primary NTS2 transcript at intron 2a (26). The corresponding truncated NTS2 mRNA encodes a 282-amino acid protein (27).

Other GPCRs encoding sequences have been shown to similarly generate truncated receptor isoforms through alternative splicing, exon skipping, or intron retention (28). Many of these splice variants, such as the truncated forms of the prostanoid

* This work was supported in part by a grant from the Canadian Institutes for Health Research. The costs of publication of this article were defrayed in part by the payment of page charges. This article must therefore be hereby marked "*advertisement*" in accordance with 18 U.S.C. Section 1734 solely to indicate this fact.
‡ Supported by a fellowship from the Fonds de la Recherche en Santé du Québec.
§ Present address: Dept. of Physiology and Biophysics, Faculty of Medicine, University of Sherbrooke, Sherbrooke, Quebec J1H 5N4, Canada.
¶ Supported by a fellowship from the Canadian Institutes for Health Research.
‖ To whom correspondence should be addressed: Montreal Neurological Institute, Dept. of Neurology and Neurosurgery, Rm. 896, 3801 University St., Montreal, Quebec H3A 2B4, Canada. Tel.: 514-398-1913; Fax: 514-398-5871; E-mail: alain.beaudet@mcgill.ca.

[1] The abbreviations used are: NT, neurotensin; GPCR(s), G protein-coupled receptor(s); TM, transmembrane domain; CHO cells, Chinese hamster ovary cells; COS-7 cells, green African monkey kidney cells; MAPK, mitogen-activated protein kinase; ERK1/2, extracellular signal-regulated kinases 1/2; DMEM, Dulbecco's modified Eagle's medium; BSA, bovine serum albumin; HRP, horseradish peroxidase; HA, hemagglutinin; RT, room temperature; CNS, central nervous system; PBS, phosphate-buffered saline; GAPDH, glyceraldehyde-3-phosphate dehydrogenase; MEK, MAPK/ERK kinase; fluo-NT, *Nα*-BODIPY-neurotensin-(2–13).

receptor EP_3 and endothelin B receptor (29, 30), differ from their full-length counterparts in their intracellular C-terminal tail. Others show a disparity in the third intracellular loop (*e.g.* the D_2 dopamine receptor variant (31)) or in the transmembrane (TM) domains (*e.g.* the D_3 dopamine receptor isoform (32)). Yet others differ from the full-length receptor in their extracellular N-terminal loop as exemplified by the truncated form of the angiotensin II receptor (33).

Splice variations may have little or no effect on ligand binding properties (34). However, some deletions, particularly in TM domains, were shown to have significant impact on ligand recognition. For example, a short variant of the 5-hydroxytryptamine 2C receptor lacking TM domains 6 and 7 was reported to be totally devoid of serotonergic binding activity (35). Similarly, the 5-TM domain isoforms of the D_3 and endothelin A receptors exhibit no ligand binding (32, 36). Shortened receptor isoforms may also display aberrant or impaired coupling, even in the face of normal ligand binding. For instance, the four alternatively spliced isoforms of the EP_3 receptor, which vary only in their C-terminal tails, couple to different G proteins and activate diverse second messenger systems (29).

The generation of alternatively spliced GPCRs may also affect the function of their full-length counterparts. Thus, coexpression of the full-length gonadotropin-releasing hormone receptor together with that of its C-terminally truncated isoform, which is incapable of ligand binding and signal transduction, was found to impair targeting of the full-length receptor to the plasma membrane (37). Finally, alternative splicing of GPCRs has been associated with a number of genetic disorders (38). For instance, splice variants of the growth hormone-releasing hormone receptors have been documented in primary human prostate carcinomas and diverse human cancer cell lines (39).

This study was initiated to determine whether the splice variant form of the NTS2 receptor originally identified in mouse brain extracts was also expressed in rat brain and to investigate the binding, internalization, and signaling properties of this receptor isoform, as compared with those of the full-length NTS2 receptor, in mammalian cells. Our results demonstrate the existence of a functional 5-TM domain variant form of NTS2 (vNTS2) in rat brain and suggest that this truncated receptor may play a role in the modulation of NT effects in the CNS.

EXPERIMENTAL PROCEDURES

Expression of Rat vNTS2 mRNA—In order to assess the expression of vNTS2 mRNA in rat CNS and spinal cord, adult male Sprague-Dawley rats (200–250 g, Charles River Breeding Laboratories, St-Constant, Quebec, Canada) were killed by decapitation. The brain and spinal cord were rapidly removed, and the areas of interest were dissected on ice. Samples were solubilized in lysis buffer (4 M guanidinium thiocyanate, 0.01 M Tris-HCl, pH 7.5, 0.97% β-mercaptoethanol), and total RNA was extracted using the SV RNA Isolation System kit (Promega, Madison, WI), according to the manufacturer's instructions. These total mRNAs (2 μg) were then reverse-transcribed at 42 °C for 1 h using the Reverse Transcription System kit (Promega, Madison, WI). First strand cDNAs were subjected to 35 cycles of PCR in a final reaction volume of 50 μl of reaction buffer (50 mM KCl, 10 mM Tris-HCl, pH 9.0, 1.5 mM $MgCl_2$, 0.1% Triton X-100, 0.02% bovine serum albumin (BSA), 200 μM dNTPs, 0.5 unit of TaqDNA polymerase) using a set of primers (5′-GAATGTGCTGGTGTCCTTCGC-3′ and 5′-ACTTGTATTTCTCCCAGGCTG-3′) derived from bases 667–1287 in the sequence reported previously (11) for the rat NTS2 receptor. The oligonucleotides used are flanking the region where the deletion occurs in the mouse vNTS2 receptor (27) and allow the amplification of fragments of predicted sizes of 620 and 439 bp, as demonstrated previously (25) in rat cerebellar granule cell cultures. As internal standard for semi-quantitative analysis, the housekeeping gene glyceraldehyde-3-phosphate dehydrogenase (GAPDH) was concurrently amplified using primers 5′-CAAGATTGTCAGCAATGCAT-3′ (sense, nucleotides 511–530) and 5′-CTTGATGTCATCATACTTGGC-3′ (antisense, nucleotides 856 to 836), which target a 346-bp sequence in the rat GAPDH gene. The ratios of NTS2 over GAPDH mRNAs and between the NTS2 receptor isoforms were determined by densitometry, using NIH Scion Image Software. Calculations and statistical analyses were performed using Excel 2000 (Microsoft) and Prism 3.02 (Graph Pad Software). Statistical analyses were performed using a one-way analysis of variance (Bonferroni's multiple comparison test). Total RNA samples were subjected to reverse transcription in the absence of the enzyme to control for intrinsic contamination by genomic DNA, and the reaction was performed without RNA to control for contamination during the experiment.

Gene Constructs—The HA-tagged cDNA encoding the rat variant NTS2 receptor was obtained through reverse transcription of vNTS2 mRNA isolated from rat brain by PCR using nucleotides (5′-ACAGAGATGGCATACCCATACGACGTCCCAGACTACGCTGAGACCAGCAGTCCGTGG-3′) and (5′-TCATACTTGTATTTCTCCCAGGCT-3′) as sense and antisense primers, respectively. The former contains the HA tag sequence followed by the 44–61-bp sequence of the rat NTS2 receptor mRNA (11), whereas the latter corresponds to the sequence 1268–1291 bp of the open reading frame of the rat *nts2* receptor gene. The predicted sizes of the amplified fragments were 1.6 kb for the full-length NTS2 and 1.4 kb for the spliced variant form of the receptor. Fidelity of PCR amplification was confirmed by DNA sequence analysis using the ABIPRISM® 3100 Genetic Analyzer in the MOBIX laboratory (McMaster University, Hamilton, Ontario, Canada). The PCR product corresponding to vNTS2 was purified from a 1% low melting agarose gel and subcloned into the pTargeT expression vector (Promega, Madison, WI).

Cell Culture and Transfections—For MAPK kinase activity and radioligand binding experiments, CHO and COS-7 cells were stably transfected with the HA-vNTS2 construct. Briefly, cells were maintained at 37 °C in a 5% CO_2 atmosphere in Dulbecco's modified Eagle's medium (DMEM) F-12 and DMEM with high glucose, respectively, supplemented with 5% fetal bovine serum in the presence of 100 units/ml penicillin/streptomycin (Invitrogen). Cells were grown in 100-mm dishes to 70–80% confluence and transfected with 4 μg of the HA-vNTS2-pTargeT plasmid by using the Lipofectamine™ transfection reagent (Invitrogen) according to the manufacturer's instructions. After 72 h at 37 °C, positive cells were selected with a FACSVantage cell sorter (BD Biosciences) following sequential labeling with a mouse monoclonal antibody (clone 12CA5) directed toward the HA epitope (1/500; Roche Applied Science) and Alexa 488-conjugated goat anti-mouse antibody (1/1000; Molecular Probes, Eugene, OR). Stable CHO (for MAPK kinase activity) and COS-7 (for radioligand binding experiments) transfectants were selected in the presence of 500 μg/ml G418.

For Western blotting and immunocytochemistry experiments, COS-7 cells were transiently transfected with 7 ml of a mixture of 100 μM chloroquine and 0.25 mg/ml DEAE-dextran containing 4 μg of plasmid DNA (HA-vNTS2, HA-NTS2 (40), untagged NTS2, or a mixture of HA-vNTS2 and untagged NTS2) in DMEM high glucose. After 2 h at 37 °C, the solution was removed, and the cells were treated for 1 min with 10% dimethyl sulfoxide in phosphate-buffered saline (PBS), rinsed twice with PBS, and returned to the 37 °C incubator in growth medium supplemented with 5% fetal bovine serum.

Immunocytochemistry on COS-7 Cells—To assess the subcellular distribution of vNTS2, COS-7 cells transfected with HA-vNTS2 cDNA were plated on poly-L-lysine-coated glass coverslips, fixed for 20 min with 4% paraformaldehyde (Polysciences, Warrington, PA) in PBS, pH 7.4, and preincubated for 30 min at room temperature (RT) with a blocking solution consisting of 5% normal goat serum, 2% BSA, and 0.1% Triton X-100 (BDH, Toronto, Ontario, Canada) in PBS. Cells were incubated overnight at 4 °C with a polyclonal antibody directed toward the 7–21-amino acid sequence in the N-terminal segment of the rat NTS2 receptor (1/25,000; made on demand by Affinity BioReagents, ABR, Golden, CO), which recognizes both short and long isoforms of the receptor (40), together with a mouse monoclonal antibody (clone 12CA5, 1/500) directed toward the HA epitope in PBS containing 1% normal goat serum and 0.05% Triton X-100. Cells were then incubated for 1 h at RT with a mixture of Alexa 594-conjugated goat anti-rabbit and Alexa 488-conjugated goat anti-mouse antibodies (1/750; Molecular Probes, Eugene, OR). For specificity controls, cells were incubated with anti-NTS2 peptide antiserum preadsorbed with the antigenic peptide.

For cell surface immunolabeling experiments, COS-7 cells expressing the HA-tagged vNTS2 receptor were stained using the Alexa 488-conjugated monoclonal anti-HA IgG (1/500; Molecular Probes, Eugene, OR) in serum-depleted medium for 1 h at 37 °C. Cells were then washed with PBS, fixed with 10% paraformaldehyde for 30 min at RT, and washed again with PBS prior to examination.

For dual immunolocalization of vNTS2 and NTS2, COS-7 cells co-

expressing HA-tagged vNTS2 and the untagged NTS2 were incubated overnight at 4 °C with mouse monoclonal anti-HA antibody in concert with rabbit NTS2 peptide antiserum (1/10,000) in PBS containing 1% NGS and 0.05% Triton X-100. This second NTS2 antiserum is directed toward a synthetic peptide (YSFRLWGSPRNPSLG) corresponding to the 397–412 predicted amino acid sequence in the C-terminal tail of the rat NTS2 receptor (custom-raised by Affinity BioReagents, ABR, Golden, CO) that specifically recognizes the full-length receptor. Cells were then incubated for 1 h at RT with a mixture of Alexa 488-conjugated goat anti-mouse and Alexa 594-conjugated goat anti-rabbit antibodies (1/750; Molecular Probes, Eugene, OR).

Cells were examined with a Zeiss 510 laser-scanning confocal microscope equipped with argon2 (488 nm) and He/Ne1 (543 nm) lasers (Carl Zeiss Micro Imaging Inc., Thornwood, NY). Images were processed using the Zeiss 510 laser-scanning microscope software and Adobe Photoshop 6.0.

Immunoprecipitation and Immunoblotting Analysis—For immunoprecipitation studies, COS-7 cells expressing either the HA epitope-tagged vNTS2 or the untagged full-length NTS2 were lysed in RIPA buffer (150 mM NaCl, 50 mM Tris-HCl, pH 7.5, 5 mM EDTA, 1% IGEPAL, 0.5% deoxycholic acid, 0.1% SDS) containing protease inhibitors (Complete™ inhibitor tablets; Roche Applied Science) and incubated for 30 min on ice. Lysates were then precleared with 5 mg of protein A-Sepharose (Sigma) for 45 min at 4 °C and incubated overnight at 4 °C with a rat monoclonal antibody (clone 3F10) directed toward the HA epitope (1/400; Roche Applied Science). The protein A-Sepharose was gently shaken in lysis buffer containing 1% BSA for 30 min at RT before use. Receptor proteins were immunoprecipitated with 3 mg of protein A-Sepharose for 2 h at 4 °C. Complexes were dissolved in Laemmli sample buffer (41) and resolved by using 10% Tris-glycine precast gels (Invitrogen). Nonspecific sites were blocked by 0.1% Tween 20 (EMD Chemicals Inc., Gibbstown, NJ) and 10% milk powder (Carnation, Don Mills, Ontario, Canada) in PBS overnight at 4 °C. Nitrocellulose membranes were then incubated with rabbit N-terminally directed NTS2 antibody (1/10,000) overnight at 4 °C, followed by horseradish peroxidase (HRP)-conjugated goat anti-rabbit antibody for 1 h at RT (1/4000; Amersham Biosciences). Specificity of antiserum was confirmed by preadsorption of the NTS2 antibody overnight with an excess of immunizing peptide (2 μg/ml of adsorbing peptide at a final antibody dilution of 1/10,000).

For cell surface labeling experiments, COS-7 cells expressing HA-vNTS2 or co-expressing HA-vNTS2 and untagged full-length NTS2 were washed with ice-cold PBS and incubated with the N-terminally directed NTS2 peptide antiserum (1/10,000) in PBS containing 0.5% BSA for 2 h at RT. Cells were then washed three times with PBS and transferred into 1.5-ml Eppendorf tubes. They were treated with 100 μl of RIPA buffer for 1 h at 4 °C, lysed, and centrifuged at 12,500 rpm at 4 °C for 30 min. The supernatants were incubated with protein A-Sepharose for 2 h at 4 °C to immunoprecipitate antibody-bound cell surface receptors. Immunoprecipitates were processed as described above. Membranes were probed with rabbit N-terminally directed NTS2 antibody (1/2000), followed by a 1-h incubation with HRP-conjugated goat anti-rabbit antibody (1/4000; Amersham Biosciences).

For heterodimerization experiments, COS-7 cells expressing the HA epitope-tagged vNTS2 together with the untagged full-length NTS2 were treated as described above. Receptor proteins were immunoprecipitated using the rat anti-HA antibody (clone 3F10; 1/400), and immunoblotting was then carried out with the N-terminally or C-terminally directed NTS2 antisera (1/10,000).

To determine which molecular forms of the vNTS2 protein are expressed in rat CNS, Western blotting experiments were performed on membranes from rat spinal cord, as this structure had been shown previously (27) to express among the highest levels of vNTS2 mRNA in the mouse. Rat spinal cord membrane preparations were obtained as described previously (40). Approximately 70 μg of protein from each sample were loaded onto 8% Tris-glycine gels and transferred to nitrocellulose membranes for immunoblotting. Membranes were incubated with the affinity-purified N-terminal specific anti-NTS2 rabbit antibody (1/1250) overnight at 4 °C in PBS containing 1% ovalbumin and 1% BSA, followed by HRP-conjugated anti-rabbit secondary antibody in PBS with 5% milk powder. Specificity of antiserum was confirmed by preadsorption with the antigenic peptide.

Receptor Binding Experiments—For radioactive ligand binding experiments, COS-7 cells expressing HA-vNTS2 were grown on 24-well plates and incubated at 37 °C in DMEM high glucose medium for 72 h before the assay. Cells were equilibrated for 10 min at 37 °C in Earle's buffer (130 mM NaCl, 5 mM KCl, 1.8 mM $CaCl_2$, 0.8 mM $MgCl_2$, HEPES 20 mM, pH 7.4) supplemented with 0.2% BSA and 0.1% glucose and incubated with 0.4 nM ^{125}I-labeled NT (1670 Ci/mmol) for 30 min at 37 °C in 250 μl of Earle's buffer containing 0.8 mM *ortho*-phenanthroline in the presence of increasing concentrations (from 10^{-10} to 10^{-3} M) of nonradioactive NT. The cells were then washed twice with Earle's buffer and harvested in 1 ml of 0.1 M NaOH, and the radioactivity content was measured in a gamma counter. IC_{50} values were determined from competition curves as the concentration of unlabeled ligand necessary to inhibit 50% of ^{125}I-labeled NT-specific binding. Nonspecific binding was defined as binding in the presence of a 10,000-fold excess of unlabeled ligand, which represented less than 1% of total counts.

For fluorescent ligand labeling, COS-7 cells expressing the HA epitope-tagged vNTS2 were grown on poly-L-lysine-treated glass coverslips and incubated at 37 °C in DMEM high glucose medium for 24 h. They were then equilibrated for 10 min at 37 °C in Earle's buffer containing 0.2% BSA and 0.1% glucose in the presence or in the absence of 10 μM phenylarsine oxide, an endocytosis inhibitor, and incubated for 30 min in the same buffer with 50 nM of *Na*-BODIPY-NT-(2–13) (Fluo-NT) in the presence or absence of 1 mM nonfluorescent NT. Cells were air-dried, mounted on glass slides with Aquamount (Polysciences, Warrington, PA), and examined by confocal microscopy as described above.

Measurement of MAP Kinase Activity—CHO cells stably expressing HA-tagged vNTS2 were split into 6-well plates and incubated for 1–2 days in DMEM-F-12 at 37 °C. Cells were then serum-starved overnight, pretreated or not with MEK inhibitors PD98059 (50 μM) (New England Biolabs, Beverly, MA) or U0126 (10 μM) (Promega, Madison, WI) for 30 min, and incubated with NT (0.1–10 μM) or levocabastine (1 μM) at 37 °C for the indicated times. The reaction was stopped by aspiration of the medium and the addition of ice-cold PBS containing 0.1 μM staurosporine and 1 mM sodium orthovanadate. After 30 min of incubation on ice, cells were lysed in 50 mM HEPES, pH 7.8, containing 1% Triton X-100, 0.1 μM staurosporine, 1 mM sodium orthovanadate, and protease inhibitors. Cell lysates were then centrifuged at 12,500 rpm for 10 min at 4 °C, and the supernatants were stored at −20 °C until use. Parallel experiments were done using untransfected cells to determine the specificity of the assay. Protein concentration was determined by the Bio-Rad procedure with BSA as standard. Samples containing 40 μg of protein were denatured in Laemmli sample buffer (41), resolved using 10% Tris-glycine precast gels, and transferred to nitrocellulose membranes (Bio-Rad). Nitrocellulose membranes were incubated overnight at 4 °C with anti-phosphorylated ERK1/2 or anti-ERK1/2 rabbit antibodies (1/1000; New England Biolabs) in PBS containing 1% ovalbumin and 1% BSA. Detection of immunoreactive proteins was accomplished by using HRP-conjugated anti-rabbit and an enhanced chemiluminescent detection system (PerkinElmer Life Sciences). To quantify the effect of NT on ERK1/2 phosphorylation, the ratios of phosphorylated ERK1/2 over total ERK1/2 levels were determined by densitometry, using NIH Scion Image software. Calculations and statistical analyses were performed using Excel 2000 (Microsoft) and Prism 3.02 (Graph Pad Software). The statistical significance of the activation of ERK1/2 between transfected and nontransfected cells was verified using the paired *t* test, and *p* values were obtained from Dunnett's tables.

RESULTS

Expression of NTS2 Receptor mRNAs in the CNS—In order to assess expression patterns of NTS2 mRNAs in rat brain and spinal cord, a set of oligonucleotide primers designed to selectively recognize the region flanking the deletion yielding vNTS2 in the mouse (27) was used for reverse transcription-PCR. As shown in Fig. 1, PCR amplification of total mRNAs yielded two bands of 620 and 439 bp, corresponding to the expected sizes of NTS2 and vNTS2 receptor fragments, respectively, in all regions examined. No signal was detected when transcribed products from homogenates were amplified with either one of the sense or antisense primers alone (not shown). Semi-quantitative analyses performed using GAPDH as an internal correction standard indicated that mRNA levels for either of the two isoforms, and hence the ratio of vNTS2 over NTS2, were not statistically different between the various regions examined (Table I).

Isolation and Molecular Characterization of the Rat NTS2 Receptor Variant Isoform—Rat vNTS2 receptor cDNA was isolated from brain tissue by reverse transcription-PCR, using a pair of sense and antisense primers corresponding to the open reading frame of the full-length NTS2 receptor. The specificity

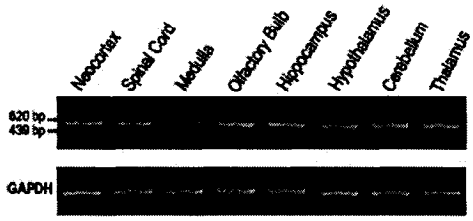

FIG. 1. **Reverse transcription-PCR analysis of NTS2 mRNAs.** Amplification of NTS2 and vNTS2 mRNAs was from various brain regions. PCRs were performed on mRNAs reverse-transcribed using primers flanking the truncated portion of NTS2. The expected sizes of the reverse transcription-PCR products were 620 and 439 bp for the full-length and spliced form of NTS2, respectively. The housekeeping gene GAPDH was also amplified and used as an internal control for semi-quantitative analyses.

TABLE I
Densitometric analysis of the regional expression of vNTS2 and NTS2 mRNAs in the rat CNS

Values represent means ± S.E. of four independent experiments. No regional difference in the expression of either isoforms is detectable ($p > 0.05$, one-way analysis of variance, Bonferroni's multiple comparison test).

Structure	Receptor to GAPDH ratio		vNTS2/NTS2
	vNTS2	NTS2	
	arbitrary units		
Neocortex	0.91 ± 0.15	0.99 ± 0.07	0.92 ± 0.15
Spinal cord	0.93 ± 0.10	1.06 ± 0.01	0.88 ± 0.11
Medulla	0.93 ± 0.10	1.03 ± 0.05	0.91 ± 0.13
Olfactory bulb	0.98 ± 0.10	1.15 ± 0.08	0.88 ± 0.14
Hippocampus	0.91 ± 0.12	1.21 ± 0.13	0.78 ± 0.16
Hypothalamus	1.09 ± 0.14	1.28 ± 0.17	0.89 ± 0.14
Cerebellum	0.73 ± 0.12	0.87 ± 0.05	0.83 ± 0.15
Thalamus	0.90 ± 0.09	1.17 ± 0.12	0.81 ± 0.14

of the amplification was verified by agarose gel electrophoresis, which revealed two bands of the expected size (full-length = 1251 bp; variant isoform = 1070 bp) (not shown). The nucleic acid sequence of vNTS2 was identical to that of the full-length NTS2 with the exception of a 181-nucleotide deletion corresponding to NTS2 base pairs 760–940. It is worth noting that the nucleotide sequence of the 5′-part of the truncated receptor shares high homology with the consensus sequence of vertebrate splice donor-acceptor sites (42). The deletion causes a frameshift in the open reading frame, leading to a premature stop codon. The short form of the rat NTS2 contains 281 amino acids, instead of 416 for the long form (Fig. 2*A*). It shows a global amino acid sequence homology of 79.9 and 77.4% with its full-length counterpart and the mouse spliced NTS2 isoform, respectively. Hydrophobicity analysis, performed according to the method of Kyte and Doolittle (BioEdit version 5.0.6), indicated that vNTS2 is a 5-transmembrane domain receptor with an intracellular C-terminal tail. The resulting protein is devoid of the last two transmembrane domains of the full-length NTS2 receptor and contains 37 unique C-terminal amino acids (Fig. 2*B*). The C-terminal domain of the variant isoform is rich in cysteine and methionine residues.

Expression of vNTS2 in COS-7 Cells—In order to investigate the pharmacological and functional properties of rat vNTS2, we established a COS-7 cell line stably expressing an HA epitope-tagged vNTS2 receptor, using cDNA transfection. Immunohistochemical analysis revealed that within these cells, the bulk of immunoreactive receptors, visualized using either HA (Fig. 3, *A* and *C*) or NTS2 N-terminally directed antibodies (Fig. 3*B*), was intracellular and concentrated in a Golgi-like structure surrounding the nucleus. No immunofluorescence signal was detected in nontransfected cells or in cells incubated in the

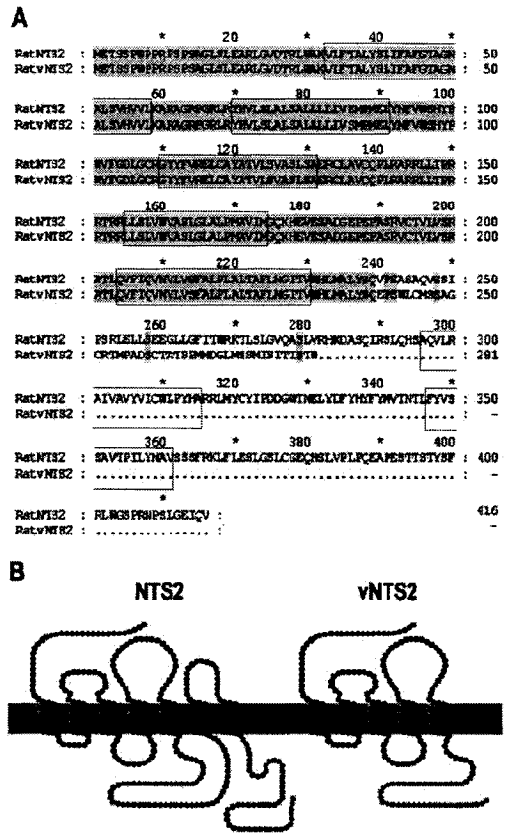

FIG. 2. **Comparison of rat full-length and variant NTS2 isoform sequences.** *A*, alignment of rat NTS2 isoform sequences. Identical sequences found in NTS2 receptor isoforms are *shaded*, and the putative transmembrane segments are *boxed*. Gaps for alignment are indicated by *dots*. The short form of NTS2 contains 281 amino acids, instead of 416 for the long form. The resulting protein is devoid of the last two transmembrane domains and contains 37 unique C-terminal amino acids. *B*, schematic representation of the secondary structure of NTS2 receptors. Common amino acids are shown in *black*. Unique amino acid residues in the sequence of NTS2 and vNTS2 are represented in *hatched* and *gray*, respectively.

absence of primary antibodies (data not shown). Preincubation of the NTS2 antiserum with its antigenic peptide completely abolished NTS2 immunolabeling (Fig. 3*D*) without affecting the HA epitope staining (Fig. 3*C*). Surface labeling studies on nonpermeabilized cells indicated that vNTS2 was poorly expressed on the cell surface (data not shown).

To confirm that the immunoreactive protein expressed in transfected cells corresponded to the variant receptor, lysates from COS-7 cells expressing the HA epitope-tagged vNTS2 receptor were immunoprecipitated with the anti-HA antibody. Immunoblotting using the NTS2 peptide antiserum revealed the presence of two distinct translation products as follows: one of ~32 kDa, corresponding to the monomeric form of the receptor as deduced from its cDNA sequence, and another of ~60 kDa, *i.e.* of the size of putative vNTS2 homodimers (Fig. 3*E*, *lane 1*). By contrast, in control COS-7 cells expressing the full-length receptor, immunoreactive bands were detected at 46 kDa, as well as around 80–85 kDa, corresponding to the size of monomeric and dimeric forms of the full-length receptor, re-

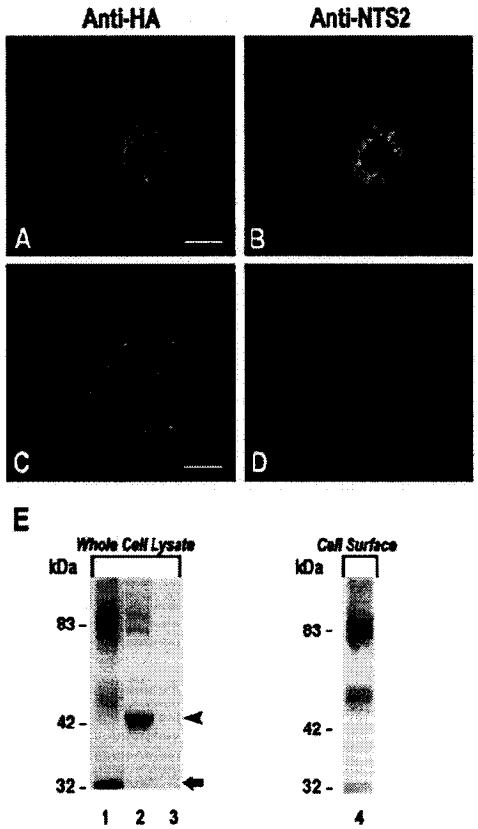

FIG. 3. **Expression of vNTS2 receptor protein in transfected COS-7 cells.** *A–D*, dual immunolabeling of COS-7 cells transfected with cDNA encoding the HA epitope-tagged vNTS2 receptor. Staining for the HA epitope (*A*) co-localizes with NTS2 immunolabeling (*B*), confirming recognition of the vNTS2 by the NTS2 antiserum. Preadsorption of NTS2 antiserum with its antigenic peptide completely abolishes NTS2 immunolabeling (*D*) in cells expressing the epitope-tagged receptor (*C*). *Scale bar*, 10 μm in *A* and *B*; 5 μm in *C* and *D*. *E*, Western blotting analysis of NTS2 receptor isoforms. Immunoprecipitation with HA antibody and blotting with N-terminally directed NTS2 antiserum of homogenates from transfected COS-7 cells (*lane 1*, COS-7/HA-vNTS2; *lane 2*, COS-7/HA-NTS2; *lane 3*, untransfected cells). In cells transfected with vNTS2, specific immunoreactive bands are evident at 32 and 60 kDa, corresponding to the molecular weights of monomeric and dimeric forms of vNTS2. The same bands were detected in cell surface labeling experiments using the N-terminally directed NTS2 antiserum (*lane 4*). In cells transfected with the full-length NTS2, immunoreactive bands are visible at 46 and 83 kDa, corresponding to the molecular weights of monomeric and dimeric forms of NTS2. *Arrow* and *arrowhead* represent the monomeric isoform of vNTS2 and NTS2, respectively. No specific band is evident in nontransfected cells (*lane 3*).

spectively (40) (Fig. 3*E*, *lane 2*). No specific bands were evident in homogenates prepared from nontransfected cells (Fig. 3*E*, *lane 3*).

To determine whether any particular molecular form of the receptor was targeted to the cell surface, COS-7 cells expressing the HA epitope-tagged vNTS2 were incubated for 2 h with the N-terminally directed NTS2 peptide antiserum, and antibody-bound cell surface receptors were separated from unbound cytoplasmic receptors by using protein A-Sepharose beads. Immunoblotting was then performed by using the NTS2 antiserum. As seen in Fig. 3*E*, *lane 4*, the cell surface fraction contained the same two forms (32 and 60 kDa) as fractions from whole cells.

Binding and Internalization Properties of vNTS2—To determine the binding properties of the short NTS2 isoform, COS-7 cells stably expressing vNTS2 were incubated with 0.4 nM ^{125}I-labeled NT for 30 min at 37 °C with increasing concentrations of nonradioactive NT. As shown in Fig. 4*A*, unlabeled NT inhibited specific ^{125}I-labeled NT binding with an IC_{50} value of 10 μM (Fig. 4*A*). No specific ^{125}I-labeled NT binding was observed in nontransfected cells (data not shown).

In order to visualize NT binding and internalization, COS-7 cells expressing vNTS2 were incubated for various periods of time with 50 nM Fluo-NT at 37 °C and were examined by confocal microscopy (Fig. 4, *B–D*). Following 30 min of incubation with the fluorescent ligand, punctate fluorescent labeling was evident throughout the cytoplasm of transfected cells, sparing the nucleus (Fig. 4, *B* and *C*). No fluorescent labeling was visible in nontransfected cells (not shown) or in transfected cells incubated with an excess of NT (Fig. 4*D*). When the incubation was carried out in the presence of the endocytosis inhibitor phenylarsine oxide, bound fluorescent molecules remained clustered on the cell surface (data not shown).

Signaling Properties of vNTS2—We then investigated whether the truncated form of the rat NTS2 receptor retained the MAPK activation (ERK1/2 pathway) properties exhibited by the long form of the receptor (24). Stimulation with NT of CHO cells stably expressing the rat vNTS2 induced the phosphorylation of ERK1/2 (p42/44^{mapk}) starting at concentrations of 1 μM (Fig. 5*A*). Time course studies in which the cells were stimulated for 1–60 min with 1 μM NT showed this effect to be rapid (<5 min) and sustained (over 1 h) (Fig. 5*B*). Densitometric analysis of the ratio of phosphorylated ERK1/2 over total ERK1/2 levels indicated that the NT-induced increase in MAPK phosphorylation was 1.4 ± 0.1-fold and reached a plateau after 15 min of stimulation (Fig. 5*C*, ●). This effect was vNTS2-mediated, as it was not observed in nontransfected cells (Fig. 5*C*, ○). A similar activation was observed following 10 min of stimulation with the NTS2 agonist levocabastine (1 μM; Fig. 5*D*). Pretreatment with selective MAP kinase kinase (MEK) inhibitors (PD98059 or U0126) significantly inhibited NT-mediated ERK1/2 phosphorylation in these cells (Fig. 5*E*).

Heterodimerization of NTS2 Receptors—In rat spinal cord membrane preparations immunoblotted with the N-terminally directed NTS2 antiserum (which recognizes both NTS2 isoforms; Fig. 6*A*), a prominent band was evident at 46 kDa, corresponding to the molecular weight of the monomeric form of the full-length NTS2 receptor detected in transfected COS-7 cells (compare Fig. 6*A* with Fig. 3*E*, *lane 2*). Surprisingly, no band was visible at 32 kDa, *i.e.* at the size expected for the monomeric form of the truncated receptor (*e.g.* Fig. 3*E*, *lane 1*). However, as in COS-7 transfected with the HA-vNTS2 (Fig. 3*E*, *lane 1*), an immunoreactive band was detected at 60 kDa, corresponding to the size of putative vNTS2 homodimers (Fig. 6*A*). An additional band was also observed at 75–85 kDa (Fig. 6*A*, *asterisk*), which might correspond to vNTS2/NTS2 heterodimers. All of these bands were absent when the antibody was pre-saturated with the immunizing peptide (not shown).

To investigate whether the species of NTS2 receptors detected at the 75–85-kDa molecular weight mark could correspond to vNTS2/NTS2 heterodimers, we co-expressed HA-tagged vNTS2 together with untagged NTS2 receptors in COS-7 cells and subjected cell lysates to Western blotting analysis. As shown in Fig. 6*B*, both monomeric and putative homodimeric forms of variant (32 and ~60 kDa, *arrows*) and full-length (46 and ~85 kDa, *arrowheads*) NTS2 receptors were detected using the N-terminally directed NTS2 peptide anti-

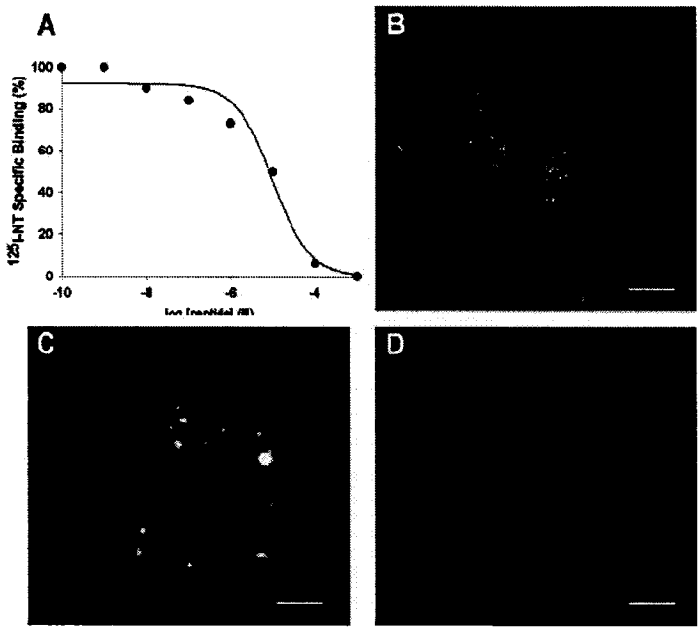

FIG. 4. **Binding and internalization of NT in COS-7 cells expressing vNTS2.** *A*, competition inhibition of ^{125}I-labeled NT binding to whole COS-7 cells stably expressing vNTS2. Cells were incubated with 0.4 nM ^{125}I-labeled NT for 30 min at 37 °C with increasing concentrations of nonradioactive NT. Binding IC_{50} = 10 μM. The results are representative of three independent experiments. *B* and *C*, confocal microscopic imaging of fluo-NT internalization in COS-7 cells expressing vNTS2. Cells were incubated for 30 min at 37 °C with 50 nM fluo-NT and air-dried. Internalized fluorescent ligand molecules are detected in the form of small endosome-like particles distributed throughout the cytoplasm. *D*, fluo-NT labeling is prevented when the incubation is performed in the presence of an excess of nonfluorescent NT. *Scale bar*, 10 μm in *B*; 5 μm in *C* and *D*.

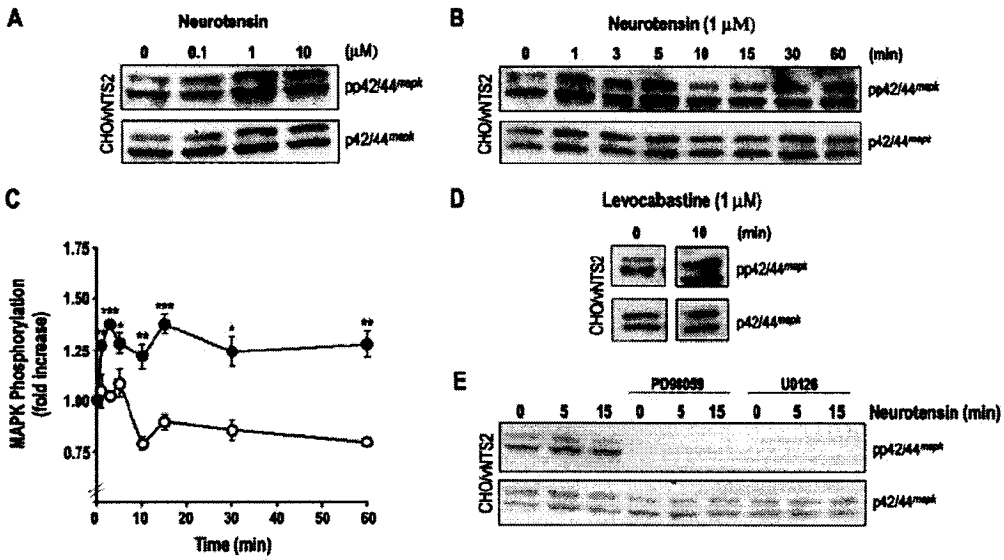

FIG. 5. **MAPK kinase signaling in CHO cells heterologously expressing vNTS2.** *A*, dose-dependent effect of NT on MAPK (ERK1/2) phosphorylation. Cells were treated for 5 min with the indicated concentrations of NT. Phosphorylation levels of MAPK were detected by immunoblotting as described under "Experimental Procedures." *Upper panels* of *A*, *B*, *D*, and *E*, phosphorylated ERK1/2; *lower panels*, total ERK1/2. *B*, time course of NT-stimulated MAPK phosphorylation in CHO cells stably expressing vNTS2. *C*, densitometric analysis of the ratio of phosphorylated ERK1/2 over total ERK1/2 levels following incubation with 1 μM of NT. Untransfected (○) and vNTS2-expressing (●) CHO cells were incubated at 37 °C for the indicated times. Values represent the means ± S.E. of five independent experiments. Transfected cell values are significantly different from nontransfected cell values at all time points as follows: *, $p \leq 0.05$; **, $p \leq 0.01$; and ***, $p \leq 0.001$. *D*, ERK1/2 phosphorylation levels in vNTS2-expressing CHO cells stimulated with levocabastine for 10 min at 37 °C. *E*, MEK inhibitors prevent ERK1/2 activation by NT in CHO cells expressing vNTS2. Cells were pretreated with PD98059 (50 μM) or U0126 (10 μM) and treated with NT (1 μM) for 5–15 min at 37 °C. The results are representative of three individual experiments, each with duplicate determinations.

serum. An immunoreactive band was also observed at the ~75-kDa mark (*asterisk*), consistent with the theoretical molecular weight of a vNTS2/NTS2 heterodimer.

Cell lysates were then subjected to immunoprecipitation with the rat anti-HA antibody. Immunoblotting of these immunoprecipitates with the N-terminally directed NTS2 antiserum

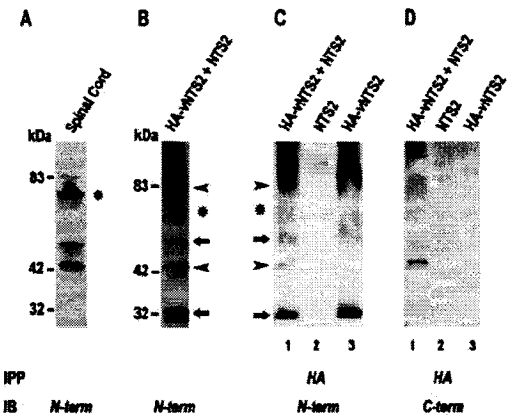

FIG. 6. **Characterization of vNTS2/NTS2 heterodimers by co-immunoprecipitation.** Immunoblotting (*IB*) analysis of NTS2 receptors in spinal cord membrane preparations (*A*) and in COS-7 cells co-expressing NTS2 and HA-vNTS2 (*B*) using a N-terminally directed NTS2 antibody. *C* and *D*, co-immunoprecipitation (*IPP*) studies on COS-7 cells heterologously expressing NTS2 (*lanes 2*), HA-vNTS2 (*lanes 3*), or a combination of both (*lanes 1*). Cells were lysed and subjected to immunoprecipitation with rat anti-HA antibody. The co-immunoprecipitates were then immunoblotted using N-terminally (*C*) or C-terminally (*D*) directed NTS2 peptide antisera as described under "Experimental Procedures." Molecular mass markers are shown to the left of *A* and *B*. Molecular masses for *B* also apply for *C* and *D*. Each illustrated blot is representative of three independent experiments. *Arrows* and *arrowheads* represent isoforms of vNTS2 and NTS2, respectively. *Asterisks* represent the putative vNTS2/NTS2 heterodimer.

showed that they contained HA-tagged vNTS2 as well as untagged NTS2 receptors, suggesting that long and short forms of NTS2 receptors physically interact (Fig. 6*C*, *lane 1*). Indeed, immunoreactive bands were detected at both 32 and 46 kDa, *i.e.* at the molecular weights of the monomeric forms of the variant and full-length receptors, as well as at ~60 kDa, corresponding to the presumptive homodimeric isoform of vNTS2 (Fig. 6*C*, *lane 1*). Higher molecular weight bands (~75 and ~110 kDa) were also evident, which may represent heteromultimeric forms of NTS2 receptors. Immunoreactive bands corresponding to monomeric and putative homodimeric forms of vNTS2 (32 and 65 kDa, respectively) were also detected in COS-7 cells transfected with the HA-vNTS2 cDNA alone (Fig. 6*C*, *lane 3*). However, no specific bands were observed in cells expressing the full-length NTS2 alone (Fig. 6*C*, *lane 2*).

Immunoprecipitates were also subjected to Western blotting analysis using the C-terminally directed NTS2 antiserum, which selectively recognizes the full-length NTS2. This antibody revealed the presence of the full-length isoform in co-transfected cells subjected to immunoprecipitation with the HA antibody, confirming that NTS2 interacts physically with vNTS2 (Fig. 6*D*, *lane 1*). No bands were detected with the C-terminally directed NTS2 peptide antiserum in immunoprecipitates from COS-7 cells expressing either NTS2 (Fig. 6*D*, *lane 2*) or HA-vNTS2 (Fig. 6*D*, *lane 3*) alone, confirming the specificity of the interaction.

To investigate whether vNTS2/NTS2 heterodimerization influenced trafficking of the truncated receptor to the cell surface, COS-7 cells co-expressing the HA epitope-tagged vNTS2 and the untagged full-length NTS2 were incubated for 2 h with the N-terminally directed NTS2 peptide antiserum, and antibody-bound cell surface receptors were separated from unbound cytoplasmic receptors by using protein A-Sepharose beads. Immunoblotting was then performed using the mouse anti-HA antibody. As seen in Table II, the density of both low (monomers) and high (dimers and multimers) molecular weight forms detected in the cell surface fraction (22 ± 2, 26 ± 3, and 52 ± 4%, respectively) was the same as in the cell fraction from cells transfected with vNTS2 alone (21 ± 2, 28 ± 4, and 51 ± 6%, correspondingly). Confocal microscopy confirmed that as in COS-7 cells transfected with vNTS2 alone (Fig. 3), the bulk of vNTS2 immunoreactivity in COS-7 co-expressing NTS2 and HA-vNTS2 was intracellular (Fig. 7*B*). Predictably, vNTS2 and NTS2 immunoreactive intracellular stores closely overlapped, in keeping with their demonstrated heterodimerization (Fig. 7, *A–C*).

TABLE II
Densitometric analysis of the effect of NTS2 expression on cell surface expression of HA-vNTS2

The relative intensity of HA-vNTS2 is expressed as percent of total surface receptor (monomer + dimer + multimer) immunoreactivity. Values represent the means ± S.E. of four independent experiments.

	HA-vNTS2 isoforms		
	Monomer	Dimer	Multimer
	%	%	%
HA-vNTS2	21 ± 2	28 ± 4	51 ± 6
HA-vNTS2 + NTS2	22 ± 2	26 ± 3	52 ± 4

DISCUSSION

In this study, we have demonstrated the presence of an alternatively spliced form of the NTS2 receptor mRNA in rat brain, comparable with the one previously identified in the mouse (27). Most importantly, we have shown that this 5-transmembrane domain truncated receptor protein is functional, in that it specifically binds and internalizes NT and is coupled to the activation of the ERK1/2 pathway.

Alternative splicing is a frequent occurrence in mammalian gene expression, contributing both to proteome diversity and to functional complexity of genomes by generating structurally distinct isoforms from a single gene (43). Nucleic acid sequence analysis demonstrated that the vNTS2 isoform results from a 181-bp deletion in the full-length cDNA that leads to a frame-shift in the reading frame, introducing a premature stop codon. The sequence of the cDNA fragment isolated showed partial sequence overlap with the previously published rat full-length NTS2 sequence (11), indicating that vNTS2 was indeed generated by alternative splicing from a donor-acceptor splice site as suggested by Sun *et al.* (26). This type of processing does not appear to be regionally selective because mRNA levels and ratios of the two isoforms did not vary significantly between the different regions examined.

Western blotting analysis of COS-7 cells transfected with cDNA encoding an HA-tagged rat vNTS2 revealed the presence of distinct translation products of ~32 and 60 kDa. The former corresponds to the molecular weight of the monomeric form of vNTS2 as deduced from its cDNA sequence, whereas the latter likely represents a homodimeric form of the receptor. Immunocytochemistry revealed that the bulk of these vNTS2 proteins were intracellular. This observation is in agreement with the results of subprograms executed by the PSORT II server (Kenta Nakai, Human Genome Center, Institute for Medical Science, University of Tokyo, Japan), which predict the subcellular localization of vNTS2 from its amino acid sequence in the endoplasmic reticulum (44.4%), intracellular vacuoles (22.2%), Golgi apparatus (11.1%), plasma membrane (11.1%), and mitochondrial compartments (11.1%). Both immunoblotting and immunocytochemical experiments suggest that the vNTS2 receptor is poorly targeted to plasma membranes. However, this restricted targeting does not appear to be linked to the molec-

FIG. 7. **Double immunolabeling of COS-7 cells co-expressing NTS2 and HA-vNTS2.** Staining with the C-terminally directed NTS2 antiserum (*A*), which exclusively recognizes the long isoform, co-localizes with immunoreactivity for the HA epitope (*B*) in co-transfected cells, as evident in the overlay (*C*).

ular species recruited to the membrane because both low (monomeric) and high (putative dimeric) molecular weight forms were detected at the cell surface.

Despite its short transmembrane span, the rat vNTS2 still specifically binds ^{125}I-labeled NT, albeit with a considerably lower affinity than the full-length receptor (IC_{50} of 10 μM *versus* 2 nM, for the full-length isoform). This result differs from those of Botto *et al.* (27), who found no specific binding of ^{125}I-labeled NT to mouse vNTS2 transiently expressed in COS-7 cells. This discrepancy may be explained by species differences, by variations in the sensitivity of the methods employed, or by the nature of the expression system. Indeed, stable transfectants might express higher levels and/or recruit more efficiently vNTS2 to the membrane than transiently transfected cells. Previous studies have shown that NT binding to rat NTS1 and human NTS2 receptors involved residues located in TM 6 and in the third intracellular loop (44, 45). These residues are lost in the variant isoform, due to the splicing of the last two TM domains of NTS2, which may explain the lower affinity of vNTS2 for NT as compared with the full-length receptor.

Confocal microscopic experiments demonstrated specific, receptor-mediated internalization of fluorescent NT. The internalized ligand was concentrated within small endosome-like organelles, a pattern consistent with earlier reports (24, 46) on internalization via the full-length NTS2 receptor. This finding suggested to us that the NTS2 variant isoform was functionally responsive to NT, as confirmed by MAPK activation experiments.

Stimulation with NT induced a rapid and sustained increase in ERK1/2 phosphorylation in CHO cells transfected with vNTS2, indicating functional coupling of the truncated receptor to the MAPK signaling pathway. Stimulation of these cells with the NTS2-specific agonist levocabastine also resulted in ERK1/2 activation. The time course of ERK1/2 activation corresponded to that observed following stimulation of the full-length receptor in a similar transfection system (24). Activation of ERK1/2 was already apparent at concentrations of NT lower than the IC_{50} (1 μM), in keeping with the detection of ligand-induced internalization at concentrations of fluo-NT of 50 nM. However, phosphorylation levels obtained following stimulation with 1 μM NT were lower in cells transfected with the vNTS2 than with the full-length receptor (1.4 *versus* 2.9-fold increase over control (24)). They were also lower than those produced in cultured rat cerebellar granule cells, which endogenously express the two NTS2 isoforms (25). These results suggest that the third intracellular loop and the C-terminal tail of the full-length NTS2 are not essential for but may play an accessory role in MAPK activation. To our knowledge, the vNTS2 is the first TM-spliced GPCR variant cloned to date that was found to maintain signaling properties. Indeed, other TM splice variants of GPCRs, such as the corticotrophin-releasing factor receptor 2, have been reported to retain their agonist binding properties but to totally lose their functional coupling (47).

Western blotting studies using an N-terminally directed NTS2 peptide antiserum revealed that the 32-kDa monomeric form of vNTS2 is not expressed in the spinal cord, whereas a band twice the size of vNTS2 is present, suggesting that the NTS2 receptor variant may exist in homodimeric form in the rat CNS. By contrast, a specific band was detected at 46 kDa, *i.e.* at the molecular weight of the full-length isoform of the receptor, indicating that in contrast to its variant isoform, the full-length receptor exists in monomeric form in rat CNS. These results are similar to those previously reported for membranes prepared from rat brain and cerebellum (40). In addition, specific bands were detected at molecular weight marks higher than the putative vNTS2 dimers. One of these was approximately twice the size of the monomeric form of the full-length receptor and was therefore interpreted as a putative NTS2 homodimer. Another migrated slightly lower, as would be expected from a vNTS2/NTS2 heterodimer. Indeed, recent biochemical, biophysical, and functional studies (48, 49) have shown that GPCR can assemble as hetero- as well as homodimeric complexes. To test whether the vNTS2 could actually associate with its full-length counterpart, we carried out immunoprecipitation experiments on COS-7 cells co-expressing HA-tagged vNTS2 and native NTS2. These experiments demonstrated that the two NTS2 isoforms did associate when co-expressed in COS-7 cells, because both receptors were pulled down using an HA antibody. Furthermore, the presence in these dually transfected cells of a band at the theoretical molecular weight of vNTS2/NTS2 heterodimers indicated that the band detected at the same level in spinal cord membranes might indeed have corresponded to a vNTS2-NTS2 heterodimer. This vNTS2/NTS2 heterodimer was stable during cell lysis and reducing Tris-glycine gel electrophoresis, suggesting that the interaction involves a noncovalent hydrophobic interface between the receptor proteins.

To investigate whether heterodimerization of NTS2 and vNTS2 receptors affected targeting of the truncated receptor to the plasma membrane, we examined by Western blot the expression of vNTS2 on the cell surface of singly transfected *versus* dually transfected cells, and we compared the immunocytochemical distribution of NTS2 and vNTS2 in dually transfected cells. By using either technique, we found that co-expression of the full-length NTS2 did not noticeably increase the cell surface density of the truncated form over that seen in cells expressing HA-vNTS2 alone, suggesting that the full-length NTS2 does not act as a chaperone protein for its shorter isoform. However, intracellular vNTS2 stores closely overlapped with those of NTS2, supporting the notion that the two receptors heterodimerize.

In summary, our results indicate that the rat vNTS2 is a functional receptor that is expressed in conjunction with the full-length NTS2 receptor throughout the CNS. Our data also indicate that this truncated 5-TM receptor does not exist in monomeric form in the rat CNS. Rather, it associates both with itself and with the full-length 7-TM receptor to form large molecular weight homo- and heterodimer species. Therefore, it is likely that these associations provide for subtle regulation of

the NT signal, as demonstrated previously (50) for the splice variant isoform of the growth hormone-releasing hormone receptor.

REFERENCES

1. Nemeroff, C. B., Osbahr, A. J., III, Manberg, P. J., Ervin, G. N., and Prange, A. J. (1979) *Proc. Natl. Acad. Sci. U. S. A.* **76,** 5368–5371
2. Kalivas, P. W., Gau, B. A., Nemeroff, C. B., and Prange, A. J., Jr. (1982) *Brain Res.* **243,** 279–286
3. Martin, G. E., Racino, C. B., and Papp, N. L. (1986) *Peptides* **1,** 333–339
4. Kinkead, B., and Nemeroff, C. B. (1994) *J. Clin. Psychiatry* **55,** Suppl. B, 30–32
5. Snijders, R., Kramarcy, N. R., Hurd, R. W., Nemeroff, C. B., and Dunn, A. J. (1982) *Neuropharmacology* **21,** 465–468
6. Rioux, F., Quirion, R., St-Pierre, S., Regoli, D., Jolicoeur, F. B., Belanger, F., and Barbeau, A. (1981) *Eur. J. Pharmacol.* **69,** 241–247
7. St-Gelais, F., Legault, M., Bourque, M. J., Rompré, P. P., and Trudeau, L. E. (2004) *J. Neurosci.* **24,** 2566–2574
8. Cape, E. G., Manns, I. D., Alonso, A., Beaudet, A., and Jones, B. E. (2000) *J. Neurosci.* **20,** 8452–8461
9. Binder, E. B., Kinkead, B., Owens, M. J., and Nemeroff, C. B. (2001) *Biol. Psychiatry* **50,** 856–872
10. Tanaka, K., Masu, M., and Nakanishi, S. (1990) *Neuron* **4,** 847–854
11. Chalon, P., Vita, N., Kaghad, M., Guillemot, M., Bonnin, J., Delpech, B., Le Fur, G., Ferrara, P., and Caput, D. (1996) *FEBS Lett.* **386,** 91–94
12. Petersen, C. M., Nielsen, M. S., Nykjaer, A., Jacobsen, L., Tommerup, N., Rasmussen, H. H., Roigaard, H., Gliemann, J., Madsen, P., and Moestrup, S. K. (1997) *J. Biol. Chem.* **272,** 3599–3605
13. Mazella, J., Zsurger, N., Navarro, V., Chabry, J., Kaghad, M., Caput, D., Ferrara, P., Vita, N., Gully, D., Maffrand, J. P., and Vincent, J. P. (1998) *J. Biol. Chem.* **273,** 26273–26276
14. Hermans, E., and Maloteaux, J. M. (1998) *Pharmacol. Ther.* **79,** 89–104
15. Vincent, J. P., Mazella, J., and Kitabgi, P. (1999) *Trends Pharmacol. Sci.* **20,** 302–309
16. Hermans, E., Maloteaux, J. M., and Octave, J. N. (1992) *Brain Res. Mol. Brain Res.* **15,** 332–338
17. Chabry, J., Labbé-Jullié, C., Gully, D., Kitabgi, P., Vincent, J. P., and Mazella, J. (1994) *J. Neurochem.* **63,** 19–27
18. Amar, S., Mazella, J., Checler, F., Kitabgi, P., and Vincent, J. P. (1985) *Biochem. Biophys. Res. Commun.* **129,** 117–125
19. Bozou, J. C., de Nadai, F., Vincent, J. P., and Kitabgi, P. (1989) *Biochem. Biophys. Res. Commun.* **161,** 1144–1150
20. Yamada, M., Watson, M. A., and Richelson, E. (1993) *Eur. J. Pharmacol.* **244,** 99–101
21. Watson, M. A., Yamada, M., Cusack, B., Veverka, K., Bolden-Watson, C., and Richelson, E. (1992) *J. Neurochem.* **59,** 1967–1970
22. Poinot-Chazel, C., Portier, M., Bouaboula, M., Vita, N., Pecceu, F., Gully, D., Monroe, J. G., Maffrand, J. P., Le Fur, G., and Casellas, P. (1996) *Biochem. J.* **320,** 145–151
23. Botto, J. M., Guillemare, E., Vincent, J. P., and Mazella, J. (1997) *Neurosci. Lett.* **223,** 193–196
24. Gendron, L., Perron, A., Payet, M. D., Gallo-Payet, N., Sarret, P., and Beaudet, A. (2004) *Mol. Pharmacol.* **66,** 1423–1430
25. Sarret, P., Gendron, L., Kilian, P., Nguyen, H. M., Gallo-Payet, N., Payet, M. D., and Beaudet, A. (2002) *J. Biol. Chem.* **277,** 36233–36243
26. Sun, Y. J., Maeno, H., Aoki, S., and Wada, K. (2001) *Brain Res. Mol. Brain Res.* **95,** 167–171
27. Botto, J. M., Sarret, P., Vincent, J. P., and Mazella, J. (1997) *FEBS Lett.* **400,** 211–214
28. Kilpatrick, G. J., Dautzenberg, F. M., Martin, G. R., and Eglen, R. M. (1999) *Trends Pharmacol. Sci.* **20,** 294–301
29. Namba, T., Sugimoto, Y., Negishi, M., Irie, A., Ushikubi, F., Kakizuka, A., Ito, S., Ichikawa, A., and Narumiya, S. (1993) *Nature* **365,** 166–170
30. Nambi, P., Wu, H. L., Ye, D., Gagnon, A., and Elshourbagy, N. (2000) *J. Pharmacol. Exp. Ther.* **292,** 247–253
31. Monsma, F. J., Jr., McVittie, L. D., Gerfen, C. R., Mahan, L. C., and Sibley, D. R. (1989) *Nature* **342,** 926–929
32. Schmauss, C., Haroutunian, V., Davis, K. L., and Davidson, M. (1993) *Proc. Natl. Acad. Sci. U. S. A.* **90,** 8942–8946
33. Nishimatsu, S., Koyasu, N., Sugaya, T., Ohnishi, J., Yamagishi, T., Murakami, K., and Miyazaki, H. (1994) *Biochem. Biophys. Acta* **1218,** 401–407
34. Minneman, K. P. (2001) *Mol. Interv.* **1,** 108–116
35. Canton, H., Emeson, R. B., Barker, E. L., Backstrom, J. R., Lu, J. T., Chang, M. S., and Sanders-Bush, E. (1998) *Mol. Pharmacol.* **50,** 799–807
36. Zhang, Y. F., Jeffery, S., Burchill, S. A., Berry, P. A., Kaski, J. C., and Carter, N. D. (1998) *Br. J. Cancer* **78,** 1141–1146
37. Grosse, R., Schoneberg, T., Schultz, G., and Gudermann, T. (1997) *Mol. Endocrinol.* **11,** 1305–1318
38. Grabowski, P. J., and Black, D. L. (2001) *Prog. Neurobiol.* **65,** 289–308
39. Rekasi, Z., Czompoly, T., Schally, A. V., and Halmos, G. (2000) *Proc. Natl. Acad. Sci. U. S. A.* **97,** 10561–10566
40. Sarret, P., Perron, A., Stroh, T., and Beaudet, A. (2003) *J. Comp. Neurol.* **461,** 520–538
41. Laemmli, U. K. (1970) *Nature* **227,** 680–685
42. Horowitz, D. S., and Krainer, A. R. (1994) *Trends Genet.* **10,** 100–106
43. Furnham, N., Ruffle, S., and Southan, C. (2004) *Proteins* **54,** 596–608
44. Barroso, S., Richard, F., Nicolas-Etheve, D., Reversat, J. L., Bernassau, J. M., Kitabgi, P., and Labbé-Jullié, C. (2000) *J. Biol. Chem.* **275,** 328–336
45. Richard, F., Barroso, S., Martinez, J., Labbé-Jullié, C., and Kitabgi, P. (2001) *Mol. Pharmacol.* **60,** 1392–1398
46. Botto, J. M., Chabry, J., Sarret, P., Vincent, J. P., and Mazella, J. (1998) *Biochem. Biophys. Res. Commun.* **243,** 585–590
47. Miyata, I., Shiota, C., Ikeda, Y., Oshida, Y., Chaki, S., Okuyama, S., and Inagami, T. (1999) *Biochem. Biophys. Res. Commun.* **256,** 692–698
48. Bouvier, M. (2001) *Nat. Rev. Neurosci.* **2,** 274–286
49. Devi, L. A. (2001) *Trends Pharmacol. Sci.* **22,** 532–537
50. Motomura, T., Hashimoto, K., Koga, M., Arita, N., Hayakawa, T., Kishimoto, T., and Kasayama, S. (1998) *Metabolism* **47,** 804–808

APPENDIX D

GenBank Report (Accession Number AY946024)


```
LOCUS       AY946024                 846 bp    mRNA    linear   ROD
22-MAR-2005

DEFINITION  Rattus norvegicus variant neurotensin receptor 2 (Ntsr2)
            MRNA, complete cds.
ACCESSION   AY946024
VERSION     AY946024.1  GI:61613030
KEYWORDS    .
SOURCE      Rattus norvegicus (Norway rat)
ORGANISM    Rattus norvegicus
            Eukaryota; Metazoa; Chordata; Craniata; Vertebrata;
            Euteleostomi;
            Mammalia; Eutheria; Euarchontoglires; Glires; Rodentia;
            Sciurognathi; Muroidea; Muridae; Murinae; Rattus.
REFERENCE   1  (bases 1 to 846)
AUTHORS     Perron,A., Sarret,P., Gendron,L., Stroh,T. and
            Beaudet,A.
TITLE       Identification and Functional Characterization of a 5-
            Transmembrane Domain Variant Isoform of the NTS2
            Neurotensin Receptor in Rat Central Nervous System
JOURNAL     J. Biol. Chem. 280 (11), 10219-10227 (2005)
PUBMED      15637074
REFERENCE   2  (bases 1 to 846)
AUTHORS     Perron,A., Sarret,P. and Beaudet,A.
TITLE       Direct Submission
JOURNAL     Submitted (28-FEB-2005) Montreal Neurological Institute,
            McGill University, 3801 University, Room 896, Montreal,
            Québec, H3A 2B4, Canada

FEATURES             Location/Qualifiers
     source          1..846
                     /organism="Rattus norvegicus"
                     /mol_type="mRNA"
                     /strain="Sprague-Dawley"
                     /db_xref="taxon:10116"
     gene            1..846
                     /gene="Ntsr2"
     CDS             1..846
                     /gene="Ntsr2"
                     /note="vNTS2; GPCR"
                     /codon_start=1
                     /product="variant neurotensin receptor 2"
                     /protein_id="AAX47307.1"
                     /db_xref="GI:61613031"
```

```
/translation="METSSPWPPRPSPSAGLSLEARLGVDTRLWAKVLFTALYSLIFA
FGTAGNALSVHVVLKARAGRPGRLRYHVLSLALSALLLLLVSMPMELYNFVWSHYPWV
FGDLGCRGYYFVRELCAYATVLSVASLSAERCLAVCQPLRARRLLTPRRTRRLLSLVW
VASLGLALPMAVIMGQKHEVESADGEPEPASRVCTVLVSRATLQVFIQVNVLVSFALP
LALTAFLNGITVNHLMALYSQEPSWLCMSSAGCRTMPADSCTATSPMMDGLMSSMISI
TISTW"

ORIGIN
        1 atggagacca gcagtccgtg gcctccgagg cccagcccca gcgcagggct
gagcctggag
       61 gcgcggctgg gcgtggacac tcgcctctgg gccaaggtgc tgttcaccgc
gctctactcg
      121 ctcatcttcg catttggcac agcgggcaat gcgctgtccg tgcacgtggt
gctgaaggcg
      181 cgggccggtc gccccgggcg cctgcgctac cacgtgctca gcctggcgct
ctcagccctg
      241 ctgctactgc tggtcagcat gcccatggag ctctacaact tcgtgtggtc
ccactaccca
      301 tgggtcttcg gcgatctggg ctgccgtggc tattacttcg tgcgcgagct
gtgcgcctac
      361 gccacagtgc tgagcgttgc cagcctaagc gcagagcgct gcctggccgt
gtgccagccg
      421 ctgcgcgccc gccgccttct caccccgcgc cgcacccgcc gcctgctgtc
actggtctgg
      481 gtcgcctctc tgggccttgc cctgcccatg gcggttatca tgggacagaa
gcacgaagtg
      541 gaaagcgcgg acggggagcc tgagcctgcc tcgcgtgtgt gcacggtgct
ggtgagccgc
      601 gccacacttc aggtcttcat ccaggtgaat gtgctggtgt ccttcgctct
ccccttggca
      661 ctcactgctt tcctgaatgg catcactgtc aaccacctga tggccctcta
ctcccaggag
      721 ccatcgtggc tgtgtatgtc atctgctggc tgccgtacca tgcccgccga
ctcatgtact
      781 gctacatccc cgatgatgga tggactaatg agctctatga tttctatcac
tatttctaca
      841 tggtga
//
```

APPENDIX E

Available online at www.sciencedirect.com
SCIENCE DIRECT
Biochemical and Biophysical Research Communications 343 (2006) 799–808
BBRC
www.elsevier.com/locate/ybbrc

Sustained neurotensin exposure promotes cell surface recruitment of NTS2 receptors

Amélie Perron [a], Nadder Sharif [a], Louis Gendron [a], Mariette Lavallée [a], Thomas Stroh [a], Jean Mazella [b], Alain Beaudet [a,*]

[a] *Montreal Neurological Institute, McGill University, Montreal, Que., Canada H3A 2B4*
[b] *Institut de Pharmacologie Moléculaire et Cellulaire, CNRS, Sophia Antipolis, 06560 Valbonne, France*

Received 1 March 2006
Available online 20 March 2006

Abstract

In this study, we investigated whether persistent agonist stimulation of NTS2 receptors gives rise to down-regulation, in light of reports that their activation induced long-lasting effects. To address this issue, we incubated COS-7 cells expressing the rat NTS2 with neurotensin (NT) for up to 24 h and measured resultant cell surface [^{125}I]-NT binding. We found that NTS2-expressing cells retained the same surface receptor density despite efficient internalization mechanisms. This preservation was neither due to NTS2 neosynthesis nor recycling since it was not blocked by cycloheximide or monensin. However, it appeared to involve translocation of spare receptors from internal stores, as NT induced NTS2 migration from trans-Golgi network to endosome-like structures. This stimulation-induced regulation of cell surface NTS2 receptors was even more striking in rat spinal cord neurons. Taken together, these results suggest that sustained NTS2 activation promotes recruitment of intracellular receptors to the cell surface, thereby preventing functional desensitization.

Keywords: Neurotensin; GPCRs; Long-term stimulation: Down-regulation; Intracellular stores: Recycling; Internalization

Neurotensin (NT) is a tridecapeptide that was shown to be involved in a variety of central and peripheral neuromodulatory effects including naloxone-independent analgesia, hypothermia, and neuroleptic-like modulation of dopaminergic pathways [1]. Most of these effects result from the specific interaction of the peptide with two cell surface G protein-coupled receptors (GPCRs) referred to as NTS1 and NTS2. The former binds NT with high affinity ($K_d = 0.2$ nM), whereas the latter binds NT with lower affinity ($K_d = 2$ nM) and is recognized by the antihistamine drug levocabastine [2,3]. Biochemical studies have indicated that NTS1 is implicated in the modulation of intracellular levels of inositol phosphates [4], cAMP [5], and extracellular signal-regulated kinases [6], whereas NTS2 induces Ca^{2+}-dependent chloride currents in *Xenopus oocytes* [7] and activates the ERK1/2 cascade, both in transfected CHO cells [8] and in cerebellar granule cells in culture [9].

Most GPCRs are subjected to regulatory processes in order to control their responsiveness to persistent agonist exposure [10,11]. Agonist-induced regulation of GPCRs usually involves receptor desensitization, due to uncoupling from G proteins, followed by receptor internalization and down-regulation. The latter is characterized by a decrease in the total number of receptors and typically involves increased turnover or reduced synthesis of receptors. In the case of the NTS1 receptor, such desensitization processes have been reported in N1E-115 cells as well as in rat cultured neurons after prolonged incubation in the presence of NT [12,13]. The disappearance of NT-binding sites was surmised to result from degradation of internalized receptors after fusion with lysosomes, since it was partially inhibited by the lysosomotropic drugs chloroquine and methylamine [13,14]. Moreover, destabilization of NTS1 mRNA was reported in N1E-115 and HT29 cells

* Corresponding author. Fax: +1 514 398 5871.
E-mail address: abeaudet@frsq.gouv.qc.ca (A. Beaudet).

0006-291X/$ - see front matter © 2006 Elsevier Inc. All rights reserved.
doi:10.1016/j.bbrc.2006.03.047

after long-term agonist exposure, suggesting that post-transcriptional events may be directly implicated in the down-regulation process [15]. Finally, it has been established that de novo synthesis is required for the recovery of NTS1 receptor-binding sites and function [12,13].

Little is known about the regulation of NTS2, except that its stimulation with NT induces long-term metabolic effects due to prolonged and sustained activation of ERK1/2, either in transfected CHO cells [8] or in neurons in culture [9]. Therefore, the present study was initiated in order to determine whether extended stimulation of NTS2 leads to a down-regulation of cell surface receptor density and/or of intracellular receptor protein levels. Our results demonstrate that cell surface NTS2 receptors are maintained following persistent exposure to NT through a recycling-independent mechanism that involves recruitment of receptors from intracellular stores.

Materials and methods

Gene constructs. The cDNA encoding the rat and human NTS2 receptors (rNTS2 and hNTS2, respectively) were obtained through reverse transcription of brain mRNA and subcloned into the mammalian expression vector pTargeT (Promega, Madison, WI) as described in [16] and [8]. The subcloning of HA-tagged NTS1 into pcDNA3 was described previously [17].

Cell culture and transfections. COS-7 cells were maintained in Dulbecco's modified Eagle's medium (DMEM) supplemented with 5% fetal bovine serum (FBS) in the presence of penicillin/streptomycin (100 U/ml; Invitrogen Burlington, ON, Canada). Cells were transiently transfected by the DEAE-dextran/chloroquine method with 4 μg of rNTS2, hNTS2, or HA-tagged NTS1 plasmid.

Receptor binding experiments. COS-7 cells expressing rNTS2, hNTS2 or HA-NTS1 were incubated with or without 1 μM NT for 1–24 h in DMEM with 2.5% FBS or Earle's buffer (130 mM NaCl, 5 mM KCl, 1.8 mM $CaCl_2$, 0.8 mM $MgCl_2$, and 20 mM Hepes, pH 7.4) for long (1–24 h) and short (0–60 min) term experiments, respectively. Cells were washed once with hypertonic acid buffer (Earle's containing 0.2 and 0.5 M NaCl, pH 4), twice with Earle's, and incubated with 0.4 nM ^{125}I-labeled NT (1670 Ci/mmol; Perkin-Elmer) for 60 min on ice in Earle's supplemented with 0.25% BSA, 0.1% glucose, and 0.8 mM *ortho*-phenanthroline. Cells were then washed twice with ice-cold Earle's, harvested in 0.1 M NaOH, and radioactivity content was measured in a gamma counter. Non-specific binding was defined as binding in the presence of a 10,000-fold excess of unlabeled ligand, which corresponded to less than 1% of total counts. Statistical comparisons between groups were performed using a Student's *t* test. Differences were considered significant for $p < 0.05$.

For experiments with recycling inhibitors, transfected COS-7 cells were equilibrated for 10 min at 37 °C in Earle's supplemented with 0.25% BSA and 0.1% glucose. Cells were then prestimulated for 30 min with 25 μM monensin (Sigma) in Earle's at 37 °C and incubated with or without 1 μM NT in the continuous presence of monensin for 60 min at 37 °C. Cells were then washed once with hypertonic acid buffer, twice with Earle's and binding with radioligand was performed as described above.

Immunoblotting analyses. COS-7 cells expressing rNTS2 were stimulated or not with 1 μM NT with or without 70 μM cycloheximide for 1 or 24 h at 37 °C and resuspended in ice-cold buffer containing 10 mM Tris–HCl, pH 8.0, and 1 mM EDTA with protease inhibitors (Complete Protease Inhibitor tablets, Roche Molecular Biochemicals, Laval, QC, Canada). Cells were then disrupted by sonication and pelleted by centrifuging at 12,000*g* for 30 min at 4 °C. Parallel experiments were done using untransfected cells as a negative control. Protein concentration was determined using the Bio-Rad method (Bio-Rad Laboratories, Mississauga, ON, Canada). Samples containing 20 μg of crude membrane proteins were denatured in Laemmli sample buffer, resolved on 10% Tris–glycine precast gels (Invitrogen), and transferred to nitrocellulose membranes (Bio-Rad). Membranes were then incubated with the NTS2 peptide antiserum (1/10,000; previously characterized in [16]) overnight at 4 °C in PBS containing 1% ovalbumin (Sigma, St-Louis, MO) and BSA, followed by HRP-conjugated anti-rabbit secondary antibody (1/3500; Amersham Pharmacia Biotech, Baie d'Urfé, QC, Canada) in PBS with 5% evaporated milk (Carnation, Don Mills, ON, Canada) for 1 h at room temperature (RT). Immunoreactive proteins were detected using an enhanced chemiluminescent system (Perkin-Elmer Life Science, Boston, MA). The effects of long-term NT exposure on rNTS2 protein levels were quantified by densitometry using Scion Image. Calculation and statistical analyses were carried out in Excel 2000 (Microsoft).

Immunocytochemistry on COS-7 cells. COS-7 cells expressing rNTS2 were stimulated or not with 1 μM NT for 1 h at 37 °C, fixed for 20 min with 4% paraformaldehyde (PFA) (Polysciences, Warrington, PA), pre-incubated for 30 min with a blocking solution (5% normal goat serum (NGS), 2% BSA, and 0.1% Triton (Sigma)), and incubated overnight at 4 °C with the NTS2 antiserum (1/25,000) alone, or in concert with either a monoclonal antibody against syntaxin 6 (1/1000; Transduction Laboratories, Lexington, KY) or guinea pig anti-PIST antibody (1/1000; gift of Dr. Hans-Jürgen Kreienkamp, Institute for Human Genetics, Hamburg, Germany). Cells were then incubated for 1 h at RT with a mixture of Alexa 488-conjugated goat anti-rabbit with either Alexa 596-conjugated goat anti-mouse or anti-guinea pig antibodies (1/750; Molecular Probes, Eugene, OR). Cells were examined with a Zeiss 510 laser scanning confocal microscope equipped with Argon2 (488 nm) and He/Ne1 (543 nm) lasers (Carl Zeiss Micro Imaging Inc., Thornwood, NY). Images were processed using the Zeiss 510 laser-scanning microscope software and Adobe Photoshop 6.0.

To quantify peripheral (as an index of cell surface) versus internal NTS2 immunolabeling in permeabilized cells, a total of 12–15 cells per condition (i.e., untreated or stimulated for 60 min with NT) from four independent experiments were randomly selected and analyzed using the ImageJ software (National Institutes of Health, Bethesda, MD). For this purpose, peripheral and intracellular compartments were delineated and integrated fluorescence densities associated with either of these two compartments were measured. Values are expressed as a percentage of the total fluorescence density (peripheral + intracellular) for each condition. Statistical comparisons between conditions were performed using a Student's *t* test.

Measurement of MAP kinase activity. COS-7 cells expressing rNTS2 were incubated at 37 °C in DMEM, 2.5% FBS with or without 1 μM NT for 24 h, serum-starved for 2 h, and then incubated with 1 μM NT for 0, 5, 15, 30 or 60 min at 37 °C. The reaction was stopped by addition of ice-cold PBS containing 0.1 μM staurosporine (Sigma) and 1 mM sodium orthovanadate. Cells were then lysed in 50 mM Hepes, pH 7.8, containing 1% Triton, 0.1 μM staurosporine, 1 mM sodium orthovanadate, and protease inhibitors. Cell lysates were centrifuged at 12,000*g* for 10 min at 4 °C and protein concentration was determined by the Bio-Rad procedure as described above. Samples containing 30 μg of protein were denatured in Laemmli buffer and resolved by using 10% Tris–glycine precast gels. Nitrocellulose membranes were incubated overnight at 4 °C with anti-phosphorylated ERK1/2 or anti-ERK1/2 rabbit antibodies (1/1000; New England Biolabs, Beverly, MA), followed by HRP-conjugated goat anti-rabbit antibody for 1 h at RT (1/4000; Amersham Pharmacia Biotech). To quantify the effect of NT on ERK1/2 phosphorylation, the ratios of phosphorylated ERK1/2 over total ERK1/2 levels were determined by densitometry using Scion Image software. Calculations and statistical analyses were performed using Excel 2000 and SigmaPlot 2001. Statistical significance of the activation of ERK1/2 between untreated and NT-prestimulated cells was determined using a Student's *t* test.

NTS2 Immunogold labeling. Adult male Sprague–Dawley rats (200–250 g; Charles River, St-Constant, QC, Canada) were anesthetized with halothane and intrathecally injected or not with NT (1200 pmol). After 20 min, rats were transaortically perfused under pentobarbital anesthesia

with a mixture of 3.75% acrolein and 2% PFA. Lumbar spinal cords were removed, fixed in 2% PFA and cut (50 μm) using a vibrating microtome. Sections were incubated in 1% sodium borohydride and cryoprotectant solution (25% sucrose and 3% glycerol) prior to snap freezing in isopentane (−70 °C), transfer to liquid nitrogen, and thawing. Sections were then incubated for 48 h at 4 °C with NTS2 antiserum (1/1800), followed by 2 h at RT with colloidal gold-conjugated goat anti-rabbit antibody (1/50; Cedarlane Laboratories, Hornby, ON, Canada). Sections were fixed with 2% glutaraldehyde and immunogold deposits were enhanced using the IntenSE kit (Amersham Pharmacia Biotech). Sections were then post-fixed with osmium tetroxide, dehydrated in ethanol, flat-embedded in Epon, counterstained with lead citrate and uranyl acetate, and examined with a JEOL 100CX transmission electron microscope. Negatives were digitized on a scanner and processed using Adobe Photoshop. Quantitative analysis of the ultrastructural distribution of NTS2 immunoreactivity was performed on three to four grids per experimental condition from three independent experiments ($n = 3$ rats). A total of 38 and 31 randomly selected labeled dendritic profiles within the superficial layers (laminae I and II) of the spinal cord from respectively non-treated and NT-injected rats were analyzed using the Neurolucida morphometry software. First, density of immunoreactive NTS2 receptor gold particles associated with selected dendrites was calculated per surface area and expressed as immunogold/silver particles per μm^2. Second, gold particles were classified as being intracellular or membrane-associated. The proportion of membrane-associated NTS2 receptors was expressed as a percentage of the total number of gold particles. Statistical comparisons between groups were performed using a Student's t test. Differences were considered significant for $p < 0.05$.

Results

Cell surface NTS2 receptors are resistant to down-regulation

To investigate the effects of prolonged incubation with NT on NTS2 cell surface density, rNTS2-expressing COS-7 cells were prestimulated with 1 μM NT for up to 24 h at 37 °C and cell surface receptor binding was carried out using 0.4 nM [^{125}I]-NT on ice. As shown in Fig. 1A, NT stimulation resulted in an immediate decrease in the density of cell surface NTS2 binding sites (50 ± 4% of baseline values after 5 min). A similar but weaker response was obtained in NTS1-expressing cells (73 ± 2% of baseline values at 5 min; Fig. 1A). Upon sustained NT exposure, NTS2 binding progressively returned to baseline values (100 ± 4% of baseline after 24 h) whereas NTS1 binding kept on decreasing (46 ± 1% of baseline after 24 h; Fig. 1B). NTS2 binding sites were also maintained at baseline levels after a 24 h stimulation with the metabolically stable NT analog JMV-431 (106 ± 6%), suggesting that maintenance of NTS2 cell surface binding sites was not due to peptide degradation (not shown). Taken together, these data show that contrary to NTS1, cell surface NTS2 binding sites are maintained following persistent agonist stimulation despite efficient internalization mechanisms.

Effect of prolonged NT exposure on NTS2 receptor protein levels

In order to determine whether prolonged exposure to NT affected total NTS2 protein levels, rNTS2-expressing COS-7 cells were stimulated with 1 μM NT for different

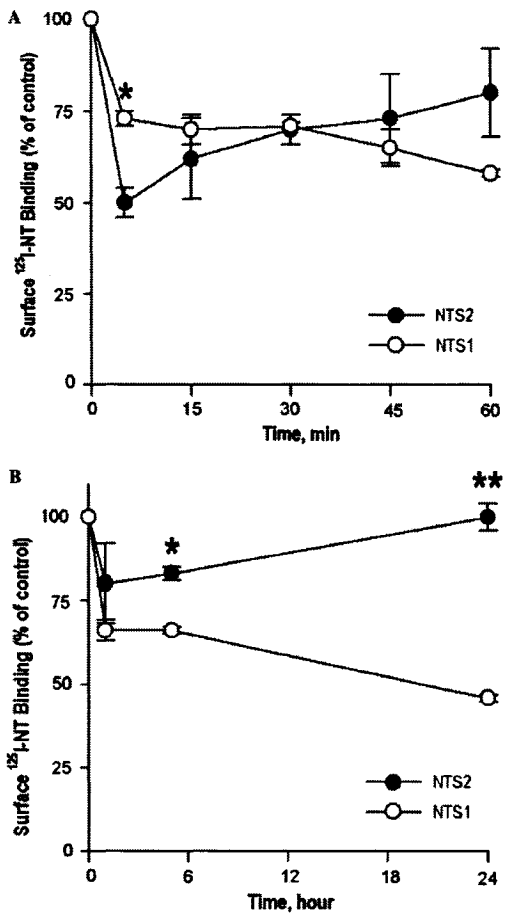

Fig. 1. Persistent agonist-induced regulation of cell surface NT receptors. COS-7 cells expressing rNTS2 (●) or NTS1 (○) were exposed to 1 μM NT for 0–60 min (A) and up to 24 h (B) at 37 °C, acid-washed, and incubated with [^{125}I]-NT on ice for monitoring cell surface receptors. The results are representative of three individual experiments ± SEM, each with triplicate determinations. Student's t tests were used to compare NT cell surface binding sites between rNTS2 and NTS1 expressing COS-7 cells. Values are significantly different at all time points with $^{*}p < 0.05$ and $^{**}p < 0.01$.

periods of time and crude membrane preparations were analyzed by Western blotting using a NTS2 peptide antiserum. As seen in Fig. 2, the total levels of immunodetected-NTS2 (45 kDa) were not significantly different after than before NT stimulation (103 ± 15% of control values after 24 h), suggesting that NTS2 is neither up- nor down-regulated following prolonged agonist exposure. To confirm that prolonged NT stimulation did not induce NTS2 neosynthesis, COS-7 cells were incubated with NT in presence of the protein synthesis inhibitor cycloheximide for up to 24 h. Immunoblotting of crude membrane preparations

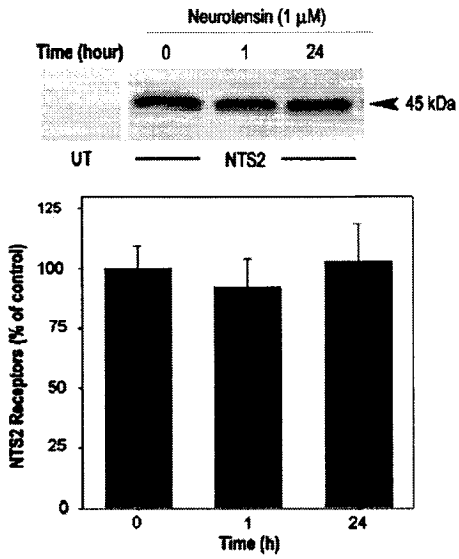

Fig. 2. Effect of NT stimulation on NTS2 receptor protein levels in COS-7 cells. COS-7 cells transiently transfected with cDNA encoding the rNTS2 receptor were stimulated with 1 μM NT for different periods of time at 37 °C and membranes were isolated as described under "Materials and methods". Similar experiments were done with untransfected (UT) cells as a negative control. Western blotting analysis was performed using the NTS2 peptide antiserum after a 10% Tris–glycine gel electrophoresis under reducing conditions and NTS2 receptor protein levels were quantified by densitometric analysis. The data represent means ± SEM of three individual experiments.

using the NTS2 peptide antiserum revealed that treatment with cycloheximide did not affect receptor protein levels (not shown).

Maintenance of cell surface NTS2 receptors is a recycling-independent process

To investigate whether receptor recycling accounted for the preservation of cell surface NTS2 receptors following prolonged NT exposure, rNTS2-expressing COS-7 cells were first preincubated with monensin for 30 min and incubated with 1 μM NT together with monensin for 1 h at 37 °C. Monensin is known to hinder late receptor recycling steps beyond the acidification of endocytic vesicles [18]. As shown in Fig. 3A monensin had little if any effect on the preservation of [^{125}I]-NT binding levels following NT exposure. Indeed, cell surface levels of NTS2 receptors represented 92 ± 8% of pre-stimulation values, which were comparable to those measured in the absence of monensin following the same stimulation period with NT (90 ± 4%).

Previous site-directed mutagenesis studies have revealed that Tyr 237 is a critical residue in the recycling process of NTS2 receptors [19]. Indeed, the human NTS2 in which a cysteine residue naturally replaces the tyrosine in position

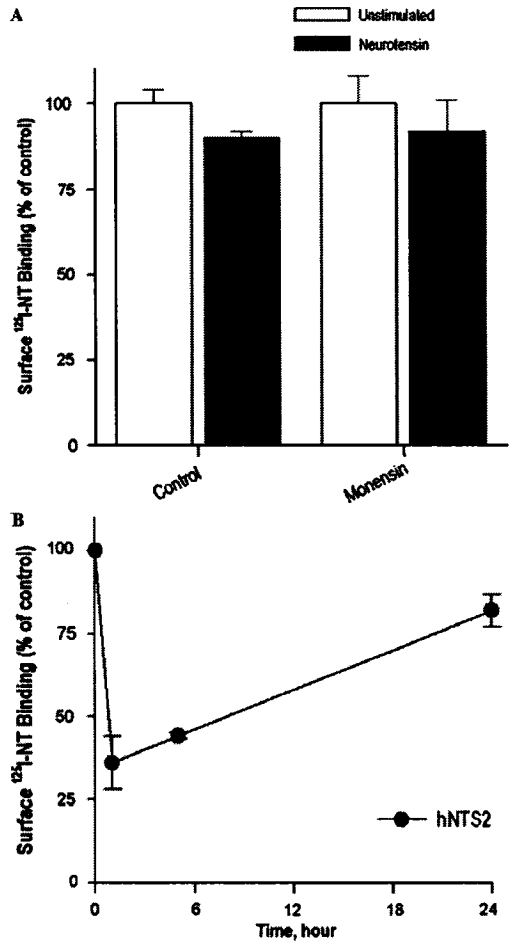

Fig. 3. Recycling is not involved in the maintenance of cell surface NTS2 binding sites. (A) COS-7 cells expressing rNTS2 were preincubated with 25 μM monensin for 30 min and stimulated with NT with the recycling inhibitor for 1 h at 37 °C. The peptide was removed by acid wash and cells were incubated with [^{125}I]-NT on ice to determine the amount of cell surface receptors. Each point is the mean ± SEM from triplicate determinations of at least two different experiments. (B) COS-7 cells expressing the non-recycling human NTS2 receptor were exposed to 1 μM NT for up to 24 h at 37 °C, acid-washed, and incubated with [^{125}I]-NT on ice for monitoring cell surface receptors. The results are representative of two individual experiments ± SEM, each with triplicate determinations.

237 does not undergo recycling following ligand-induced internalization [19]. In order to study further the potential implication of receptor recycling in the maintenance cell surface NTS2 receptors, hNTS2-expressing COS-7 cells were prestimulated with 1 μM NT for up to 24 h at 37 °C and cell surface receptor binding was carried out by using 0.4 nM [^{125}I]-NT on ice. As shown in Fig. 3B, NT stimulation resulted in rapid decrease in the density of cell surface

human NTS2 binding sites (36 ± 8% of baseline values after 5 min), suggesting efficient ligand-induced internalization. However, human NTS2 receptors also progressively resurfaced upon extended agonist exposure (82 ± 5% of baseline after 24 h) despite their inability to undergo recycling [19]. Taken together, these results suggest that receptor recycling does not account by itself for the maintenance of cell surface NTS2 receptors, but that other mechanisms must be brought into play.

Effect of long-term NT stimulation on NTS2 receptor trafficking and function

In order to visualize the effect of NT stimulation on NTS2 intracellular trafficking, transfected COS-7 cells were incubated in the presence or absence of 1 μM NT for 60 min at 37 °C and the distribution of immunolabeled receptors was examined by confocal microscopy. Immunostaining of non-stimulated, permeabilized cells revealed a prominent juxtanuclear pool of NTS2 receptors as well as small peripheral, presumably membrane-associated, receptor clusters (Fig. 4A). To ensure that the localization of the receptors was not due to an idiosyncratic feature of COS-7 cells, we repeated the experiments using CHO cells stably expressing rNTS2. As in COS-7 cells, NTS2 exhibited a predominantly intracellular distribution (not shown). Following 60 min stimulation with NT at 37 °C, intracellular immunoreactive receptors were no longer concentrated next to the nucleus, but became scattered throughout the cytoplasm in the form of small vesicle-like clusters (Fig. 4A). However, there was no apparent change in the density of cell surface receptor clusters (Fig. 4A, arrowheads). Indeed, quantitative image analysis confirmed that there was no difference in the relative density of peripheral immunolabeling before and after NT stimulation (15.3 ± 1.8% versus 15.9 ± 3.6%, respectively; $p > 0.95$; Fig. 4B). These data suggest that receptor activation results in a redistribution of intracellular receptor stores without any apparent loss of cell surface receptors.

To ascertain whether NTS2 receptors present at the cell surface following prolonged NT exposure were functional, rNTS2-expressing COS-7 cells were preincubated or not with 1 μM NT for 24 h at 37 °C and serum-starved for 2 h without the agonist. ERK1/2 phosphorylation was then measured in response to subsequent pulse stimulations with NT. As shown in Fig. 5, NT induced a rapid (<5 min) and sustained phosphorylation (over 1 h) of ERK1/2, irrespective of whether cells had been preincubated or not with NT for 24 h. Moreover, densitometric analysis of the ratio of phosphorylated ERK1/2 over total ERK1/2 levels indicated that NT pretreatment did not significantly influence the agonist-induced ERK1/2 activation (5.2 ± 1.6 versus 4.6 ± 0.6-fold increase in ERK1/2 phosphorylation levels at 5 min in cells pretreated or not with NT, respectively; $p > 0.95$). This effect was NTS2-mediated since it was not observed in untransfected cells (not shown). Thus, these data indicate that NTS2 receptors maintained at the cell surface following sustained ligand exposure are truly functional.

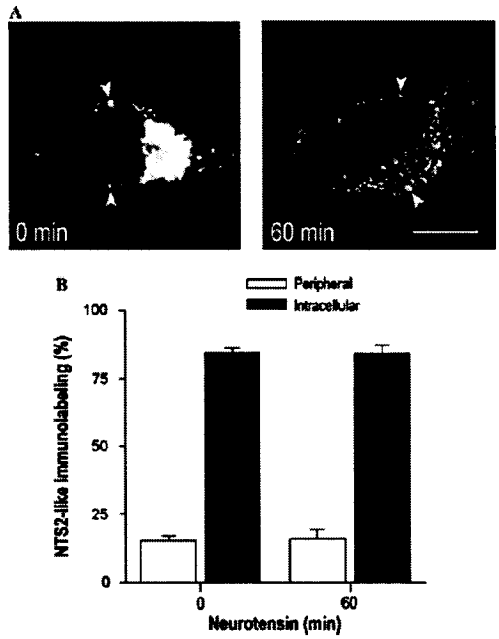

Fig. 4. NT-induced intracellular redistribution of NTS2 receptors in COS-7 cells. (A) rNTS2-expressing COS-7 cells were stimulated or not with 1 μM NT for 60 min at 37 °C. Immunolabeling was then performed on permeabilized cells by using the NTS2 peptide antiserum. Scale bar = 5 μm. (B) Quantitative analysis of NTS2-like immunoreactive staining densities in COS-7 cells stimulated or not with NT. Data are expressed as a percentage ± SEM of integrated density values associated with peripheral (including cell surface) versus intracellular compartments over total fluorescence (representative of four independent experiments).

Golgi apparatus and TGN as putative sources of newly recruited NTS2 receptors

To investigate putative intracellular sources for the membrane recruitment of NTS2 receptors, we co-localized NTS2 with the molecular markers syntaxin 6 or PIST, using dual labeling immunocytochemistry in rNTS2-expressing COS-7 cells. Previous studies have shown that syntaxin 6 is present mainly in the trans-Golgi network (TGN) and participates in vesicular trafficking between the TGN and endosomes [20], whereas PIST (PDZ domain protein interacting specifically with TC10) is known to be associated with the Golgi apparatus [21]. In unstimulated cells (Figs. 6A–F), NTS2 immunoreactivity (Figs. 6A and D) was largely intracellular and concentrated in a compact juxtanuclear structure that was immunopositive for endogenous syntaxin 6 (Fig. 6B) and PIST (Fig. 6E), as shown in overlays (Figs. 6C and F). These data strongly suggest that

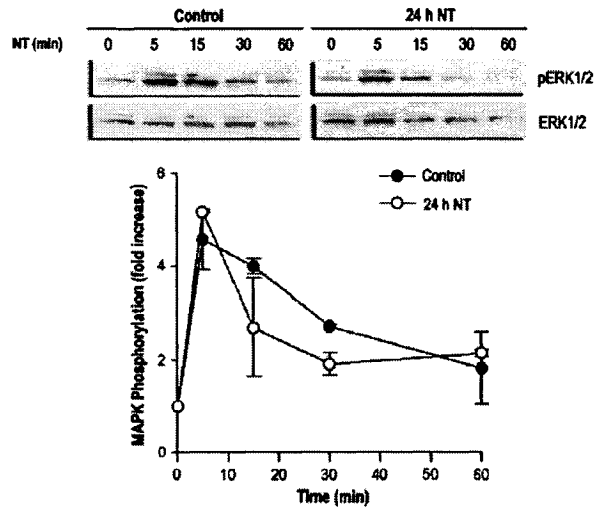

Fig. 5. Effect of persistent stimulation with NT on ERK1/2 phosphorylation in COS-7 cells heterologously expressing rNTS2. Cells were pretreated (○) or not (●) with 1 μM NT for 24 h at 37 °C and subsequently incubated with 1 μM NT for the indicated periods of time (0–60 min). ERK1/2 activity was determined by the ratio of the densitometric analysis of phosphorylated ERK1/2 over total ERK1/2 levels expressed as fold increase over control. Data represent the means ± SEM of two individual experiments, each with triplicate determinations.

NTS2 localizes primarily to the TGN/Golgi complex. This observation was confirmed by the fact that disassembly of the Golgi complex by Brefeldin A induced a total dispersion of NTS2 through the cytoplasm (data not shown). Following a 1 h-incubation with 1 μM NT (Figs. 6G–L), NTS2 immunolabeling was still noticeable in the TGN/Golgi where it remained co-localized with syntaxin 6 (Fig. 6H) and PIST (Fig. 6K). However, NTS2 was also apparent in vesicle-like structures distributed throughout the cytoplasm of the cells. These fluorescent clusters were partially immunopositive for syntaxin 6, but not for PIST, as shown in overlays (Figs. 6I and L). Similar experiments using the anti-lamp1 antibody as a molecular marker revealed that NT exposure did not induce the trafficking of NTS2 receptors to lysosomes for degradation (not shown). Taken together, these data suggest that NTS2 receptors targeted to the plasma membrane subsequent to NT stimulation could originate from the TGN/Golgi.

Effect of NT stimulation on cell surface NTS2 receptor density in rat spinal cord neurons

To determine whether the preservation of cell surface NTS2 receptors observed following sustained stimulation of transfected cells in vitro also occurred in neuronal cells in vivo, we examined by immunoelectron microscopy the fate of NT-stimulated NTS2 receptors in neurons of the superficial layers of the rat spinal cord, which had previously been reported to contain high concentrations of NTS2 receptor immunoreactivity [22]. In both stimulated and unstimulated conditions, the bulk of NTS2 immunoreactivity was associated with dendritic shafts, branches, and branchlets (Figs. 7A and B). In saline-injected rats, NTS2 immunolabeling within these dendrites was associated mostly with intracellular vesicles and organelles (Fig. 7A). Only a small fraction of immunogold particles was found on the plasma membrane (4.7 ± 2.6% of total; Fig. 7C). Following 20 min exposure to intrathecal NT, there was a considerable increase in the proportion of immunogold–receptor complexes associated with the plasma membrane (35.1 ± 8.5% of total; Figs. 7B and C). By contrast, the density of immunoreactive receptors (immunogold particles/μm^2) was not statistically significantly different between NT- (4.6 ± 2.3 particles/μm^2) and saline-injected (8.2 ± 4.7 particles/μm^2) animals ($p > 0.95$; Student's t test), indicating that the NT-induced change in plasma membrane receptor density was a trafficking event.

Discussion

In the present study, we have demonstrated a preservation of cell surface NTS2 receptor densities following prolonged exposure to NT. This preservation did not depend on receptor neosynthesis or recycling, but appeared to involve recruitment of spare receptors from intracellular stores to the plasma membrane.

Sustained activation of most GPCRs triggers a time-dependent decline of cell surface receptors. This process, which reverses upon agonist removal, is of direct clinical relevance as it accounts in part for cellular desensitization to a variety of GPCR-acting drugs [23]. As confirmed in

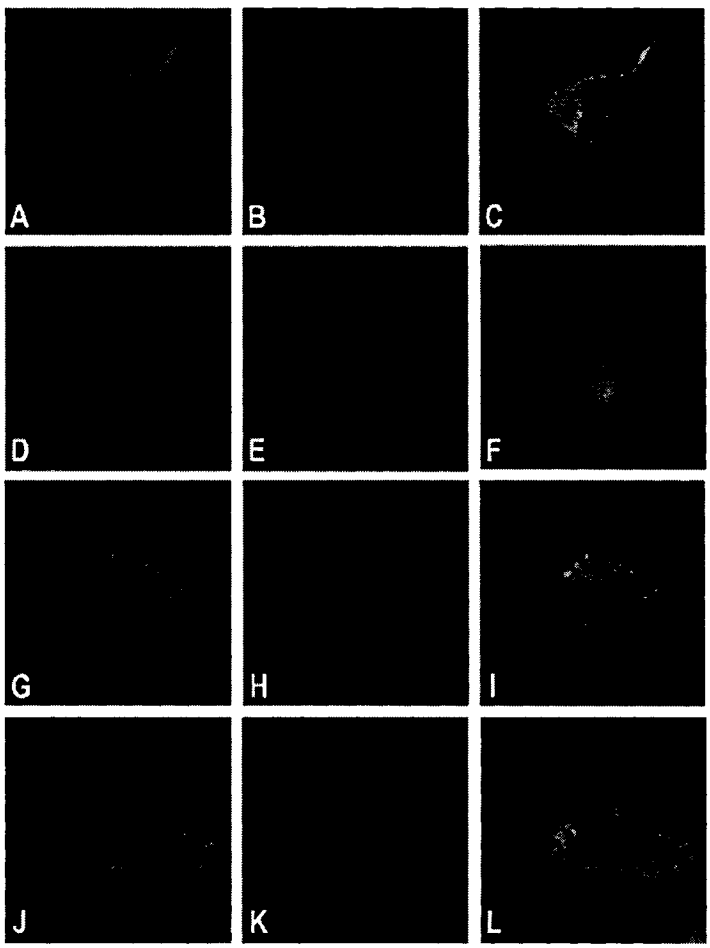

Fig. 6. Dual immunolabeling of NTS2 and trans-Golgi network markers in COS-7 cells. Confocal microscopic images of cells transiently expressing rNTS2 preincubated (G–L) or not (A–F) with 1 μM NT for 1 h at 37 °C. In unstimulated cells, NTS2 labeling with the NTS2 peptide antiserum (A,D) co-localizes with immunoreactivity for the TGN/Golgi markers syntaxin 6 (B) and PIST (E) in the perinuclear zone as evident in the overlays (C,F). Following incubation with NT, NTS2 immunostaining is punctate and dispersed throughout the cell. Part of NTS2-positive vesicles also exhibit syntaxin 6 (H) but not PIST (K) immunoreactivity as shown in the merged images (I,L). All images were acquired using the same parameters and represent three different experiments.

the present study, agonist stimulation of NTS1 likewise resulted in a loss of cell surface receptors that is known to occur through internalization and lysosomal degradation (reviewed in [15]). In the case of NTS2, stimulation with NT was found here to first induce a rapid decrease in cell surface receptor density (i.e., 50% by 5 min). This decrease was previously shown by us [9] and others [24] to be due to ligand-induced receptor internalization and, accordingly, to be entirely abolished in the presence of sucrose or phenylarsine oxide, which inhibits internalization. However, this decrease was short-lived and, in spite of persistent ligand exposure, NTS2 receptors rapidly resurfaced. Indeed, binding activity recovered to 80% of pre-stimulation levels by 1 h and to 100% after 24 h of stimulation with NT. This reinstatement of cell surface receptors cannot be ascribed to ligand degradation as the same phenomenon was observed when the incubation was carried out with the protease-resistant NT analog JMV-431, instead of NT. The cell surface binding sites maintained during persistent NT exposure corresponded to functional NTS2 receptors, since NT-induced ERK1/2 phosphorylation levels in cells exposed to NT for 24 h were

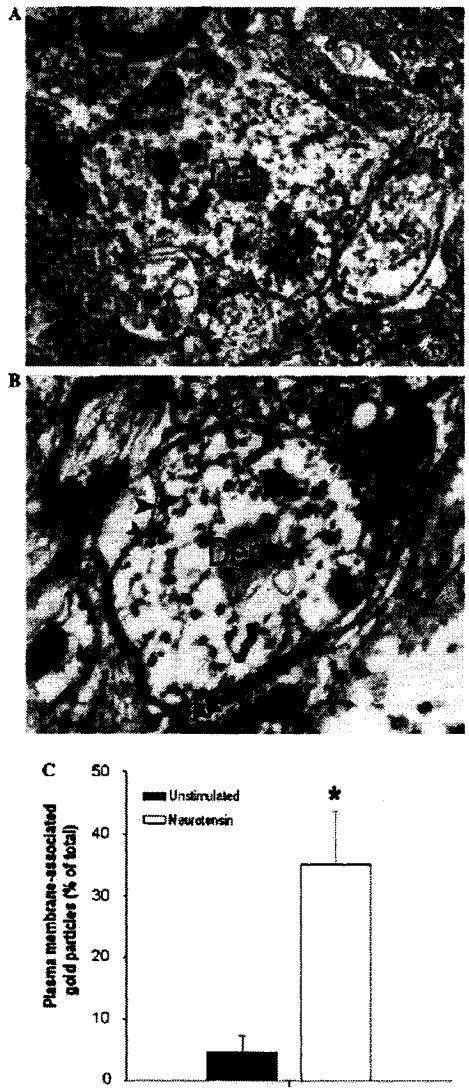

Fig. 7. Electron microscopic detection of NTS2 immunoreactive receptors in superficial laminae of the rat lumbar spinal cord. (A) In the absence of the agonist, gold particles (i.e., NTS2 immunolabeling) are mainly intracellular and poorly associated with dendritic (Den) plasma membranes. (B) In the presence of NT, numerous immunogold particles are associated with dendritic plasma membranes (arrowheads). (C) Effects of NT exposure on membrane-associated/total NTS2. The asterisk indicates a significant difference ($p < 0.05$) from control.

comparable to those measured in control cells and were similar to those previously reported in rat cerebellar granule cells [9] and transfected CHO cells [8].

Maintenance of cell surface receptors in response to sustained activation has been documented for a limited number of GPCRs including the β_3-adrenergic receptor [25], somatostatin receptor subtype 1 [26], and AT_2 angiotensin II receptors [27]. It has also been shown for the single transmembrane domain receptor NTS3, following prolonged stimulation with NT [28,29]. Cell surface receptor densities are known to result from the equilibrium between receptor internalization, recycling, and recruitment from intracellular stores [30]. In the case of NTS2, recycling of internalized receptors, demonstrated under different experimental conditions [24,31], did not appear to account significantly for the reinstatement of the plasma membrane receptor population after prolonged NT exposure. Indeed, cell surface receptor recovery was not affected by blockade of receptor recycling with monensin nor by replacing rat NTS2 with the non-recycling human NTS2 [19]. Neither did the maintenance of cell surface NTS2 receptor densities appear to require receptor neosynthesis since NTS2 protein levels, as measured by Western blotting, remained unchanged following NT exposure with or without the protein synthesis inhibitor cycloheximide.

Immunocytochemistry revealed that under baseline conditions, the bulk of NTS2 proteins were intracellular (i.e., $84.7 \pm 1.8\%$ of total receptors in basal conditions). This observation is in agreement with the results of subprograms executed by the PSORT II server (Kenta Nakai, Ph.D., Institute for Medical Science, University of Tokyo, Japan), which predicted the subcellular localization of NTS2 from its amino acid sequence to be poorly localized to the plasma membrane (22.2%) and possibly confined to intracellular stores such as the endoplasmic reticulum (33.3%), Golgi apparatus (11.1%), intracellular vacuoles (22.2%), and mitochondrial compartments (11.1%). However, confocal microscopic experiments on permeabilized cells demonstrated that NT induced an extensive redistribution of NTS2 receptors from the TGN/Golgi complex (syntaxin 6 and PIST-positive) to vesicle-like structures, suggesting that the maintenance of surface NTS2 receptors involved mobilization of spare receptors from internal stores. Although syntaxin 6 was mainly concentrated in the TGN, it was also detected in the NTS2-containing vesicles that formed as a result of NT exposure. This co-localization is consistent with previous results showing that syntaxin 6 co-localizes broadly with the early endosomal autoantigen EEA1 in BHK-21 cells and may therefore be implicated in TGN to endosomes trafficking [32]. Interestingly, an earlier study in NTS2-expressing cerebellar granule cells had demonstrated that following prolonged NT stimulation, internalized fluorescently labeled NT was targeted to a syntaxin 6-positive juxtanuclear compartment, corresponding to the TGN [9]. It is therefore possible that internalized NT is targeted to the TGN and serves as a triggering signal for the translocation of resident NTS2 receptors from this compartment to the cell surface, implying a dynamic regulation of subcellular protein localization.

The physiological and pharmacological relevance of the present results was confirmed by immunogold electron

microscopic studies of the superficial laminae of the rat spinal cord. Intrathecal injection of NT resulted in a sevenfold increase in the proportion of immunoreactive NTS2 receptors associated with dendritic plasma membranes as compared with saline-injected controls. This increase in the density of plasma membrane-associated NTS2 was not accompanied by a statistically significant increase in the overall receptor population, suggesting that, as in our in vitro studies, the NT-induced increase of NTS2 receptors at the plasma membrane of dorsal horn neurons was a trafficking event. These results are reminiscent of the enhanced recruitment of δ-opioid receptors (DOR) to the plasma membrane of dendrites in the same superficial laminae of the dorsal horn following either prolonged morphine treatment [33] or chronic inflammation [34]. However, whereas this enhanced DOR targeting was heterologously mediated through stimulation of μ-opioid receptors [35], the present increase in NTS2 externalization likely results from stimulation of NTS2 receptors themselves. The present results may, therefore, explain the highly potent, long-lasting antinociceptive effects of the NTS2-specific agonist JMV-431 in tests of spinal analgesia [22].

In conclusion, we have demonstrated that cell surface NTS2 receptors are resistant to down-regulation following persistent exposure to NT. By inference from the patterns of intracellular distribution of NTS2 receptors observed using confocal and electron microscopy, we propose that the maintenance of cell surface NTS2 receptors is due in part to the recruitment of spare receptors from internal stores. This stimulation-induced regulation of cell surface NTS2 receptors was even more striking in rat spinal cord neurons in vivo (sevenfold increase in cell surface receptor density) than in transfected COS-7 cells in vitro (return to baseline). Such maintenance of NTS2 bioavailability upon prolonged agonist treatment might prove of great importance for the use of NTS2-selective agonists for the treatment of chronic pain.

Acknowledgments

The authors are grateful to Dr. Hans-Jürgen Kreienkamp for the anti-PIST antibody and Naomi Takeda for secretarial help in the preparation of this article.

References

[1] J.P. Vincent, J. Mazella, P. Kitabgi, Neurotensin and neurotensin receptors, Trends Pharmacol. Sci. 20 (1999) 302–309.
[2] K. Tanaka, M. Masu, S. Nakanishi, Structure and functional expression of the cloned rat neurotensin receptor, Neuron 4 (1990) 847–854.
[3] P. Chalon, N. Vita, M. Kaghad, M. Guillemot, J. Bonnin, B. Delpech, G. Le Fur, P. Ferrara, D. Caput, Molecular cloning of a levocabastine-sensitive neurotensin binding site, FEBS Lett. 386 (1996) 91–94.
[4] M.A. Watson, M. Yamada, B. Cusack, K. Veverka, C. Bolden-Watson, E. Richelson, The rat neurotensin receptor expressed in Chinese hamster ovary cells mediates the release of inositol phosphates, J. Neurochem. 59 (1992) 1967–1970.
[5] M. Yamada, M.A. Watson, E. Richelson, Neurotensin stimulates cyclic AMP formation in CHO-rNTR-10 cells expressing the cloned rat neurotensin receptor, Eur. J. Pharmacol. 244 (1993) 99–101.
[6] C. Poinot-Chazel, M. Portier, M. Bouaboula, N. Vita, F. Pecceu, D. Gully, J.G. Monroe, J.P. Maffrand, G. Le Fur, P. Casellas, Activation of mitogen-activated protein kinase couples neurotensin receptor stimulation to induction of the primary response gene Krox-24, Biochem. J. 320 (Pt 1) (1996) 145–151.
[7] J. Mazella, J.M. Botto, E. Guillemare, T. Coppola, P. Sarret, J.P. Vincent, Structure, functional expression, and cerebral localization of the levocabastine-sensitive neurotensin/neuromedin N receptor from mouse brain, J. Neurosci. 16 (1996) 5613–5620.
[8] L. Gendron, A. Perron, M.D. Payet, N. Gallo-Payet, P. Sarret, A. Beaudet, Low-affinity neurotensin receptor (NTS2) signaling: internalization-dependent activation of extracellular signal-regulated kinases 1/2, Mol. Pharmacol. 66 (2004) 1421–1430.
[9] P. Sarret, L. Gendron, P. Kilian, H.M. Nguyen, N. Gallo-Payet, M.D. Payet, A. Beaudet, Pharmacology and functional properties of NTS2 neurotensin receptors in cerebellar granule cells, J. Biol. Chem. 277 (2002) 36233–36243.
[10] P. Tsao, M. von Zastrow, Downregulation of G protein-coupled receptors, Curr. Opin. Neurobiol. 10 (2000) 365–369.
[11] S.S. Ferguson, Evolving concepts in G protein-coupled receptor endocytosis: the role in receptor desensitization and signaling, Pharmacol. Rev. 53 (2001) 1–24.
[12] E. Donatodi Paola, B. Cusack, M. Yamada, E. Richelson, Desensitization and down-regulation of neurotensin receptors in murine neuroblastoma clone N1E-115 by [D-Lys8] neurotensin (8–13), J. Pharmacol. Exp. Ther. 264 (1993) 1–5.
[13] E. Hermans, M.A. Vanisberg, M. Geurts, J.M. Maloteaux, Down-regulation of neurotensin receptors after ligand-induced internalization in rat primary cultured neurons, Neurochem. Int. 31 (1997) 291–299.
[14] F. Vandenbulcke, D. Nouel, J.P. Vincent, J. Mazella, A. Beaudet, Ligand-induced internalization of neurotensin in transfected COS-7 cells: differential intracellular trafficking of ligand and receptor, J. Cell Sci. 113 (Pt 17) (2000) 2963–2975.
[15] E. Hermans, J.M. Maloteaux, Mechanisms of regulation of neurotensin receptors, Pharmacol. Ther. 79 (1998) 89–104.
[16] P. Sarret, A. Perron, T. Stroh, A. Beaudet, Immunohistochemical distribution of NTS2 neurotensin receptors in the rat central nervous system, J. Comp. Neurol. 461 (2003) 520–538.
[17] C. Labbé-Jullié, S. Barroso, D. Nicolas-Eteve, J.L. Reversat, J.M. Botto, J. Mazella, J.M. Bernassau, P. Kitabgi, Mutagenesis and modeling of the neurotensin receptor NTR1. Identification of residues that are critical for binding SR48692, a nonpeptide neurotensin antagonist, J. Biol. Chem. 273 (1998) 16351–16357.
[18] B. Tycko, C.H. Keith, F.R. Maxfield, Rapid acidification of endocytic vesicles containing asialoglycoprotein in cells of a human hepatoma line, J. Cell Biol. 97 (1983) 1762–1776.
[19] S. Martin, J.P. Vincent, J. Mazella, Recycling ability of the mouse and the human neurotensin type 2 receptors depends on a single tyrosine residue, J. Cell Sci. 115 (2002) 165–173.
[20] J.B. Bock, J. Klumperman, S. Davanger, R.H. Scheller, Syntaxin 6 functions in trans-Golgi network vesicle trafficking, Mol. Biol. Cell 8 (1997) 1261–1271.
[21] W. Wente, T. Stroh, A. Beaudet, D. Richter, H.J. Kreienkamp, Interactions with PDZ domain proteins PIST/GOPC and PDZK1 regulate intracellular sorting of the somatostatin receptor subtype 5, J. Biol. Chem. 280 (2005) 32419–32425.
[22] P. Sarret, M.J. Esdaile, A. Perron, J. Martinez, T. Stroh, A. Beaudet, Potent spinal analgesia elicited through stimulation of NTS2 neurotensin receptors, J. Neurosci. 25 (2005) 8188–8196.
[23] B.L. Roth, D.L. Willins, W.K. Kroeze, G protein-coupled receptor (GPCR) trafficking in the central nervous system: relevance for drugs of abuse, Drug Alcohol Depend. 51 (1998) 73–85.
[24] J.M. Botto, J. Chabry, P. Sarret, J.P. Vincent, J. Mazella, Stable expression of the mouse levocabastine-sensitive neurotensin receptor

in HEK 293 cell line: binding properties, photoaffinity labeling, and internalization mechanism, Biochem. Biophys. Res. Commun. 243 (1998) 585–590.
[25] R.F. Thomas, B.D. Holt, D.A. Schwinn, S.B. Liggett, Long-term agonist exposure induces upregulation of beta 3-adrenergic receptor expression via multiple cAMP response elements, Proc. Natl. Acad. Sci. USA 89 (1992) 4490–4494.
[26] N. Hukovic, M. Rocheville, U. Kumar, R. Sasi, S. Khare, Y.C. Patel, Agonist-dependent up-regulation of human somatostatin receptor type 1 requires molecular signals in the cytoplasmic C-tail, J. Biol. Chem. 274 (1999) 24550–24558.
[27] D.T. Dudley, R.M. Summerfelt, Regulated expression of angiotensin II (AT2) binding sites in R3T3 cells, Regul. Pept. 44 (1993) 199–206.
[28] V. Navarro, S. Martin, P. Sarret, M.S. Nielsen, C.M. Petersen, J. Vincent, J. Mazella, Pharmacological properties of the mouse neurotensin receptor 3. Maintenance of cell surface receptor during internalization of neurotensin, FEBS Lett. 495 (2001) 100–105.
[29] A. Morinville, S. Martin, M. Lavallée, J.P. Vincent, A. Beaudet, J. Mazella, Internalization and trafficking of neurotensin via NTS3 receptors in HT29 cells, Int. J. Biochem. Cell Biol. 36 (2004) 2153–2168.
[30] J.A. Koenig, J.M. Edwardson, Endocytosis and recycling of G protein-coupled receptors, Trends Pharmacol. Sci. 18 (1997) 276–287.
[31] C. Debaigt, H. Hirling, P. Steiner, J.P. Vincent, J. Mazella, Crucial role of neuron-enriched endosomal protein of 21 kDa in sorting between degradation and recycling of internalized G-protein-coupled receptors, J. Biol. Chem. 279 (2004) 35687–35691.
[32] A. Simonsen, J.M. Gaullier, A. D'Arrigo, H. Stenmark, The Rab5 effector EEA1 interacts directly with syntaxin-6, J. Biol. Chem. 274 (1999) 28857–28860.
[33] C.M. Cahill, A. Morinville, C. Hoffert, D. O'Donnell, A. Beaudet, Up-regulation and trafficking of delta opioid receptor in a model of chronic inflammation: implications for pain control, Pain 101 (2003) 199–208.
[34] C.M. Cahill, A. Morinville, M.C. Lee, J.P. Vincent, B. Collier, A. Beaudet, Prolonged morphine treatment targets delta opioid receptors to neuronal plasma membranes and enhances delta-mediated antinociception, J. Neurosci. 21 (2001) 7598–7607.
[35] A. Morinville, C.M. Cahill, M.J. Esdaile, H. Aibak, B. Collier, B.L. Kieffer, A. Beaudet, Regulation of delta-opioid receptor trafficking via mu-opioid receptor stimulation: evidence from mu-opioid receptor knock-out mice, J. Neurosci. 23 (2003) 4888–4898.